

GEOLOGY, GEOCHEMISTRY AND GEOCHRONOLOGY
OF THE SPRINGDALE GROUP, AN EARLY SILURIAN
CALDERA IN CENTRAL NEWFOUNDLAND

CENTRE FOR NEWFOUNDLAND STUDIES

**TOTAL OF 10 PAGES ONLY
MAY BE XEROXED**

(Without Author's Permission)

MARYLOU COYLE



National Library
of Canada

Bibliothèque nationale
du Canada

Canadian Theses Service Service des thèses canadiennes

Ottawa, Canada
K1A 0N4

The author has granted an irrevocable non-exclusive licence allowing the National Library of Canada to reproduce, loan, distribute or sell copies of his/her thesis by any means and in any form or format, making this thesis available to interested persons.

The author retains ownership of the copyright in his/her thesis. Neither the thesis nor substantial extracts from it may be printed or otherwise reproduced without his/her permission.

L'auteur a accordé une licence irrévocable et non exclusive permettant à la Bibliothèque nationale du Canada de reproduire, prêter, distribuer ou vendre des copies de sa thèse de quelque manière et sous quelque forme que ce soit pour mettre des exemplaires de cette thèse à la disposition des personnes intéressées.

L'auteur conserve la propriété du droit d'auteur qui protège sa thèse. Ni la thèse ni des extraits substantiels de celle-ci ne doivent être imprimés ou autrement reproduits sans son autorisation.

ISBN 0-315-65314-0

**GEOLOGY, GEOCHEMISTRY AND GEOCHRONOLOGY
OF THE
SPRINGDALE GROUP,
AN EARLY SILURIAN CALDERA IN
CENTRAL NEWFOUNDLAND**

by

(c) Marylou Coyle

**A thesis submitted to the School of Graduate Studies
in partial fulfillment of the
requirements for the degree of
Doctor of Philosophy**

**Department of Earth Sciences
Memorial University of Newfoundland
St. John's, Newfoundland**

1990

ABSTRACT

Volcanic-sedimentary facies and structural relationships of the Silurian Springdale group in west central Newfoundland are indicative of a large collapse caldera, with an area of more than 2,000 km². Basaltic flows, andesite flows and pyroclastics rocks, silicic ash-flow tuffs, high -silica rhyolite domes, and volcanically derived debris-flows and breccias and mesobreccias, fluviatile red sandstones and conglomerates make up the group. Five new uranium/lead zircon dates provided in this study show for the lowermost ash-flow tuff of the group an age of $432.4 \pm 1.7/-1.4$ Ma, the Burnt Berry rhyolite dome of 430.8 ± 2 Ma, and the topmost Indian River ash-flow tuff of 425 ± 3 Ma, as well the age of 427 ± 2 Ma for both the King's Point complex and the Cape St. John Group.

The Springdale Group is bounded on the east and west by up-faulted basement rocks which include gneisses, amphibolites and pillow lavas derived from Lower Ordovician volcanic rocks, and in the northwest unconformably overlies the equivalent less metamorphosed Lower Ordovician submarine volcanics. These margins are intruded by cogenetic and younger granitoid rocks. The volcanic rocks form a calc-alkaline series, although gaps in silica

content between 52 to 56%, 67 to 68%, and 73 to 74% separate them into four groups, basalts, andesites-dacites, rhyolites, and high-silica rhyolites.

The high-silica rhyolites are chemically comparable to melts thought to form the upper parts of large layered silicic magma chambers of epicontinental regions. Such an environment is also suggested by the large area of the Springdale caldera, and the probability that it is one of at least five calderas which make up a large Silurian volcanic field. An epicontinental tectonothermal environment for central Newfoundland in Silurian-Devonian times is readily explained by the fact that this magmatic activity followed a period of destruction and closure of the Lower Paleozoic Iapetus Ocean, with trapped heat and basaltic magma causing large scale crustal melting in an overall transpressional tectonic regime.

ACKNOWLEDGEMENTS

I am grateful to Dr. D. F. Strong for suggesting and supervising this study, without his inspiration, intelligence and persistence the Springdale caldera would still be unfound. I also thank Drs. B. J. Fryer and D. H. C. Wilton for serving on my supervisory committee. I especially thank Dr. T.P. Krogh for welcoming me to his laboratory at the Royal Ontario Museum for the zircon dating, and to Dr. R. Tucker for assistance with the mass spectrometry. I thank Dr. K. L. Currie for his support of this project, Drs. P. Erdmer , J. Van Birkle, and J. Tuach for helicopter support, S. J. P. Burry, D. Dingwell, D. and L. Kontak, H. Sandeman, D. Machin, M. Basha, E. Lambert, D. Gibbons, C. Saunders, H. S. Swinden, P. Roberts, and D. Taylor for field assistance, J. O'Sullivan and Esso Minerals Ltd., A. A. Burgoyne and R. Hewton of Brinco Mining, D. McInnes and Steve Walker of Noranda Mines Ltd., and "Scotty" of Viking Helicopters Ltd. for logistic support; G. Andrews, D. Press, G. Veinott, Drs. H. Longerich and S. Jackson for chemical analyses; and S. J. P. Burry and L. Nolan for drafting.

I am grateful to the Newfoundland and Labrador Department of Forestry at Springdale and Pinns Brook for the use of their aerial photographs, and Kreuger Paper Co. in Corner Brook for maps and road access. This study was funded by the Geological Survey of Canada through Canewf Resources Ltd. (Project no. 840024), with additional support from Memorial University of Newfoundland and the Natural Sciences and Engineering Research Council of Canada (Operating Grant no. A7975 to D.F. Strong). The thesis would not have met the deadline without the extraordinary support from Joan Burry and Heather Seviour.

I thank Terry Heard of Equity Silver Mines Ltd. and Matthew Blecha of Tech Corporation Ltd. for their help and support during the mineral assessment phases of the project, and particularly for the geophysical surveys which were so useful in refining the geological interpretations.

Thank you especially to my loving family and my friends for their encouragement and support during this study.

TABLE OF CONTENTS

ABSTRACT-----	ii
ACKNOWLEDGEMENTS-----	iv
TABLE OF CONTENTS-----	vi
LIST OF FIGURES-----	viii
LIST OF PLATES-----	x
LIST OF TABLES-----	xv
LIST OF APPENDICES-----	xv
CHAPTER 1 - INTRODUCTION-----	1
1.1. Statement of the Problem-----	1
1.2. Appalachian/Caledonian Silurian Volcanic Sequences	4
1.3. Calderas and Ash-Flow Tuffs-----	7
CHAPTER 2 - GEOLOGY OF THE SPRINGDALE GROUP-----	17
2.1. Introduction-----	17
2.2. Local Geological Setting of the Springdale Group--	20
2.3. Unit 1-----	31
2.4. Unit 2-----	32
2.5. Unit 3-----	39
2.6. Unit 4-----	40
2.7. Unit 5-----	42
2.8. Unit 6-----	46
2.9. Unit 7-----	50
2.10. Unit 8-----	52
2.11. Unit 9-----	60
2.12. Unit 10-----	63
2.13. Domes and Vent Centres of the Springdale Caldera--	66
2.14. Intrusive Rocks-----	92
2.15. Structural Geology-----	93
2.15.1. Faults-----	93
2.15.2. Folds-----	105
2.16. Detailed Geology, Springdale Central Map Area (Map 2)	105
2.16.1. Geophysics-----	105
2.16.2. Geology-----	109
2.17. Detailed Geology of the Springdale East map Area	
(Maps 3 and 4)-----	112
2.17.1. Geophysics-----	112
2.17.2. Geology-----	119
2.18. Summary and Discussion-----	124

CHAPTER 3. PETROGRAPHY OF THE ROCKS OF THE SPRINGDALE CALDERA-----	127
3.1. Introduction-----	127
3.2. The Mafic Flows-----	129
3.3. The Intermediate Flows-----	140
3.4. Pyroclastic (Ash-flow) Tuffs-----	144
3.5. Dacitic Domes-----	154
3.6. High-Silica Rhyolitic Domes, Dykes and Sills-----	157
CHAPTER 4. CHEMISTRY OF SPRINGDALE GROUP IGNEOUS ROCKS-----	163
4.1. Introduction-----	163
4.2. Mafic Rocks-----	169
4.3. Intermediate Rocks (Andesite-Dacite)-----	189
4.4. Felsic Rocks (Rhyodacite-Rhyolite)-----	192
4.5. Silicic Rocks (High-Silica Rhyolite)-----	194
4.6. Summary and Conclusions-----	202
CHAPTER 5. GEOCHRONOLOGY-----	206
5.1. Introduction-----	206
5.2. Results-----	208
5.2.1. Springdale Group, Unit 1 (Sample Zr-11)-----	208
5.2.2. Springdale Group, Burnt Berry Dome (Zr-7)-----	212
5.2.3. Springdale Group, Unit 10 (Sample Zr-3)-----	217
5.2.4. King's Point Complex (Sample KP-1000)-----	222
5.2.5. Cape St. John Group (Sample CSJ-10)-----	223
5.3. Discussion-----	229
5.4. Summary-----	236
CHAPTER 6. MINERALIZATION POTENTIAL-----	241
6.1. Introduction-----	241
6.2. Calderas and Mineralization-----	241
6.3. Epithermal Deposits-----	242
6.4. Appalachian Silurian-Devonian Caldera Suites-----	253
6.5. The Springdale Caldera-----	258
6.6. Summary-----	261
CHAPTER 7.7. SUMMARY, INTERPRETATIONS AND CONCLUSIONS-----	262
7.1. Introduction-----	262
7.2. Chemistry-----	266
7.3. Geochronology-----	267
7.4. Caldera Evolution-----	269
7.5. Tectonic Controls-----	283
7.6. Economic Potential-----	284
7.7. Conclusion-----	286
REFERENCES-----	288

LIST OF FIGURES

- Figure 1.1.** Distribution of Silurian-Devonian rocks in the northern Appalachians and northern Britain.
- Figure 1.2.** Tectonic setting of the Springdale Group.
- Figure 1.3.** Tectonic settings of the Taupo and Oslo rift calderas.
- Figure 1.4.** A generalized ash-flow caldera cycle.
- Figure 2.1.** Tectonic setting of the Springdale Group.
- Figure 2.2.** Silurian volcano-plutonic suites of the Springdale area.
- Figure 2.3.** Simplified geological map of the Springdale caldera.
- Figure 2.4(a to c)** Cross sections of domes and tephra deposits.
 (d). Pre-eruptive (A) and eruptive (B) stages for Vulcanian activity.
 (e). Cross section through a rhyolite dome.
 (f). Interpretation of the features of Johnson's Lookout.
- Figure 2.5(a).** Major faults of western Newfoundland.
 (b). Reconstruction of the major fault zones of the Springdale region.
 (c). Geology and major faults of the northern edge of the Springdale caldera.
 (d). Linear-enhanced Landsat digital image of the Springdale caldera.
- Figure 2.6.** Aeromagnetic map of the Springdale Central map area.
- Figure 2.7(a).** Aeromagnetic anomaly map of the Springdale East map area, northern half.
 (b). Aeromagnetic anomaly map of the Springdale East map area, southern half.
- Figure 4.1** Histograms of silica distribution in all (165) analysed samples from the Springdale Group.

- Figure 4.2. Classification of volcanic rocks of the Springdale Group in terms of silica and a number of "immobile" trace elements.
- Figure 4.3. Chemical classification of the Springdale Group basalts.
- Figure 4.4. Classification of Springdale Group basalts based on the variation of FeO^*/MgO .
- Figure 4.5. Pearce and Cann discrimination diagrams applied to the Springdale Group basalts.
- Figure 4.6. Covariation diagrams for a number of trace elements in the Springdale Group mafic rocks.
- Figure 4.7. Extended rare earth element plots for Springdale Group mafic rocks.
- Figure 4.8. Extended rare earth element diagrams for the four groups of mafic, intermediate, felsic and silicic rocks of the Springdale Group.
- Figure 4.9. Extended rare earth element plots for Springdale Group intermediate (a), felsic (b) and silicic (c) rocks
- Figure 4.10. K/Rb in the Springdale Group intermediate rocks (a) and mafic rocks (b).
- Figure 4.11. Classification of Springdale Group felsic rocks according to the scheme of Pearce et al. (1984).
- Figure 4.13. Variation of selected elements with niobium in the rhyolites of the Springdale Group.
- Figure 5.1. Concordia plot for sample ZR-11. Springdale Group, Unit 1.
- Figure 5.2. Concordia plot for zircon sample no. Zr-7, Burnt Berry Dome.
- Figure 5.3. Concordia plot for zircon sample no. Zr-3, Indian River Tuff.
- Figure 5.4. Concordia plot for zircon sample no. KP-1000, King's Point Complex.

- Figure 5.5. Concordia plot for zircon sample no. CSJ-10, Cape St. John Group.
- Figure 5.6 Summary of the U/Pb zircon dates produced in this study.
- Figure 6.1. Idealized model of epithermal precious metal deposits.
- Figure 6.2. Calderas of the San Juan volcanic field.
- Figure 6.3. Generalized geology of the Creede and San Luis calderas, the Creede mining district, and schematic representation of the Creede hydrothermal system.
- Figure 6.4 Generalized geology of the Platoro and Summitville calderas.
- Figure 6.5. Distribution of reported epigenetic gold mineralization in Newfoundland.
- Figure 7.1. Schematic outline of the main structural elements of the Springdale caldera.
- Figure 7.2. Schematic outline of the sequence of events which produced the Springdale caldera and its products.
- Figure 7.3 Schematic outline of events leading to generation of caldera-forming units.

LIST OF PLATES

- Plate 2.1. Helicopter views of folded ridges of Springdale sandstones.
- Plate 2.2(a). Redbeds of the Springdale Group.
- (b). Gently-dipping Springdale Group sandstones.
- Plate 2.3. Foliated amphibolite of Unit A.
- Plate 2.4(a). Lithic clasts and biotite phenocrysts in glassy groundmass with crystal fragments, Unit 1.
- (b). Perlitic, spherulitic and eutaxitic textures in clasts of Unit 1.
- Plate 2.5(a,b). Coarse laharic breccia of Unit 2.
- (c). Grossly bedded megabreccias of Unit 2.
- (d). Volcanic conglomerate in megabreccia collapse blocks.
- (e). Partially abraded blocks in a microbrecciated "frothy" matrix of Unit 2.

- Plate 2.6. Photomicrograph of glomerocrystic andesite of Unit 3.
- Plate 2.7(a). Weakly welded dacitic lapilli tuff of Unit 4.
(b). Welded part of Unit 4.
- Plate 2.8. Flat-topped ridge of basalt flows of Unit 5.
- Plate 2.9(a). Zone of plagioclase phenocryst concentration in basalt of Unit 5.
(b). Basalt flow-top breccia.
- Plate 2.10. Welded basal zone of Unit 6, with large flattened pumice bombs.
- Plate 2.11. Large lithophysae in ash-flow tuff of Unit 6.
- Plate 2.12. Flat-lying orientation of welding and flattened pumice in Unit 6.
- Plate 2.13(a). Ash-flow tuff of Unit 7.
(b). Flow-banding in densely welded very fine-grained dacitic ash-flow tuff of Unit 7.
- Plate 2.14. Rhyolitic ash-flow tuff of Unit 8.
- Plate 2.15. Vitric tuff member of Unit 8.
- Plate 2.16. Pyroclastic breccia of Unit 8.
- Plate 2.17. Small "dykelet" of mafic magma entraining some droplets of felsic melt in ash-flow tuff of Unit 8.
- Plate 2.18. Burnt Berry Rhyolite dome (Unit C).
- Plate 2.19. Typical sequence of Springdale "redbeds" (Unit 9).
- Plate 2.20. Ripple marks on the surface of a bedding plane in sandstone of Unit 9.
- Plate 2.21. Eutaxitic texture in ash-flow tuff of Unit 10.
- Plate 2.22. Microlites of riebeckite in groundmass of rhyolite from Burnt Berry dome.
- Plate 2.23. Convoluted flow-foliation in the Burnt Berry dome (Unit C).

- Plate 2.24. Autobrecciation in gas-rich zones of the Burnt Berry dome.
- Plate 2.25. The eastern side of Johnson's Lookout.
- Plate 2.26. Autoclasification of flow-banded dacite of Johnson's Lookout.
- Plate 2.27. Columnar joints and cooling fractures along the eastern scarp of Johnson's Lookout.
- Plate 2.28. Greyish layers of isotropic dacite (left) with little or no fracture/autoclasification.
- Plate 2.29. Polymictic cobble conglomerate of Unit 9.
- Plate 2.30. Glassy pilotaxitic-textured dacite with flow-aligned plagioclase laths.
- Plate 2.31. Small amphibole laths in Wolf Head dacite.
- Plate 2.32. Splay-like intrusions of lithophysae dykes
- Plate 2.33. Micro-fractures off-setting flow banding of Burnt Berry rhyolite.
- Plate 2.34. Waterfall on cliffs of the west Brook dome.
- Plate 2.35. Vent breccia.
- Plate 3.1. Amygdale showing complex array of secondary minerals.
- Plate 3.2. Glomeroporphyritic basalt
- Plate 3.3a. Plagioclase-phyric cumulate basalt.
- Plate 3.3b. As above with crossed polars.
- Plate 3.4 Ophitic basalt
- Plate 3.5. Subophitic texture.
- Plate 3.6. Same as sample above, shows albite twinning in the feldspars (4x, XPL).
- Plate 3.7. Porphyritic basalt.

- Plate 3.8. Olivine pseudomorphs rimmed with chlorite.
- Plate 3.9a. Radial array of amygdale minerals
- Plate 3.9b. Amygdale and groundmass showing diverse secondary minerals.
- Plate 3.10. Example of amygdale with prenite, epidote and chlorite.
- Plate 3.11. Surface of intermediate lava flow (andesite).
- Plate 3.12. Typical andesite with porphyritic texture.
- Plate 3.13. Magmatic biotite.
- Plate 3.14. Banded, unwelded crystal lithic tuff.
- Plate 3.15. Example of perlitic fractures in the groundmass and devitrified clasts.
- Plate 3.16. Crystal-lithic-vitic tuff with well preserved fiamme.
- Plate 3.17. Welded crystal-lithic tuff showing basaltic fragment and feldspar crystal.
- Plate 3.18. Example of moderately welded portion of Unit 6 with silicic lithic fragment.
- Plate 3.19. Variation in welding across a microscopic field from Unit 6.
- Plate 3.20. Unwelded vitric tuff from Unit 7 with well preserved pumice.
- Plate 3.21. Alternating flow bands of glassy groundmass and pumice.
- Plate 3.22. Fine crystal-vitric tuff from Unit 8 with small black fiamme.
- Plate 3.23. Black glassy pumice disaggregated in a felsic ashy groundmass.
- Plate 3.24. Disequilibrium feldspar in the groundmass of a mixed tuff within Unit 8.

- Plate 3.25. Vitric shards.
- Plate 3.26. Pumice from dome carapace
- Plate 3.27. Excellent example of eutaxitic texture in crystal-rich tuff.
- Plate 3.28. Same as photograph above with more detail.
- Plate 3.29. Typical glassy nature of the dacitic domes.
- Plate 3.30. Microphenocryst of feldspar.
- Plate 3.31. Autobrecciated dacite.
- Plate 3.32. Glassy rhyolite.
- Plate 3.34. Granulation along microfracture.
- Plate 3.35a. Devitrification spherule.
- Plate 3.35b. Same as above with crossed polars.
- Plate 5.1. SEM split-screen photo of ZR-11
- Plate 5.2. ZR-11 photo of unabraded sample morphology
- Plate 5.3. Photo of abraded fraction of zircons ZR-11
- Plate 5.4. Zr-7 photos unabraded
- Plate 5.5. ZR-7 abraded pop of zircons
- Plate 5.6. Zr-3 photos.
- Plate 5.7. Photos of kp-1000.
- Plate 5.8. CJS-10 photos.
- Plate 5.9. Biotite intensely altered to hematite, sericite, chlorite and epidote.
- Plate 5.10. Elongate zircon crystals in sample CSJ-10.
- Plate 5.11. Strongly abraded zircon prisms.
- Plate 5.12a. Cored zircon crystal.

Plate 5.12b. As above, with crossed nicols.

LIST OF TABLES

- Table 1.1. Summary of the characteristics of collapse calderas.
- Table 5.1. Summary of U/Pb isotopic data for zircon geochronology.
- Table 5.2. Summary of available radiometric dates of relevant suites in central Newfoundland.
- Table 6.1. Characteristics of adularia-sericite type and acid-sulfate type deposits.

LIST OF APPENDICES

- APPENDIX A - Summary Petrographic Tables for Selected Rocks of the Springdale Group.
- APPENDIX B - Springdale Group Sample Locations (Universal Transverse Mercator Coordinates)
- APPENDIX C - Analytical Procedures for Major and Trace Elements (AA, XRF, ICP-MS)
- APPENDIX D - Analytical Data for Rocks of the Springdale Group
- APPENDIX E - Laboratory Procedures for Uranium/Lead Zircon Dating

IN POCKET

- Map 1
Map 2
Map 3
Map 4

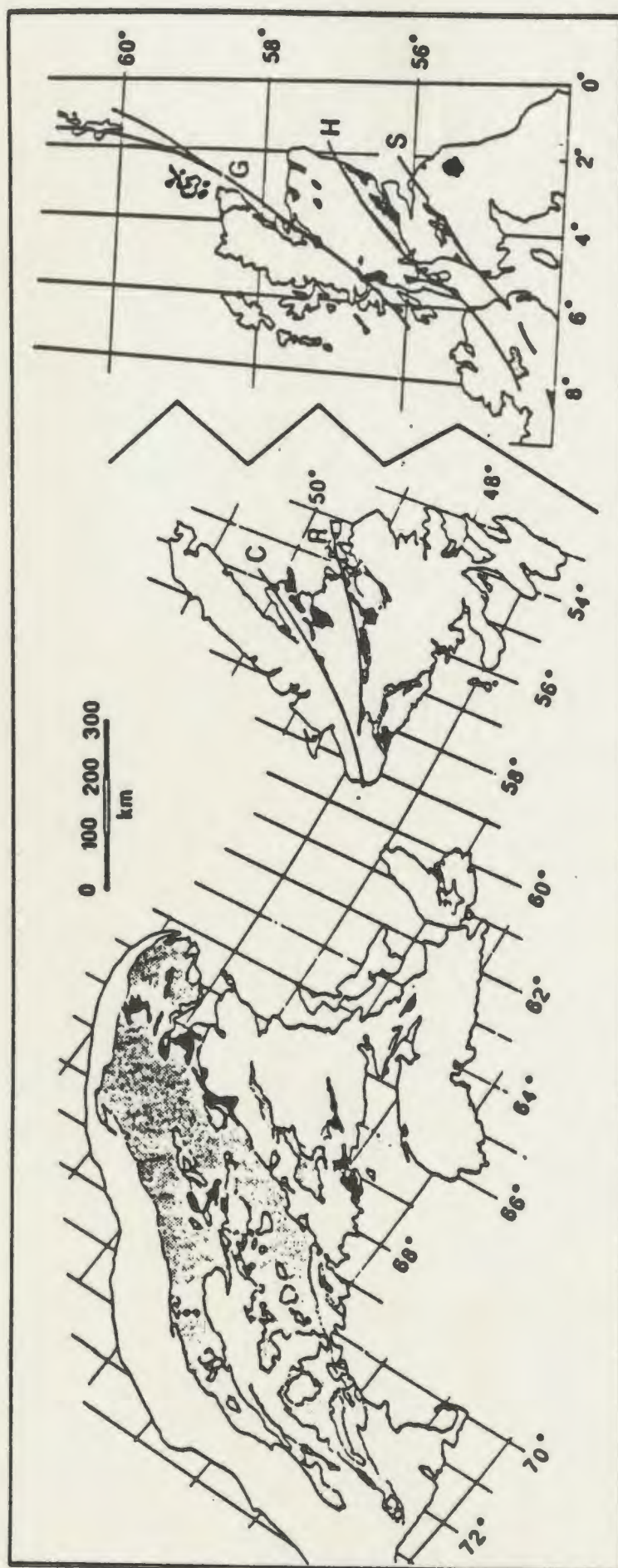
INTRODUCTION

1.1. Statement of the Problem

Calderas are the topographic and volcanological manifestations of shallow magma chambers, which result from deeper-seated thermal processes ultimately reflecting global scale tectonic activity. Accordingly, the documentation of ancient calderas and their products provides essential insights into the magmatic and tectonic evolution of ancient terranes. Since the Silurian-Devonian volcanic belts of the Appalachians are variably eroded, the recognition of such features is enhanced by the variety of structural levels at which they are now exposed. They thus have much to offer for understanding the tectono-thermal evolution of the Appalachian orogen, especially since such volcanic sequences are known throughout the orogen, at least from Scotland to Maine (Fig. 1.1).

The purpose of this study is to characterize and attempt to understand the magmatic and tectonic processes which controlled the development of the Springdale Group, newly recognized by the author as comprizing a full caldera assemblage (Coyle and Strong, 1987). It is based on about twelve months of geological mapping over a three year period, petrographic study of some 400 thin sections, 165 whole-rock chemical analyses, and radiometric dating of five samples by the U/Pb (zircon) method. The study also included some work on correlative sequences in western Newfoundland.

Figure 1.1. Distribution of Silurian-Devonian volcanic (black) and sedimentary (shaded) rocks in the northern Appalachians (Williams, 1980), and of correlative volcanic and sedimentary rocks of northern Britain (Thirlwall, 1981). Lines show major faults in Britain (GG = Great Glen; HB = Highland Boundary; SU = Southern Uplands) and Newfoundland (C = Cabot; R = Reach).



1.2. Appalachian/Caledonian Silurian Volcanic Sequences

Throughout much of Scotland and northern England (Fig.1.1), volcanic rocks are associated with the Silurian-Devonian Old Red Sandstone series of continental sediments. They have received contrasting interpretations, basically centering on whether they were subduction-related or not. Stillman and Francis (1979) considered them to be continental, with any relation to subduction being unlikely, although they did recognize them as a high-K calc-alkaline suite. Others, e.g. Groome and Hall (1974), French et al. (1979), Thirlwall (1981), interpreted the chemistry of these suites as requiring a subduction-related origin, although not all characteristics of subduction are present.

Similar controversies surround the correlative rocks in Maine and Quebec. The Lower Devonian Piscataquis volcanic belt of Maine (Fig. 1.1) was interpreted by Rankin (1968) as part of "a real island arc system", and he suggested that garnet phenocrysts in the rhyolites reflect their "generation from partial melting of sediments in the deeper parts of the Appalachian geosyncline". He subsequently rejected this interpretation (Rankin, 1980), although he did not suggest any precise alternative. Other Silurian-Devonian volcanic-sedimentary sequences of Maine (e.g. the Spider Lake volcanics, the Hedgehog Formation, the Debouille Stock, the Five-mile Brook Formation) may

Correlative rocks along strike in Quebec and northern New Brunswick contain a larger proportion of basaltic and andesitic rocks, and recent studies in Quebec have provided new interpretations. According to Laurent and Belanger (1984), Silurian-Devonian volcanism of the Gaspé area took place within an intracontinental or continental border regime of compression, and was controlled by strike-slip faults. They suggest that the volcanic rocks differ from those of arc-trench systems, being rich in Ti, P and other incompatible elements. They proposed a tectonic model analogous to that of the Alpine system in northern Anatolia and Iran, where Quaternary volcanism is associated with major transcurrent fault zones. This transpressional model provides an elegant resolution to the problem of contrasting Siluro-Devonian volcanic types, and is comparable to that suggested by Strong (1980) for similar-aged granitoid rocks throughout the orogen.

The Springdale Group occurs near the western margin of Newfoundland's lower Paleozoic Central Mobile Belt (Figs. 1.1 and 1.2). Despite their extent and potential importance to understanding mid-Paleozoic magmatic activity in the Appalachians, no volcanological or geochemical studies have previously been carried out on rocks of the Springdale Group. This study provides the first geochemical data for the Springdale Group, and demonstrates that they are calc-alkaline and comparable to orogenic calc-alkaline suites of circum-Pacific regions (cf. Ewart, 1982).

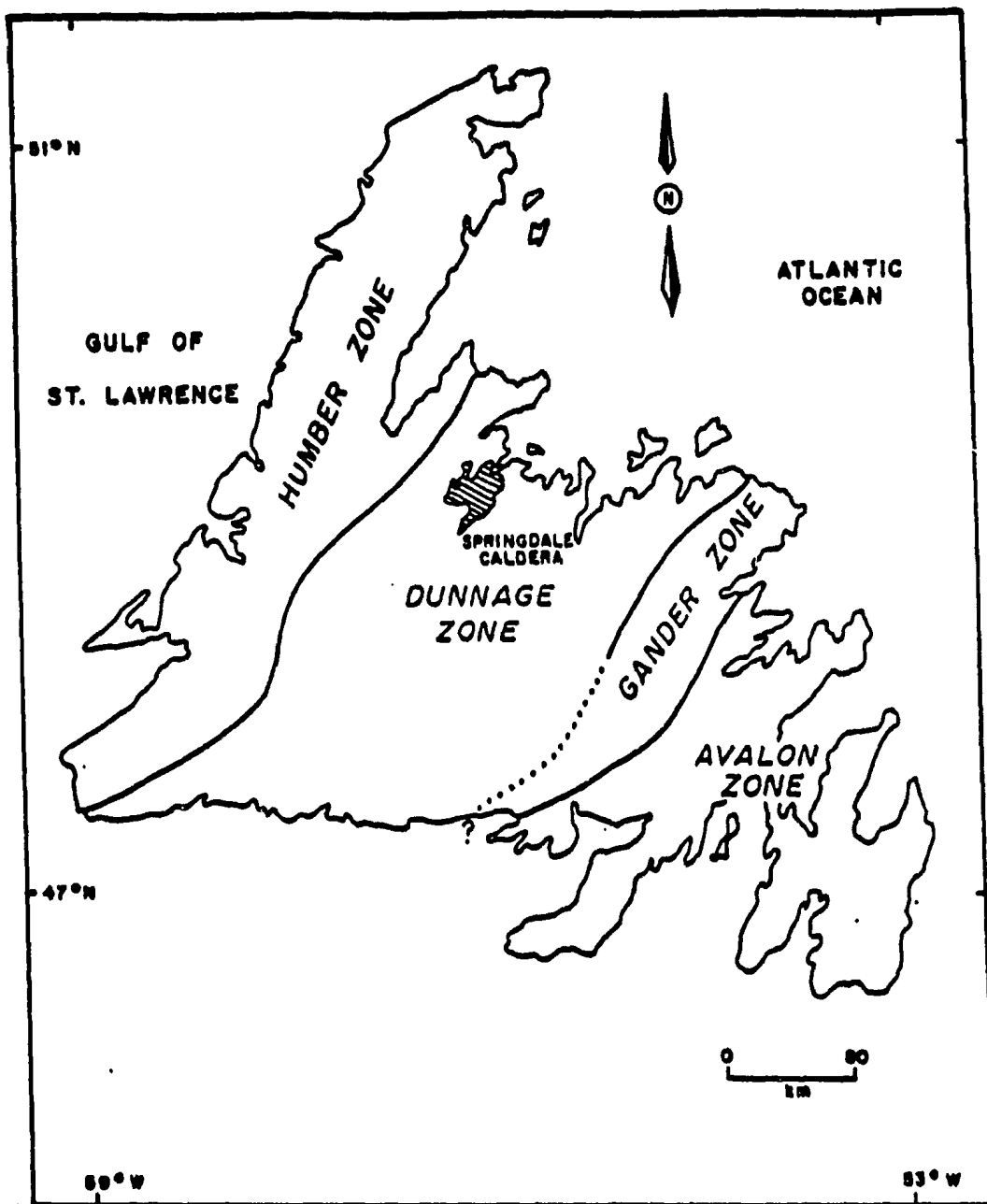


Figure. 1.2. Setting of the Springdale Group within the tectonic-stratigraphic subdivisions of central Newfoundland (modified from Hibbard, 1983).

However the Group also includes a suite of high-silica rhyolites which are similar to the high-silica rhyolites derived from large layered siliceous magma chambers of continental regions such as the Basin and Range area of southwest U.S.A. (cf. Lipman et al., 1978). The Springdale caldera is unlike any found with orogenic calc-alkaline suites in that its large size, representing a minimum eruption volume between 10^3 and 10^4 km³, is matched only by the largest epicontinental calderas, like those of the southwestern USA. This, as do the high-silica ash flow compositions, implies a similar tectono-thermal environment for Silurian-Devonian times in west-central Newfoundland.

1.3. Calderas and Ash-Flow Tuffs

Before presenting the interpretation that the volcanic, plutonic and sedimentary facies of the Springdale Group described below represent the products of caldera collapse and fill, it is useful to review the features and terminology upon which the conclusions are based.

"Epicontinental-type" calderas are characterized by large diameters and associated eruptions of large volumes of pyroclastic material. Smith (1979) estimated relationships between these two parameters and developed the correlation between volumes of eruption and volumes and compositions of the associated magma chambers. In general large calc-alkaline systems produce vertically zoned

pyroclastic eruptions, and in fact all products exceeding 1 km³ are compositionally zoned (Hildreth, 1981). Within such systems processes such as crystal fractionation, thermodiffusion, volatile and liquid complexing and many others may occur and produce specialized fractionates such as high-silica rhyolitic magma.

Such large systems are well-represented by the zoned ash flow sheets of the western U.S.A., e.g. the Bishop tuff, the San Juan volcanic field, and different levels of exposure of the salient tectonic features of caldera and subsidence structures are seen in many other areas, e.g. the Oslo Graben (Ihlen et al., 1982), the Arabian Shield (Roobol and White, 1986), and the Taupo depression (Cole, 1985). They occur as arrays situated within, outside or along rifts or other major structural discontinuities which can reflect an overall plate tectonic regime from separation to collision, in the latter case local extension being produced in the back-arc environment (Fig. 1.3).

Collapse calderas are defined as being produced by the collapse of a magma chamber roof due to the eruption of the magma as pyroclastic and lava flows (Bates and Jackson 1980). These eruptive products are characterized by near-source and intermediate-source facies rocks that accumulate both within and outside the caldera walls. Cunningham and Steven (1979) have termed these the intracaldera facies and the caldera outflow facies, respectively, related to eruption and outflow of

Figure. 1.3. Tectonic settings of the calderas in the Taupo depression (Cole, 1985) and the Oslo rift (Ihlen et al., 1982; Russell and Smythe, 1983).

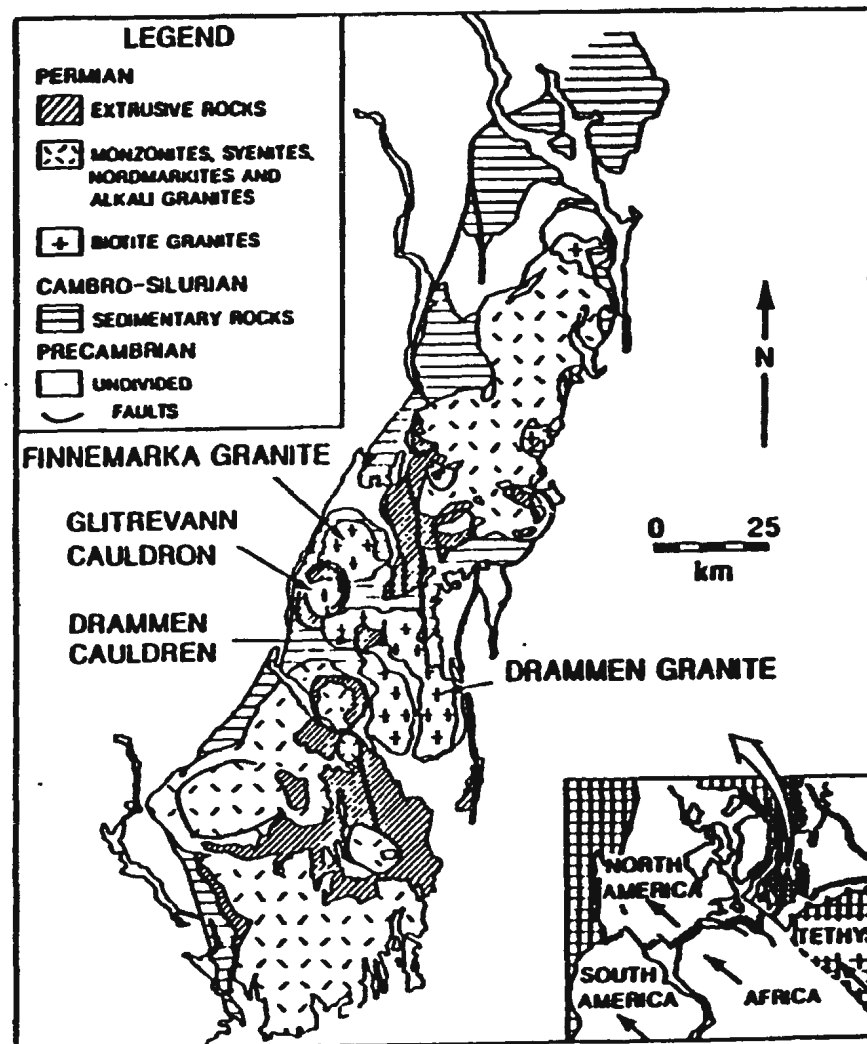
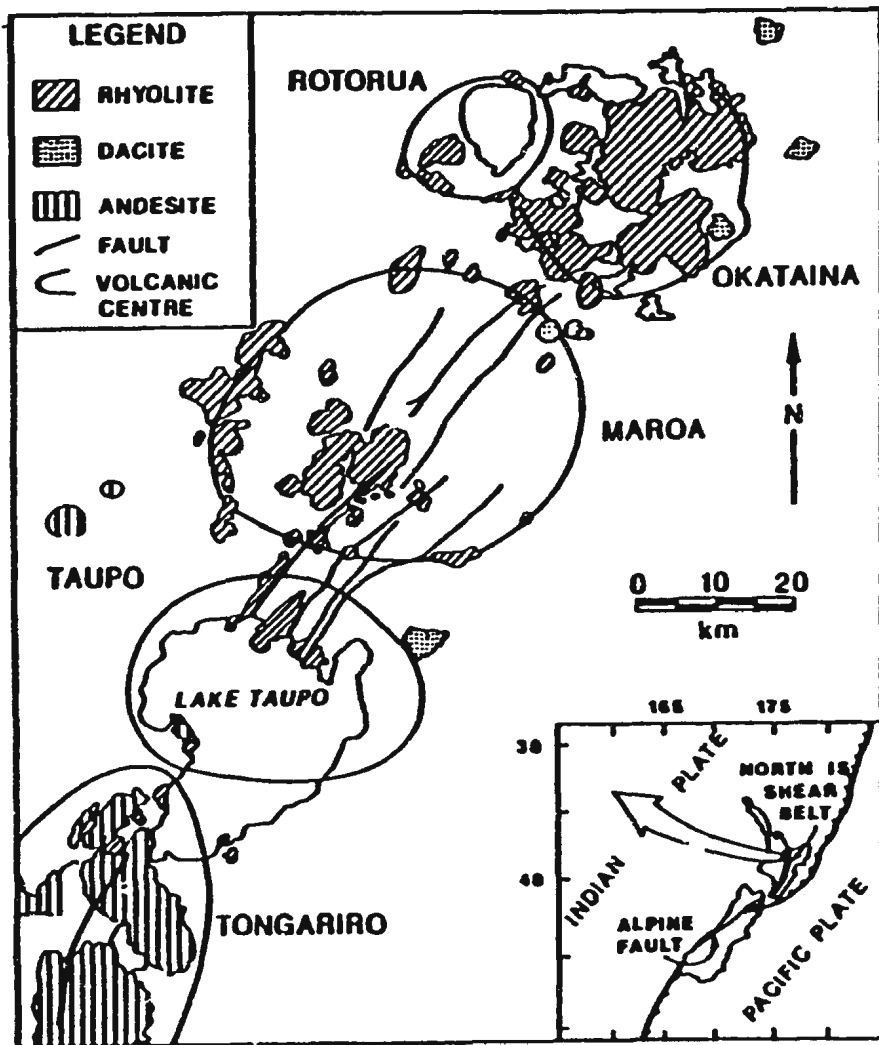
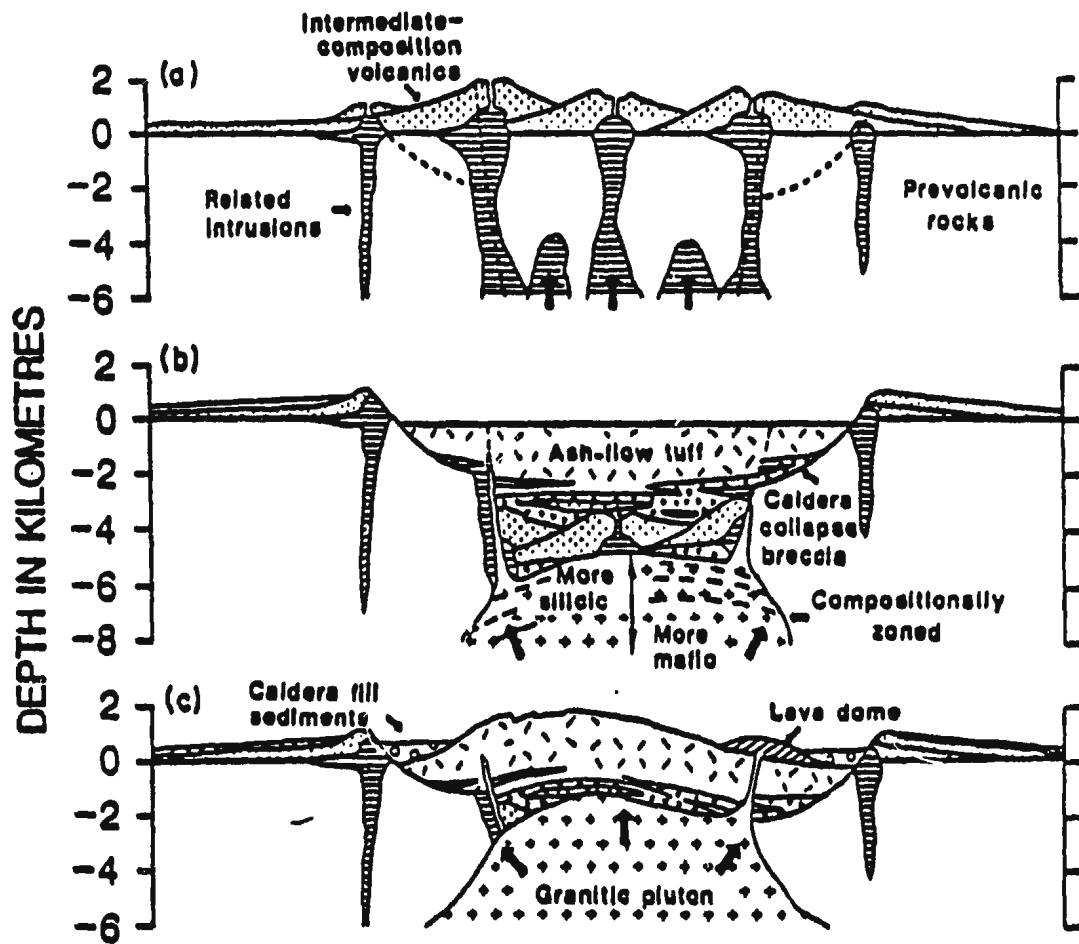


Figure 1.4. A generalized ash-flow caldera cycle based on a composite of features from a number of calderas (after Lipman, 1984). (a) "Pre-collapse volcanism. Clustered intermediate- composition strato-volcanoes form over isolated small high-level plutons that mark the beginning of accumulation of a batholith-sized silicic magma body that will feed ash-flow eruptions. Uplift related to emplacement of the plutons leads to the development of arcuate ring fractures which form the sites of subsequent caldera collapse (dotted lines). Heavy arrows indicate upward movement of magma. (b) Caldera geometry just after ash flow eruptions and concurrent caldera collapse. Central area of clustered earlier volcanoes caves into collapsed caldera. Intracaldera tuff ponds during subsidence and is an order of magnitude thicker than cogenetic outflow ash-flow sheet. Initial collapse along ring faults is followed by slumping of over- steepened caldera walls and accumulation of voluminous collapse breccias that interfinger with ash-flow tuffs in the caldera fill sequence. Caldera floor subsides asymmetrically and is tilted to the left side of the diagram. Main magma body underlies entire caldera area and is compositionally zoned prior to eruption, becoming more mafic downward. (c) Resurgence and post-caldera deposition. Resurgence is asymmetrical, with greatest uplift in area of greatest prior collapse. Extensional graben faults form over crest of the dome. Some resurgent uplift is accommodated by movement along ring faults in the sense opposite that during caldera subsidence. Magma body has risen into volcanic pile and intrudes cogenetic intracaldera welded tuff. Original caldera floor has been almost entirely obliterated by rise of the magma chamber to near the level of pre-volcanic land surface. Caldera moat is partly filled by lava domes and volcanoclastic sediments. Hydrothermal activity and mineralization become dominant late in the cycle."



pyroclastic material with concurrent collapse of the source area. Such collapse may be followed by development of a resurgent cauldron as shown in Fig. 1.4(c), or there may be continuous collapse without resurgence, i.e. just stages (a) and (b) of Fig. 1.4.

As described by Fisher and Schmincke (1984, p. 361), "the intra-caldera facies within the subsided area may include ignimbrite deposits measuring hundreds of meters in thickness. If resurgence occurs, the resulting moat may be filled by pyroclastic rocks, lava flows, lake sediments, epiclastic volcanic sediments, and particularly by landslide or talus breccias from the caldera wall. The caldera-outflow facies is characterized by ignimbrite sheets that may extend for many tens of kilometers outside the caldera. Resurgence may occur without filling, and filling may occur without resurgence. Moreover, fills within calderas can be derived from younger ash flows from any nearby younger source."

Other important features to be noted are the presence of associated marginal ring or linear faults considered to form the major conduits of eruption, and to control location of late intrusions and/or "nesting" in complex areas. Perhaps the most diagnostic signature of these complex structures is the combination of post-caldera collapse volcanic facies, associated plutonics and specific structural elements such as ring dykes and structural

boundaries of the caldera-collapse block. Preservation of all caldera features is rare and it is often necessary to make comparisons between a number of reasonable models for the interpretation of a given caldera and its setting. The general features by which calderas might be recognized are summarized in Table 1.1.

Table 1.1. Summary of the characteristics of collapse calderas. Note that any one of these features may occur unrelated to a caldera, so these criteria should be used as a group rather than singly (after Panze et al., 1988).

1. Extensive rock units of lavas, breccias, and lahars of intermediate composition (andesite, dacite, quartz latite).
2. Intra-caldera ash-flow accumulation. Large thicknesses (500-2000 m) of silicic ash-flow tuffs (quartz latites, rhyolites). Often ponds within collapsing caldera.
3. Large-volume (greater than 100 km^3) ash-flow units eruption causes collapse).

Table 1.1. (Continued).

4. Landslide or slump breccia deposits (mass wasting from caldera walls). May consist of very large blocks (greater than 1 km) or unusual (exotic) breccias.
5. Intracaldera volcanic rocks and volcaniclastic sedimentary rocks.
6. Curved zones of faulting, fracturing, and brecciation (ring fracture zone).
7. Regional propylitic alteration with local occurrence of argillic, sericitic, and advanced argillic alteration.
8. Resurgent doming evidence by:
 - a. outward dip of intracaldera units
 - b. central graben
 - c. plutonic or hyabyssal resurgent magma
9. Ring-fracture domes of rhyolite and/or quartz latite.

Table 1.1. (Continued).

10. Structural depression marked by collapsed block.
11. Radial and/or concentric fault, drainage, and topographic patterns.
12. Clustering of mineral occurrences.
13. Circular patterns on high-altitude photographs or remote imagery.
14. Geochemistry: The distribution of metal values (Au, Ag, Cu, Mo, Pb, Zn, etc.) may aid in defining caldera structures.
15. Geophysics. Gravity, magnetics, resistivity, and radiometrics may show evidence of caldera structure.

2. GEOLOGY OF THE SPRINGDALE GROUP

2.1. Introduction

This thesis is based on fieldwork carried out mainly on the Springdale Group, a sequence of volcanic and sedimentary rocks located near the town of Springdale (lat. $49^{\circ}30'N$, and long $56^{\circ}5'W$) a prosperous distribution centre for the mining and fishing industries of west central Newfoundland (Fig. 2.1). The area is found on NTS map sheets Springdale (sheet 12H/8), the Great Gull Pond (sheet 12H/1), King's Point (12H/9), and Topsails (12H/2).

Ancillary detailed work was carried out in the Sheffield Lake Group on the adjoining map sheet to the west (Sheffield Lake sheet 12H/7), so as to assess its continuity with the Springdale Group. Reconnaissance investigations were also made of the King's Point, MicMac Lake, and Cape St. John Groups in order to compare them to the Springdale Group (Fig. 2.2). Brief visits were also made to the Sops Arm area for the same purpose.

The mapping was generally recorded at 1:12,500 scale, and at larger scales where outcrop was sufficient or geological features justified it, using both orthophotomaps and coloured air photographs for field control. In general the exposure is moderate, with local ridges surrounded by poor exposure, and excellent river coverage. Access to the area is fair with many gravel roads provided throughout the

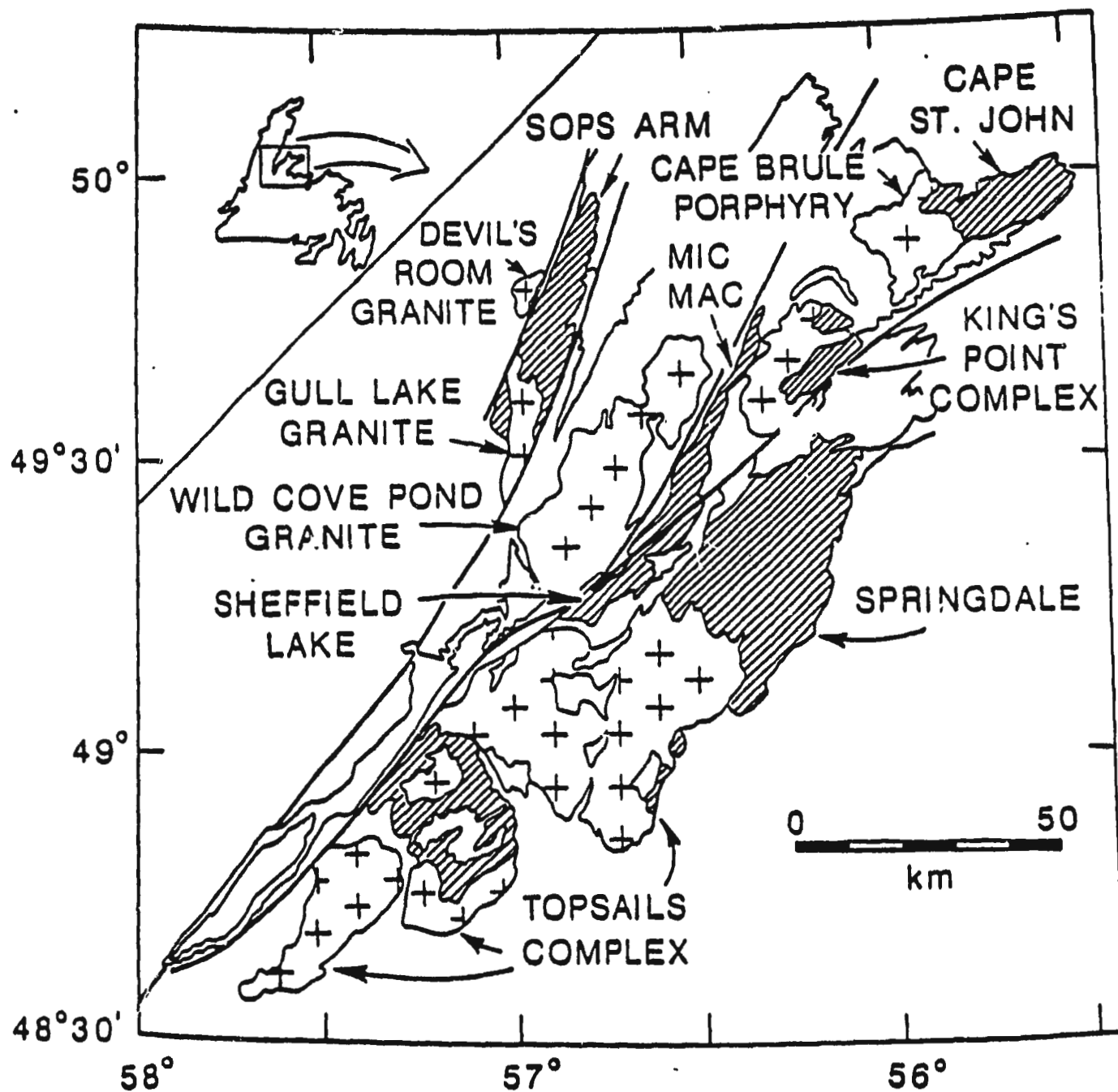


Figure 2.2. Silurian volcano-plutonic suites of the Springdale area.

area by logging operations. Much of the mapping was carried out by foot aided by the use of four wheel drive vehicles and was followed up with helicopter traverses where outcrop was limited over wide areas or where access was difficult. Final maps were constructed at a scale of 1:100,000, with larger scales used where details are illustrative of important lithological relationships and structure.

This thesis contains (in pocket) one summary map at 1:000,000 scale (Map 1), with more detailed maps at 1:10,000 for areas where geophysical data were available, termed the Springdale central (Map 2) and Springdale east (Maps 3 and 4) areas.

2.2. Local Geological Setting of the Springdale Group

The geology of the island of Newfoundland, at the northern extremity of the Appalachian orogen, has been reviewed by numerous writers (e.g. most recently by Swinden et al., 1989; Williams et al., 1988) and so need not be repeated here. The essential feature is that Precambrian rocks are known to underly platformal Paleozoic sedimentary rocks on both the western (Humber Zone) and eastern (Avalon Zone) sides of a central (Dunnage) zone of volcanic, plutonic and sedimentary rocks thought to have formed through the development and destruction of Cambro-Ordovician oceanic and island arc sequences, which were

then overlain and intruded by the Silurian and younger rocks (Fig. 2.1). Williams et al. (1988), on the basis of contrasts in geological, metallogenic and isotopic characteristics, subdivided the Dunnage Zone into two subzones, the Notre Dame and Exploits Subzones northwest and southeast, respectively, of a tectonic boundary which they termed the "Red Indian Line" (Fig. 2.1). Currie and Piasecki (1989) have suggested that differences in metamorphic grade and lithological assemblages justify further subdivision of central Newfoundland, with the designation of three more subzones.

Williams (1967) recognized nine different belts of Siluro-Devonian rocks on the island of Newfoundland which are not restricted by any of the zone boundaries described above. The largest of these are the Springdale, belt in the Notre Dame Subzone, and the Botwood belt in the Exploits Subzone. The Springdale belt extends continuously for 60 km, and possibly a further 100 km southwestward if volcanic inliers within the Topsails Complex are included (see Fig. 2.2 of Whalen and Currie, 1983), and reaches a maximum width of 35 km across the centre of the belt (Fig. 2.2). It is also correlated with rocks of the King's Point Complex and the Cape St. John Group, found up to 50 km to the north and the MicMac, Sheffield Lake and Sops Arm Groups to the west (Fig. 2.2). The Springdale Group (Fig. 2.2) is not fossiliferous, so that prior to this study its Silurian age

was only indirectly inferred through correlation with the fossiliferous Botwood belt. Chandler and Dunning (1983) compared the Springdale Group with rhyolites of southern Newfoundland which yielded zircon date of 431 ± 5 Ma. This correlation was subsequently supported by a U/Pb zircon date of $429 \pm 6/-5$ Ma from an ash flow tuff of the Springdale Group (Chandler et al., 1987).

Rocks of the Springdale Group generally show no penetrative deformation, but are folded about a northerly-plunging synformal axis (see Plate 2.1). Sedimentary rocks of the Group are gently dipping (Plate 2.1, 2.2.b), but locally inclined up to 50° on either side of the fold axis (Fig. 2.2.a). If all units were folded to the same degree, this would indicate across-strike structural shortening of up to about 20%, contributing to the present elongate distribution pattern of the Group.

Although the radiometric dates (Chapter 5) indicate that the numbering sequence for the map units described below is indeed in chronological order, such volcano-facies stratigraphy is typified by abrupt truncation and wedging out of lithological units. Correlation of volcanic and sedimentary markers are made even more difficult by the discontinuous exposure in the area. Dramatic variation in the eruptive facies precludes

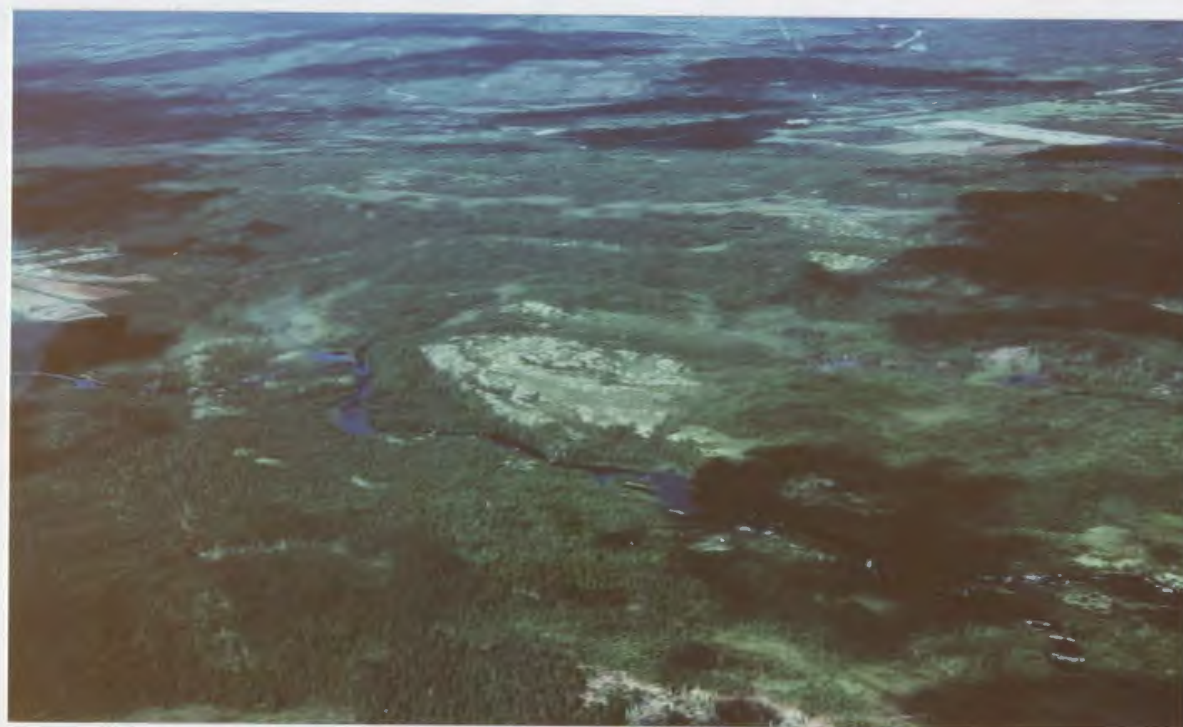


Plate 2.1. Helicopter views of folded ridges of Springdale sandstones. Location is south of Springdale and north of the junction of routes 1 and 391, with views from the northeast (a) and east (b).



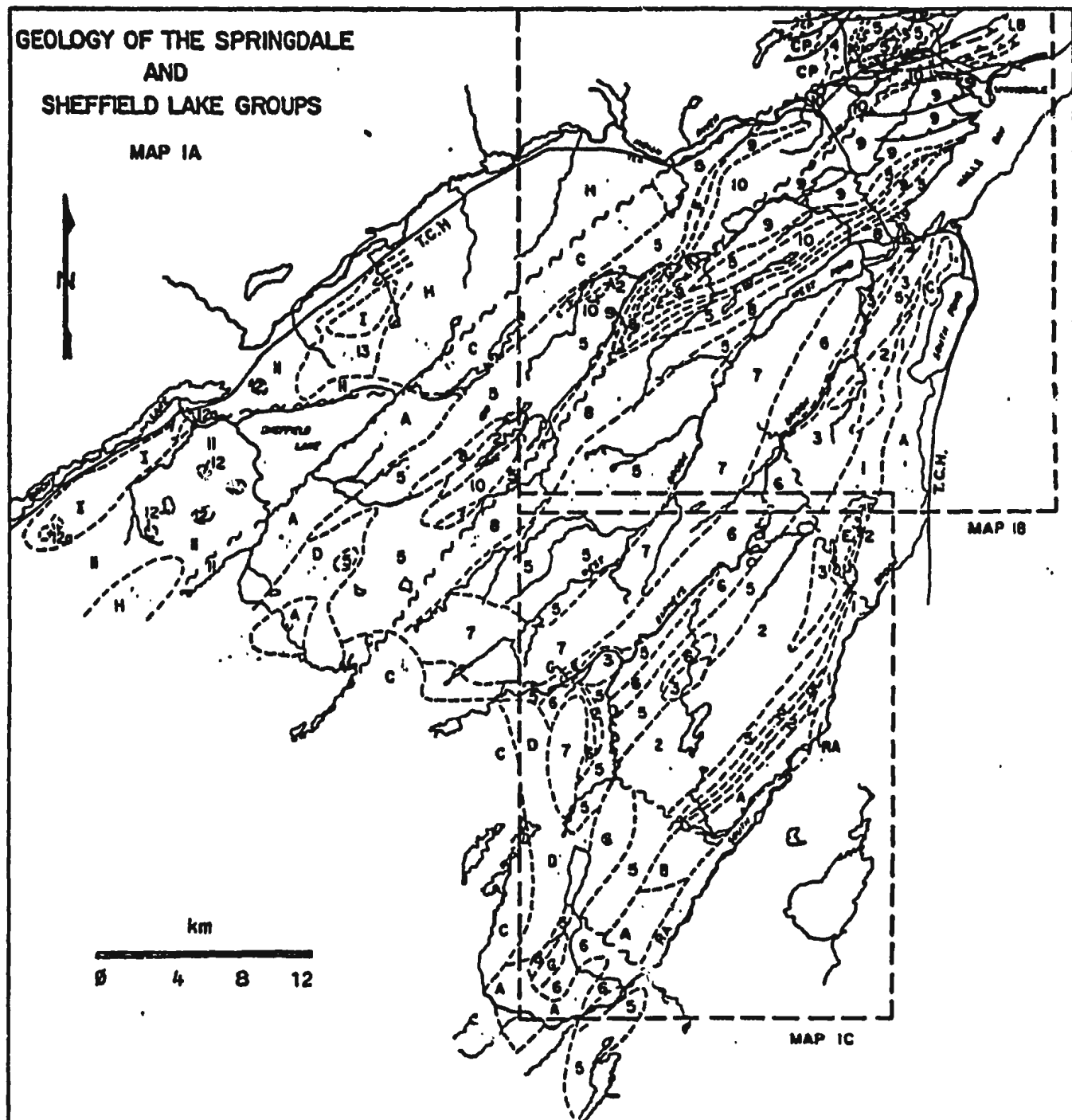
Plate 2.2(a). Red sandstones of the Springdale Group (Unit 9) on the east limb of the central syncline. On Route 1, viewing north.



Plate 2.2(b). Gently-dipping Springdale Group sandstones (Unit 9) exposed on Burnt Berry Brook north of the Route 1 (viewing south).

reliable correlation and stratigraphic control except where noted. Accordingly, the units are presented as lithological divisions, and not necessarily in a stratigraphic sequence, in the legend of Figure 2.3 and Map 1.

The eastern and western boundaries of the Group (Fig. 2.3; Map 1), although intruded by granitoid rocks, mark early boundary faults along which the Group was down-dropped, and which partially controlled volcanism, sedimentation, and intrusion of the granitoids. Along its eastern boundary, rocks of the Group lie unconformably on, or are faulted against, a basement of foliated granodiorite, diorite and tonalite which correlates with the Mansfield Head complex (Bostock et al., 1979) and the Hungry Mountain complex (Thurlow, 1981). Whalen and Currie (1983a, b) also show rocks of the Hungry Mountain complex on the southwestern margin of the Group. Whalen et al. (1987) provided a U/Pb zircon date of 467 ± 8 Ma for tonalite of the Hungry Mountain Complex, comparable to a date of 456 ± 3 Ma given by Dunning et al. (1989) for the vast tonalite terrane intruded by the Topsails and other Silurian rocks to the southwest, and to the date of 463 ± 5 Ma for the Burlington Granodiorite (Hibbard, 1983) which is intruded by the Silurian King's Point Complex to the northwest (Fig. 2.2). All of these granitoids have zircons inherited from older Precambrian rocks.



**Figure 2.3. Geological map of the Springdale caldera
(reduced from Map 1A, in pocket).**

LEGEND

4. Felsic to intermediate, dominantly dacitic, ash flow tuff.
Crystal-lithic and lapilli ash-flow tuffs; clasts of andesite, rhyolite, angular and flattened pumice; variably welded.
3. Andesitic to dacitic flows. Locally plagiophyric, massive to flow-foliated to brecciated; local intrusions of massive andesite.
2. Mesobreccia. Laharic flows, tuffites and pepperites, volcanic conglomerates and breccias, red sandstones.
1. Welded, lithic-crystal tuff. Plagioclase and K-feldspar, accessory biotite, quartz, and rare opaques, clasts of granophyre, plagiophyric basalt, andesite, ultramafics, and jasper.

INTRUSIVE and BASEMENT ROCKS

- I. Quartz-K-feldspar porphyry. Orange to green, with sodic amphibole oikocrysts and minor cegrine and altered fayalite.
- H. Granite to quartz syenite. Red medium-grained plagioclase, K-feldspar and amphibole porphyritic. Granophyric textured; heavily altered.
- G. Rhyolite domes, dykes and sills. High-silica. Microphenocrysts of quartz and feldspar, with finely disseminated riebeckite in groundmass; flow-foliated, auto-brecciated, zones of intense development of spherules and other indications of gas-streaming.
- F. Felsic microporphyry sills and dykes.
- E. Microdiorite. Black, fine-grained, massive.
- D. Granite. Medium to coarse grained; characterized by quartz and pink feldspar with finer grained crystals of black amphibole, intruded by finer grained whitish grey granite, with locally riebeckite pegmatite and abundant amphibole-linedmiarolitic cavities and fractures; offshoots of the Topsails Complex.
- C. One-feldspar granite. White to red, medium to coarse grained, equigranular with amphibole \pm sodic pyroxene; in large part peralkaline.
- B. Granite, granodiorite, minor diorite. May in part be correlative with the Twin Lakes Complex.
- A. Amphibolite, diorite, granodiorite, granite. Foliated amphibolite and gabbro occurring as large screens and xenoliths in foliated diorite and granodiorite; intruded by variably deformed tonalite and amphibolite-biotite granite; intruded or net veined by a pale fine-grained granite.
- RA. Roberts Arm Group. Mafic to felsic submarine volcanic rocks.
- CP. Catchers Pond Group. Mafic to felsic submarine volcanic rocks.
- LB. Lushs Bight Group. Mafic, ophiolite-related submarine volcanic rocks.

LEGEND (cont'd.)CARBONIFEROUS

14. Red to grey mudstones to pebble conglomerates with local carbonate cement.

SILURIAN-(DEVONIAN?)SHEFFIELD LAKE GROUP

13. Andesite. Aphyric to plagioclase-microphyric.
 12a. Vitric tuff. Orange to red, welded. Characterized by large sodic amphibole oikocrysts with rare resorbed K-feldspar phenocrysts.
 12. Ash-flow tuff. Massive, maroon, aphanitic to flow-banded quartz- and feldspar-phyric.
 11. Red and brown crystal, vitric and lithic-rich ash-flow sheets.
Laharic, fault and gas-breccias. Rhyolite domes and dykes. Minor basalt.

SPRINGDALE GROUP

10. Crystal-lithic tuff. Densely welded and massive large phenocrysts of quartz and feldspar, clasts of mafic and rare ultramafic lithologies.
 9. Clastic sedimentary rocks. Red conglomerate, sandstone, and sandy siltstone, local caliche horizons; cross-bedding, ripples, laminations, rip-up horizons, scour channels, etc. indicate stream-flood and proximal and distal fluvial origin; clasts essentially volcanic or plutonic provenance.
 8. Rhyolitic vitric ash-flow tuffs and breccias. Welded, devitrified, locally massive; areas of unwelded vitroclastic tuffs with large individually devitrified shards with axiolitic texture; locally passes into sandstones; alternating thin basaltic and silicic bands in some horizons.
 7. Dacitic to rhyolitic ash-flow tuffs, vitroclastic breccia and domes. Massive, vitric, strongly welded; curvilinear joint surfaces in the domes, with internal plastic shear zones, local brecciation, and flow folds; tuffs locally porphyritic, with small euhedral plagioclase and rare quartz phenocrysts in glassy matrix.
 6. Silicic ash-flow tuffs. Crystals, lithic fragments, and vitroclasts; basal lithophysae-rich horizons, grading up into a partially welded crystal-lithic lapilli tuff; broken phenocrysts of plagioclase, K-feldspar and quartz; flattened pumice bombs up to a metre long; clasts of silicic volcanics, andesite and rarely basalt.
 5. Mainly basaltic flows, some of intermediate composition. Locally plagiophytic; with amygdaloids of quartz, calcite and chlorite; variably altered. Note that map units include large areas of no outcrop.

These basement rocks are grouped as Unit A on Figure 2.3 and Map 1, on the eastern and western margins of the map area. In the east they extend from South Pond southwards to Joe Glodes Pond for at least 45 km along a faulted unconformable contact. In the west they are exposed as an up-faulted block, and as roof pendants within the Topsails Complex. These rocks range from amphibolite and diorite through granodiorite and granite in composition. The former are mainly foliated amphibolite and gabbro occurring as large screens and xenoliths in foliated diorite and granodiorite. Green and black, medium- to fine-grained diorite, with hornblende and biotite, are intruded or net-veined by a pale fine-grained granite, with a typical tectonic fabric emphasized by amphibole alignment (Plate 2.3). These are locally intruded by variably deformed tonalite and amphibole-biotite granite. Intrusive contacts are intermittently exposed, and are locally fault-modified, but it is clear that both the basement rocks and the Springdale Group were intruded by granitoid rocks.

Three groups of Lower Ordovician volcanic rocks form the basement along the northern margin of the Springdale Group. They are the Lushs Bight, Catchers Pond and Buchans/Roberts Arm Groups, all Arenig in age. Zircons from the Buchans Group yield an age of $473 \pm 3/-2$ Ma (Dunning et al., 1987). The Lushs Bight Group is dominated by basaltic pillow lavas and dikes representing the upper parts of



Plate 2.3. Foliated amphibolite of Unit A, taken near the southern end of South Pond.

Iapetus oceanic crust, and it is assumed that the deeper parts of such ophiolitic suites were the source of ultramafic clasts within the ash flows of the Springdale Group. Silicic pyroclastic rocks are found with the pillow lavas of the Catchers Pond and Buchans/Roberts Arm Groups, which are generally interpreted as of island arc/back arc origin (e.g. Swanson et al., 1981; Kean, 1988).

In general it can be said that the volcanic and plutonic rocks of the Springdale Group have had access to a variety of source rocks for their derivation and contamination, including subducted Precambrian continental crust and overlying platformal sediments, Cambro-Ordovician oceanic crust and mantle, and early Ordovician island arc/back arc volcanic rocks and associated sediments. Their influence on the Springdale rocks can be seen in the following descriptions.

2.3. Unit 1

Unit 1 is located along the eastern margin of the map area, and extends as an elongate lens towards the south, to at least 15 km southwest of South Pond (Fig. 2.3; Map 1). It is the lowermost recognized of the volcanic units, is intruded by younger granitoid rocks (unit E), and has a fault-modified unconformable relationship with the older granodiorite (Unit A) to the east.

Unit 1 is a moderately welded, crystal-lithic tuff, commonly highly fractured or sheared along its eastern margin. It differs from the other overlying ash-flows in that fractured and broken crystals of both plagioclase and K-feldspar are present, along with accessory biotite, quartz, and rare opaques (Plate 2.4a). The lithic component includes clasts of plagiophyric basalt, andesite, ultramafics, red jasper, granophyre and perlitic felsic fragments. The matrix includes shards, rock and crystal fragments and partially welded eutaxitic pumice lapilli (Plate 2.4b). The occurrence of two feldspars and biotite in the crystal component of this tuff suggest that it was erupted from water-saturated magma chamber, perhaps relatively deeper than those of the later ash flows.

2.4. Unit 2

Unit 2 is a distinctive and complex assemblage of clastic rocks forming a composite unit, best developed as elongate lenses along the eastern margin of the caldera (Fig. 2.3; Map 1). These eastern exposures form two main bands. The northernmost is about 8 km long and only metres wide in the north, expanding southwards to cover an irregularly shaped lobate area about 1 km wide. The southern band is seen as separate elongate ridges, in contact with basement rocks, extending the unit for a further 18 km. The western equivalent is found in two

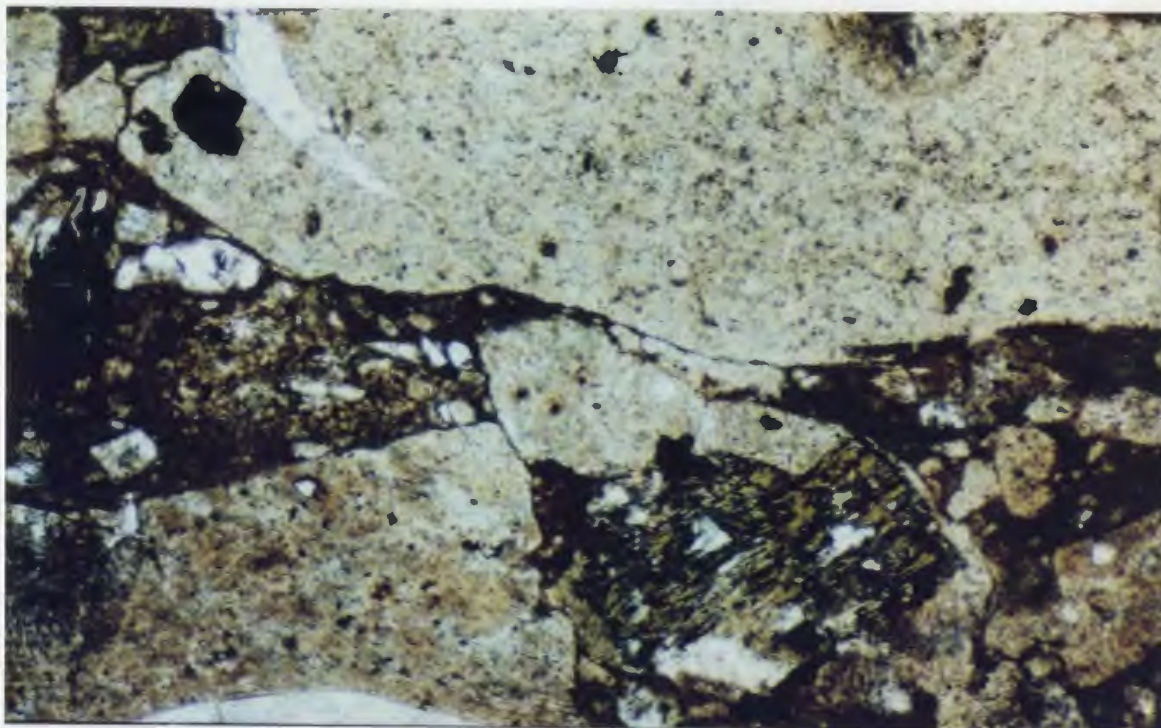


Plate 2.4(a). Lithic clasts and biotite phenocrysts in glassy groundmass with crystal fragments, Unit 1.

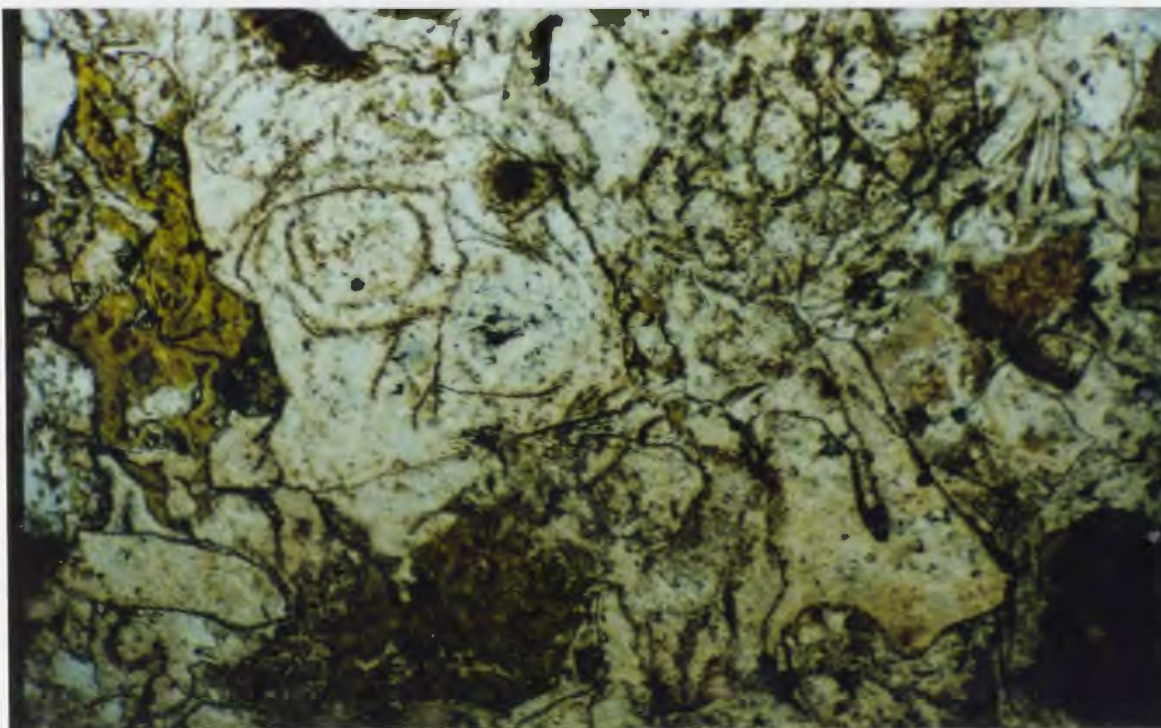


Plate 2.4(b). Perlitic, spherulitic and eutaxitic textures in clasts of Unit 1.

separate smaller exposures, a northern one about 1 km², and a southern one about 1 by 5 km. Smaller areas of this lithology have been mapped in the western parts of the caldera, and other elongate lenses in the south central parts of the area indicate that this lithology has been generated throughout the deposition of most other units of the Springdale Group.

It is dominated by mesobreccias, laharic flows, with tuffites and peperites, volcanic conglomerates and local red sandstones, and volcanic explosion breccias (Plates 2.5a-e). The term mesobriccia is used as defined by Lipman (19) for a complex caldera-margin clastic assemblage including a range of blocks up to 1km across. In general the volcanoclastic lithologies are characterized by poor sorting and massive to very coarse bedding. The lahars have dominantly sub-angular blocks in a locally vesicular muddy or ashy matrix. Both the coarse and fine fractions of these deposits are compositionally variable from basalt to rhyolite. Bedding is commonly absent in the lahars, but where present it is reversely graded, with the finer basal horizon much thinner than the overlying coarse beds. The laharic flows locally exhibit imbrication of elongate clasts (Plate 2.5a).

The tuffites are composed of predominantly pyroclastic debris and reworked volcanic clasts, and can be subdivided into tuffaceous conglomerates and tuffaceous breccias. Boulders in the tuffites are not as large as those of the lahars, but are also commonly subangular to

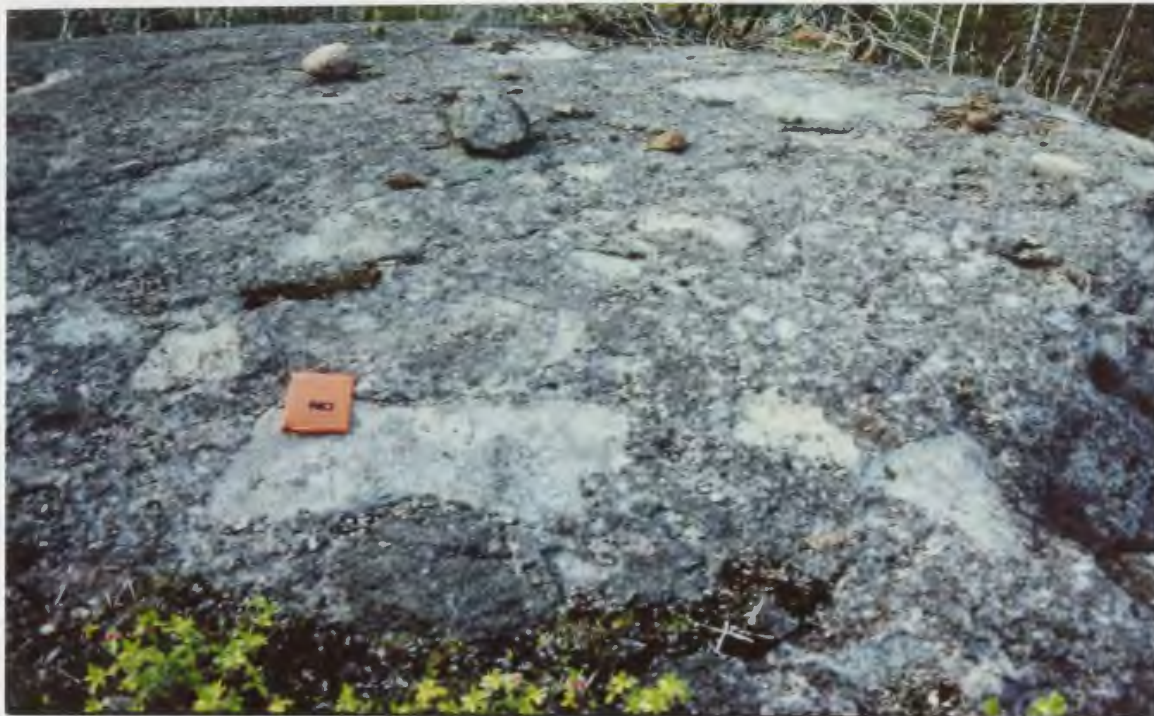


Plate 2.5(a,b). Coarse laharic breccia of Unit 2, west of South Pond on the eastern margin of the map area.

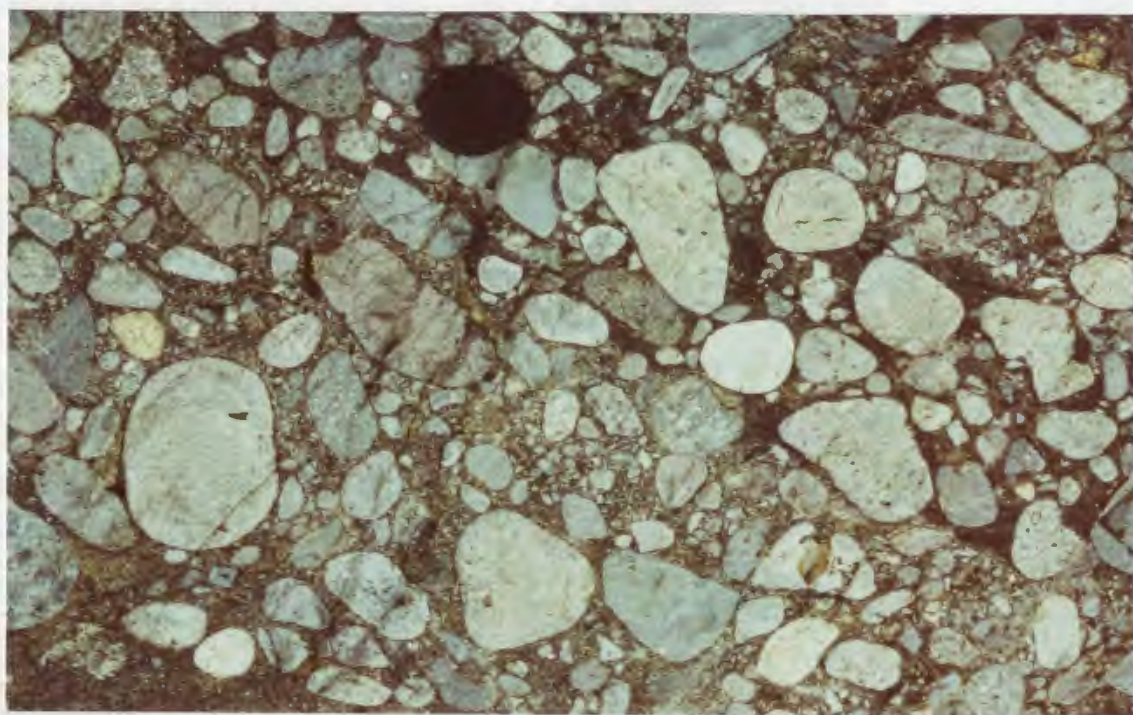


Plate 2.5(c). Coarsely bedded mesobreccia block of Unit 2 along southeast margin of the caldera. It contains both epiclastic volcanic debris and reworked material.



Plate 2.5(d). Volcanic conglomerate in mega-breccia collapse blocks found along the northwest margin of the caldera.

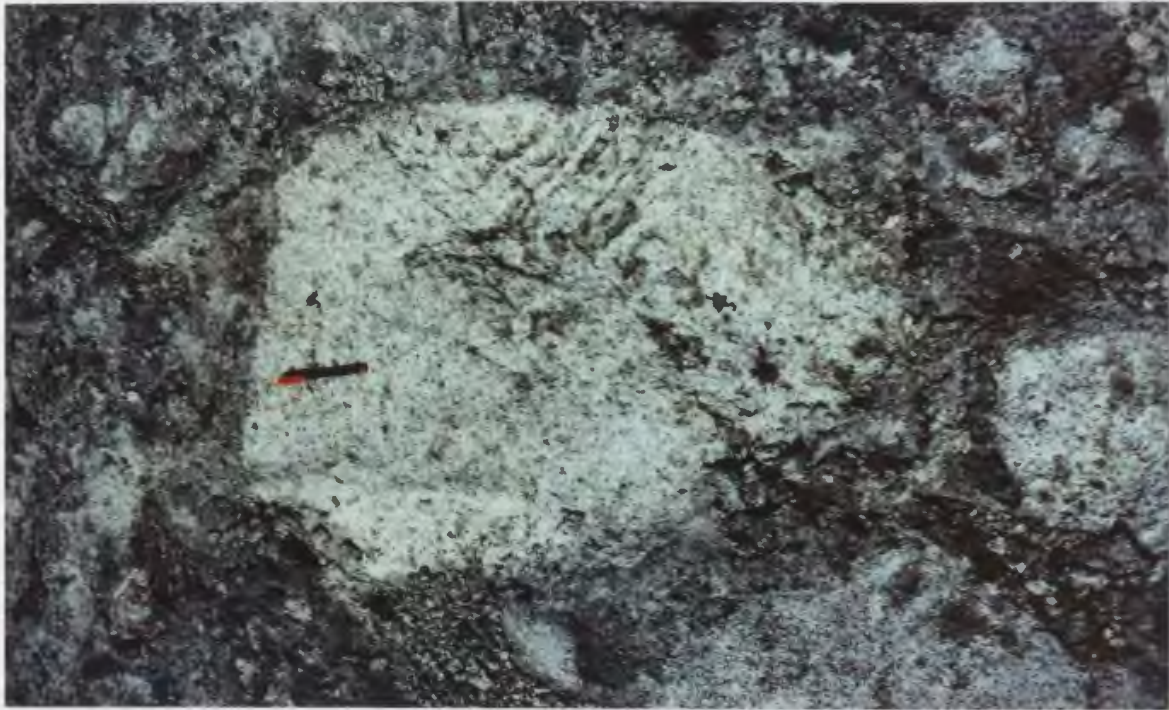


Plate 2.5(e). Partially abraded blocks in a microbrecciated "frothy" matrix of Unit 2, near Barney's Brook.

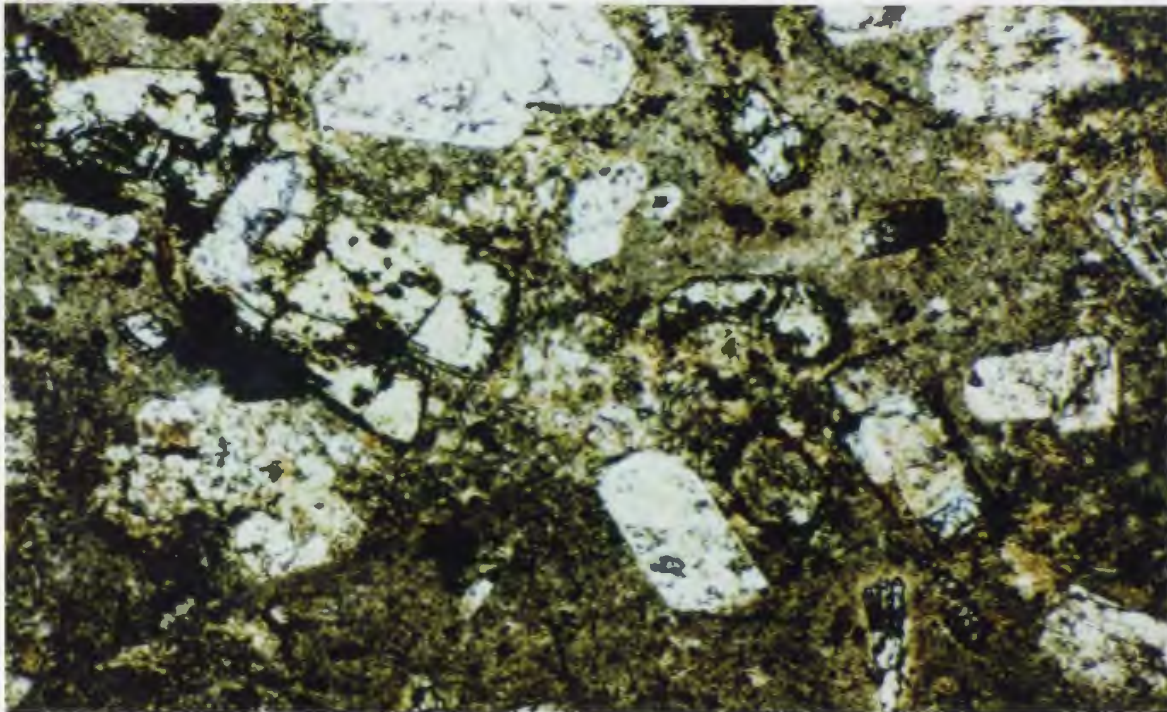


Plate 2.6. Photomicrograph of glomerocrystic andesite of Unit 3. Mineralogy includes clinopyroxene, plagioclase, minor olivine replaced by serpentine in a trachytic groundmass with opaques and oxides.

and bombs to rhyolitic tuffs of varied texture. The matrix is dominated by vitric shards and broken crystals, with minor lithic fragments, and is locally vesicular, presumably due to de-watering during and after deposition (Plate 2.5b).

The peperites are composed of fine- to medium-grained volcanogenic sandstones which have been baked and oxidized by injection of basaltic and intermediate lavas. They contain a range of detritus, including cobbles and pebbles of underlying flows, breccias, and pyroclastic deposits.

Volcanic conglomerates differ from the above lithotypes in that they have been more extensively reworked, sorted and redeposited as clastic sediments. They contain large, subrounded to rounded boulders and cobbles in a sand-sized matrix (Plate 2.5c). Most of the clasts are of silicic volcanics, with some of andesite and basalt. Sorting in these conglomerates ranges from poor to good. Bedding is common, and may be thick and structureless, thin and finely laminated, or crossbedded (Plate 2.5d). These deposits commonly show normal grading, especially obvious in scour fills or channel deposit horizons of red arkosic sandstones interbedded with the more silicic and well-bedded conglomerate horizons.

Rocks which are very similar to monomictic lahars are interpreted to be degassing explosion breccias because of their microbrecciated matrix, in contrast to the muddy

laharic matrix. They are commonly composed of intermediate or basaltic volcanic material, as both clasts and matrix (Plate 2.5e). Bedding is commonly absent and the fabric is isotropic, or shows "streaming" from the gas brecciation process.

Unit 2 was produced by a mixture of volcanic and sedimentary processes. The predominant feature in all subunits is the large size of the clasts, suspended in a finer matrix, i.e. a strongly bimodal size distribution. These lithologies represent facies developed during volcanic activity, ranging from near-source explosion deposits, to more distal, fluvially reworked sediments. Some debris flows may have been activated on unstable slopes and rapidly deposited, whereas others could have had long periods of reworking. The lithologies of unit 2 are similar to those seen at caldera margins and, as discussed below, this unit is important as a marginal facies marker for the Springdale caldera.

2.5. Unit 3

Unit 3 includes intermediate flows, flow breccias, and intrusive rocks. They are distributed along the eastern and southern border of the caldera in a belt about 24 km long and up to 3 km wide (Fig. 2.3, Map I). A number of isolated exposures are also found in the central and western parts of the map area. Unit 3 is interbedded with

units 1, 2, 4, and 5, and intrudes unit 5. It consists of intermediate composition (dacite, andesite) non-vesicular flows, commonly very aphanitic but locally with glomerocrystic aggregates of plagioclase and phenocrysts of altered mafic minerals (olivine? and hornblende? Plate 2.6). The massive to strongly flow-foliated flows are typically brecciated. Intrusions of massive diorite are also found.

The flows and intrusions of unit 3 represent a period of volcanism dominated by andesitic-dacitic chemistry, unlike the other major lava flows which are of basaltic composition. A minor phase of this unit consists of interbanded silicic and mafic compositions on the scale of centimetres and smaller, suggesting that some of these intermediate rocks may have been formed by mixing of more mafic and silicic magmas.

2.6. Unit 4

Unit 4 forms a narrow band, about 500 m. wide, of intermediate ash-flow tuff, extending from southern Hall's Bay for about 10 km toward the SSW (Fig. 2.3; Map 1; also Fig. 2.7.a). It overlies unit 3 and is succeeded by basaltic flows of unit 5, and may be locally gradational into unit 6. It ranges in composition from rhyolite to andesite, although it is predominantly dacite. Its lithologies include pyroclastic breccia, crystal-lithic and lapilli ash-flow tuffs.



Plate 2.7(a). Weakly welded dacitic lapilli tuff of Unit 4 (northern Barney's Brook).



Plate 2.7(b). Welded part of Unit 4 (south of route 1 on power line).

In the lithic-dominated portions, the cognate clasts are andesite and aphanitic rhyolite in an ashy matrix. These lithic tuffs are generally layered, tend to have reverse grading, and vary in their degree of welding. The tuff breccias contain angular and flattened pumice clasts (>65 mm long) in an ashy matrix, with minor lithic clasts, and also show variable degrees of welding (Plate 2.7). The lapilli tuff has pumice lapilli up to 65 mm long, in a welded ashy matrix. These lithologies tend to be discontinuous along strike.

2.7. Unit 5

Unit 5 consists mainly of basaltic flow rocks which occur throughout the map area (Fig. 2.3; Map 1), with prominent exposures along the coast of Hall's Bay, along Barney's, Burnt Berry, and West Brooks, and to the southwest on flat-topped hills (Plate 2.8). They are interbedded with the other lithologies, are intruded by younger granitoid rocks of the Topsails Complex, and rest disconformably upon and are faulted against the basement rocks.

These flows are typically aphanitic, with notable local concentrations of plagioclase phenocrysts (Plate 2.9). They range from non-vesicular to highly vesicular, with amygdales of quartz, calcite and chlorite. The flows are variably altered throughout the entire Springdale Group



Plate 2.8. Flat-topped ridge composed of a sequence of basalt flows of Unit 5 (southwest corner of the map area, viewing east).



Plate 2.9(a). Coarsely porphyritic vesicular basalt, Unit 5.



Plate 2.9(b). Typical features of basaltic flows, with tabular base and vesicular top, Unit 5.



Plate 2.9(c). Basalt flow-top breccia; looking down at the top surface of the lava flow. Clasts of basalt suspended in a rubbly matrix of rock flour and some sandy dykes generated as flows incorporate wet sediments.

and the secondary assemblages show no systematic geographic variation, except along the eastern margins of the map where they have the greatest diversity of secondary minerals.

2.8. Unit 6

Unit 6 consists of silicic ash-flow tuffs, exposed continuously along Barney's Brook, in conformable contact with basaltic flows of unit 4 (Plate 2.10a), over a strike length of 14 km with a maximum width of 3 km (Fig. 2.3; Map 1). The unit has been extended southwards from a discontinuous exposures for an additional 30 km, with maximum width of 6 km in the extreme south of the map area (Plate 2.10b). These ash flows are reddish-brown to grey and display varying proportions of crystals, lithic fragments, and spectacular flattened vitroclasts (Plate 2.11a). In the north along Barney's Brook the basal part of the unit is a thick lithophysae-rich horizon resting on irregular flow tops of the basaltic Unit 5. The individual lithophysae may be as large as 10 cm in diameter, with central cavities partially or completely filled with radiating quartz crystals, microlites, and chalcedony (Plate 2.11b). This horizon grades up into a partially welded crystal-lithic lapilli tuff. In the south Unit 6 has an extensive area where lithophysae for dykes and tubes formed where gas-charged fluids were injected along



Plate 2.10(a). Shows the clear contact between basaltic flows of Unit 5 in the foreground and Unit 6 in middle and background. Photograph taken on the northern part of Barney's Brook, viewing south-southwest.



Plate 2.10(b). Contact between Units 5 and 6, as well as large sill intruded along bedding. Photograph taken in the south part of Barney's Brook, viewing south.



Plate 2.10(c). Close-up of sill at contact shown in 2(b).



Plate 2.11(a). Welded basal zone of Unit 6 with large flattened pumice bombs.



Plate 2.11(b). Large lithophysae in ash-flow tuff, Unit 6.



Plate 2.11(c). Coalesced lithophysae forming gas-charged dykes and tubes injecting along the upper contact of Unit 6.

the contact with a dacite sill (Plate 2.11c). The phenocrysts are plagioclase, K-feldspar and quartz, which are commonly broken and concentrated in the matrix in preference to the pumice vitroclasts. A crude bedding is defined by flattening of pumice lapilli up to a metre long (Plate 2.12), as well as by their concentration.

The densely welded parts of Unit 6 are maroon to brown ash-flow tuffs, with phenocrysts of plagioclase, K-feldspar and quartz, with streaky variations in relative proportions. A welding lamination is seen on weathered surfaces, but on fresh surfaces they look massive and structureless. The welded zones are locally extremely massive and have the superficial appearance of an intrusive quartz-feldspar porphyry. Unit 6 includes a number of pyroclastic flow units, each characterized by different proportions of lithic and vitroclastic clasts. They cooled as a simple cooling unit suggesting that the ash flows followed one another in rapid succession, with no substantial development of internal thermal gradients.

2.9. Unit 7

Unit 7 is found along West Brook and across the south central parts of the map area. This unit is dacitic to rhyolitic, and includes massive, strongly welded vitric ash-flow tuffs, vitroclastic breccias and domes. The massive tuffs are locally porphyritic, with small euhedral flow-aligned plagioclase and rare quartz phenocrysts in a

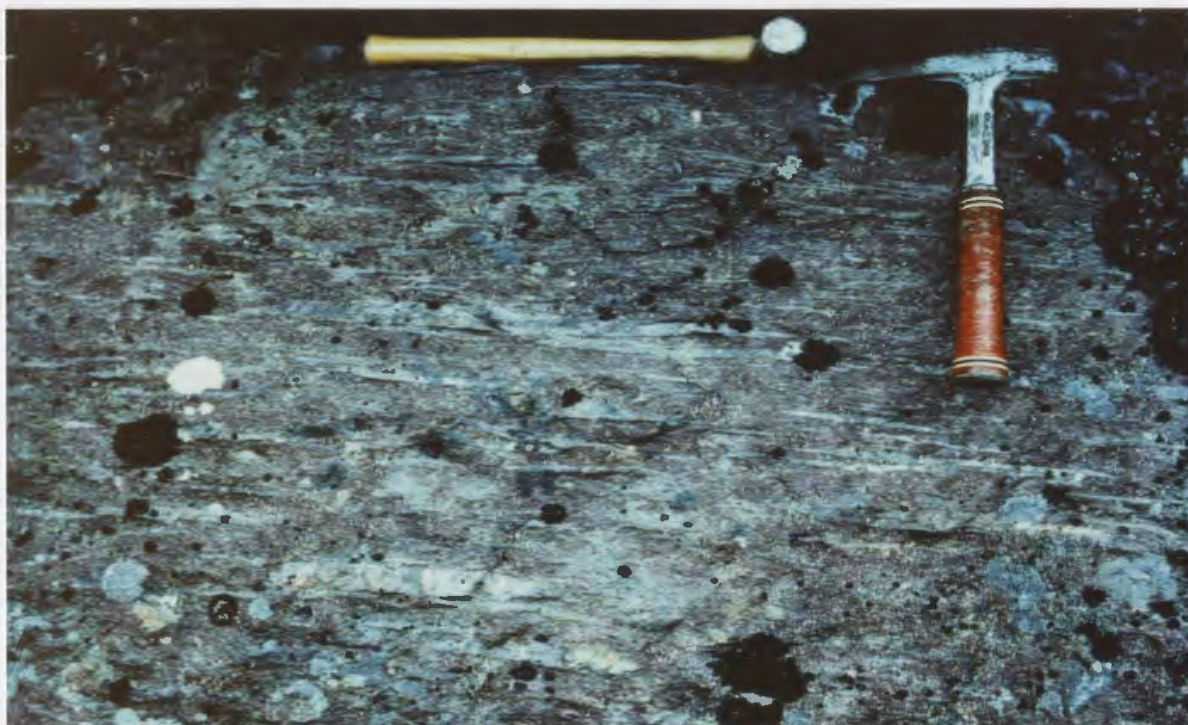


Plate 2.12. Flat-lying orientation of welding and flattened pumice in Unit 6.

brown to maroon glassy matrix. Welding can be observed on weathered surfaces and is apparently flat-lying in the southern exposures (Plate 2.13a) of this unit and becomes more steeply inclined towards the north (Plate 2.13b). Curviplanar joint surfaces are very common in the massive portions of the unit, and internal plastic shear zones and local brecciation can be seen, as well as flow folds; features indicative of domes. Petrographic studies show that the welded vitroclastic breccia of Unit 7, with very angular variably flow-folded and chaotically oriented "pumice fragments", represents the autobrecciated debris of cooling domal intrusions in the vicinity of contacts with their cogenetic pyroclastic apron (Plate 2.13c).

2.10. Unit 8

Unit 8 is a rhyolitic ash-flow tuff sequence extending throughout the centre of the map area (Fig. 2.3; Map 1), mappable with the aid of the geophysical maps in a number of separate fault-bounded lenses and bands about a synformal axis, despite the intermittent exposures. Because the exposures are intermittent, it is not possible to measure thicknesses in a straightforward manner. However, the map pattern allows for some inferences, based on the regional variations in dip as measured on clearly exposed bedding criteria. The band of Unit 8 as seen on the northwestern limb is less than 1 km wide and extends for 14



Plate 2.13(a). Photograph on Great Gull Pond map sheet, viewing south, showing Unit 7 in the left background, Unit 6 in the medium, and an igneous breccia phase of Unit 2 in the foreground.



Plate 2.13(b). Ash-flow tuff of Unit 7 exposed on West Brook, with moderately-dipping welding fabric visible on weathered surface.

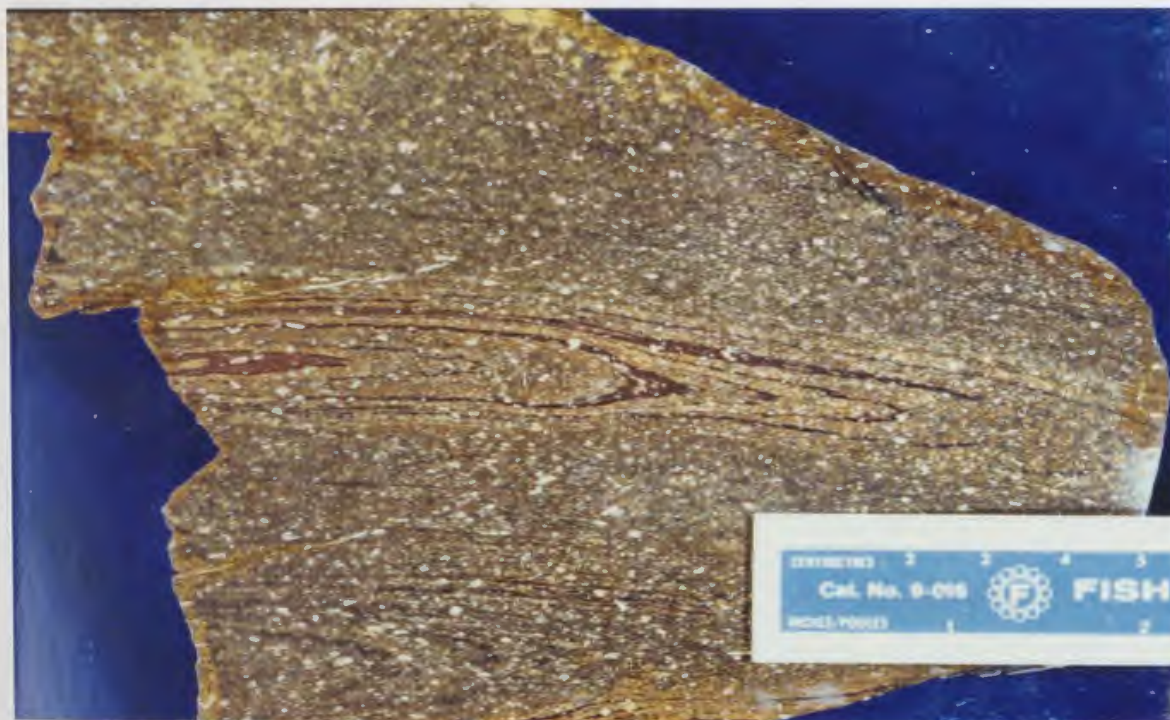


Plate 2.13(c). Large block of flow-banded densely welded very fine-grained dacitic ash-flow tuff of Unit 7 found in carapace of dome on West Brook.

km from the fold closure. Exposures on the southeastern limb form two horizons separated by red sandstones. The outer one is about 40 km long, several 100 m wide in its northern extremity and broadens toward the southwest to 2 km. The inner band is only several 100 m or less wide and 7 km long. Another band of this lithotype is found in the western part of the map area, about a km wide and six long.

Unit 8 includes an assemblage of devitrified, variably welded, pink and red rhyolitic ash-flow tuffs and breccias (Plate 2.14), displaying a variety of rheomorphic features. Since this ash-flow tuff grades into a sandstone at a few localities, it may be part of a complex rather than a simple cooling unit. Certain parts of this unit are very massive due to intense welding, others not strongly devitrified, and all have internal auto- or gas-breccias with clasts of plastically deformed rhyolitic lava and pumice (Plate 2.15). Others consist of unwelded vitroclastic tuffs with large individually devitrified shards (Plate 2.16), each showing independent development of spherules.

A few outcrops of unusual vitroclastic breccias within Unit 8 are interpreted as a dome apron or carapace, although exposure is inadequate to determine its geometry. Mixed magmas are found within the breccias, with alternating thin basaltic and silicic bands (Plate 2.17). Near central Burnt Berry Brook the silicic tuffs are intruded by a rhyolitic dome, the Burnt Berry Dome (Unit C, Plate 2.18).



Plate 2.14. Rhyolitic ash-flow tuff of Unit 8. Moderately welded with red fiamme in a white weathered matrix.



Plate 2.15(a). Pyroclastic breccia of Unit 8. Note plastic deformation of clasts.



Plate 2.15(b). Unwelded pyroclastic breccia with angular cognate and accidental lithic clasts.

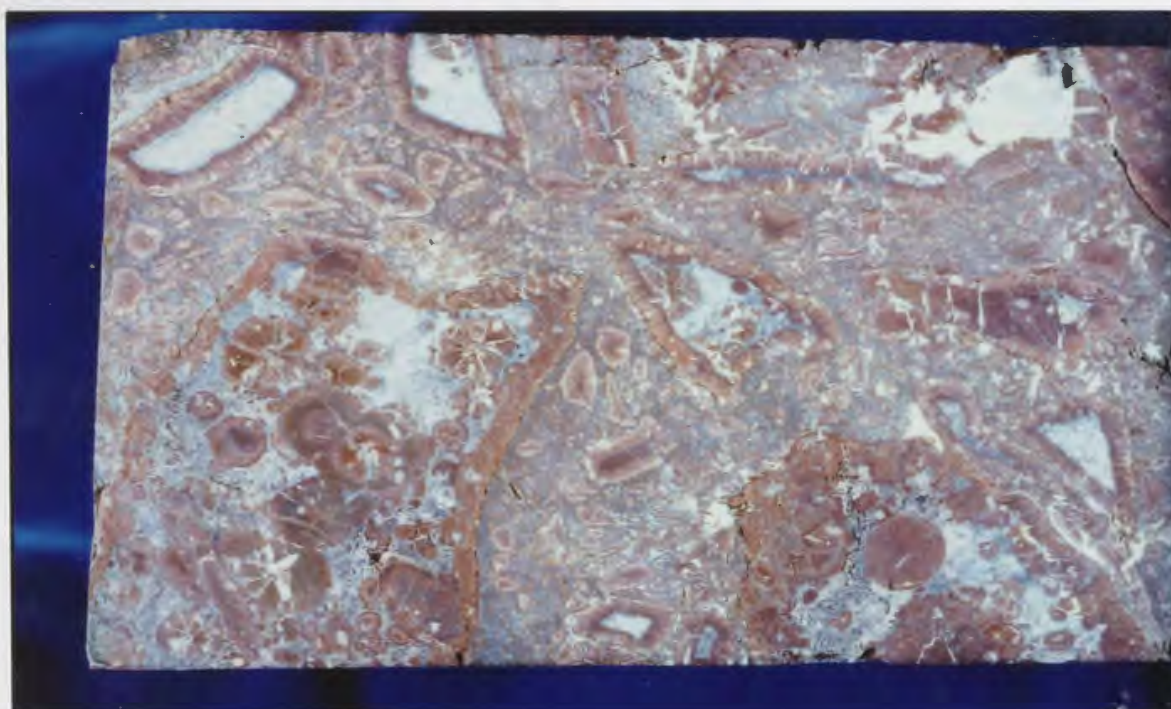


Plate 2.16(a). Breccia of Unit 8, with pink glassy clasts in a siliceous matrix, probably a dome carapace breccia derived from the cooling surface of a still mobile dome.

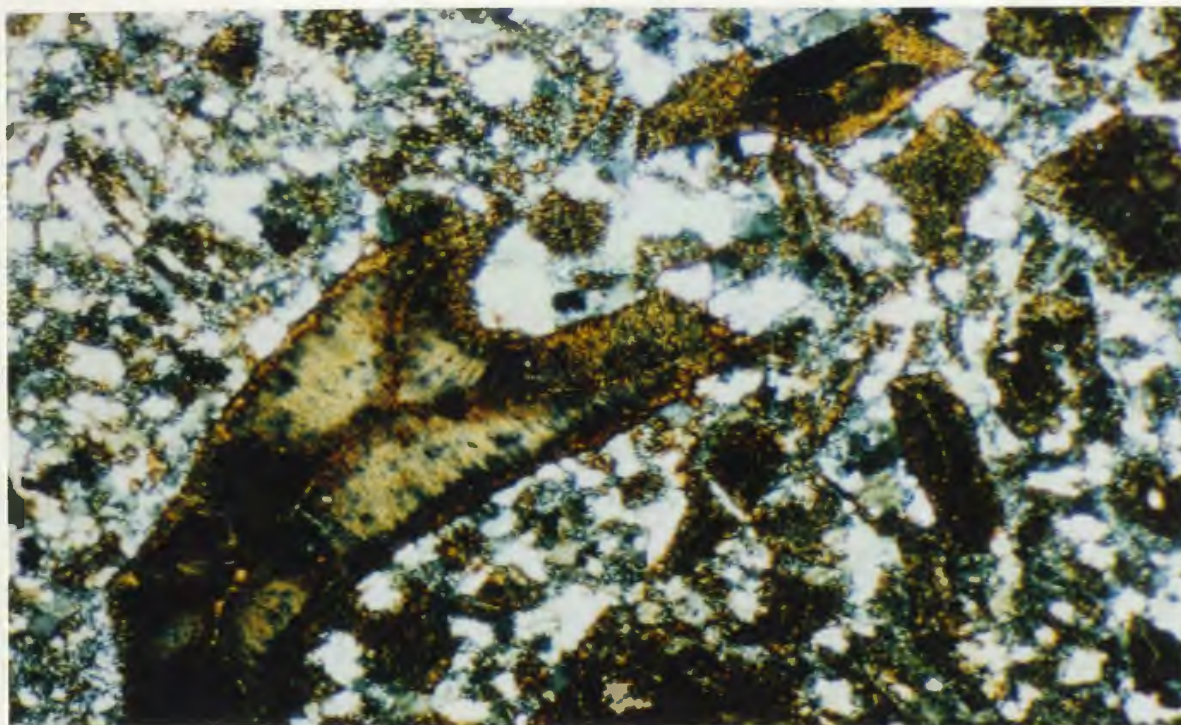


Plate 2.16(b). Photomicrograph of sample shown in Plate 2.16(c). The vitric clasts are individually devitrified with axiolitic texture.



Plate 2.17(a). Small "dykelet" of mafic magma entraining some droplets of felsic melt, in ash-flow tuff of Unit 8.

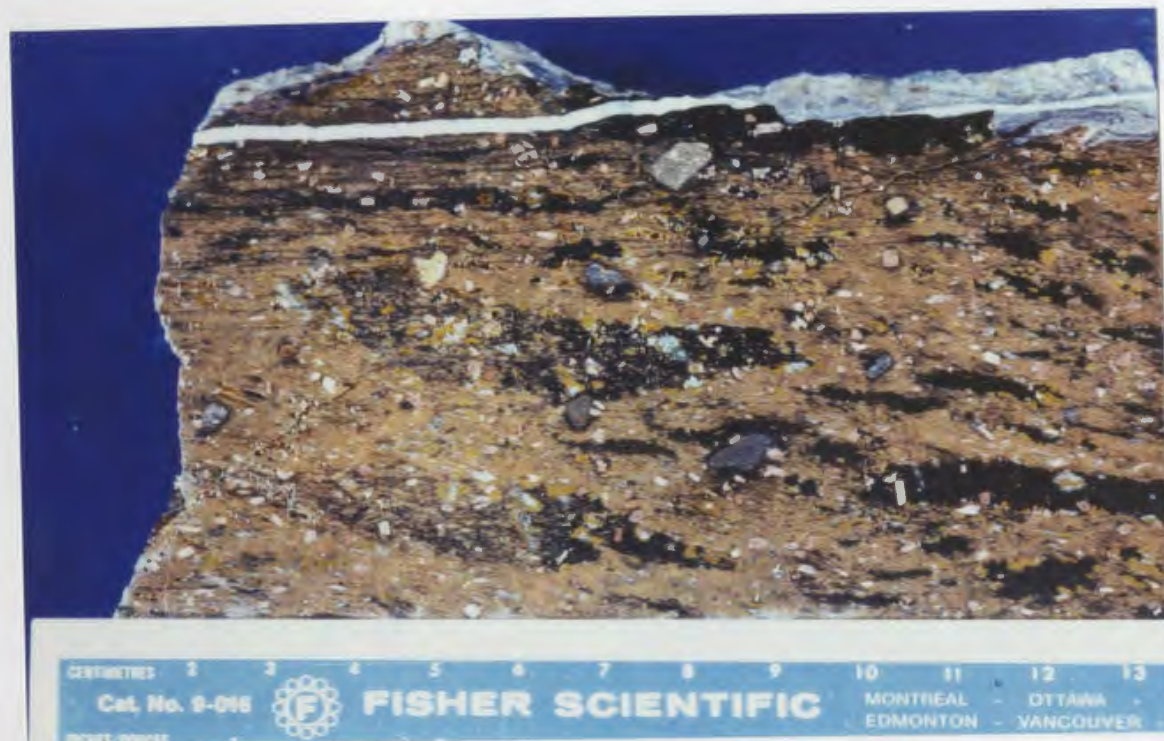


Plate 2.17(b). Ash-flow tuff of Unit 8. The black pumice clasts are mildly welded, in a crystal-lithic matrix which contains abundant mafic xenocrysts.

2.11. Unit 9

Unit 9 comprises a sequence of redbed sedimentary rocks distributed in the central portion of the synform (Fig. 2.3; Map 1). As with Unit 8, estimates of its boundaries can only be inferred from the distribution patterns, as seen on Figure 2.3. It forms belts up to 25 km long, 3 km wide in the northeast and narrowing to 500 m at the inner fold closure. An outer band of sediments are disposed about the central synclinal axis over a distance of 20 km and width between 2 and 0.5 km. Unit 9 is interbedded with units 5, 8 and 10, and grades into unit 8 in a few locations.

These sedimentary rocks have been described in detail by Wessel (1975). In general they consist of two types of conglomerate, sequences of sandstones, and sandy siltstones with localized development of caliche (Plate 2.19). Structures such as cross-bedding, ripples, laminations, rip-up horizons, scour channels, and many other sedimentary features are present (Plate 2.20a). Wessel (1975) suggested that they represent stream-flood and proximal and distal fluvial deposits.

Distinctive polymictic cobble conglomerates are found at local contacts with the volcanic rocks of the Springdale Group. These conglomerates are commonly massive to poorly bedded, with bedding marked by sandy scour channels which pinch and swell and obscure true bedding orientations. The



Plate 2.18. Rhyolite dome (Unit C) found on upper Burnt Berry Brook.



Plate 2.19. ("Newfoundland Gothic"!) Typical sequence of Springdale "redbeds" (Unit 9). Thick basal pebble conglomerate fining up to fine-grained sandstone beds capped with caliche. Photo taken on coastline in town of Springdale.

larger clasts may be imbricated and large-scale coarsening upward sequences can be recognized. The subrounded to subangular cobbles consist predominantly of aphanitic and porphyritic rhyolites, intermediate volcanics, and rarer basaltic and granitoid clasts (Plate 2.20b). The cobbles are supported in a medium-grained pale beige to maroon sandy matrix composed of the same lithic material plus abundant alkali feldspar and quartz.

Pebble conglomerates delineate basal portions of sandy cycles, thus occurring repeatedly throughout the sequence, and are usually massive and indurated, with little recognizable grading or other internal structures. Pebbles in this conglomerate are subrounded, and composed of silicic volcanic rocks, red and green cherts, and rare ultramafic, basaltic, and granitoid clasts. These pebbles are supported in a fine- to medium-grained matrix of subangular sand which is composed of the same lithic components as the pebbles and a high proportion of quartz and feldspar.

2.12. Unit 10

Unit 10 is an orange to brown, densely welded crystal-lithic tuff found mainly in the interior of the central syncline, and in one other exposure in the southwestern part of the area (Fig. 2.3; Map 1). The larger

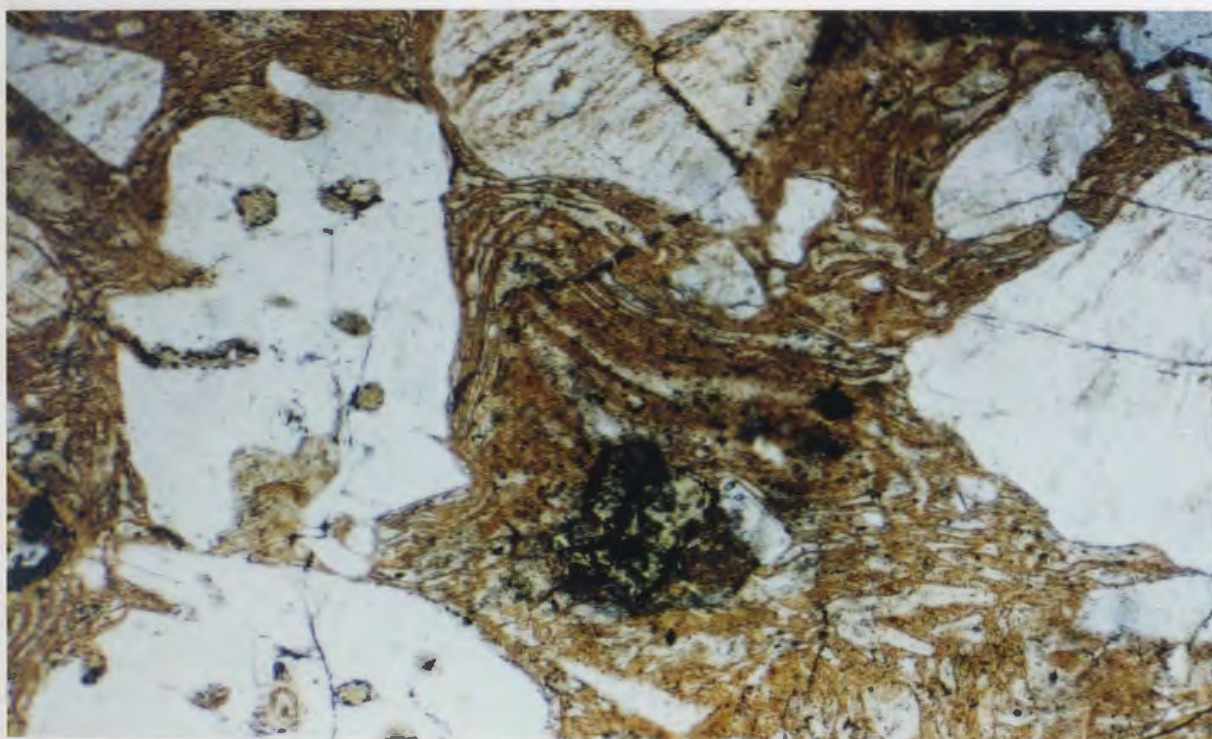


Plate 2.20(a). Ripple marks on the surface of a bedding plane in sandstone of Unit 9.



Plate 2.20(b). Polymictic conglomerate. Note weathering rims on some cobbles.

Plate 2.21. Eutaxitic texture in a crystal ash-flow tuff of Unit 10. Note resorbed quartz and feldspar and typical Y and X-shaped bubble wall shards in matrix.



synclinal exposure trends northeast for 18 km, with the northwestern limb formed by a broader band as wide as 2.5 km in the centre and narrowing both northwards and southwards. The southeastern limb is up to 1 km wide, becoming less than 150 m at its northern limit on the coast of Halls Bay. The southwestern exposures form a belt about 6 km long by 1.25 km wide.

This crystal tuff is very massive and so strongly welded as to look like an intrusive porphyry. It has large phenocrysts of quartz and feldspar, clasts of mafic and ultramafic lithologies, and does not demonstrate many fluidal characteristics. The feldspars are often zoned and fractured, and together with the quartz can constitute up to 60% of the rock. The crystals are found in a red, brown or orange vitric aphanitic matrix. The lithics are commonly angular, and may have reaction halos, especially around the ultramafic clasts (Plate 2.21).

2.13. Domes and Vent Centres of the Springdale Caldera

Unit C is a glassy rhyolite with microphenocrysts of quartz and feldspar, and may contain finely disseminated bluish-green amphibole and hematite in the groundmass (Plate 2.22). This unit comprises rhyolitic dykes, sills and high-silica domes. Such domes are found as a number of separate roughly oval exposures in the southern and central parts of the map area (Fig. 2.3, Map 1), as an elongate

lens intersected by Burnt Berry Brook, and as an isolated exposure, cut by intermediate dykes, near Barney's Brook.

The rhyolite domes have similar compositions and textures, and intrude Units 3, 6 and 8, as well as the microdiorite of unit B,. They are flow-foliated, with extreme convolution shown by fluidal folds (Plate 2.23) and disruption of flow banding (Plate 2.23b), auto-brecciated and contain zones of intense development of spherules and other indications of gas-streaming. Auto-brecciated aprons composed of disrupted fragments of the dome are considered to be part of this unit. They are not reworked clasts in any sense and are commonly found in a glassy matrix which represents magma injected into the cooled rind along the margins of the domes (Plate 2.24). Curvilinear jointing and ductile flow-shear features are found within the body of the domes.

At least three main centres of eruption can be recognized in the Springdale Caldera which are now manifested as domes and/or plugs and vent complexes, each with distinctive features and emplacement characteristics.

Domes can be described as "steep-sided, rounded extrusions of highly viscous lava squeezed out from a volcano, and forming dome-shaped or bulbous masses of congealed lava above and around the volcanic vent" (Bates and Jackson, 1980). Although this definition is accurate for most "exogenous" domes in which the lava is extruded at

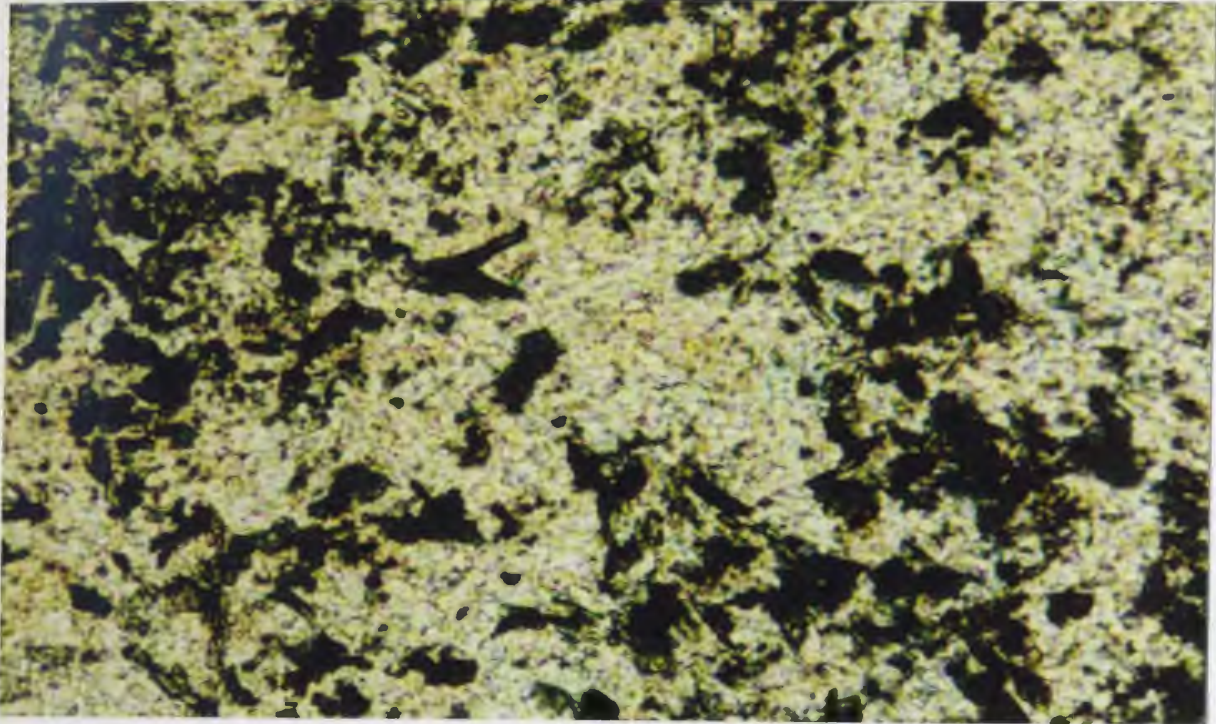


Plate 2.22. Microlites of riebeckite in groundmass of rhyolite from Burnt Berry Dome.



Plate 2.23(a). Fluidal flow folds in Burnt Berry Dome.



Plate 2.23(b). Convoluted flow-foliation in the Burnt Berry Dome. (Unit C).



Plate 2.24. Autobrecciation in gas-rich zones of the Burnt Berry Dome.

the dome surface, another type of emplacement behavior is preserved as "endogenous" domes wherein the fresh lava is added to the interior of the structure and may not reach the surface. There is a continuum of physical characteristics between these types of domal structures as well as their associated lateral lava flows and co-genetic pyroclastic deposits, as shown in Fig. 2.4, which should be followed in the following descriptions and discussion.

The Mount Saint Helens eruption of 1980 has allowed for observations of the actual physical mechanisms of dome emplacement and related pyroclastic eruption (Swanson et al., 1987). It was noted there that periods of endogenous inflation alternated with exogenous extrusion and explosive eruption, direct evidence that a dome site can be a vent source which is subsequently plugged with the non-explosive viscous lava of the subjacent magma reservoir.

Dome systems typically occur around the margins of calderas and may be distributed along arcuate or linear features which define the fracture systems related to the collapse and emplacement history of the caldera. Collapse geometry as well as chemical composition, volatile content of the magma, and surface conditions (e.g. wet or dry emplacement) control the distribution of domes and vents.

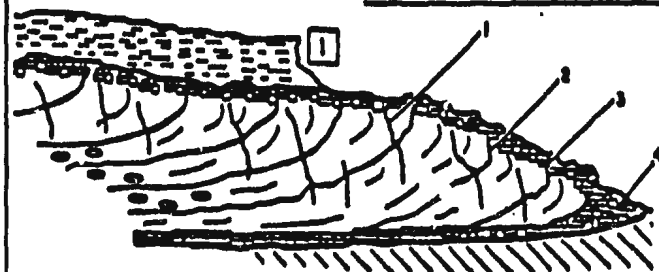
Although more detailed geophysical interpretations are made in the following sections, it is expedient to make passing reference to the geophysical maps in discussing the

Figure 2.4. Schematic interpretations of the features seen in domes and tephra deposits of the Springdale caldera.

- (a). Johnson's Lookout, based on Burt and Sheridan's (1987) description of "Mexican-type" rhyolite flows. 1. Internal fractures that cut flow banding; 2. Flow banding; 3. vitrophyric carapace breccia (See also Unit 8 and Plates 2.15(a,) and 2.16(a); 4. breccia beneath and at the front of the flow.
- (b). Tuff ring and lava cone with overflowing lava plug. Note inward-dipping bedding of the tuff-cone, as observed in Plate 2.29(b) (after Heiken and Wohletz, 1987).
- (c). Hypothetical cross section through a rhyolite dome showing the steepening and overturning of flow foliations as the upper contact or carapace is approached (after Burt and Sheridan, 1987).
- (d). Schematic illustration of pre-eruptive (A) and post-eruptive (B) stages for vulcanian activity, showing the crater-fill and vent breccia seen on West Brook (See Plate 2.35) (modified from Heiken and Wohletz, 1987).

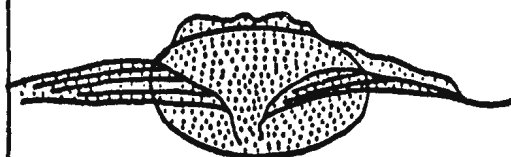
JOHNSON'S LOOKOUT

73



(a)

TUFF RING AND TUFF CONE
WITH OVERFLOWING LAVA PLUG

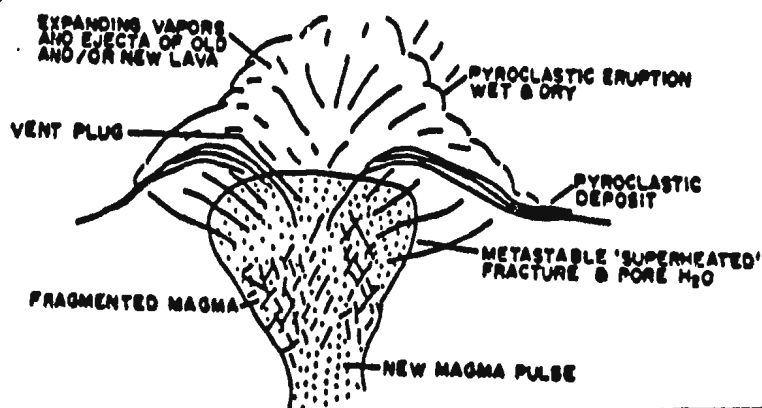


WOLF HEAD COMPLEX

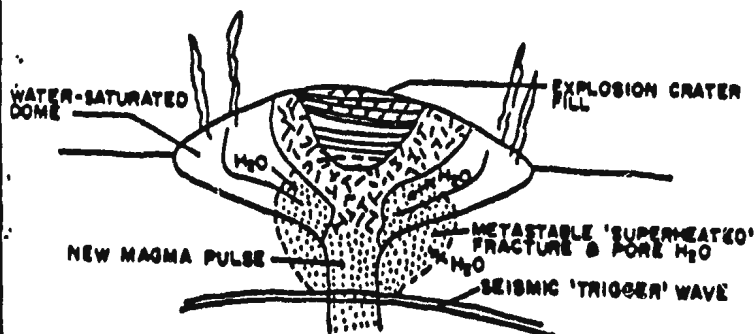
(b)

A.

(d)

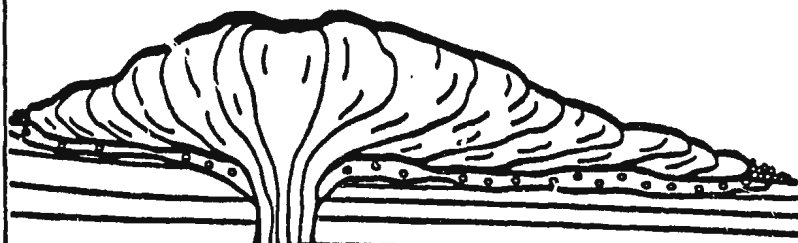


B.



WEST BROOK DOME & VENT

BURNT BERRY DOME



(c)

domes. For example, the bounding fractures can be inferred from the total field aeromagnetic map (Fig. 2.7a). Buried plutons along the margins can also be inferred with the use of these magnetic data and the limited outcrop (Fig. 2.7 and maps 3 and 4 below).

At each end of one such lineament on the eastern margin of the caldera two elongate domal structures or spines are present. These structures represent dome/plug facies which delineate the fissure system along which the major caldera-forming ash flow tuffs erupted. The two features are named Johnson's Lookout and Wolf Head (Map 1a). They are described separately although they could represent two points of emplacement along a dyke feeder that may have erupted simultaneously. Also the present structural configuration has not preserved these features at the same erosional level and therefore different depths are represented at each feature. Although late stage volcanic and sedimentary facies cover most of the feeder system to Johnson's Lookout and Wolf Head, the lineament upon which these two features are found can be traced along a trend on the geophysical maps (see Fig. 2.7, below).

Johnson's Lookout is a prominent topographic feature which occurs along the eastern margin of the Springdale Caldera. As mentioned above it appears to be the source or vent area for at least one ashflow eruption in the caldera, based on the facies variation of the ash flow

Plate 2.25(a). The eastern side of Johnson's Lookout; view towards the northeast.



Plate 2.25(b). The eastern side of Johnson's Lookout.

tuff preserved around this feature and the chemistry of the tuff in comparison to that of Johnson's Lookout Spine itself. The feature is a massive spine roughly 800 feet above sea level with a vertical rise of 50 feet (Plate 2.25a,b). It trends in a northeasterly direction and the prominent feature is about 750 metres long. The main feature is surrounded by adjacent, topographically prominent outcrops that are composed of both the massive dacitic composition (66.80 % silica) domal material and brecciated apron material consisting of autoclastic fragments either produced by auto-injection and fracturing of the melt along cooling joints or spalling of cooled rind material along the flanks of the feature (Plate 2.26). These rock types are pervasive in the vicinity of Johnson's Lookout (Johnson's Lookout) for a range of 2 km along the trace length of the elongate northeasterly direction and across the short axis direction of less than one km in outcrop distribution (Fig. 2.4a). Both geophysical data and mapping show a wider distribution of the pyroclastic deposit which appears to be a cogenetic ashflow or proximal deposit to this source area (Fig. 2.7, maps 3 and 4 below).

A number of characteristics of Johnson's Lookout suggest that a magma reservoir drove the melt upward and in part outward from a deeper source and cooled at or near the surface. Not all of the plug/dome/apron features are preserved, but enough are to reconstruct the basic elongate orientation and primary features of the spine.



Plate 2.26. Autoclasification of flow-banded dacite of Johnson's Lookout. Note fine flow-banding marked by devitrification spots.



Plate 2.27. Columnar joints and cooling fractures along the eastern scarp of Johnson's Lookout.

Johnson's Lookout is composed of aphyric glassy dacitic material with plagioclase crystals, and has zones or regions of color bands and cleaved cooling joints. These cleaved areas appear to radiate around the structure although the greatest portion of them are found along the southeastern flank of the feature. Along some of these congealed joints, localized autobrecciation is observed, which suggests that they may be primary flow channels in a solidifying carapace. In plan view along the top of Johnson's Lookout they are steeply dipping and are at most 10 centimetres wide. These steeply dipping or locally inclined joints divide the spine into elongate columnar masses (joints) up to a few metres across (Plate 2.27).

These features can readily be observed along the eastern scarp of Johnson's Lookout. The scale and irregularity of these joints would suggest that they represent vertical shrinking fractures. Also observed is at least one set of subhorizontal or curvilinear sheeting joints. Where the Johnson's Lookout slopes off to the north and south, oblique cuts through these "fractures" show a distinctive kinking pattern with centimetre-wide repetitions of the peaks. The orientation of the kinking is broken up in domains or fracture blocks along the dominant joints. Small-scale flow banding is also present and where it has become brecciated, pieces of the flow-banded glass are rotated or pushed aside and rest in an isotropic glassy

groundmass. Where the flow-banding is well developed, devitrification spots or blebs overprint the banding and are more pervasive.

On the eastern scarp vertical striations are seen which are similar to those produced by shearing of viscous and solid siliceous melt during intrusion. The eastern scarp appears to be the limit of solid melt material of the spine and may thus approximate the fracture along which the melt was injected against wall rock (that is now eroded away). Late stage fluids may have accentuated these features either as conduits for melt emplacement or later as fluids passed through the fractures. Near the base of Johnson's Lookout a swarm of "dykes" appears to feed up into the surface of the structure. These dykes or pipes have distinct margins, appear stony or more grainy than the spine matrix but are chemically and physically equivalent with the glassy dacitic material. However they cross-cut the preexisting fabrics. Veining associated with these small scale intrusions may suggest a late vapor-phase or residual at the waning stage of dome emplacement.

In thin section, the color bands or layering appear to be alternating areas of greater or lesser parallel cracks or discrete fractures. Where the fracturing is dense and they are aligned or in conjugate sets, the band has a reddish stain due to an oxidation of the iron-rich microlites. The greyish layers are either massive isotropic

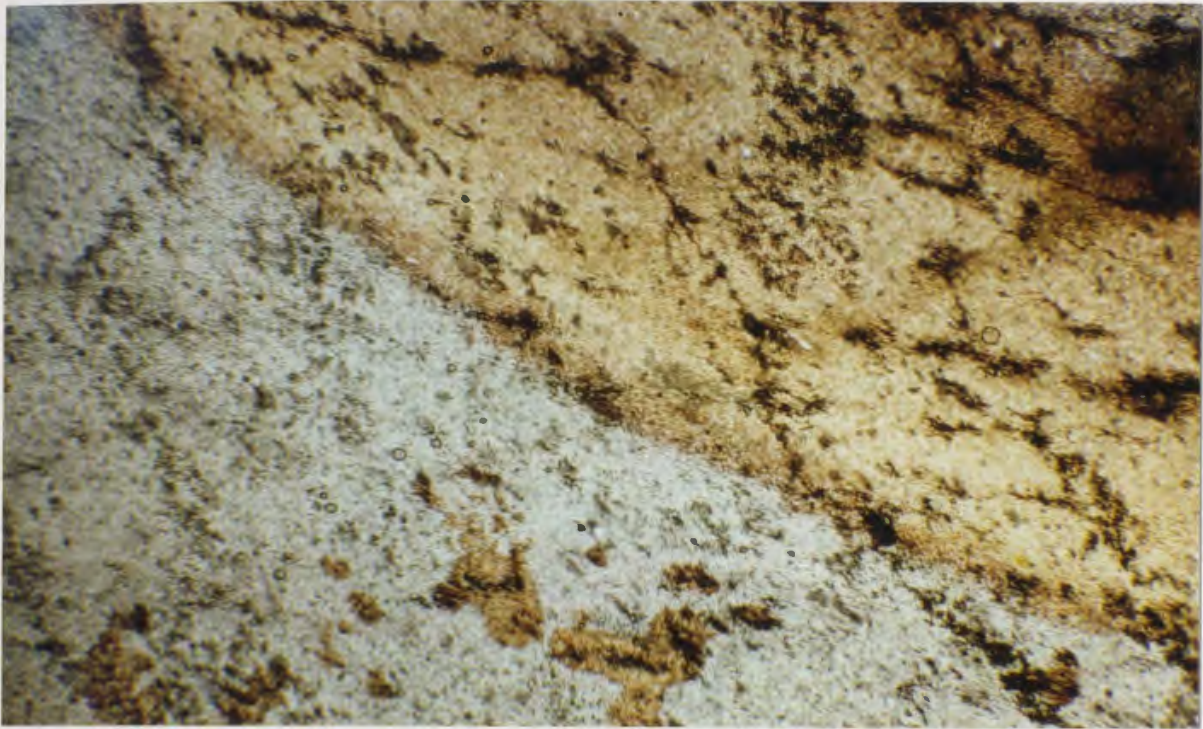


Plate 2.28. Greyish layers of isotropic dacite (left) with little or no fracture/autoclasis, with oxidized band in upper right displaying conjugate microfractures with microlites aligned oblique to fractures.



Plate 2.29(a). Eastern scarp of the Wolf Head peninsula, view to southwest.

glass with little or no fracture/autoclasis, or bands of uniformly shattered dacitic melt in a relatively unaltered state (Plate 2.28). These variations may represent primary shear planes along which the melt flowed.

Wolf Head is a small peninsula in the southern part of Hall's Bay which divides a section of water known as West Bottom from Goodyear's Cove (Wolf Cove). The feature trends northeasterly and is just over one kilometer in length, less than 500 m wide, and rises out of the sea over 65 metres at it's highest point (Map 1). The main body of Wolf Head is composed of brownish to maroon massive dacite that has greasy to glassy surfaces. The most prominent cliff face on the east side of the peninsula displays a gross bedding which is composed of large angular blocks in a brecciated dacitic matrix (Plate 2.29a). The bedded blocky material forms a skin along both the eastern and western scarps of the peninsula (Plate 2.29b). Massive and autobrecciated material composes the central core and for this reason the brecciated material is interpreted as a fallback breccia along the margins of an original vent fracture which was subsequently plugged with viscous melt at the cessation of eruption (Fig. 2.4b).

This sequence of events is also indicated by the occurrence of an ash-flow tuff (Unit 4) which originates from and centres on Wolf Head, and overlies some pre-eruptive andesite flows that are found along the very

Plate 2.29(b). Base of the Wolf Head vent, looking north.
Note Coarse bedding in the vent breccias seen in
cliff. Red andesite flows underlying these breccias
are seen in the left foreground.



base of the cliffs and in the general vicinity (see Maps 3 and 4). Wolf Head is along strike from Johnson's Lookout and is virtually identical in terms of its physical characteristics and geochemistry. It is inferred that Wolf Head and Johnson's Lookout represent distinct locations of ash-flow tuff eruption (either contemporaneous or at least cogenetic) along an original fracture vent system on the eastern edge of the Springdale Caldera. Some prominent jointing surfaces run lengthwise along the extent of the peninsula and two prominent joints cut across it. No major displacement appears to have taken place across these joints, although one fracture set forms a bench on the eastern side, separating the massive material from the blocky intrusion breccia, and may represent some original instability along the emplacement wall.

In thin section the bulk of samples are glassy pilotaxitic-textured dacite with flow aligned plagioclase laths (Plate 2.30). The majority of samples show little evidence of heavy alteration although clots of carbonate and alteration of the plagioclase is typical. Where the rock appears brecciated along flow fractures, as in Johnson's Lookout, the areas of brecciation are zones where microlites are oxidized along parallel and conjugate fractures (Plate 2.31).

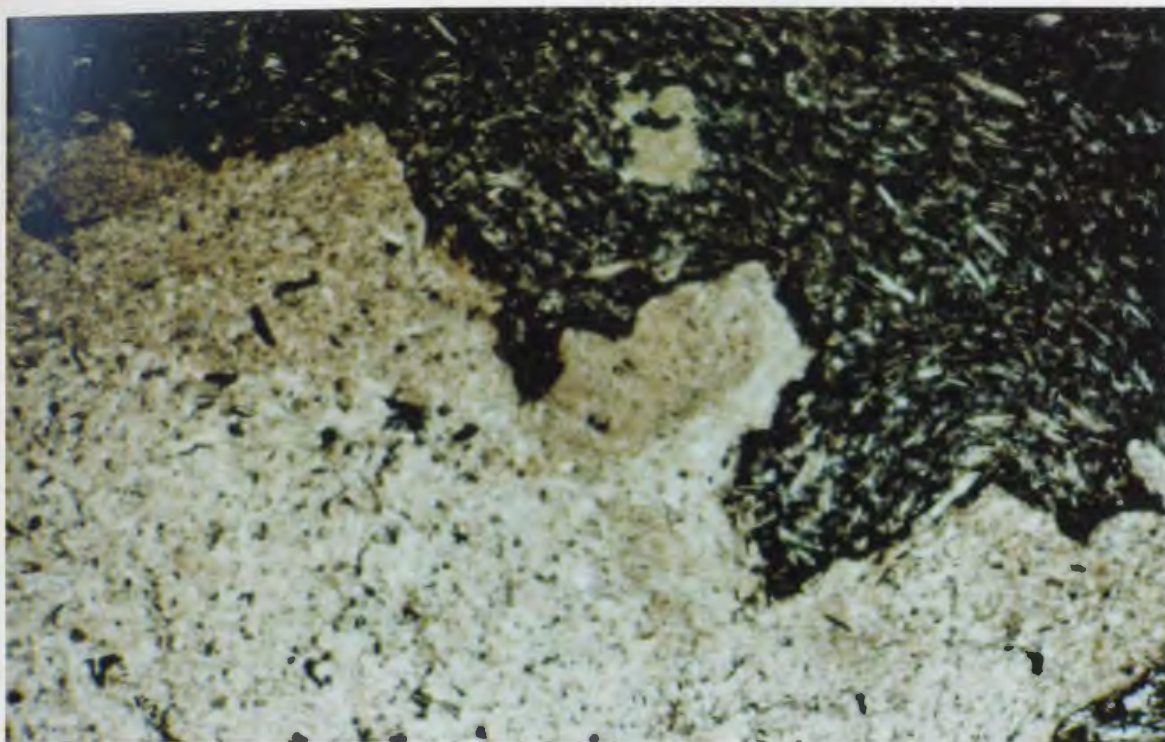


Plate 2.30. Glassy pilotaxitic-textured dacite with flow-aligned microlites, Wolf Head.

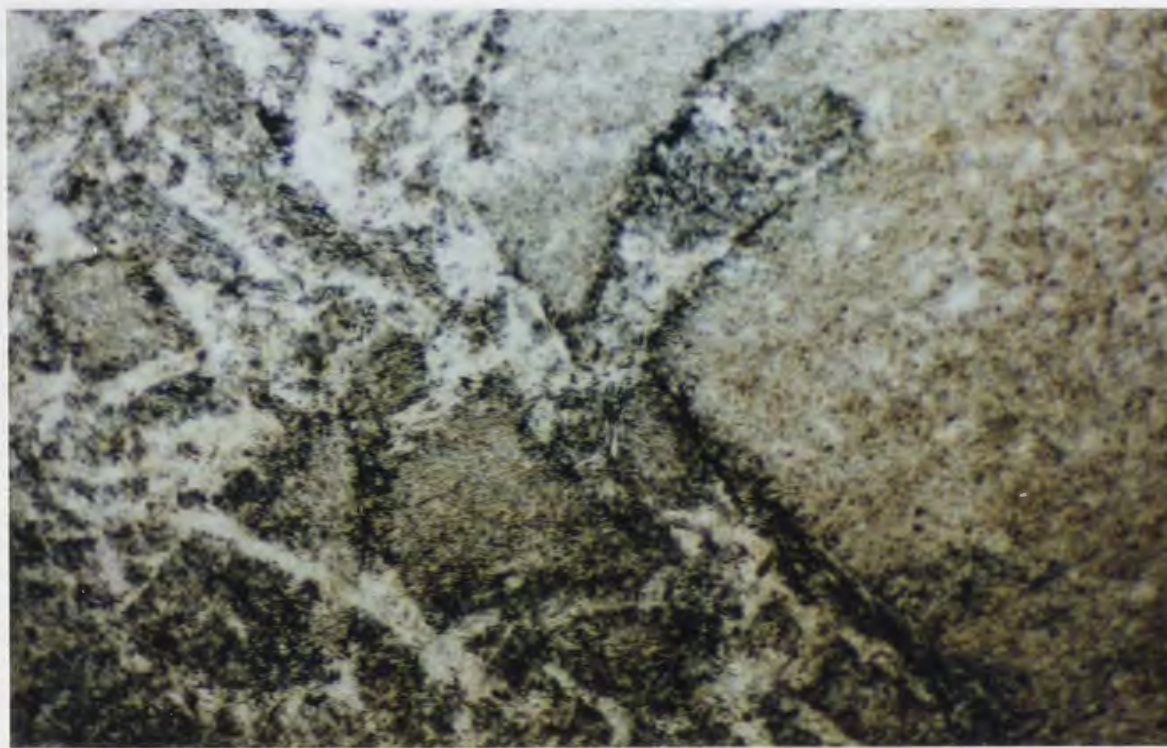


Plate 2.31. Autobrecciated Wolf Head dacite.

The Burnt Berry Dome is located near the central region of the caldera and is seen to intrude ashflow tuffs and basaltic flow rocks of the late-stage caldera fill. This dome appears to have two "lobes" which may represent two coalesced plugs or may be a single structure that has been deformed by folding and faulting. The outcrop in this vicinity is very poor except for the river section along the Burnt Berry Brook (for which the dome is named). A wide variety of physical characteristics can be noted in the brook where the dome is exposed for over 750 metres. The contact between it and adjacent lithologies is not actually exposed.

Recent exploration trenching in the area has exposed a northwest-trending fault where two units, an ash-flow tuff (Indian River Tuff, Unit 10) and a lens of red sandstone and pebble conglomerate (Unit 9) are rotated to near vertical position along the edge of the Burnt Berry Dome. This section of the caldera fill was interpreted as representing a late keystone block with a high degree of both vertical and strike-slip faulting. This may have been accompanied by emplacement of the dome along fractures produced by slight upwarping from asymmetrical resurgence beneath the caldera. This faulting and the more complicated fault and geophysical patterns in the central caldera area (see Map 3 and Fig. 2.6 below) support this interpretation.

The Burnt Berry dome is made up of pink to brown glassy rhyolite. Good examples of curvilinear joint surfaces are found throughout, and zones of flow-foliation or banding are common (Fig. 2.4c). In plan view domains of metre-scale columnar joint complexes are seen, and flow-generated breccias are common along congealed fractures. Near the margins of the structure, splay-like intrusions of lithophysae dykes (Plate 2.32) and gas-breccias are found that bud off as irregular or radiating fracture sets.

In thin section the rhyolite is extremely fine-grained to glassy with a spherulitic texture developed throughout from devitrification of the glassy matrix. Phenocrysts of plagioclase and quartz are found along with zircon. Where gas-brecciation is prevalent, thin sections show an abundance of miarolitic cavities now infilled with drusy quartz. Small fractures off-set flow banding, on a scale from thin section (Plate 2.33) to outcrop-scale, typically filled with quartz and minor calcite and fluorite.



Plate 2.32. Splay-like intrusions of lithophysae dykes

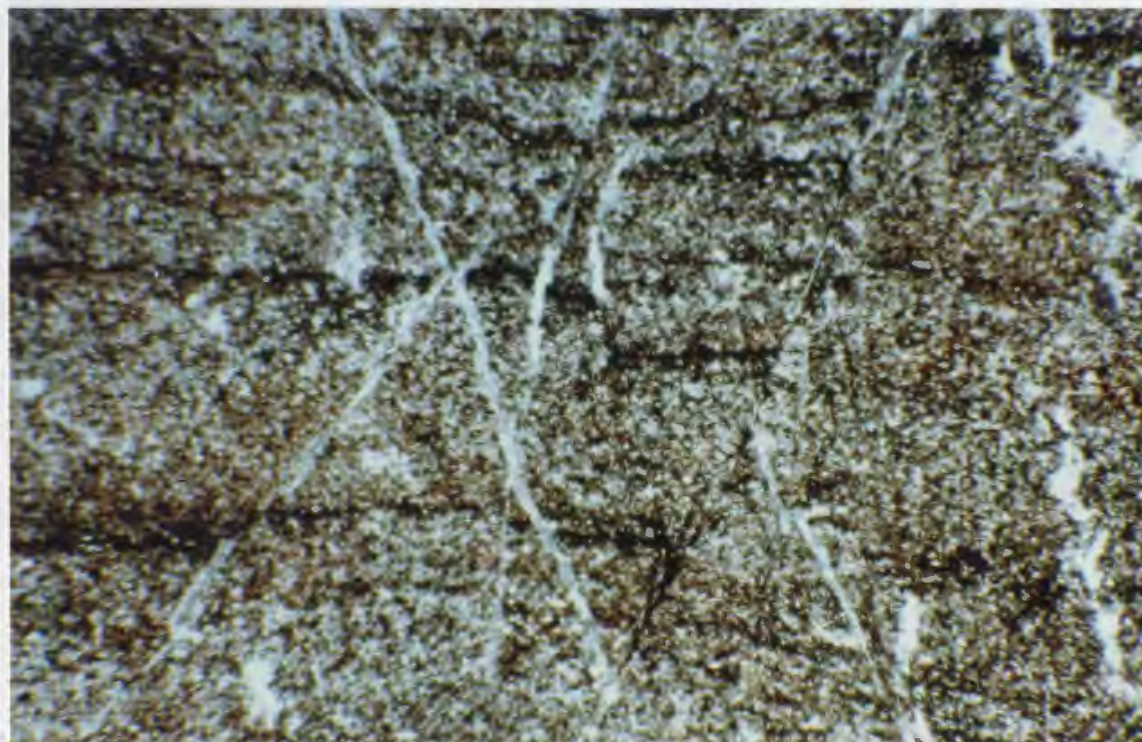


Plate 2.33. Micro-fractures off-setting flow banding of Burnt Berry rhyolite.

A few other rhyolitic domes occur in the Springdale caldera. One is partially exposed on the southern part of Barney's Brook on the Great Gull Pond Sheet (12H/1). This dome is roughly 500 m in diameter and shows most of the features described for the Burnt Berry Dome above, as well as a well defined autobrecciated apron. This dome is fed by a number of massive rhyolitic dykes that were heavily gas-charged and in some cases these dykes contain gas tubes. In this area there is also a massive sill of rhyolitic composition sandwiched between two pyroclastic units, and many of the gas-charged dykes are seen to "feed" into the sill.

Two other rhyolite domes have been identified in the southeastern part of the map area. They can be seen on Map 1 and are generally ovoid with more gently sloping contact relationships with the surrounding units (i.e. they are not steep-sided plug-like intrusions at their current level of exposure). These two larger domes, one near Misery Hill, and the other to the south of it, have well preserved aprons and may represent exogenous flow domes with their lateral flows preserved. These domes appear to be emplaced in a concentric pattern around the Topsails intrusion to their south. The volcanic sequence in this area is tilted up toward the north by the intrusion of the Topsails Granite.

The West Brook Dome, like the Burnt Berry Dome, is named for the brook along which it is exposed and where it forms prominent waterfall outcrops (Plate 2.34). The West Brook Dome is found in close association with its cogenetic pyroclastic deposits and because of the structural disposition and relief variation in the area of exposure almost a complete cross-section can be reconstructed.

I have included the West Brook Dome into unit 7 along with its surrounding pyroclastic deposit (ash-flow tuff). It is dacitic (62.8% silica), brown to maroon with obvious pink stained plagioclase crystals in a dense glassy matrix. A thick ash-flow tuff of this composition with variable welding orientation, is mapped along the main banks of West Brook. Its contact with the surface of the dome is demarcated by a coarse apron of blocky autobreccia which is composed of angular blocks (45cms and greater) of flow-banded and flow-folded dacite (Plate 2.13c), identical with the domal material beneath this carapace. The blocks are in a matrix of the same composition and in places the breccia appears to be flow aligned. The dome is beneath this autoclastic autobreccia but in part is overlain directly by the welded tuff of the same composition. The base of the tuff unit is a coarse pyroclastic deposit in some places which grades up into a fine ash-flow tuff. Where the coarse pyroclastic breccia is preserved, large pumice bombs are seen along



Plate 2.34. Waterfall on cliffs of the West Brook dome.

Plate 2.35. Vent breccia exposed in cliffs of the West Brook dome.



with some accidental lithic material such as angular, dense rhyolite clasts. The dome is exposed for 50 metres along its surface and in cross section for more than 10 metres.

In part the dome is massive, but areas of extensive shearing and ductile/brittle fracture are also preserved where the dense glassy matrix appears to form discrete closely spaced and sheeted flow planes. The sheeting is produced by alternating bands of dense glassy material and granular gas-charged material and are curvilinear to concentric around the more massive core of the dome. The massive material of the dome appears to plug a vent structure at the base of the lowest waterfall.

In the gorge formed by the West Brook Falls, the wall opposite the falls has a distinctive hackly fracture and forms a large V-shaped structure up the wall. The interior of the V-shape is filled with large angular blocks of dacitic material in a fine, ashy, reddish matrix (Plate 2.35). The walls around this V-shape are the massive dacitic composition matrix of the dome material. At the top of the "V", the vent breccia is overlain by a lens of fine red sandstone, similar in composition to the breccia matrix. This is all capped by several basaltic flows. This feature is interpreted as a preserved vent through which was erupted the surrounding pyroclastic deposit and which was eventually plugged and quenched by the intrusion of the West Brook Dome, closely analogous to the events of the

1980 Mount St. Helens eruption (Swanson et al., 1985). It was subsequently filled with the silty debris and covered (and preserved by) basaltic flows.

2.14. Intrusive Rocks

The intrusive rocks around the margins of the Springdale Group have not been studied in any detail, but they were sampled and their approximate contacts with the volcanic units have been delineated. Some of the information about these rocks has been compiled from Whalen et al. (1983), Thurlow (1981), Kalliokoski (1955, 1953) and Coyle et al. (1985)

Units B and C appear to be genetically related to the Springdale volcanic rocks. Unit B is a black massive microdiorite exposed near both margins of the group. It is intruded by dykes and sills of unit C, (but may be relatively contemporaneous) and intrudes units A and 3. Unit D may also intrude it in the west, although this contact is obscured by faulting.

Units D and E, the younger granitoid rocks, were intruded along faults bounding the Springdale Group in the east and west, and truncate much of the stratigraphy in the south. These are part of the Topsails Complex which extends over tens of km southwards (Whalen and Currie, 1983a, b). These intrusions exhibit contact aureoles of major extent and intensity, indicated by the regional aeromagnetic maps,

although they have not been mapped in this study. Along the northwestern boundary with the volcanic rocks, the granites tend to be highly deformed and altered, possibly resulting from the faulting responsible for uplift and elimination of units 1 to 7 in this area. Most previous workers (e.g. Taylor et al., 1980; Whalen et al., 1983a) considered the granites of both Units D and E to be offshoots of the Topsails Complex.

2.15. Structural Geology.

2.15.1. Faults

In order to interpret the main faults affecting the Springdale Group it is useful to review the major faults which have affected the general area and their relative importance with regard to the Springdale and other correlative groups. The many faults of central and western Newfoundland have received variable attention and differing interpretations, depending upon the perspective and background, as well as the objectives of the particular investigator (e.g. see reviews by Dean and Strong, 1976; Hibbard, 1983; Van der Pluijm, 1986). Recent mapping of the Silurian volcanic and associated rocks, particularly those of the Springdale and King's Point calderas (Coyle and Strong, 1985, 1986; Coyle et al., 1985, 1986; Kontak and Strong, 1986; Mercer et al., 1985), has shown that several different styles of faulting can be recognized, reflecting a changing stress regime with time.

The most important and continuous fault system of the area is the Long Range - Baie Verte fault system (Fig. 2.1), first recognized by Murray and Howley (1881) and named by Wilson (1962) as the Cabot Fault. Because in the north this Cabot Fault splays into a number of branches, which are the main subject of this review, it is referred to here as the Cabot Fault Zone, with each of its branches discussed under their individual names. On the scale of the Appalachian-Caledonian orogen, attention has been focussed on the Cabot Fault Zone because of its correlation with the Great Glen Fault of Scotland, both of which have been interpreted as a major crustal break related to the ancestral Lower Paleozoic Iapetus ocean margin (Wilson, 1966). Wilson (1962) correlated the Cabot Fault with others as far south as Boston, but it is more fundamentally correlated with faults further west, the "Baie Verte - Brompton Line" of Williams and St. Julien (1982), i.e. with emphasis on its earliest role as the Iapetus ocean-continent suture.

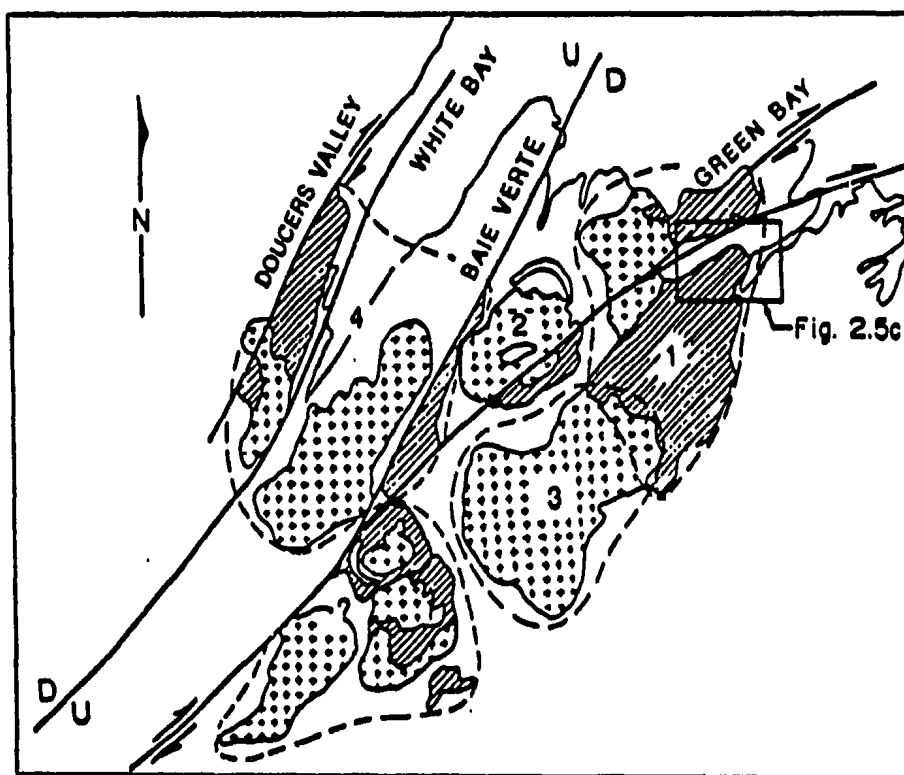
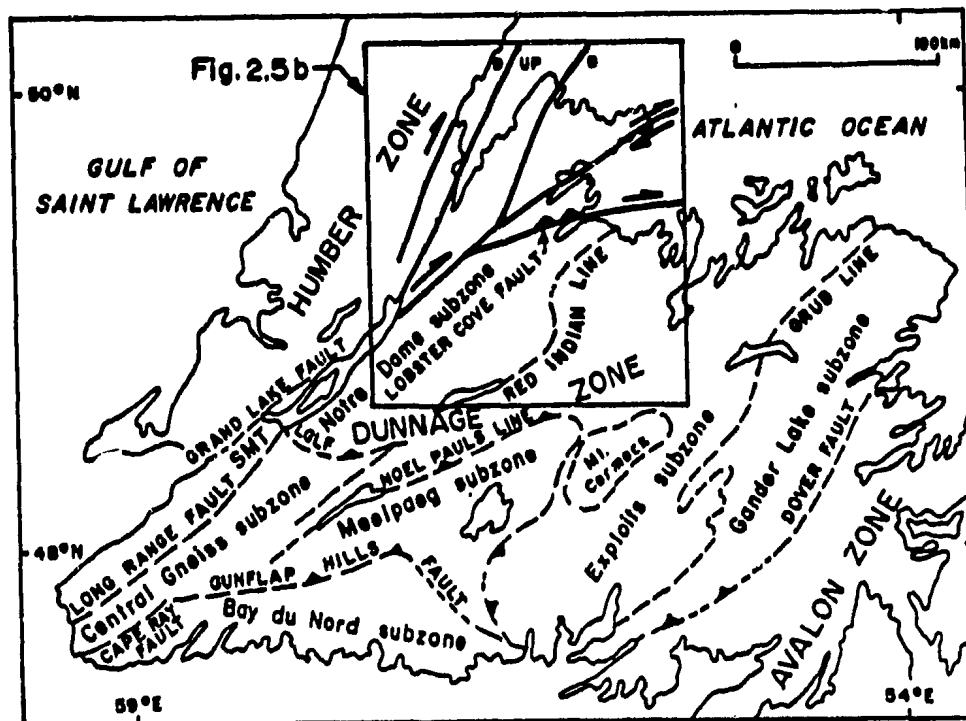


Figure 2.5(a). The major faults of western Newfoundland (modified from Currie and Piasecki, 1989). (b). Reconstruction of the major fault zones of the Springdale region (See Fig. 2.2 for further details).

The general evidence is strong that the Cabot-Great Glen Fault system has been intermittently active throughout the development of the Appalachian-Caledonian orogen, with style of movement changing from rifting and normal faulting when Iapetus was formed in the latest Precambrian, to obduction and thrusting during closure and destruction of Iapetus in the Middle Ordovician, to variable extents and senses of strike-slip faulting following closure, i.e. from the late Ordovician to the Carboniferous. Early or pre-Devonian sinistral displacement of up to 104 km, along with some eastward down-dropping, has been demonstrated along the Great Glen Fault by Kennedy (1946), but megametre-scale displacements suggested from paleomagnetic studies (e.g. Kent and Opdyke, 1978; Van der Voo and Scotese, 1981; Dewey, 1982) have not been supported by more detailed investigation in Scotland (Smith and Watson, 1983) or in Newfoundland (Irving and Strong, 1984, 1985).

There are five splays of the Cabot Fault system which are important for understanding the Silurian magmatic activity of west central Newfoundland. They are named, from west to east, the Doucer's Valley, White Bay, Baie Verte, Green Bay, and Lobster Cove faults (Fig. 2.5a,b). The local faults within and surrounding the Springdale Caldera (especially splays of the Lobster Cove fault) are discussed in more detail following description of each of the above.

Doucer's Valley Fault: Lock (1969) suggested that the Devil's Room and Gull Lake Granites (Fig. 2.2) are correlative, and were separated by a dextral displacement of about 15 km along the Doucer's Valley fault. This interpretation is supported by similar radiometric age dates around 400 Ma (reviewed below). Similar-aged ash-flow tuffs of the Sops Arm Group (Fig. 2.5b) are interbedded with fossiliferous middle to late Silurian marine sediments (Lock, 1972), and it is suggested that these are genetically related to the intrusive rocks, together making up part of what can be termed the Sops Arm caldera.

The White Bay Fault, also termed the Hampden Fault (Webb, 1969; Belt, 1969) and the Cabot Fault (Wilson, 1962; Hibbard, 1983), has variable significance at different positions along strike, emphasizing the difficulty of generalizing about major fault zones. With regard to this thesis, the main concern is its effect on the Silurian igneous suites of the White Bay area. The Wild Cove Pond Granite might be tentatively correlated with the Sop's Arm Group and associated intrusions because of its similar biotite K/Ar date of 392 ± 16 Ma (Wanless et al., 1972), and its lithological/geochemical similarities (Hibbard, 1983; D.F. Strong, unpubl. data). There is no indication of lateral displacement along the White Bay fault, and it is suggested that exposure of the relatively coarser grained Wild Cove Pond Igneous Suite in juxtaposition with the Sops

Arm and MicMac Lake volcanic rocks result from uplift of the Wild Cove Pond suite as a central horst (here termed the "Fleur de Lys horst") between these two faults (Fig. 2.5b). This is also indicated by the much higher metamorphic grade of country rocks (the Fleur de Lys Supergroup) within this block than those outside it, and further south by direct contact between the metamorphic rocks and Carboniferous sedimentary rocks (Hibbard, 1983). The latter relationship indicates that the White Bay Fault was active into the Carboniferous, and may have controlled Carboniferous sedimentation to some degree (Hyde, 1979).

The Baie Verte Fault is best known for its role as the main suture between rocks of the Iapetus Ocean and the North American continent, and its relevance for the Silurian magmatism may be less obvious. The main Silurian evidence of this fault is a deformation of pyroclastic rocks of the MicMac Lake Group. It also separates them from the Wild Cove Pond Igneous Suite, obscuring any correlation between them. The MicMac Lake Group might at first glance be considered part of the King's Point Complex, and has historically been correlated with the volcanic rocks associated with the Springdale Group redbeds, but MicMac conglomerates contain clasts of black glassy comenditic tuffs that are typical of the King's Point volcanic rocks, suggesting that the MicMac are younger than the King's Point. Furthermore, the 427 Ma age of the King's Point, as

discussed below, is substantially older than the MicMac Rb/Sr whole rock dates of 404 ± 24 Ma (Wanless, in Neale and Kennedy, 1967) and 386 ± 15 Ma (Pringle, 1978). Thus, it seems more probable that the MicMac Lake Group is correlative with the late Silurian Sops Arm Group and associated intrusive suites which make up the Sops Arm caldera. If this interpretation is valid, it means that post-Silurian movement on the Baie Verte Fault was mainly vertical, i.e. forming the east side of the Fleur de Lys horst.

The Green Bay Fault was first noted by Neale et al. (1960) and later named by Upadhyay et al. (1971). According to Hibbard (1983) it truncates the Wild Cove Pond Igneous Suite, the Baie Verte Fault and the MicMac Lake Group. Along the shore of Green Bay it is exposed as a steep scarp in excess of 330 metres, where the eastern margin of the King's Point Complex is juxtaposed against the Lush's Bight Group ophiolitic rocks. Both the deeper level of erosion and the higher altitude of the west side of the fault accords with vertical uplift along it, but it appears that its dextral motion is more important. Hibbard (1983, p. 188) has reviewed the evidence provided by previous workers for dextral displacement of at least 25 km, up to a maximum of 100 km. As suggested below (Chapter 5), such an interpretation would result in the juxtaposition of the Springdale and Cape St. John Groups which, along with other evidence, implies that their origin may have been related to the same caldera.

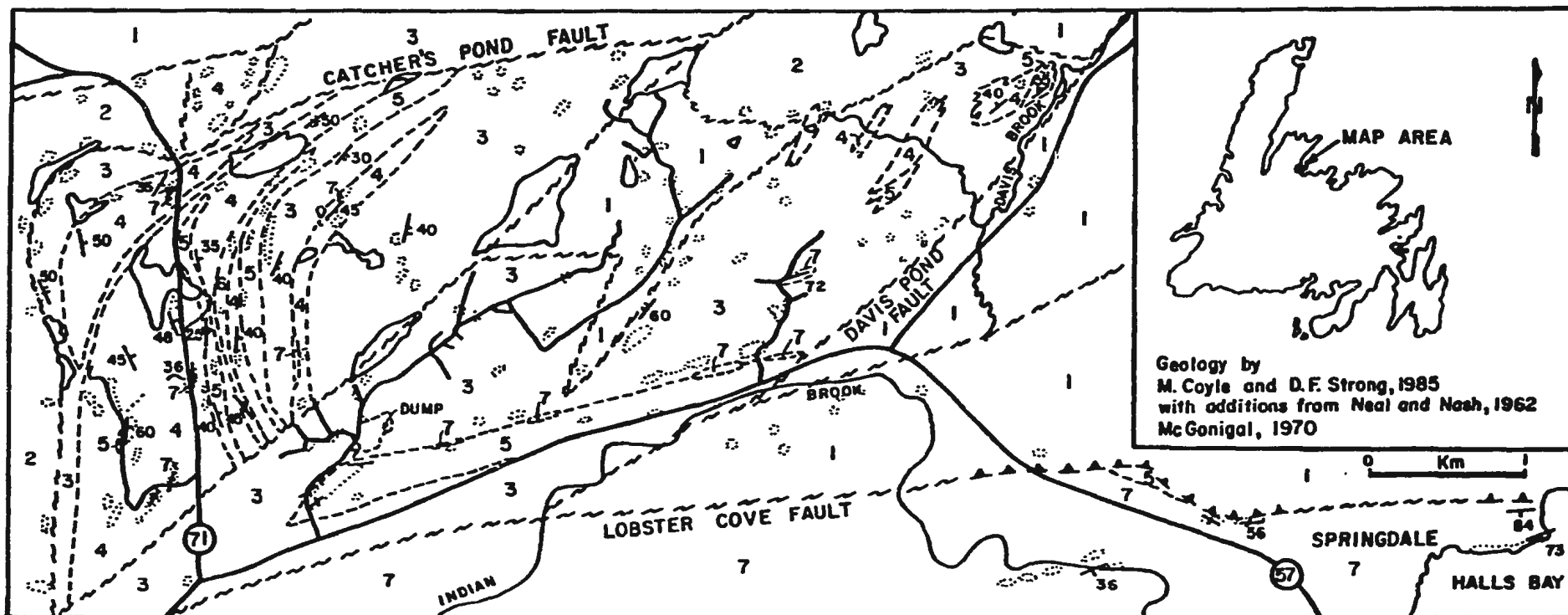
Support for such displacement is also given by the compelling similarities between the oikocrystic comendites and porphyries of the King's Point Complex and the Sheffield Lake Group (Coyle et al., 1986). The similarity between these unique rocks strongly suggest that the two were part of the same King's Point caldera, which was also dissected and displaced about 50 km by the dextral movement along the Green Bay Fault. This fault was also active until at least the Lower Carboniferous, as seen by deformation of Lower Carboniferous strata along its full extent.

The Lobster Cove Fault: Like most of these faults, the Lobster Cove Fault has received differing interpretations, especially at different places along its length. These were reviewed by Dean and Strong (1977), who concluded that across Notre Dame Bay it is mainly a thrust fault which has been folded into a vertical to slightly overturned orientation. In the Springdale area it has not been folded, and can be seen in cliff faces to be a gently northward-dipping thrust fault. Two new features of the Lobster Cove fault have been recognized by this study. It oversteps several mappable units of the Springdale Group, i.e. sandstones, basaltic flows and the interbedded Indian River ash-flow tuff. Furthermore, it exhibits a number of splays which separate imbrications within a duplex structure of the Lushs Bight Group, formed by ramping at a bend in the fault.

The detailed map of the northern margin of the Springdale caldera (Fig. 2.6) shows a simplified "football-shaped" structure to the north of the Lobster Cove fault which encloses marginal fault blocks of the caldera, some retaining limited internal stratigraphy. This feature really comprises a complex assemblage of juxtaposed fault blocks disposed about an asymmetrical fold axis with an axial planar fault axis, all of which is sandwiched between the Lobster Cove Fault to the south and several east-west trending faults which divide this duplex from others in the Catcher's Pond Group to the north (Fig. 2.5.c).

Along its western extension, the Lobster Cove Fault changes orientation to a more north-south direction parallel to the dextral and vertical faults, and may also change in sense of movement. To the east the fault is straight, and has been interpreted by Calon and Szybinski (1988) as having a dominantly dextral sense of motion, at least during part of its history. They also interpret the thrusting in the Springdale area as resulting from a contractional duplex in the otherwise dextral strike-slip fault, supporting the basic interpretation made earlier by the author (Coyle and Strong, 1986). An age of 425 Ma for the Indian River Tuff (discussed in Chapter 5) predates at least this dextral movement along the Lobster Cove Fault, which Calon and Szybinski suggest was synchronous with the overlying caldera-fill sedimentation.

Figure 2.5(c). Geology and major faults of the northern edge of the Springdale caldera (See Fig. 2.5b and Map 1 for location).



LEGEND

SPRINGDALE GROUP: 7 - RED SANDSTONE AND CONGLOMERATE; 6 - RHYOLITE AND CRYSTAL TUFF; 5 - WELDED QUARTZ - FELDSPAR CRYSTAL-LITHIC TUFF; 4 - CONGLOMERATE; 3 - BASALT.

PRE-SPRINGDALE GROUP: 2 - CATCHERS POND GROUP; 1 - LUSHS BIGHT GROUP;

SYMBOLS: ▲▲ THRUST FAULT; ~~~ FAULT (unknown displacement); --- GEOLOGICAL CONTACT; OUTCROP; ~~~ ROAD; BEDDING OR FLATTENING IN PYROCLASTIC ROCKS (▲ inclined; ▼ vertical); BEDDING IN SEDIMENTARY ROCKS (▲ inclined; ▼ vertical; ▴ overturned); CONTACT OR FLOW STRUCTURE IN BASALT (▲ inclined; ▼ vertical).

The demonstrable syn-caldera dextral motion on the Lobster Cove and other faults contrasts with the suggestion by Currie and Piasecki (1989) that Silurian faulting in the area was sinistral, although the latter do recognize that this sense of motion could have been reversed "prior to Carboniferous time". It must be pointed out that the extensional nature of the Springdale caldera does not favour the locally compressional stress regime which would have resulted from sinistral motion in the Silurian, at least during caldera formation. Clearly further detailed studies will be necessary to determine precisely both the timing and sense of motion on these faults.

All of the fault patterns described above are reflected in the smaller scale faults within the Springdale Caldera recognized by this study. A number of thrust faults within the upper sedimentary rocks of the Springdale Group give some confidence in inferring similar faults to explain discontinuities in less distinctive units within the caldera. Within the sedimentary rocks of the Springdale Group there are two main thrusts which truncate sedimentary trends (Fig. 2.3; Map 1), clearly visible on geophysical maps (e.g. the total field aeromagnetic map, Fig. 2.5.c). The northernmost of these appears to have developed along the Burnt Berry syncline, which it cuts and displaces along its southernmost extent. The southern of the two marks the approximate southeastern boundary of the redbed sedimentary caldera infill (Unit 10).

2.15.2. Folds

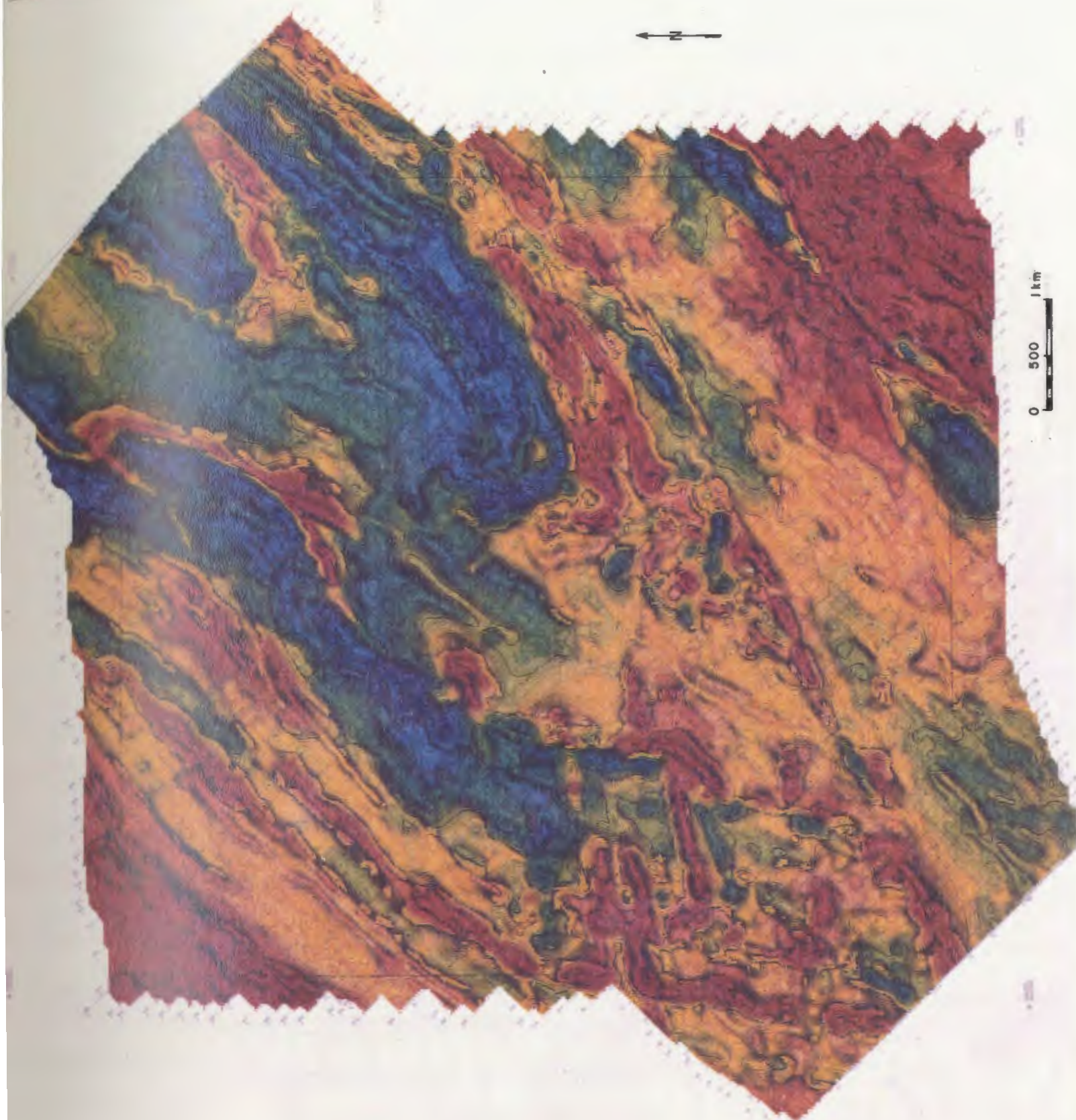
Deformation of the Springdale Group was dominated by one major fold, an open syncline with its axis trending southwestward through the western part of the caldera (Fig. 2.3; Map 1). It is particularly easy to recognize in the north over a distance of about 30 km, e.g. where the caldera-fill redbeds are intersected by the Trans-Canada highway. To the south it becomes more difficult to trace, but it can be seen from the geological map pattern to extend for at least another 30 km, where it is truncated by a NE-trending fault. This pattern is seen on the aeromagnetic map (Fig. 2.6) where, as discussed below, magnetic lineaments indicate faulting oblique to and along the hinge of this asymmetrical fold. The synclinal axis is also complicated by a thrust/strike-slip fault trending northeast along Saunders Brook.

2.16. Detailed Geology, Springdale Central Map Area (Map 2)

2.16.1 Geophysics

Total field aeromagnetic maps were produced by Aerodat Ltd. under contract to Equity Silver Mines Ltd. as part of a mineral exploration program under the author's supervision. They provide ancillary evidence for some of the main structures of the caldera, and two have been selected for specific discussion.

Figure 2.6. Total field aeromagnetic map of the Springdale
Central map area (See also Map 2, in pocket).



The aeromagnetic map for the Springdale Central map area (Fig. 2.6) exhibits high positive anomalies in the northwest and southeast corners of the map area which are inferred, or can locally be demonstrated, to result from granitic intrusions, as shown on Map 2. Next to the granite contact in the northwest are seen several distinct bands of intermediate level positive anomalies, reflecting the interbedded tuffs, basaltic flows and sandstones. The centre of the map area is marked by a broad low magnetic swath interrupted by two narrow higher magnetic bands which clearly outline the main synclinal/anticlinal structure shown on Figure 2.3.

The southern half of the map area is marked by a generally positive magnetic character, with a strong northeast-trending anomaly which separates a broadly low-relief area in the southeast from a complex high-relief area to the northwest. This abrupt change in character is most readily interpreted as the result of faulting, and its parallelism with thrust faults outside the map area (e.g. the Lobster Cove fault) suggests a similar origin, although it might equally have some relation to the resurgent updoming postulated for this area. There are a number of shorter sub-parallel lineaments between this fault and the main low-relief synclinal area, and it may be that they represent faults of the same type. It is also possible that the magnetic character of these lineaments, although

ultimately fault-controlled, is the result of intrusions which are not exposed at the surface. Contours on maps of apparent resistivity and VLF-EM total field intensity (not included in this thesis) generally confirm the magnetic indications, with the fold structures and main fault zones clearly evident.

2.16.2. Geology

The Springdale Central map area (Map 2) is underlain by volcanic, intrusive and sedimentary rocks which represent intra-caldera fill facies erupted and deposited during the waning stages in the evolution of the Springdale Caldera. These rock types range in composition from basaltic flows to rhyolitic ash-flow tuffs and domes. They are disposed about a north-northeast trending fold axis which plunges to the north. This fold axis has been augmented by axial faulting oblique to and along the hinge of this asymmetrical fold, and local thrust faulting occurs along the same structure to the north of this figure, within the caldera. The area is also complicated by the thrust/strike-slip fault which trends northeasterly along Saunders Brook. The area has been domed up by later intrusions exposed as silicic domes in the vicinity of Burnt Berry and Saunders Brooks. The more detailed scale of Map 2 (discussed below), in conjunction with the geophysical data, allows for some refinement of the distribution and structure of the units shown on Map 1.

The basaltic flow rocks of Unit 5 can be distinguished as at least five different folded and faulted lenses within the stratigraphic sequence. They are interbedded with both the sedimentary and pyroclastic units, and are intruded by rocks of the Burnt Berry Dome.

The rhyolitic ash-flow tuff of Unit 8, which extends throughout the centre of the caldera, is divisible (Map 2) with the aid of the geophysical maps into a number of separate fault-bounded lenses and bands about the synformal axis, despite the intermittent exposures. It includes an assemblage of mostly devitrified, welded, pink and red rhyolitic ash-flow tuffs and breccias, displaying a variety of rheomorphic features. Certain parts of this unit are very massive due to intense welding, and others consist of unwelded vitroclastic tuffs with large individually devitrified shards with perfectly preserved axiolitic textures, as described above. Other parts of the ash-flow breccias are not strongly devitrified, and all have internal auto- or gas-breccias with clasts of plastically deformed rhyolitic lava and pumice. Mixed magmas are found within the breccias, with alternating thin basaltic and silicic bands. These silicic tuffs are intruded by the Burnt Berry rhyolitic dome.

Unit 9 is divisible into a number of thin lenses of redbed sedimentary rocks which clearly outline the syncline and part of the anticline in this area. It is very

extensive outside the area of Map 2, forming belts up to 25 km long, 3 km wide in the northeast and narrowing to 500 m at the inner fold closure. An outer band of sediments is disposed about the central synclinal axis over a distance of 20 km and widths between 2 and 0.5 km. Unit 9 it is interbedded with units 5, 8 and 10, and appears to grade into unit 8 in a few localities. As described above, these sedimentary rocks in the area of Map 2 include conglomerate, red sandstones, and sandy siltstones with localized caliche.

Unit 10, the orange-brown crystal-lithic Indian River Tuff forms four separate lenses in the interior of the central syncline, interbedded with and overlying unit 9, i.e. is the youngest unit of the area. As described in Chapter 2, the larger synclinal exposure extends northeasterly outside of Map 2 for a distance of 18 km to the coast of Halls Bay. Unit C is a glassy rhyolite with microphenocrysts of quartz and feldspar, locally with finely disseminated bluish-green amphibole in the groundmass, forming dykes, sills and high-silica domes best exposed as an elongate lens intersected by Burnt Berry Brook, i.e. the Burnt Berry Dome.

The large positive magnetic highs on the northwest and southeast corners of the total field magnetics map (Fig. 2.6) were both interpreted above as indicating granitic intrusions. The northwestern was already

identified as the marginal granite Unit D. That of the southeast was not indicated on the larger-scale Map 1 or Figure 2.3, but a number of granitic outcrops were identified, and it is inferred that the magnetic anomaly indicates a substantial pluton there. Hence it is also shown as Unit D on Map 2.

2.17. Detailed Geology of the Springdale East Map Area (Maps 3 and 4)

2.17.1. Geophysics

Two adjoining total field aeromagnetic maps are shown in Figure 2.7 for the northern (Fig. 2.7a) and the southern (Fig. 2.7b) parts of the Springdale east map area. These are accompanied by the geological Maps 3 and 4 (in pocket). The most outstanding feature of the total field magnetic intensity map for the northern half is the large oval-shaped magnetic high which ranges from a high of 57800, consistently zoned outwards for a radial distance of about 3 km to a low of 54480 nanoTeslas. Although there are slight variations within this zone which might reflect lithological variations, it generally overrides any known lithological boundaries and hence defies definitive explanation. Nevertheless, the pattern and shape, and its similarity to the anomalies of known intrusive aureoles, e.g. those surrounding the Topsails Granite which intrudes the Springdale caldera to the south, compels one to suggest that it must be the reflection of a buried pluton.

Figure 2.7(a). Total field aeromagnetic anomaly map of the Springdale East map area, northern half. Adjoins Figure 2.7(b) to the west (bottom). See also Map 3 (in pocket).

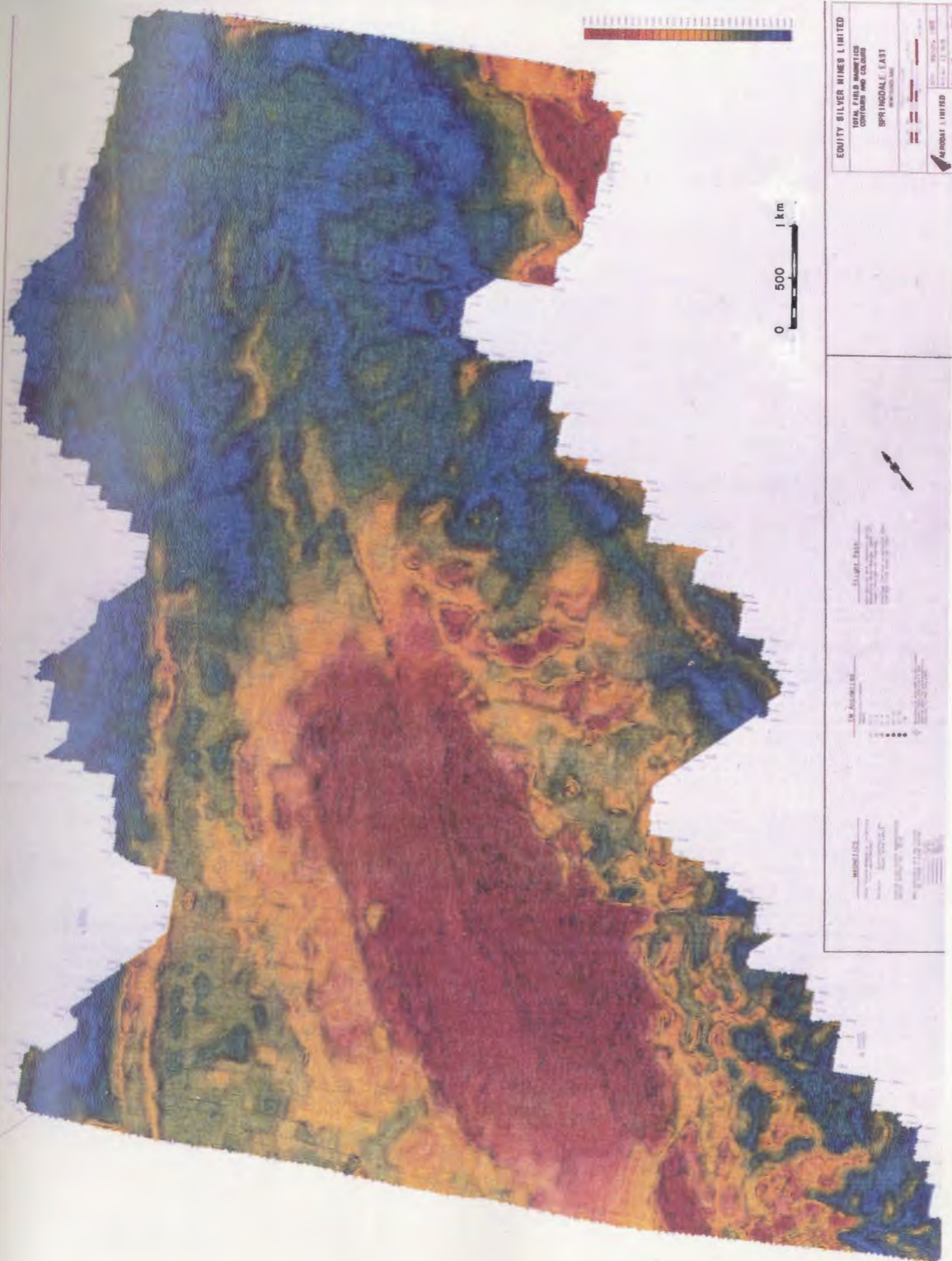
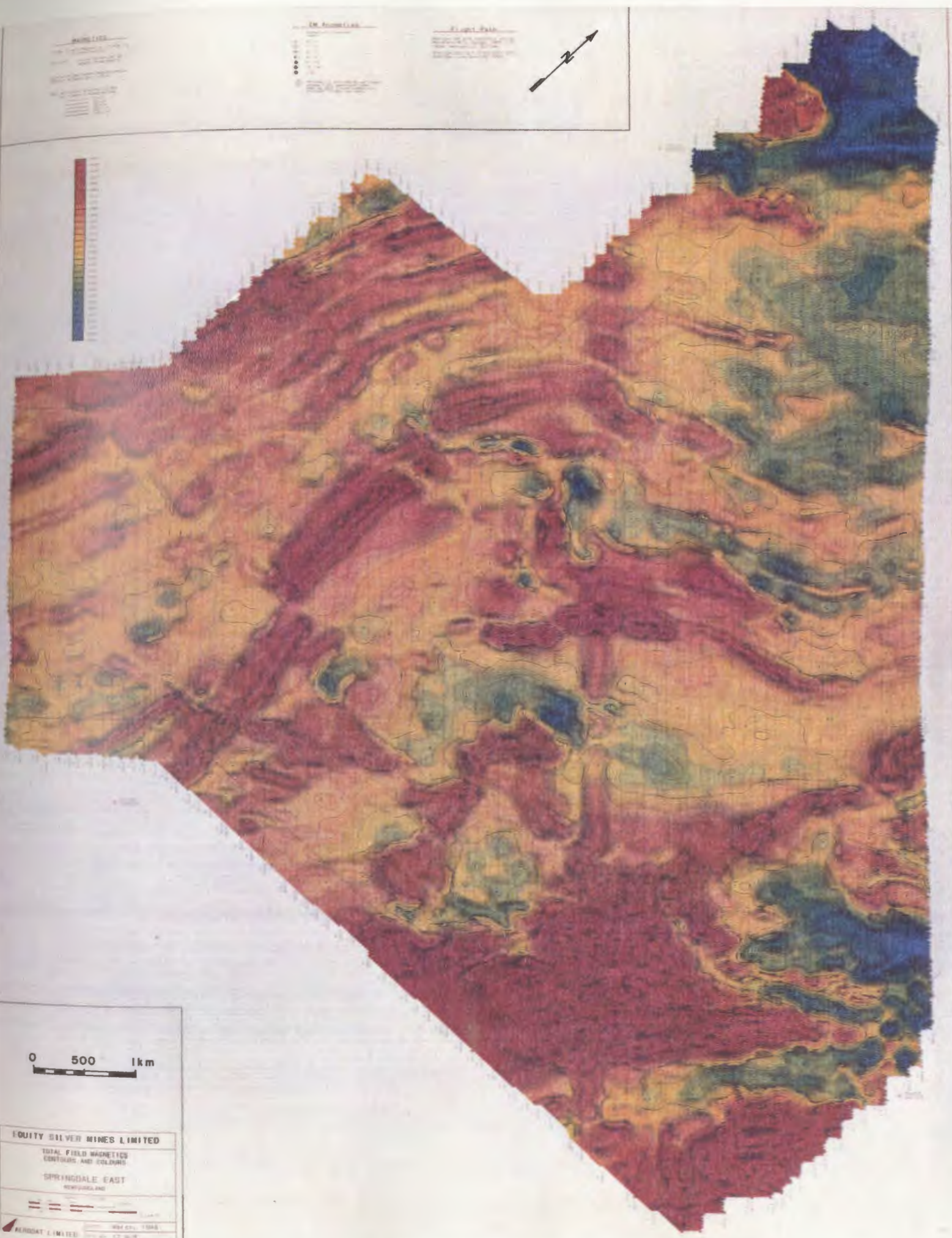


Figure 2.7(b). Total field aeromagnetic anomaly map of the Springdale East map area, southern half. Adjoins Figure 2.7(a) to the east (top). See also Map 3 (in pocket).



Although some magnetic effects are seen around and within the South Pond Granite in the northeastern part of Figure 2.7a, they are much weaker, possibly the result of a number of factors including the different depth of exposure (i.e. magnetic roof-rocks removed, and steep sides giving a narrow aureole). Both the apparent resistivity and the VLF-EM total intensity maps support this interpretation, showing clearly the South Pond granite contact. A major positive linear anomaly of intermediate range clearly outlines the distribution of intermediate composition rocks of unit 4 (See Map 3). Several linear magnetic lows within both the caldera rocks and the basement Unit A are interpreted as indicating fault zones which have also been identified in the field by fault gouge and breccias. In general the caldera rocks have low magnetic relief, with low-level lineaments delineating contacts between units. The basement rocks on the eastern edge of the map area have a much more complex relief, reflecting their much more complex geology.

Coyle and Strong (1986) speculated that the dioritic plug of unit B and the andesitic flows dipping away from it (See cross-section B-B', Fig. 2.3), along with laharic and other lithologies, indicate the former presence of a strato-volcano. This interpretation is spectacularly supported by the total field aeromagnetic map shown in Figure 2.7b, which shows a clear-cut series of concentric

alternating high and low magnetic bands around the granodiorite body (see Map 4). This intrusion is itself on the edge of an irregular-shaped broad magnetic high. Together these features are readily interpreted as indicating a large intrusive volcanic centre with concentrically disposed flows, pyroclastics, sediments and sills, as shown in Map 4 (in pocket). Equally outstanding are the series of structures which radiate out from this centre, which are clearly analogous to the radial faults and dyke swarms which are seen in more recent stratovolcanos (e.g. the Summer Coon volcano of the San Juan Mountains in Colorado (Lipman, 1976)). It is also clear from these structures that they were synvolcanic, since there is clearly some relative fault displacement across them, both the radial and concentric, all of which are typical features of up-doming effects around central volcanoes. Although outcrops in this area are sparse, there are a few distinct magnetic lows which can be seen from several exposures to be represented, on surface at least, by rhyolite domes. In one exposure it can be seen that the radiating magnetic high is represented on surface by diabase dykes.

2.17.2. Geology

Detailed attention was focussed on the Springdale East map area because it includes the critical facies of the eastern caldera margin, including mass wasting deposits or mesobreccias located and generated at the caldera walls; a complex of caldera margin emplacement-related intrusions; and a post- emplacement granitic stock with associated dykes and hydrothermal system. The geology of the eastern margin is complex, with a wide variety of pyroclastic facies varying in both composition and physical characteristics. Also this margin hosts two domal/spine complexes (Johnson's Lookout and Wolf Head, described above) and their associated pyroclastic aprons. The pyroclastic assemblages are interbedded with mafic and intermediate composition lava flows and some local sedimentary rocks derived from these lithologies.

The lithologies of the Springdale East (northern) area are grouped into five units on Figure 2.3 and Map 1 (Units 1-5), recognizable on the regional 1:100,000 scale, but the combination of the larger scale and the newly available geophysical data allow for eight subdivisions on Map 3. This map also includes the intrusive unit D which is related to the development of the caldera, and the foliated granodioritic complex intruded by tonalite (unit A) which is the local basement lithology and not related to the genesis of the caldera. The eight subdivisions shown on Map 3 can be described as follows.

Unit 1 is a welded crystal-lithic tuff of metaluminous affinity (plagioclase, K-feldspar, biotite, quartz) which is locally deformed along its eastern contact with the basement by both shearing and small-scale southeastward-directed thrusting. It is also intruded by unit D, a granitic stock on the northern limit of the map, where it displays brittle deformation caused by the intrusion.

Unit 2, the mesobreccias, is located along the eastern to central portion of the map and oriented roughly in a northeasterly direction. In the northern map (2.7b) the mesobreccias are associated with and are distributed in a lobate manner around Johnson's Lookout (part of Unit 3, described in detail above). Unit 3 can be recognized both in outcrop and on the aeromagnetic map as forming a northerly-trending belt extending over 14 km. Using the geophysical maps with detailed geological mapping, it can be divided into subunits 3a, 3b, and 3c. The first is the massive porphyritic andesite and dacite intrusions and flows which exhibit the lowest magnetic signature. The second (3b), although lithologically similar to unit 4, is marked by resistivity and magnetic lows, and a weak argillic and carbonate-chlorite alteration. Unit 3c forms the dacitic autoclastic apron with ashy reworked volcanic debris. Unit 3 marks the major magmatic conduit on the caldera margin, possibly also the eruption sites for the other ash-flow tuffs (units 1, 3b and c, and 4), as 3

well as hydrothermal alteration systems which might be buried by these units. The latter is indicated where more heavily altered rocks are exposed by deeper erosion along the banks of Barney's Brook. Unit 4 is a dominantly intermediate composition lithic/lapilli ash-flow tuff with variable welding. In part, this tuff hosts thick sections (~2m) of porous, moderately to strongly altered, lithophysae zones. This unit can be traced up to its possible vent source, Wolf Head.

Unit 5a consists of thin flows of basaltic andesites, generally massive and aphyric to trachytic-textured, with plagioclase and minor amphibole phenocrysts, and abundant accessory altered magnetite. Unit 5b is mainly thick basaltic flows with massive bases grading up to vesicular tops and flow-top breccias, typically with plagioclase phenocrysts, with amygdales of quartz, calcite and chlorite.

The exposed geology of the Springdale East southern area (Map 4) is similar to that of the north, except that in addition to Units 1, 2, 3, 4, and 5, Units 6 and B are also seen. Indeed, Unit 6 may be at least in part equivalent to Unit 4, although Unit 4 in the north has such distinctive lithological and geophysical characteristics that it is retained for present purposes.

Unit 6 consists of silicic ash-flow tuffs, exposed continuously along Barney's Brook, in conformable contact with basaltic flows of Unit 4, over a strike length of 14 km with a maximum width of 3 km. They have been extended southwards from discontinuous exposures outside of Map 4 for an additional 30 km, with maximum width of 6 km in the extreme south of the map area. These ash flows are reddish-brown to grey and display varying proportions of crystals, lithic fragments, and vitroclasts. Along Barney's Brook the basal part of the unit is a thick, lithophysae-rich, horizon resting on irregular flow tops of the basaltic Unit 5. The individual lithophysae may be as large as 10 cm in diameter, with central cavities partially or completely filled with radiating quartz crystals, microlites, and chalcedony. This horizon grades up into a partially welded crystal-lithic lapilli tuff. The phenocrysts are plagioclase, K-feldspar and quartz, commonly broken and concentrated in the matrix in preference to the pumice vitroclasts. A crude bedding is defined by flattening of the pumice lapilli, which can be as long as 50 cm, and by concentrations of the large vitroclasts.

The densely welded parts of Unit 6 are maroon to brown ash-flow tuffs, with phenocrysts of plagioclase, K-feldspar and quartz, which vary in relative proportions in a streaky manner. A welding lamination is seen on

weathered surfaces, but on fresh surfaces they look massive and structureless. The welded zones are locally extremely massive and have the superficial appearance of an intrusive quartz-feldspar porphyry. Unit 6 includes a number of pyroclastic flow units, each characterized by different proportions of lithic and vitric clasts. They cooled as a simple cooling unit, suggesting that the ash flows followed one another in rapid succession, with no substantial development of internal thermal gradients.

Units B and C appear to be genetically related to the Springdale volcanic rocks. Unit B is a black massive microdiorite exposed near both margins of the group. It intrudes units A and 3, and is contemporaneous with or intruded by dykes and sills of unit C. Unit C is a glassy rhyolite with microphenocrysts of quartz and feldspar, and locally contains finely disseminated bluish-green amphibole in the groundmass, and is seen as dykes, sills and high-silica domes. These rhyolitic lithologies intrude Units 3, 6 and 8, as well as the microdiorite of unit B, and have similar compositions and textures. They are flow-foliated, with extreme convolution seen as fluidal folds and disruption of flow banding, auto-brecciated and contain zones of intense development of spherules and other indications of gas-streaming. Auto-brecciated aprons composed of disrupted fragments of the dome are included in this unit. They are not reworked clasts in any sense, and are commonly found in a glassy matrix which represents

magma injected into the cooled rind along the margins of the domes and sills. Curvilinear jointing and ductile flow-shear features are found within the body of the domes.

2.18. Summary and Discussion

The Springdale Group comprises a sequence of ash-flow tuffs, basaltic and andesitic flows and pyroclastics, rhyolite domes and intrusive centres, mesobreccias, and clastic sediments, all of which are typical of those found in caldera sequences throughout the world. Their distribution within a topographic depression and their appropriate disposition about this depression lead to the interpretation that the Group forms a classic caldera of a similar scale and characteristics to those of epicontinental regions such as the southwestern United States. The Springdale caldera is part of a larger volcanic field.

In such large volcanic fields a number of overlapping centres and/or calderas are commonly found together, especially within a particular period of geological time, e.g. about 4 million years in the San Juan field of Colorado (Steven and Lipman, 1976). At least three such centres, and possibly more, can be demonstrated in west-central Newfoundland, with the various volcanic and intrusive exposures representing different structural levels of the individual calderas and subjacent plutons.

For example in the King's Point complex, a composite ring dyke (Neale and Nash, 1966; Kontak and Strong, 1986) provides clear evidence for cauldron subsidence, the complex representing a caldera exposed at a depth intermediate between that of the Springdale caldera and the Topsails complex.

Although it is fairly clear from the above descriptions that an abundance of volcanic facies typical of cauldron subsidence and related pyroclastic volcanism are represented in the Springdale and correlative groups, their extent, and indeed the great extent of similar-aged magmatism throughout central Newfoundland, indicates that the tectonic controls of magmatism as well as caldera collapse were of regional significance. It is well known that calderas are in many case locally controlled by basement structures, and it is probable that those of west-central Newfoundland, with their NE-trending elongate shapes and pattern of distribution are ultimately related to the NE-trending faults and other structures seen in the basement rocks (Fig. 2.5).

Because Silurian-Devonian magmatic activity in Newfoundland followed closure of Iapetus (e.g. Strong, 1977, 1980), and the recognition that these Silurian calderas are located along the paleo-suture zone, it was suggested (Coyle and Strong, 1987) that this was due to melting of the subducted continental crust, with intrusion

and ascent focussed by the inherent structural weaknesses at the suture. Most correlative rocks in the orogen, from Scotland to at least as far south as Maine, are also found near this or other suture zones. For example Laurent and Belanger (1984) have suggested that Silurian volcanism of the Quebec Appalachians was produced in an overall dextral strike-slip tectonic regime, and numerous authors (e.g. Van der Pluijm and Van Staal, 1988, and references therein) have suggested a dextral strike-slip regime for the northern Appalachians. Given that such large calderas demand an extensional environment, at least locally, it can be suggested that such extension would be most readily produced in local pull-apart basins in this dextral regime. This would imply that the oblique sinistral closure of the "Iapetus II" of Van der Pluijm and Van Staal (1988) would have taken place before Springdale volcanism, possibly coinciding with the 438 Ma "island arc type intrusive rocks" of the Rainy Lake complex (Whalen et al. (1987)).

3. PETROGRAPHY OF THE ROCKS OF THE SPRINGDALE CALDERA

3.1 Introduction

The Springdale Group rocks represent a volcano-plutonic complex which is best described as a caldera as it has all of the inherent and definitive characteristics that are indicative of the collapse-explosive volcanicity seen in most modern and ancient calderas. It consists of a suite of pyroclastic rocks, domes and their associated deposits, both mafic and intermediate lava flows and sedimentary rocks as well as granitic rocks along the margins of the volcanic complex. The rocks range in composition from basalt through high-silica rhyolite as described in chapter 4.

This chapter deals with the petrographic descriptions of the volcanic rocks and associated domal intrusions. It does not deal with the late-stage, redbed sedimentary rocks in the northern part of the caldera nor the granitic suites that are found to the caldera's south and along the eastern and western margins. For the purposes of this chapter the rocks are divided as follows; mafic flows, intermediate flows, pyroclastic ash-flow tuffs, dacite domes, and high silica domes, dykes and sills.

The rocks of the Springdale caldera are remarkably well preserved with respect to primary textures and mesoscopic characteristics. They also preserve evidence of a pervasive propylitic alteration otherwise described as low greenschist metamorphism. However, areas of extensive or intense alteration at the surface are rare and limited to discrete localities. The alteration can be traced out of such zones into fresh examples of the host rock type.

A total of 440 thin sections were made and studied in the course of this thesis. Three hundred and twenty samples are directly related to the Springdale Caldera with the following distribution: 90 basalts, 15 andesites, 40 dacitic dome/autobreccias/dykes, 35 high-silica rhyolitic dome/sills/dykes, 105 pyroclastic rocks, 20 epiclastic/mass wasting deposit rocks, 10 late-stage redbed sedimentary rocks, and 5 marginal granitic rocks. An additional 20 thin sections were made in the course of the zircon geochronology discussed in chapter 5, and the remaining 100 thin sections represent the Sheffield Lake Complex to the west of the Springdale caldera which was mapped and studied during the summer of 1986 but is only made reference to in this thesis in terms of its local relationships to the Springdale caldera.

Appendix A is a generalized table of selected, representative petrographic descriptions which is meant to give a few "type" examples from each petrographic group as outlined above. It is not a full nor exhaustive list of all rock types or the full array of samples collected or thin-sectioned within the scope of this thesis study. It does provide however a realistic representation of the range of petrographic features for each group.

3.2 The Mafic Flows

The Springdale basalts are dominantly distributed in three belts as shown on Map 1A and described in chapter 2. They are however interbedded with most of the other lithologies of the caldera throughout the complete range of the volcanic stratigraphy and therefore such relationships suggest that there were conduits to mafic composition magma throughout the evolution of the caldera. This relationship is also displayed in rocks that have a mixture of mafic material within dominantly felsic ash-flow tuffs, as described for parts of units 3 and 8. The significance of this observation will be discussed in chapter 7.

The mafic rocks can be classified into four different types as follows: 1)plagioclase + olivine + clinopyroxene-phyric basalts, 2)plagioclase + clinopyroxene-phyric basalts, 3)plagioclase-phyric basalts, 4)plagioclase + olivine-phyric basalts, in descending order of abundance.

A full range of grain sizes are found within each of the four groups of basalts. In general the thin, single basaltic flows are aphanitic with tabular and non-vesicular basal portions which grade up to highly vesicular (amygdaloidal), (see Plate 3.1) rubbly tops. When a series of flows are stacked up in succession the middle flows are phaneritic and typically porphyritic with ophitic, subophitic or glomeroporphyritic (Plate 3.2) texture in thin section. The coarser grained nature of central flows is probably due to slower cooling and crystallization as well as concentration of fluids there. The plagioclase-phyric basalts typically display trachytic texture.

Along the western and southeastern margins of the caldera a few isolated outcrops of coarsely plagioclase-phyric "cumulate" basalts (Plates 3.3 a, b) are found and boulders of this rock type are found throughout the glaciated low-lying depression which now topographically defines the Springdale caldera.

It is difficult to determine the sequence of crystallization within the basalts because of alteration of some phenocryst phases and the groundmass. However the majority of flows have ophitic (Plate 3.4) to subophitic texture (Plates 3.5) which would suggest the coprecipitation of the phases involved (i.e. plg-cpx, plg-cpx-ol, and in a few rare cases plg-ol).

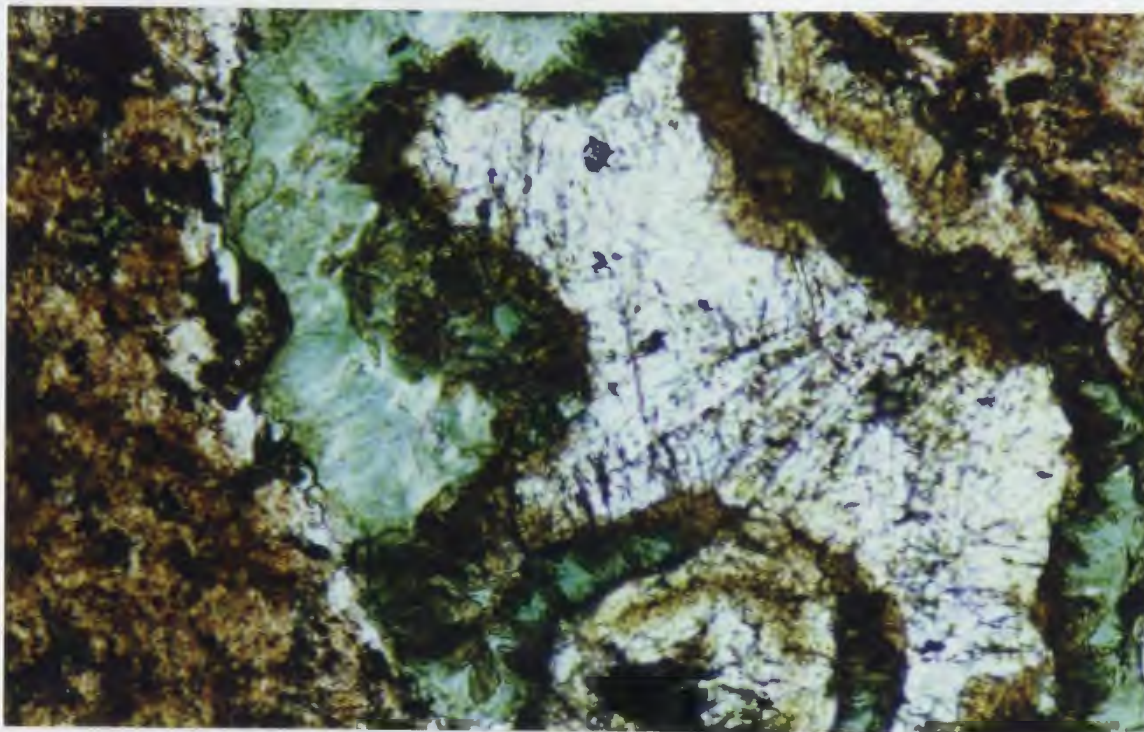


Plate 3.1. Amygdale showing complex array of secondary minerals. Radiating clear sprays in core are prenite, rimmed with chlorite and clotty patches of brownish epidote (DS-86-10A, 10X, PPL.)

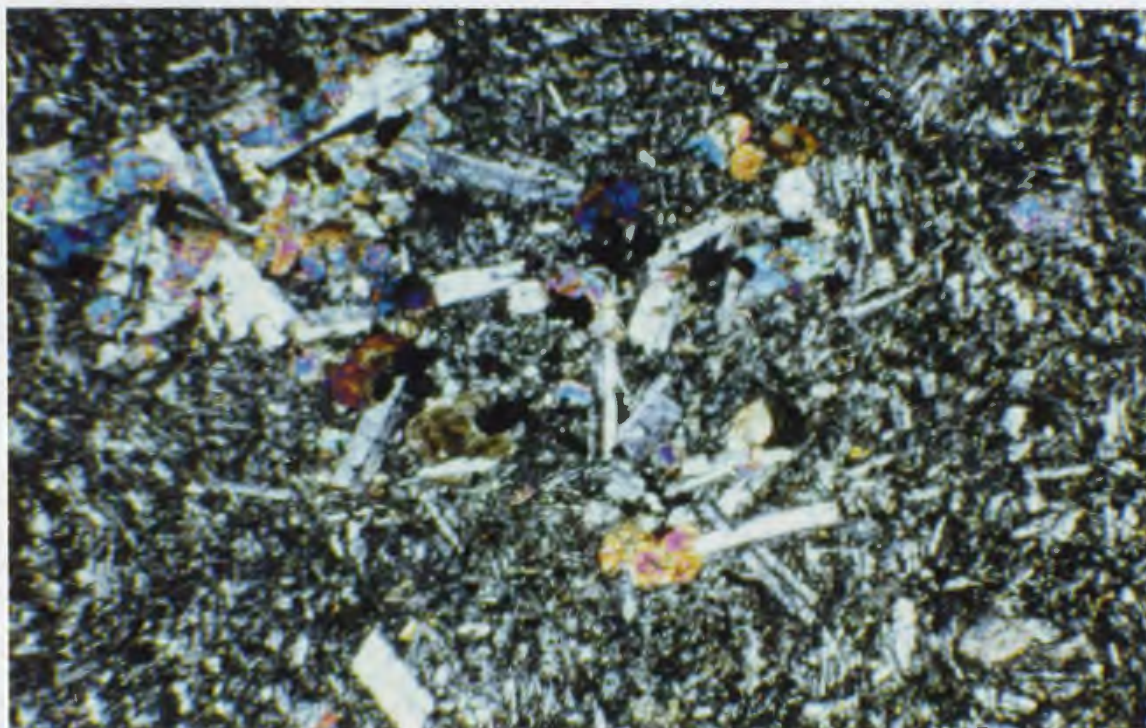


Plate 3.2. Glomeroporphyritic basalt with twinned plagioclase laths, clinopyroxene (medium birefringence) in a seriate groundmass (3-6-35A, 1x, XPL).

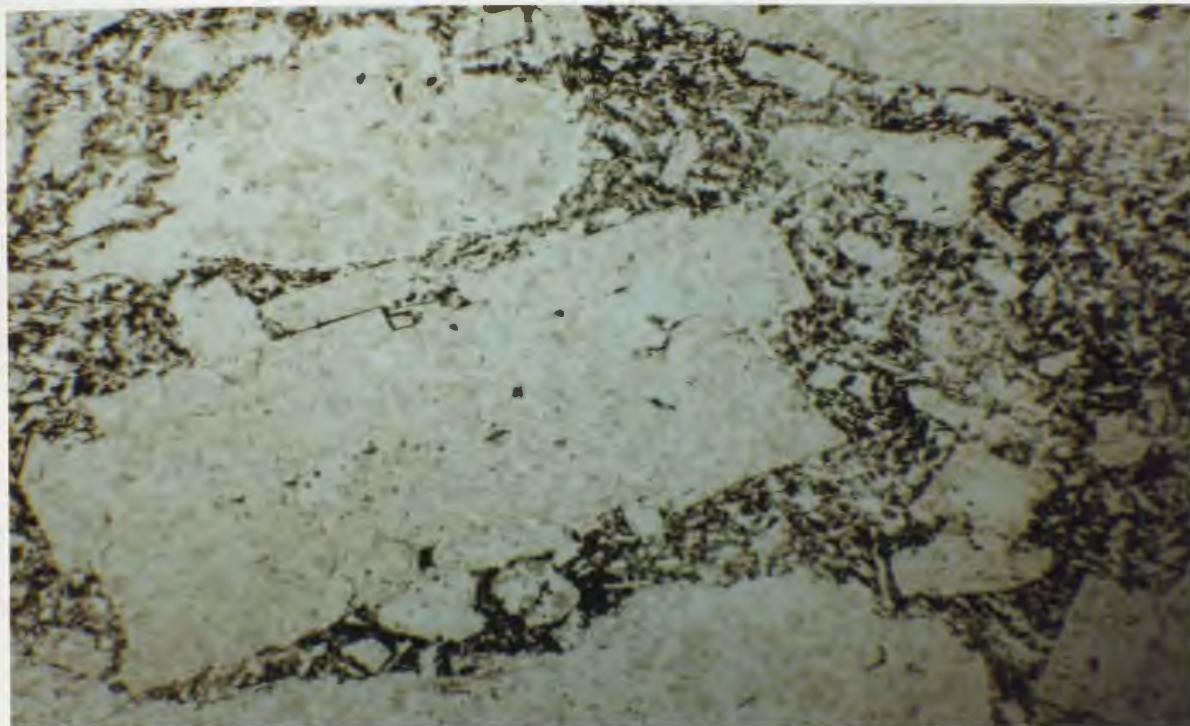


Plate 3.3a. Plagioclase-phyric cumulate basalt, plagioclase crystals exceed 1 cm in length. (DS-84-5, 1X, PPL)



Plate 3.3b. As above with crossed polars.

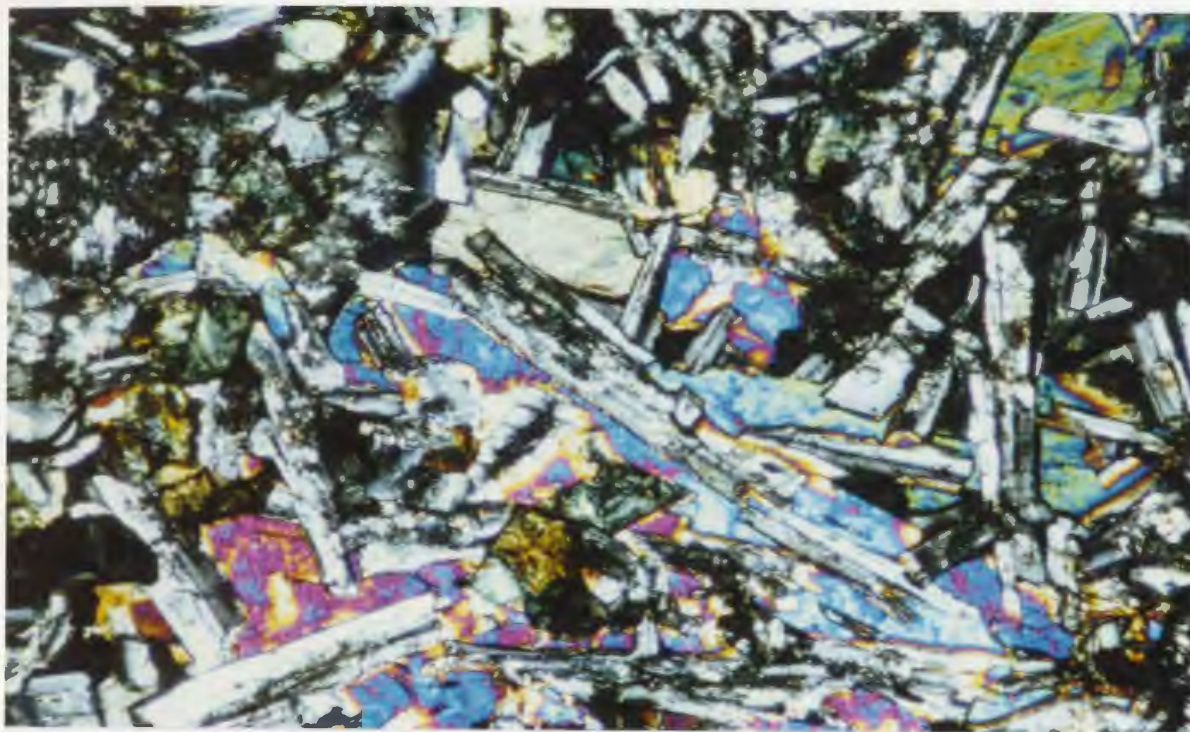


Plate 3.4 Ophitic basalt with plagioclase, clinopyroxene, and olivine in a brown interstitial glass.

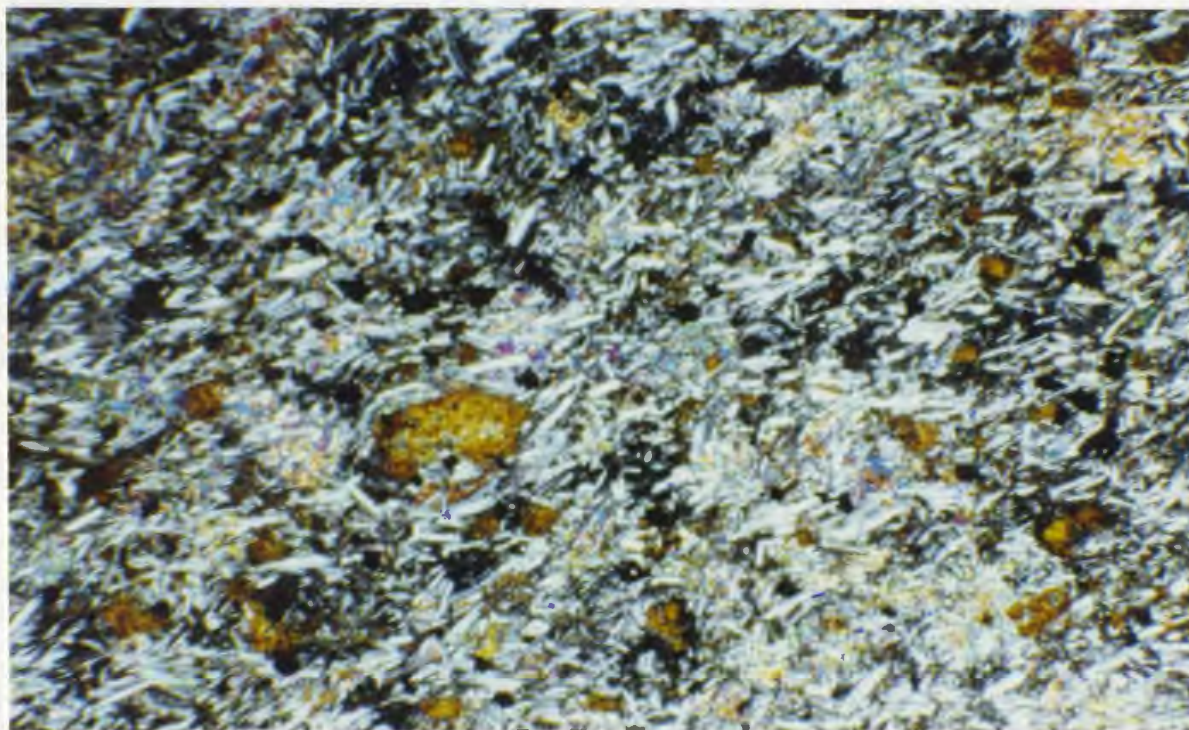


Plate 3.5. Subophitic texture with plagioclase, clinopyroxene in a felty groundmass (HS-71, 1x, XPL)

of flows (and their chemistry, see chapter 4) are typical of the sub-alkaline, calc-alkaline series summarized by Ewart (1982). Exception to this is notable only in a few flows found in the King's Point Road section on the north western margin of the caldera. There, the basalts are more mafic and may represent a late stage caldera fill event which tapped a deeper source within the evolved and devolatilized magma chamber.

The plagioclase phenocrysts are typically completely albitized and albite twinning is ubiquitous (Plate 3.6). Some samples were probed and the majority of feldspars probed are pure albite. A few zoned feldspars gave primary plagioclase compositions of $An_{(60-70)}$. The clinopyroxene phenocrysts appear relatively unaltered in thin section, with a pale grey-green color in plane light (Plate 3.7). There was little variation in the compositions of clinopyroxenes selected for probing, typical low-titanium augites. The olivine phenocrysts in the basalts are ubiquitously altered to one or more of the following secondary minerals as simple or complex intergrowths: iddingsite, chlorite and/or epidote (Plate 3.8).

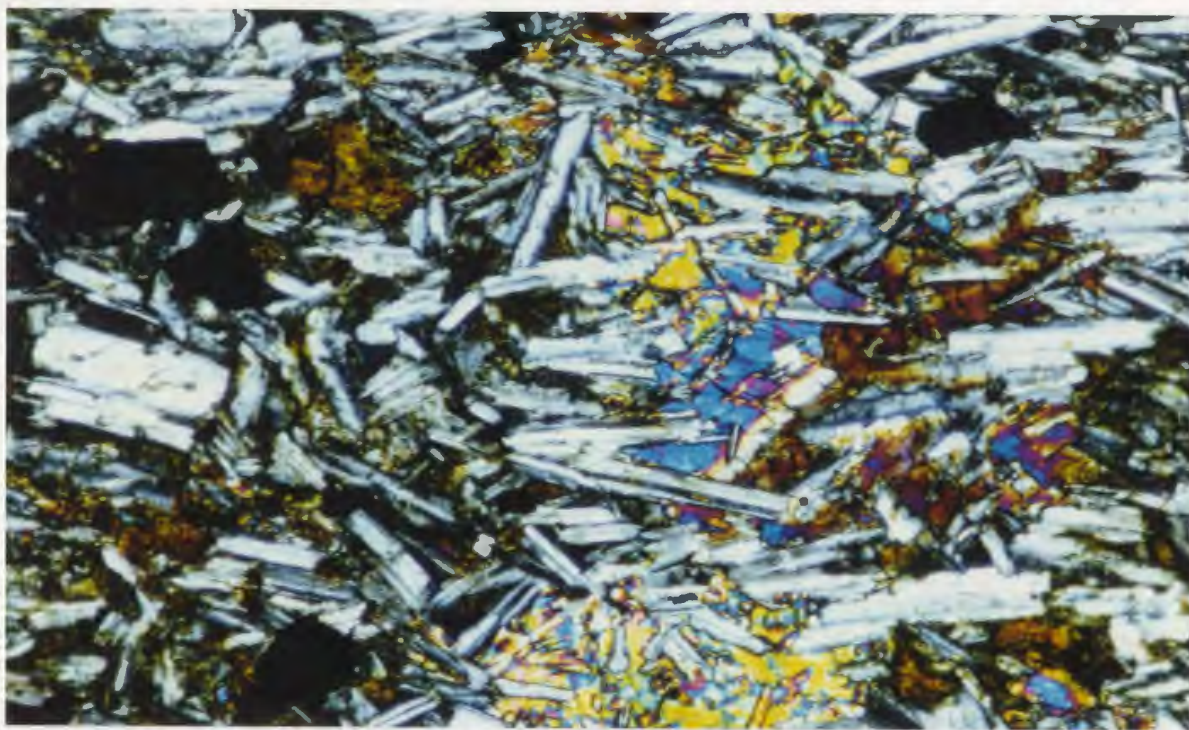


Plate 3.6. Same as sample above, shows albite twinning in the feldspars (4x, XPL).

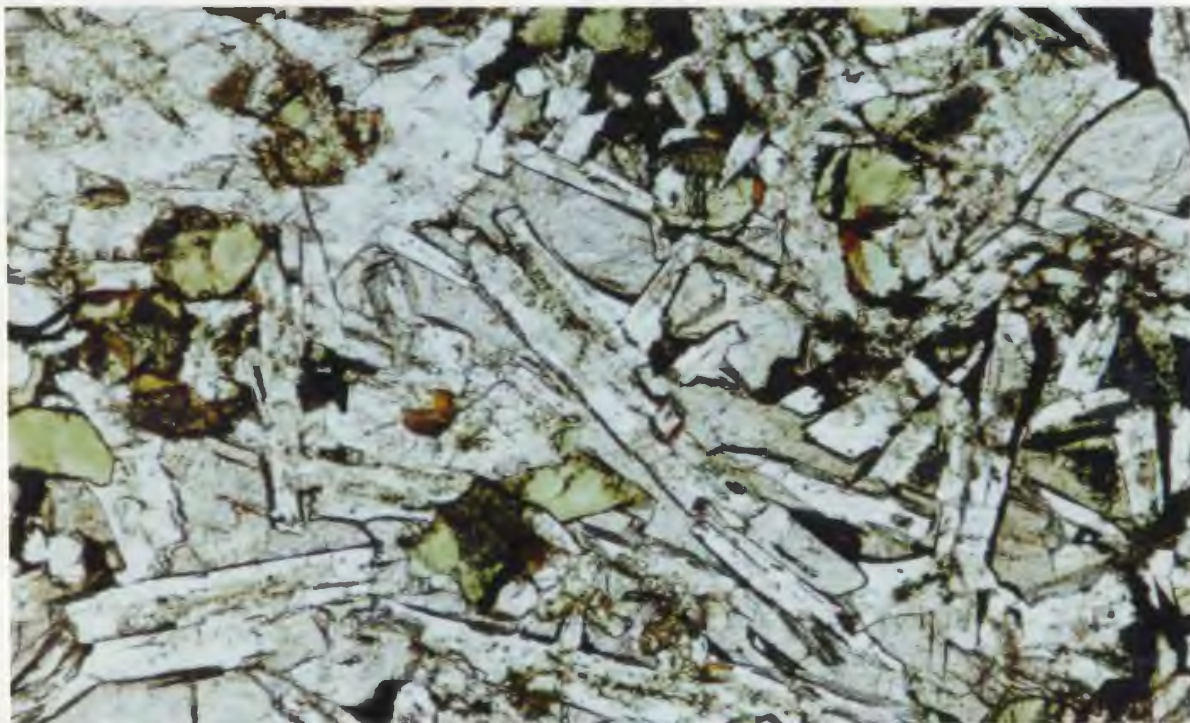


Plate 3.7. Porphyritic basalt showing pale grey clinopyroxene crystals (HS-109, 4x, PPL).

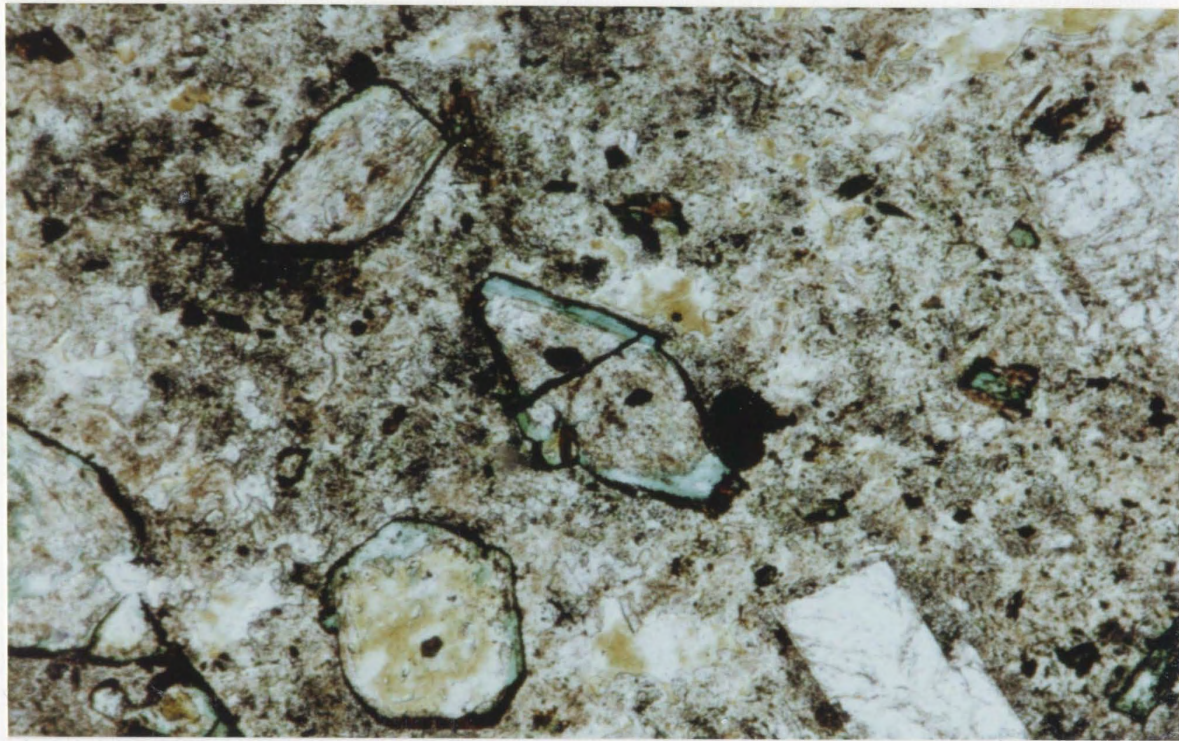


Plate 3.8. Olivine pseudomorphs rimmed with chlorite
(C4-68, 4x, PPL).

The secondary mineral phases seen in the basalts are numerous and varied in abundance. The basalts that are found along the eastern margin of the caldera are altered to the greatest intensity within the suite as a whole. However, the alteration is extremely variably even within a given flow. It appears that along the eastern margin the rocks have undergone at least one phase of hydrothermal alteration associated with the intrusion of both a buried granitic pluton and a higher level exposed granite in the northeast. This alteration is concentrated in both the phenocrysts and groundmass, and appears to superimpose a more highly acid-type, focused alteration (i.e. quartz-sericite-chl) (Plate 3.9 a,b) onto the more regional "volcanic" or syngenetic alteration that involved groundwaters and produced less acid alteration products (i.e. calcite, carbonates, oxides etc.). Many of the alteration types are noted in Appendix A. Veins of calcite, epidote and quartz are seen to be locally confined within basaltic flows and where such veining is found large vugs and amygdales of the same compositions are also found (Plate 3.10).

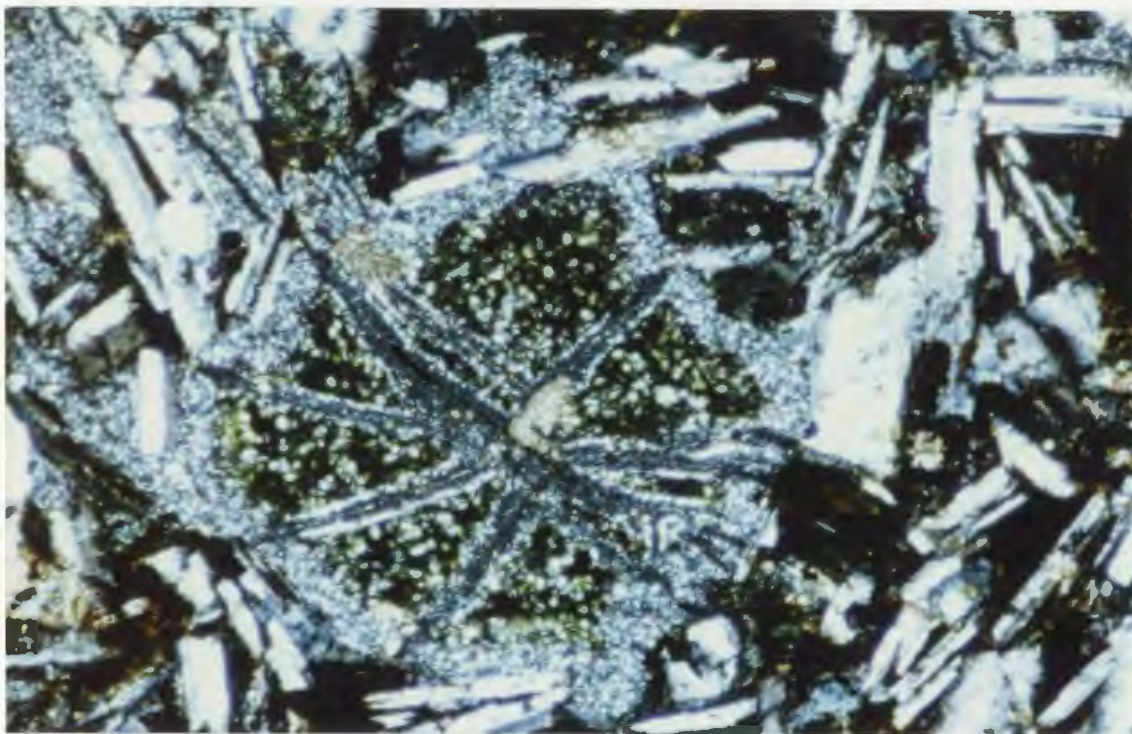


Plate 3.9a. Radial array of amygdale minerals with carbonate in the core and rim, and chlorite in the centre (3-6-11, 4x, PPL).

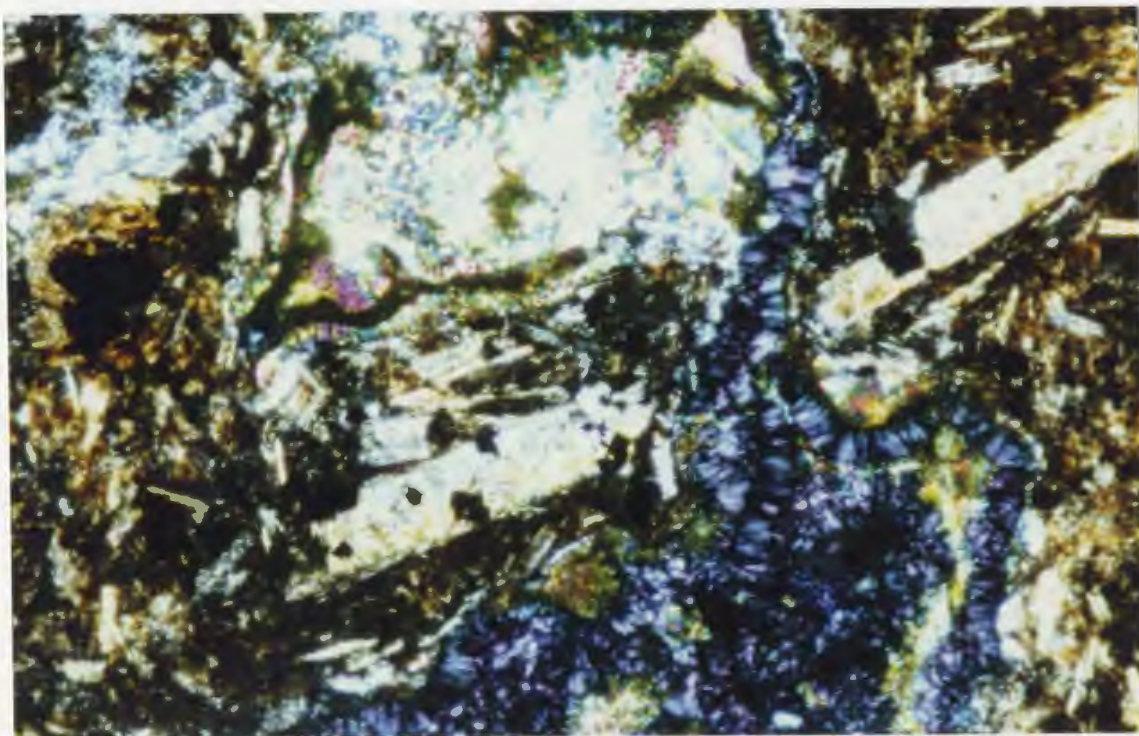


Plate 3.9b. Amygdale and groundmass showing diverse secondary mineral assemblage including chlorite, calcite and epidote (DS-86-10A, 4x, PPL)

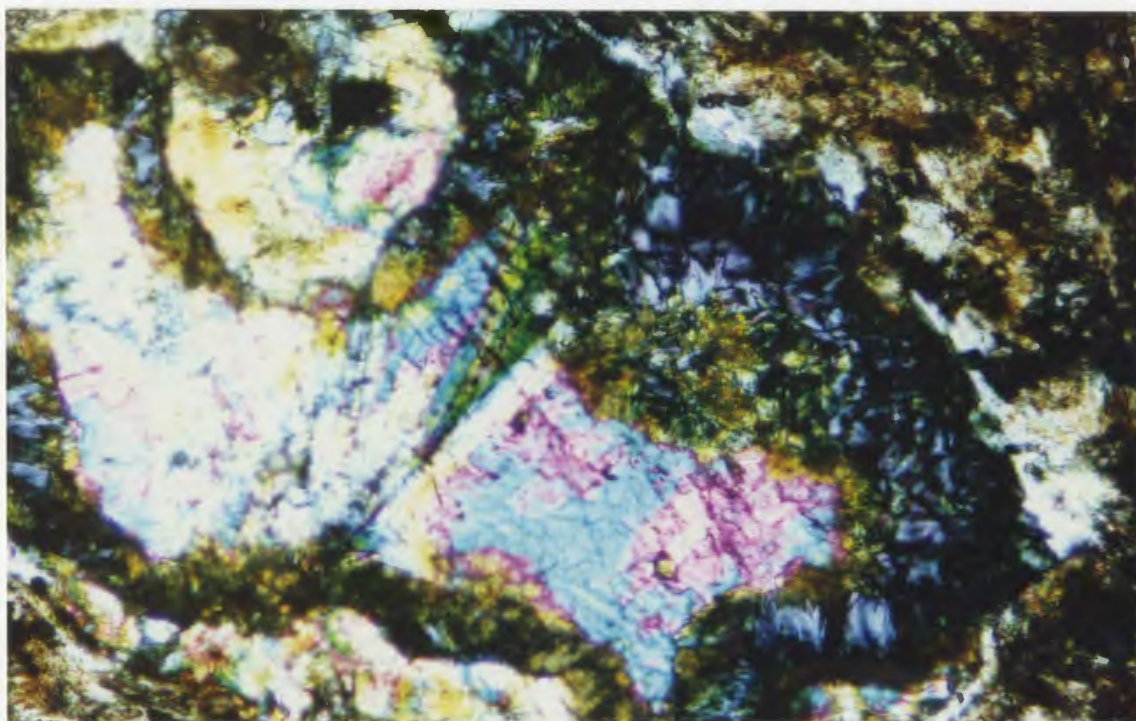


Plate 3.10. Example of amygdale with prenite, epidote and chlorite (DS-10A, 10x, XPL).

3.3 The Intermediate Flows

The intermediate flows of the Springdale caldera are typically massive, tabular flows with columnar jointing (Plate 3.11). They are thicker than discrete basaltic flows of the caldera and individual andesite flows can only be indentified by a very slight variation in granularity when stacked upon one another. The andesites are commonly associated with interbedded laharic flows and rubbly debris flows that are composed of material derived from an intermediate source in a silty or muddy matrix.

The intermediate flows are grouped into unit 3 on maps 1a-c, they are found along the eastern margin of the caldera intermittently for at least 60 kilometers. One source for these flows was a stratovolcano which is found on the southeastern edge of the Springdale sheet (see Fig. 2.7b and Map 4). The andesites dip away from this volcanic centre which is plugged by a diorite stock and intruded by a plexus of radial dykes and sills which are beautifully displayed by the aeromagnetic survey (Fig. 2.7). It appears that this stratovolcano is only partially preserved within the topographic margin. On the southwestern margin of the Springdale caldera in one of the large megga-breccia blocks a mass of andesitic material is also seen and may indeed be another source area for intermediate flows that are sporadically seen in the southwestern part of the caldera.



Plate 3.11. Surface of intermediate lava flow (andesite). Displays good polygonal cross-sections of columnar joints in the flow.

The andesites are pale brownish-purple and are porphyritic or glomeroporphyric. The textures vary very little, but some of the more aphanitic flows have a trachytic texture.

The andesites have phenocrysts of feldspar, clinopyroxene, pseudomorphs of olivine, +/- amphibole and opaques. The crystallization sequence cannot be determined with certainty for these rocks. The phenocrysts are randomly distributed. However, as with the mafic flows, plagioclase is the dominant phase and probably precipitated first (Plate 3.12). The feldspars range from equant blocky or stubby prisms to elongate blades and are typically altered and can be complexly zoned or embayed. Clinopyroxene phenocrysts are typically a pale grey-green with high relief and show good examples of polysynthetic twinning. Olivine phenocrystic and microphenocrystic pseudomorphs have been replaced by serpentine/iddingsite, chlorite and clots of opaques (probably magnetites.). Amphibole phenocrysts are less abundant than the other mafic phenocrysts but when seen have typically been replaced by chlorite. The phenocrysts are set in a fine hyalopilitic groundmass with little evidence of groundmass crystals or may less typically have either a pilotaxitic to trachytic texture. The groundmass is typically oxidized and may have patchy areas of carbonate or chlorite.

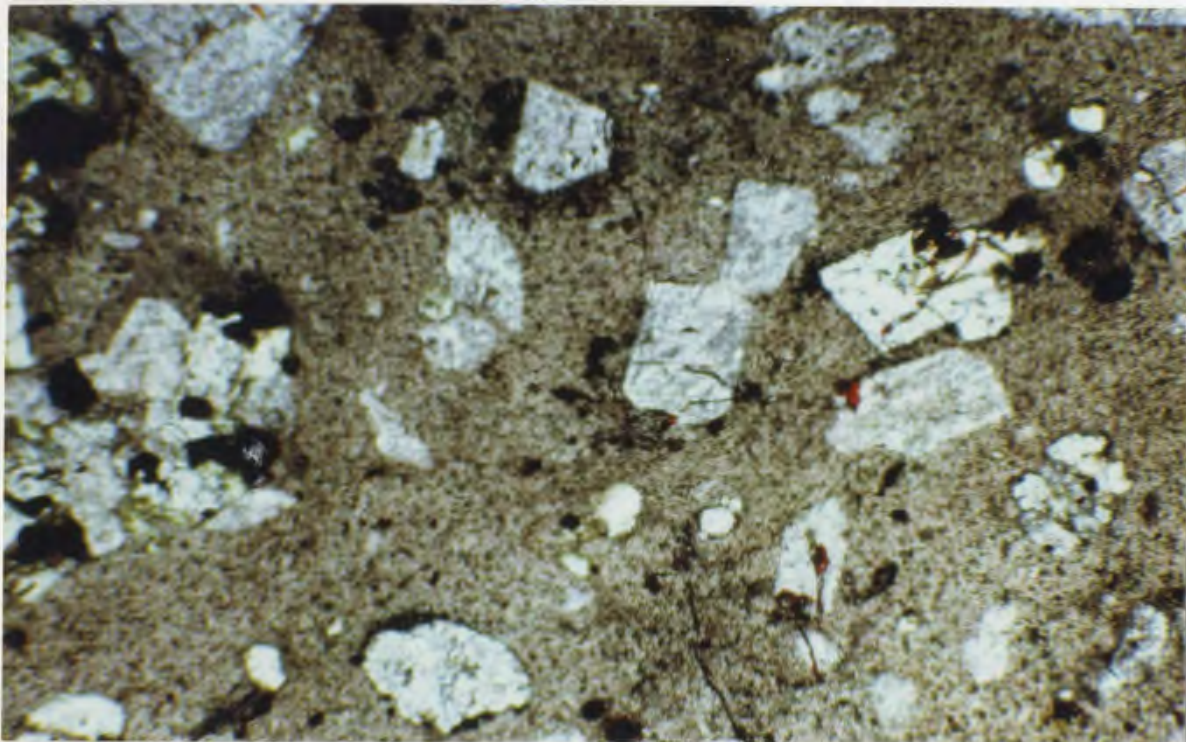


Plate 3.12. Typical andesite with porphyritic texture. Sample C4-19 shows blocky altered feldspars with higher relief grey amphibole and smaller pseudomorphs of olivine (brighter, with dark rims) seen in upper right and lower left corners. (C4 - 19, 4x, PPL)

3.4 Pyroclastic (Ash-flow) Tuffs

The pyroclastic rocks of the Springdale caldera are by far the most diverse and variable assemblage of rocks in the suite. They not only comprise six separate units (1,4,6,7,8,10) but the variation "within" each unit is considerable. Ash-flow tuffs are an admixture of crystal, vitric, and lithic debris in an ashy matrix. The proportions of these constituents varies not only laterally but vertically as well. The degree of welding in a given unit imparts dramatic textural differences in rocks of very similar bulk composition. Crystal fragments, shards and accidental material are typically entrained into parts of the flow whereas equivalent "pristine" facies of the same unit may not contain such debris. As ash-flows are subject to the dynamics of physical as well as chemical variation (i.e. proximal to distal facies of a given unit, and chemical zonation in a given tuff), a spectacular range of variability is found.

The pyroclastic rocks are also devitrified (no examples of glass were recovered during this thesis study) and the devitrification also imparts a superimposed texture to some of the pyroclastics. Excellent examples of devitrification spherules and axiolites are seen in thin section. One hundred and five pyroclastic rocks were sectioned and therefore the petrographic features will be grouped according to dominant textural differences seen

throughout the range of pyroclastic rocks as well as any special, or interesting features. The tuffs all contain broken crystals of feldspar, (+/- quartz). The feldspars are probably sanidines, but most are altered to some degree. Also it appears that some xenocrysts including feldspars may have been entrained into parts of the tuffs, therefore it is difficult to determine "true" mineralogical associations. The quartz and feldspars are commonly embayed and may have melt inclusions. In tuffaceous rocks the pumice can preserve the original phenocrysts which crystallized in the magma chamber whereas groundmass crystals and fragments may have accidental origins. Thus in order to define the various ash-flow tuff units of the caldera emphasis was placed on the pumice where possible.

Unit 1 is the only tuff in the caldera which appears to have magmatic mica (biotite), shown in Plate 3.13. The biotite is partially replaced by chlorite and has abundant inclusions. Unit 1 also preserves good examples of unwelded zones, as well as a wide variety of lithic fragments including some which made up the roof rocks to the magma chamber prior to eruption (Plate 3.14). Excellent examples of perlitic fractures are also seen in the groundmass and within fragments of this tuff (Plate 3.15).

Unit 4 has a high proportion of mafic and intermediate lithic fragments and contains some phenocrysts (xenocrysts ?) of clinopyroxene. It has feldspar phenocrysts which are heavily altered and resorbed or

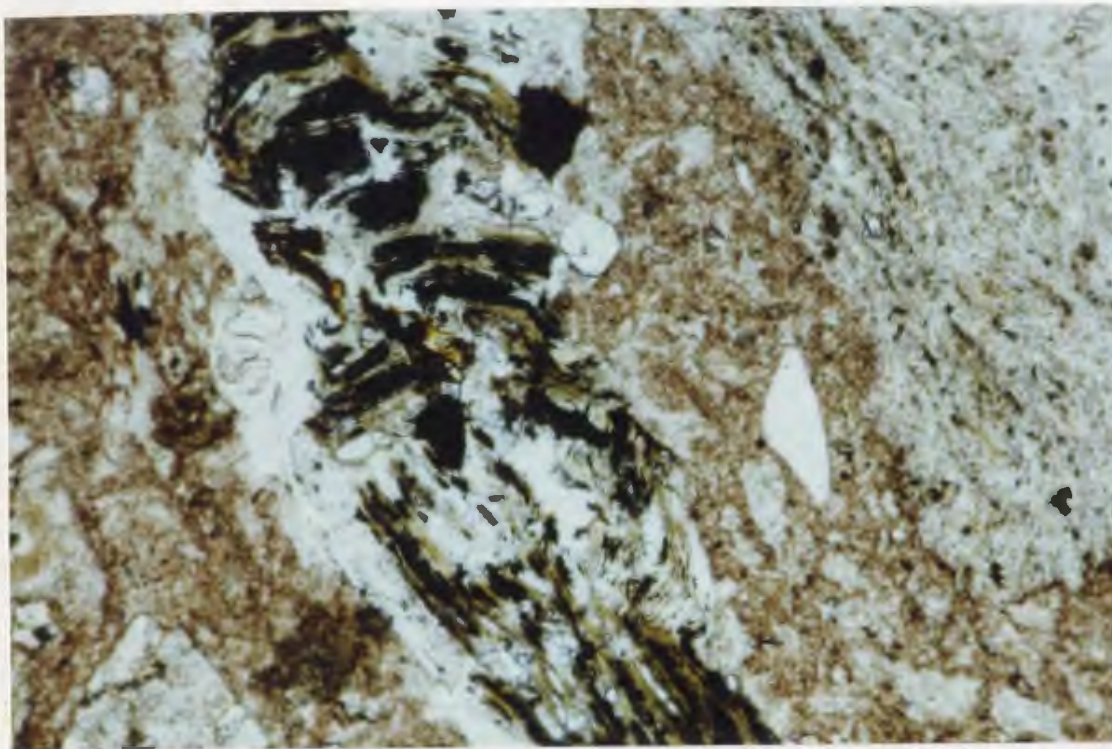


Plate 3.13. Magmatic biotite in unwelded portion of Unit 1
(C4-288, 4x, PPL)

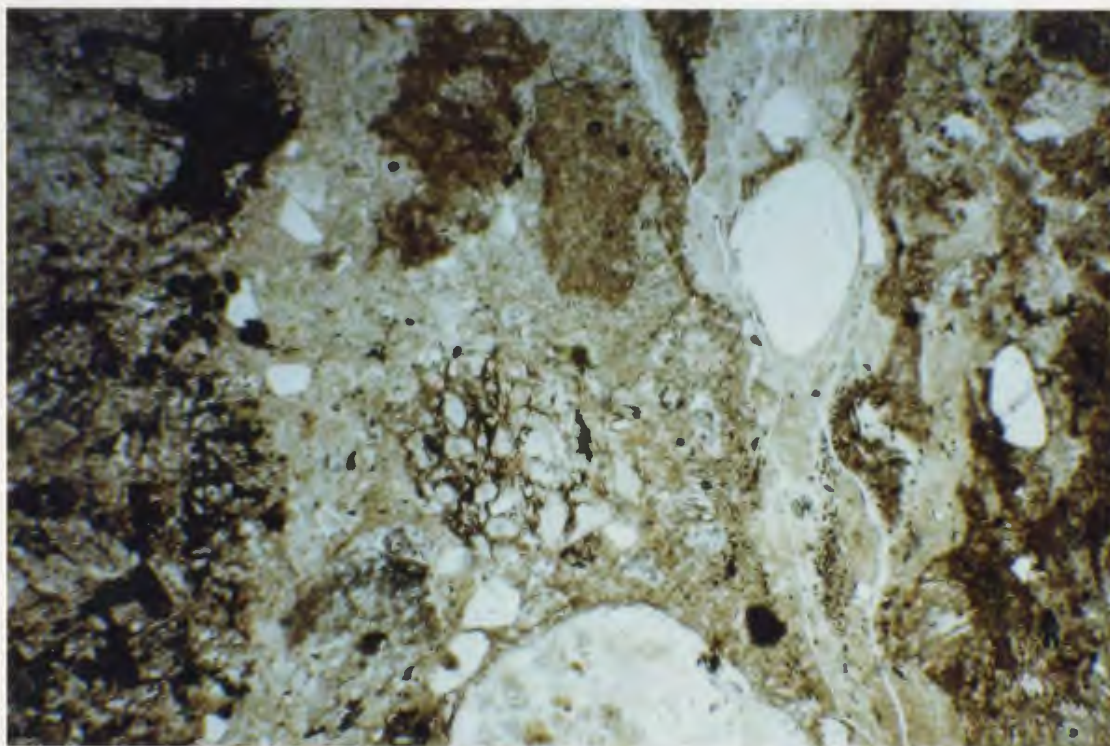


Plate 3.14. Banded, unwelded crystal lithic tuff of Unit 1
(C4 - 285, 1x, PPL).

embayed but does not contain quartz phenocrysts. The tuff has a chloritic alteration of the groundmass and therefore may contain fragments or microlites of mafic phases such as amphibole or clinopyroxene which have altered to chlorite (Plate 3.16). This unit has concentrations of large pumice bombs as described in chapter 2. It is a crystal, lithic, vitric tuff and these elements can be seen in plate 3.16.

Unit 6 is an extensive ash-flow tuff with a great array of features. It has a variety of lithic clasts ranging in composition from basalt through rhyolite and therefore appears to have sampled the surface of the caldera as it was being emplaced (Plates 3.17 and 3.18). It has both plagioclase feldspar and altered K-feldspar along with quartz phenocrysts. Welding is variable in this unit and even on a microscopic scale welding "density" varies around the lithic fragments and juvenile pumice fragments (Plate 3.19)

Unit 7 consists of rhyodacitic crystal-vitric tuffs that tend to be massive in outcrop and have a pale brownish-purple vitreous luster. There is at least one dome/vent complex associated with this unit found on West Brook and described in chapter 2. The tuffs are plagioclase phyric with rare quartz phenocrysts. In thin section the tuffs are fine and glassy with nicely preserved "inflated", as well as, flattened pumice. Lithic fragments although present are not abundant and dominantly felsic (Plate 3.20). Overlying the dome on West Brook a

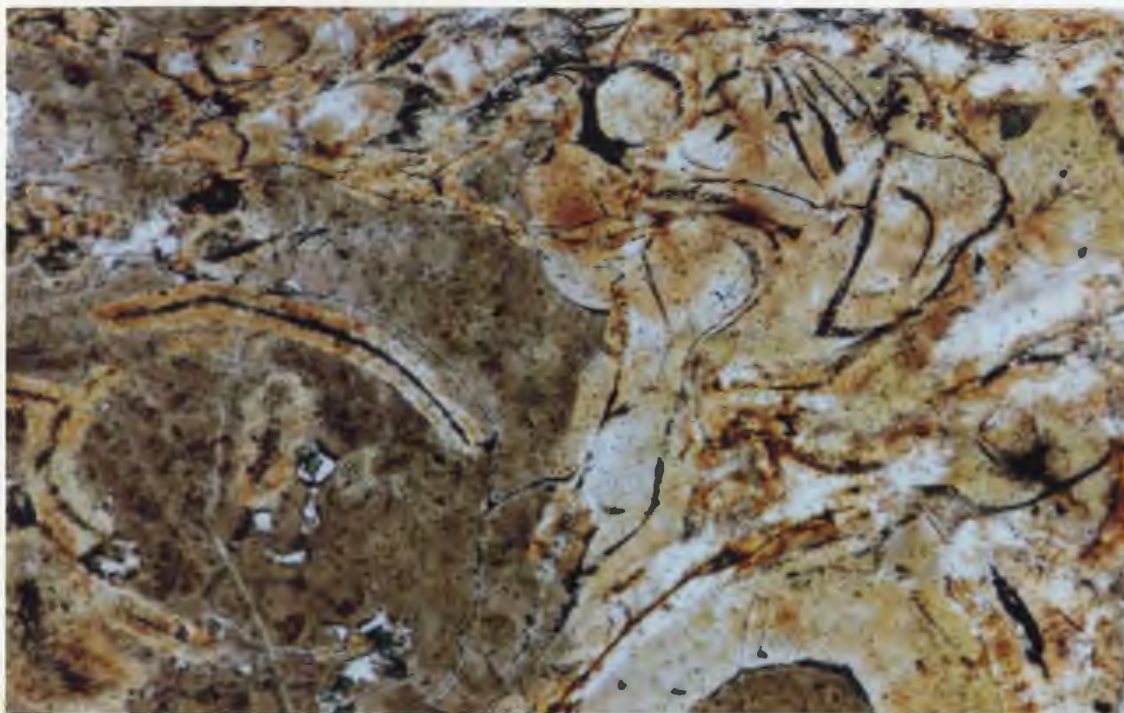


Plate 3.15. Example of perlitic fractures in the groundmass and devitrified clasts within Unit 1 (C4-285, 4x, PPL)

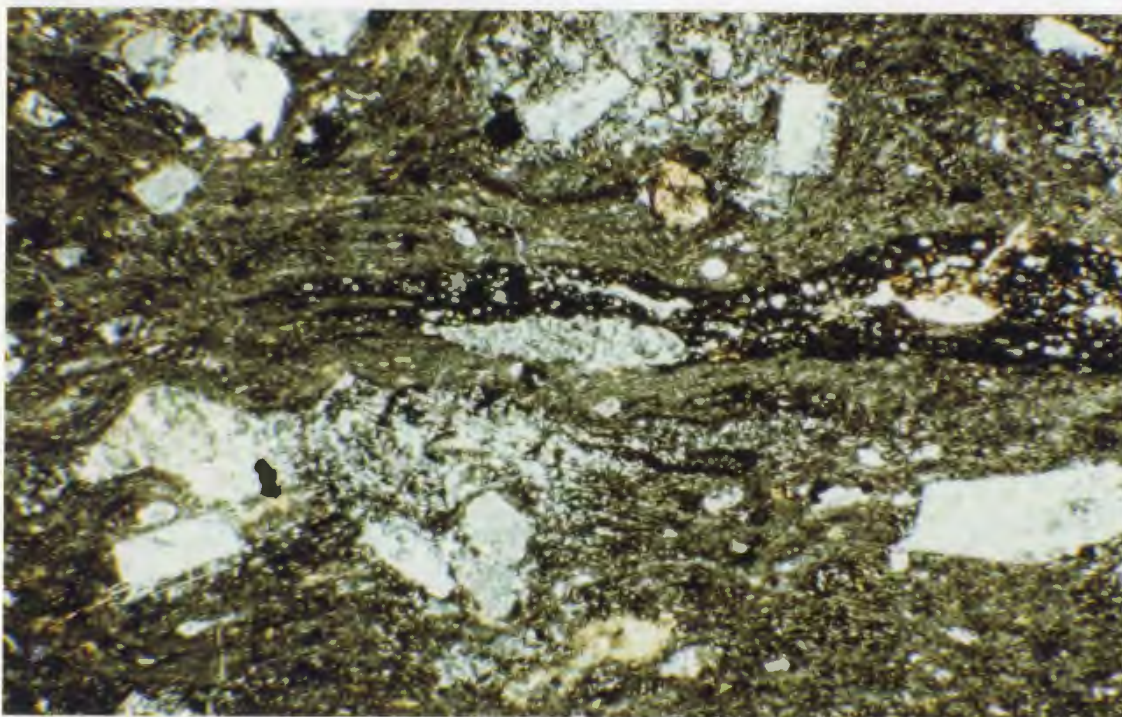


Plate 3.16. Crystal-lithic-vitic tuff from Unit 4 with well preserved fiamme in centre of the photograph in a chloritic groundmass (C4-186, 1x. XPL).

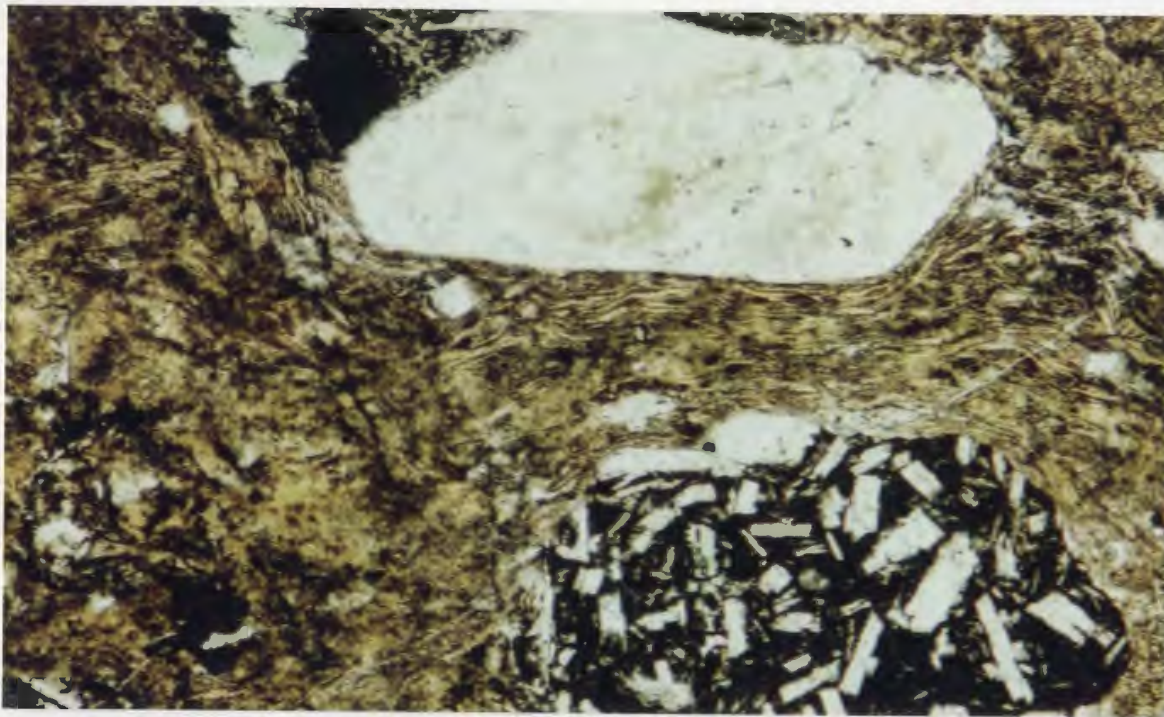


Plate 3.17. Welded crystal-lithic tuff from unit 6 showing basaltic fragment and feldspar crystal; welding is intensified around clasts (C4-97, 4x, PPL).

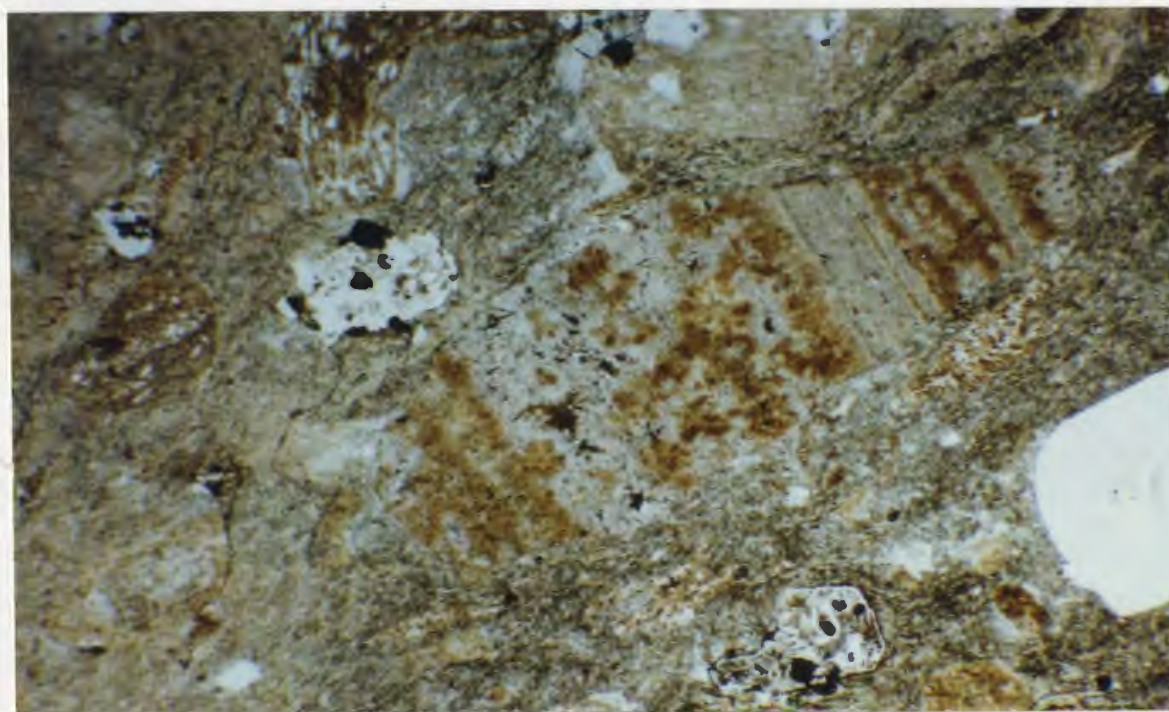


Plate 3.18. Example of moderately welded portion of Unit 6 with silicic lithic fragment in the centre of the photograph. Note devitrification in the lithic clast (C4-90, 1x, PPL).

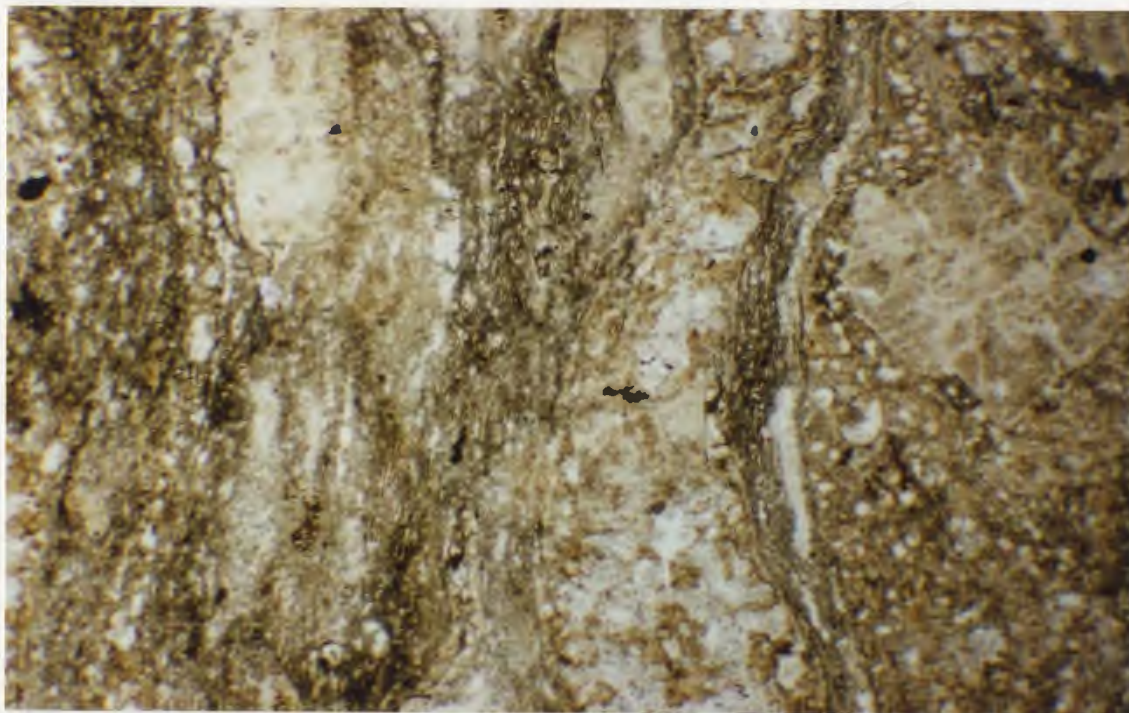


Plate 3.19. Variation in welding across a microscopic field from Unit 6 (C4-207, 1x, PPL).

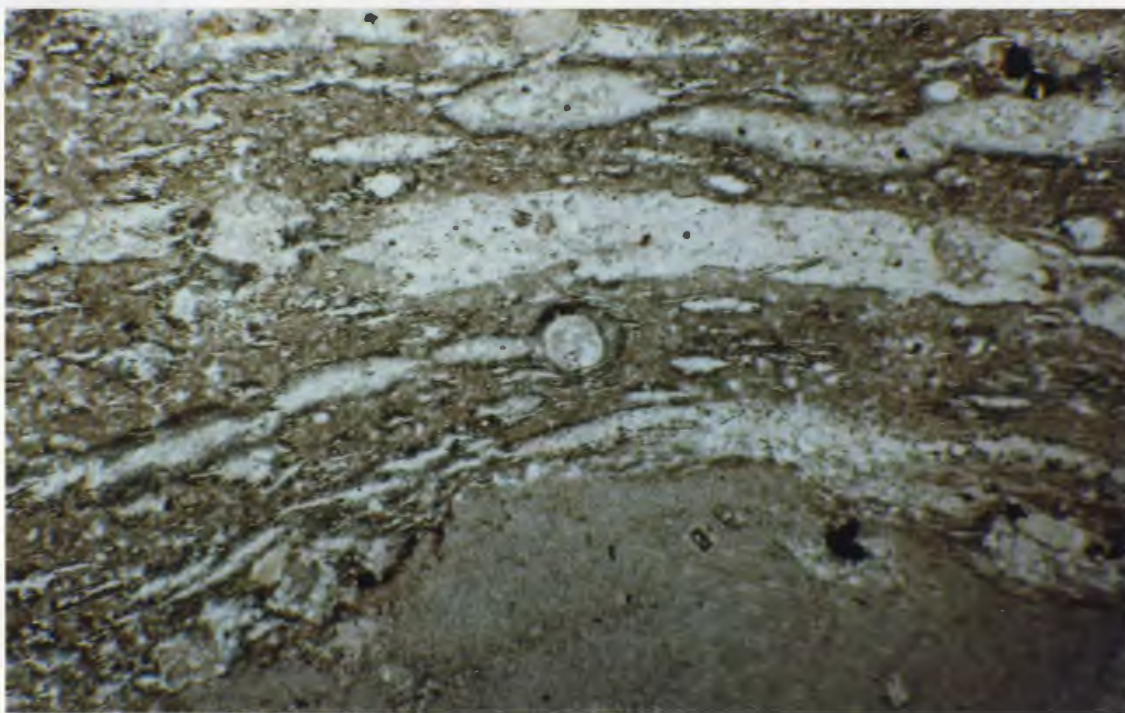


Plate 3.20. Unwelded vitric tuff from Unit 7 with well preserved pumice (white) in a fine-grained groundmass (grey). Felsic lithic clast seen at bottom of the photograph (C4-230, 1x, PPL).

coarse "autoclastic" breccia is seen. This breccia contains angular blocks of flow banded material. The flow banding is actually folded and can be seen as variation in color on weathered surfaces. These bands in thin section appear to be alternating glassy groundmass and pumice. Therefore the pumice was being incorporated into a glassy or ashy flow being deposited at the surface of the dome. Plate 3.21 displays this relationship, but as can be seen in the thin section, no obvious glassy shards are seen in the groundmass between the darker, porphyritic pumice.

Unit 8 is a complex rhyolitic ash-flow tuff and contains areas of magma-mixing. It has altered feldspars and quartz phenocrysts. Unit 8 is distributed around the Burnt Berry Dome and may have been associated with the late-stage emplacement of it. It is a fine crystal-vitric tuff with scarce lithic debris and small black fiamme (Plate 3.22). The coarser parts of this unit have millimeter sized bands of mafic material or "dykelets". They appear to brecciate the felsic matrix. However, clots of the mafic melt are also seen disaggregated in the felsic material (Plate 3.23). In these instances mafic xenocrysts are also abundant and disequilibrium textures can be seen in the feldspars (Plate 3.24).

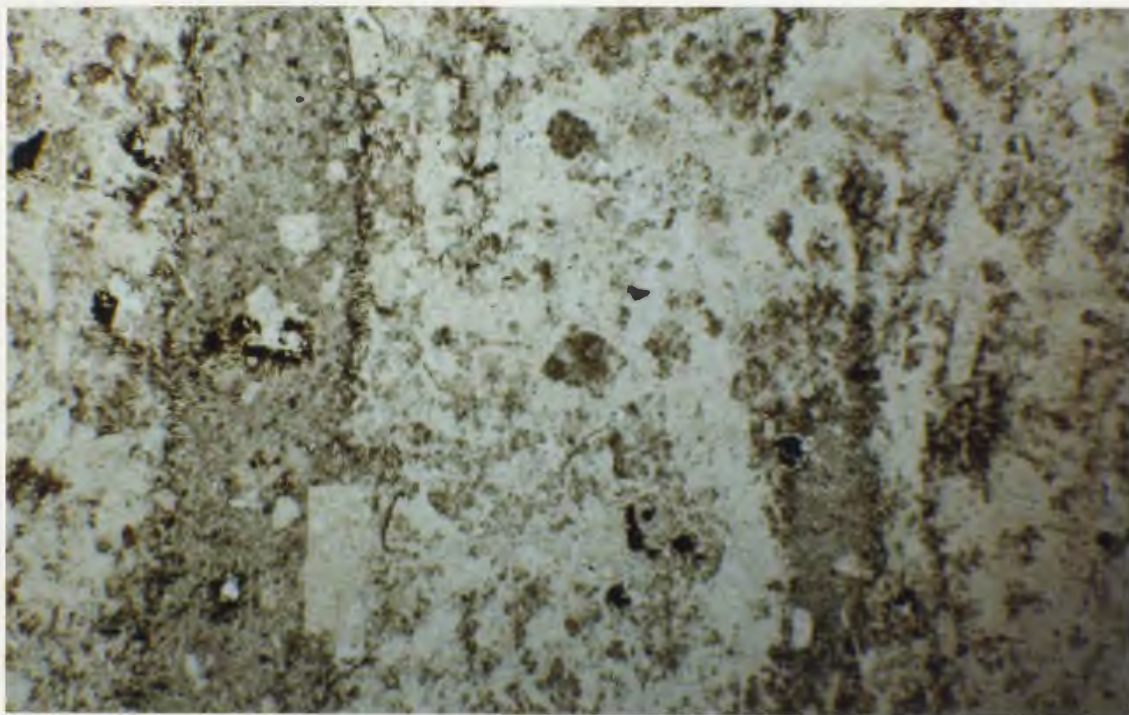


Plate 3.21. Alternating flow bands of glassy groundmass (white) and pumice (grey) which have concentrations of phenocrysts. Sample from Unit 7 dome apron/breccia (C4-233D, 1x, PPL).

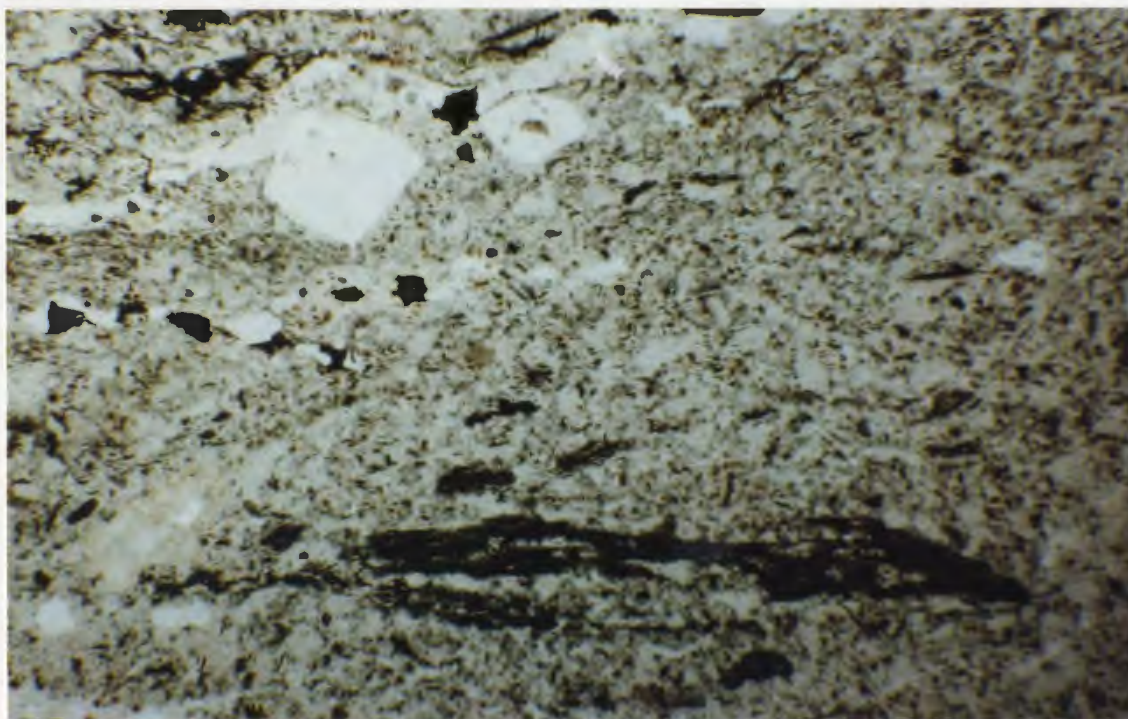


Plate 3.22. Fine crystal-vitric tuff from Unit 8 with small black fiamme (C4-301, 1x, PPL).

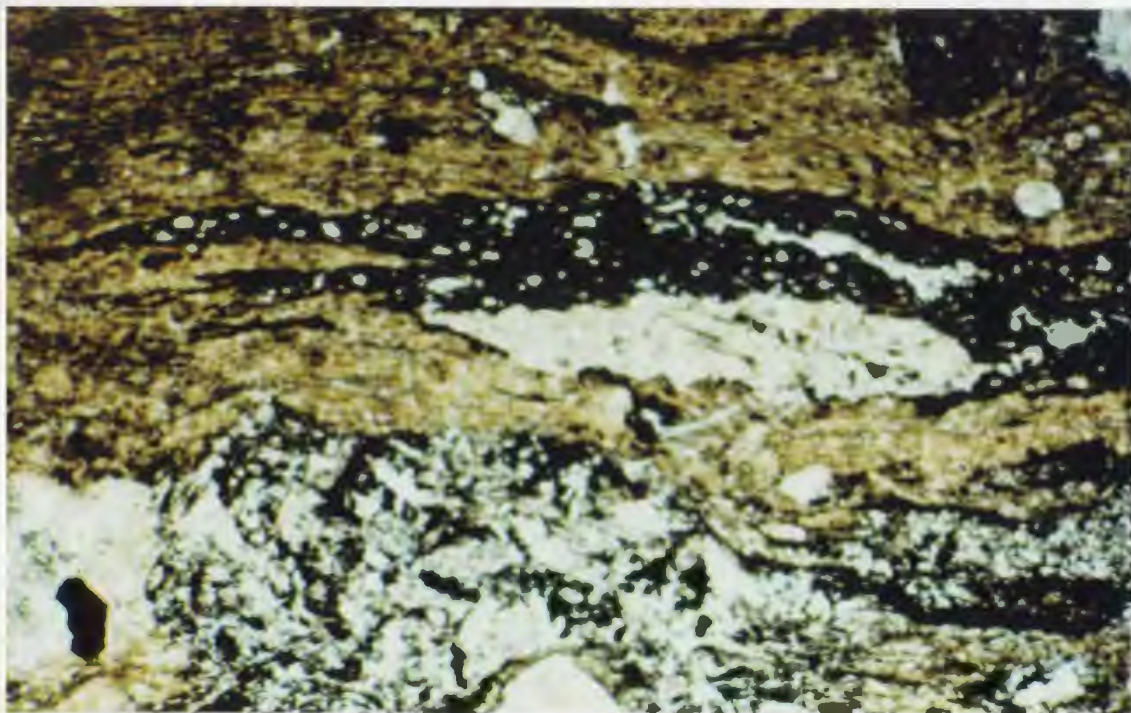


Plate 3.23. Black glassy pumice disaggregated in a felsic ashy groundmass (C4-298, 4x, PPL).

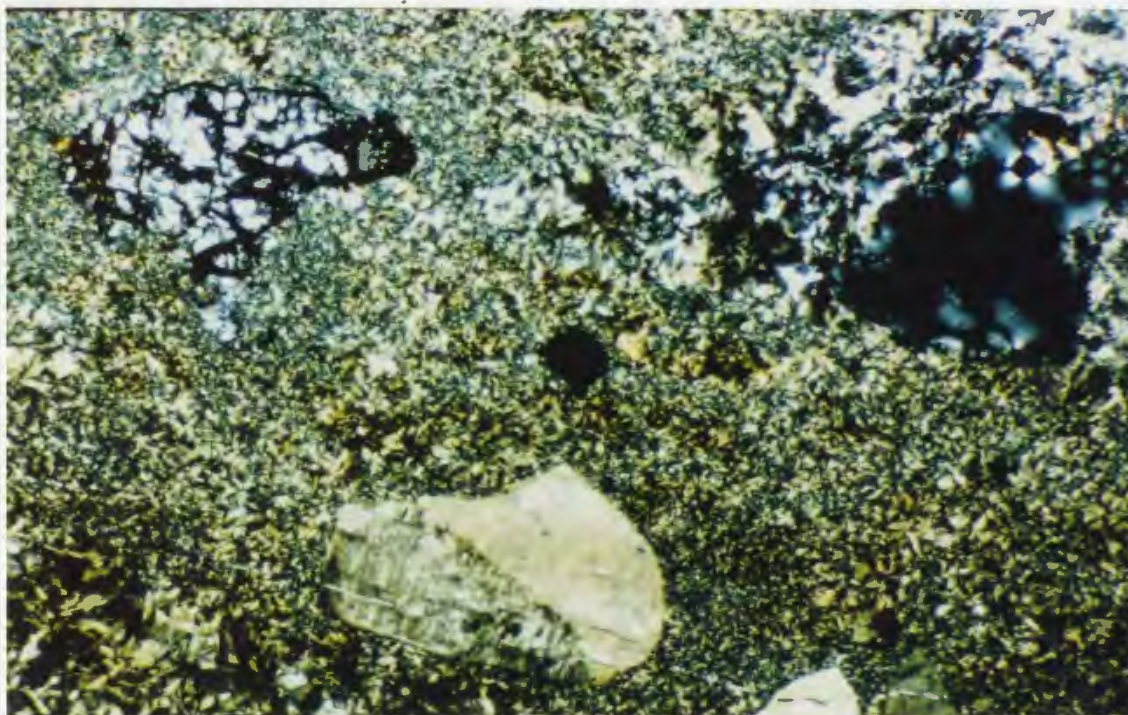


Plate 3.24. Disequilibrium feldspar in the groundmass of a mixed tuff within Unit 8. An olivine xenocryst is also seen in the upper left corner (C4-296, 10x, PPL).

Unit 8 also contains a few outcrops of rhyolitic material which is wholly composed of vitric clasts which are individually devitrified (Plate 3.25). The shards are angular with beautiful axiolitic and spherulitic devitrification textures. Some of the vitric clasts are fibrous and may represent some juvenile material (pumice) that is related to a small ashy deposit around the dome (Plate 3.26). Such features are characteristic of dome carapaces and are similarly interpreted as being compositionally similar.

Unit 10 is a crystal rich ash-flow tuff which is an outflow from the King's Point caldera. It is interbedded with the Springdale caldera's late-stage sedimentary fill and basalt flows. It covers all of the Springdale caldera volcanic and domal rocks. Unit 10 is massive and contains xenoliths of serpentinite and jasper. In thin section the tuff displays a beautiful eutaxitic texture with abundant phenocrysts of quartz and feldspar. Most of the phenocrysts are embayed and have melt inclusions (Plate 3.27 and 3.28).

3.5 Dacitic Domes

Chapter 2 describes the occurrences and types of dacite domes found within the Springdale Caldera. The dome rocks are typically hyalopilitic to pilotaxitic with rare microphenocrysts. Very little variation is seen in this suite, except for slightly different alteration products

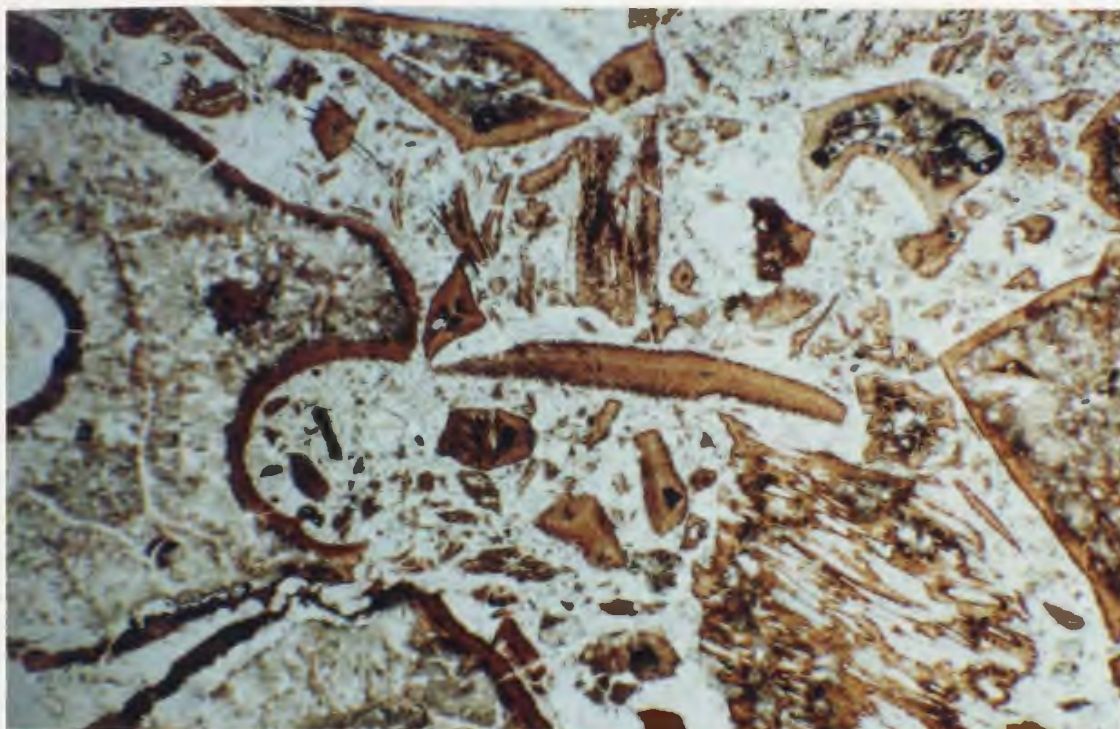


Plate 3.25. Vitric shards with axiolitic and spherulitic devitrification suspended in a glassy rhyolitic matrix. Represents a dome carapace (EL-304b, 1x, PPL).

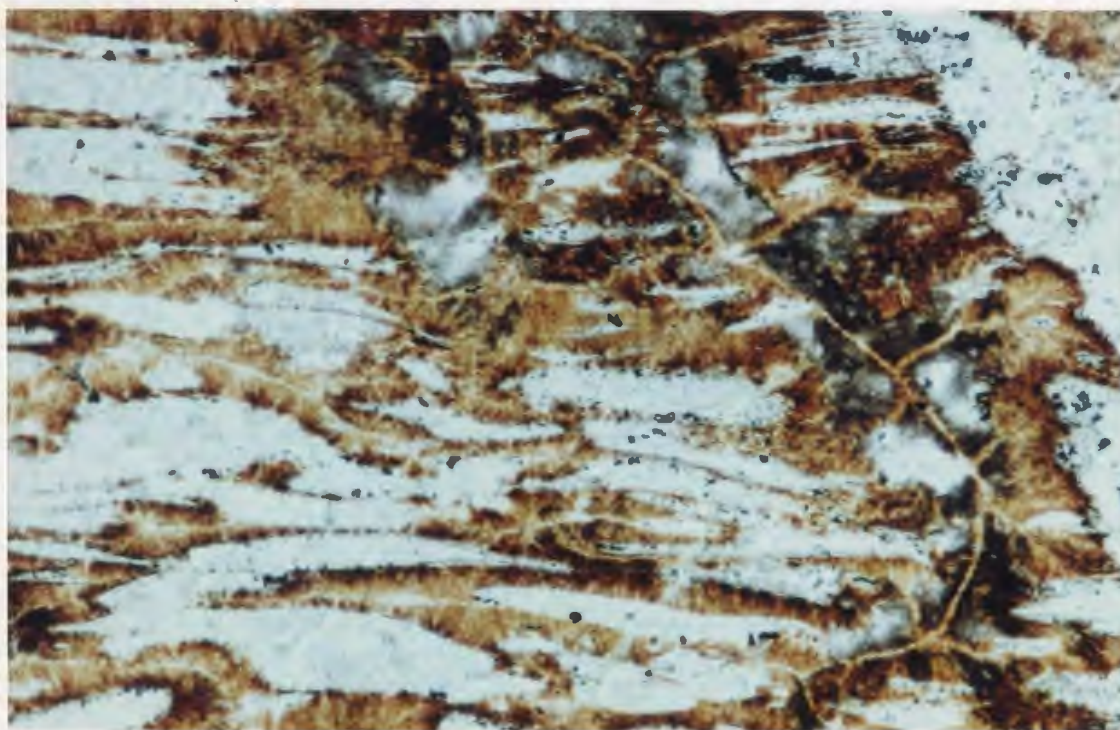


Plate 3.26. Pumice from dome carapace (EL-304b, 10x, PPL).

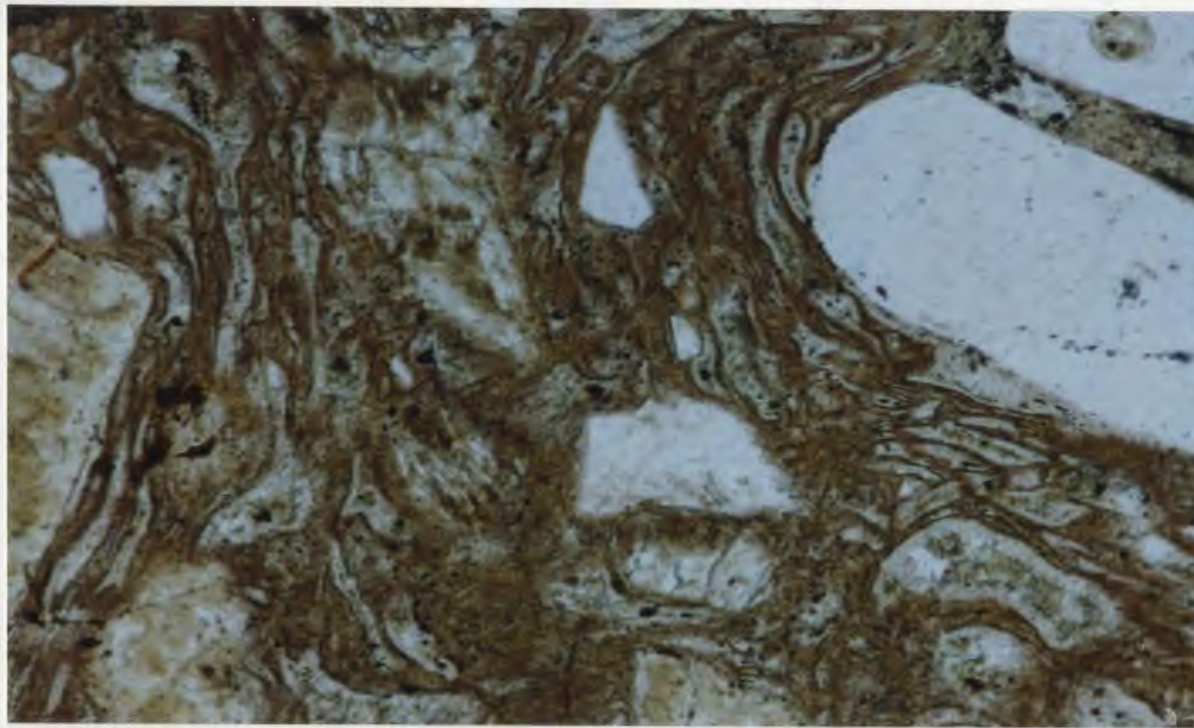


Plate 3.27. Unit 10, excellent example of eutaxitic texture in crystal-rich tuff. Note embayed quartz crystals with melt inclusions (C4-241, 4x, PPL).

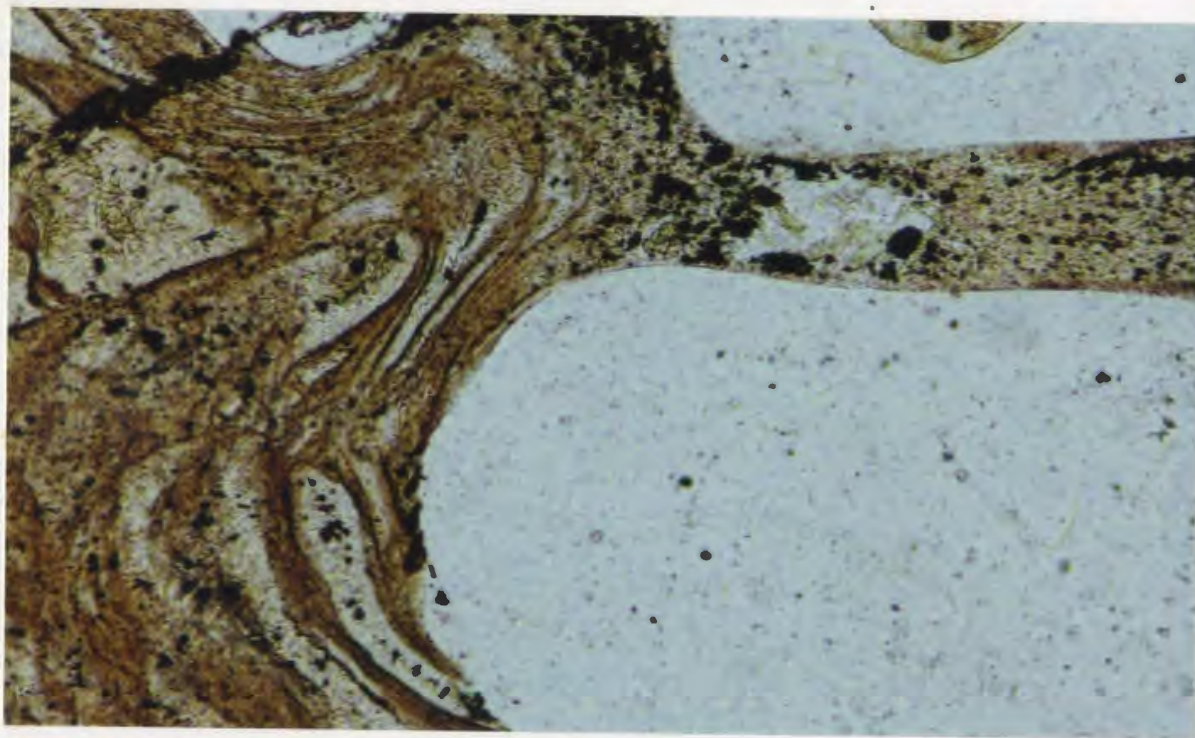


Plate 3.28. Same as photograph above with detail of the welded bubble-wall shards around the edge of the quartz phenocryst (C4-241, 10x, PPL).

which are related more to the regional propylitic alteration than to inherent magmatic differences in the domes. Plate 3.29 shows a typical example of the glassy nature of the domes with flow-aligned microlites and domains of oxidation. The microphenocrysts are typically altered feldspars lathes, and concentrations of oxides in the groundmass cluster around the phenocrysts (Plate 3.30). Examples of autobrecciation in the groundmass is typical along the margins of the domes as well as locally within the body of it. The groundmass is more pervasively altered around the autoclats as these areas become more permeable after fracturing (Plate 3.31).

3.6 High-Silica Rhyolitic Domes, Dykes and Sills

The Springdale caldera hosts at least one high-silica rhyolite dome called the Burnt Berry Dome. A second is found at the southern margin of the caldera (Misery Hill), but it has an extensive apron which covers most of the glassy domal material. The Burnt Berry Dome is a pink, curvilinear jointed mass with sheeting and variations in volatile content evidenced by alternating dense glassy bands and more granular zones of lithophysae dykes and miarolitic cavities. In thin section it is very fine-grained with microlites defining flow-banding orientations. The flow banding can be laminar or highly convolute (Plate 3.32). The glass is devitrified and patchy

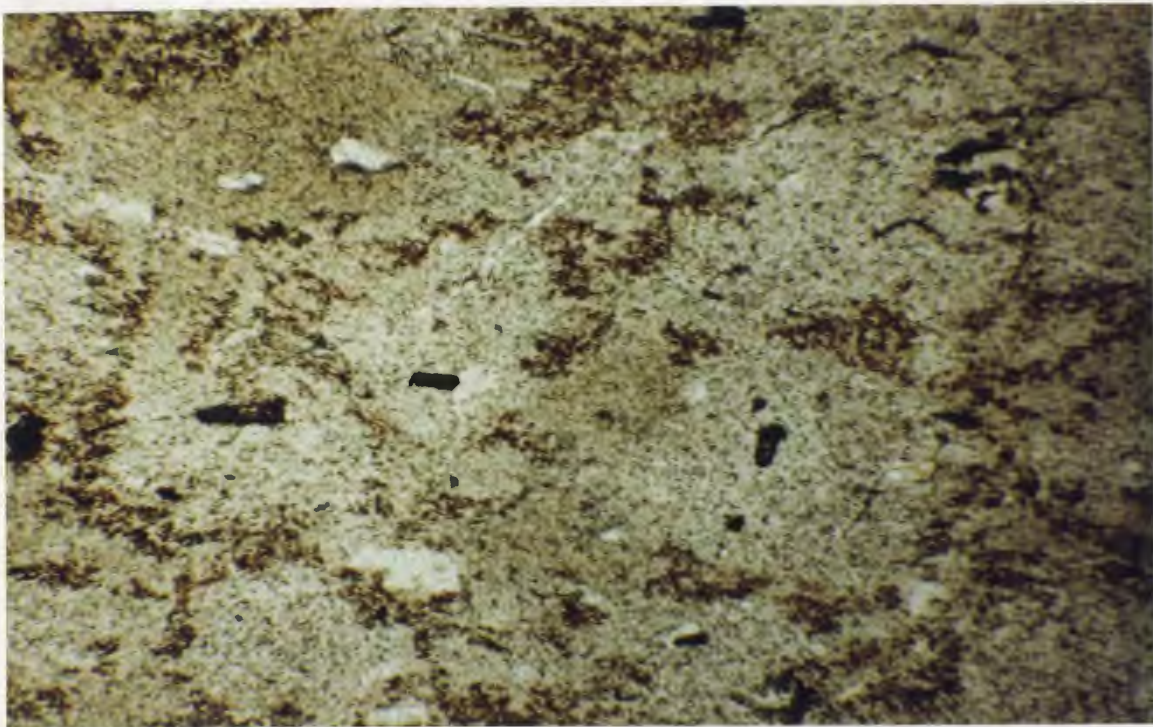


Plate 3.29. Typical glassy nature of the dacitic domes (C4-209, 1x, PPL).

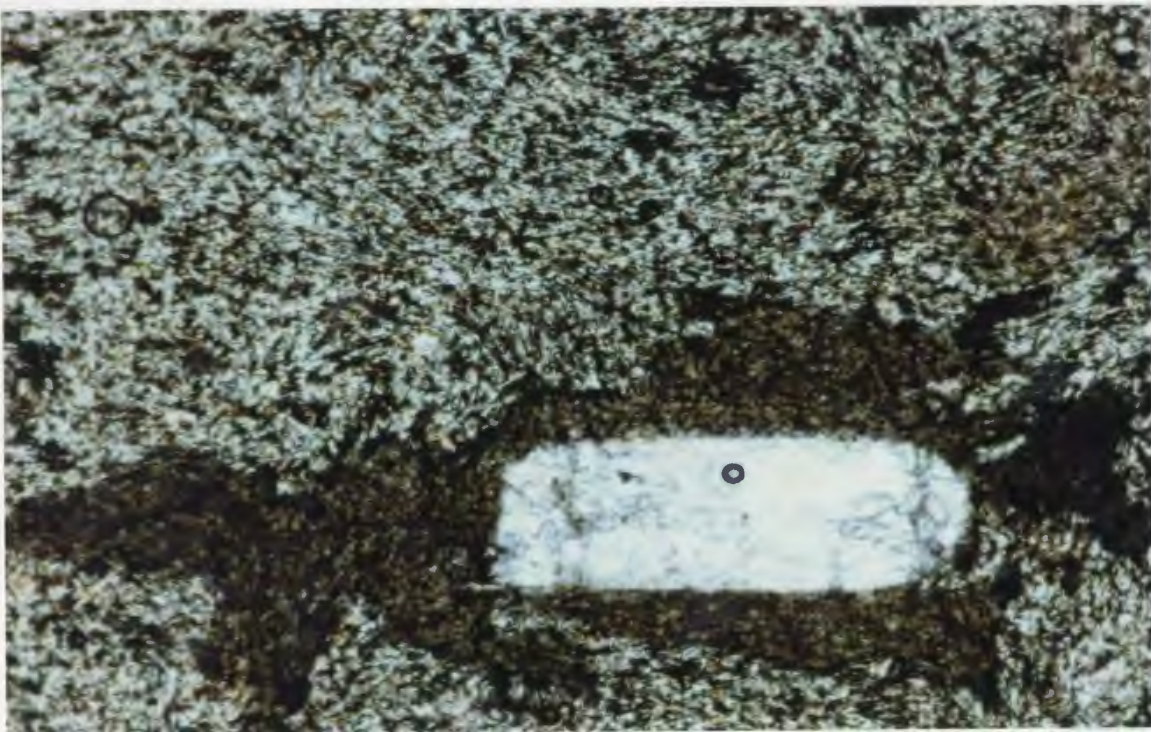


Plate 3.30. Microphenocryst of feldspar in a pilotaxitic groundmass (C4-253b, 4x, PPL).

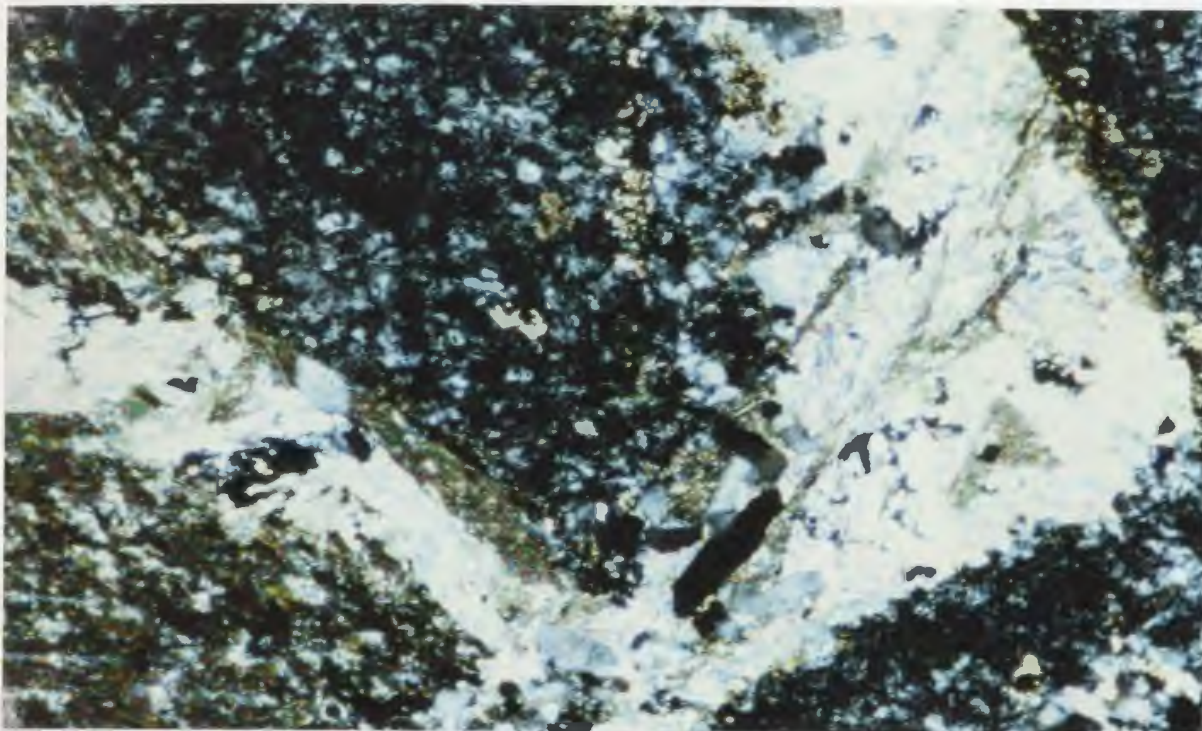


Plate 3.31. Autobrecciated dacite. Fragment is surrounded by calcite and fibrous sericite at it's edge (C4-266, 4x, XPL).



Plate 3.32. Burnt Berry Dome, glassy rhyolite with flow aligned microlites (EL-325b, 10x, PPL).

as well as spherulitic devitrification is seen (Plate 3.33). Radial devitrification nucleates on perlitic fractures in the groundmass and small microfractures of brecciated glass result from the intersection of flow lobes where they have different cooling rates (Plate 3.34).

Where lithophysae coalesce to form dykes, large spectacular devitrification spherules form and can be seen in Plate 3.35.

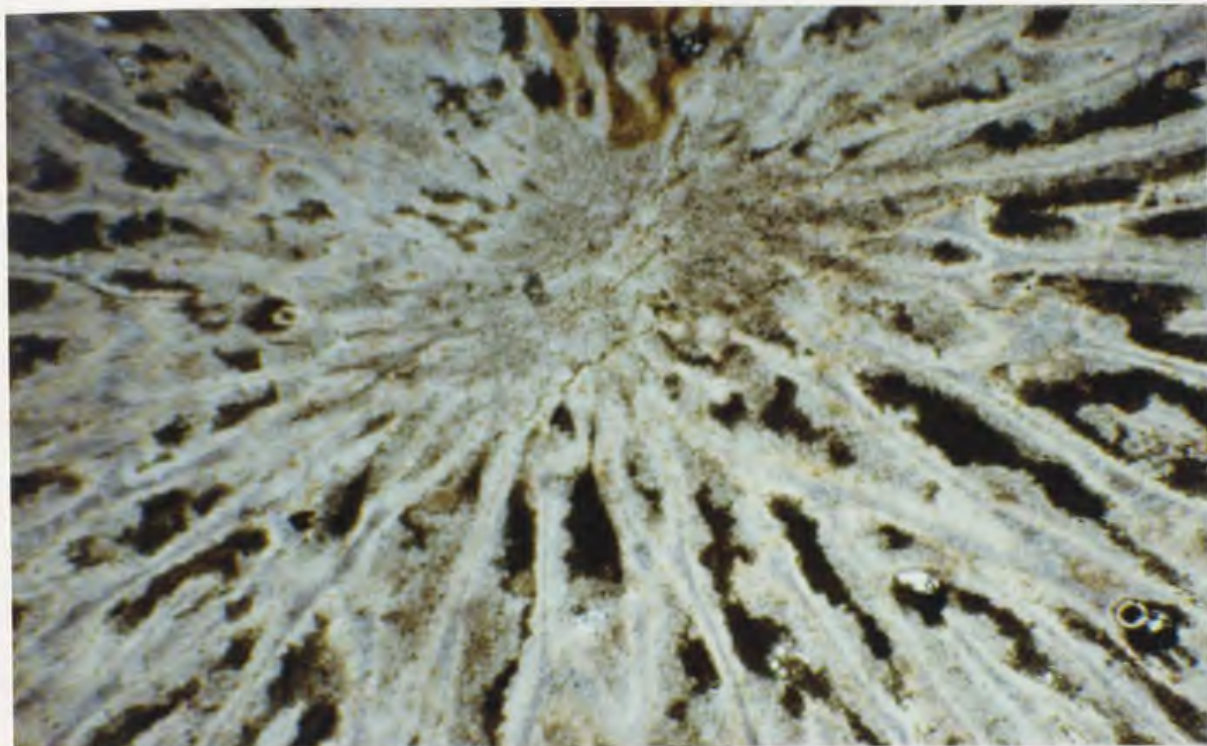


Plate 3.35a. Large radial devitrification spherule produced in gas rich high-silica dykes (DS-20, 1x, PPL)

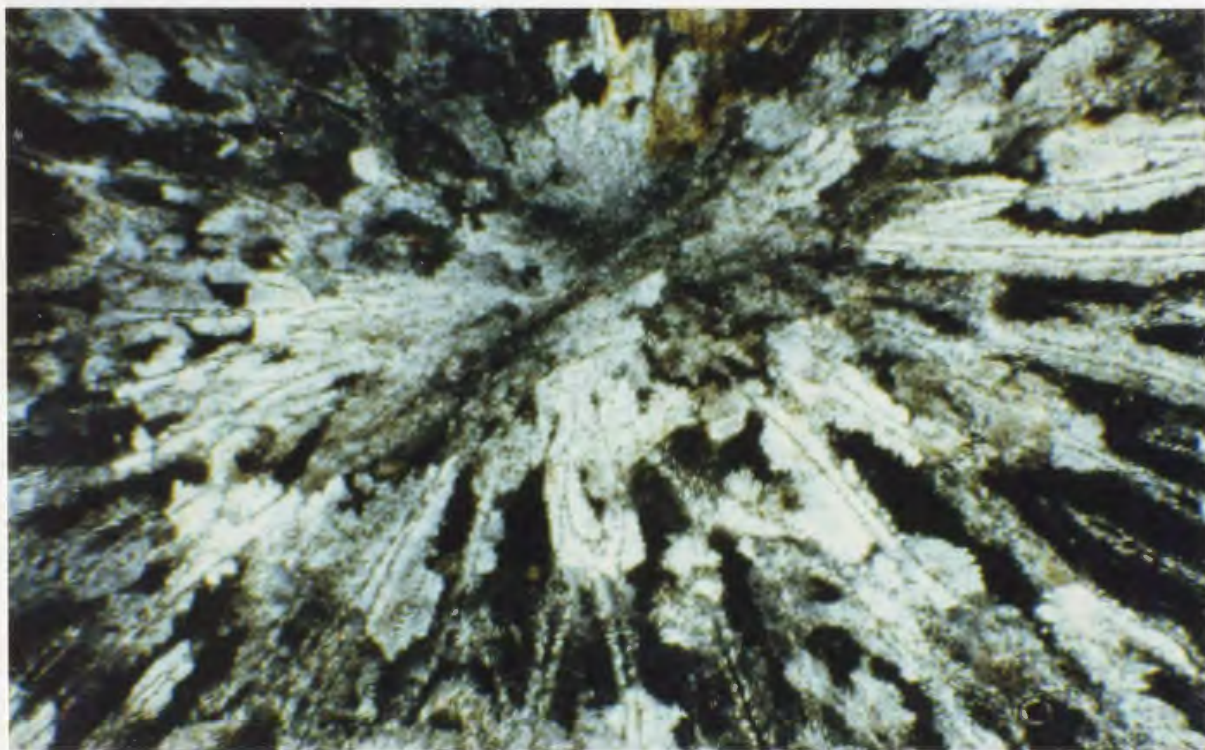


Plate 3.35b. Same as above except with crossed polars.



Plate 3.33. High-silica rhyolite with radial devitrification. Groundmass alteration phases include calcite and epidote (EL-325b, 4x, PPL).

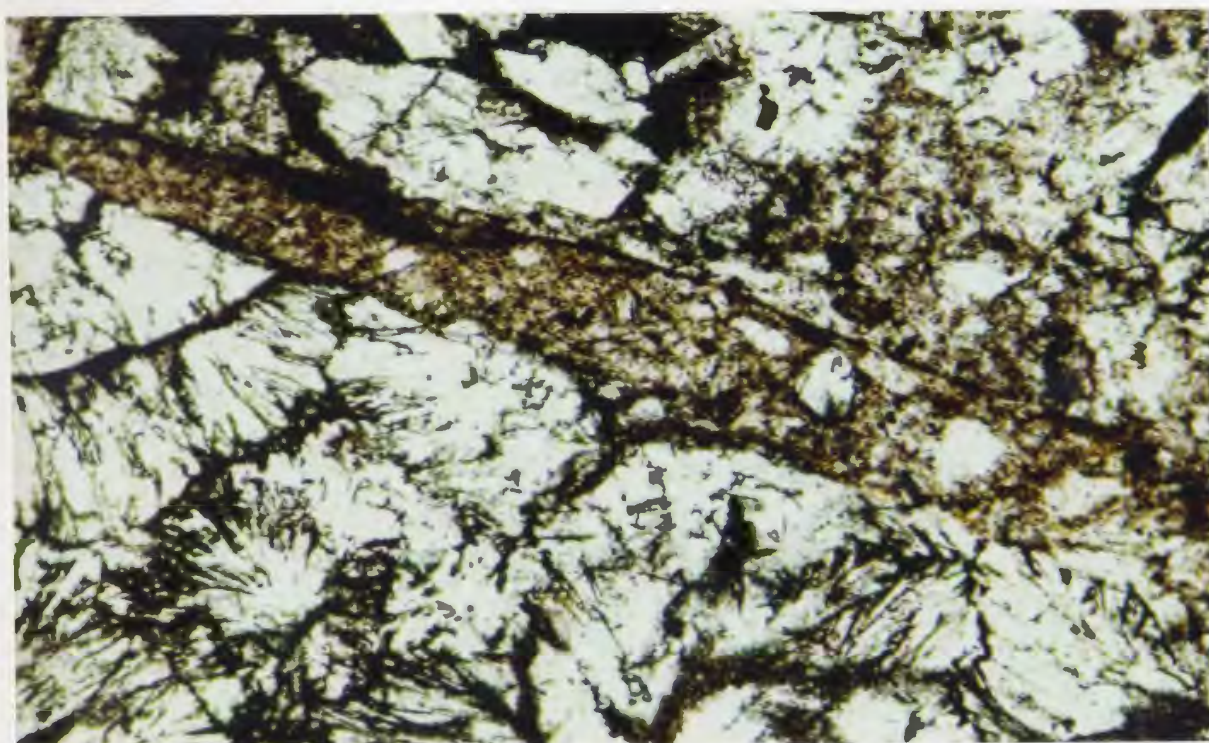


Plate 3.34. Granulation along microfracture within the dome. Good perlitic fractures are also seen in this section (EL-325b, 10x, PPL).

4. CHEMISTRY OF SPRINGDALE GROUP IGNEOUS ROCKS

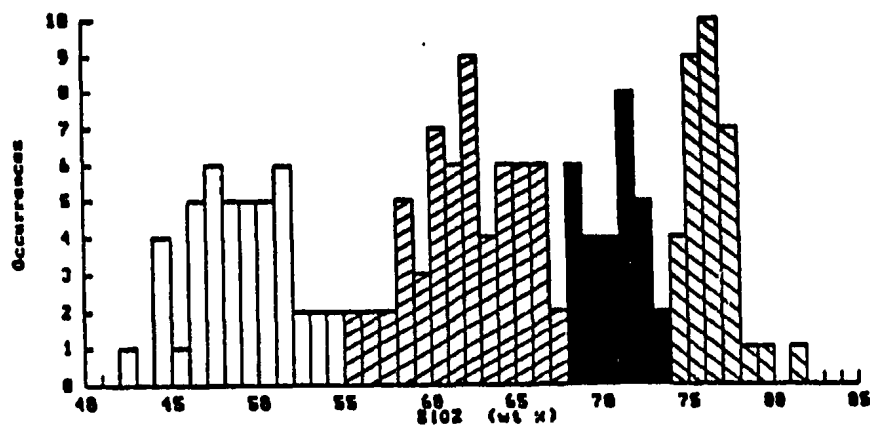
4.1. Introduction

Of some 1500 samples collected from the rocks described above, 165 have been analysed for the major element oxides by atomic absorption and 18 trace elements by X-ray fluorescence techniques. Twenty-four of these samples were also analysed by inductively coupled plasma - mass spectrometry (ICP-MS) for 14 rare earth elements and an additional 10 trace elements. Of the total, 155 samples are of volcanic and associated intrusive rocks from throughout the map area, and the others are from lithologies not directly related to the Springdale Group. Care was taken to exclude any rocks containing xenoliths or lithic clasts or amygdales, or which show evidence of exceptional alteration. Analytical methods are described in Appendix C and the data are presented in Appendix D.

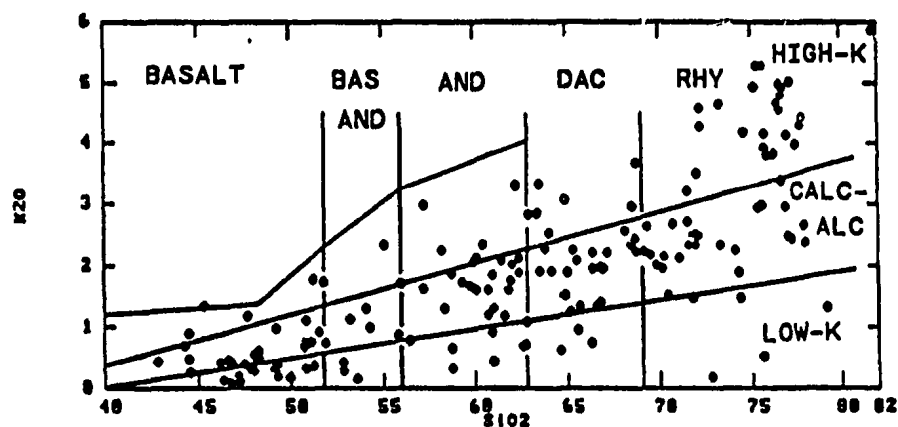
Although an attempt is made to understand the petrogenesis of these rocks, it should be noted that this was not the primary purpose of this thesis. Hence, the suggested petrogenetic model might well be refined by more detailed isotopic, mineralogical other studies specifically designed for that purpose.

A histogram of silica distribution (Fig. 4.1.a) demonstrates a range of lithologies from basalts to

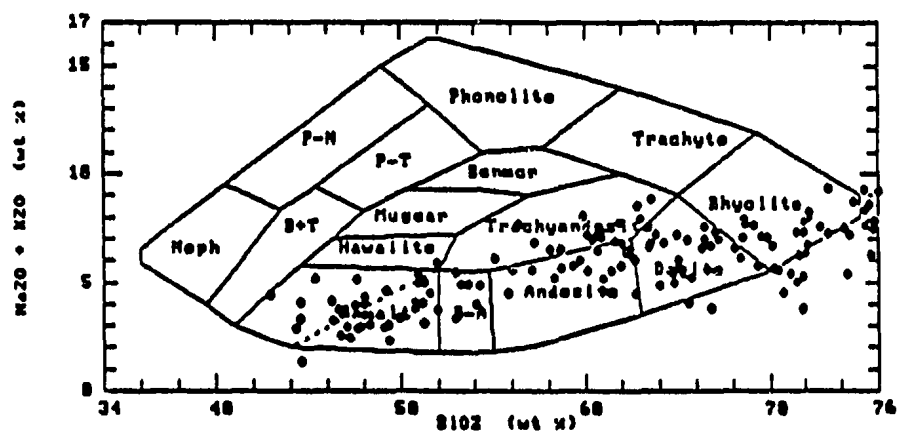
Figure 4.1(a). Histogram of silica distribution in all (165) analysed samples from the Springdale Group. Classification based on (b) K_2O content (after Peczerillo and Taylor, 1976), (c) total alkalies (after Cox *et al.*, 1979), and (d) total alkalies (after Middlemost, 1985). The fields numbered in (d) identify rock types as follows: 1. Nephelinite; 2. Phonolite; 3. Alkali trachyte; 4. Pantellerite; 5. Comendite; 6. Basanite; 7. Alkali picrite; 8. Alkali olivine basalt; 9. Trachybasalt; 10. Trachyandesite basalt; 11. Trachyandesite; 12. Trachyte; 13. Trachydacite; 14. Trachyrhyolite; 15. Alkali rhyolite; 16. Picrite; 17. Tholeiitic basalt; 18. Andesite basalt; 19. Andesite; 20. Andesite dacite; 21. Dacite; 22. Rhyolite dacite; 23. Rhyolite.



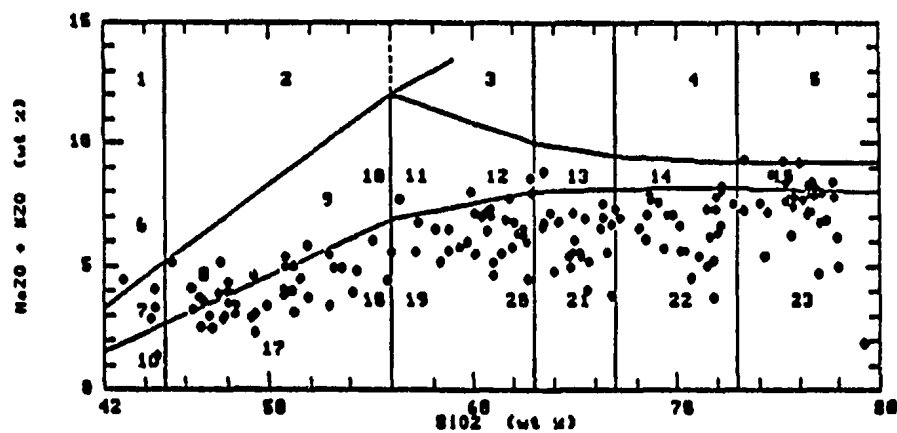
(a)



(b)



(c)

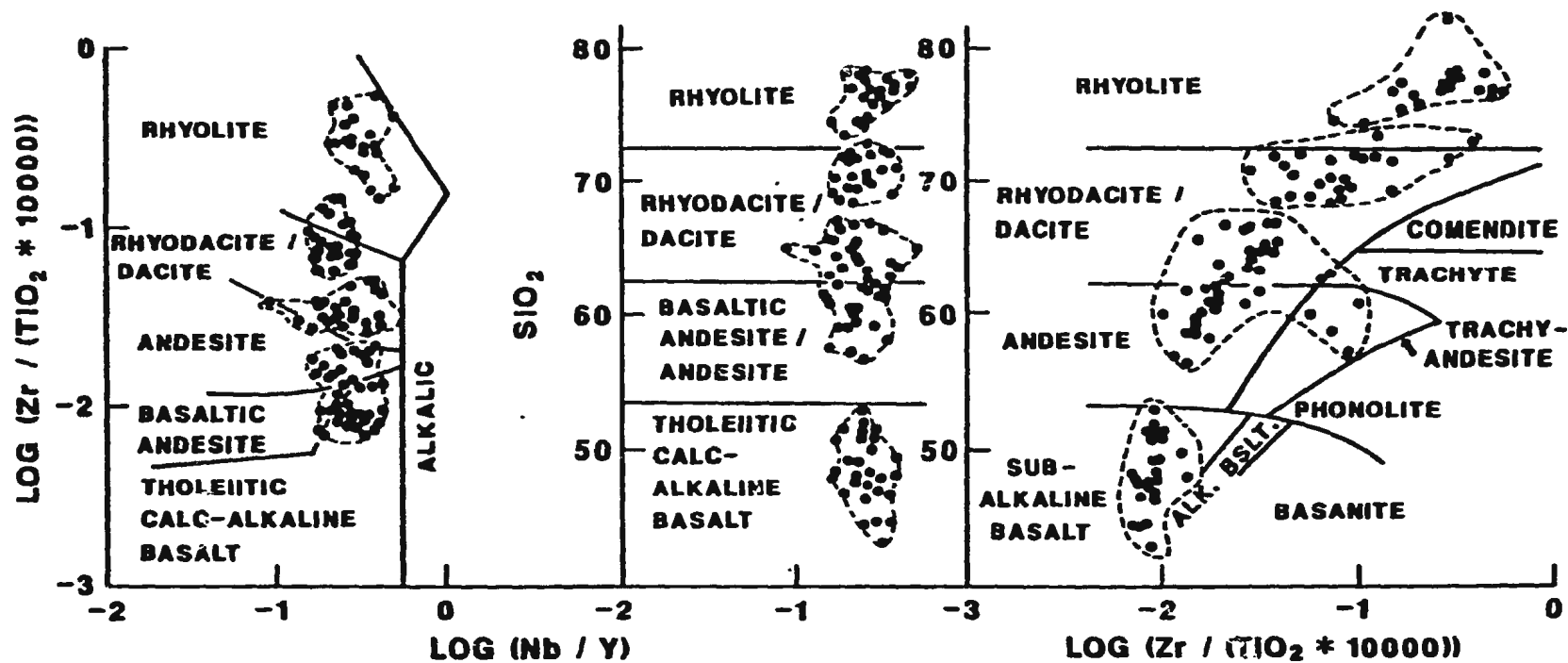


(d)

high-silica rhyolites. It appears from Figure 4.1(a) that these rocks fall into four groups separated by silica gaps at 52-58%, 67-68% and 73-74% SiO_2 . For the purposes of the following discussion these groups are referred to as the mafic, intermediate, felsic and silicic groups. The latter two are equivalent to low-silica and high-silica rhyolites, but the precise volcanic terminology to be used for these rocks would depend upon the particular classification scheme applied, as seen in Figures 4.1(b,c,d).

In the terminology of Cox et al. (1979), the lowest-silica group are basalts and basaltic andesites, the intermediate group are andesites and dacites, and both of the higher-silica groups are rhyolites. Using the Peccerillo and Taylor (1976) plot of K_2O vs. SiO_2 (Fig. 4.1.b), these rocks would be clearly classified as a calc-alkaline suite ranging from basalts through andesites and dacites to the low-silica rhyolites. The high-silica rhyolites show a much wider range of K_2O up to more than 6%, and would thus be termed high-K rhyolites. This is a characteristic primary feature of high-silica magmas with more than 74% SiO_2 , and in many cases is associated with economic mineralization (see review by Tuach et al., 1986). Although some of the lower-silica rocks also have anomalous K_2O concentrations, these result from secondary redistribution of alkalis in the volcanic rocks as a whole, and cannot be used to classify the Springdale Group as a high-potassium suite. In terms of the total alkalis vs. silica diagrams (Figs. 4.1.c,d), the

Figure 4.2. Classification of volcanic rocks of the Springdale Group in terms of silica and a number of "immobile" trace elements (boundaries after Winchester and Floyd, 1977).



data show a typically silica-saturated suite, with a few of the more altered basalts and andesites plotting in the undersaturated fields of alkali basalt and trachyandesite-trachyte, respectively.

Other elements less mobile than alkalis (Fig. 4.2) also show the sub-alkalic nature of the Springdale Group. With regard to the precise terminology, however, the Winchester and Floyd (1977) boundaries based on these elements and SiO_2 content are different from those of Fig. 4.1 and some of the rocks are grouped under different names. For example, using the plot of Zr/Ti vs. SiO_2 , the silica gap at basaltic andesites is spanned by the basaltic rocks, the andesites are classified as dacites, and the low-silica rhyolites are classified as rhyodacites-dacites. Given that tectonic classifications of volcanic rocks are commonly based on geochemical characteristics for particular petrochemical groupings rather than precise rock names, the Springdale group geochemical data is discussed below in terms of the four groups identified above, i.e. mafic, intermediate, felsic and silicic.

4.2. Mafic Rocks

Numerous classification schemes have been proposed to distinguish between different types of basaltic rocks as a means of understanding their petrogenetic history (e.g. Yoder and Tilley, 1964; MacDonald and Katsura, 1964; BVSP, 1981) or their tectonic setting (e.g. Pearce and Cann,

1972; Shervais, 1982; Meschede, 1986). For the purpose of this thesis it is more important to try and identify the tectonic setting in which the basalts were produced, rather than to carry out a detailed assessment of their petrogenetic history, which would require more comprehensive data, such as Nd/Sm and other isotopic systems, than could be obtained in the course of this study.

As was shown in Figure 4.1, the mafic rocks are sub-alkaline. Using the Irvine and Baragar AFM classification (Fig. 4.3.a) they are grouped as dominantly calc-alkaline. However, on the Al-[Fe+Ti]-Mg diagram of Jensen (1979) they are shown to be tholeiitic (Fig. 4.3.b). These inconsistencies are also seen when other major elements are used, e.g. the Ti-Mn-P diagram of Mullen (1983) where the Springdale Group mafic rocks straddle at least three tectonic classification boundaries (Fig. 4.3.c). The same is seen with immobile trace elements (Fig. 4.3.d), with most samples plotting within the fields of within-plate tholeiites and volcanic arc basalts, and a few within the field of primitive mid ocean ridge basalts.

Using the different combinations of SiO_2 , TiO_2 and FeO^*/MgO given by Myashiro (1974) one is led to suggest that, despite substantial overlap (Fig. 4.4.a), these rocks are essentially tholeiitic (Fig. 4.4.b,c). Using the immobile trace elements Zr and Y with Ti, most of

Fig. 4.3. All data for the Springdale Group plot as a calc-alkaline suite according to (a) the classification of Irvine and Baragar (1971), but as a tholeiitic suite according to (b) that of Jensen (1979). The mafic rocks overlap several fields in terms of both (c) minor elements (after Mullen, 1983) and (d) high field strength (immobile) trace elements (after Meschede, 1986). Abbreviations are as follows:

- (b) TR - Tholeiitic rhyolite; TD - Tholeiitic dacite; TA - Tholeiitic andesite; CR - Calc-alkaline rhyolite; CD - Calc-alkaline dacite; HFT - High-Fe tholeiite; HMT - High magnesium tholeiite; BK - Basaltic komatiite; PK - Peridotitic komatiite (after Jensen, 1979).
- (c) CAB - Calc-alkaline basalt; IAT - Island arc tholeiites; MORB - Mid-ocean ridge basalts; OIA - Ocean island andesites; OIT - Ocean Island tholeiites (after Mullen, 1983).
- (d) AI, AII - Within-plate alkaline basalts; AII, C - Within-plate tholeiites; B - Primitive mid ocean ridge basalts; C, D - Volcanic arc basalts; D - Normal mid ocean ridge basalts (after Meschede, 1986).

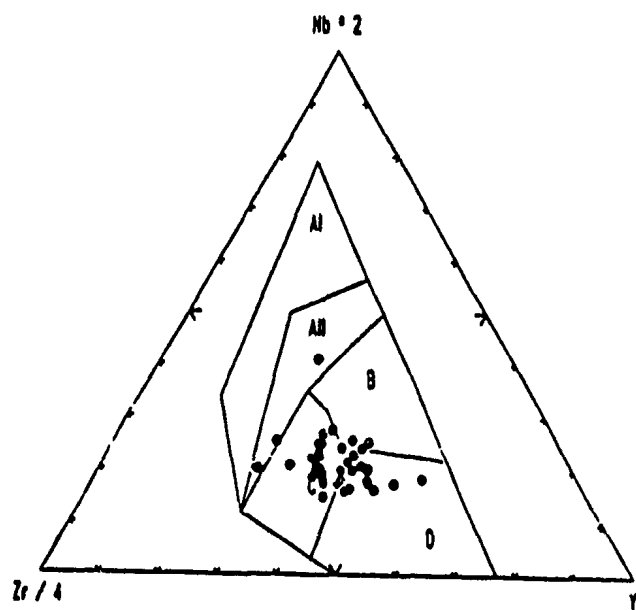
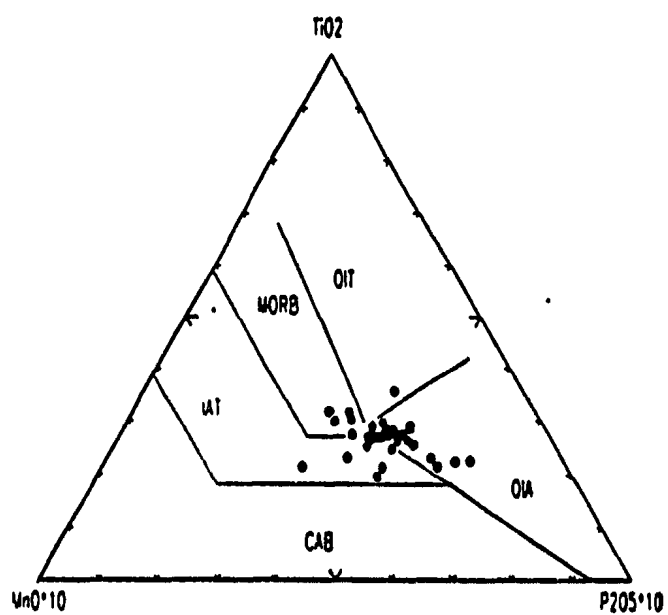
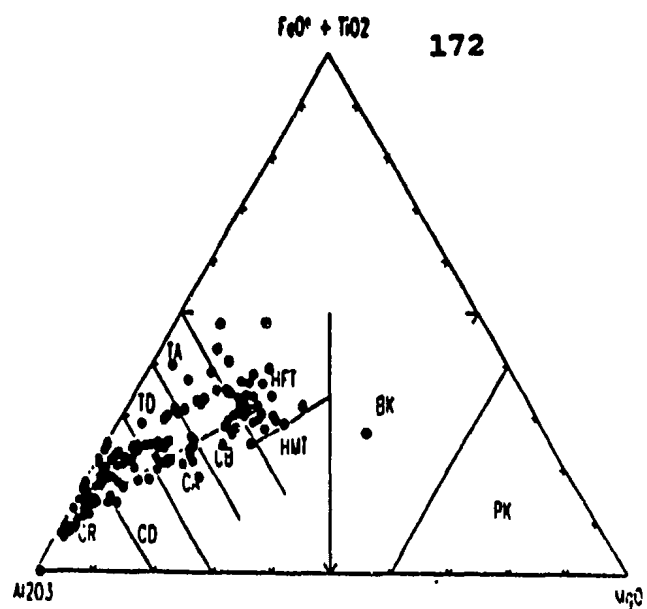
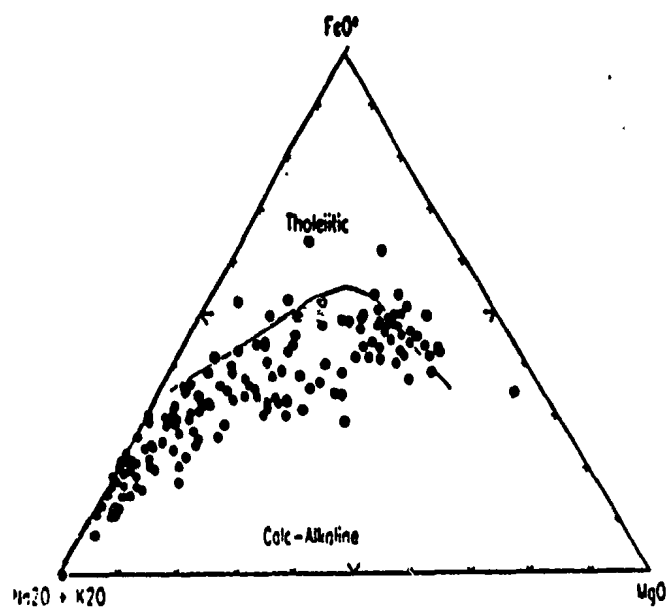


Figure 4.4. Classification of Springdale Group basalts based on variations in FeO^*/MgO as proposed by Myashiro (1974).

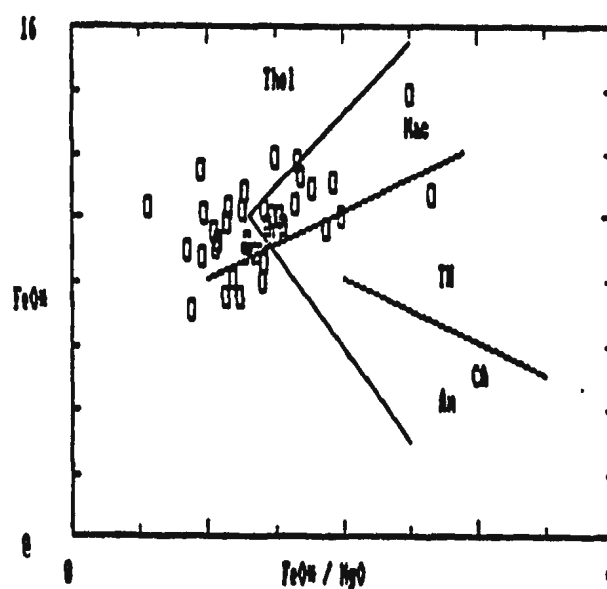
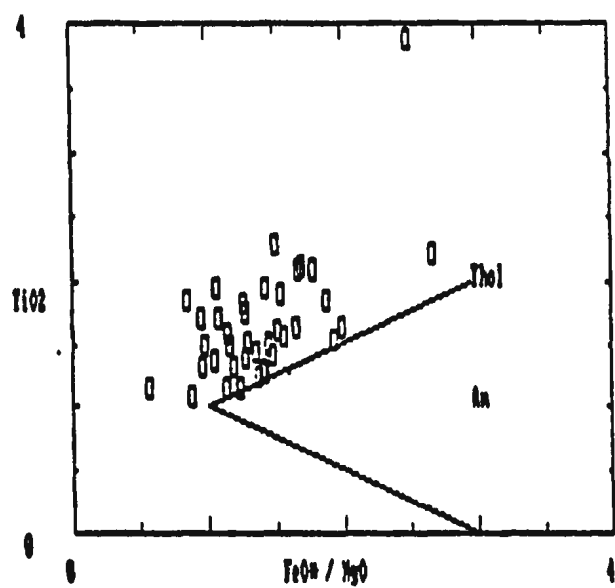
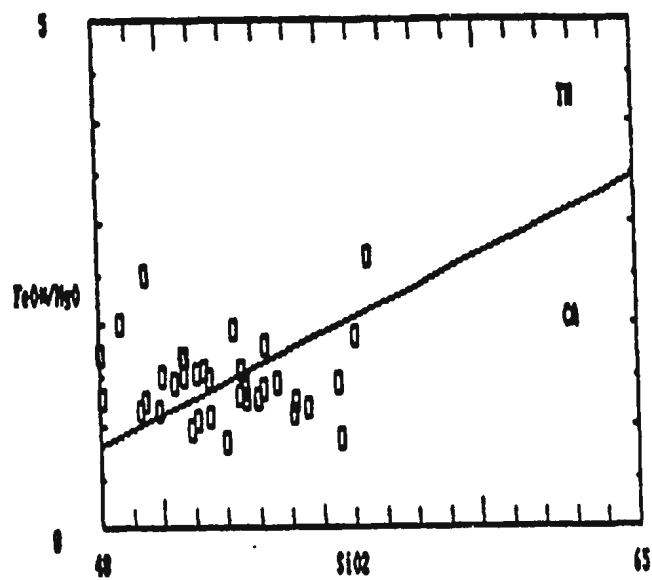
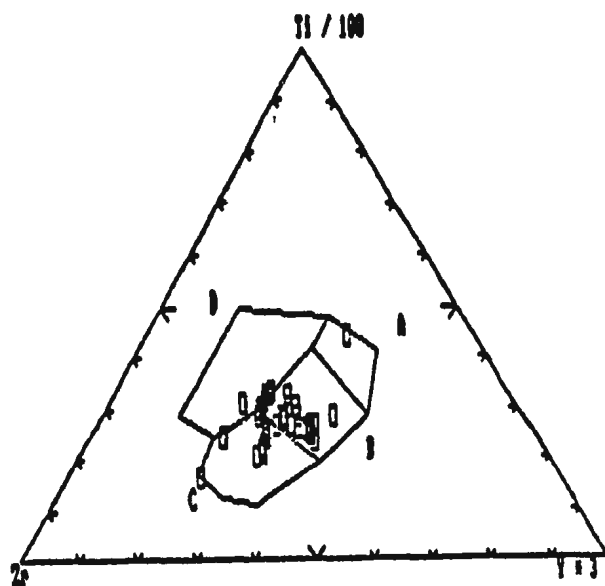
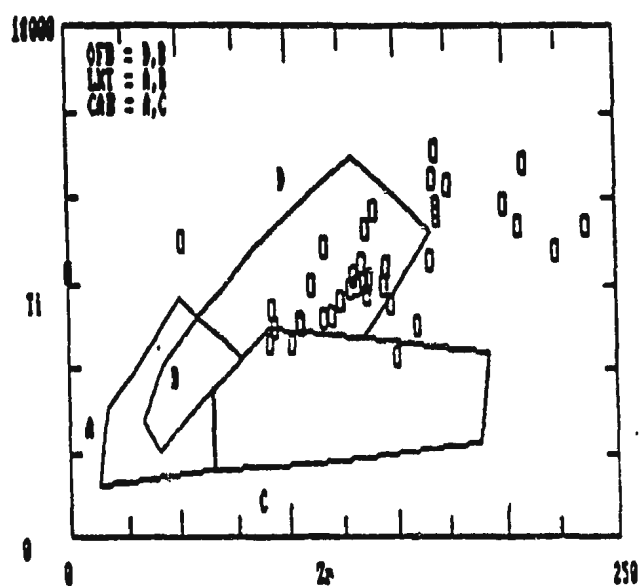


Figure 4.5. Using the discrimination diagrams proposed by Pearce and Cann (1973) the Springdale Group basalts would classify as mostly as calc-alkaline basalts and a few within plate basalts (a), or as mostly ocean floor basalts with no calc-alkaline trend (b). They likewise plot as ocean floor basalts according to the classification of (c) Shervais (1982) and (c) Pearce (1975). Abbreviations are as follows:

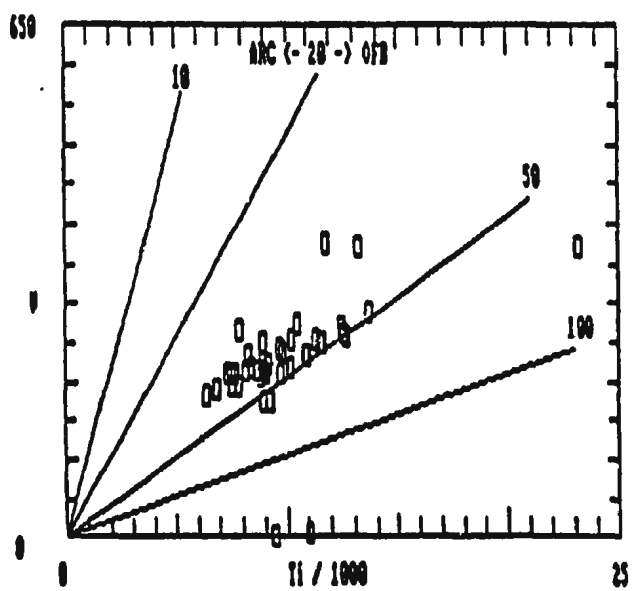
- (a) A, B - Low-K tholeiites; B - Ocean floor basalts; B, C - Calc-alkaline basalts; D - Within plate basalts.
- (b) A, B - Low-K tholeiite; A, C - Calc-alkaline basalt; B, D - Ocean floor basalt.
- (c,d) ARC - Island arc basalts; OFB - Ocean floor basalts; LKT - Low - K tholeiites.



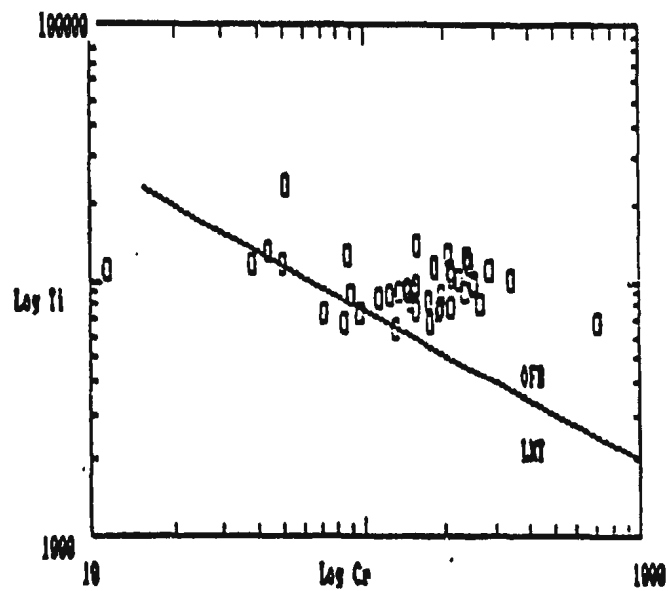
(a)



(b)



(c)



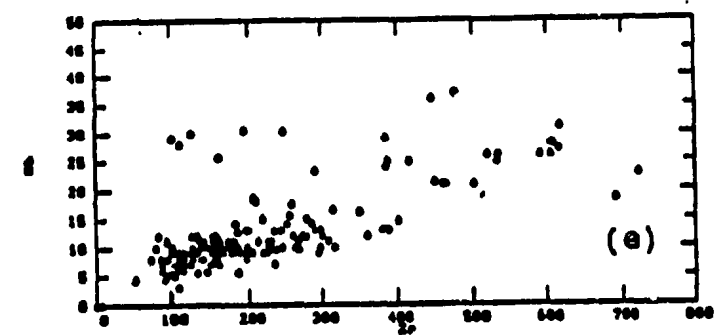
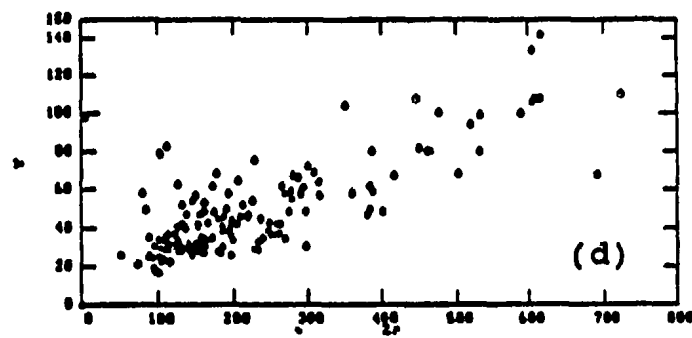
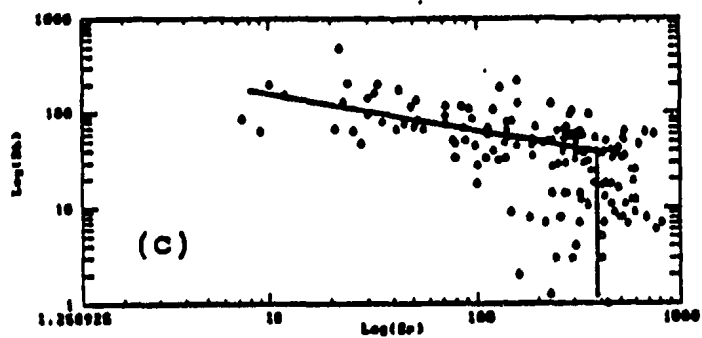
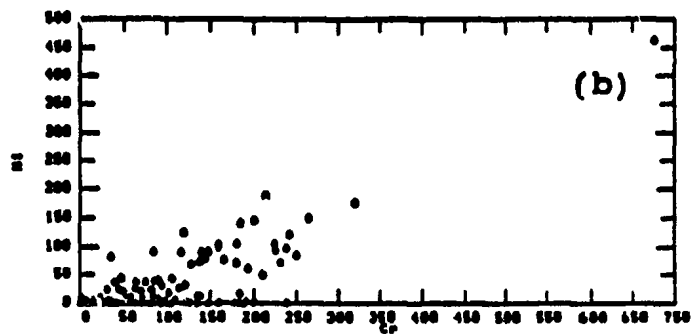
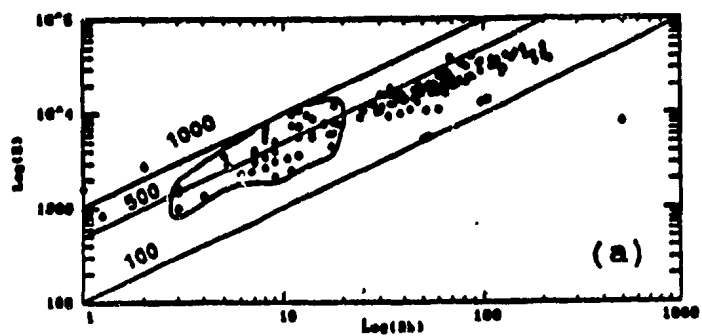
(d)

these data plot mainly within the calc-alkaline basalt field (Fig. 4.5.a), but in the classification based on two of these same three elements, Ti-Zr (Fig. 4.5.b), they plot mostly within the field of ocean floor basalts and show no indication of a calc-alkaline trend.

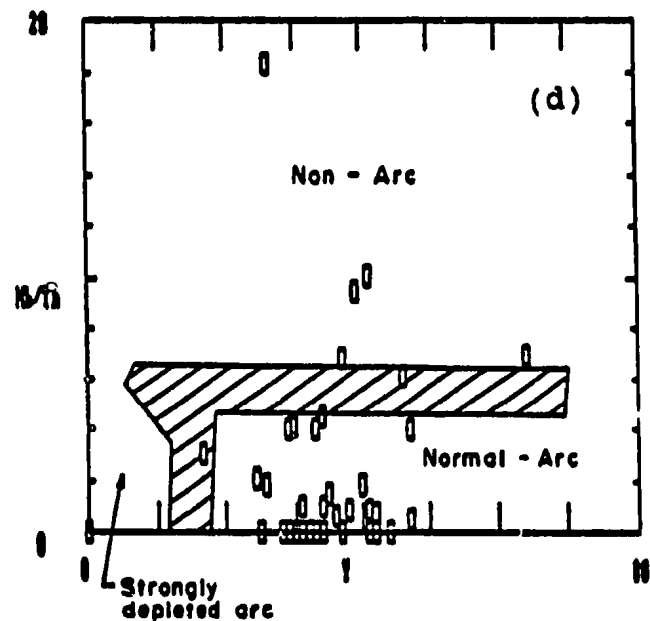
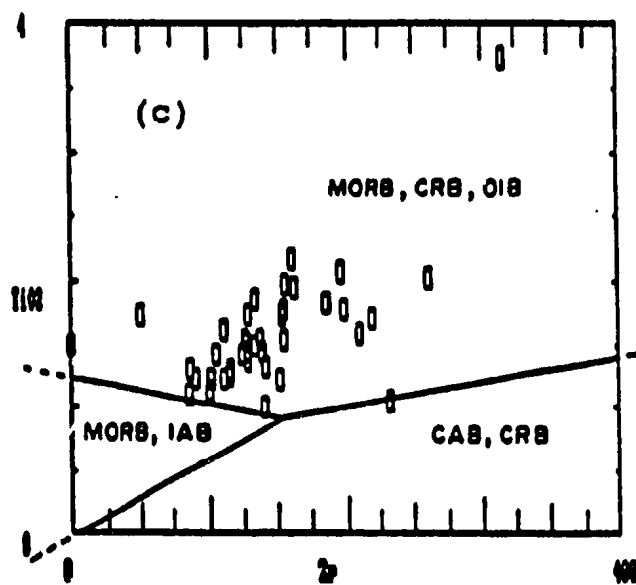
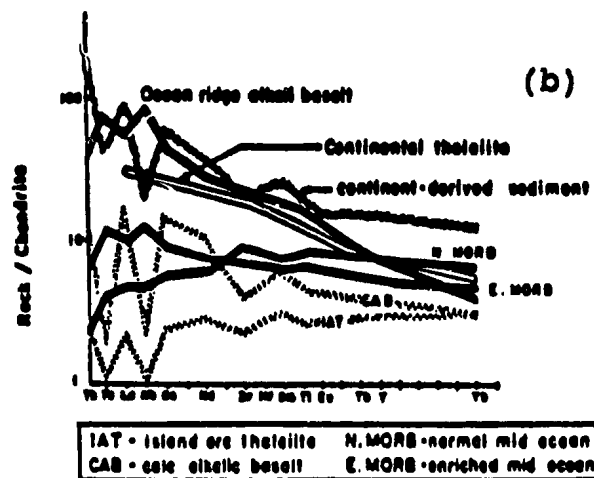
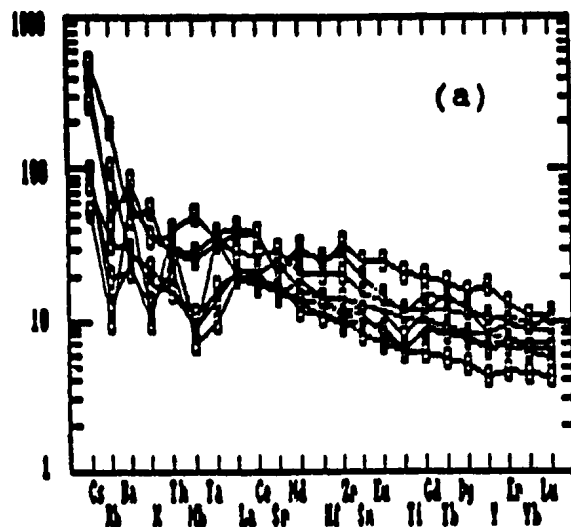
Although the geological setting of the Springdale Group clearly precludes an origin on the ocean floor, it is interesting that the basalts do have characteristics of ocean floor basalts (Fig. 4.5.c,d). This is not unique for Silurian mafic rocks of central Newfoundland, as the Mount Peyton Gabbro, which intrudes the Botwood Group, is geochemically similar to those of ocean floor basalts (Strong, 1979). It may be that both of these suites were derived from melts produced through continued sub-crustal activity of the same Iapetus spreading center which was earlier active in the Ordovician and, according to most tectonic models for central Newfoundland (e.g. see review by Swinden et al., 1979), would have been over-ridden by both ophiolitic and arc material by closure of Iapetus.

With regard to the petrogenesis of the Springdale Group mafic rocks, the generally high K/Rb ratios around 500 (Fig. 4.6.a) can be taken to reflect the original mantle ratios, since it is well known that crustal rocks average K/Rb ratios around 230 (Taylor, 1966) or lower (Lambert et al., 1976). However, the Ni and Cr contents (Fig. 4.6b) indicate that these basalts are not primitive magmas derived directly from the mantle, but had

Figure 4.6. Covariation of a number of trace elements in the Springdale Group mafic rocks. In (a) basalts plot within the enclosed field, and numbers refer to K/Rb ratios of 1000, 500, 100. In (c) the lower vertical line is through the mafic rocks and symbolizes olivine and clinopyroxene fractionation (i.e. no Sr variation); the abrupt change in slope of the upper line reflects the depletion of Sr and slight Rb enrichment by plagioclase fractionation.



- Figure 4.7. (a) Extended rare earth element plots for Springdale Group mafic rocks, with concentrations normalized to primitive mantle data of Sun (1982).
- (b) Typical extended rare earth element plots for continental flood basalts (after Thompson et al. (1983, 1984), other basalt types (after Sun, 1982), and continent-derived oceanic sediment (after Hole et al. (1984) (modified from Swinden et al. (1989).
- (c,d) Proposed distinctions between different basalt types proposed by (c) Condie et al. (1987) and (d) Swinden et al. (1989).
- Abbreviations are as follows: IAT - Island arc tholeiite; CAB - Calc-alkaline basalt; N-MORB - Normal mid-ocean ridge basalt; E-MORB - Enriched mid-ocean ridge basalt; OIB - Ocean island basalt; CRB - Continental rift basalt.



undergone significant fractionation of olivine and possibly pyroxene.

The rare earth elements (Fig. 4.7a) exhibit a range of chondrite-normalized ratios for La between 20 and 40, and for Lu between 5 and 10, with relatively straight-line negative slopes similar those of continental tholeiites (Thompson et al., 1983, 1984; Fig. 4.7b). They do not exhibit significant europium anomalies, indicating that plagioclase was not an important component in the genesis of these mafic rocks, although plagioclase is present as a phenocryst phase in most samples.

Because of the abundance of andesites in the Springdale Group, it is important to evaluate the possible importance of subduction in the generation of this sequence. An attempt at this can be made by means of the extended REE plots shown in Figure 4.7(b). Swinden et al. (1989) have reviewed the characteristics of "arc signatures" and "non-arc signatures" of basalts, supporting the conclusions of Wood et al. (1979) and Sun (1980) that subduction-related mafic rocks are depleted in the high-field-strength elements including the heavy rare earth elements and particularly Nb and Ta, and are enriched in the low-field-strength elements, including the light rare earth elements, with a definitive thorium enrichment relative to lanthanum. These features are shown for different basaltic types on the extended REE plots as a

negative anomalies for Nb and Th (Fig. 4.7.b), and allow for a distinction between different suites as shown in Figure 4.7(c). It can be seen from Figure 4.7(c) and 4.7(a) that some of the Springdale Group mafic rocks show the Nb depletion and Th enrichment, which might be taken to suggest that they were produced by subduction-related processes. However, other samples of the Group show non-arc patterns, and actually form a continuum across the supposed boundary between the arc and non-arc fields (Fig. 4.7.c). Furthermore, these rocks have Zr-TiO₂ ratios of tholeiites formed in extensional regimes such as mid-ocean ridges, continental rifts or oceanic islands, and are unlike those of calc-alkaline basalts or island arc basalts (Fig. 4.7.d).

These features suggest that other explanations for these anomalies should be considered, for example crystal fractionation and/or contamination of the basaltic magmas during their ascent by the sediments and continental crust previously subducted during closure of Iapetus, not necessarily their partial melting during an active subduction process. Figure 4.8(a) shows extended REE plots for the mafic rocks normalized to continental crust, with most REE enriched by a factor between 1 and 2, slightly positive Ti and some Nb anomalies. The Th and some Nb ratios are lower than those of continental crust. The other LFSE ratios are generally lower than 1, but in these and the other diagrams the scatter of these elements is taken

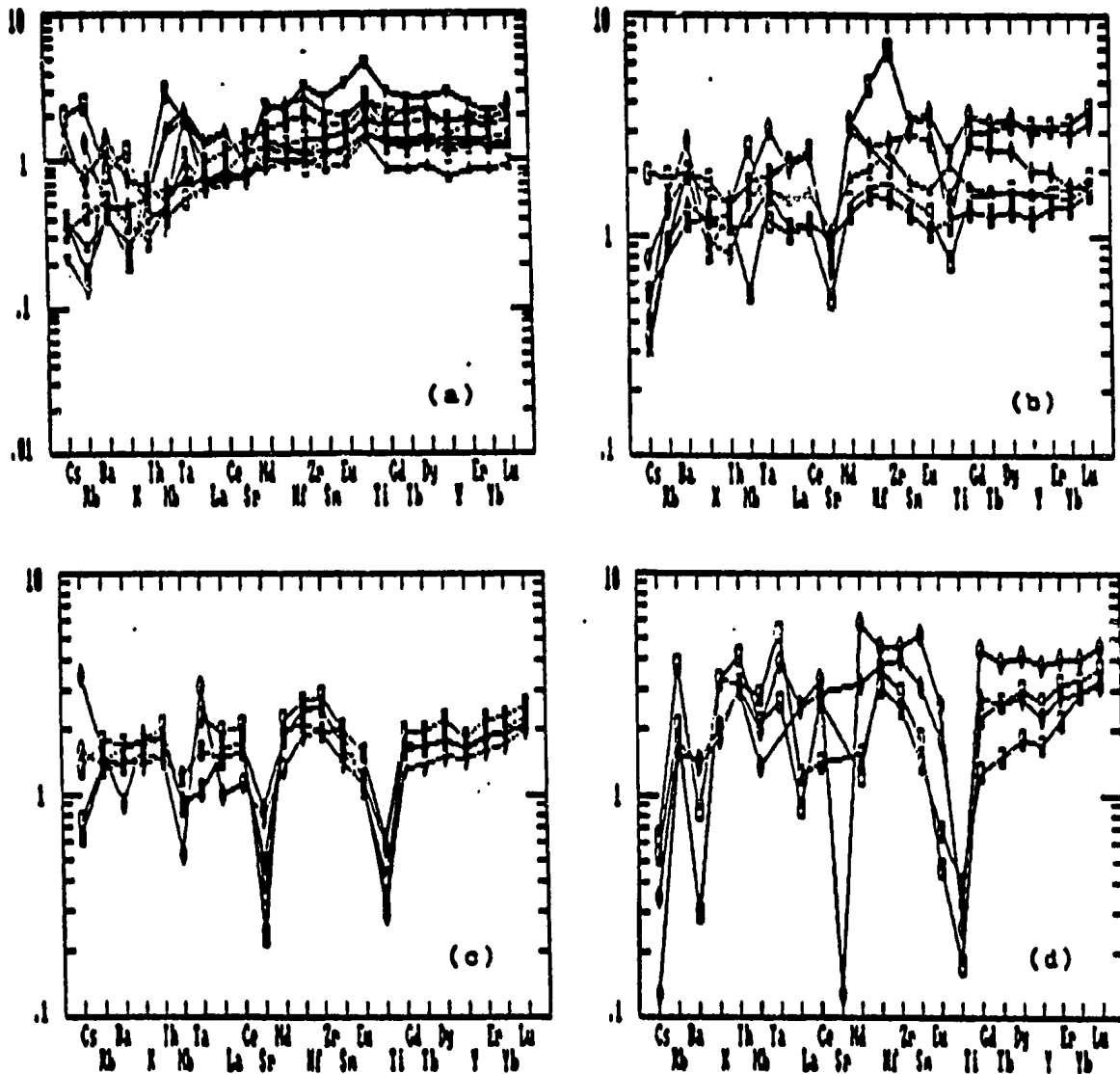


Figure 4.8. Extended rare earth element diagrams for the four groups of mafic, intermediate, felsic and silicic rocks of the Springdale Group, normalized to the average continental crust of Taylor and McLennan (1985).

as reflecting alteration, i.e. precluding their use as reliable petrogenetic indicators.

If contamination by continental crust has influenced the compositions of the mafic rocks, one might reasonably expect it to have had some control on the other rock types as well, with at least the intermediate (granodiorite-like; i.e. similar to average continental crust in major elements, e.g. Taylor and McLennan, 1985) rocks being progressively more similar to continental crust. When normalized to continental crust, however, most elements of the intermediate (Fig. 4.8.b) and felsic rocks (Fig. 4.8.c) are seen to be enriched by factors between 1 and 2, except for strong depletions of Sr and Ti in the latter group and Nb in several samples of each.

Although the intermediate and felsic rocks are discussed in more detail below, comparison of their REE patterns with those of the basalts does clarify the interpretation of the latter.

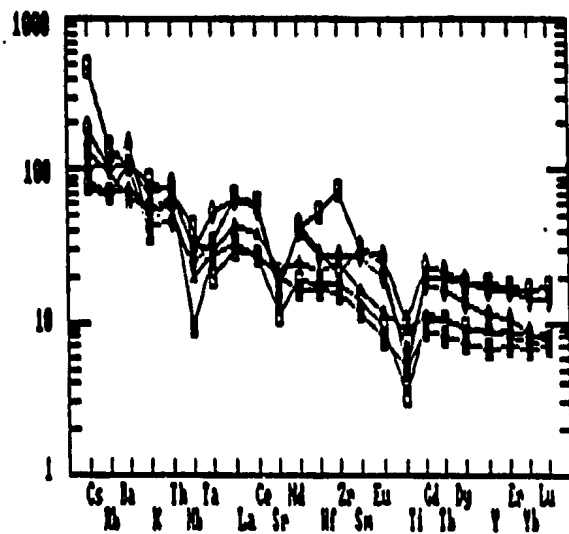
The chondrite-normalized extended REE plots for the intermediate (Fig. 4.9.a) and felsic rocks (Fig. 4.9.b) show more clearly the continuum from the mafic patterns, with the negative Nb and positive Th anomalies progressively increased. These trends are also accompanied by progressive enhancement of Ti, Sr and Eu anomalies, features which are readily explained by fractionation, along with the olivine and clinopyroxene discussed above,

of plagioclase and Fe-Ti oxides, both of which occur as phenocryst phases in these rocks. In other words, the continuum of patterns, including the increasing Nb anomalies, from the mafic to felsic rocks suggests that these patterns, including those of the mafic rocks, are all the result of fractionation and not partial melting processes, and therefore cannot be reliably used as indicators of arc or non-arc origin.

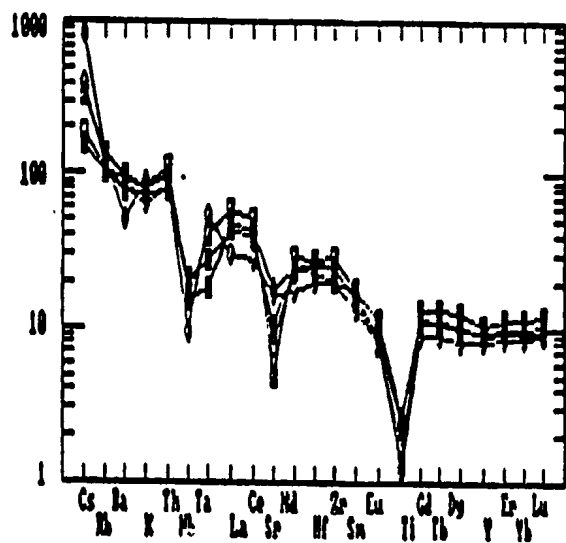
The corresponding changes in the HFSE such as Zr, Hf, Nb and Y with total REE are illustrated in Figures 4.6(d,e), with strong correlations which can be interpreted as due to zircon and magnetite fractionation.

In general, it seems reasonable to suggest that the Springdale Group basalts are tholeiites, with similarities to ocean floor basalts, possibly produced by the Iapetus spreading centre which was over-ridden during closure in the late Ordovician, analogous to the southwestern United States where the East Pacific Rise was over-ridden by continental crust of the American plate (Atwater, 1970; Gans *et al.*, 1989). The Newfoundland situation would have differed only in that the over-riding material would have been an assemblage of North American Precambrian (Grenville) continental crust and the Lower Paleozoic oceanic and arc sequences, all of which were juxtaposed by closure of Iapetus (see Swinden *et al.*, 1989, for a review). The original primary basaltic compositions were modified during passage through this crust by fractionation

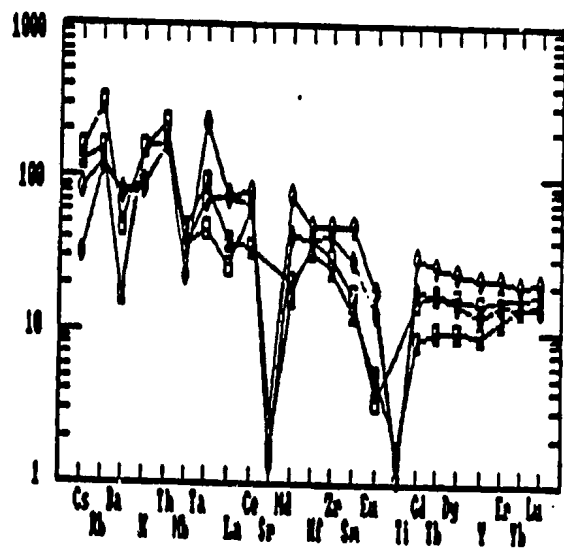
Figure 4.9. Extended rare earth element plots for Springdale Group intermediate (a), felsic (b) and silicic (c) rocks, with concentrations normalized to primitive mantle data of Sun (1982).



(a)



(b)



(c)

of olivine, clinopyroxene, some Fe-Ti oxides and zircon, with plagioclase becoming important in the andesites and more silicic compositions. This fractionation could well have been accompanied by limited contamination from the crustal rocks, as well as mixing with more silicic crustal melts. (analogous to the model for crystallization during mixing proposed by McBirney, 1984, p. 158, Fig. 5-14)

4.3. Intermediate Rocks (Andesite-Dacite)

The "intermediate" rocks of the Springdale Group are defined as those with silica values falling between gaps in the data at 56 and 69% SiO_2 , essentially the andesites and dacites (Fig. 4.1.a). They plot mainly within the calc-alkaline field in terms of K_2O vs. SiO_2 , although several altered samples are found within the fields of high-K andesites (Fig. 4.1.b). The data nevertheless tend towards the higher-K side of the calc-alkaline field, with a trend comparable to those of suites ranging from an extensional setting such as Iceland to subduction settings such as the island arcs of the Southwest Pacific (Ewart, 1979). Given the extensional tholeiite nature of the basaltic rocks discussed above, and the abundance of high-silica rhyolites, it is unlikely that the Springdale Group andesites were produced in a subduction setting. This is also in accord with the above interpretation that the tectonic setting of the Springdale Group was analogous to that of the Basin and Range province where, in an

extensional tectonic setting, voluminous andesites were also produced (Gans et al., 1989).

The petrogenesis of andesites has been a subject of controversy since at least the 1920s, with Fenner's (1926) suggestion of an origin by mixing of felsic and mafic magmas in contrast to Bowen's (1928) interpretation of an origin by crystal fractionation. Although these two extremes are still the dominant hypotheses, it appears from the available evidence that the Springdale Group andesites accord with McBirney's (1984) conclusion that "andesite is a derivative magma, and its parent is basaltic", although the transition from parent to derivative might have been brought about in a number of ways. For example, it was shown above that the REE and other trace element concentrations and distribution patterns of the Springdale Group form a continuum from the basalts through andesites to dacites which can be explained by fractionation of olivine, clinopyroxene, Fe-Ti oxides, zircon and plagioclase, and possibly with limited crustal contamination. Given that none of these phases except plagioclase should affect the K/Rb ratios, it is useful to compare the K/Rb ratios for these mafic and intermediate groups (Fig. 4.10). It can be seen from Figure 4.10(a) that there is some overlap between the basaltic and intermediate rocks. However, the intermediate rocks fall into two groups, one similar to the basalts with K/Rb between 1000 and 300, and one more enriched in K and Rb with a more

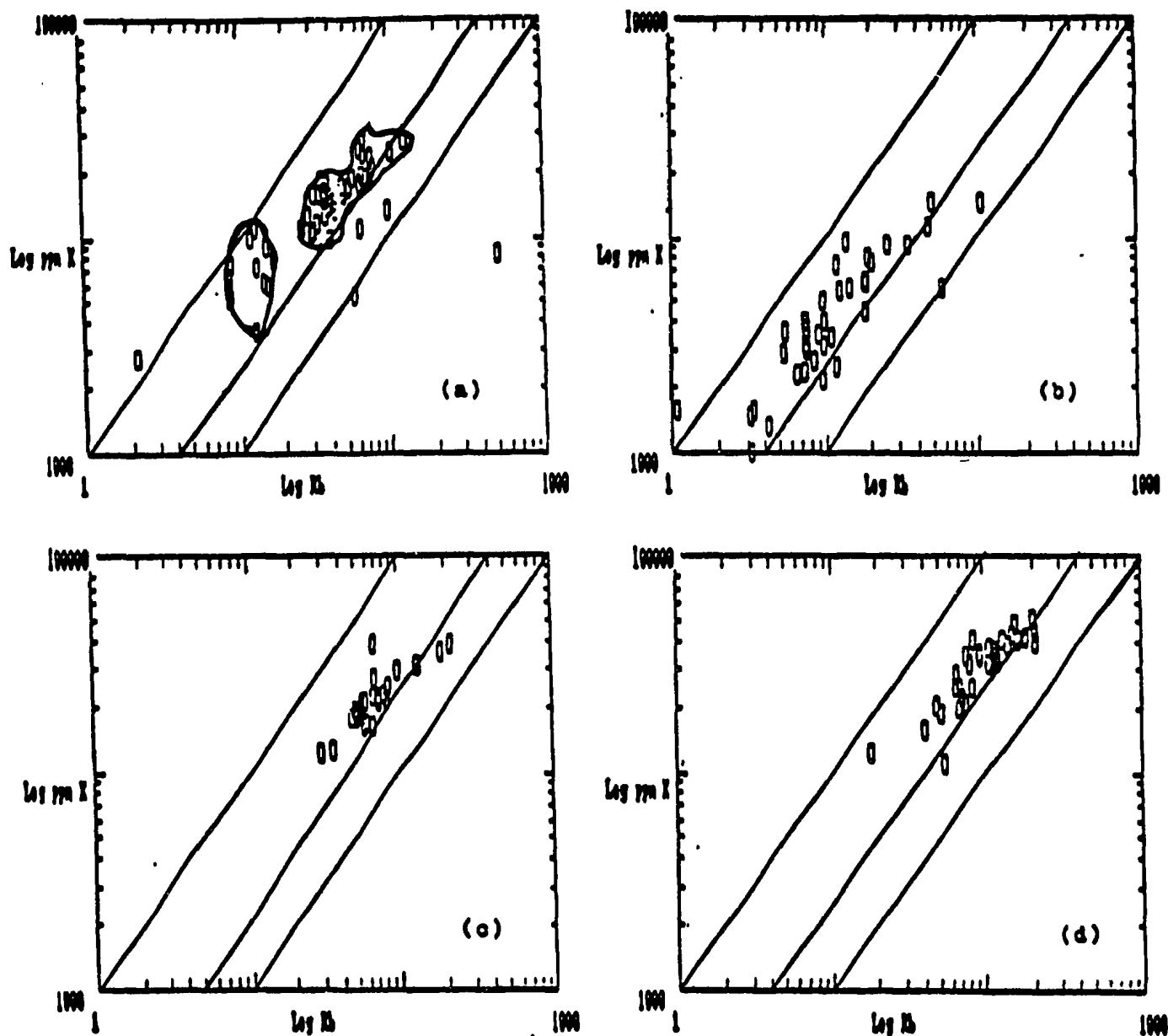


Figure 4.10. K/Rb in the Springdale Group intermediate (a), mafic (b), felsic (c) and silicic rocks (d). The enclosed area in (a) is for most of the basalts shown in (b).

restricted K/Rb range between 500 and 300. The latter lies directly on a trend to the felsic and silicic rocks, and might be explained as resulting from the beginning of fractionation of plagioclase in the suite. This has also been shown more clearly in Figure 4.6(c) where, despite the fact that the Sr and Rb data are independently scattered due to alteration, there is an abrupt kink in the Rb-Sr curve which marks the beginning of plagioclase fractionation within the mafic rocks. As expected, the HFSE such as Zr and Nb maintain their positive correlation within the intermediate group as was seen in the mafic group, indicating that there was no change in the fractionating phases which controlled their distribution, i.e. oxides and zircon (Fig. 4.6.d,e).

4.4. Felsic Rocks (Rhyodacite-Rhyolite)

The "felsic" rocks of the Springdale Group are defined as those which fall between the silica gaps at 69 and 74% SiO_2 (Fig. 4.1.a), i.e. rhyolites-rhyodacites, on a direct continuation of the trend from the intermediate rocks in virtually all diagrams (e.g. $\text{K}_2\text{O}-\text{SiO}_2$, Fig. 4.1.b). They have lower K/Rb ratios than the intermediate rocks, around 300 (Fig. 4.10.c), but exhibit the same positive HFSE correlations and ratios (Fig. 4.6.d,e). Using the classification schemes of Pearce *et al.* (1984) (Fig. 4.11.a) these rocks

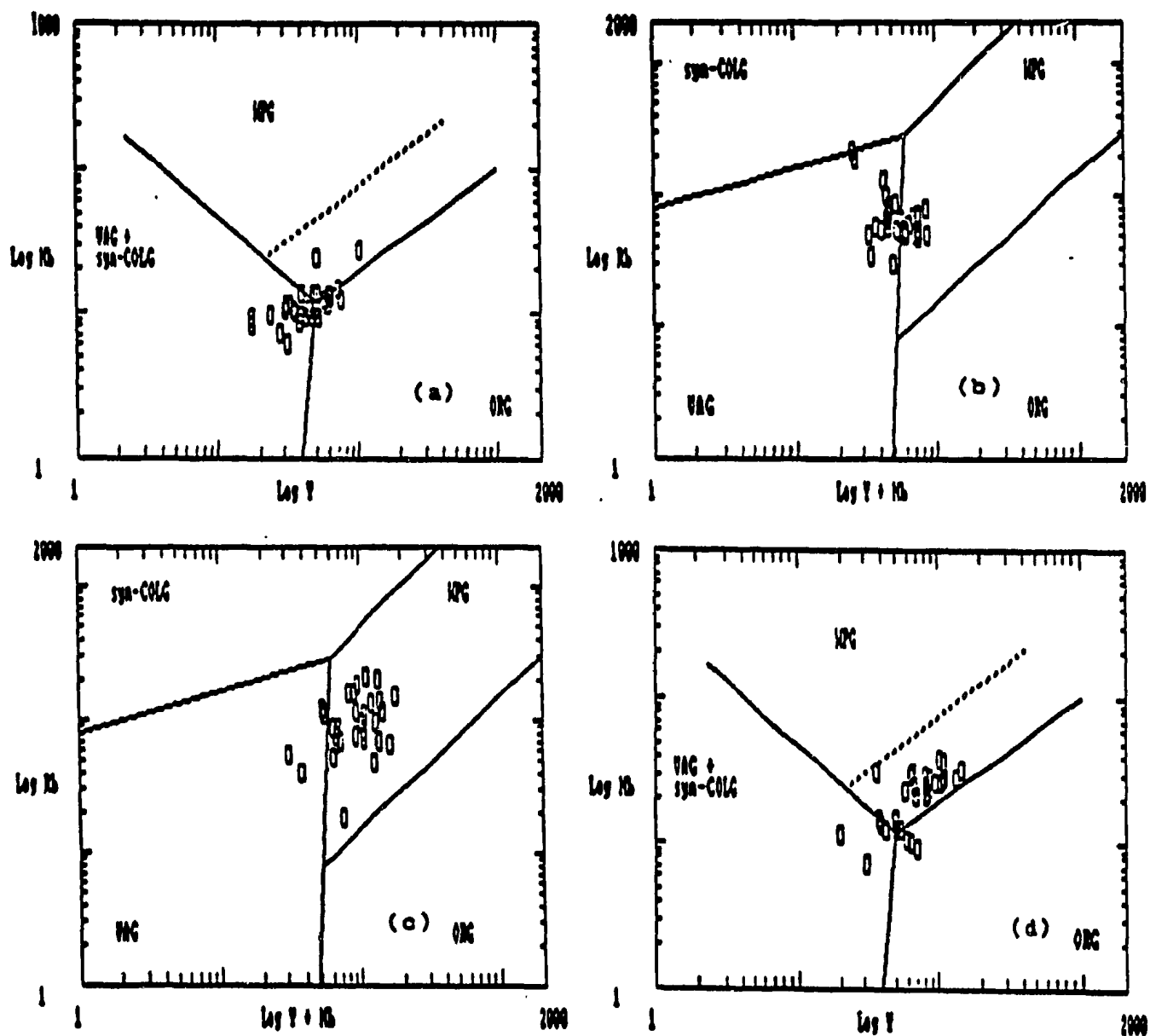


Figure 4.11. Classification of Springdale Group felsic (a,b) and silicic (b,c) rocks according to the scheme of Pearce *et al.* (1984).

straddle all three boundaries between volcanic arc/syn-collisional granites, ocean ridge granites and within plate granites, and the boundaries between volcanic arc granites and within plate granites (Fig. 4.11b). The ocean ridge granites can be excluded because the Springdale felsic rocks have equilibrated in a relatively shallow crustal magma chamber, and are also geochemically continuous with the rest of Springdale Group volcanic rocks. According to Figures 4.11 (c and d), however, these felsic rocks are within plate granites, a classification which is in accord with their tectonic setting.

4.5. Silicic Rocks (High-Silica Rhyolite)

The distinctive group of high-silica rhyolites, with more than 74% SiO_2 (Fig. 4.1.a), are closely similar to the "within-plate granites" of Pearce *et al.* (1984), although a sub-group of these samples straddle the boundary with volcanic arc granites (Fig. 4.11.d,e), as do the felsic rocks (Fig. 4.11a,b). These rocks are also similar to those which are found as late-stage domes and zoned ash-flow tuffs derived from the tops of differentiated magma chambers in continental calderas (e.g. Hildreth, 1979). The Springdale Group high-silica rhyolites are also mostly associated with small domes and their pyroclastic aprons which have been emplaced late in the sequence, although no detailed studies of individual ash flows have been conducted to determine their degree of zonation.

The high-silica rhyolites mostly exhibit the same positive covariance between the HFSE, although they are somewhat more enriched in these elements (Fig. 4.12a,b). They also differ in that some samples are substantially enriched in elements like Nb and Y over Zr. This was also indicated for the rare earth elements, particularly the heavy REE, in Figure 4.8d. Although these rocks also exhibit even more depleted Nb, Sr and Ti anomalies with respect to other elements on these extended REE diagrams than the less silicic rocks, i.e. reflecting even greater fractionation of plagioclase and opaque oxides, the overall enrichments of REE and associated elements require additional processes for their explanation.

The high-silica rhyolites and the lower-silica felsic rocks are compared in more detail in Figure 4.13, where a number of trace elements are plotted against niobium. These elements are typically strongly enriched or depleted not only in high-silica rhyolites (e.g. Hildreth, 1979) but also in peralkaline granites (e.g. Taylor et al., 1981). It is clear from Fig. 4.13 that there is virtually a complete separation of the two types in terms of their Nb contents, as well as Zr, Sr and Y. The high-silica rhyolites also tend to have higher concentrations of Rb and Zn, but there is some overlap of the two groups.

Figure 4.12(a).

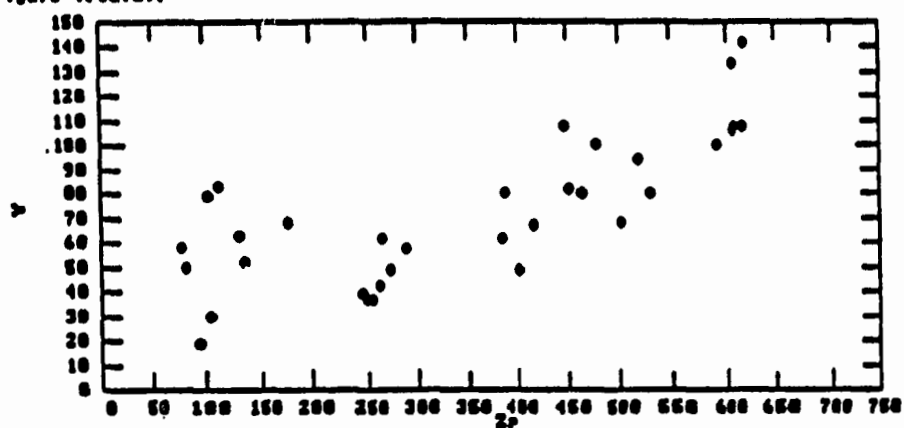


Figure 4.12(b).

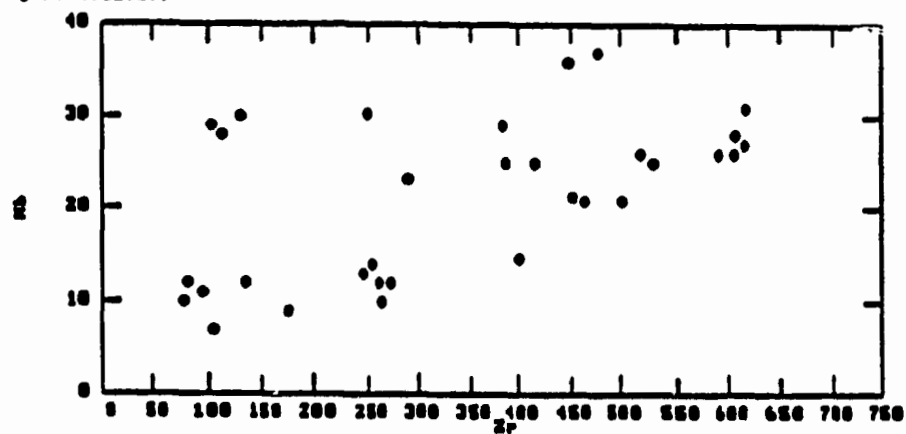


Figure 4.12. Covariation of Y (a) and Nb (b) with Zr in Springdale Group silicic rocks.

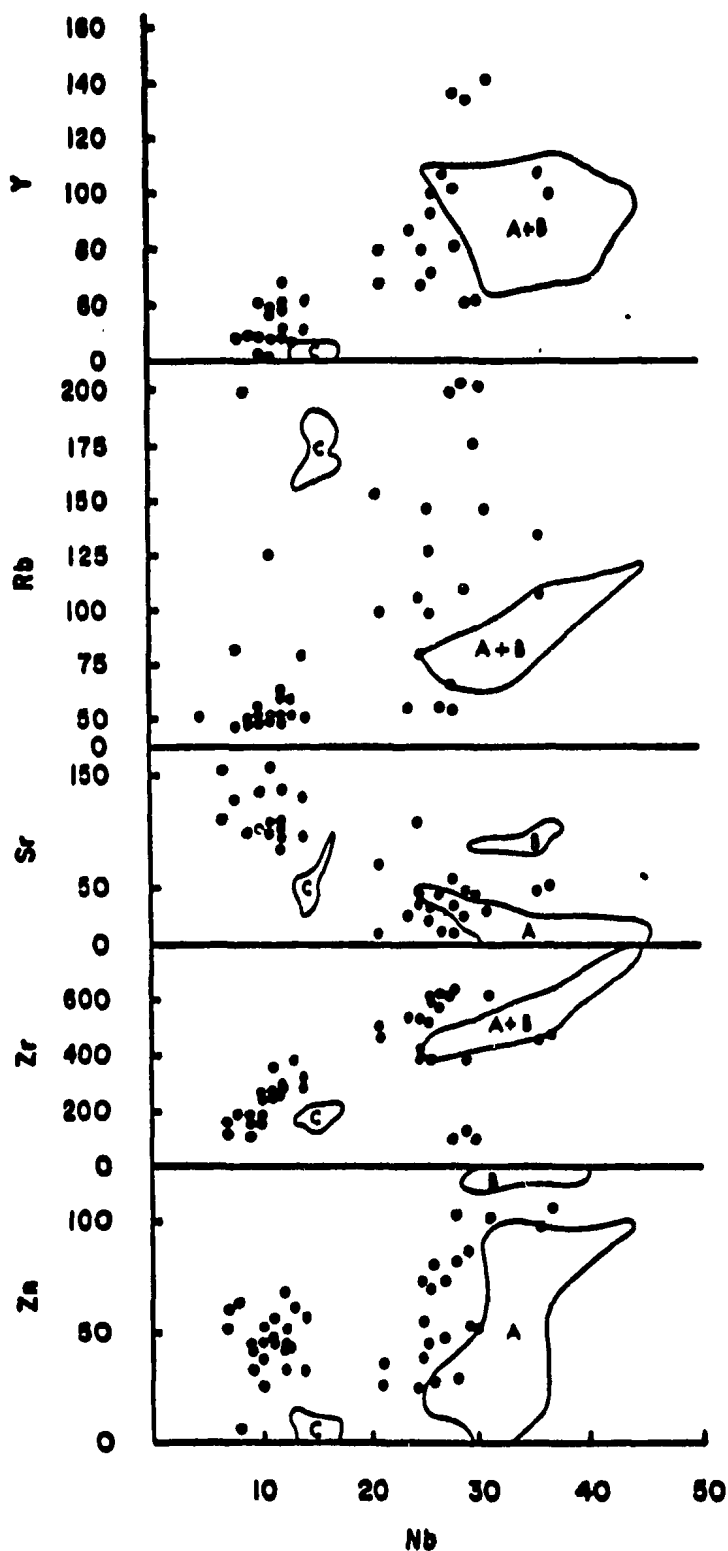


Figure 4.13. Variation of selected elements with niobium in the high-silica (circles) and low-silica (dots) rhyolites of the Springdale Group. Fields from the Kings Point area are shown for ignimbrites and porphyries (A), quartz-feldspar dykes (B), and granitic rocks (C) (from Kontak and Strong, 1986).

Of greater interest is the strong correlation of Nb with Zn, a feature which seems to be unique to peralkaline rocks such as those of the adjoining Topsails (Taylor et al., 1981) and King's Point (Kontak and Strong, 1986). Given that the peralkalinity of the King's Point complex (and Sheffield Lake Group) is at least partly a result of metasomatic (fensitization) processes near intrusive contacts (Taylor et al., 1981; Strong and Taylor, 1984; Mercer et al., 1985; Strong and Coyle, 1987), these patterns in the high-silica rhyolites of the Springdale Group may suggest that similar intrusions are associated with the Springdale, and that similar metasomatic processes were operative. Although such intrusions are not exposed, these features support the suggestion in Chapter 2 of a similar evolutionary history for the King's Point, Topsails and Springdale systems.

The genesis of high-silica magmas has been intensively discussed in the current literature. Hildreth (1979, 1981) has focussed attention on high-level, high-silica magma chambers, interpreting compositional variation in ash-flow tuffs as indicating their source from a large layered magma chamber. Recent models suggest that the layering may arise from a process of thermogravitational diffusion (Hildreth, 1979, 1981) or through convective fractionation (Rice, 1981; Sparks et al., 1984; Tuach et al.; 1988).

Geochemical trends in the Devonian Ackley Granite of eastern Newfoundland led Tuach et al. (1988) to infer a similarity of processes to those operating for the Bishop Tuff magma chamber, i.e. with geochemical zonation in the upper parts of the Ackley magma chamber developed in a silicate liquid with small proportions of crystals, like that of the Bishop Tuff. They further noted that at least two distinct processes seem to have operated in the Ackley Granite magma chamber, producing a greater variability and higher concentrations of U, F, Y, Nb, Rb, and lower concentrations of Sr and Ba, at above 74% SiO₂, precisely as seen for the Springdale Group rocks with greater than 74% SiO₂.

As reviewed by Tuach et al. (1988), such trends might be attributed to crystal/melt fractionation by mechanical processes such as crystal settling or filter-pressing, but such an explanation for both the scatter and enrichment/depletion would require either a sudden change in partition coefficients, or the appearance of new phases for both fractionation and accumulation. Although it is possible that the former could happen, e.g. due to melt depolymerization and complexing by elements of high ionic potential (e.g. Hess, 1980; Watson, 1979), Tuach et al. did not find any evidence for fractionation of the accessory minerals which would be necessary to bring about such changes.

Burnham (1967) has demonstrated that a number of the elements of interest would be partitioned into a volatile phase which coexisted with a silicate melt, and it may be that such a process is operative in high-level magma chambers. Again, however, Tuach et al. (1988) have convincingly dismissed this process because, among other reasons, they could demonstrate that the element enrichments are only the end-products of processes which formed smooth trends observable over a much larger area of the Ackley Granite where there is no physical evidence for volatile activity. While the ash-flow volcanism of the Springdale Group of course provides abundant evidence of volatiles, the Ackley system does demonstrate that such volatiles are not necessarily controls of the observed element patterns in the high-silica rhyolite domes. Their suggestion "that volatile exsolution was another result of the magmatic concentration mechanisms within the magma chamber, rather than a cause of the range of features" seems equally applicable to the Springdale magma chamber(s).

There is no reason to assume anything other than that the Springdale Group high-silica rhyolites were derived from a layered magma chamber like that envisioned by Hildreth (1979), with a high-silica LIL and HFS element-enriched top overlying less silicic magma. This does not necessarily require that Hildreth's model of

liquid-state diffusion was operative, and indeed it has met considerable opposition in the recent literature from both experimental (Lasher et al., 1982) and theoretical (Michael, 1983) points of view. Tuach et al. (1988) preferred a process of concentration of elements in a high-silica roof zone by convective circulation of the magma, involving roof-ward convection of fluid away from crystals forming at the walls of the magma chamber where cooling was fastest and crystallization most effective.

Tuach et al. (1988) pointed out that this removes one of Hildreth's (1979) major objections to crystal fractionation, i.e. the necessity to remove unreasonably large proportions of crystals. Michael (1983) also pointed out that fractionation of 65-70% of the observed phases could explain the variations in the Bishop Tuff (e.g. extreme Ba and Sr depletion) and Sparks et al. (1984) demonstrated that side-wall crystallization provides an acceptable physical mechanism. As with the process of thermogravitational diffusion expounded by Hildreth (1979, 1981), the convective fractionation model of Sparks et al. (1984) could be self-enhancing in that the zone of crystallization would become depleted in Ba and Sr and enriched in volatiles and LIL-HFS elements. The later lowest-density material to rise to the top of the magma chamber would produce the most evolved high-silica rhyolites, thus accounting for their presence in the

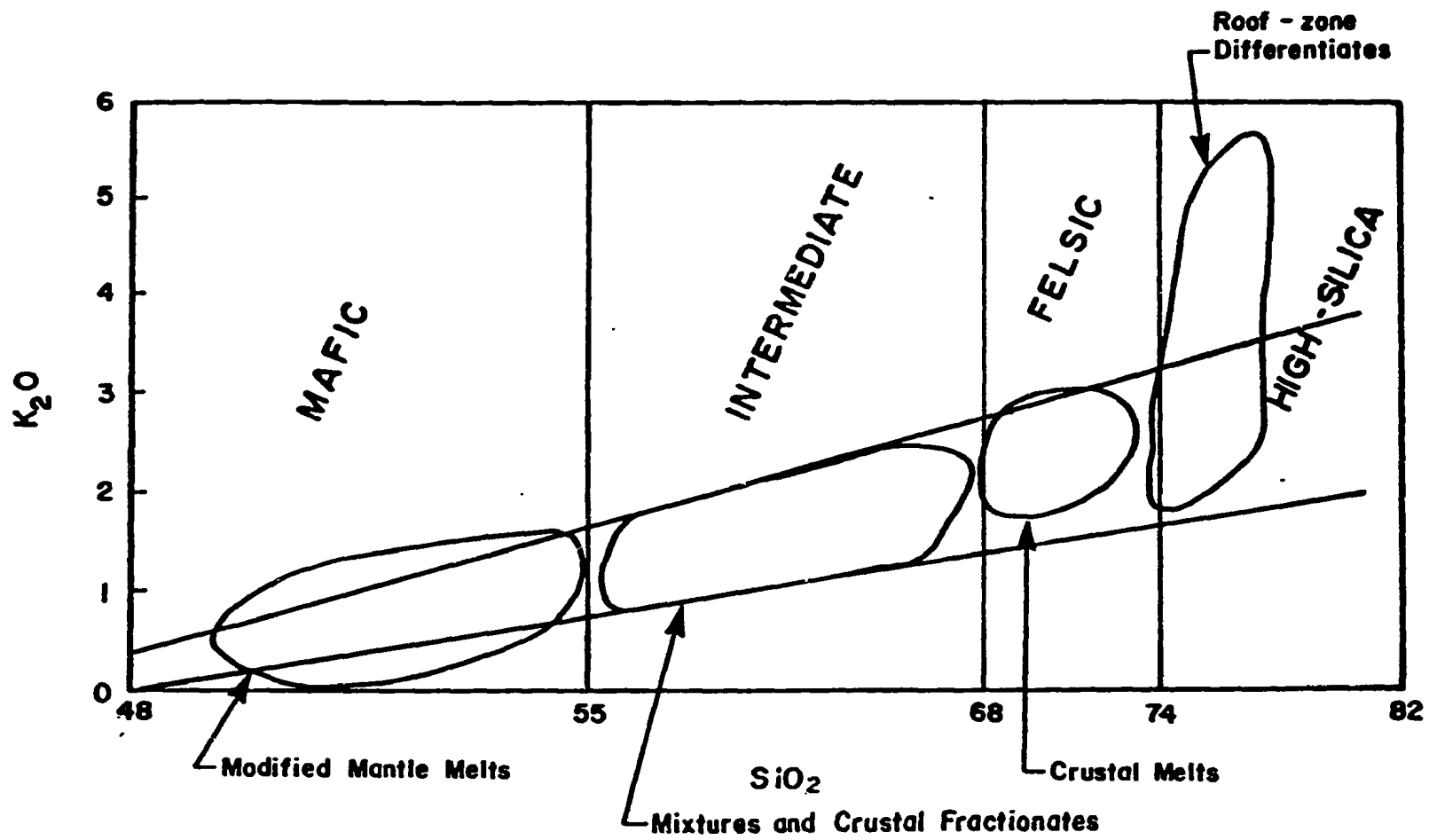
late-stage domes. The similarity of these patterns to those observed in the King's Point and Topsails peralkaline rocks would suggest that similar processes were operative there, that is that the metasomatic effects are the result of fluids produced at the end-stages of convective fractionation within the magma chambers.

4.6. Summary and Conclusions

The Springdale Group data, as shown in Figure 4.1(a), are naturally divisible into four groups based on silica values, viz. "mafic" (basalts and basaltic andesites), "intermediate" (basaltic andesites, andesites and dacites), "felsic" (dacites and rhyodacites), and "silicic" (rhyolites and high-silica rhyolites). The first three groups form a typical calc-alkaline trend which can be interpreted as having been produced by fractionation of olivine, clinopyroxene, plagioclase, Fe-Ti oxides and zircon. The fourth group, found mostly as late-stage domes, is typical of high-silica rhyolites produced in the late stages of development in the roof zones of large magma chambers, and are interpreted to have been similarly produced by processes dominated by convective fractionation. These latter rocks, along with other geochemical characteristics of the less silicic rocks (e.g. the basalts being non-arc tholeiites) suggest that the Springdale Group was formed in an extensional environment

which included continental crust. The preferred genetic interpretation of these rocks is schematically outline in Figure 4.14.

Figure 4.14. A schematic representation of the genesis of the Springdale Group volcanic rocks. The basalts from primary mantle melts modified by olivine \pm clinopyroxene during ascent. The felsic rocks are crustal melts produced by heat from the mantle melts during their ascent through the crust. These two types of melt accumulated in a shallow magma chamber and produced the intermediate compositions by a combination of magma mixing and fractionation of olivine - clinopyroxene - plagioclase - Fe-Ti oxides. The high - silica rocks were produced by accumulation in the roof zone of the magma chamber of low - viscosity, gas - charged melts which could have formed by a combination of processes including side - wall crystallization, thermogravitational diffusion and volatile transport.



5. GEOCHRONOLOGY

5.1. Introduction

The method of precise U/Pb zircon dating (Krogh, 1982) offers a particularly powerful, perhaps the only, method for attacking the problems associated with establishing the internal stratigraphy and external correlations of altered non-fossiliferous Paleozoic felsic volcanic sequences. This approach was used in the present study to obtain five new zircon dates. These are for samples from the lowermost and uppermost ash-flow tuffs and an intermediate-aged rhyolite dome of the Springdale Group within the caldera, a syenite from the King's Point Complex, and an ash-flow tuff from the Cape St. John Group. These units were dated for the primary objective of bracketing the ages of individual units of the Springdale caldera, as an independent check on their relative ages based on geological observations and interpretations, and to determine the time span over which the caldera was active. The second important objective was to determine the ages of associated volcano-plutonic sequences in order to evaluate proposed correlations and volcanic/plutonic/tectonic interpretations based on these correlations in Newfoundland and elsewhere in the orogen.

The data are summarized in Table 5.1 and Figures 5.1 to 5.5, and details of the method are given in Appendix 5.

Table 8.1. Summary of the U/Pb isotopic data for zircon geochronology.**Springdale Group and Related Rocks**

FRACTIONS No. Properties (1)	CONCENTRATIONS			ATOMIC RATIOS						AGE(Ma)
	Wt. [mg]	U [ppm]	Pb common [pg]	^{206}Pb	^{207}Pb	^{208}Pb	^{206}Pb	^{207}Pb	^{207}Pb	
				^{204}Pb	^{206}Pb	^{208}Pb	^{206}Pb	^{207}Pb	^{206}Pb	

Springdale Eruptive Rocks**I Welded Lithic-Crystal Tuff [ZR-11]**

1 Zircon ONM+M1,-100+200,cl,n,A	0.130	1312	73	10 028	0.05874	0.16281	0.06802	0.5260	432
2 Zircon ONM,-100+200,cl,p,A	0.044	1145	31	6 733	0.05859	0.14770	0.06848	0.5245	434
3 Zircon M3,-100+200,os,cr,NA	0.174	1289	182	5 888	0.05788	0.17887	0.06724	0.5148	434
4 Zircon M3,-100200,cr,p,NA	0.050	1284	54	4 785	0.05811	0.16478	0.06868	0.5043	433

II Lithic-Crystal Tuff [ZR-3]

5 Zircon 1NM+M,-300,be,sh,LA	0.075	1636	298	1 785	0.05323	0.13748	0.06822	0.5208	428
6 Zircon ONM,-100+200,be,s,p,A	0.042	1545	84	2 835	0.05869	0.12539	0.06842	0.5227	428
7 Zircon ONM,-200+325,be,s,p,LA	0.044	2185	103	3 791	0.05863	0.02733	0.06839	0.5231	432
8 Zircon 1NM,-100+200,be,s,p,A	0.046	1332	58	4 338	0.05861	0.12372	0.06802	0.5313	446

Springdale Intrusive Rocks**III Burnt Berry High-Silica Dome [ZR-7]**

9 Zircon 1NM+M,100,+200,be,p,A	1.480	73	48	6 564	0.05887	0.15081	0.06877	0.5257	430
10 Zircon ONM,-200+325,eu,be,A	0.237	74	18	4 840	0.05838	0.15212	0.06880	0.5258	430
11 Zircon 1M,-100+200,be,s,p,A	0.220	73	33	2 008	0.05918	0.15807	0.06870	0.5256	432

King's Point Complex**IV Granite-Quartz Syenite [KP-1000]**

12 Zircon 1NM,-100+200,eu,s,A	0.098	224	11	8 188	0.05548	0.21844	0.06880	0.5230	427
15 Zircon 1M,-100+200,s,y,p,A	0.080	268	12	5 334	0.05578	0.22808	0.06838	0.5218	428

Cape St. John**Welded Lithic Tuff [CSJ-10]**

16 Zircon ONM,-300+325,cr,n,A	0.116	163	10	6 267	0.55408	0.16108	0.06883	0.5236	428
17 Zircon 1M,-300+325,cr,n,A	0.131	209	37	3 180	0.58840	0.17488	0.06843	0.5230	430
18 Zircon 1M,-100+200,s,p,A	0.030	163	16	1 538	0.64788	0.17080	0.07320	0.6200	864
19 Zircon 1M,-100+200,s,s,p,A	0.121	179	13	7 828	0.57038	0.14588	0.07821	0.7636	828

NOTES:

- (1) NM, M = non-magnetic, magnetic at indicated degree of tilt of Frantz isodynamic separator (at 1.6A and 0° slope); 1.35M = magnetic at 10° slope at 1.35A 100, 200 = size in mesh; py = pale-yellow; cl = clear; eu = euhedral; ov = oval shaped, resorbed; pr = prismatic; oc = contains visible core; t = turbid; b = brown; pb = pale brown; or = cracked; f = faceted; s = subhedral; db = dark brown; m = milky; rb = red-brown.
- (2) concentrations are known to $\pm 0.5\%$ for sample weights over 1 mg, $\pm 1\text{-}2\%$ for sample weights between 1.0 and 0.2 mg, and $\pm 5\%$ for sample weights less than 0.1 mg.
- (3) corrected for 0.117 mole fraction of common Pb in the ^{206}Pb spike.
- (4) measured ratio relative to total radiogenic Pb.
- (5) corrected for fractionation and blank; U blank = 2 pg; Pb blank = 10pg; Pb and U fractionation correction = 0.1%/amu ($\pm .05\%$).
- (6) corrected for fractionation, spike, blank, and initial common Pb; error for zircon is estimated at 0.25% for Pb/U and 0.1% for $^{207}\text{Pb}/^{206}\text{Pb}$ at the 2-sigma level (errors are estimated from replicate analyses); error for titanite and rutile is estimated at 0.5% for Pb/U and 0.1% for $^{207}\text{Pb}/^{206}\text{Pb}$.

5.2. Results

5.2.1. Springdale Group, Unit 1 (Sample Zr-11)

Sample no. Zr-11 was taken from Unit 1, the lowermost of the volcanic units within the Springdale caldera. In general this unit comprises a moderately welded, lithic-crystal tuff, commonly highly fractured or cleaved along its eastern margin. It differs from most of the other overlying ash flows in that fractured and broken crystals of both plagioclase and K-feldspar are present, along with accessory biotite, quartz, and rare opaques. The lithic clasts include plagiophyric basalt, andesite, serpentinite, jasper, and granophyric, perlitic and other felsic clasts. The matrix includes shards, rock and crystal fragments, and partially welded eutaxitic pumice lapilli. The actual sample from which the zircons were separated was taken from a finer grained ashy lithology of the unit in an attempt to avoid lithic debris and thus lessen the possibility of zircon xenocrysts.

In thin section this sample is seen to be a fine-grained recrystallized ashy portion of Unit 1, representing a lithic-poor or distal facies of this unit. It shows little evidence of primary welding textures or vitric clasts although such features were noted on the outcrop. The thin section is composed of groundmass quartz and feldspar (albite) in roughly equal portions. The groundmass has abundant sericite alteration, both as

individual sheaves projecting into cavities, as intergrowths along grain boundaries, and as alteration of the feldspars. Small epidote needles are seen as a common alteration product. Zircon can be seen in this thin section only under the highest magnifications, not surprisingly in this sample which contains only 133 ppm Zr (see Appendix D, sample 3-6-8).

Each sample was examined with the scanning electron microscope and analysed with the energy dispersive microprobe in order to ensure an adequate zircon population for age-dating. Plate 5.1 is a split-screen photograph of sample Zr-11 showing a typical back scatter electron image on the top half with three zircons present. The bottom half is an X-Ray map for Zr which identifies the three crystals of zircon.

The zircon population of sample Zr-11 was relatively small (i.e. low yield) and the zircon crystals are small (-100- \rightarrow +200 mesh), thin, elongated clear prisms with cracks running the length of the crystal (see Plate 5.2). The sample showed no evidence of cores and therefore only light abrasion was necessary to remove the problems of surface leaching and lead loss. Four fractions were run to establish a truly concordant point (See Table 5.1 for weights and other pertinent data). The first two fractions were picked from the M 3⁰ yield so as to preserve the small M1⁰ and NM fractions and to bracket the Pb

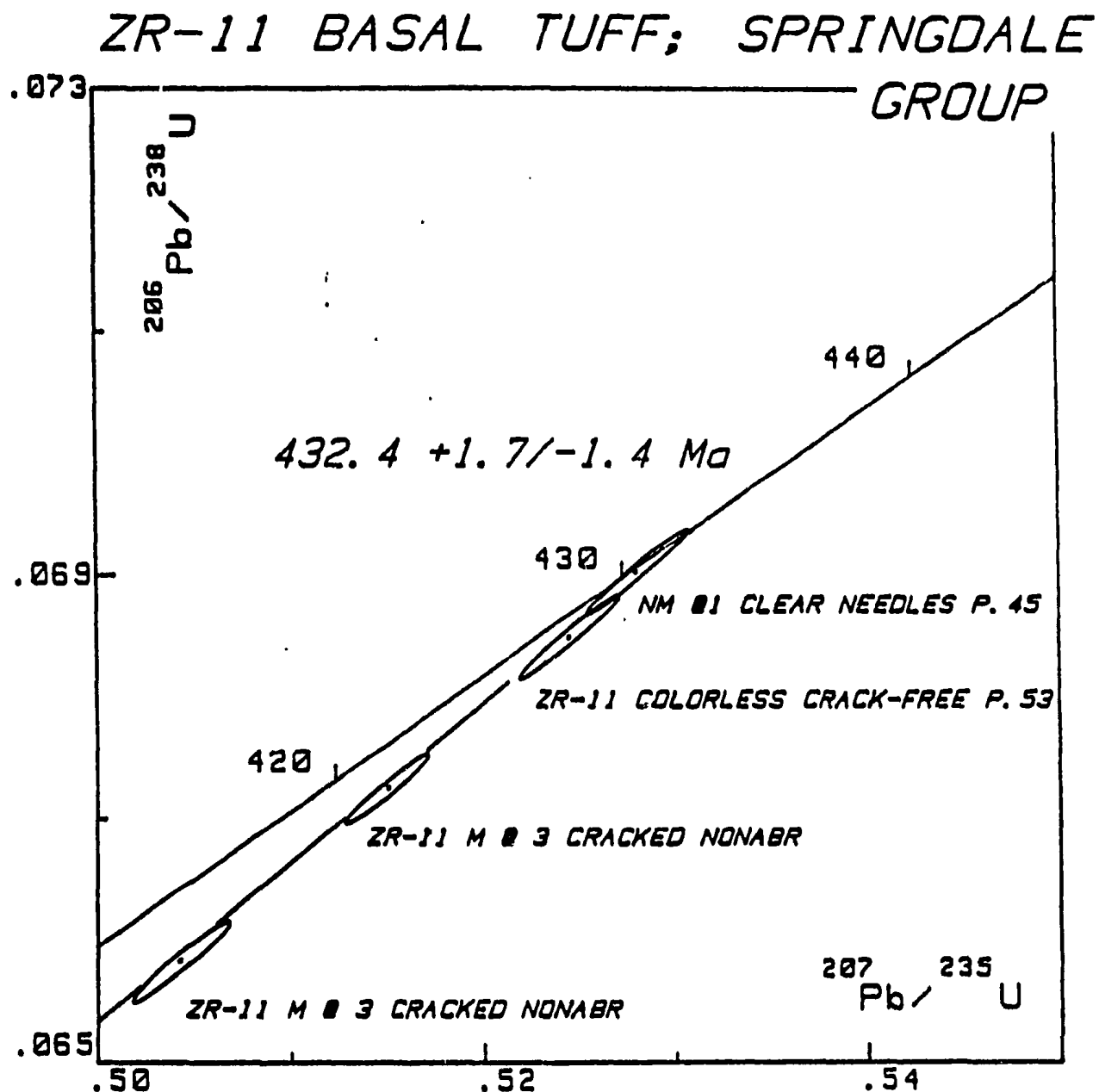


Fig. 5.1. Concordia plot for sample ZR-11. Springdale Group, Unit 1.

Plate 5.1. Split-screen photograph of sample Zr-11 showing a typical back scatter electron image on the top half, with three zircons present. The bottom half is an X-Ray dot map for Zr which identifies the three crystals of zircon.

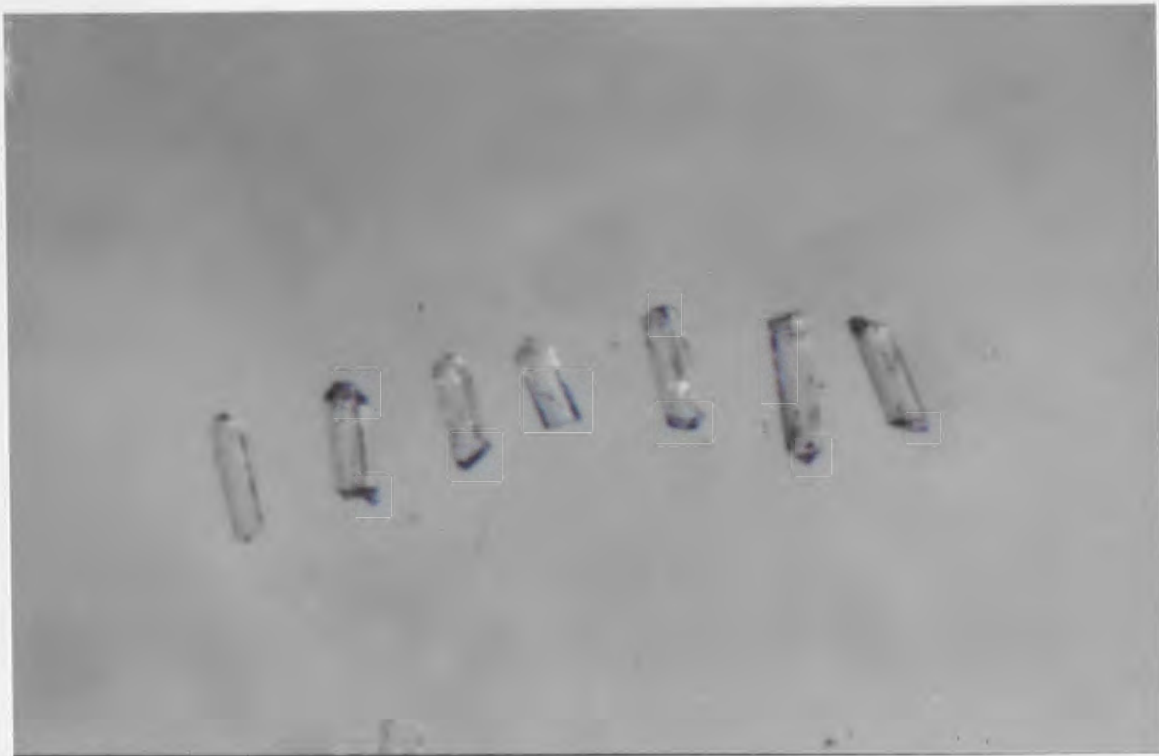
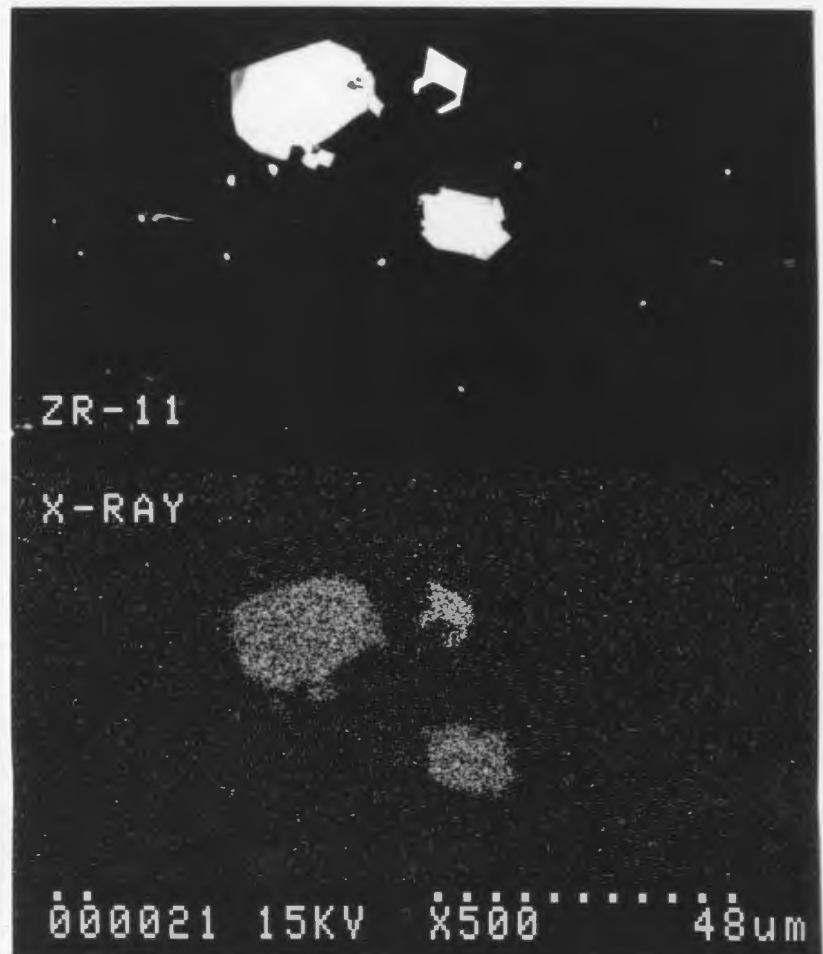


Plate 5.2. Small (-100->+200 mesh), thin, elongated clear zircon prisms with cracks running the length of the crystal. Sample Zr-11.

concentrations for spiking the final fractions properly. This method is typically employed to produce a "lead-loss line" with limited zircons. The final fraction was abraded and produced clear, relatively crack-free, glassy elongate ovals (See Plate 5.3) which plotted on concordia. Figure 5.1 shows the relationships between the various fractions on the concordia diagram, based on regression calculation carried out as outlined by Davis (1982), with errors on the calculated ages quoted at the 95% confidence level. The clear abraded fractions plot directly on concordia at an estimated age of $432.4 \pm 1.7/-1.4$ Ma, with the cracked non-abraded fractions and a discordant abraded fraction all plotting linearly away from it along a lead loss line.

5.2.2. Springdale Group, Burnt Berry Dome (Zr-7)

Sample Zr-7 was taken from the Burnt Berry Dome, a rhyolite dome which was interpreted to have been emplaced in the middle stages of the Springdale caldera sequence, although with its high-silica composition and proximity to late-stage caldera in-fill lithologies, it appears to be a late-stage feature, as is typical for high-silica domes observed in other such calderas. As described above, these rocks are flow-foliated with extreme convolution seen as fluidal folds and disruption of flow banding, auto-brecciated and contain zones of intense development of lithophysae and other indications of gas-streaming. These

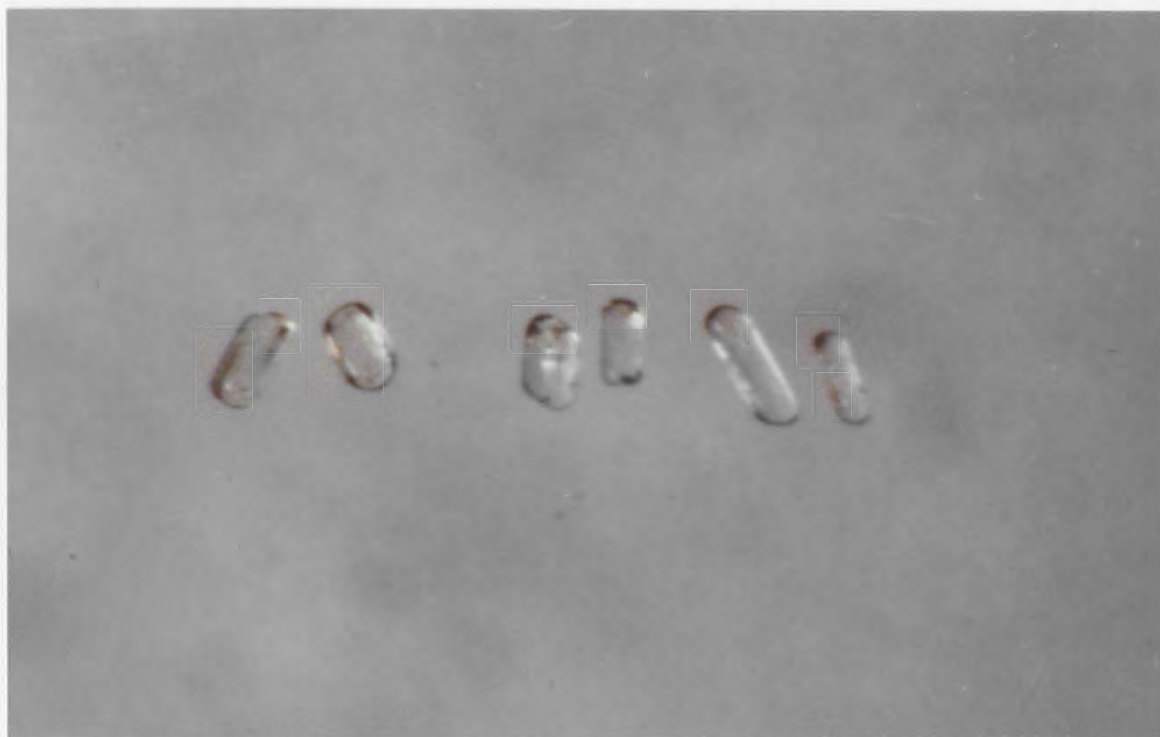


Plate 5.3. Selection of the final abraded fraction used for dating - clear, relatively crack-free, glassy abraded prisms - of zircon from Unit 1, sample no. Zr-11.

rocks were earlier suggested to be correlative with younger granitoid rocks which were intruded along faults bounding the Springdale Group in the east and west, and truncate much of the stratigraphy in the south as part of the Topsails Complex (Coyle and Strong, 1986).

In thin section the Burnt Berry Dome is made up of devitrified fine "glassy" rhyolite with granophyric texture, microphenocrysts of K-feldspar are common. Patches and sprays of hematite are characteristically disseminated as microlites in the groundmass. Sample no. Zr-7 from which the zircons were extracted has a typical devitrification mosaic texture under crossed polars (intergrowths of quartz and feldspar). Devitrification spherules (radiating axiolitic sprays of quartz and feldspar) are common and in general the section shows a predominance of granophyric patches. Resorbed and hematite-stained phenocrysts of K-feldspar are common. Zircons are distributed as isolated blocky crystals throughout the thin section, with no preference for the granophyric groundmass or phenocrysts.

The zircon population obtained from sample ZR-7 consists of stubby, vitreous, clear, beige, euhedral prisms (Plate 5.4) with no evidence of cores or cracks, i.e. no suggestion of inheritance or alteration. With strong abrasion the zircons are well polished clear crack-free ovals as seen in Plate 5.5 and accordingly they plot directly on concordia, with an estimated age of 400.8 ± 2 Ma (see Fig. 5.2 and Table 5.1).



Plate 5.4. Selection of the zircon population obtained from sample ZR-7 consists of stubby, vitreous, clear, beige, euhedral, prisms with no evidence of cores or cracks.

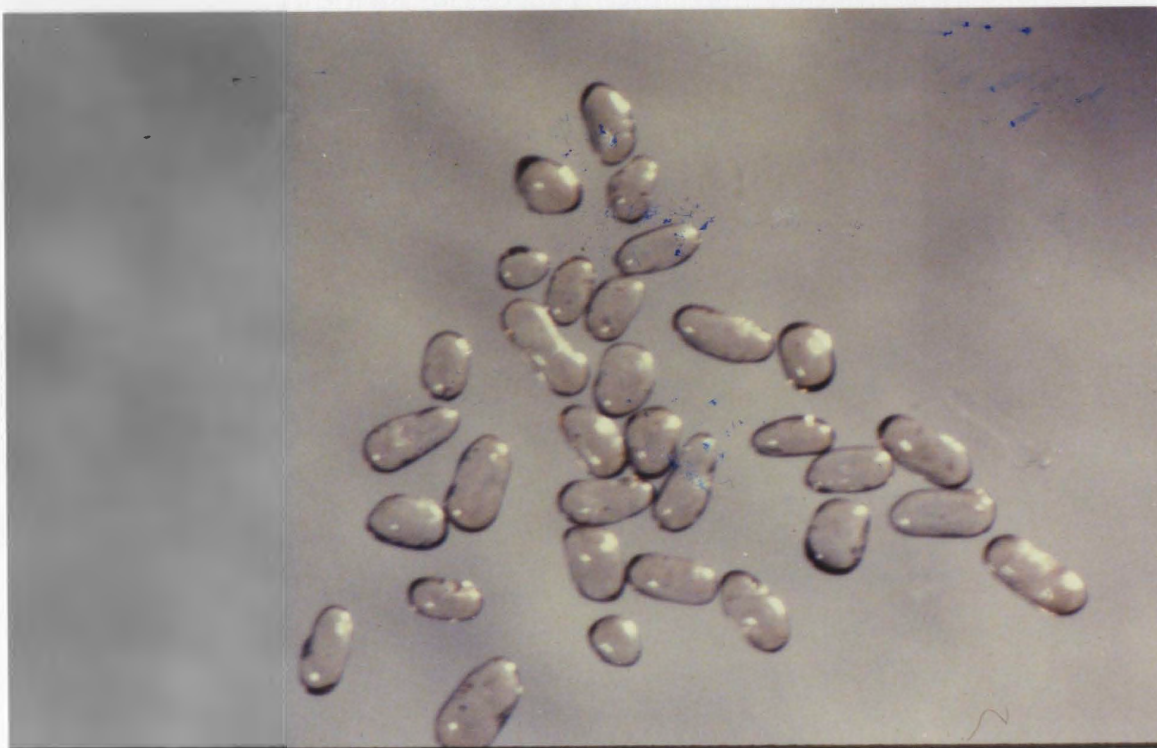


Plate 5.5. Strongly abraded, well polished, beige crack-free ovals of zircon from Burnt Berry dome sample Zr-7.

ZR-7 BURNTBERRY DOME

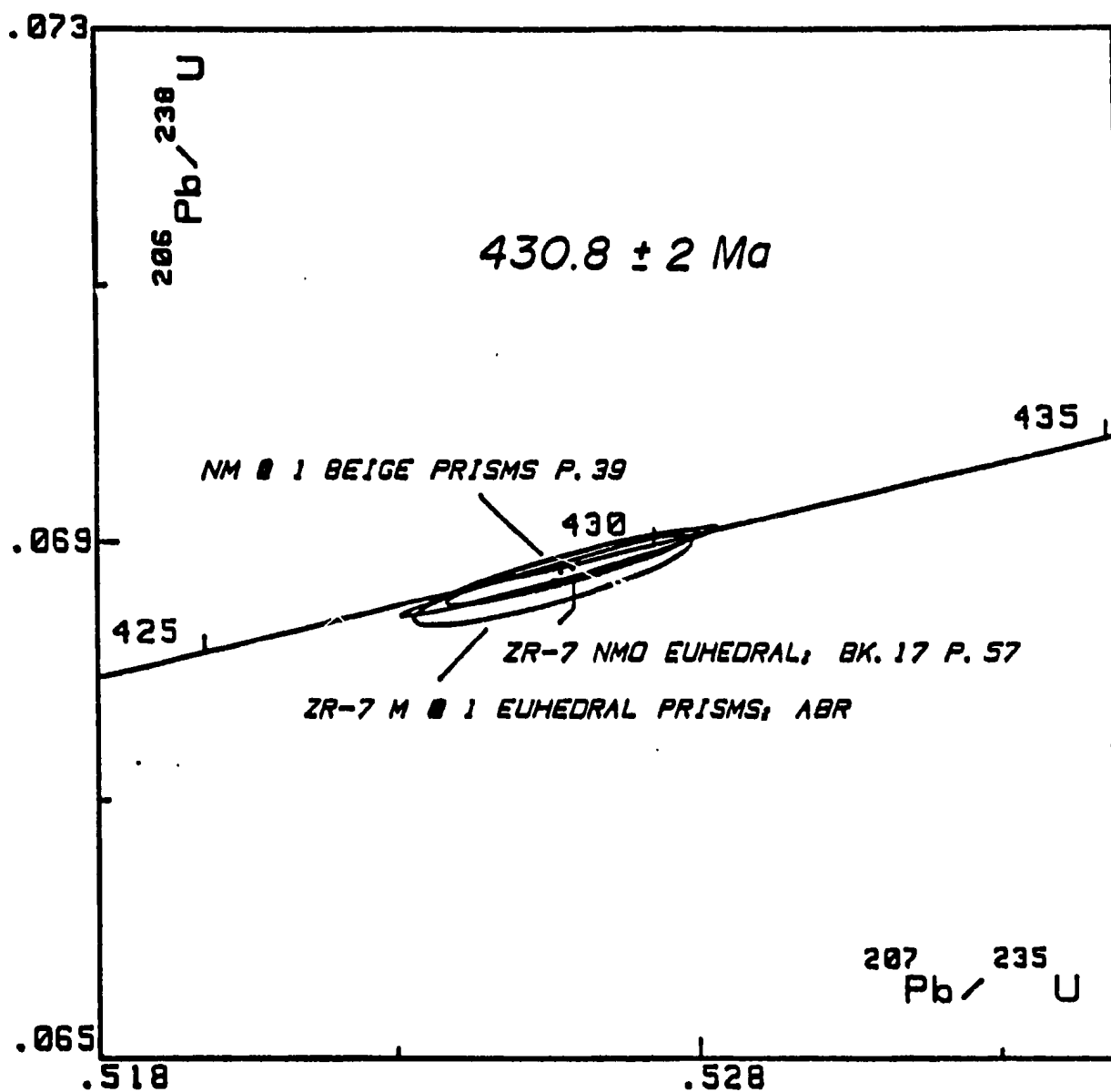


Figure 5.2. Concordia plot for zircon sample no. Zr-7, Burnt Berry Dome.

5.2.3. Springdale Group, Unit 10 (Sample Zr-3)

Sample no. Zr-3 was taken from Unit 10, the Indian River Tuff, an orange to brown crystal-lithic tuff found mainly in the interior of the caldera but overlapping its margin in the northwest. This crystal tuff is very massive and generally strongly welded, with abundant (up to 60%) large phenocrysts of quartz and feldspar, and clasts of jasper, mafic and ultramafic lithologies. It caps the volcanic sequence of the caldera and is interbedded with red sandstones of the caldera-fill stage of development, and is seen to directly overly basement rocks of the Lushs Bight Group outside the northwestern margin of the caldera. Its similarity to phases of the King's Point Complex led Coyle and Strong (1987) to suggest that it was in fact derived from the King's Point and not the Springdale caldera. This unit was dated at $429 \pm 6/-5$ Ma by Chandler et al. (1987), who suggested that one discordant sample reflected inheritance from older xenocrysts which they observed as cores in euhedral zircons.

In thin section (Plate 5.6) sample no. ZR-3 from which the zircon was taken is spectacularly phenoclastic with large broken and resorbed phenocrysts of quartz, K-feldspar and plagioclase comprising (in roughly equal proportions) about 60% of the rock with about 10% vitric and lithic clasts in a moderately welded eutaxitic matrix littered with fine crystal fragment debris. Melt inclusions

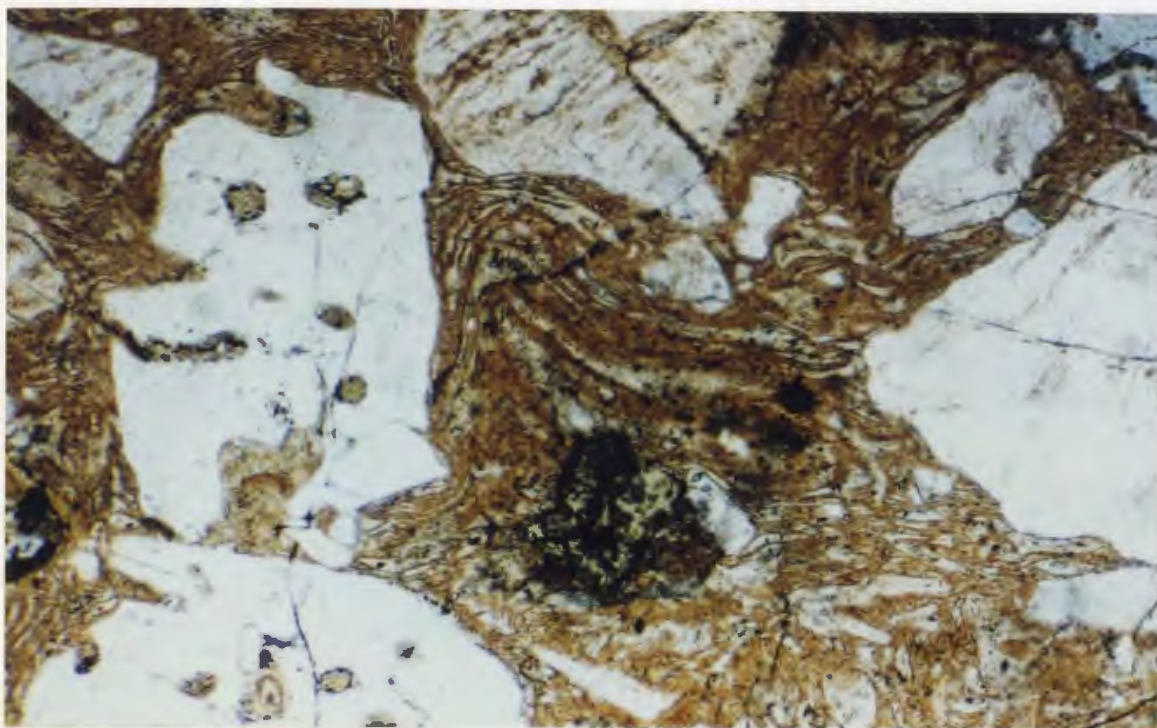


Plate 5.6. Photomicrograph of sample no. ZR-3. Large broken and resorbed phenocrysts of quartz, K-feldspar and plagioclase, with vitric and lithic clasts in a moderately welded eutaxitic matrix littered with fine crystal fragment debris.

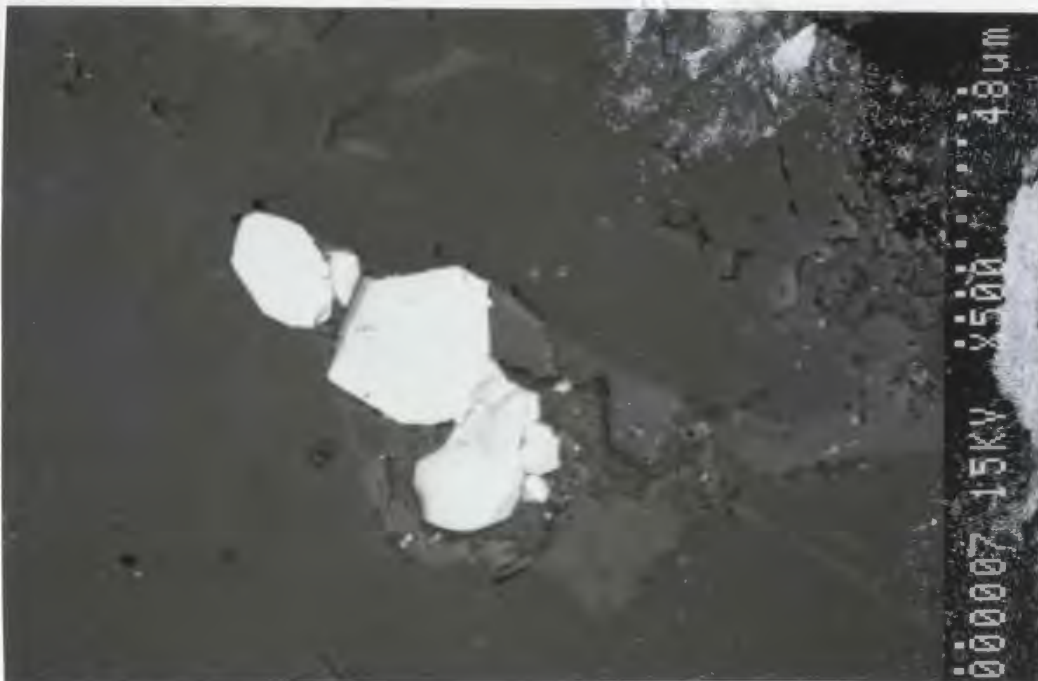


Plate 5.7. Crystal clusters of zircon identified in sample Zr-3, using the scanning electron microscope; back-scattered electron image.

are abundant in the quartz phenocrysts and rare in the feldspar phenocrysts. Both the matrix and feldspar phenocrysts have been oxidized and lightly sericitized. Zircon crystals tend to be small and difficult to detect in the oxidized groundmass. They are, however, readily detectable as individual crystals, fragments and clusters using the scanning electron microscope (Plate 5.7).

The zircons separated from sample Zr-3 were all stubby to blocky euhedral prisms, with some containing darker cores, as observed by Chandler et al. (1987). Both the clear crystals and clear beige shards and tips of cored crystals were used for dating (Plate 5.8), and one crystal was abraded for analysis of the core to assess inheritance. As shown in Figure (5.3), all fractions except the core plot on or near concordia, giving an estimated age of 425 ± 3 Ma. This is 4 Ma younger than the age estimated by Chandler et al. (1987), but the higher precision suggests that this younger date is preferable. This is supported by the fact that the core sample dated in this study is, like the discordant sample of Chandler et al., offset from concordia to indicate an inherited age of 1346 ± 230 Ma. While this age is not readily identified in the known potential Precambrian source rocks of the region, the precision on the "inheritance age" is not adequate to assess precisely, any such origin. Nevertheless, it is not unreasonable that zircons of this age would be found in rocks which are precursors to the Grenville basement seen

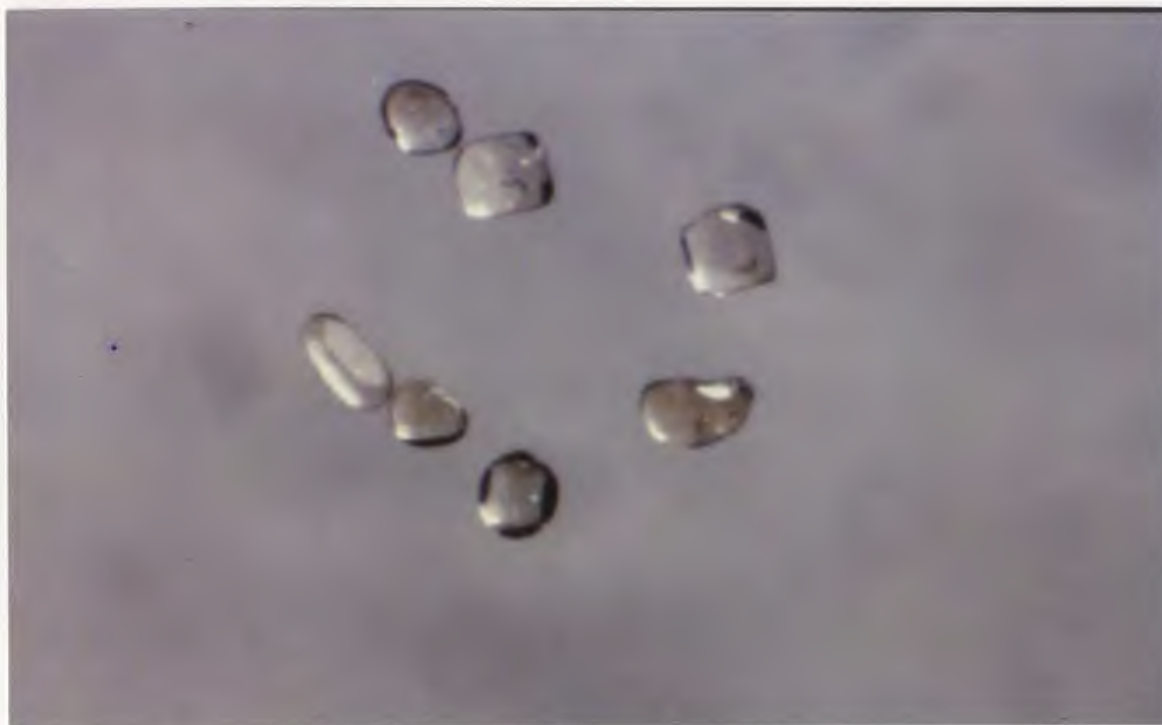


Plate 5.8. Clear crystals and clear beige shards and tips of cored crystals of sample Zr-3, Unit 10.

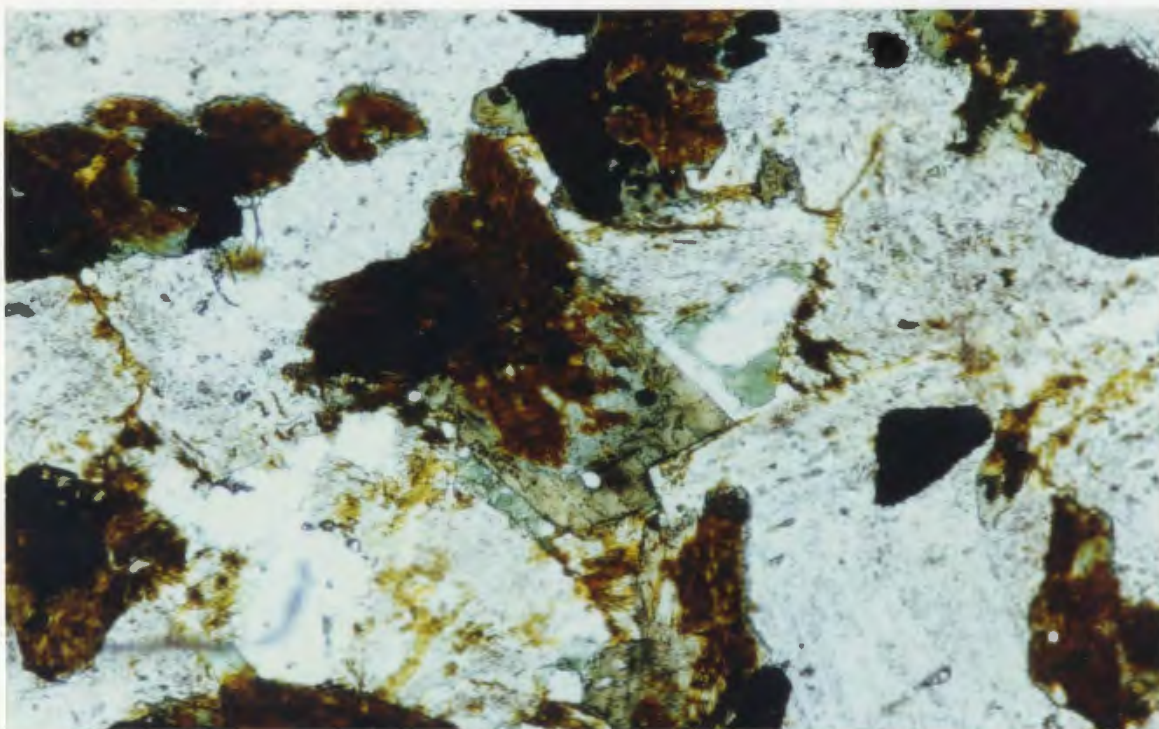


Plate 5.9. King's Point Complex, sample no. KP-1000.
Biotite intensely altered to hematite, sericite, chlorite and epidote, with rim overgrowths of sodic amphibole.

ZR-3 CRYSTAL LITHIC TUFF

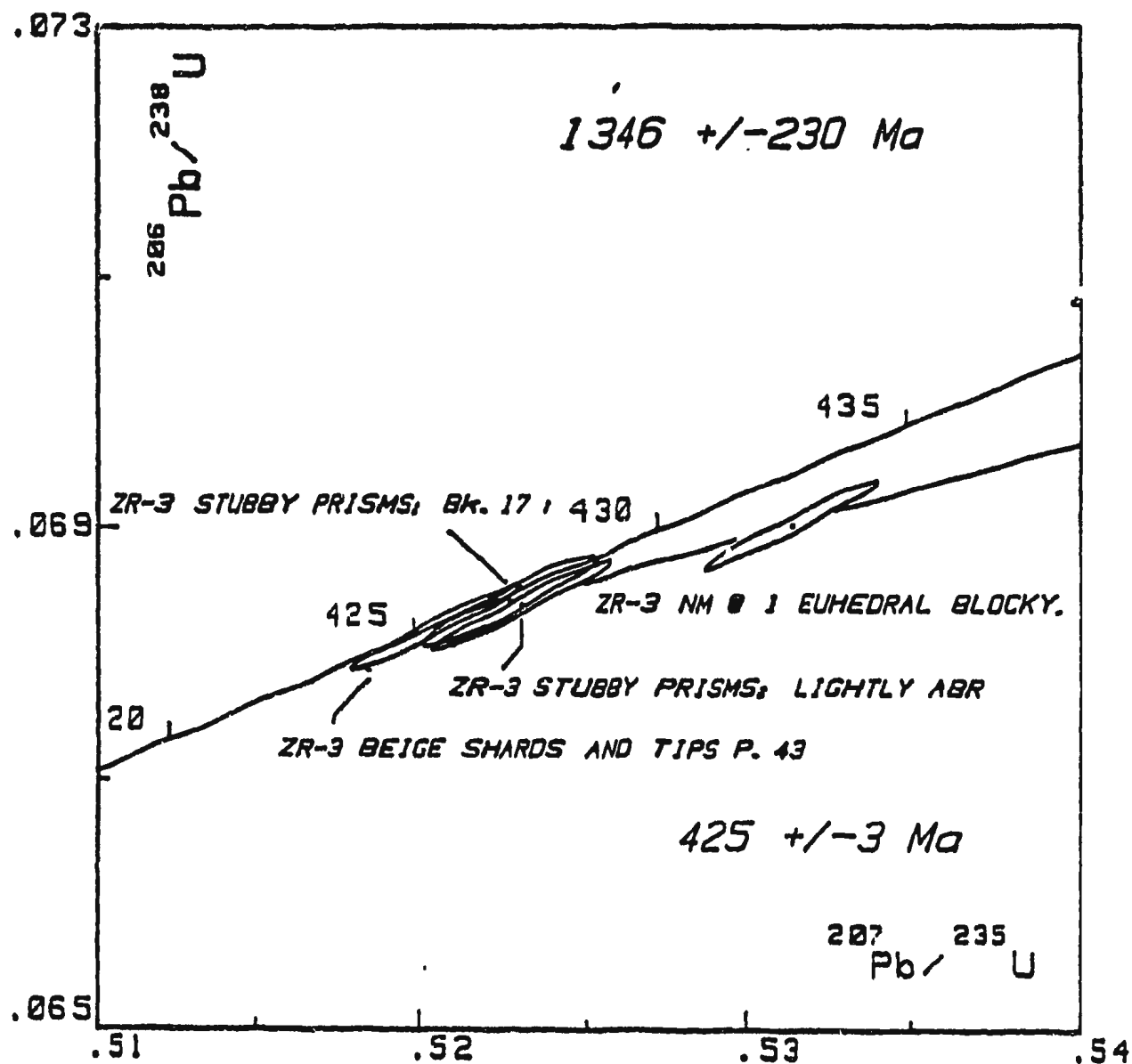


Figure 5.3. Concordia plot for zircon sample no. Zr-3, Indian River Tuff.

to the west of the Springdale Group and inferred to be beneath it by previous workers. These observations support the interpretation from other independent geochemical data that these rocks were derived from underlying continental crust, as is typical for such large siliceous volcanic terranes.

As described above, the striking similarity between the Indian River Tuff of the Springdale Group and some rocks of the King's Point complex suggests that this tuff is an outflow facies of the King's Point caldera. If this is so, its position at the top of the Springdale Group indicates that the King's Point complex (or at least this phase of it) is somewhat younger than, but overlapping in time with the Springdale caldera volcanism.

5.2.4. King's Point Complex (Sample KP-1000)

The sample dated from the King's Point Complex, no. KP-1000, is a holocrystalline quartz syenite with very large (up to 1 cm long) phenocrysts of K-feldspar in a coarse granular to granophyric groundmass of intergrown quartz, K-feldspar, plagioclase, biotite, magnetite, and accessory apatite and calcite. Alteration of the feldspars is characterized by hematitic and sericitic dusting. The biotite is more intensely altered to hematite, sericite, chlorite and epidote. A particular feature of this sample is the replacement of the biotite by sodic amphibole (riebeckitic arfvedsonite) (Plate 5.9). The zircons occur as large stubby crystals which tend to cluster with the biotites.

Zircons obtained from KP-1000 were stubby euhedral prisms, without cores or alteration. They plot on concordia with an estimated age of 427 ± 2 Ma (Fig. 5.4).

5.2.5. Cape St. John Group (Sample CSJ-10)

The Springdale Group biotite-bearing ash flows, intermediate andesitic-dacitic flows and pyroclastic deposits, and the basaltic flows are similar to lithologies of the Cape St. John Group and the Cape Brule porphyry which grades into the volcanic suite. If these three suites are correlative, it is possible that they are related to the same caldera, with part of the Cape Brule porphyry forming a sub-volcanic pluton.

Two samples were selected for dating, one of ash-flow tuff at the contact with the Cape Brule porphyry (CSJ-6) and one from ash-flow tuff presumed to be stratigraphically higher (CSJ-10). Both of these occur in the north central parts of these units, where they have been subjected to variable degrees of deformation. Both units are characterized by an abundance of lithic clasts including those derived from the underlying ophiolite suite, jasper, basalt and ultramafics, similar to those found in the Indian River Tuff.

Zircons obtained from CSJ-6 were highly altered and cored, and the single sample which looked to be suitable for analysis was found to be highly discordant due to inheritance and multiple zircon populations. Thus no age

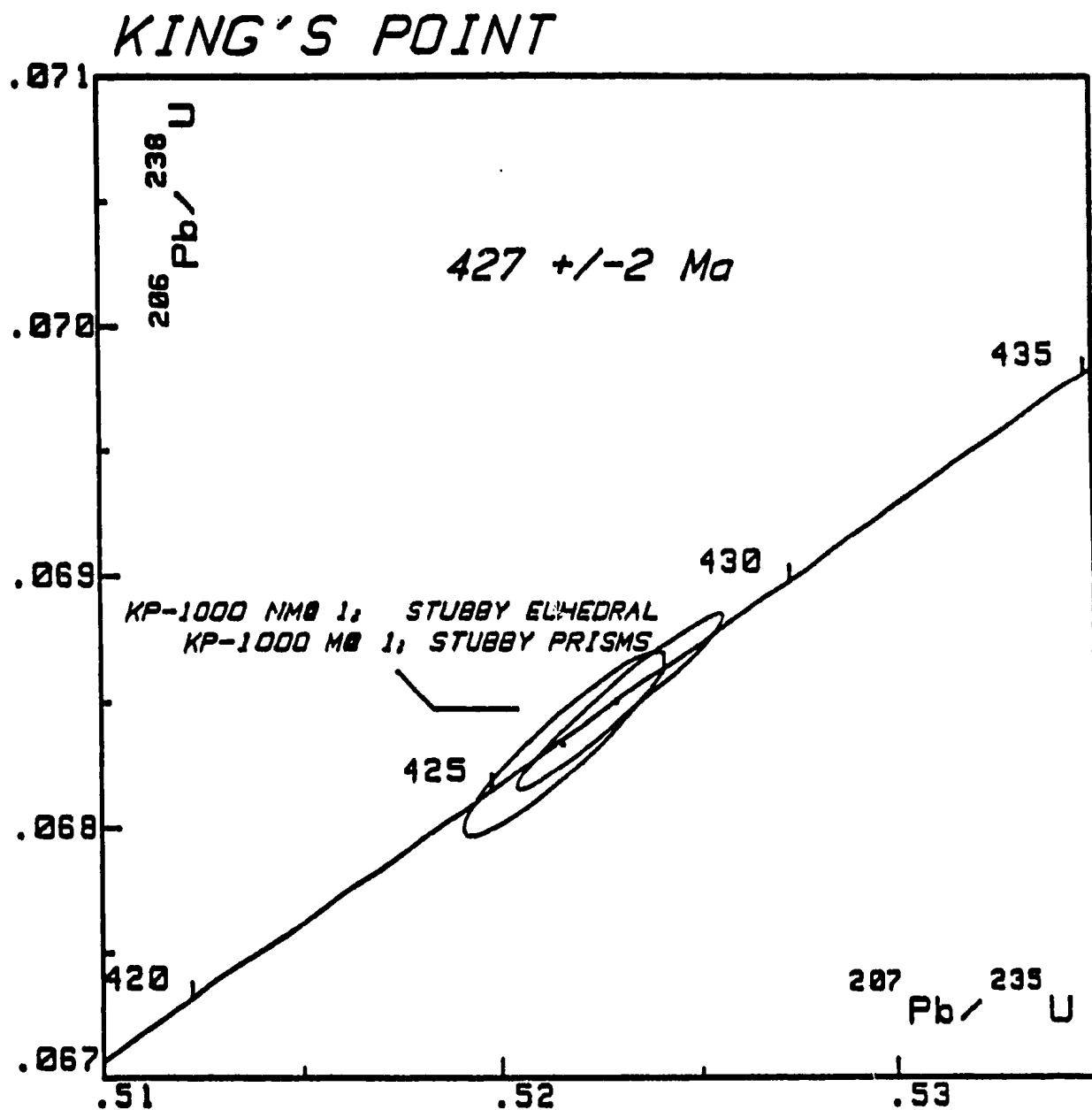


Figure 5.4. Concordia plot for zircon sample no. KP-1000, King's Point Complex.

estimate from that sample was possible within the scope of this project. Thus efforts were focused on the more suitable sample no. CSJ-10.

In thin section sample CSJ-10 is an intensely sericitized and carbonatized crystal lithic ash-flow tuff. Phenocrysts of albite K-feldspar and quartz are almost completely replaced by sericite. Primary groundmass textures are destroyed and a faint tectonic cleavage is defined by undulose domains of sericite and carbonate. The most obvious zircons seen in thin section are stubby crystals overgrowing obvious cores. Other, much smaller zircon crystals, are yellow-brown and more elongate (Plate 5.10).

The zircons of sample CSJ-10 form three populations, stubby euhedral crystals with xenocrystic cores, slender prisms, and cracked needles. The needles appeared to be most suitable for dating, and strongly abraded samples of the best cracked needles (Plate 5.11) plotted on concordia with an estimated age of 427 ± 3 Ma (Fig. 5.5). The prisms and euhedral crystal populations are both strongly discordant, plotting on a chord with its lower intersect at the 427 Ma date and an upper intersect with the very approximate date of $2287 +98 -88$ Ma.



Plate 5.10. Small yellow-brown elongate zircon crystals in sample CSJ-10.

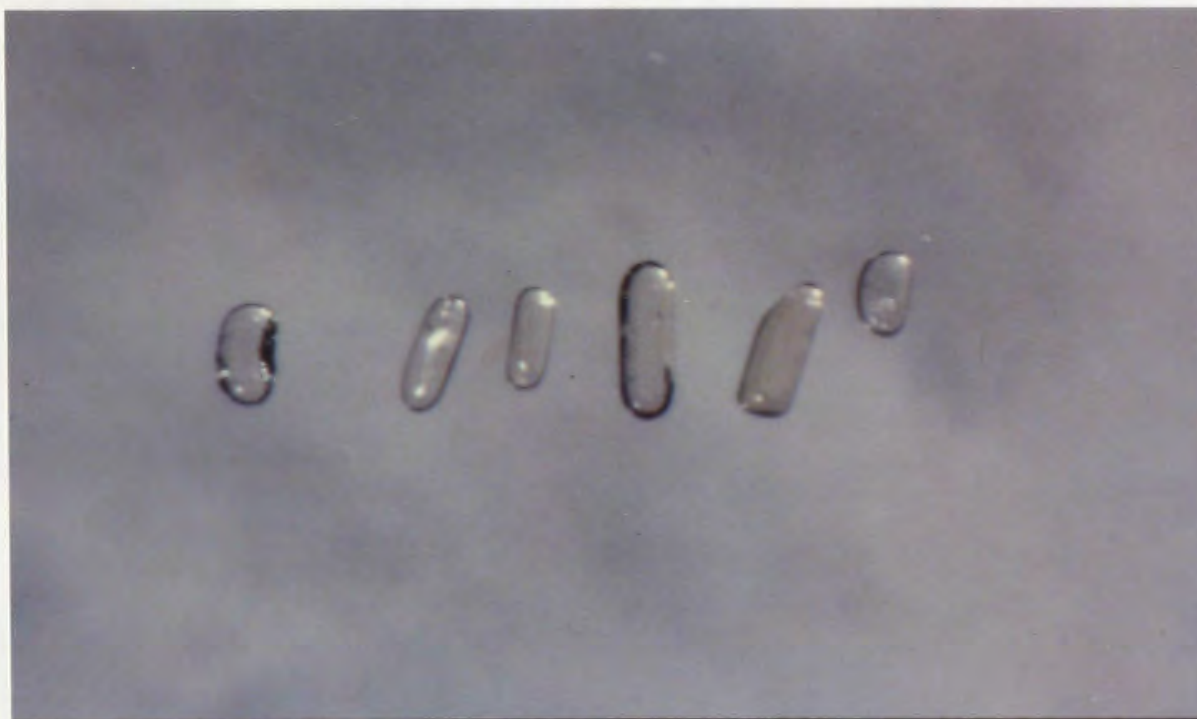


Plate 5.11. Strongly abraded samples of the best zircon prisms of sample CSJ-10 used for dating.

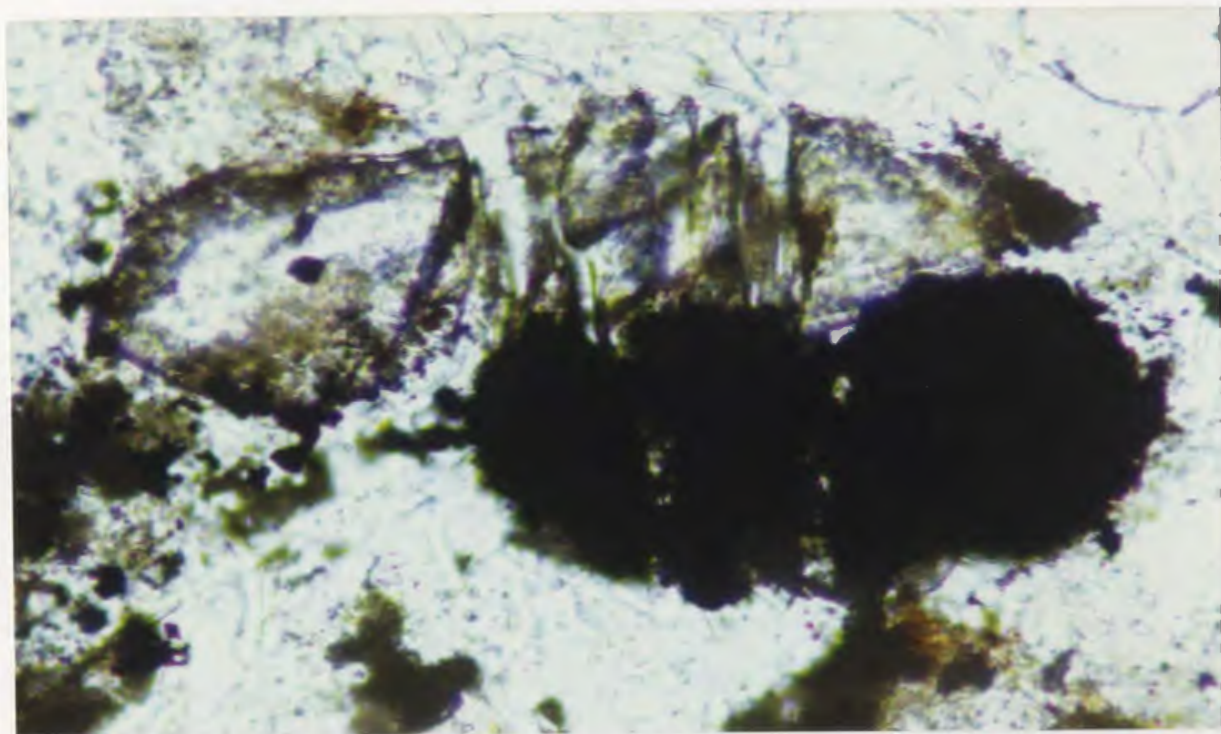


Plate 12(a). Photomicrograph of cored zircon crystal in sample CSJ-10 (plane light, 20x).

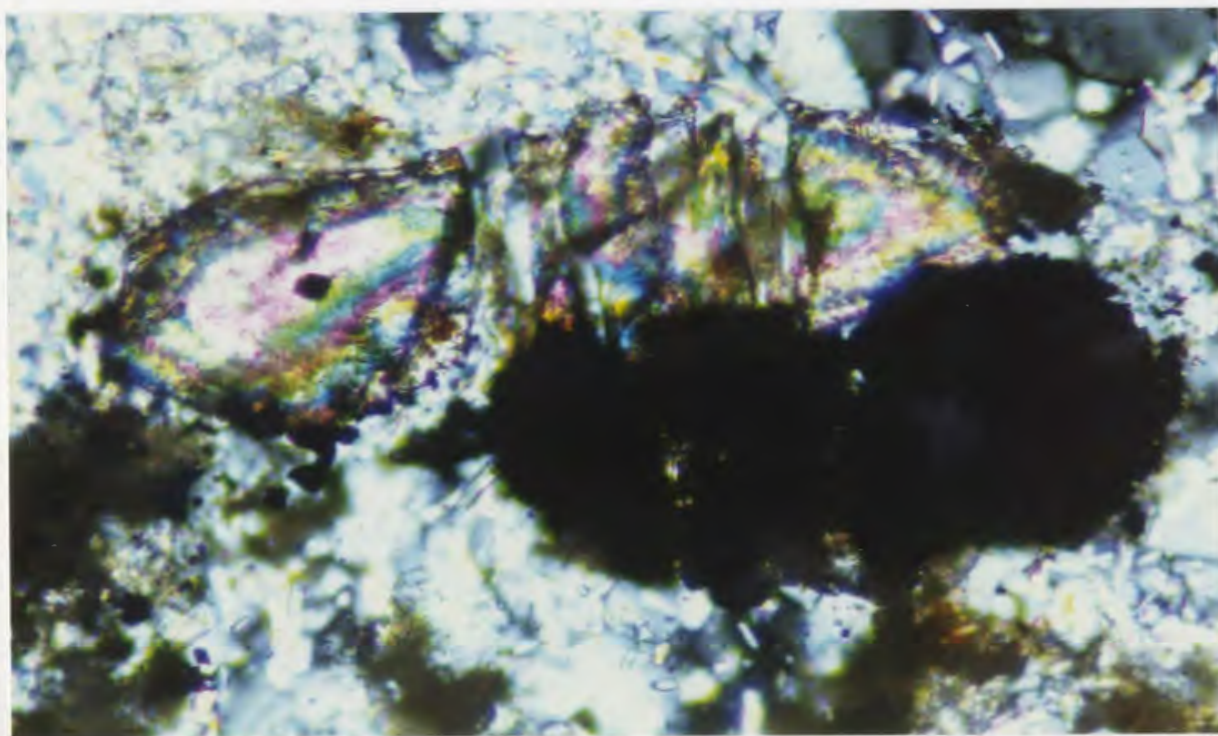


Plate 12(b). As above, with crossed nicols.

CAPE ST. JOHN SAMPLES

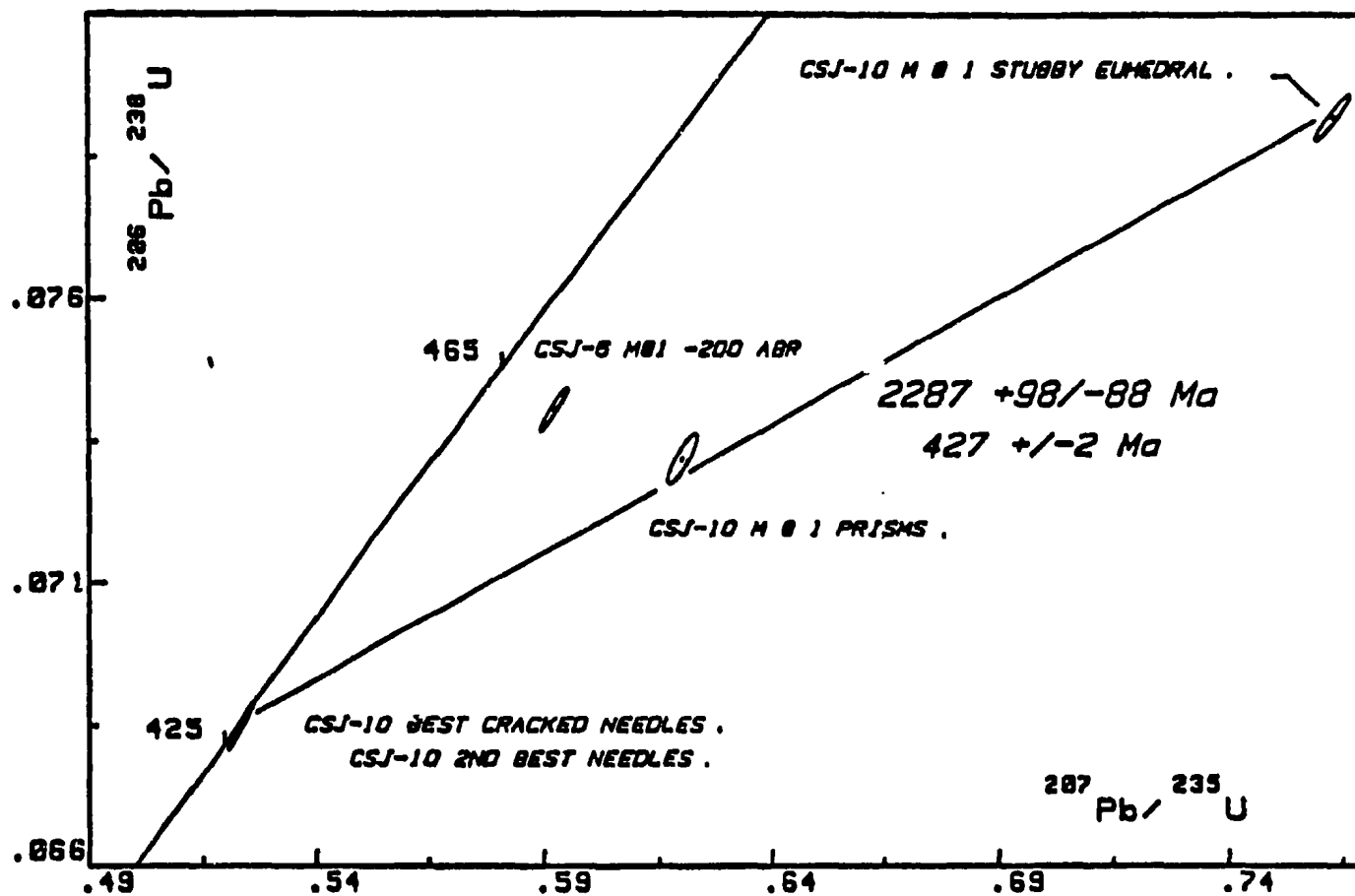


Figure 5.5. Concordia plot for zircon sample no. CSJ-10, Cape St. John Group.

No source rocks with the older age are known in the Appalachians, so it would not be advisable to attach very great significance to it without much more investigation of the inheritance. The similarity of the younger date, 427 Ma, with that of the King's Point syenite and the Indian River Tuff, as well as their close lithological similarity, suggest that the three are closely correlative, and that all three were derived from the King's Point magma chamber. Nevertheless, it is clear that much more work is necessary to determine just where in the Cape St. John stratigraphy the dated tuff occurs, and indeed just what is the stratigraphy of the Cape St. John Group.

5.3. Discussion

Although the stratigraphic sequence shown in Figure 2.3 and Map 1 for the volcanic and sedimentary units within the Springdale caldera was assigned with some uncertainty because of the discontinuous exposure, the radiometric dates of this study do confirm that the sequence is correct. These dates are summarized in Figure 5.6.

It was suggested in Chapter 2 that the Springdale, Cape St. John, Mic Mac Lake, Sops Arm and Sheffield Lake Groups and the King's Point and Topsails Complexes have many features in common, and form a volcanic field (the "Springdale volcanic field") of nested calderas on a scale comparable to those of large epicontinental volcanic

<u>SPRINGDALE GROUP</u>	<u>CORRELATIVE SUITES</u>
Indian R. Tuff, Unit 10 (ZR-3) 425 \pm 3 Ma	
	King's Point (KP-1000) 427 \pm 2 Ma Cape St. John (CSJ-10) 427 \pm 2 Ma
Burnt Berry Dome (ZR-7) 430.8 \pm 2 Ma Basal Tuff, Unit 1 (ZR-11) 432.4 \pm 1.7/-1.4 Ma	

Figure 5.6. Summary of the U/Pb zircon dates produced in this study.

terrane (Figure 2.2). The latter have been documented as being active for tens of millions of years, although the actual caldera-forming events may be much shorter-term. For example, the entire San Juan volcanic field, i.e. calderas and associated ash flows, were formed over a period of only seven million years (Steven and Lipman, 1976), although other magmatic activity of the area extended over a longer period of 35 million years (Lipman et al., 1976). The 7 Ma time span of the Springdale, King's Point and Cape St. John ash-flow volcanism accords well with that of comparable volcanic fields, but it is important to also assess it in their context within the Appalachian orogen.

Radiometric dates for the Baie Verte Peninsula and other suites relevant to this study are summarized in Table 5.2. Different techniques have been used for these dates and hence do not have precisely the same geochronological/geological meanings, some have large errors, and some are not consistent with field relations. They do, nevertheless, provide some indication of the timing and sequence of events in this area.

Ash-flow tuffs of the Sops Arm Group are interbedded with fossiliferous marine sediments of Middle to Late Silurian age (Lock, 1972; Berry and Boucot, 1970), overlapping the age of the Devil's Room and the Gull Lake granites which give a combined U/Pb zircon date of $398 \pm 27/-7$ Ma and Pb/Pb dates on apatites, sphenes and

K-feldspars of about 405 Ma (Erdmer, 1986 and pers. comm.), and the K/Ar date of 392 ± 16 Ma for the Wild Cove Pond Granite (Wanless et al., 1972). R. F. Cormier (pers. comm., 1989) also reported a Rb/Sr date of 401 ± 8 Ma for the lower rhyolite of the Sop's Arm Group. Clasts of King's Point-like comendite within conglomerates of the Mic Mac Lake Group imply that they are also younger than the King's Point caldera, and it is tentatively suggested that they are correlative with the Sop's Arm Group.

Altogether, these rocks appear to comprise a cogenetic volcanic-plutonic suite, tentatively interpreted as making up the Sops Arm caldera. It can be seen from Figure. 2.2 that separation of the Devil's Room and Wild Cove Pond Granites implies a dextral displacement of about 15 km along the Doucer's Valley fault, as suggested by Lock (1969), and this has been allowed for in Figure 2.5(b). There is no strong evidence for lateral displacement along either the White Bay or Baie Verte Faults, and it can be suggested that exposure of the relatively coarse-grained (i.e. deeper-seated) Wild Cove Pond Igneous Suite in juxtaposition with the Sops Arm and Mic Mac Lake volcanics can be explained by their vertical uplift as a central horst between these two faults (Fig. 2.5.b). This is also indicated by the much higher metamorphic grade of Fleur de Lys Supergroup country rocks within this block than those outside it (Hibbard, 1983).

On the southern boundary of the Springdale Group (Fig. 2.2), the Topsails Complex has both peralkaline and metaluminous granitoid suites (Taylor et al., 1980, 1981), and according to the map of Whalen and Currie (1983b), there are a number of volcanic-plutonic assemblages within the Topsails Complex. The distribution of some of these in circular patterns suggest that the complex includes at least two calderas.

The U/Pb dates provided by Whalen et al. (1987) for zircons from different units of the Topsails Complex, one of which they correlate with (indeed term) a "Springdale Group rhyolite", at 427, 429 and 429 Ma (Table 5.2), are all within the range of 432 to 425 Ma obtained for samples within the Springdale Group sensu stricto (i.e. within the caldera), and indeed for the King's Point and Cape St. John Group. Whalen and Curry have also combined samples from a number of units within what they term the "Topsail's terrane" to produce a composite Rb/Sr "whole rock" isochron date of 429 Ma. Although the validity of this approach (i.e. combining samples which could have been derived from different magma sources) is questionable, it is notable that the date does correspond with the zircon dates. To the extent that it is reliable, and given that Rb/Sr dates can be readily re-set (e.g. Kontak et al., 1988), this "isochron" can be taken to indicate that there was no subsequent thermal event to re-set this date. On the Baie

Verte peninsula, however, the numerous argon 40/39 dates provided by Dallmeyer (1977; in Hibbard, 1983; Table 5.2.) suggest that there was re-setting of the argon system of biotite as recently as 343 Ma, and a similar explanation may obtain for the Rb/Sr dates as young as 324 Ma.

The Cape Brule porphyry was dated by Mattinson (1977) at 475 ± 15 Ma. However, as reviewed by Hibbard (1983) this porphyry intrudes post-tectonically the Burlington Granodiorite, and thus must be younger than its preferred age of ~460 Ma. From its transitional relationship and similarity to the Cape St. John Group, Hibbard suggested that they were equivalent, an interpretation which I support. The Cape St. John Group has produced a wide range of Rb/Sr radiometric dates, from 353 ± 15 to 441 ± 50 Ma (Pringle, 1978), and from 385 ± 15 to 520 ± 40 Ma (Bell and Blenkinsop, 1978), and a zircon U/Pb date of 475 ± 10 Ma was reported by Mattinson (1977). Hibbard's suggestion and interpretation that "the 441 ± 50 Ma date seems to fit best with the age of formation of the Group", and that "the 475 ± 10 Ma date may reflect the age of an inherited zircon, as zircon morphology analyses were not conducted on this sample". This interpretation is supported by the new data of this study.

The basement rocks of the region all appear to be related to early Ordovician plutonic and volcanic rocks produced in an oceanic or island arc regime, with some

dates subsequently affected by the Silurian-Devonian caldera-forming events. For example, the Burlington Granodiorite exhibits Rb/Sr dates of 434 ± 10 Ma (Pringle, 1978) and 494 ± 39 (Hibbard, 1983, quoting Dallmeyer), and a U/Pb zircon date of 461 ± 40 Ma (Hibbard, 1983, quoting Dallmeyer). Mattinson (1977) provided U/Pb dates of 434 ± 9 Ma on sphene and a Pb/Pb date of 461 ± 15 Ma for the Burlington Granodiorite. The inconsistency and large errors cast some doubt on the validity of most of these dates, but the deformed state of the Burlington Granodiorite prior to intrusion of the King's Point Complex suggests that the date of 434 (so close to the more precise King's Point zircon dates of this study) is especially dubious. Indeed, its similarity may indicate that some of the common intrusions from the King's Point Complex were mistakenly sampled as Burlington Granodiorite. The range of 461 Ma to 494 Ma may be possible, but the younger date seems more consistent with other basement rocks to the Silurian sequences of the area.

For example, zircon from gabbro of the Betts Cove ophiolite, intruded by the Burlington Granodiorite, was dated by Dunning and Krogh (1985) at $488.6 +3.1/-1.8$ Ma. Dunning et al. (1987; Table 2)) provided precise U/Pb zircon dates for basement rocks around the Springdale caldera. Rhyolite of the Roberts Arm Group, directly overlain by the basal tuffs of the Springdale Group, was dated at 473 ± 2 Ma. South and east of the Springdale

Group, rhyolite of the Buchans Group was dated at $473 \pm 3/-2$ Ma and of the Victoria Lake Group at $462 \pm 4/-2$ Ma. The deformed and metamorphosed Mansfield Cove complex plagiogranite, also directly overlain by the basal tuffs of the Springdale Group, was dated at 479 ± 3 Ma.

It is important to emphasize that the tectonomagmatic event which produced the Springdale Group was widespread throughout central Newfoundland, in the Exploits as well as the Notre Dame Subzone. For example, rhyolites at King George IV Lake in southern Newfoundland have yielded an Early Silurian U/Pb zircon date of 431 ± 5 Ma (Chandler and Dunning, 1983). Dunning *et al.* (1988, 1989) have reported precise zircon ages between 428 and 435 Ma for granites, rhyolites and gabbros for southwestern Newfoundland, and an age of 423 Ma for the Stony Lake rhyolite, a dome-dominated caldera suite which unconformably overlies the Botwood Group in central Newfoundland.

5.4. Summary

The new dates provided in this study are the first available for the Springdale caldera ss, although less precise dates have been provided by earlier workers for samples inferred to be part of the Springdale Group. They bracket the age of the caldera between the lowermost ash-flow tuff at 432 Ma and the uppermost ash-flow tuff at

425 Ma. A rhyolite dome within the caldera dates at 431 Ma, as would be expected from its position in the middle of the stratigraphic sequence. This study is also the first successful of many attempts to provide a precise date for the Cape St. John Group and the King's Point Complex, both at 427 Ma. The precision of these dates shows great potential for volcanological studies which were previously impossible in such ancient non-fossiliferous volcanic sequences. They also allow for correlation with other suites of central Newfoundland, identifying a major tectonothermal event tightly focussed around 430 ± 5 Ma.

Table 5.2. Radiometric dates available for Paleozoic volcanic and plutonic rocks of central Newfoundland.

<u>Stratigraphic Unit</u>	<u>Method</u>	<u>Age</u>	<u>Reference</u>
Dunamagon Granite	Rb/Sr	425 +/-10	Pringle (1978)
		366 +/-10	
		368 +/-10	
		343 +/-10	
	U/Pb zircon	460 +/-12	Mattinson (1977)
		435 +/-15	
	K/Ar	355 +/-15	Wanless <u>et al.</u> (1972)
	⁴⁰ Ar/ ³⁹ Ar (biotite)	345 +/-5	
	"	343 +/-5	
	"	344 +/-5	"
Burlington Granodiorite	Rb/Sr	434 +/-10	Pringle (1978)
	Rb/Sr	494 +/-34	Hibbard (1983)
	U/Pb zircon	461 +/-15	Hibbard (1983)
	U/Pb sphene	434 +/-9	Mattinson (1977)
	U/Pb apatite	345 +/-30	Mattinson (1977)
	Pb/Pb zircon	451 +/-5	Mattinson (1977)
	⁴⁰ Ar/ ³⁹ Ar (hornblende)	463 +/-5	Hibbard (1983)
		418 +/-5	Hibbard (1983)
		417 +/-8	Hibbard (1983)
		414 +/-5	Hibbard (1983)
		413 +/-5	Hibbard (1983)
		412 +/-5	Hibbard (1983)
		406 +/-5	Hibbard (1983)
		414 +/-10	Hibbard (1983)
		412 +/-10	Hibbard (1983)
		409 +/-10	Hibbard (1983)
	⁴⁰ Ar/ ³⁹ Ar (biotite)	345 +/-5	Hibbard (1983)
		343 +/-5	Hibbard (1983)
		380	Lowden <u>et al.</u> (1963)
		386 +/-15	Pringle (1978)
		404 +/-24	Neale & Kennedy (1967)
Micmac Lake Group	Rb/Sr	386 +/-15	Pringle (1978)
	Rb/Sr	404 +/-24	Neale & Kennedy (1967)
Cape St. John Group	Rb/Sr	353 +/-15	Pringle (1978)
	Rb/Sr	441 +/-50	Pringle (1978)
	Rb/Sr	385 +/-15	Bell & Blenkinsop (1978a)
	Rb/Sr	520 +/-40	Bell & Blenkinsop (1978a)
	U/Pb zircon	475 +/-10	Mattinson (1977)

Table 5.2 (continued)
Stratigraphic Unit

Stratigraphic Unit	Method	Age	Reference
Cape Brule Porphyry	Rb/Sr	484 +/-25	Pringle (1978)
	Rb/Sr	334 +/-14	Bell & Blenkinsop (1977)
	U/Pb zircon	475 +/-10	Mattinson (1977)
Seal Island Bight Syenite	Rb/Sr	324 +/-25	Bell & Blenkinsop (1977)
	U/Pb	435 +/-15	Mattinson (1977)
Rattling Brook Group	K/Ar	362	Lowden (1961)
Wild Cove Pond	K/Ar	365	Lowden (1961)
Igneous Suite	K/Ar	384 +/-16	Wanless <u>et al.</u> (1972)
Partridge Point Granite	K/Ar	368 +/-16	Wanless <u>et al.</u> (1972)
East Pond Metamorphic Suite	40Ar/39Ar	394 +/-5	Dallmeyer (1977)
Old House Cove Group	40Ar/30Ar	383 +/-5	Dallmeyer (1977)
	" "	388 +/-5	"
	" "	388 +/-5	"
	" "	400 +/-5	"
	" "	416 +/-5	"
"	" "	421 +/-5	"
"	" "	419 +/-5	"
"	" "	429 +/-10	"
Rattling Brook Group	" "	373 +/-5	"
	" "	375 +/-5	"
	" "	394 +/-5	"
	" "	398 +/-5	"
Hungry Mountain Complex	U/Pb zircon	2090 +/-75	Whalen <u>et al</u> (1987)
		467 +/-8	"
Hinds Brook Granite	U/Pb zircon	460 +/-10	"
Rainy Lake complex	" "	438 +/-8	Whalen <u>et al</u> (1987)
Springdale Group	" "		
rhyolite	" "	429 +/-4	"
Topsails amphibole granite	U/Pb zircon	429 +/-3	"
Topsails quartz-K-feldspar porphyry	" "	427 +/-3	"
Betts Cove Complex (trondhjemite)	U/Pb zircon	463 +/-6	Dunning & Krogh (1985)
(gabbro)	U/Pb zircon	488.6 +/-3.1/-1.8	"
Buchans Group (rhyolite)	U/Pb zircon	473 +/-2	Dunning <u>et al.</u> (1987)
Roberts Arm Group (rhyolite)	U/PB zircon	473 +/-2	"
Mansfield Cove Complex (plagiogranite)	U/Pb zircon	479 +/-3	"

Table 5.2 (continued)

<u>Stratigraphic Unit</u>	<u>Method</u>	<u>Age</u>	<u>Reference</u>
Victoria Lake Group (rhyolite)	U/Pb zircon	462 \pm 4/-2	"
Devils Room Granite	U/Pb zircon		Erdmer (1986; & pers. comm.)
Burgeo Batholith	U/Pb zircon	428 415 \pm -2	Dunning <u>et al.</u> (1988)
Port aux Basques Gneiss	U/Pb titanite	412 \pm -2	"
Little Passage Gneiss	U/Pb zircon	423 \pm -3	"
Post-tectonic North Bay Granite	"	398 \pm -3	"
Stony Lake Rhyolite	"	423 \pm -3	"
Main Out Mafic		431 \pm -2	"
Boogie Lake Mafic		435 \pm 5/-2 Ma	"
Rhyolites in Red Beds		438 \pm 3/-2 Ma	"
Cape Ray Granite		428 \pm -41	Dunning <u>et al.</u> (1989)
King George IV Lake red felsic flow		431 \pm -5	Chandler & Dunning (1983)
"Spingdale Group Rhyolite"		429 \pm 6/-5	Chandler <u>et al.</u> (1987)

6. Mineralization Potential

6.1. Introduction

The potential economic importance of this study hinges upon the fact that epithermal precious metal deposits are dominantly associated with calderas, and thus the newly-recognized Springdale caldera should have some potential for such mineralization which would not have been investigated prior to that recognition. Given that the only such exploration to date has been that generated by the author, and the true economic potential has therefore not been assessed fully, it is useful to provide a brief overview of the main characteristics of epithermal deposits and other mineralization aspects of calderas, as well as a brief review of correlative rocks and associated mineralization in Newfoundland.

6.2. Calderas and Mineralization

As reviewed in Chapter 1, large collapse-type calderas and associated subjacent intrusive assemblages are produced by the collapse of a magma chamber roof due to eruption of the magma as pyroclastics and lava flows. These eruptive products are characterized by near-source and intermediate-source facies rocks that accumulate both within and outside the caldera walls. Such collapse may be followed by development of a resurgent cauldron or there may be continuous collapse without resurgence. The

intra-caldera facies may include ash-flow deposits measuring hundreds of metres in thickness. If resurgence occurs, the resulting moat may be filled by pyroclastic rocks, lava flows, lake sediments, epiclastic volcanic sediments, and particularly by landslide or talus breccias from the caldera wall. The caldera-outflow facies is characterized by ash-flow sheets that may extend for many tens of kilometres outside the caldera. Other important features to be noted are the presence of associated marginal ring or linear faults considered to form the major conduits of eruption, and to control location of late intrusions and/or "nesting" in complex areas. Perhaps the most economically important signature of these complex structures is the combination of post-collapse volcanic facies, associated plutonics and specific structural elements such as ring dykes and structural boundaries of the caldera-collapse block, and in many cases blocks and faults associated with late resurgence, particularly within graben structures of keystone blocks.

6.3. Epithermal Deposits

Buchanan (1981) suggested a general model for epithermal precious metal mineralization (Fig. 6.1), based on a compilation of more than sixty gold-silver vein deposits in unmetamorphosed volcanic to sub-volcanic environments, which has been used with some modification for numerous subsequent studies. One particularly detailed

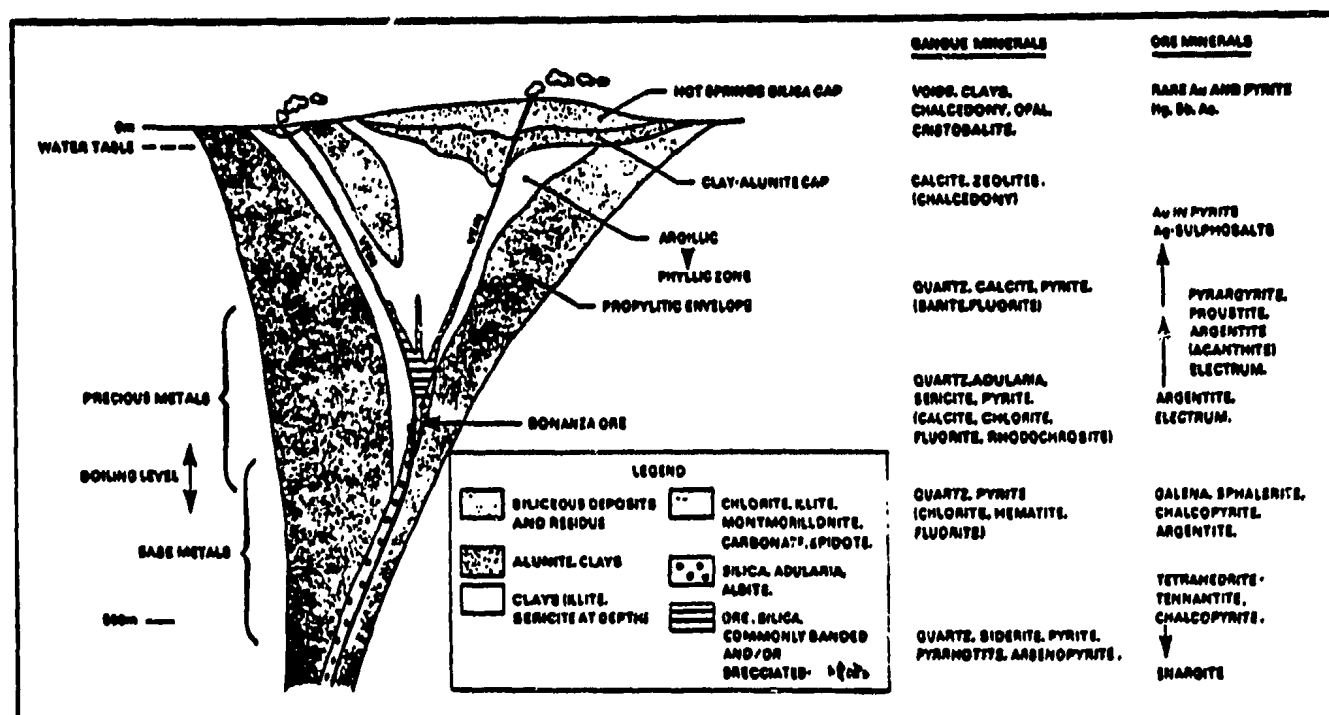


Figure 1. Idealized model of epithermal precious metal deposits (after Buchanan, 1981).

study of a smaller number (16) of these deposits by Heald et al. (1987) showed that two types of epithermal deposits can be distinguished, mainly on the basis of vein and alteration mineral assemblages, as indicated in Table 6.1. The two types are well illustrated by examples from the San Juan volcanic field of Colorado (Fig. 6.2), namely Creede and Summitville.

The adularia-sericite type (e.g. Creede, Eureka, Lake City I), is generally found in a regional structural setting along the margins of calderas, although other structurally more complex volcanic environments may also be associated, e.g. along fault zones (e.g. Colqui) of different types within the calderas or within domes (e.g. Silver City, De Lamar). There is a large range in size of these deposits, from close to 200 sq. m. for Guanajuato, Mexico (silver and base metals), to smaller areas of around 10 m.. The paleodepths of mineralization may range from 300 to 1500 metres, with vertical ranges of mineralization on the order of 400 to 700 metres. The importance of the volcanic setting is primarily one of providing the plumbing system and heat to drive circulating hydrothermal fluids, so that virtually any rock type may be a favourable host for mineralization. The adularia type deposits are characterized by the presence of vein adularia and sericite, with chlorite, manganese minerals, with base metal sulfides, sulfosalts, and native silver and gold. The

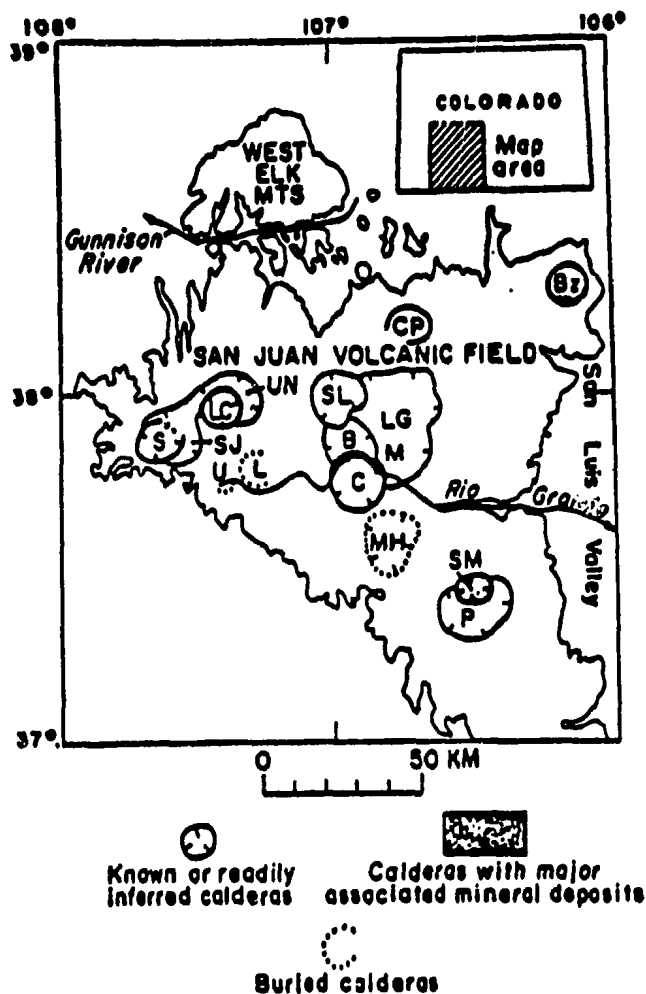


Figure 6.2. Calderas of the San Juan volcanic field.

Abbreviations are as follows: S - Silverton; LC - Lake City; CP - Cochetopa Park; Bz - Bonanza; LG - La Garita; SL - San Luis; B - Bachelor; C - Creede; MH - Mount Hope; P - Platoro; SM - Summitville; L - Lost Lake; U - Ute Creek; SJ - San Juan; UN - Uncompahgre; M - General Location of the Mammoth Mountain caldera. From Hayba *et al.* (1985; after Steven and Eaton, 1975).

TABLE 6.1. Characteristics of the adularia-sericite type and acid-sulfate type deposits (compiled from Heald et al., 1986).

	<u>Acid Sulfate</u>	<u>Adularia-Sericite</u>
Structural setting	Intrusive centers, 4 out of the 5 studied related to the margins of calderas	Structurally complex volcanic environments, commonly in calderas
Size length:width ratio	Relatively small equidimensional	Variable; some very large usually 3:1 or greater
Host rocks	Rhyodacite typical	Silicic to intermediate volcanics
Timing of ore and host	Similar ages of host and ore (<0.5 m.y.)	Ages of host and ore distinct (>1 m.y.)
Mineralogy	Enargite, pyrite, native gold, Electrum, and base-metal sulfides Chlorite rare No selenides Mn-minerals rare Sometimes bismuthinite	Argentite, tetrahedrite, tennantite, native silver and gold, and base-metal sulfides chlorite common selenides present Mn gangue present no bismuthinite
Production data	Both gold- and silver-rich deposits Noteworthy Cu production production	Both gold- and silver-rich deposits variable base-metal
Alteration	Advanced argillic to argillic (\pm - sericitic) Extensive hypogene alunite Major hypogene kaolinite No adularia	Sericitic to argillic Supergene alunite occasional kaolinite abundant adularia
Temperature	200° to 300°C ¹	200° to 300°
Salinity	1 to 24 wt% NaCl eq. ²	0 to 13 wt% NaCl eq.
Source of fluids	Dominantly meteoric, possibly significant magmatic component	Dominantly meteoric
Source of sulfide sulfur	Deep-seated, probably magmatic	Deep-seated, probably derived by leaching wallrocks deep in system
Source of lead	Volcanic rocks or magmatic fluids	Precambrian or Phanerozoic rocks under volcanics

¹ Limited data, possibly unrelated to ore.² Salinities of 5 to 24 wt% NaCl eq. are probably related to the intense acid-sulfate alteration which preceded ore deposition.

ratio of gold to silver is highly variable, and there appears to be a continuum from base metal-silver rich districts to the b.m.-poor/Au-rich deposits, although a low ratio is more common. Wall-rock alteration is in general marked by silica, sericite, K-feldspar, chlorite, near the veins, grading outwards into a broader propylitic alteration which may have substantially preceded mineralization and be unrelated to it.

Although all of these features are not fully illustrated by the Creede mining district (Fig. 6.3), these deposits are especially important in that they have been studied in great detail (Hayba et al., 1985). They actually occur within a set of fractures forming a graben structure between the Creede and the San Luis calderas, and are hosted by the intracaldera fill of the older resurgent Bachelor caldera (Fig. 6.3.a,b). Radiometric dating of the alteration minerals has shown that the mineralization formed about one million years after the youngest volcanic event, and is inferred to have been deposited by hydrothermal fluids driven by and unexposed pluton which interacted with groundwaters of the area (Fig. 6.3.c).

Acid-sulfate deposits have a similar structural setting to some adularia-sericite deposits, but the presence of intrusive centres, particularly ring-fracture volcanic domes on the margins of calderas, appears to be a critical genetic factor, as seen in Figure 6.4. These

Figure 6.3(a). Generalized geology of the Creede and San Luis calderas in relation to the Bachelor (B) and La Garita calderas and to the Creede mining district. (b).

Generalized geology of the Creede mining district (location shown in (a)). (c). Schematic representation of the Creede hydrothermal system, where upwelling plume (within the 200°C isotherm), driven by inferred sub-surface pluton, displaces and interacts with groundwater to deposit ore.

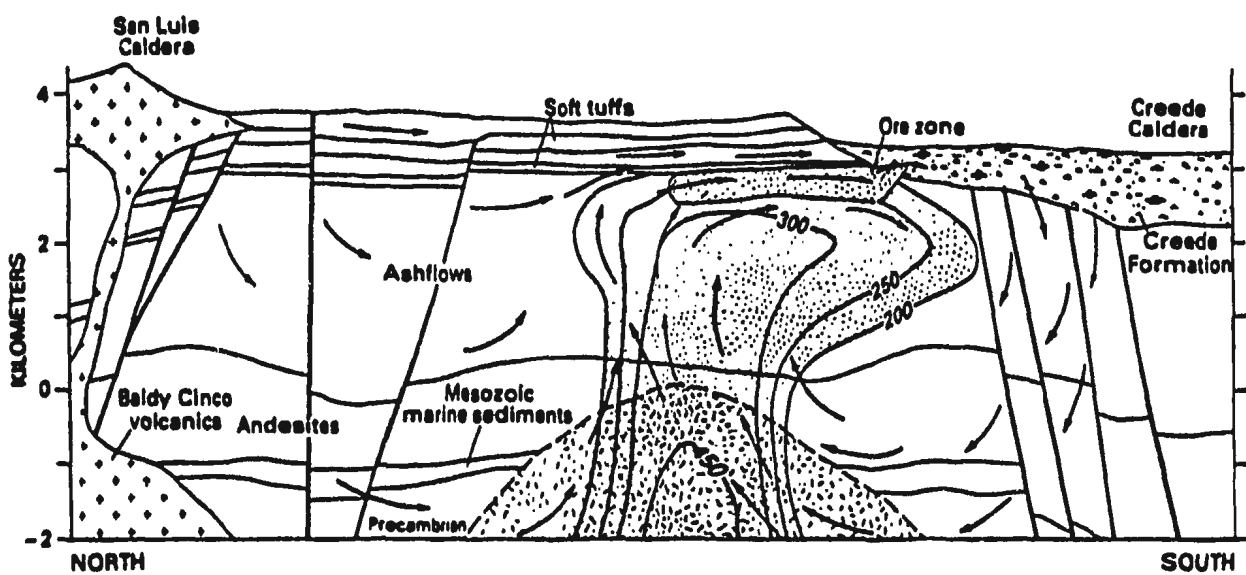
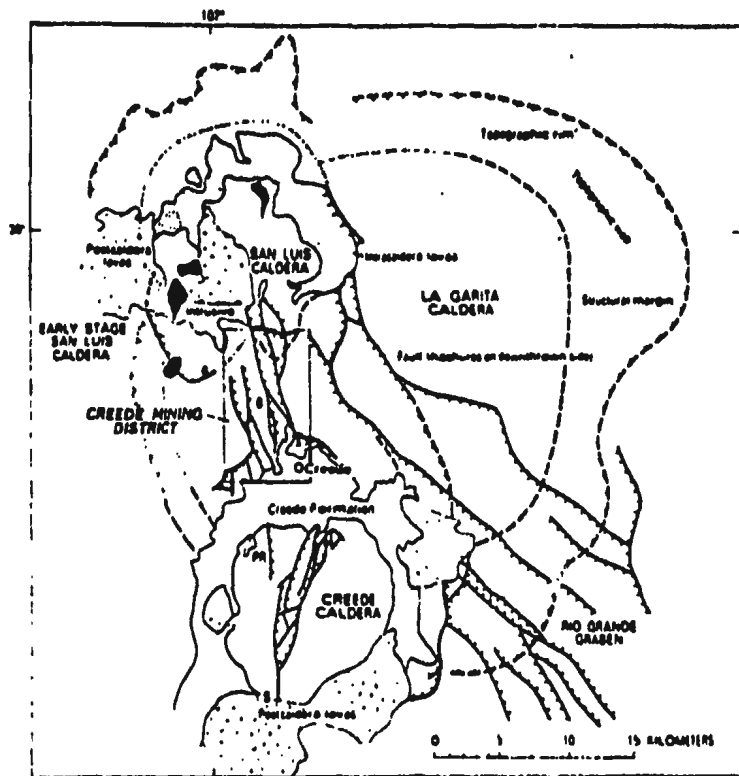
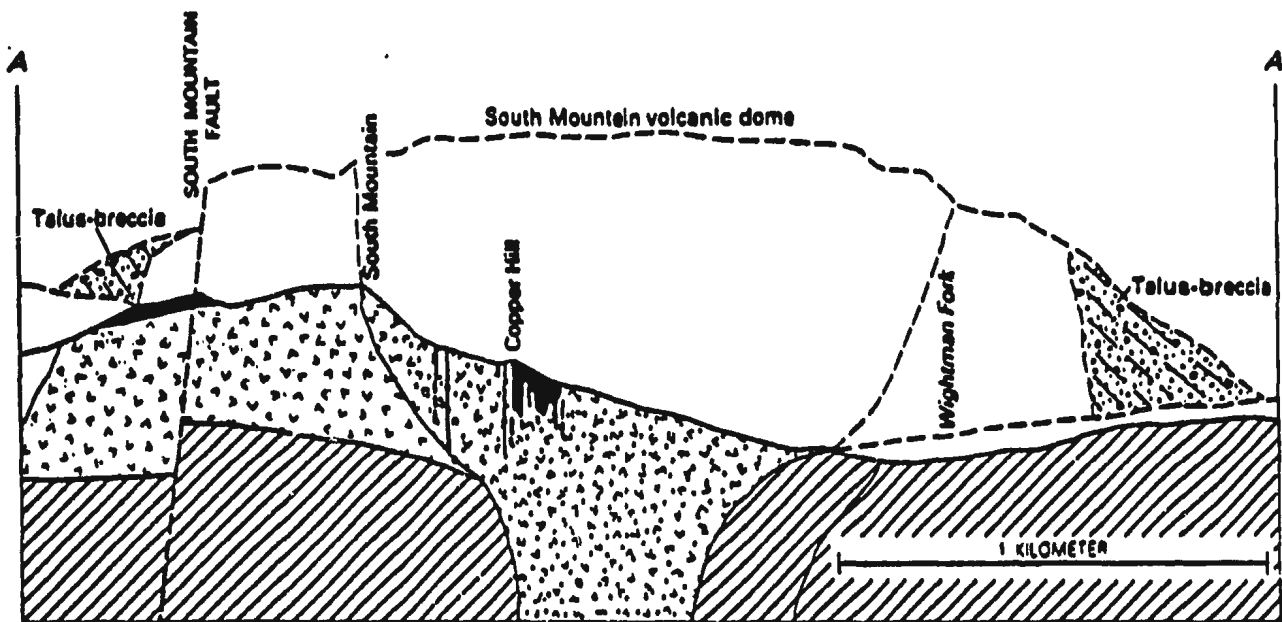
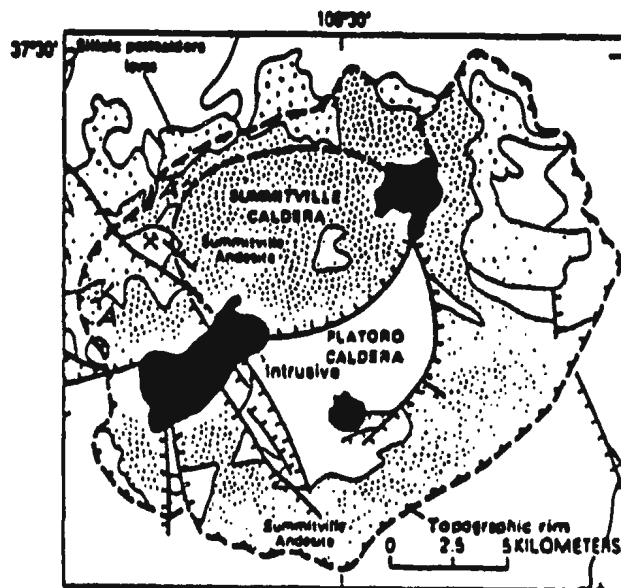


Figure 6.4(a). Generalized geology of the Platoro and Summitville calderas, showing location of Summitville mining district (pick and hammer) and the cross-section A-A' of the restored South Mountain volcanic dome and mineralization shown in (b). (All from Hayba et al., 1985, and references therein).



EXPLANATION

- Crepsy Mountain Rhyolite 20.2 m.y.
- Coarse porphyry

- South Mountain Quartz Latite 22.9 m.y.
- Quartz-silunite 22.3 m.y.

- Summitville Andesite ~29 m.y.
- Altered area

deposits tend to be smaller than the adularia-sericite deposits, with a less elongated surface expression (e.g. only about 2 x 1.5 km at Goldfield, Nevada), and a shorter vertical extent of generally less than 500 metres. They are also different in that the host rocks are almost exclusively porphyritic rhyodacite, although at Julcani some ore is hosted by dacite, and at Goldfield by trachyandesite and rhyolite as well as the rhyodacite.

This, together with the close age relationship between mineralization and intrusion, suggests a closer genetic relationship than for the adularia-sericite type. The acid-sulfate types are characterized by the occurrence of the vein mineral assemblage enargite + pyrite \pm covellite, with ore occurring as either native gold and electrum, with sulfosalts, sulfides, and tellurides. Gold/silver ratios tend to be high, reflecting the high proportion of free gold and gold-bearing minerals. The wall-rock alteration is marked by advanced argillic alteration with the ore, with kaolinite, alunite and silica near the veins, and argillic and sericitic alteration surrounding the advanced argillic, passing outwards into propylitic alteration.

The Summitville district (Fig. 6.4) differs somewhat from the above-noted examples in having relatively lower proportions of silver, lead and zinc. The mineralization is located in the South Mountain volcanic dome on the

northwestern edge of the Platoro caldera and the southwestern edge of the younger nested Summitville caldera, at a major fault zone which cuts across both calderas (Fig. 6.4.a). The dome is made up of quartz-latite rich in K-feldspar and smaller plagioclase phenocrysts. The mineralization is localized along the core of the dome in a series of irregular pipes and veins of quartz and alunite which mostly replace the quartz latite (Fig. 6.4.b). As reviewed by Hayba et al. (1985), it is generally agreed that a magmatic vapour phase was the dominant fluid responsible for Summitville mineralization, but it is not clear how important was interaction with groundwater as a cause for deposition.

6.4. Appalachian Silurian-Devonian Caldera Suites

Preservation of all caldera features is rare and it is often necessary to make comparisons between a number of reasonable models for the interpretation of a given caldera and its setting. Nevertheless, there are numerous examples of such rocks in the Silurian-Devonian terranes of the northern Appalachians, both in and outside of Newfoundland, to indicate that caldera-type volcanism was prevalent during this time, and correspondingly that caldera-type mineralization is also to be found. Examples which warrant detailed investigation are the Lower Devonian Piscataquis volcanic belt, the Spider Lake volcanics, the Hedgehog

Formation, the Debouille Stock, the Five-Mile Brook Formation, all in Maine. Similar-aged rocks in Quebec and northern New Brunswick appear to include a larger proportion of basaltic and andesitic rocks, hence being more tenuously related to calderas.

The Springdale and King's Point volcano-plutonic complexes, occurring along the western margin of Newfoundland's Lower Paleozoic Central Volcanic Belt, are two of nine separate Silurian subarea volcanic-sedimentary-plutonic suites found on the island (See Fig. 2.2). Despite their extent and potential importance to understanding post-orogenic magmatic activity in the Appalachians, prior to the present study they have not been targets for mineral exploration based on caldera models. The Springdale Group can be traced for at least 60 km along strike, and possibly a further 100 km southwestward, and reaches a maximum width of 35 km across the centre of the belt. The King's Point Complex, somewhat more deeply eroded than the Springdale, has a greater proportion of intrusive rocks exposed, with a mixture of both peralkaline and metaluminous granites, syenites and ash-flow tuffs. Comparable Silurian volcanic-plutonic rocks occur in the Cape St. John Group to the north, and the Mic Mac, Sheffield Lake and Sops Arm Groups to the west.

Tuach et al. (1988) reviewed the full range of gold mineralization types in Newfoundland (Fig. 6.5), so only the briefest of comments are necessary here. The most important of the epithermal types, and the only one currently being mined, is the Hope Brook deposit, which contains about 11 million tons of ore grading at 4.54 g/t. It consists of an ore lens about 60 by 400 m in a 5-km long zone of pyrophyllite-sericite-silica alteration, with fine-grained gold disseminated with pyrite and chalcopyrite associated with tellurides, bismuthenite, cassiterite, native silver, and elevated values of Sb, Ag and Sn. These are hosted by a sequence of felsic tuffs, volcanoclastic sediments, and granitic rocks of the LaPoile Group, and Tuach et al. (1988) list numerous other prospects within this sequence. Nevertheless, there is some inconsistency in the age estimates for this sequence, with the subaerial felsic volcanic rocks of the La Poile Group dated at 426 to 419 Ma, comparable in age to the Springdale Group, whereas the "stratified rocks of the Group" must be older than the 563 ± 4 Ma determined for the Roti Granite which is thought to intrude it (Dunning et al., 1988).

The Cape Ray deposit is perhaps the next most promising of these deposits, with about a million tons grading at 5.75 g/t gold, occurring as lenses within mylonitic rocks of the Cape Ray Fault Zone. The Main Zone of mineralization is associated with quartz veins within

- Epigenetic Gold - **DEPOSITS AND OCCURRENCES** **IN** **NEWFOUNDLAND**

VEN DEPOSITS

A Unaltered

B Epithermal

Major Deposit

Prospect (mining, prospecting)

Occurrences, anomalous gold, reported occurrences

Ultramafic rocks (peridotite, carbonates)

Hydrothermal alteration features (high alumina, sericite, carbonates)

Faults, fractures, thrusts, etc.

Lineaments with associated gold potential

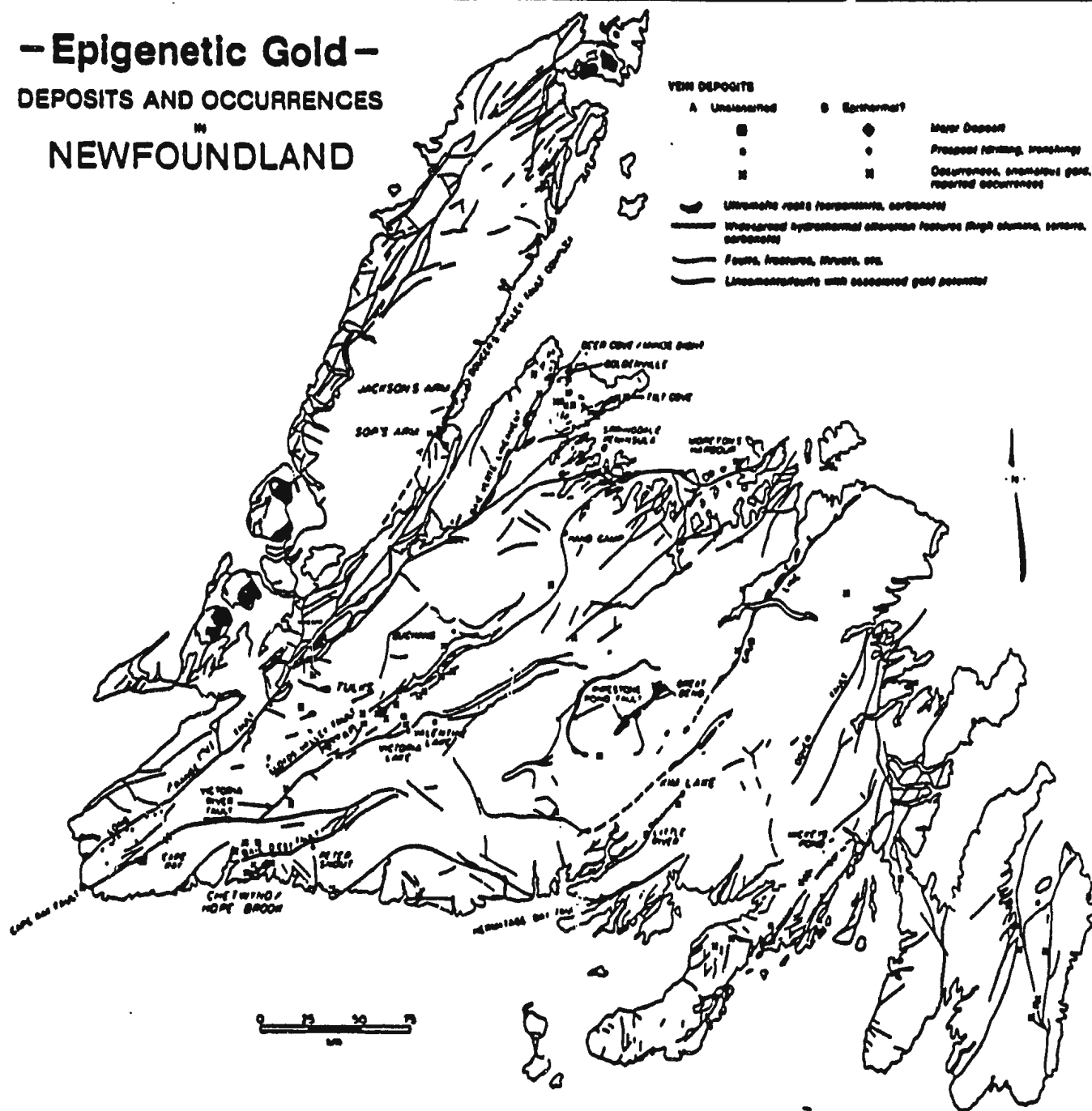


Figure 6.5. Distribution of reported epigenetic gold mineralization in Newfoundland (after Tuach et al., 1988).

mylonitized graphitic sediments, mafic and felsic tuffs. The Windowglass Hill zone consists of sheeted and stockwork quartz veins in albitized brecciated graphitic granite of the Devonian Windowglass Hill Granite. In both deposits, the gold is associated with galena, chalcopyrite, sphalerite and pyrite within the quartz veins. Clearly, this mineralization would have formed at a substantially deeper level than the Hope Brook deposit, with the fault zone providing the necessary plumbing system for the mineralizing fluids.

Both faults and volcanic structures have controlled the different types of gold mineralization associated with the Silurian-Devonian caldera-related rocks of Western White Bay. The Jackson's Arm gold mineralization is associated with intense potassic alteration of a range of rock types ranging from Late Precambrian granites and sediments to Early Devonian granites. In the most intensely altered areas gold and sulfides are associated with fine grained albite, Fe-carbonate, quartz, and arsenopyrite. At Unknown Brook gold is associated with quartz-carbonate-alkali feldspar-pyrite veins in a deformed lithophysae zone of the Upper Silurian Sops Arm Formation (not a conglomerate bed, as suggested by Tuach et al., 1988). The Browning Mine is found in deformed and brecciated quartz veins associated with intensely Fe-carbonatized-sericitized fine-grained schistose tuffs of the Sops Arm Formation.

In summary, many of the volcanic sequences which are similar to and in some cases directly correlative with the Springdale Group are known for significant gold mineralization, lending support to the proposition that the latter may also have some exploration potential.

6.5. The Springdale Caldera

Some of the following is based upon observations made while the author supervised an exploration program in the Springdale Caldera during the summer of 1988, developed on the basis of the epithermal/epigenetic models discussed above. This activity was focussed on the two main areas within the Springdale caldera described in Chapter 2, Springdale Central and Springdale East. Other exploration work was done as part of that program outside the caldera in the King's Point and Sheffield Lake Complexes, but it is not included in this thesis. Each of these areas was assessed by the author with exploration for sites of alteration and/or mineralization, and geological mapping at 1:10,000 scale, as shown in Maps 1 to 3. This exploration and mapping was augmented by geophysical (aeromagnetic, EM and IP) surveys as discussed in Chapter 2.

The main indicator of potentially economic mineralization in most geological environments is secondary alteration, and this is especially true for caldera environments. Three areas of alteration were located in the

Springdale caldera, all being limited in areal distribution, mainly because of poor exposure. The most promising alteration type of the Springdale Central area was found along the eastern side of Burnt Berry Brook (Map 2) where rubbly outcrop and scree are exposed along a small woods road. The alteration is found along a sub-vertical fault trending Northwest, moderate to strong sericitic in porcelanitic tuffs in contact with redbed sedimentary rocks, and ranges from weak to moderate argillic alteration in spherulitic zones within silicic volcanics. An exploration grid was centered in this area for geochemical soil sampling, and gold grains were recognized in the till.

A second area of interest in this central part of the caldera occurs as local quartz veining and hydrothermal brecciation of the volcanics and granite. Another area of possible interest is along the Saunders Brook fault where a regular and lengthy EM conductor is found although the available outcrop along the brook is relatively pristine except for calcite/quartz/epidote veining in the basalt flows and very local small scale veining and brecciation in the rhyolite of the Burnt Berry Dome.

The Springdale East area was identified as a caldera-margin target since, as reviewed above, this is a favoured setting for epithermal gold deposits, especially the sericite-adularia type. The caldera marginal facies are well-exhibited here, including mass wasting deposits or

mesobreccias located and generated at the caldera margin, margin-related intrusions, and a post-emplacement granitic stock with associated dykes and hydrothermal system. The "ring fault", or fracture faults which demarcate the structural margin of the caldera in the north and the topographic margin further south, typically act as conduits for the circulation of fluids, both groundwaters and those generated in the magma chamber at time of caldera foundering and collapse, have obvious potential for ore deposition.

One rock sample of Unit 1 was anomalous for gold in the vicinity of South Pond, and stream-silt samples in this area also proved anomalous for gold and associated trace elements. In the vicinity of Johnson's Lookout stream samples from tributaries of Barney's Brook which drain Unit 2 have anomalous gold, arsenic and zinc. Unit 4 hosts some of the strongest alteration in the Springdale East area (Map 3), with thick (~2m) porous lithophysae zones moderately to strongly altered with quartz-pyrite veining in limonitic/argillic alteration zones.

In the southeastern part of the Springdale East area (Map 4), Unit 2 is dominantly conglomeratic or a reworked facies of the marginal mesobreccias exposed further north along strike. Here Unit 2 is intruded by Units B and C, and the conglomerates are weakly to moderately altered (silica, hematite, amphibole, chlorite and pyrite). One rock sample

was anomalous for gold (>5 ppb) and four others from this unit, in this vicinity were also anomalous for arsenic (5 ppm) and antimony (>1 ppm). Stream silt samples from this area also provided anomalies in all these elements plus zinc. The intrusive units in this area are not significantly altered, except for minor pyrite seen in both the microdiorite and felsic sill and dykes that cut the conglomerates.

6.6. Summary

It is clear from both the geological mapping for the main part of this thesis study, as well as the limited subsequent exploration, that there are a number of indications of alteration and geochemical anomalies which were predicted on the basis of typical models for caldera style mineralization. These are obviously important as indicators of mineral potential and warrant much more intensive exploration and investigation. They are perhaps equally important to this study in that they provide yet another line of evidence in support of the interpretation that the Springdale Group represents the products of a large collapse caldera.

7. SUMMARY, INTERPRETATIONS AND CONCLUSIONS

7.1. Introduction

The purpose of this study was to characterize and attempt to understand the magmatic and tectonic processes which controlled the development of the Springdale Group, newly recognized by the author as comprizing a full caldera assemblage, occurring along the western margin of Newfoundland's lower Paleozoic Central Mobile Belt (Coyle and Strong, 1985, 1987). This study provides the first geochemical data for the Springdale Group, and demonstrates that they mimic some calc-alkaline trends comparable to orogenic calc-alkaline suites of circum-Pacific regions (cf. Ewart, 1982). However, they also include tholeiitic basalts, and a suite of domes, intrusions and pyroclastic rocks which are similar to the high-silica rhyolites derived from large layered siliceous magma chambers of continental regions. Furthermore, the Springdale caldera is unlike any found with orogenic calc-alkaline suites in that its large size, representing a minimum eruption volume between 10^3 and 10^4 km³, is matched only by the largest epicontinental calderas, like those of the southwestern USA. This, along with the high-silica rhyolite compositions, implies a similar epicontinental tectonothermal environment for Silurian-Devonian times in west-central Newfoundland.

The Springdale Group exhibits virtually the full range of features which characterize such calderas (listed in Table 1.1), namely [uncertain examples in square brackets]:

Extensive rock units of lavas, breccias, and lahars of intermediate composition (andesite, dacite, rhyodacite).

Intra-caldera ash-flow accumulation. Large thicknesses of silicic ash-flow tuffs (dacite, rhyolite).

Landslide or slump breccia deposits (mass wasting from caldera walls), with very large blocks and unusual (exotic) breccias.

Intracaldera volcanic rocks and volcanoclastic sedimentary rocks.

Curved zones of faulting, fracturing, and brecciation (marginal fracture zone).

Regional propylitic alteration with local occurrence of argillic, sericitic, and advanced argillic alteration.

Resurgent doming evidence by:

- a. [outward dip of intracaldera units];
- b. central graben [inferred];
- c. plutonic or hyabyssal resurgent magma;

Ring-fracture domes of rhyolite and dacite (e.g. Wolf Head, Johnson's Lookout).

Structural depression marked by collapsed blocks.

[Radial and/or concentric fault, drainage, and topographic patterns.]

[Clustering of mineral occurrences.]

[Circular patterns on high-altitude photographs or remote imagery.]

[Geochemistry: The distribution of metal values (Au, Ag, Cu, Mo, Pb, Zn, etc.) may aid in defining caldera structures.]

Geophysics. [Gravity], magnetics, resistivity, [and radiometrics] show evidence of caldera structure.

The Springdale Group extends continuously for 60 km, and possibly a further 100 km southwestward, and reaches a maximum width of 35 km. It is correlated with rocks of the King's Point Complex and the Cape St. John Group, found up to 50 km to the north, and the MicMac, Sheffield Lake and Sops Arm Groups immediately to the west. Rocks of the Springdale Group are folded about a main northerly-plunging synformal axis locally marked by a steeply-dipping spaced fracture cleavage. Sedimentary rocks of the Group are gently dipping, but locally inclined up to to 50° on either side of the fold axis, possibly indicating across-strike structural shortening of up to about 20%, inferred to contribute to the present elongate distribution pattern of the Group. A schematic outline of the main structural elements of the caldera is shown in Figure 7.1.

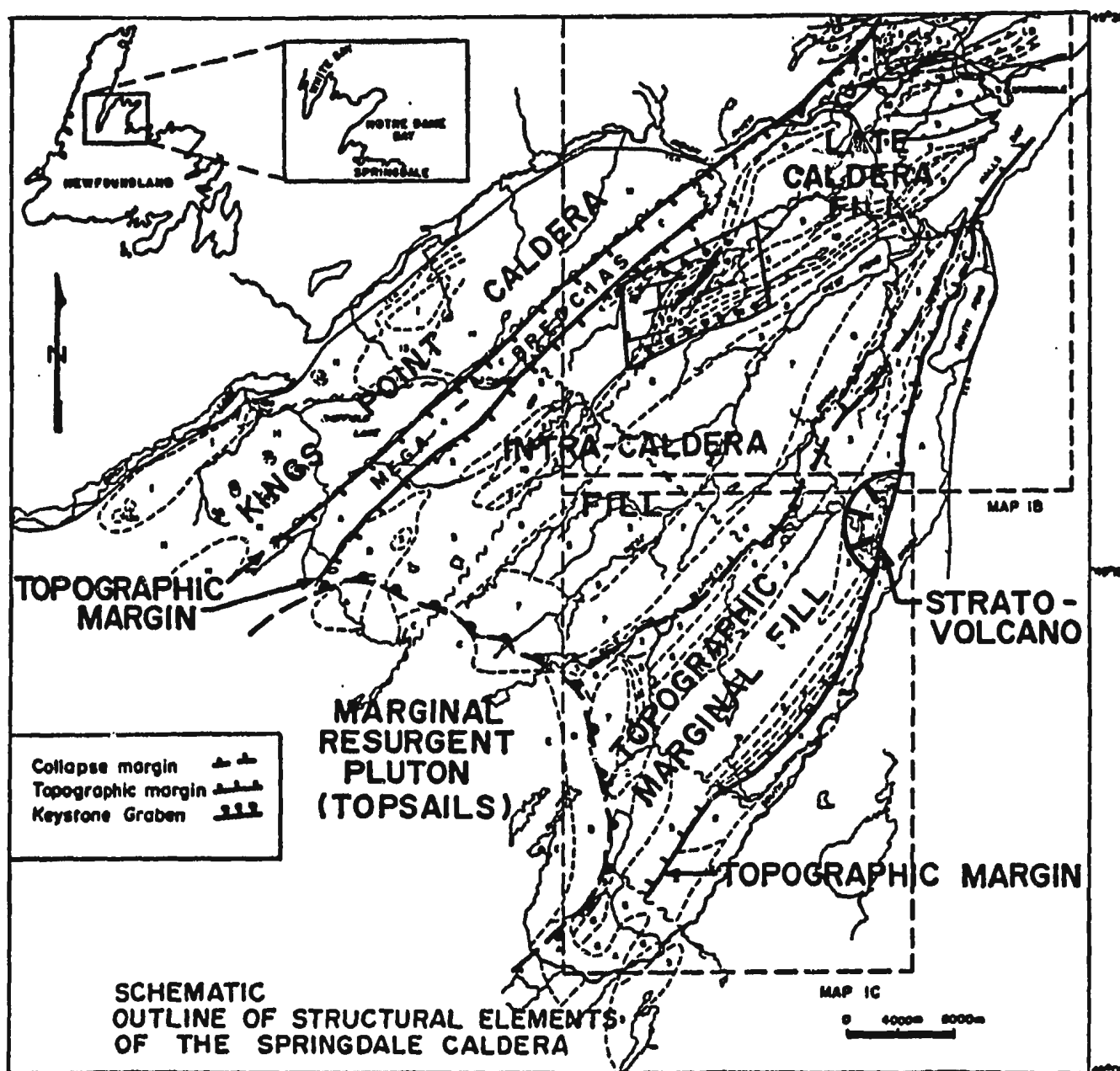


Figure 7.1. Schematic outline of the main structural elements of the Springdale caldera.

The eastern and western boundaries of the Group, although intruded by granitoid rocks, mark early boundary faults along which the Group was down-dropped, and which partially controlled volcanism, sedimentation, and intrusion of the granitoids. Along its eastern boundary rocks of the Group lie unconformably on, or are faulted against, a basement of metamorphic rocks derived from Lower Ordovician (467 - 456 Ma) island arc volcanic sequences. The volcanic rocks of the Springdale Group show evidence for a variety of source rocks for their derivation and contamination, from continental (Precambrian zircon cores) to oceanic crust (ultramafic to cherty lithic clasts in ash flows).

7.2. Chemistry

The Springdale Group data are divisible into four groups based on silica contents, viz. "mafic" (basalts and basaltic andesites), "intermediate" (basaltic andesites, andesites and dacites), "felsic" (dacites and rhyodacites), and "silicic" (rhyolites and high-silica rhyolites). The first three groups form a typical calc-alkaline trend which can be interpreted as having been produced by fractionation of olivine, clinopyroxene, plagioclase, Fe-Ti oxides and zircon. The fourth group, found mostly as late-stage domes, is typical of high-silica rhyolites produced in the late stages of development in the roof zones of large magma chambers, and are interpreted to have been produced by

processes dominated by convective fractionation. These latter rocks, along with other geochemical characteristics of the less silicic rocks (e.g. the basalts being non-arc tholeiites) suggest that the Springdale Group were formed in an extensional environment which included continental crust.

7.3. Geochronology

Five new precise U/Pb zircon dates have been determined for the Springdale Group in this study. These are for samples from the lowermost and uppermost ash-flow tuffs and an intermediate-aged rhyolite dome of the Springdale Group within the caldera, a syenite from the King's Point Complex, and an ash-flow tuff from the Cape St. John Group. These units were dated for the primary objective of bracketing the ages of individual units of the Springdale caldera, as an independent check on their relative ages based on geological observations and interpretations, and to determine the time span over which the caldera was active. The second important objective was to determine the ages of associated volcano-plutonic sequences in order to evaluate proposed correlations and volcanic/plutonic/tectonic interpretations based on these correlations in Newfoundland and elsewhere in the orogen.

Clear abraded fractions plot directly on concordia at an estimated age of $432.4 \pm 1.7/-1.4$ Ma, with cracked non-abraded fractions and a discordant abraded fraction all plotting linearly away from it along a lead loss line, i.e. with no evidence of contamination from older zircons. Strongly abraded zircons from the Burnt Berry dome also plot directly on concordia, with an estimated age of 430.8 ± 2 Ma.

All fractions except crystal cores separated from sample Zr-3, the Indian River Tuff, plot on or near concordia, giving an estimated age of 425 ± 3 Ma. The core sample is offset from concordia to indicate an inherited age of 1346 ± 230 Ma. This age would be found in rocks which are precursors to the Grenville basement seen to the west of the Springdale Group and inferred to be beneath the King's Point caldera from which the tuff is considered to have originated.

Zircons obtained from the King's Point Complex, stubby euhedral prisms without cores or alteration, plot on concordia with an estimated age of 427 ± 2 Ma. Zircons obtained from the Cape St. John Group form three populations, stubby euhedral crystals with xenocrystic cores, slender prisms, and cracked needles. Strongly abraded samples of the best cracked needles plotted on concordia with an estimated age of 427 ± 3 Ma. The prisms and euhedral crystal populations are both strongly

discordant, plotting on a chord with its lower intersect at the 427 Ma date and an upper intersect with the very approximate date of $2287 \pm 98 - 88$ Ma.

The new precise dates provided in this study, the first available for the Springdale caldera ss, bracket the age of the caldera between the lowermost ash-flow tuff at 432 Ma and the uppermost ash-flow tuff at 427 Ma. A rhyolite dome within the caldera dates at 431 Ma, as would be expected from its position in the middle of the stratigraphic sequence. This study is also the first successful of many attempts to provide precise dates for the Cape St. John Group and the King's Point Complex, both at 427 Ma. The precision of these dates shows great potential for volcanological studies which were previously impossible in such ancient non-fossiliferous volcanic sequences. They also allow for correlation with other suites of central Newfoundland, identifying a major tectonothermal event tightly focussed around 430 ± 5 Ma.

7.4. Caldera Evolution

Ten broad units were mappable in the Springdale Group at the scale of this study. They are interpreted as having the following volcanological significance, as illustrated in Figure 7.2.

Figure 7.2. Schematic outline of the sequence of events which produced the Springdale caldera and its products (based on Smith and Bailey, 1968, from Fisher and Schmincke, 1984).

- I. Regional tumescence, propagation of ring and radial fractures with possible apical graben subsidence. Eruptions from radial or ring fractures. Erosion of the volcanic highland with sediments deposited on flanks and surrounding lowland areas.
- II. Major ash-flow eruptions with flows extending tens of miles beyond the volcano.
- III. Caldera collapse. Ash flow deposits within the caldera form part of the intra-caldera facies along with avalanches and slides from caldera wall. Ash-flow deposits beyond the caldera walls form the dominant rock of the outflow facies.
- IV. Pyroclastic eruptions, domes and lava flows occur on caldera floor of some calderas and occur with continuing deposition of slides, fans, and lake deposits.

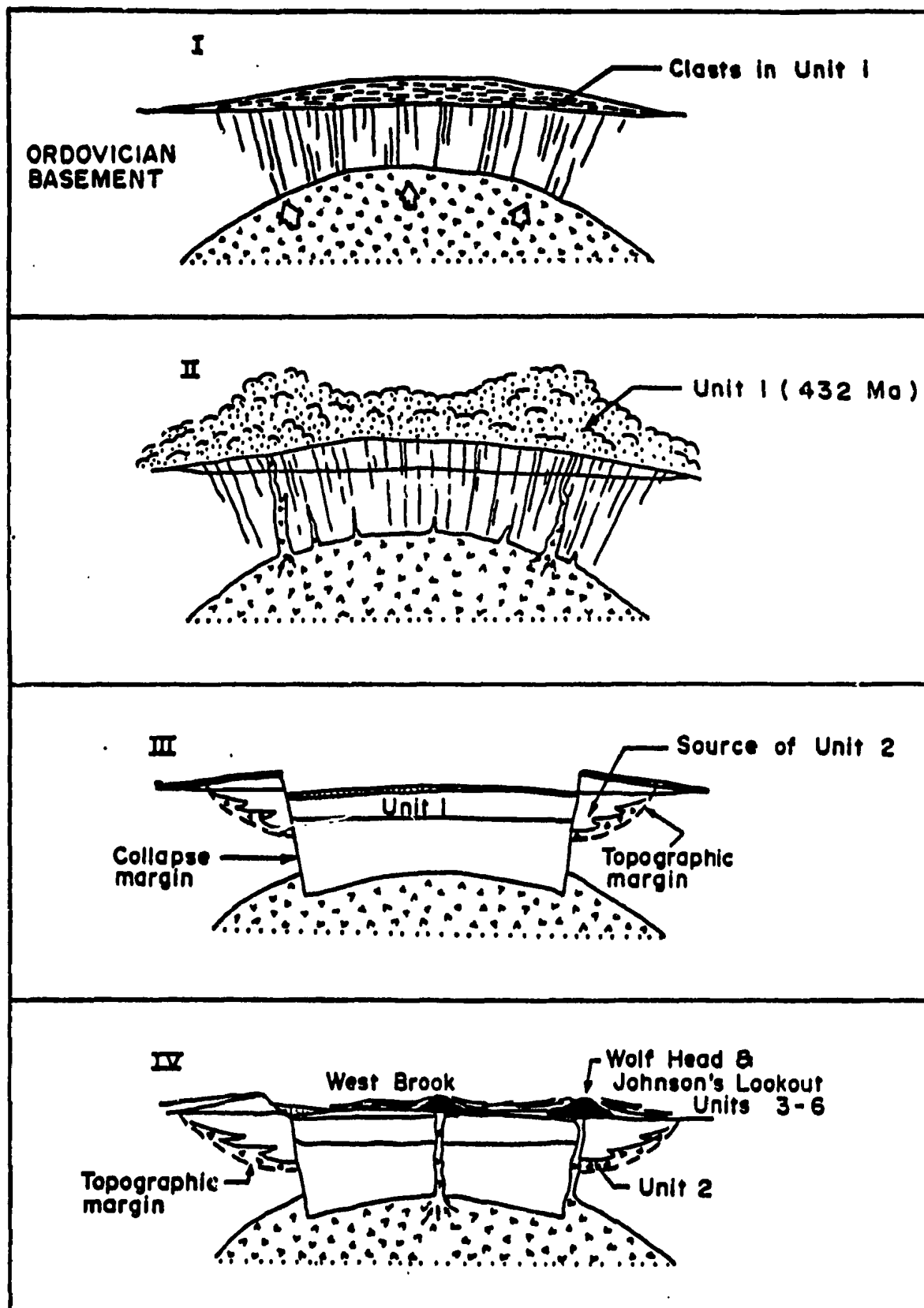
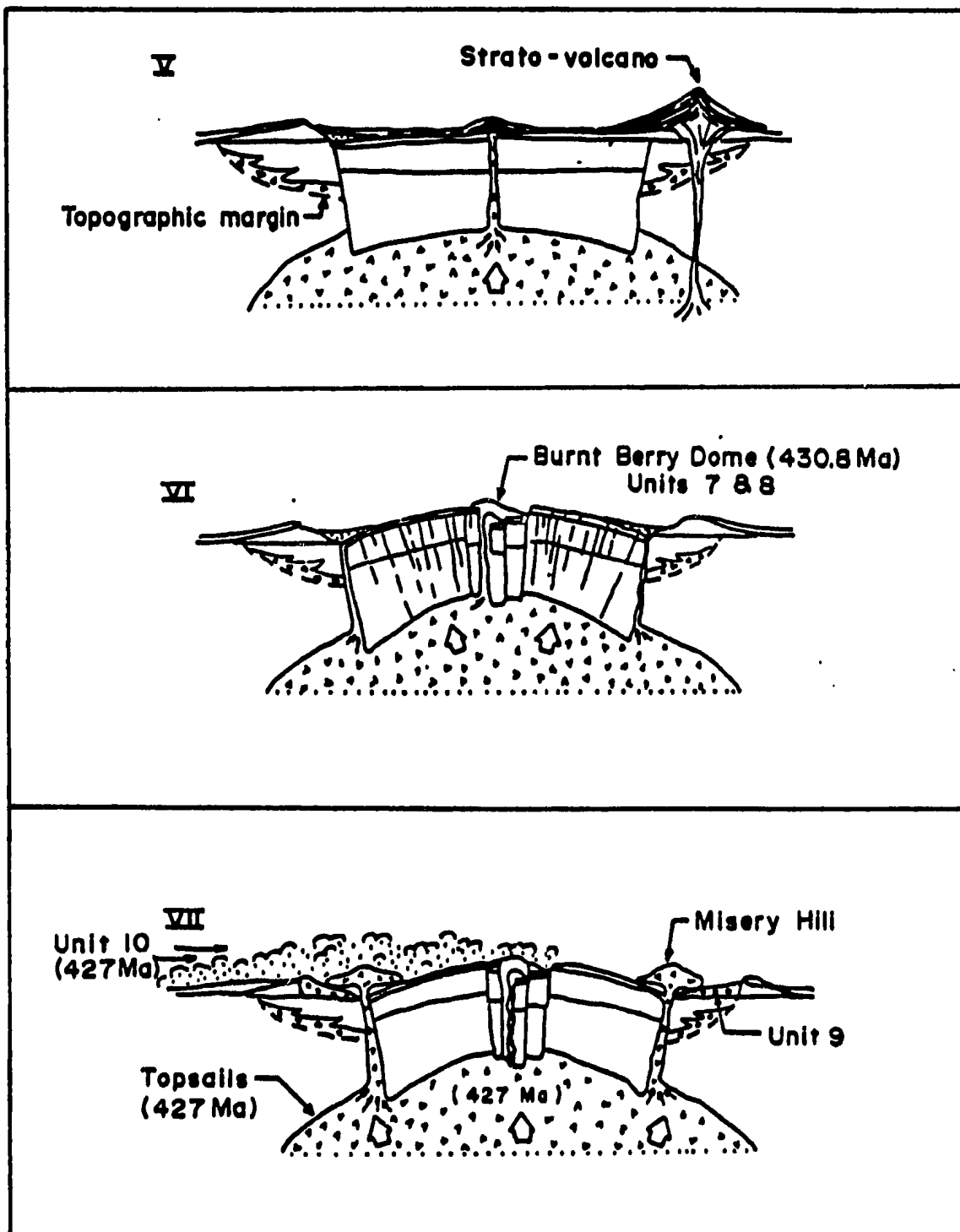


Figure 7.2 (continued). Schematic outline of the sequence of events which produced the Springdale caldera and its products.

- V. Eruption of stratovolcano with andesitic flows and pyroclastics concentrically dispersed around a central dioritic pluton.**

- VI. Resurgent doming and possible ring-fracture volcanism and/or eruption or intrusion in dome fractures.**

- VII. Continued resurgence and intrusion/eruption of silicic domes and basaltic lava flows. Caldera fill from non-volcanic sedimentary processes continues. Incursion of ash-flow tuffs from adjacent calderas (King's Point, Topsails?) are interbedded with other caldera-fill material.**



Stage I

Clasts of plagiophyric basalt, granophyre and perlitic felsic clasts found in Unit 1, and these are taken as evidence of the volcanic activity during the pre-collapse stage of regional tumescence.

Stage II

Unit 1, dated at 432 Ma, is the earliest erupted ash flow and is thus taken to represent the product of initial evacuation of the Springdale magma chamber. The abundance and variety of lithic clasts (basalt, andesite, ultramafics, jasper) indicate that the roof of this magma chamber was essentially the ophiolitic and island arc material which forms the basement to the Springdale Group and is common around the caldera margins.

Stage III

Unit 2 is dominated by mesobreccias, laharic flows, with tuffites and peperites, volcanic conglomerates and local red sandstones, and volcanic explosion breccia. In general the volcanoclastic lithologies are characterized by poor sorting and massive to very coarse bedding. The lahars have dominantly sub-angular blocks in a locally vesicular muddy or ashy matrix. Both the coarse and fine fractions of these deposits are compositionally variable from basalt to rhyolite.

The rocks of Unit 2 are considered to represent the major unit deposited by collapse and erosion of the caldera walls following the initial collapse due to the eruption of Unit 1. However, these lithologies clearly represent facies developed during different stages of volcanic activity, and range from near-source explosion deposits to debris flows to more distal, fluviially reworked sediments. Some debris flows may have been activated on unstable slopes and rapidly deposited, whereas others contain clasts which suggest longer periods of reworking.

Stage IV

This caldera stage was one of pyroclastic eruptions and lava flows on the caldera floor, as described by Fisher and Schminke (1984), but it is taken as the stage during which most of the rocks within the caldera, i.e. Units 3 to 6, were deposited.

Unit 3, occurring mainly as an extensive belt along the east side of the caldera, consists of intermediate composition (dacite, andesite) flows, domes and intrusions. They represent a period of non-explosive volcanism dominated by andesitic-dacitic chemistry, although a minor phase of this unit consists of silicic and mafic compositions interbanded on the scale of centimetres and smaller, suggesting that these intermediate rocks may have been formed by mixing of more mafic and silicic magmas.

Unit 4 is also intermediate in composition, but it occurs as a narrow band of ash-flow tuff extending over a distance of 10 km, overlying unit 3 and succeeded by basaltic flows of unit 5. It is predominantly dacite, but ranges in composition from rhyolite to andesite. The tuff breccias contain large angular and flattened pumice clasts and the lapilli tuff has pumice lapilli up to 65 mm long, and these lithologies tend to be discontinuous along strike. These features are taken to indicate a near source for these rocks, probably the same fracture system which fed the rocks of the adjacent Unit 3.

Basaltic flows of Unit 5 occur as three dominant bands, one on each side of the caldera and one in the centre. Although outcrop of the less resistant basaltic rocks is generally poor, those of the western belt form particularly striking ridges exposing multiple flows typical of fissure eruptions. It is probable that all three bands were erupted through fissures, possibly in the caldera floor, but dominantly along the margins as appears to be typical for calderas. A number of later basaltic flows are also found in the northern part of the caldera interbedded with the late caldera-fill redbeds of Stage VI.

Silicic ash-flow tuffs of Unit 6 occur in discontinuous exposures for more than 30 km within the caldera. These ash flows are particularly characterized by basal thick lithophysae-rich horizons, with individual

lithophysae as large as 10 cm in diameter. This indicates that these ash flows trapped substantial fluid during eruption, possibly from the rivers and lakes which would have been forming in these intermediate to late stages of caldera evolution. Different ash flows cooled as a simple cooling unit, suggesting that they followed one another in rapid succession.

Stage V

Although probably overlapping in time with Stage IV, Stage V is isolated in order to emphasize the small central volcano originally identified on the basis of andesitic lava flows apparently emanating from a central dioritic pluton, and subsequently affirmed by aeromagnetic data. The latter shows a near-perfect pattern of concentric and radial lineaments from the central pluton which compels an interpretation in terms of concentric flows and ring dykes with presumably co-genetic radial dykes.

Stage VI

Units 7 and 8, occurring as broad bands through the central part of the caldera, is dominated by massive, strongly welded vitric ash-flow tuffs, vitroclastic breccias and domes. The massive tuffs and domes are locally porphyritic, with small euhedral flow-aligned plagioclase and rare quartz phenocrysts. These rocks mark a change in composition of ash-flow tuffs from the andesitic to dacitic compositions of Stage IV to rhyolitic-dacitic rocks which suggest either or both of more advanced differentiation of

the magma chamber, or the tapping of more siliceous (shallower) portions of it. The latter would accord with the fact that these rocks are found in the centre of the caldera, i.e. where the shallower parts of the magma chamber would be tapped, as shown in Figure 7.2.

Welding in Unit 7 is flat-lying in its southern exposures and becomes more steeply inclined towards the north where the Burnt Berry and West Brook Domes are exposed. These features together are taken to indicate that both Units 7 and 8 heralded the period of resurgence shown in Stage 8. Mixed magmas within the breccias of Unit 8 are interpreted as resulting from mixing of the shallow silicic lavas with the late basaltic lavas interbedded with the caldera-fill sediments. The date of 430.8 for the Burnt Berry dome gives a time-span of 2.2 million years for development of the caldera to this stage.

Stage VII

Stage VII appears simple as it is shown in Figure 7.1, but it actually includes four important components. Unit 9 comprizes a sequence of redbed sedimentary rocks distributed in the central portion of the Springdale syncline. It forms belts up to 25 km long, disposed about the central synclinal axis over a distance of 20 km, and records the activity of fluvial and lacustrine processes within the caldera, with clast assemblages representing virtually all lithologies produced during the caldera

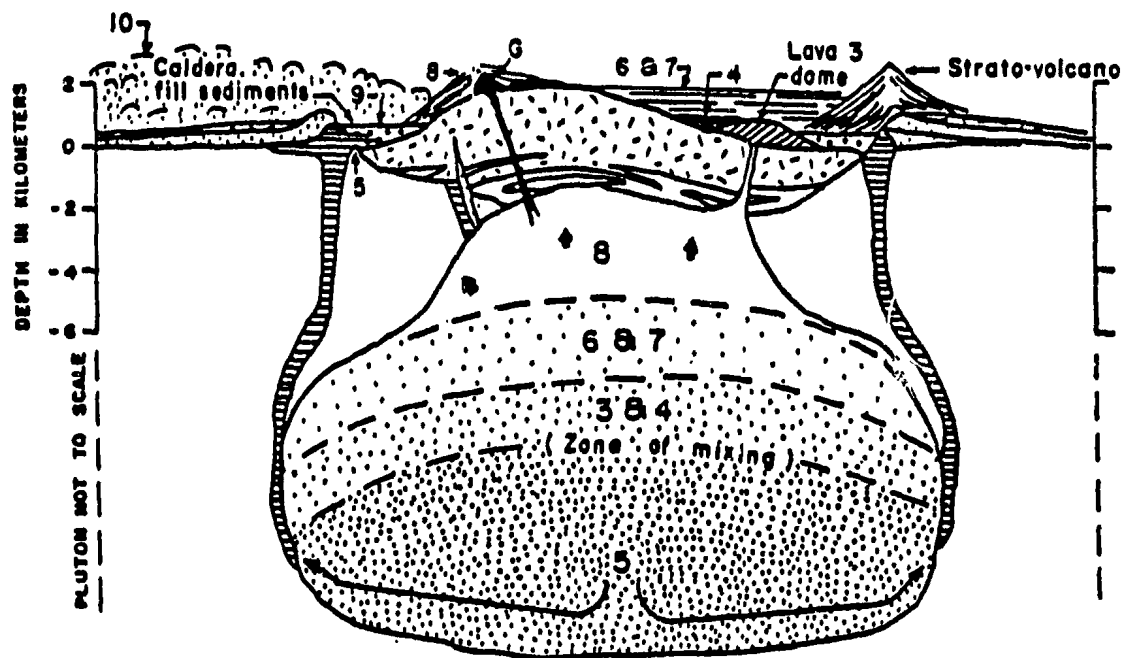
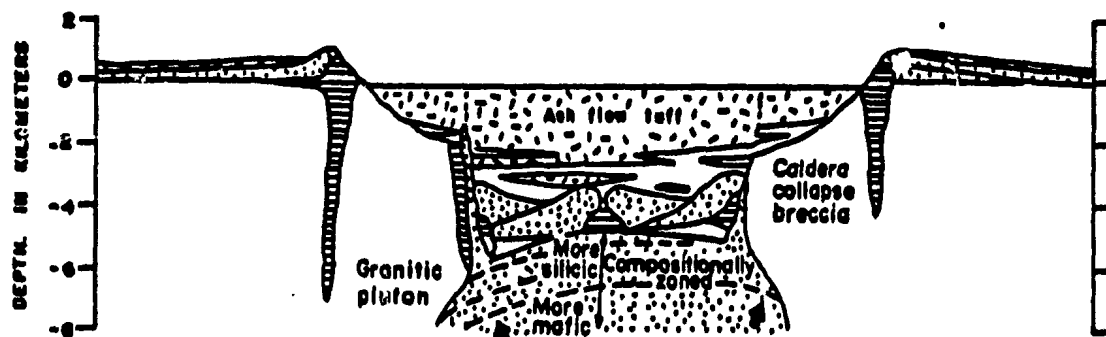
development. These sedimentary rocks are interbedded with basaltic flows, not shown on Fig. 7.2(VII). Unit 10, the Indian River Tuff, occurs throughout the interior of the central syncline in the north of the caldera, and in one other exposure in the southwestern part of the caldera, and has been interpreted as being an outflow facies of the adjacent King's Point caldera. It is comparable to Unit 1 of the Springdale caldera in that it has clasts of mafic, ultramafic and cherty lithologies, indicating that like the Springdale caldera, the roof of the King's Point magma chamber consisted of the Ordovician oceanic crust and arc sequences.

The third element of Stage VII is represented by rhyolitic domes such as that of Misery Hill and others in the southern parts of the caldera. These are inferred to be offshoots of the Topsails pluton which truncates the southwestern part of the caldera, because of their concentric distribution with respect to its intrusive contact. Although the estimated age of 427 Ma for the Topsails complex is not as precise or reliable as those provided by the present study, its similarity to the date of 427 Ma provided by this study for both the King's Point caldera and the Cape St. John Group attests to the climactic importance of this time in the development of the "Springdale volcanic field" of western Newfoundland.

Lithologies produced by the earliest caldera-forming events (Fig. 7.2) are summarized in Figure 7.3(a), and later lithologies in Figure 7.3(b). They appear to show a pattern of eruption which can be related to depth within the magma chamber, also shown on Figure 7.3(b). It is assumed that the Springdale magma chamber was layered, with the most siliceous melts at the top, the basaltic melts rocks at the bottom, and intermediate compositions in a zone of mixing as outlined in Figure 4.14, based on the magma chamber models proposed by many workers (e.g. Hildreth, 1981). Unit 1 was so contaminated with accidental roof material that no samples were chemically analysed, but one might assume that the magma came from the roof zone.

During Stage IV intermediate compositions of Units 3 to 6 were erupted from within the zone of mixing. Likewise, in Stage V, the marginal strato-volcano was erupted from a marginal feeder tapping into the andesitic magma-mixing levels. The rift basalts (Unit 5) were erupted mainly through marginal fractures which tapped deep into the basaltic magma at the caldera bottom. The more silicic magmas of Units 7 and 8 (Stage VI) were erupted from the, by now, highly differentiated top of the magma chamber. Stages VI and VII marked the final emptying of the chamber by eruption of the late caldera-fill basalts. The other eruptions of Stage VII came from the adjacent King's Point (Unit 10) and Topsails (silicic domes and granites) calderas.

Figure 7.3. A schematic outline of the events associated with generation of (a) the early caldera-forming (Units 1 and 2), and all later lithologies (b). Based upon a layered magma chamber, with the most siliceous magma at the top, the basaltic magma at the bottom, and intermediate compositions in a zone of mixing between the two. Numbers and arrows within the chamber suggest the site of origin of the material reaching surface.



7.5. Tectonic Controls

Syn-caldera dextral motion on the Lobster Cove and other faults of the area suggest that the Springdale caldera, indeed the whole volcanic field from Cape St. John to topsails, was generated in a transpressional tectonic environment. This followed closure and destruction of the Cambro-Ordovician Iapetus Ocean, when continental crust was juxtaposed against that of the ocean basin. Evidence for this juxtaposition is seen in both the King's Point and Cape St. John rocks, where ophiolitic clasts are included along with zircons derived from continental crust. No such zircons are found within rocks of the Springdale Group, possibly indicating that it occurs to the east of the ancient continental margin.

Deformation of the Springdale Group was dominated by one major fold, an open syncline. This, along with other minor folds and both thrust and strike-slip faults allow for east-west shortening of the order of 20 to 30%, which in turn explains the present elongate shape of the caldera.

Location of the Springdale volcanic field straddling the continent-ocean suture zone leads to the suggestion that this volcanism was focussed by the inherent structural weaknesses at the suture. Most correlative rocks in the orogen, from Scotland to at least as far south as Maine, are also found near this or other major tectonic boundaries, with a similar dextral strike-slip tectonic

regime. Given that such large calderas demand an extensional environment, at least locally, it can be suggested that such extension would be most readily produced in local pull-apart basins in this dextral regime.

7.6. Economic Potential

Epithermal precious metal deposits are commonly associated with calderas, and the Springdale caldera should have similar potential. The adularia-sericite type of epithermal deposits are generally found in a regional structural setting along the margins of calderas, although other structurally more complex environments may also be associated, e.g. along fault zones of different types within the calderas or within domes. The importance of the volcanic setting is primarily one of providing the plumbing system and heat to drive circulating hydrothermal fluids, so that virtually any rock type may be a favourable host for mineralization. Acid-sulfate types of deposits have a similar structural setting to some adularia-sericite deposits, but the presence of intrusive centres, particularly ring-fracture volcanic domes on the margins of calderas, appears to be a critical genetic factor.

The Springdale caldera, prior to the present study, has not been a targets for mineral exploration based on caldera models, although there are numerous examples of caldera-related gold mineralization in correlative rocks in central Newfoundland, e.g. Hope Brook and Sops Arm areas.

Three areas of alteration were located in the Springdale caldera. The most promising was found along the eastern side of Burnt Berry Brook, where the alteration is moderate to strong sericitic in porcelanitic tuffs, and ranges from weak to moderate argillic alteration in spherulitic zones within silicic volcanics. This locality is within the area interpreted to mark the main keystone graben area related to resurgence, a favourable environment in many calderas. Gold grains were found in the till of this area. Other zones of interest in this area are seen as local quartz veining and hydrothermal brecciation of the volcanics and granite, and along faults where EM conductors are found.

In the eastern collapse margin area of the caldera, one rock sample of Unit 1 was found to be anomalous for gold, and stream-silt samples also proved anomalous for gold and associated trace elements. In the vicinity of Johnson's Lookout stream samples from tributaries of Barney's Brook which drain Unit 2 have anomalous gold, arsenic and zinc. Unit 4 hosts some of the strongest alteration in the area, with thick (~2m) porous lithophysae zones moderately to strongly altered with quartz-pyrite veining in limonitic/argillic zones.

In the southeastern part of the collapse margin area one rock sample of Unit 2 was anomalous for gold (>5 ppb) and four others were also anomalous for arsenic (5 ppm) and antimony (>1 ppm). Stream silt samples from this area also provided anomalies in all these elements plus zinc.

It is clear from both the geological mapping for the main part of this thesis study, as well as the limited subsequent exploration, that there are a number of indications of alteration and geochemical anomalies which were predicted on the basis of typical models for caldera style mineralization. These are obviously important as indicators of mineral potential and warrant much more intensive exploration and investigation. They are perhaps equally important to this study in that they provide yet another line of evidence in support of the interpretation that the Springdale Group represents the products of a large collapse caldera.

7.7. Conclusion

The Springdale Group of north central Newfoundland consists of volcanic and sedimentary rocks produced through the formation and evolution of a large epicontinental type caldera. These events took place over a five million year period in the early Silurian between 430 and 427 Ma. The Springdale caldera is at least partly correlative with the nearby King's Point caldera, the Cape St. John Group (caldera?) and the Topsails complex (caldera?), samples from all three also dated at 427 Ma. These together make up part of an extensive early Silurian volcanic field, here termed the Springdale Volcanic Field. The scale of these calderas and their abundant highly siliceous volcanic rocks

suggest that they were formed in a substantially thickened epicontinental type of crustal regime, presumably produced through crustal thickening following closure of the Cambro-Ordovician Iapetus Ocean.

The main accomplishment of this thesis has been the recognition and documentation of the Springdale Caldera. With further detailed study, it and its correlatives promise to yield greater insights into Appalachian tectonic and magmatic processes. It also exhibits most of the characteristics which make it a prime target for the discovery of epithermal precious mineral deposits.

REFERENCES

- Atwater, T., 1970. Implications of plate tectonics for the tectonic evolution of western North America. *Geol. Soc. Amer. Bull.* 81, pp. 3513-3536.
- Bates, R. L. and Jackson, J. A. 1980. *Glossary of Geology* (Second Edition) American Geological Institute, Falls Church, Virginia.
- Bell, K. and Blenkinsop, J., 1978. U-Pb ages of some crystalline rocks from the Burlington Peninsula, Newfoundland, and implications for the of Fleur de Lys metamorphism: discussion. *Canadian Journal of Earth Sciences*, Vol. 15, pp. 1208-1210.
- Bell, K., Blenkinsop, J. and Strong, D. F., 1977. The geochronology of some granitic bodies from eastern Newfoundland and its bearing on Appalachian evolution. *Canadian Journal of Earth Sciences*, 14, pp. 456-476.
- Belt, E. S., 1969. Newfoundland Carboniferous stratigraphy and its relation to the Maritimes and Ireland. In *North Atlantic Geology and Continental Drift*. Edited by M. Kay. American Association of Petroleum Geologists, Memoir 12, pp. 734-753.
- Berry, W. B. N. and Boucot, A. J. (eds.), 1970. Correlation of the North American Silurian rocks. *Geological Society of America Special Paper No. 102*, 289p.

- Bostock, H. H., Currie, K. L., and Wanless, R. K. 1979. The age of the Roberts Arm Group, north central Newfoundland. *Canadian Journal of Earth Sciences*, **16**, pp. 599-606.
- Bowen, N. L., 1928. *The Evolution of the Igneous Rocks*. Dover Publications, Inc., New York, 332p.
- Buchanan, L. J., 1981. Precious metal deposits associated with volcanic environments in the southwest. In *Relations of Tectonics to Ore Deposits in the southern Cordillera*, edited by W. R. Dickson and W. D. Payne. Arizona Geological Society, vol. 14, pp. 237-262.
- Burnham, C.W., 1967. Hydrothermal Fluids at the Magmatic Stage. In *Geochemistry of Hydrothermal Ore Deposits*. Edited by H.L. Barnes. Holt, Rinehart and Winston, N.Y., pp. 34-76.
- Burt, D. M., and Sheridan, M. F., 1987. Types of mineralization related to fluorine-rich silicic lava flows and domes. In *The Emplacement of Silicic Domes and Lava Flows*. Edited by J. H. Fink, G. S. A., Special Paper 212, pp 103-110.
- Calon, T. J. and Szybinski, Z. A., 1988. Lobster Cove Fault: dextral strike slip fault system. GAC, MAC, CSPG Program with Abstracts, vol. 13, p. A17.
- Chandler, F. W. and Dunning, G. R. 1983. Fourfold significance of an early Silurian U-Pb zircon age from rhyolite in redbeds, southwest Newfoundland, N.T.S. 12A/4. *Current Research, Geological Survey of Canada Paper* 83-1B, pp. 419-421.

- Chandler, F. W., Sullivan, R.W., and Currie, K.L., 1987. Age of the Springdale Group, western Newfoundland, and correlative rocks - evidence for a Llandovery overlap assemblage in the Canadian Appalachians. Transactions of the Royal Society of Edinburgh, Earth Sci., vol. 78, pp. 41-49.
- Church, W. R. and Stevens, R.K., 1971. Early Paleozoic ophiolite complexes of the Newfoundland Appalachians as mantle -oceanic crust sequences. Jour. Geophy. Res. vol. 76, pp. 1460-1466.
- Cole, J. W. 1985. Taupo-Rotorua Depression : an ensialic marginal basin of North Island, New Zealand. pp. 109-119 in Kokelaar, B. P. and Howells, M. F. (eds.) Marginal Basin Geology, Geological Society of London.
- Coyle, M. and Strong, D.F., 1987. Geology of the Springdale Group: a newly discovered Silurian caldera in central Nfld. Can. J. Ea. Sci., 24, 1135-1148.
- Coyle, M. and Strong, D. F., 1986. Geology of the southern and northern margins of the Springdale caldera, Newfoundland. Current Research, Geological Survey of Canada Paper 86-1A pp. 499-506.
- Coyle, M., Strong, D. F. and Dingwell, D. B. 1986. Geology of the Sheffield Lake area. Current Research, Geological Survey of Canada Paper 86-1A pp. 455-459.

- Coyle, M., Strong, D.F., Gibbons, D., and Lambert, E. 1985. Geology of the Springdale Group, central Newfoundland; in Current Research, Part A, Geological Survey of Canada, Paper 85-1A, p. 157-163.
- Cox, K. G., Bell, J. D. and Pankhurst, R. J., 1979. The Interpretation of Igneous Rocks, George Allen and Unwin, London, 450p.
- Cunningham, C. G. and Steven, T. A., 1979. Mount Belknap and Red Hills Calderas and associated rocks, Marysvale Volcanic Field, west-central Utah. U. S. Geol. Surv. Bull. 1468, pp. 1-34.
- Currie, K.L. and Piasecki, M.A.J., 1989. Kinematic model for southwestern Newfoundland based upon Silurian sinistral shearing. Geology, v. 17, p. 938-941.
- Davis, D. W., 1982. Optimum linear regression and error estimation applied to U-Pb data. Canadian Jour. of Earth Sciences, vol. 19, pp. 2141-2149.
- Dallmeyer, R. D., 1977. $^{40}\text{Ar}/^{39}\text{Ar}$ age spectra of minerals from the Fleur de Lys terrane in northwest Newfoundland: their bearing on chronology of metamorphism within the Appalachian orhotectonic zone. Jour. of Geology, vol. 85, pp.89-103.
- Dean, P. L. and Strong, D. F., 1977. Folded thrust faults in Notre Dame Bay, Central Newfoundlands. Amer. Jour. Sci., vol. 277, pp. 97-108.

- Dean, P. L. and Strong, D. F., 1976. Geological maps of the Notre Dame Bay region, Central Newfoundland. Open File 1:50,000 series, Nfld Dept. Mines and Energy, St. John's , and Geol. Surv. Can. Ottawa.
- Debon F. and LeFort P., 1983. A chemical-mineralogical classification of common plutonic rocks and associations.
- Degrace, J. R., Kean, B. F. and Hsu, E. and Green, T. 1976. Geology of the Nippers Harbour Map area (2E/13) Newfoundland. Newfoundland Department of Mines and Energy Report 76-3, 73 pp.
- Dunning, G.R. and Krogh, T.E., 1985. Geochronology of ophiolites of the Newfoundland Appalachians. Can. Jour. Earth Science, vol. 22, pp. 1659-1670.
- Dunning, G. R., Wilton, D. H.C. and Herd, R. K., 1989. Geology, geochemistry and geochronology of a taconic batholith, southwestern Newfoundland. Trans. of the Royal Society of Edinburgh, vol. 80, Part 2, pp. 159-168.
- Dunning, G. R., Krogh, T. E., O'Brien, S. J., Colman-Sadd, S. P., and O'Neill, P., 1988. Geologic framework of the Central Mobile Belt in southern Newfoundland and the importance of Silurian orogeny. Geol. Assoc. of Canada, Program with Abstracts, volo. 13, p. 34.
- Dunning, G. R., Kean, B. F., Thurlow, J. G. and Swinden, H. S., 1987. Geochronology of the Buchans, Roberts Arm and Victoria Lake Groups and Mansfield Cove Complex, Newfoundland. Can. J. Earth Sci., vol. 24, pp. 1175-1184.

- Erdmer, P., 1986. Geology of the Long Range Inlier, Sandy Lake map area, (12/H) west Newfoundland. Current Research Part B, Geological Survey of Canada Paper 86-1B, p. 19-27, and G.S.C. Open File 13-10 Map with marginal notes.
- Fenner, C. N., 1929. The crystallization of basalts. American Journal of Science, vol. 18, pp. 225-253.
- Fisher, R. V. and Schmincke, H.-U, 1984. Pyroclastic Rocks. Springer-Verlag, Germany, 472p.
- French, W. J., Hassan, M. D., and Westcott, J. 1979. The petrogenesis of Old Red Sandstone volcanic rocks of the western Ochils, Stirlingshire. In: Harris, A.L., Holland, C.H. and Leake, B.E. (eds.), The Caledonides of the British Isles - reviewed. Special Publication of the Geological Society of London, 8, pp. 635-642.
- Gans, P.B., Mahood, G. A., and Schermer, E., 1989. Syn-extensional magmatism in the Basin and Range Province; a case study from the eastern Great Basin. Geological Society of America Special Paper No. 233.
- Gill, J. B., 1981. Orogenic Andesites and Plate Tectonic. Springer-Verlag, Berlin, 389p.
- Ewart, A., 1982. The mineralogy and petrology of Tertiary-Recent orogenic volcanic rocks: with special reference to the andesitic-basaltic compositional range. In R.S. Thorpe (ed.) Andesites, John Wiley & Sons., pp. 25-95.

- Groome, D.R. and Hall, A., 1974. The geochemistry of the Devonian lavas of the Lorne Plateau, Scotland. *Mineralogical Magazine*, 39, pp. 621-640.
- Hayba, D. O., Bethke, P. M., Heald, P. and Foley, N.K., 1985. Geologic, mineralogic, and geochemical characteristics of volcanic-hosted epithermal precious-metal deposits. In *Geology and Geochemistry of Epithermal Systems*, edited by B. R. Berger and P. M. Bethke. *Reviews in Economic Geology*, vol. 2, pp. 129-167.
- Heald, P., Foley, N. K. and Hayba, D. O. 1987. Comparative anatomy of volcanic-hosted epithermal deposits: acid-sulfate and adularia-sericite types. *Econ. Geol.* vol. 82, pp.1-26.
- Heiken, G. and Wohletz, K., 1987. Tephra deposits associated with domes and lava flows. In *The Emplacement of Silicic Domes and Lava Flows*. Edited by J. H. Fink, G. S. A., Special Paper 212, pp. 55-76.
- Hess, P.C., 1980. Polymerisation model for silicate melts. In *Physics of magmatic processes*. Edited by R. B. Hargraves. Princeton University Press, pp. 3-48.
- Hibbard, J., 1983. Geology of the Baie Verte Peninsula, Newfoundland. Newfoundland Department of Mines and Energy Memoir 2, 279 pp.
- Hildreth, E.W., 1981. Gradients in silicic magma chambers: Implications for lithostatic magmatism. *Journal of Geophysical Research*, 86, pp. 10153-10192.

- Hildreth, E. W., 1979. The Bishop Tuff: Evidence for the origin of compositional zonation in silicic magma chambers. Geological Society of America Special Paper 180, pp. 43-76.
- Hyde, R. S., 1979. Geology of Carboniferous strata in portions of the Deer Lake Basin, western Newfoundland. Nfld. Deot. Mines and Energy, Mineral Development Division, Report 79-6, 43p.
- Ihlen, P. M., Tronnes, R. and Vokes, F. M., 1982. Mineralization, wall rock alteration and zonation of ore deposits associated with the Dramman granite in the Oslo Region, Norway. In: Metallization Associated with Acid Magmatism, edited by A. M. Evans. John Wiley, Chichester, pp. 111-136
- Irvine, T. N., and Barager, W. R. A., 1971. A guide to the chemical classification of the common volcanic rocks. Can. Jour. Earth Sci., vol. 8, pp. 523-548.
- Irving, E., and Strong, D. F., 1984. Palaeomagnetism of the Early Carboniferous Deer Lake Group, western Newfoundland: no evidence for mid-Carboniferous displacement of "Acadia". Earth and Planetary Science Letters, vol. 69, pp. 379-390.
- Irving, E., and Strong, D. F., 1984. Paleomagnetism of rocks from the Burin Peninsula, Newfoundland: hypothesis of Late Paleozoic displacement of Acadia criticized. Jour. Geophys. Res. v. 90, 1949-1962.

- Jenson, L. S., 1976. A new cation plot for classifying subalkalic volcanic rocks. Ont. Dept. of Mines, Misc. Paper 66.
- Kalliokoski, J. 1955. Gull Pond, Newfoundland (Second Preliminary Map); Geological Survey of Canada Paper 54-4.
- Kalliokoski, J. 1953. Springdale, Newfoundland: Geological Survey of Canada Paper 53-5, 4 p.
- Kean, B. F., 1988. Regional geology of the Springdale Peninsula. In The Volcanogenic Sulphide Districts of Central Newfoundland, edited by H. S. Swinden and B. F. Kean. Geol. Assoc. Canada, Mineral Deposits Section, pp. 74-79.
- Kennedy, W. Q., 1946. The Great Glen Fault. Geol. Soc. London Quart. Jour. vol. 102, pp. 41-72.
- Kent, D. V. and Opdyke, N. D., 1978. Paleomagnetism of devonian Catskill red beds: evidence for motion of coastal New England-Canadian Maritime region relative to cratonic North America. Jour. Geophysical Research, vol. 83, p. 4441.
- Kontak, D. J. and Strong, D. F., 1986. The King's Point volcano-plutonic complex, Newfoundland. Current Research Geological Survey of Canada pp. 465-470.
- Kontak, D. J., Tuach, J., Strong, D. F., Archibald, D. A., and Farrar, E., 1988. Plutonic and hydrothermal events in the Ackley Granite, southeast Newfoundland, as indicated by total fusion $^{40}\text{Ar}/^{39}\text{Ar}$; geochronology. Can. J. Earth Sci., 25, 1151-1160.

- Krogh, T. E., 1973. A low contamination method for the hydrothermal decomposition of zircon and extraction of U and Pb for isotopic age determinations. *Geochimica et Cosmochimica Acta*. 37: 485- 494.
- Krogh, T. E., 1982. Improved accuracy of U-Pb zircon ages by the creation of more concordant systems using an air abrasion technique. *Geochimica et Cosmochimica Acta*, 46, pp. 637-649.
- Krogh, T. E. and Davis, G. L., 1975. The production and preparation of ^{205}Pb for use as a tracer for Isotope Dilution analysis. *Carnegie Institution of Washington Yearbook* 74, p. 416-417.
- Laurent, R. and Belanger, J., 1984. Geochemistry of Silurian-Devonian alkaline basalt suites from the Gaspé Peninsula, Quebec Appalachians. *Maritime Sediments and Atlantic Geology*, 20, pp. 67-78.
- Lambert, R. St. J., Chamberlain, V. E., and Holland, J. G. 1976. The geochemistry of Archean rocks. pp. 377-387 in Windley, B. F. (Ed.) *The Early History of the Earth*. John Wiley & Sons, 619 pp.
- Leshner, C. E., Walker, D., Candela, P., and Hayes, J. F., 1982. Soret fractionation of natural silicate melts of intermediate to silicic composition. *Geological Society of America, Abstracts with Programs*, 14, p. 545.

- Lipman, P. W., 1976. Caldera-collapse breccias in the western San Juan Mountains, Colorado. *Geol. Soc. Am. Bull.*, vol.87, pp. 1397-1410.
- Lipman, P. W., Doe, B. R., Hedge, C. E., Steven, T. A., 1978. Petrologic evolution of the San Juan volcanic field, southwestern Colorado: Pb and Sr isotope evidence. *Geological Society of America Bulletin*, 89, pp. 59-82.
- Lipman, P. W., Fisher, F. S., Mehnert, H. H., Naeser, C.W., Luedke, R. G., and Steven, T. A., 1976. Multiple ages of mid-Tertiary mineralization and alteration in the western San Juan Mountains, Colorado. *Econ. Geol.*, 71, pp. 571-588.
- Lock, B.E., 1972. Lower Paleozoic history of a critical area: eastern margin of the St. Lawrence Platform in White Bay, Newfoundland, Canada. *International Geological Congress 24th. Montreal, section 6*, p. 310-324.
- Lock, B.E., 1969. The Lower Paleozoic geology of western White Bay, Newfoundland. Unpublished Ph.D. thesis, Cambridge University, England, 343 pages.
- MacDonald, G. A. and Katsura, T., 1964. Chemical composition of Hawaiian lavas. *Jour. Petrology*, vol. 5, pp. 82-133.
- Maniar, P. D. and Piccoli, P. M., 1989. Tectonic discrimination of granitoids. *Geol. Soc. of Amer. Bull.*, vol. 101, pp.635-643.
- Mattinson, J. M., 1977. U-Pb ages of some crystalline rocks from the Burlington Peninsula, Newfoundland, and implications for the age of Fleur de Lys metamorphism. *Canadian Journal of Earth Sciences*, Vol. 14, pp 2316-2324.

- McBirney, A. R., 1984. *Igneous Petrology*. Freeman Cooper & Co., San Francisco, 504p.
- Mercer, B., Strong, D. F., Wilton, D. H. C. and Gibbons, D., 1985. The King's Point volcano-plutonic complex, western Newfoundland. Current Research, Part A, Geological Survey of Canada Paper 85-1A, Report 8.
- Meschede, M., 1986. A method of discriminating between different types of mid-ocean ridge basalts and continental tholeiites with the Nb-Zr-Y diagram. *Chemical Geology*, Vol. 56, pp. 207-208.
- Michael, P.J., 1983. Chemical differentiation of the Bishop Tuff and other high-silica magmas through crystallization processes. *Geology*, 11, pp. 31-34.
- Middlemost, E.A.K., 1985. *Magmas and Magmatic Rocks*, Longman Group Limited, Essex. - pp.
- Mullen, E. D., 1983. MnO/TiO₂/P₂O₅: a minor element discriminant for basaltic rocks of oceanic environments and its implications for petrogenesis, *Earth and Planetary Science Letters*, vol. 62, pp. 53-62.
- Murray, A. and Howley, J. P., 1881. Report of the Geological Survey of Newfoundland from 1864 to 1880. Geological Survey of Newfoundland, Publication, 536 p.
- Myashiro, A., 1974. Volcanic rock series in island arcs and active continental margins. *Amer. Jour. of Sci.*, vol. 274, pp. 321-355.
- Neale, E.R.W. 1962. King's Point area, Newfoundland; Unpublished manuscript.

- Neale, E. R. W. and Kennedy, M. J., 1967. Relationship of the Fleur de Lys Group to younger groups of the Burlington Peninsula, Newfoundland. In *Geology of the Atlantic Region*. Edited by E.R. W. Neale and H. Williams. Geological Association of Canada, Special Paper 4, pp. 139-169.
- Neale, E.R.W., and Nash, W.A. 1963. Sandy Lake (east half), Newfoundland; Geological Survey of Canada, Paper 62-28, 40 p.
- Neale, E.R.W., Nash, W.A., and Innes, G.M. 1960. King's Point, Newfoundland; Geological Survey of Canada, Map 35-1960.
- Panze, A. J., Cruson, M. G., and Watkins, T. A., 1983. Gold-silver deposits of the San Juan Mountains, Colorado. 1983 Mining Yearbook, Colo. Mining Assoc., Denver, pp. 64-73.
- Peacock, M. A., 1931. Classification of igneous rock series. *Jour. of Geology*, vol. 39, pp. 54-67.
- Pearce, J.A. 1983. Role of the sub-continental lithosphere in magma genesis at active continental margins. In *Continental Basalts and Mantle Xenoliths*, C.J. Hawkesworth and M.J. Norry (eds.), Shiva Publishing Limited, pp.230-249.
- Pearce, J.A. 1975. Basalt geochemistry used to investigate past tectonic environments on Cyprus. *Tectonophysics*, vol.25, pp. 41-67.

- Pearce, J.A. and Cann, J.R., 1973. Tectonic setting of basic volcanic rocks determined using trace element analyses. *Earth and Planetary Science Letters*, vol.19, pp. 290-300.
- Pearce, J.A. and Norry, M.J., 1979. Petrogenetic implications of Ti, Zr, Y and Nb variations in volcanic rocks. *Contributions to Mineralogy and Petrology*, vol., 69, pp. 33-47.
- Pearce, T.H., Gorman, B.E. and Birkett, T.C., 1977. The relationship between major element chemistry and tectonic environment of basic and intermediate volcanic rocks. *Earth and Planetary Science Letters*, vol. 36, pp. 121-132.
- Pearce, J.A., Harris, N.B.W. and Tindle, A.G., 1984. Trace element discrimination diagrams for the tectonic interpretation of granitic rocks. *Journal of Petrology*, vol. 25, pp.956-983.
- Peccerillo, A. and Taylor, S. R., 1976. Geochemistry of Eocene calc-alkaline volcanic rocks from the Kastamonu area, northern Turkey. *Contributions to Mineralogy and Petrology*, 58, pp. 63-81.
- Pringle, J., 1978. Rb-Sr ages of silicic igneous rocks and deformation, Burlington Peninsula, Newfoundland. *Canadian Journal of Earth Sciences*, Vol. 15, pp. 293-300.

- Rankin, D. 1968. Volcanism related to tectonism in the Piscataquis volcanic belt, an island arc of Early Devonian age in north-central Maine. *in* Zen, E-An, Hadley, White and Thompson (eds). *Studies of Appalachian Geology: Northern and Maritime*. Wiley Interscience, N. Y., pp. 355-369.
- Rice, A., 1981. Convective Fractionation: A mechanism to provide cryptic zoning (macrosegregation), layering, crescumulates banded tuffs and explosive volcanism in igneous processes. *Journal of Geophysical Research*, 86, no. B1, pp. 405-417.
- Roobol, M. J. and White, D. L. 1986. Cauldron-subsidence structures and calderas above Arabian felsic plutons: a preliminary survey. *Journal of African Earth Sciences*, vol. 4, pp. 123-134.
- Russell, M.J. and Smythe, D.K., 1983. Origin of the Oslo Graben in relation to the Hercynian-Alleghanian orogeny and lithospheric rifting in the North Atlantic. *Tectonophysics*, 94, 457-572.
- Shervais, J. W., 1982. Ti-V plots and the petrogenesis of modern and ophiolitic lavas. *Earth and Planetary Science Letters*, vol. 59, pp. 101-118.
- Smith, R. L., 1979. Ash flow magmatism. *Geological Society of America Special Paper* 180, pp. 5-27.
- Smith, D.I. and Watson, J., 1983. Scale and timing of movements on the Great Glen fault, Scotland. *Geology*, v. 11, p. 523-526.

- Sparks, R. S. J., Huppert, H. E., and Turner, J. S., 1984. The fluid dynamics of evolving magma chambers. Phil. Trans. Royal Soc. of London, A310, pp. 511-534.
- Steven, T. A. and Eaton, G. P., 1975. Environments of deposition in the Creede mining district, San Juan Mountains, Colorado: I. Geologic, hydrologic and geophysical setting. Economic Geology, vol. 70, pp. 1023-1037.
- Steven, T.A. and Lipman, P.W. 1976. Calderas of the San Juan volcanic field, southwestern Colorado. U. S. Geological Survey Professional Paper 958, pp. 1-35.
- Stillman, C. J. and Francis, E. H. 1979. Caledonide volcanism in Britain and Ireland. in Harris, A.L., Holland, C.H. and Leake, B.E. (eds.) The Caledonides of the British Isles - reviewed. Special Publication of the Geological Society of London 8, pp.
- Strong, D.F. (1985): Mineral deposits associated with granitoid rocks of eastern Canada and western europe: a review of their characteristics and their depositional controls by source rock compositions and late-stage magmatic processes. p. 248-257 in R.P Taylor and D.F. Strong (eds.), Granite-Related Mineral Deposits, Extended Abstracts of Papers Presented at the Canadian Institute of Mining and Metallurgy Conference, September 15-17, 1985, Halifax, Canada.

- Strong, D. F., 1981. Ore deposit models - 5: A model for granophile mineral deposits. *Geoscience Canada*, 8, pp. 155-161.
- Strong, D. F., 1980. Granitoid rocks and a associated mineral deposits of eastern Canada and western Europe. *Geological association of Canada Special Paper* 20, pp. 741-769.
- Strong, D. F. 1977. Volcanic regimes of the Newfoundland Appalachians. *in*: Baragar, W. R. A., Coleman, L. C., Hall, J. M. (eds.) *Volcanic Regimes in Canada*, *Geological Association of Canada Special Paper* 16, pp. 61-90
- Strong, D. F. and Taylor, R. P. .1984. Magmatic-subsolidus and oxidation trends in composition of amphiboles from silica-saturated peralkaline igneous rocks. *Tschermaks Mineralogische und Petrographische Mitteilungen*, 32, pp. 211-222.
- Sun, S.-S., 1982. Chemical composition and origin of the Earth's primitive mantle, *Geochim, Cosmochim. Acta*, vol. 46, pp. 179-192.
- Sun, S.-S., 1980. Lead isotope study of young volcanic rocks from mid-ocean ridges, ocean islands and island arcs. *Phil. Trans. Roy. Soc. London*, vol. 297, pp. 409-445.

- Swanson, D. A., Dzurisin, D., Holcomb, R. T., Iwatsubo, E. Y., Chadwick, W. W. Jr., Casadevall, T. J., Ewert, J. W., and Heliker, C. C., 1987. Growth of the lava dome at Mount St. Helens, Washington, (USA), 1981-1983. In The Emplacement of Silicic Domes and Lava Flows. Edited by J. H. Fink, G. S. A., Special Paper 212, pp.1-16.
- Swanson, E. A., Strong, D.F., and Thurlow, J. G., (eds.), 1981. The Buchans Orebodies: Fifty Years of Geology and Mining. Geol. Assoc. Can. Special Paper No. 22, 350p.
- Swinden, H.S., Jenner, G.A., Kean, B.F., and Evans, D.T.W., 1989. Volcanic rock geochemistry as a guide for massive sulphide exploration in central Newfoundland. Current Research (1989) Newfoundland Department of Mines, Geological Survey of Newfoundland, Report 89-1, pp. 201-219.
- Taylor, R. P., Strong, D. F. and Fryer, B. J. 1981. Volatile control of contrasting trace element distributions in peralkaline granitic and volcanic rocks. Contributions to Mineralogy and Petrology, 77, pp. 267-271.
- Taylor, R. P., Strong, D. F., and Kean, B. F. 1980. The Topsails igneous complex: Silurian-Devonian peralkaline magmatism in western Newfoundland; Canadian Journal of Earth Sciences, 17, pp. 425-439.
- Taylor, S. R., 1965. The application of trace element data to problems in petrology. Physics and Chemistry of the Earth, vol. 6, pp. 133-213.

- Taylor, S.R. and McLennan, S.M., 1985. The Continental Crust: Its Composition and Evolution. Blackwell, Oxford, 312 pp.
- Taylor, S. R. and McLennan, S. M., 1981. The composition and evolution of the continental crust: rare earth element evidence from sedimentary rocks. Phil. Trans. Roy. Soc. London A301, pp 381-399.
- Thirlwall, M. F., 1981. Implications for Caledonian plate tectonic models of chemical data from volcanic rocks of the British Old Red Sandstone. Journal of the Geological Society, 139, pp. 123-138.
- Thompson, R.N., Morrison, M.A., Dickin, A.P. and Hendry, G.L., 1983. Continental Flood Basalts ... arachnids rule OK? In Continental Basalts and Mantle Xenoliths. Edited by C. J. Hawkesworth and M.J. Norry. Shiva Publishing Company, Nantwick, UK., pp. 158-185.
- Thompson, R.N., Morrison, M.A., Hendry, G.L., and Parry, S.J., 1984. An assessment of the relative roles of crust and mantle in magma genesis: an elemental approach. Philosophical Transactions of the Royal Society of London, vol. A310, pp. 549-590.
- Thurlow, J. G., 1981. The Buchans Group: Its stratigraphic and structural setting. In The Buchans Orebodies: Fifty years of Geology and Mining. Edited by E. A. Swanson, D. F. Strong and J. G. Thurlow. Geol. Assoc of Canada Special Paper No. 22, pp.79-90.

- Tuach, J., Dean, P.L., Swinden, H.S., O'Driscoll, C.F., Kean, B.F. and Evans, D.T.W., 1988. Gold Mineralization in Newfoundland: A 1988 Review. In Current Research, Nfld., Dept. of Mines, Mineral Development Division, Report 88-1, pp. 279-306.
- Upadhyay, H. D., Dewey, J. F., and Neale, E.R. W., 1971. The Betts Cove ophiolite complex, Newfoundland: Appalachian oceanic crust and mantle. Geol. Assoc. Canada Proc., vol. 24, p. 161-167.
- Van der Pluijm, B. A., 1986. Geology of eastern New World Island, Newfoundland: An accretionary terrane in the northeastern Appalachians. Geol. Soc. Amer. Bull., vol. 97, pp. 932-945.
- Van der Pluijm, B. A. and Van Staal, C. R., 1988. Characteristics and evolution of the Central Mobile Belt, Canadian Appalachians. Jour. of Geology, vol. 96, pp. 535-547.
- Van der Voo, R. and Scotese, C., 1981. Paleomagnetic evidence for a large (2000 km) sinistral offset along the Great Glen Fault during Carboniferous times. Geology, vol. 9, pp. 583-589.
- Wanless, R. K., Steven, R. D., Lachance, G. R., and Delabio, R. N. 1972. Age determinations and geological studies: K/Ar isotopic ages. Report 10. Geological Survey of Canada, Paper 71-2, pp. 89-93.

- Watson, E.B., 1979. Zircon saturation in felsic liquids. Experimental results and applications to trace element geochemistry. Contributions to Mineralogy and Petrology, 70, pp. 407-419.
- Webb, G. W., 1969. Paleozoic wrench faults in Canadian Appalachians. In North Atlantic Geology and Continental Drift. Edited by M. Kay. American Assoc. of Petroleum Geologists, Memoir 12, pp. 754-786.
- Wessel, J. M. 1975. Sedimentary Petrology of the Springdale and Botwood Formations, Central Mobile Belt, Newfoundland, Canada. unpubl. Ph. D. thesis, University of Massachusetts, 216 p.
- Whalen, J. B., and Currie, K. L. 1983a. The Topsails igneous terrane of western Newfoundland. In Current Research, part A. Geological Survey of Canada, Paper 83-1A, pp.15-23.
- _____. 1983b. Geology of the Topsails igneous terrane, western Newfoundland. Geological Survey of Canada, Open File Map 923.
- Whalen, J.B., Currie, K.L. and Chappell, B.W., 1987. A-type granites: geochemical characteristics, discrimination and petrogenesis. Contributions to Mineralogy and Petrology, vol. 95, pp. 407-419.
- Williams, H., 1980. Tectonic Lithofacies Map of the Appalachians. Memorial University of Newfoundland.
- Williams, H. 1967: Island of Newfoundland; Geological Survey of Canada Map 1231A.

- Williams, H., and Hatcher, R. D., Jr., 1983. Appalachian suspect terranes. Geological Society of America, Memoir 158, pp. 33-53.
- Williams, H. and St-Julien, P. 1982. The Baie Verte - Brompton Line: Early Paleozoic continent-ocean interface in the Canadian Appalachians. In Major Structural Zones and Faults of the Northern Appalachians. Edited by P. St-Julien and J. Beland. Geological Association of Canada, Special Paper 24, pp. 177-207.
- Williams, H., Colman-Sadd, S. P., and Swinden, H. S., 1988. Tectonic-stratigraphic subdivisions of central Newfoundland. Geological Survey of Canada, Current Research, Part B, Paper 88-1B, pp. 91-98.d
- Williams, H., Dickson, W. L., Currie, K. L., Hayes, J. P., and Tuach, J., 1989. Preliminary report on a classification of Newfoundland granitic rocks and their relations to tectonostratigraphic zones and lower crustal blocks. Geological Survey of Canada, Current Research, Part B, Paper 89-1B, pp. 47-53.
- Williams, H., Piasecki, M. A. J. and Colman-Sadd, S. P., 1989. Tectonic relationships along the proposed central Newfoundland Lithoprobe transect and regional correlations. Geological Survey of Canada, Current Research, Part B, Paper 89-1B, pp. 55-66.
- Wilson, J. T., 1962. The Cabot Fault. Nature, Vol. 195, pp. 135-138.

- Wilson, J. T., 1966. Did the Atlantic close and then re-open?
Nature, Vol. 211, pp. 676-681.
- Winchester, J.A. and Floyd, P.A., 1977. Geochemical
discrimination of different magma series and their
differentiation products using immobile elements. Chemical
Geology, vol. 20, pp.325-343.
- Wood, D.A., 1980. The application of a Th-Hf-Ta diagram to
problems of tectonomagmatic classification and to
establishing the nature of crustal contamination.
- Wood, D. A., Joron, J.-L., and Treuil, M., 1979. A re-appraisal
of the use of trace elements to classify and discriminate
between magma suites erupted in different tectonic
settings. Earth and Planetary Science Letters, vol. 50, pp.
326-336.
- Yoder, H. S. and Tilley, C. E., 1962. Origin of basalt magmas:
an experimental study of natural and synthetic rock
systems. Jour. of Petrology, vol.3, pp. 342-532.

APPENDIX A

SUMMARY PETROGRAPHIC

TABLES FOR SELECTED

ROCKS OF THE

SPRINGDALE GROUP

9

--64

A summary of petrographic data for rocks of the Springdale area.

PRIMARY

SECONDARY

Sample No	Fieldname	Phenocrysts + clasts						Groundmass						Anal.	Gen. Comnts.
		Ol	Cpx	Plg	Bl	Xeno	Opaq	Textures, etc.	Olk	Chl	Ser	Cal	OxS	Oth	
194 288	Basalt	hm >5%	y >5%	y 5- 10%				Felty/diabasic Plg, hm, & Cpx intergrown. >75%				y	hm	y	The olivines have Cpx rims; many of the olivines have gone to hematite.
CA-279C 311	Plg- phyric basalt	chl serp Fe- oxs.		prn ?				Med-coarse seriate texture Glass replaced by opaques and oxides.		y			hm	prn opq	n Vesicular w/ chl in- filling the vesicles. Plg. phenocrysts heavily altered to pranhite. Olivines have oxide "rims".
DS-84-2 K.Pt.Rd.	Porphy- ritic basalt	chl Q	epd opaq	ser cal				Basaltic, ser- iate texture with prominent green color.		y	y	y	y	epd	n Replacement of both groundmass and pheno- crysts by intergrown chl, cal & Q.
MS-48 484	Basalt			y				Med-coarse diabasic tex- ture w/ quench Cpx and Plg.		y		y		y probe	Vesicular w/ chl and cal alteration.
CA-178C 173	Vesicular basalt	? chl		y few				Med-coarse diabasic texture w/ Plg, Cpx inter- grown but Cpx resorbed.			y	y	hm	opq	n Well rounded vesicles contain cal, chl, Q; pervasive alteration to ser & cal; some groundmass Q.
CA-255A 278	Basaltic auto- breccia	y Ox, serp chl, cal.		y cal				Flow-top? auto-bx; bas. frags. in micro- cryst. g'mass		y		y	hm	opq	n some basaltic fragments could be xenolithic; g'mass silicified.
CA-167B 167	Vesicular basalt			y few				Fine trachytic texture. Most of the Plg phenocrysts altered to cal.		y		y		opaq Q	n Vesicles streamed out w/ Q rims; chl & cal centers.
DS-28 468	Hornfised basalt	y chl serp		y ser cal				Some remnant g'mass Cpx; tremolite		y	y	y	hm	prn opaq	y Vesicles w/ chl, prn Some complexly zoned, others homogeneous.
EL-341B 522	Basalt							Poikilitic Plg -Cpx texture.			y			hm mt	n A highly vesicular basalt flow.

1. / A summary of petrographic data for rocks of the Springdale area.

PRIMARYSECONDARY

e No	Fieldname	Phenocrysts + clasts					Groundmass					Oik	Chl	Ser	Cal	OxS	Oth	Anal.	Gen.Cmnts.
		Ol	Cpx	Plg	Sl	Xeno	Opaq	Textures, etc.											
112 .Pt.Rd.	Basalt							Diabasic tex w/ Plg and Cpx		y						hm		y	Vesicles infilled w/ chl (Berlin Blue)
187	Basalt							Felty / dia- basic texture, Plg. & Ol->serp, black needles ?ilm.		y				y		y		y	Complete alteration of groundmass to Cal & Chl. Many vesicles infilled w/ Q, Chl, Cal pump. Veinlets of cal throughout.
28	Basalt	y	y	y				Diabasic text Plg, Cpx, Ol- phyric. Hm stain Also Apatite.							y	hm	apat	y	Oxidation fronts. Vesicles infilled w/ cal and pump alteration.
			serp														Serp		
			hm														pump		
		5%	28%	58%													opaq		
71 428	Basalt	y		y				Felty/diabasic texture w/Plg Cpx intergrown but aligned (trachytic fluidal). Plg-phyric palkilitic cpx.		?				y		y	y	y	A patchy yellow mineral is seen in groundmass, stained chl and epidote. Iddingsite, & serp. replace olivine.
			Cal														Fe- oxs	opaq	
			Fe- oxs														mt	epid	
			18- 28%																
7u 14	Basalt	y		y				Lathy/Felty tex Vesicles w/pren rims & chl, pump cores or all chl/serp. Resorbed cpx.		y						y	serp	y	Microphenoxs of Ol, replaced by serp and Fe-oxides.
			serp														hm		
																	opq?		
-6 .Pt.Rd.	Vesicular basalt	y		y				Quench/dia- basic texture. Intergrown Plg & Cpx.		y	?			y		y	Q	n	Highly vesicular infilled w/ Chl & a carbonate mineral, epid and Q. Pervasive- ly chloritized. High degree of silici- fication.
			opq														hm	epid opaq	

No	Fieldname	PRIMARY					Textures, etc.	SECONDARY								Gen. Cmnts.
		Ol	Cpx	Plg	Bl	Xeno		Opaq	Oik	Chl	Ser	Cal	OxS	Oth	Anal.	
190 95	Plg-phyric basalt	chl		y				Highly porphyritic w/ large Plg & Ol phenocrysts in a seriate/trachytic groundmass of Plg, Cpx, & altered glass.			y		epd	y	Most phenocrysts are aligned within the matrix. The "glass" is replaced by 2nd. alteration particularly needles of Fe-oxides.	
3 .Pt.Rd.	Basalt	y	?	y				Basaltic/seriate texture w/ high % of phenocrysts.	y	y	y	hm	epid	n	Heavily altered.	
		chl		ser								pyr	?			
		Qtz	cal													
		cal	epid.													
KS-84-5 1.Pt.Rd.	Basalt	y		y				Basaltic/seriate texture. Groundmass ser, "glass" replaced by oxides, opaques and chl.	y	y	y	hm	pump	n	Altered vesicular basalt. Vesicles are quite large w/ cal, Q and possible pump.	
		chl		ser								opq	Q			
		cal														
-181 148	Basaltic flow-top breccia (Andes?)	y	micro	?				Mixed glassy streaks or flow w/in a flow. (basaltic). Fragments of basaltic glass and auto-breccia w/in matrix.	y			y	?	y	Tremolite may also replace Ol. Very quenched texture in the "matrix" which surrounds auto-brecciated fragments. High degree of oxidation. Could be mixed magmas.	
		serp	pheno	prn								hm	al-	probe		
		Fe-	cryst										an-			
		oxs											ite			
													w/in			
													Plg			
													pre			
													opq			
183 150	Basaltic flowtop breccia							Hydrothermal alteration.			y		pre	n	Completely overgrown w/ prehnite & pump like a cob-web.	
													pump	probe		
24-180 147	Basaltic andesite	chl	y	ep				Seriate/diabas. texture. Blocky Plg. Oxidized.	y		y	hm	ep	y	Ves. w/ pump. cores and cal. rims, some all calcite.	
		cal		cal												
19	Basalt	ox		y				Felty microcryst g'mass with quench Cpx.	y		y	hm		n	Ves. w. cal rims, chl cores. Groundmass chl & ox and opatite.	
		idd.														
		serp														
-188	Basalt	serp		cal				Seriate, felty g'mass, irreg. ox	y		y	hm	epd	n	Altered w/ chl g'mass opatite.	
													pump			

A summary of petrographic data for rocks of the Springdale area.

PRIMARY							SECONDARY								
Le No	Fieldname	Ol	Phenocrysts + clasts				Groundmass Textures, etc.	Olk	Chl	Ser	Cal	OxS	Oth	Anal.	Gen.Cmts.
			Cpx	Plg	Bi	Xeno									
232a 48	Contact between basalt and sandstone			y			Diabasic/ seriate text- ure. Recrystal- lization by patchy ser, Q, also random "blotchy" Q, and cal aggregates.			y	y			n	Irregular contact of probe basalt flow on top of Springdale sandstone. Little "intermixing" between the lith- ologies.
IS-25 165	Basaltic auto- breccia?		y	y			Igneous breccia w/trachytic textured basalt fragments cem- ented by a frothy host matrix. Some fragments have Plg pheno- chrysts, others Plg and Cpx.	y			y	hm	epid	n	Some of the basaltic probe fragments could be xenoliths (ie. foreign).
IS-84-7 C.Pt.Rd.	Basalt	y serp chl opaq					Medium-coarse diabasic basalt subophitic Cpx. Ol phenocrysts	y			y	y hm	serp	y	Few vesicles infilled w/ cal and chl. Cal veinlets.
IS-38 193	Basalt	y chl serp	y	y	y		Harrisitic w/ poikilitic Cpx. Plg phenocrysts are commonly flow aligned.	y			y	y hm		y	High proportion of Cpx.
IS-189 C.Pt.Rd.	Basalt	y Mi- cro serp chl		y			Diabasic Plg w/ poikilitic Cpx. Plg has sericitized cores.	?					?	y epd	Vesicular w/ chl and strange spherical structures in the vesicles. These are bright green high w/ relief, some sort of epid? granular aggreg

Table 1. (continued) A summary of petrographic data for rocks of the Springdale area.

Sample No	Fieldname	Ol	PRIMARY				Groundmass Textures, etc.	SECONDARY						Anal.	Gen. Cmnts.
			Cpx	Plg	Bi	Xeno		Opaq	Oik	Chl	Ser	Col	OxS		
CA-217 223	Basaltic Andesite	y	y	y			Groundmass heavily oxidized. Porphyritic with severe alteration. Mixing?				y			y	Aggregates of Plg & Cpx magnetically resorbed. Cpx shows polysynthetic twinning. High % of opaques.
CA-166 162	Basaltic Andesite	y serp chl		y col ser			Very fine felty groundmass w/ zoned Plg phenocrysts most altered to col & ser. Minor silicification. Opqs & hm.	y	y	y	y	epd hm mt opqs	y ? probe	y	Vesicular w/ blue-green chl (berlin blue). High relief yellow mineral is possibly epidote. Magnetite shows 111 twin lamelle and are altered to hm.
CA-0818 122	Basaltic Andesite	? chl 10% to 20%	y 5% to 10%	y ser 30%			Felty/trachytic texture. Few glomero-porphyrific aggregates, composed of Plg Cpx and Ol.			y	y	hm pat- chy		y	In general many Plg phenocrysts are altered to ser. and heavily included. Fresh chl seems to be replacing a primary phenocryst .Ol?
CA-233A 244	Andesite			y col ser			Fine Trachytic/felty groundmass w/ Plg phenocrysts aligned or sub-aligned.	y	y	y	hm		y probe		Very patchy alteration. Groundmass extensively calcified and minor silicification. Few small vesicles.
HS-116 446	Basaltic andesite	serp ox.		ser chl			Microcrystalline devit. glass.	y	y		hm	serp	y		Abund. clear Plg in devit. & ox. g'mass.
CA-076 115	Basaltic Andesite	chl serp	y	y			Felty, patchy oxidation. Ol abundant and fewer Cpx & Plg.	y		y	hm	serp qtz	y		A few vesicles w/ chl.

1 continued) A summary of petrographic data for the basaltic and andesitic rocks of the Springdale area.

No	Fieldname	Ol	PRIMARY				Groundmass Textures, etc.	SECONDARY							Gen.Cmnts.
			Cpx	Plg Bi	Xeno	Opaq		Oik	Chl	Ser	Cal	OxS	Oth	Anal.	
12A	Andesite/ dacite	? cal chl		ser	y xeno- chrys- tic frag- ments : :		Microcrystal- line w/inter- grown Q. & F'spar and ser- chl.		y	y	y	hm	pump	y	The rock is either a crystal porphyry or flow. The xenoliths are resorbed and commonly consist of felsic crystal por- phyry. The groundmass is "chilled" against the xenoliths/crysts.
4-312B	Andesite/ dacite porphyry			ser	mafic phase Amphb re- place- ed by chl.		Glomerocrystic w/Plg and relic amphi- bole aggregates Q, fine chl and epidote inter- grown in ground mass.		y	y	y		epd & Q	n	See sample number 312A for comparison.
-019 50	Andesite	mt serp 10%	y 30%	y		y	Glomerocrystic Plg, Cpx & Ol. w/oxides. Felt groundmass.			y		mt hm	serp carb	y probe	Olivines replaced by serp and Fe-ox, chl. Polysynthetically twinned cpx[see 208]
24-276 306	Andesite/ dacite plag- phyric flow	? serp		cal			Fine felted flow aligned texture. Plg alteration to cal.				y	hm	Q opaq chl	n	Also same chl and Q alteration.
CA-102 149	Dacite/ andesite	y		y	Plg Cpx		Quench texture matrix w/few Plg, Cpx xeno- crysts; commonly replaced and in- cluded heavily. Ol micropheno- crysts re- placed by cal chl, minor serp.		y		y		serp	y	Plag & Ol form glam- erocrysts in a quench matrix. Also single xtls of Plg & Cpx distributed random- ly.

A summary of petrographic data for the basaltic and andesitic rocks of the Springdale area.

No	Fieldname	PRIMARY						SECONDARY						Anal.	Gen.Comnts.	
		Ol	Cpx	Plg	Bi	Xeno	Opaq	Textures, etc.	Oik	Chl	Ser	Cal	OxS			Oth
-314	Andesite	y chl		y				Very few glom- eroporphyritic aggregates of Plg & chlorite in a trachytic matrix of Plg & chloritized groundmass.		y					n probe	Areas of the ground- mass demonstrate flow alignment of skeletal Plgs xtl's but other places are more randomly orientated. F'spar phenocrysts; are also present which are highly sericitized.
275	Andesite/ dacite		cal					Superfine glass w/ few phenocrysts of K-spar?		y	y	y			y	A "cleavage" is seen in this rock type. Sericitization develops along it. Alteration patchy.
-068	Andesitic basalt	y chl	y	y				Felted/quench texture. Chl alteration pervasive. Hornfelsed		y		y		opaq	y probe	Ol also alters to of talc- carbonate. Cpx has rims of chl, cores talc.
167C	Andesite			y few				Fine felty/ trachytic texture w/ alignment of Plg laths common. Quench- ed groundmass Cpx.					hm blot ches		y	Extremely homogenous. The "blotches" are common and random- ly distributed. They may represent the oxidation of a primary phenocryst phase?
-208 14	Andesite	y serp	y	y			mt	Glomerocrystic Cpx, Plg, Ol in trach. g'mass.		y		y	hm		y probe	Polysynthetically twinned cpx.
-099	Andesite	? serp	y	y				Felty w/ paik- ilitic aggre- gates of Plg. Cpx and poss- ible Ol. Ground mass Chl.		y			hm opq serp	y probe	Larger (low relief) laths of chl have a pale blue anomalous color. Disseminated opaques.	

A summary of petrographic data for rocks of the Springdale area.

Le No	Fieldname	PRIMARY					SECONDARY									Anal.	Gen.Comnts.
		Phenocrysts + clasts					Groundmass										
		Ol	Cpx	Plg	Si	Xeno	Opoq	Textures, etc.	Olk	Chl	Ser	Cal	OxS	Oth			
108	Andesite	y	y	y				Diabasic/felted Vesicles rimmed with opaques and heavily oxidized. Commonly cored w/ pump.		y	y	y	y	opq y hm pump probe		Many of the Plg are zoned and the rims are altered to cal. Randomly distributed hematite blotches.	
		?	micro ser pheno														
C4-0708 109	Vesicular basalt	?	y	y				Felty/trachytic hyalopilitic groundmass. Glomeropor- phyritic w/ resorbed Plg. Cpx and Ol. Oxidation "rims" surround these aggregates.		y			hm	pump n serp		Amygdules consist of pump, chl, and serp. They commonly have oxidation "rims".	
			Fe- oxs														
C4-98 145	Basalt	y	y	y				Fine diabasic/ seriate texture.					hm		y pump	Plg-phyric homogen- ously textured basalt.	
			serp 15%	20%													
C4-179 183	Vesicular basalt	ox. chl		ser cal				Glassy, heavily ox. Quench cpx rosettes, needles feathery pl.		y		y	hm	opaq y cubes needles		Vesicles have cal/chl cores, thin chl rims. Pl-rich cumulate.	
C4-264A 289	Basaltic conglomer- ate.							Most fragments fairly angular. Intersertial chl.		y		y	hm	pump n in some frag		Basaltic clastic rock Sand-sized fragments of various basalt types ranging from aphyric to Plg-phyric and differently altered.	
C4-811 15	Scor- iacious basalt			y cal				Highly recryst- allized ground- mass of Q and Adularia? Alteration is patchy.		y		y	hm	adul y ?		Very excessive alteration. High % of Plg.	

A summary of petrographic data for rocks of the Springdale area.

Is No	Fieldname	Ol	PRIMARY				Groundmass Textures, etc.	SECONDARY						Anal.	Gen. Cmmts.
			Cpx	Plg	Bi	Xeno		Opaq	Oik	Chl	Ser	Col	OxS		
222A	Vesicular basalt			y	also chl			Fine diabasic texture w/ Plg, oxs and opqs. Groundmass chl and cal. Plg phenocrysts have sieve tex- ture with ser alteration. Most are zoned, and heavily in- cluded. Some are completely sericitized.	y	y	y	hm	opq	y	Vesicles have irreg- ular shapes w/ fine chl rims & col inter- iors, also aggregate chl. Long Prismatic crystals are also seen?
-211 17	Dacite/ andesite	? Fe- oxs		y				Felty/Trachytic plitaxitic texture. Opaques & biotite flake in groundmass, after Cpx?		y	y	y		y	Patchy alteration and calcification. Few "intact" pheno- chrysts of Plg with good albite and peri- cline twinning.
-278 7	Dacite auto- breccia		y					Fine felted texture with recrystall- ization to Q, cal and chl alteration.	y	y	y	hm	Q need Kspr les.	n	Altered autobreccia. Alteration is predominantly found within the matrix between fragments. Small fractures/ veins filled w/ Q and cal.
4-186 53	Diorite							Med-grained dioritic tex., interlocking albite rimmed Plg, green Hbl is replaced by biotite & actinolite. Also magmatic zircon and apatite.		y	y		y	n	Plg has core alter- ation to ser and cal.

No	Fieldname	Q	PRIMARY				Groundmass	Textures, etc.	Oik	Chl	SECONDARY				Anal.	Gen.Cnts.
			Kspar	Plg	Oth	Vitr					Lith	Ser	Col	OxS		
1690	Felsic welded tuff	y	ser	col			Bas. and Ands.	Fine shards in glass with eutaxitic texture. Pervasive alteration to col and oxides obscured the texture.			y	y	hm opq	serp	n	Crystal-lithic tuff with Plg, K-spar and lithic fragments. Lithophysae with Q and radial microlites in devitrified rims.
4-1708	Welded crystal vitric tuff	y	y San	y An	y			Eutaxitic tex. with fiamm that are recrystallized to granular Q. Larger fiamm altered to carbonate. Alkali f'spars resorbed, sanidine displays perthitic tex.			y	y	hm fine dis- per- sed.		probe	The two feldspars suggest subsolidus conditions thus considerable depth of formation. A more calcic feldspar is present replaced by ser. Q-ser veinlets.
-173	Welded crystal-vitric-lithic tuff		rare San		y		Bas thru Rhy	Eutaxitic crystals often broken. Two distinct types of fiamm are seen one of recrystallized polygonal Q. and pale's hair. Other fibrous, may be cognate lithic fragments. Alteration dominated by cal.			y	y		Q	n	Lithic frags. are predominantly basaltic with a variety of phenocryst assemblages including Ol-phyric, Plg-phyric; aphyric trachytic andesite and rhyolite. Lithophysae have cal-Q cores with ser rims.

PRIMARYSECONDARY

Phenocrysts + clasts

Groundmass

le No	Fieldname	Q	Kspar	Plg	Oth	Vitr	Lith	Textures, etc.	Oik	Chl	Ser	Cal	OxS	Oth	Anal.	Gen. Cmnts.
174	Welded vitric tuff	re- sor- bed	San cal ser			y		Eutaxitic texture beautifully developed. Patchy zones of cal and oxs alteration nucleate around phenocrysts. Fiam rare and are recrystal- lized Q and ? albite.			y	y	hm ab	Q n		This unit grades into a spherulitic zone where most of the oxidizing fluids were generated.
-231A	Welded massive rhyolitic tuff		San ser	An				Very fine/ glassy with suggestion of alignment or welding marked by streaky cal oxs, and app alteration. Few pumice suggest- ive of intru- sive nature as as is the eu- hedral nature of the seriate but rare phenocrysts.			y	y	hm	?		Found in contact with a rhyolitic breccia may be a flow dome?
299	Dome apron	rare	y				Few Bas	Intergrown Q and albite re- crystallized as devitrifica- tion texture. Secondary al- bitization. Spherules of hematite stain feldspar, pump are common.					hm ab	pump ? ab		Very near a dome and this unit is composed of rhyolitic frags. many of which have perlitic cracks sug- gestive of massive glassy intrusives.

PRIMARYSECONDARY

Is No	Fieldname	Q	Phenocrysts + clasts				Groundmass Textures, etc.	Oik	Chl	SECONDARY				Anal.	Gen. Cmts.
			Kspar	Plg	Oth	Vitr	Lith			Ser	Cal	OxS	Oth		
4-163	Crystal-lithic tuff	re-sorbed			Mus	y	y	Fine devitrified matrix with numerous frags with granophyric, graphic & merikitic textures. Other frags are rhyolitic w/perlitic cracks or fibrous. Altern		y		hm apq	Q ?		This is a high-level porphyry which has erupted thus it has both cognate and foreign clasts derived from local rocks. Also some "chilled" frags which represent margin of intrusion.
4-185	Lithic tuff	y	y			y	Bas thru Rhy	Glassy quenched matrix w/patchy pervasive alteration in both frags. and matrix, pumice are rare. Carbonitization and varied in individual lithic clasts.		y	y		n		Lack of eutaxitic texture suggests no welding as does the unflattened pumice. In the field a flattening was observed which suggests welding however. Some bomb size frags.
4-224	Felsic lahar or sandy pyroclastic						Wide variety	A granular rock with good sorting. Matrix is altered and thus features such as glass shards are obscured if there. Most lithic clasts are felsic volcs., also Bas Andesitic. Alteration depends on lithology.	y	y	y	hm	pump Q	n	Difficult to access the genesis of the rock due to the fine "dust-like" matrix. Most fragments touch each other with recrystallized aggregates of Q between. In places matrix looks "quenched".

Table 1. (cont'd.) Petrographic descriptions of rocks of the Springdale Area.

Sample No	Fieldname	Q	PRIMARY				SECONDARY								Gen.Cmnts.
			Phenocrysts + clasts			Lith	Textures, etc.	Olk	Chl	Ser	Col	OxS	Oth	Anal.	
Kspar	Plg	Oth	Vitr												
24-385A	Andesitic breccia		y		Fe-oxs serp Opq	Bas And Fels	Trachytic/vesicular fragments in a heavily carbonitized and oxidized groundmass. Difficult to determine the nature of matrix due to alteration and fine grain size			y		hm opq	n	There may be foreign clasts as well which are felsic. Vesicles filled with chl and small rims of col. Some vesicles replaced by Q. May be a separate Opq phenocryst phase.	
24-96	Basaltic laharic breccia			Opq		Main-ly Ande-site	Glossy, replaced by opqs. Altered to carbonate and Fe-oxides.		y	y	hm		n	Most of lithic frags. have trachytic to felty texture. They range from ophyric to Plg-phyric with varied states of alteration.	
24-167B	Basaltic laharic breccia "peperite"	Q				Main Bas. few Ands. and rare Fels. volc clast	A clastic rock with a fine felsic silty groundmass composed of Q, feldspar and mica. The frags. are "infiltrated" by the muds especially the vesicles. Frags are altered to carbonates and Fe-oxides.	y		y	y hm opq		n	Fragments are predominantly mafic with a range of textures and phenocryst assemblages. There appears to be some auto-brecciation in the basaltic clasts and may represent contemporaneous lavas flows during deposition of this unit.	
24-192A	Basaltic laharic breccia	Q	y	Mus ser		Bas thru Rhy	Polyolithic fine to med. grained muddy-ashy matrix. Crystal frags. range from euhedral to granophyric.		y	y	hm opq	n		Similar to other basaltic breccias in the area.	

1. (cont'd.) Petrographic descriptions of rocks of the Springdale Area.

ield No./ .No.	Fieldname	Q	PRIMARY						SECONDARY								Gen.Cmnts.
			Phenocrysts + clasts						Groundmass								
			Plg	Ksp	Oth	Xeno	Opq	Textures,etc.	Oik	Chl	Ser	Cal	OxS	Oth	Anal.		
24	Barney's Brk tuff	n	y	n	zir	ol	hm,mg	eutax w/abun ser,cal,devitrif. texts.Fiame(2 types)	2nd n	y	y	y	y		y	welded lith, vit. tuff,abun lithics many basaltic. Veinlets ser, cal.	
C4-283	Barney's Brk tuff	n	y	n	zir	ol	hm,mg	as above	n	y	y				y	As above	
C4-93	Barney's fault	y	y	n	?	n	hm	fault breccia poss. intrusion	n	n	y	n	y	sil	y	In o'crop fz w/devit. spherules and gauge	
C4-287	Barney's Brk. tuff	n	y	n	y	ol	hm,mg	eutax.as 284, flat pumice	n	y	y	y	y		y	Abun vitric clasts fewer basaltic clasts	

APPENDIX B

SPRINGDALE GROUP

SAMPLE LOCATIONS

(UNIVERSAL TRANSVERSE MERCATOR COORDINATES)

APPENDIX B: SPRINGDALE GROUP SAMPLE LOCATIONS.

Sample Number	Easting	Northing	Sample Number	Easting	Northing	Sample Number	Easting	Northing
d83	514877	5458773	C4022A	547685	5478820	C4312A	558195	5458410
d82	515232	5458426	C4022B	547660	5478820	C4312B	558165	5458395
d81	515316	5458385	C4023A	547965	5478560	C4313A	558010	5458350
d57	517307	5459363	C4023B	547940	5478560	C4313B	558045	5458350
d56	517249	5459358	C4024A	548255	5477960	C40314	558540	5456620
d55	517184	5459360	C4024B	548280	5477960	C4315A	558255	5458640
d60	516519	5459284	C4024X	548230	5477955	C4315B	558210	5458640
d61	516298	5459206	C4025-	548240	5474850	C40316	554930	5457890
d62	516645	5458822	C4026A	547390	5473580	C40317	559680	5457675
d63	516807	5458801	C4025X	548220	5477930	C4318A	560590	5459480
d64	517569	5459085	C4026B	547355	5473580	C4318B	560555	5459480
d67	517649	5459427	C4026X	548225	5474850	C4319A	560495	5459465
d66	518026	5459621	C4027A	547165	5473240	C4319B	560460	5459460
d53	518836	5460999	C4027B	547190	5473240	C4320-	560490	5459150
d52	518990	5461102	C4027C	547135	5473240	C40321	560340	5460045
d51	519208	5461111	C4028-	546800	5473130	C40322	559999	5457485
d59	519501	5461420	C4029-	547130	5472990	C40323	559675	5458950
d50	519500	5461416	C4030-	550720	5473390	C40324	559015	5457850
d49	519589	5461480	C4031-	550890	5471245	C40325	556500	5457495
d48	519694	5461532	C4032-	549115	5470620	C40326	556930	5457950
d47	519740	5461487	C4033-	549400	5477070	C40327	556090	5458250
d46	519865	5461624	C4034-	549920	5476930	C40328	556120	5457750
d45	519889	5461698	C4035A	550285	5476920	C40329	554520	5458190
d44	519782	5461672	C4035B	550260	5476920	C40330	555190	5460550
d18	522969	5460501	C4035C	550225	5476920	C40331	555250	5466080
d17	522967	5460280	C4036A	550285	5476840	C4332A	550995	5459010
d16	523009	5460149	C4036B	550250	5476840	C4332B	550956	5459020
d15	523165	5459897	C4037-	549020	5475450	C4332C	550910	5459000
d14	523261	5459893	C4038-	548360	5475000	C4333A	538955	5456060
d13	523316	5459947	C4039-	547790	5474875	C4333B	538920	5456040
d12	523110	5460286	C4040A	548045	5474495	HS0029	543620	5465060
d11	523094	5460375	C4040B	548010	5474495	HS0031	545220	5466325
35211	523014	5460533	C4040C	547985	5474495	HS032A	545310	5466815
35210	523004	5460372	C4040D	547650	5474495	HS032B	545370	5466845
35212	523006	5460242	C4041-	548015	5474390	HS0035	545785	5467305
35213	523068	5460290	C4042-	546800	5472785	HS0036	546015	5467975
35214	523118	5459968	C4043-	545740	5472275	HS0037	546175	5468100
35215	523353	5459768	C4044-	545420	5472105	HS0038	551490	5455860
d89	523555	5464341	C4045-	545150	5471320	HS0039	551390	5455780

APPENDIX B: SPRINGDALE GROUP SAMPLE LOCATIONS.

Sample Number	Easting	Northing	Sample Number	Easting	Northing	Sample Number	Easting	Northing
d88	523442	5464015	C4046-	544450	5471020	HS0040	552520	5456935
d20	523162	5462386	C4047-	547050	5472700	HS0041	551860	5463520
d21	523258	5462466	C4048-	546550	5472020	HS042A	551890	5463675
d22	523926	5463389	C4049-	546420	5471830	HS042B	551855	5463675
d23	524003	5463587	C4050-	546050	5470290	HS0044	551665	5464000
d24	524222	5463879	C4051-	550110	5475925	HS0045	551655	5464070
d25	524437	5464039	C4052-	550670	5473475	HS047A	551690	5464135
d38	524361	5464189	C4053-	550690	5473415	HS047B	551655	5464135
d26	524379	5464282	C4054A	550895	5473175	HS047C	551616	5464135
d39	524364	5464391	C4054B	550870	5473175	HS0048	551625	5464200
d19	524116	5462285	C4055-	551085	5472895	HS0049	551665	5464350
3590	524014	5465128	C4056A	546670	5467390	HS0050	551790	5464495
3591	524003	5465077	C4056B	546650	5467390	HS0051	551820	5464645
3592	524047	5465025	C4056C	546615	5467390	HS0053	552005	5465150
3593	523988	5464953	C4056D	546695	5467390	HS054A	551695	5464245
3594	524025	5464921	C4057-	547095	5466850	HS054B	551656	5464245
3595	524152	5464883	C4058-	546245	5465700	HS054C	551610	5464245
3596	524306	5464792	C4059-	546690	5465230	HS0055	551720	5464430
3597	524358	5464761	C4060-	549605	5466010	HS0056	551815	5464525
35100	524282	5464733	C4061A	551550	5470530	HS057A	551895	5464800
c563	524392	5464552	C4061B	551515	5470530	HS057B	551870	5464800
c562	524414	5464582	C4062-	552015	5467150	HS0059	552080	5465225
35102	524520	5464555	C4063-	549980	5463490	HS0061	552310	5465815
c564	524698	5464523	C4064A	551935	5463420	HS062A	552395	5465000
c565	524731	5464458	C4064B	551900	5463420	HS0063	552465	5466190
35103	525117	5464444	C4065-	553155	5459730	HS0064	555520	5468395
35104	525227	5464444	C40066	563860	5472925	HS0065	554395	5468145
35106	525456	5464559	C467A-	563860	5472725	HS0066	552830	5467520
35107	525519	5464549	C4067B	563815	5472730	HS067A	552590	5467380
35108	525738	5464714	C4067C	563785	5472725	HS067B	552555	5467380
35117	525945	5464847	C40068	563760	5472610	HS0068	554000	5467105
35116	526130	5464882	C4069A	563765	5472620	HS0069	553695	5466550
35114	526224	5464794	C4069B	563520	5472520	HS0070	553535	5466285
35114	526234	5464777	C4070A	563075	5470475	HS0071	553180	5466160
35115	526224	5464783	C4070B	563105	5470495	HS0072	558490	5466290
35114	526302	5464742	C40071	563015	5470320	HS0074	558235	5466115
35113	526537	5464686	C40072	563055	5470160	HS0075	558085	5466285
3550	526650	5464675	C40073	563315	5470500	HS0077	558480	5466675
3545	526719	5464633	C40074	563245	5470280	HS0078	557745	5465395

APPENDIX B: SPRINGDALE GROUP SAMPLE LOCATIONS.

Sample Number	Easting	Northing	Sample Number	Easting	Northing	Sample Number	Easting	Northing
3546	526696	5464654	C40075	562925	5470140	HS0080	557170	5464935
3540	526652	5464620	C40076	562930	5469945	HS0082	556925	5464780
3548	527063	5464034	C40077	562800	5469690	HS0084	555940	5464050
c535	527883	5463036	C40078	562765	5469445	HS0086	555565	5463210
3566	527529	5463013	C40079	561215	5468320	HS0087	564420	5473290
c534	527211	5463176	C4080A	564155	5473345	HS0088	564785	5473210
3575	535659	5459588	C4080B	564190	5473340	HS0093	561035	5460280
3574	535074	5459738	C4081A	561450	5465410	HS094A	560560	5460140
3573	535137	5461266	C4081B	561415	5465415	HS094B	560435	5460155
3564	524584	5461047	C40082	561500	5465140	HS096A	560460	5459810
3563	524431	5461155	C40083	561380	5465020	HS096B	560415	5459810
3586	525234	5461838	C40084	561290	5464860	HS0098	560385	5459570
3585	525224	5461931	C40085	561425	5464830	HS0116	555930	5468985
3583	525160	5462047	C40086	561545	5464820	HS0118	557080	5470285
3584	524817	5462173	C40087	561505	5464610	HS0119	558110	5471125
c552	524928	5462259	C4088A	559090	5464040	HS0120	559970	5470930
35241	524827	5461176	C4088B	559160	5464090	HS0121	560000	5470400
c553	526028	5461118	C47173	561415	5465415	HS0123	559300	5469500
c554	526488	5460981	C4088C	559220	5464110	HS0126	558890	5468640
3588	526381	5460941	C40089	555605	5460495	DM0032	555720	5474390
3587	526235	5460874	C40090	555560	5460610	DM0034	556000	5473940
c540	526924	5461523	C4091A	555555	5460705	DM0035	556120	5474200
c539	527405	5461421	C4091B	555500	5460700	DM0037	557910	5474215
c538	527260	5461290	C4092A	555495	5461305	DM0039	559380	5475550
c537	527157	5461155	C4092B	555440	5461400	DM0040	557180	5476180
3560	527027	5461030	C4092C	555415	5461375	DM0029	557310	5479550
3561	527000	5460938	C40093	555370	5461320	DS0020	537485	5458165
c547	527485	5460310	C40094	555345	5461280	DS0021	537710	5458025
c5466	527076	5459158	C40095	555430	5461220	DS0022	537925	5457635
3570	527111	5459146	C40096	555385	5461190	DS0023	538420	5460775
3571	527028	5459022	C40097	555345	5461150	DS0024	538375	5461130
35200	530863	5455497	C40098	564090	5473250	DS0025	538010	5461010
d70	533307	5470272	C40099	564000	5472995	DS0026	537725	5462205
d71	533271	5470426	C40100	564005	5472995	DS0027	540440	5461690
d73	532945	5470267	C40101	563745	5472300	EL301A	554915	5472595
d74	532763	5470180	C40102	563750	5472615	EL201B	554960	5472595
d75	532471	5469981	C40103	563710	5472510	EL302A	554865	5472310
d76	532238	5469824	C40104	564650	5472420	EL302B	554810	5472310
d77	531568	5469639	C40105	564160	5471100	EL303-	552995	5469410

APPENDIX B: SPRINGDALE GROUP SAMPLE LOCATIONS.

Sample Number	Easting	Northing	Sample Number	Easting	Northing	Sample Number	Easting	Northing
d78	531294	5469537	c40106	564005	5470960	EL304A	552946	5469490
d79	531248	5469305	c40107	563920	5470945	EL304B	552990	5469490
d80	531257	5469110	c40108	563810	5470990	EL305-	554965	5470675
c576	531329	5468573	c40159	538200	5458000	EL306-	554950	5473210
c575	532450	5467686	c40160	538020	5457890	EL307A	555385	5475370
35122	532283	5467424	c40161	537620	5460185	EL307B	555340	5475370
35123	531815	5467790	c40162	537575	5460280	EL308A	555765	5474400
35124	531611	5468100	c40163	538440	5462630	EL308B	555725	5474400
35125	531573	5468345	c40165	556800	5464280	EL309-	556190	5473985
35217	542756	5435488	c40166	557300	5464805	EL310-	557585	5473970
35218	543118	5437054	c4167A	557535	5465020	EL311-	558215	5473850
35219	543699	5436886	c40168	557700	5465180	EL312-	557555	5473620
35220	544267	5438090	c4169A	557755	5465220	EL313-	557060	5472990
la1	545062	5439019	169B	557700	5465220	EL314-	552745	5472380
la2	545041	5438849	c4167B	557588	5465020	EL315-	552310	5471710
la3	544999	5438685	c4167C	557508	5465020	EL316-	552215	5471820
la4	545060	5438673	c4169C	557670	5465220	EL317-	552280	5471880
la5	545363	5438301	c4169D	557635	5465220	EL318-	548585	5470000
la6	545218	5437930	c4170A	557726	5465250	EL319A	547955	5471690
la7	545220	5435692	c4170B	557777	5465250	EL319B	547990	5471690
la8	546016	5435485	c4170C	557800	5465200	EL320-	548050	5471800
la9	546300	5435380	c40171	557840	5465250	EL321-	548510	5472500
la10	546815	5435343	c40172	557900	5465375	EL322-	550100	5473115
35221	546427	5440222	c40173	557990	5465315	EL323-	550400	5473175
35208	544785	5442976	c40174	558215	5465850	EL324-	550645	5473095
c5201	545063	5444751	c40175	558490	5466300	EL325A	550755	5473395
c622	551662	5443884	c4176A	558650	5466370	EL325B	550796	5473395
c614	556656	5452751	c4176B	558610	5466370	EL325C	550710	5473395
35233	546832	5447698	c40177	558690	5466490	EL326-	551015	5473460
35207	546217	5447883	c40178	558900	5466980	EL327-	551345	5473660
c5202	546020	5448242	c40179	558890	5467200	EL328A	551950	5472595
35232	546798	5448500	c40180	560010	5468250	EL328B	551996	5472595
a1	545409	5448592	c4181A	560250	5468250	EL328C	551915	5472595
a2	545467	5448864	c40181	560210	5468250	EL329-	552005	5472560
a3	545324	5449190	c40182	560540	5469220	EL330-	546980	5472590
a4	545697	5449313	c40183	560730	5469690	EL331-	547020	5472600
a5	545736	5449516	c40184	560700	5469880	EL332-	547850	5471410
a6	545390	5450010	c40185	560750	5469910	EL333A	547590	5471095
a7	545264	5450170	c40186	560790	5469990	EL333B	547515	5471095

APPENDIX B: SPRINGDALE GROUP SAMPLE LOCATIONS.

Sample Number	Easting	Northing	Sample Number	Easting	Northing	Sample Number	Easting	Northing
a8	545048	5450161	C40187	560850	5470120	EL334-	547690	5470910
a9	544865	5450888	C40188	560690	5470200	EL335-	547225	5470090
a10	545001	5451053	C40189	560700	5470280	EL336-	546545	5467395
a11	545204	5451112	C40190	560610	5470400	EL337A	546560	5467460
a12	545420	5451286	C40191	560520	5470500	EL337B	546505	5467460
a13	545578	5451547	C4192A	560495	5470700	EL338-	545980	5467930
a14	545786	5452046	C4192B	560450	5470700	EL339A	546355	5468460
35226	545930	5452179	C40193	557930	5464790	EL339B	546390	5468460
35227	545947	5452251	C40194	555520	5462390	EL340-	546745	5469030
35228	546223	5452582	C40195	555450	5462350	EL341A	546990	5469260
35229	547079	5451712	C40196	555450	5462290	EL341B	546945	5469260
c5203	546961	5451388	C40197	555400	5462100	EL901A	548140	5478735
35230	546890	5451248	C40198	555430	5461900	EL901B	548185	5478735
35231	546796	5451078	C40199	555450	5461710	EL337C	546515	5467460
3520	542978	5450502	C40200	555450	5461590	EL373-	556730	5479280
3521	543056	5450484	C40201	555450	5461400	EL374A	554095	5480145
c522	542895	5450450	C40202	555480	5461250	EL374B	554070	5480145
3522	543754	5450829	C40203	555480	5461250	EL375-	554215	5479685
3523	543733	5450923	C40204	555390	5461230	EL376-	555020	5479680
c523	543797	5450858	C40205	555390	5461230	EL377-	553930	5479595
3524	543867	5450871	C40206	555350	5461200	EL378A	554095	5479690
3526	543921	5450864	C40207	555300	5461090	EL378B	554066	5479690
3525	543926	5450804	C40208	564620	5474790	EL378C	554010	5479690
3527	544043	5450881	C40209	564885	5475400	EL379A	564495	5479220
3528	544135	5450961	C40210	564790	5475430	EL379B	564456	5479220
3529	544327	5451155	C40211	564960	5475720	EL379C	564410	5479220
3530	544502	5451332	C40212	565090	5475750	EL380-	565530	5479485
3533	544583	5451364	C40213	565010	5475690	EL381-	564530	5479235
3534	544961	5451444	C40214	565040	5475610	EL383-	563810	5479195
3535	545262	5451633	C40215	565000	5475500	EL384-	563815	5479320
c4344	544775	5451318	C40216	564930	5475510	EL385-	563920	5479510
c4343	541642	5453260	C40217	562820	5473090	EL386A	564066	5479625
c4342	540698	5452873	C40218	563120	5474040	EL386B	564005	5479625
c4341	540168	5452302	C40219	563300	5474060	EL387-	561695	5476590
c4340	539554	5452982	C40220	563500	5474005	EL388-	561590	5476645
c4340	539597	5453022	C4221A	563790	5474120	EL389A	562460	5476055
c4339	538815	5454386	C4222A	562885	5473250	EL389B	562425	5476055
c4338	538617	5453463	C4222B	562846	5473300	EL390-	564890	5478445
c4337	537837	5452770	C4222C	562810	5473310	EL391-	564810	5478480

APPENDIX B: SPRINGDALE GROUP SAMPLE LOCATIONS.

Sample Number	Easting	Northing	Sample Number	Easting	Northing	Sample Number	Easting	Northing
c4336	537276	5452730	C40223	562950	5473370	EL392-	564690	5478505
3634	543191	5433278	C40224	562930	5473405	EL393-	564615	5478500
3639	544570	5430757	C40225	562885	5473410	EL394-	562700	5478010
3640	545110	5431614	C40226	562800	5473410	EL395-	562520	5478010
3641	545737	5429741	C40227	563115	5473400	EL396-	562425	5477780
3642	545444	5428575	C40228	562720	5472920	EL397A	559625	5476380
3635	545781	5433422	C40229	565510	5474630	EL397B	559555	5476500
3636	545898	5433434	C40230	551350	5463500	EL398-	558885	5476025
c625	546008	5433392	C4231A	551685	5464195	EL406-	562895	5476395
3638	546234	5433146	C4232A	551695	5464110	EL407-	564300	5477600
3637	547489	5433983	C4232B	551656	5464110	EL408-	564395	5477700
3633	549046	5435719	C4232C	551610	5464110	EL409-	564520	5477725
3632	549401	5435888	C4231B	551605	5464195	EL410A	564565	5477710
3631	552611	5440710	C4233A	551695	5464100	EL410B	564500	5477710
3630a	553802	5442230	C4233B	551656	5464100	EL411-	563035	5476325
3630b	553818	5442254	C4233C	551617	5464100	EL412-	557480	5473415
3630c	556979	5447272	C4233D	551570	5464040	EL413-	558180	5473975
3644	547581	5439671	C4234A	551895	5463625	EL414-	558695	5474200
3545	547849	5440499	C4234B	551850	5463710	EL415-	564660	5478875
3646	548260	5441350	C40235	551795	5463750	EL416-	559020	5476690
3647	548827	5442050	C4236A	551765	5463850	EL417-	557350	5480500
3648	547995	5445394	C4236B	551725	5463910	EL418A	557275	5480420
3649	547706	5444140	C42237	551290	5462920	EL418B	557230	5480420
3658	546558	5447907	C40238	551290	5462920	EL432-	554590	5478175
3625	553226	5443911	C40239	551205	5471600	EL433-	554635	5480675
3624	552306	5443954	C4240A	551055	5471505	EL434-	553395	5478495
3623	551768	5444899	C4240B	551016	5471505	EL435-	553825	5479000
3627	550616	5444812	C4240C	551090	5471505	EL436-	554555	5480490
3629	550012	5449865	C40241	548790	5469850	EL437-	554375	5480330
c623	550287	5449720	C40242	549100	5470490	EL438-	552795	5479020
3628a	550402	5450271	C40243	549196	5470790	EL439-	552380	5478080
3628b	550385	5450446	C40244	549205	5470905	EL440-	551430	5477995
3618	558295	5448633	C40245	549350	5471300	EL441-	552315	5478115
3619	557991	5449571	C4246A	549185	5471600	EL442-	551475	5477520
3616	558549	5453077	C4246B	549205	5471115	EL443-	552200	5477330
3615	558040	5453384	C4247A	548755	5470380	EL444A	551885	5476110
3614	558116	5453396	C4247B	548790	5470380	EL444B	551880	5476110
3613a	558131	5453865	C40248	548725	5471300	EL445-	552685	5476620
3613b	558149	5453830	C4249A	548595	5471295	EL446-	554165	5480230

APPENDIX B: SPRINGDALE GROUP SAMPLE LOCATIONS.

Sample Number	Easting	Northing	Sample Number	Easting	Northing	Sample Number	Easting	Northing
3612	558260	5455081	C4249B	548630	5471350	EL447A	553855	5480030
3611	559430	5454948	C4249C	548650	5471400	EL447B	553800	5480030
3610a	560020	5455210	C40250	560905	5464670	EL448-	554725	5480500
3610b	560042	5455176	C40251	560775	5464170	EL457-	562950	5478810
3620	554046	5452002	C40252	560700	5464165	EL458-	562750	5478650
3621	552769	5451711	C4253A	560240	5464385	EL459A	552590	5469380
3622	553295	5450760	C4253B	560285	5464385	EL459B	552545	5469380
3650	549237	5451832	C40254	560195	5464380	EL459C	552515	5469290
3651	551926	5454721	C4255A	559755	5464280	EL469A	541155	5467520
3652	551300	5454519	C4255B	559710	5464280	EL469B	541190	5467520
3653	550685	5453513	C40256	559565	5465200	EL470-	555450	5470950
3654	551720	5455211	C40257	559365	5465030	G4043-	554425	5480820
ds861	546292	5452139	C4258A	559280	5465020	G4044A	554705	5480860
ds861	546606	5452546	C4258B	559250	5464960	G4044B	554750	5480860
ds861	546740	5452701	C40259	561080	5466905	G4045-	553740	5480130
ds861	547167	5452789	C40260	561090	5466710	G4046A	553855	5480135
ds861	547504	5452611	C40261	560700	5466550	G4046B	553890	5480135
3655	552282	5455330	C40262	560190	5466270	G4047-	555680	5480595
3656	551782	5455674	C40263	560120	5466190	G4048-	562745	54802625
3601	557151	5456813	C4264A	559935	5466120	G4049-	562790	5480325
3617	558428	5459537	C4264B	559980	5466020	G4050-	561250	5476005
c610	559323	5455831	C40265	559765	5465855	G4051-	560730	5476550
3609a	559379	5455934	C40266	559945	5465765	G4052-	560720	5476600
3609b	559405	5455949	C4267A	560470	5465355	G4053-	560705	5476920
3602	561363	5459902	C4267B	560425	5465395	G4054A	560775	5477530
3603	561045	5460016	C40268	560470	5465300	G4054B	560700	5477530
3604	560853	5460193	C40270	559195	5465100	G4055A	560664	5477810
3605a	560441	5460126	C40271	559230	5465165	G4055B	560620	5477810
3605b	560434	5460095	C4271A	559230	5465165	G4056-	559500	5478640
3607	560645	5459243	C4271B	559250	5465205	G4033-	560320	5480795
3608	561146	5459067	C4272A	558930	5465585	G4034-	562695	5479720
3665	543468	5477729	C4272B	558960	5465545	G4035-	561990	5480380
c643	541534	5476560	C4273A	558540	5465000	G4036-	561690	5480530
3663	541250	5476509	C4273B	558515	5465035	G4040-	565960	5480510
3662	541140	5476496	C4275X	559220	5464225	G4041A	566750	5481295
3661	541068	5476511	C40275	559295	5464185	G4041B	566795	5481295
3660	541070	5476444	C40276	557915	5464895	G4042A	566665	5480390
c642	541049	5476349	C40277	558100	5464935	G4042B	566690	5480390
3664	541217	5476417	C40278	557050	5464345	G4021-	567210	5481710

APPENDIX B: SPRINGDALE GROUP SAMPLE LOCATIONS.

Sample Number	Easting	Northing	Sample Number	Easting	Northing	Sample Number	Easting	Northing
c640a	561199	5479886	C4279A	557715	5463990	G4022-	567400	5481995
c640b	561628	5479823	C4279B	557775	5464015	G4024-	567185	5481725
c640c	561602	5479949	C4279C	557835	5464045	G4025-	567045	5481895
c640d	561864	5480043	C4274A	559770	5466695	G4026-	567415	5482820
c640e	562003	5480226	C4274B	559725	5466695	G4029-	560990	5477060
c640f	562097	5480309	C4274C	559690	5466630	G4030-	560920	5477220
c641a	562258	5480503	C4273C	558470	5465005	G4031-	560805	5477600
c641b	562380	5480635	C40266	559885	5465675	G4032-	560260	5479320
c641c	562621	5480802	C4280A	557585	5463290	G4011-	567470	5482430
c641d	562185	5480646	C4280B	557530	5463260	G4012-	567650	5482300
c641e	562058	5480481	C4280C	557495	5463230	G4013-	567690	5482330
c641f	561758	5480311	C40281	550815	5474410	G4014-	567325	5482560
C4002B	567435	5482580	C40282	550885	5474460	G4015-	567325	5482500
C4002A	567410	5482580	C40283	550915	5474495	G4016-	567695	5482190
C4002D	567390	5482580	C40284	562980	5469690	G4017-	567690	5482130
C4003A	559955	5480590	C40285	563205	5469805	G4018-	567675	5482185
C4003B	559920	5480590	C40286	563100	5469405	G4019-	567685	5481980
C4004A	559985	5480720	C40287	562880	5469560	G4020-	567550	5481875
C4004B	559960	5480720	C40288	562810	5469005	G4001-	565850	5479600
C4005A	555905	5480650	C40289	562775	5468830	DM0066	546230	5472195
C4006-	563730	5479020	C40290	563405	5468810	DM0068	546100	5471435
C4007A	565665	5479480	C40291	564620	5473090	DM0069	545620	5469305
C4007B	565690	5479480	C4292A	549130	5472030	DM0070	547005	5472875
C4008-	565520	5479090	C4292B	549280	5472075	DM0073	558595	5456820
C4009-	565560	5479230	C4292C	549360	5472070	DM0076	558550	5455595
C4010-	565930	5479720	C40293	549500	5472275	DM0042	551890	5463450
C4011-	564890	5475240	C40294	549505	5472085	DM0043	551850	5463400
C4012-	564950	5475340	C4295A	548645	5471450	DM0045	551710	5463300
C4013A	553975	5474080	C4295B	548720	5471540	DM0046	551665	5463220
C4013B	553950	5474080	C40296	548730	5471740	DM0047	551530	5462535
C4014-	550600	5468720	C40297	548415	5470950	DM049A	551255	5462595
C4015A	551545	5464740	C40298	548340	5471195	DM049B	551290	5462595
C4015B	551520	5464740	C40299	548255	5471150	DM0051	551210	5462360
C4u16A	551565	5463470	C40300	548300	5471285	DM0053	551150	5462205
C4016B	551540	5463470	C40301	548205	5471205	DM0054	564260	5472760
C4016C	551515	5463470	C40302	548125	5471150	DM0055	564335	5472550
C4016D	551500	5463470	C40303	562810	5464515	DM0057	564270	5472220
C4016E	551580	5463475	C40304	561475	5460640	DM058A	564180	5472080
C4016F	551470	5463480	C4305A	558580	5459500	DM0059	564020	5471750

APPENDIX B: SPRINGDALE GROUP SAMPLE LOCATIONS.

Sample Number	Easting	Northing	Sample Number	Easting	Northing	Sample Number	Easting	Northing
C4017-	562095	5464110	C4305B	558640	5459490	DM0060	564095	5471750
C4018-	562620	5465660	C4305C	558610	5459425	DM0061	564580	5471395
C4019-	564096	5474525	C40306	558260	5459280	DM0062	564695	5472010
C4020A	550865	5478560	C40307	558275	5459250	DM063A	546540	5472890
C4020B	550840	5478560	C40308	558400	5459100	DM0064	544900	5472170
C4020C	550815	5478560	C40309	558295	5458875	DM0065	546500	5472200
C4021A	548725	5478750	C40310	558000	5458780			
C4021B	548700	5478750	C40311	558350	5458580			

APPENDIX C

ANALYTICAL PROCEDURES

FOR MAJOR AND

TRACE ELEMENTS

(AA, XRF, ICP-MS)

APPENDIX C

Analytical Procedures for Major and Trace Elements.

Samples for analysis were chosen to exclude as much as possible any secondary material such as weathering, alteration, veins, amygdales, lithic clasts (in ash-flow tuffs), etc. These samples were crushed into chips and then pulverized for 2-3 minutes using a tungsten carbide puck mill to produce a powder of approximately -100 mesh.

Major elements, except for phosphorous, were determined on a Perkin-Elmer Model 370 atomic absorption spectrometer with digital readout, by G. Andrews in the Memorial University Department of Earth Sciences, using her well-established methods based on those described by Langmuir and Paus (1968). Phosphorus was determined colorimetrically using a Bausch and Lomb Spectronic 20 Colorimeter, based on a modification of the method described by Shapiro and Brannock (1962). Loss on ignition was determined by weighing approximately one gram of the powdered sample into a porcelain crucible and heating it to approximately 1000°C for about 90 minutes to volatilize S, CO₂, H₂O etc. Analytical errors are estimated at <5% for all major elements except MnO, MgO, LOI (<8%), and TiO₂ and P₂O₅ (<20%).

Most trace elements (Pb, U, Th, Rb, Sr, Y, Zr, Nb, Ga, Zn, Cu, Ni, La, Ti, Ba, V, Ce, Cr) were determined using a Phillips 1450 X-Ray fluorescence (XRF) spectrometer with a rhodium tube. Sample pellets for trace element analysis were made by mixing 10 g of powdered sample with approximately 1.5 g of bakelite binding resin, compressing the mixture and baking the resulting pellet for ten minutes at 200°C. Samples were run in batches of nine with U.S.G.S. standard W-1 run as a tenth sample. A monitor saturated with trace elements was used to calibrate the machine against standard values and correct for instrument drift. Precision (2-sigma) is within 10% for most of these trace elements, increasing to higher percentages for those in very low concentrations of about 10 ppm or less.

Most of the above trace elements, as well as the rare earths and Sc, Bi, W, Mo, Cs, Li, Ta, and Hf were determined by Drs. H. Longerich and S. Jackson with inductively coupled plasma - mass spectrometry (ICP-MS) using the following procedures. A standard HF/HNO₃ digestion of a 0.1 g sample aliquot; analysis of the solution by inductively coupled plasma mass spectrometry (ICP-MS) using the method of standard addition to correct for matrix effects. Any sample material that did not dissolve in HF/HNO₃ was attacked with HCl/HNO₃. Any samples that did not dissolve fully even after multi-acid attack (usually due to presence of graphite, sulphides,

chromite etc.) and required filtering of insoluble residue prior to analysis are indicated (none for this study). Zircon may not always dissolve completely so that Zr and Hf values from ICP-MS should be considered minimum concentrations. The W data are also invalid because the samples were crushed using tungsten carbide-lined equipment.

A reagent blank (RBK) and a sample of the CANMET geological reference standard SY-2 (syenite) were prepared and analysed with the samples. Reagent contamination is insignificant and reagent blank concentrations were not subtracted from sample concentrations. One or more of the sample solutions were analysed in duplicate (DUP) in each analytical run (18 solutions) and no significant differences were detected. Sample detection limits were at the ppb level for all elements except Li which was less than 2 ppm. All determinations for standard SY-2 were within <5% of the accepted values (compiled from Govindaraju, 1984, Geostandards Newsletter (Special Issue), 8, 3, except for the REE data from Doherty and Vander Voet, 1985, CJS, 30, 135) and the average values (23 runs) determined in our laboratory (SY-2 MUN).

APPENDIX D

ANALYTICAL DATA

FOR ROCKS OF

THE SPRINGDALE

GROUP

Sample Name	C4-187	DS-20	HS-38	HS-42B	HS-57A	HS-63	HS-71	HS-109	HS-112	HS-114
Mg Number	54	64	55	55	52	58	58	63	63	56
SiO2	46.20	44.30	49.10	50.70	47.60	49.20	50.70	48.30	47.80	51.20
TiO2	1.71	1.40	1.40	1.44	1.52	1.42	1.44	1.28	1.22	1.22
Al2O3	14.70	16.50	16.00	15.50	16.30	15.60	15.70	15.10	16.00	15.90
Fe2O3	1.50	1.58	1.53	1.50	1.62	1.42	1.48	1.49	1.36	1.37
FeO	7.66	8.05	7.82	7.63	8.26	7.24	7.54	7.59	6.94	6.97
MnO	0.19	0.17	0.11	0.24	0.15	0.14	0.15	0.15	0.11	0.11
MgO	5.88	9.65	6.37	6.24	5.88	6.61	6.90	8.51	8.46	5.81
CaO	7.92	8.64	10.00	9.14	7.36	7.54	8.28	8.98	8.94	9.80
Na2O	3.67	2.20	2.63	3.15	3.97	3.62	3.31	2.58	2.67	2.80
K2O	0.42	0.69	0.31	0.68	1.17	0.98	0.74	0.49	0.30	0.36
P2O5	0.33	0.20	0.24	0.35	0.28	0.23	0.24	0.15	0.20	0.18
LOI	8.55	3.45	2.74	2.03	4.04	3.97	1.28	3.29	3.36	1.66
Cr	165	184	116	128	144	141	138	251	181	147
Ni	77	141	90	68	77	77	74	84	104	92
Sc	0	0	0	0	0	0	0	0	0	0
V	223	235	197	207	197	197	168	202	181	198
Cu	23	106	63	308	8	7	42	32	22	46
Pb	16	1	2	28	0	16	3	0	13	6
Zn	65	102	53	61	68	69	53	54	61	54
Bi	0	0	0	0	0	0	0	0	0	0
W	0	0	0	0	0	0	0	0	0	0
Mo	0	0	0	0	0	0	0	0	0	0
K	0	5727	0	0	0	0	0	0	0	0
Rb	8	53	0	12	13	18	18	7	11	0
Cs	0	0	0	0	0	0	0	0	0	0
Ba	179	162	158	247	354	356	229	199	264	220
Sr	258	273	394	327	418	425	373	216	351	411
Tl	0	0	0	0	0	0	0	0	0	0
Ga	16	16	14	16	12	13	17	10	14	14
Li	0	0	0	0	0	0	0	0	0	0
Ta	0	0	0	0	0	0	0	0	0	0
Nb	11	7	9	8	9	8	8	6	8	10
Hf	0	0	0	0	0	0	0	0	0	0
Zr	153	105	123	139	126	127	127	87	110	101
Ti	2	8393	1	1	1	1	1	1	1	1
Y	42	30	38	47	41	41	33	35	36	34
Th	16	0	10	2	0	10	0	4	13	11
U	19	0	6	11	0	0	3	29	12	10
La	27.00	13.00	12.00	28.00	16.00	7.00	14.00	22.00	20.00	16.00
Ce	29.00	32.00	43.00	2.00	34.00	38.00	0.00	21.00	24.00	26.00
Pr	0.00	5.00	0.00	0.00	0.00	0.00	0.00	0.00	0.00	0.00
Nd	0.00	21.20	0.00	0.00	0.00	0.00	0.00	0.00	0.00	0.00
Sm	0.00	5.00	0.00	0.00	0.00	0.00	0.00	0.00	0.00	0.00
Eu	0.00	1.60	0.00	0.00	0.00	0.00	0.00	0.00	0.00	0.00
Gd	0.00	6.00	0.00	0.00	0.00	0.00	0.00	0.00	0.00	0.00
Tb	0.00	1.40	0.00	0.00	0.00	0.00	0.00	0.00	0.00	0.00
Dy	0.00	7.50	0.00	0.00	0.00	0.00	0.00	0.00	0.00	0.00
Ho	0.00	1.80	0.00	0.00	0.00	0.00	0.00	0.00	0.00	0.00
Er	0.00	3.80	0.00	0.00	0.00	0.00	0.00	0.00	0.00	0.00
Tm	0.00	51.00	0.00	0.00	0.00	0.00	0.00	0.00	0.00	0.00
Yb	0.00	3.50	0.00	0.00	0.00	0.00	0.00	0.00	0.00	0.00
Lu	0.00	0.70	0.00	0.00	0.00	0.00	0.00	0.00	0.00	0.00
Be	0.00	0.00	0.00	0.00	0.00	0.00	0.00	0.00	0.00	0.00

Sample Name	C4-179	C4-189	C4-190	HS-48	DS-84-7	DS-84-9	C4-279A	C4-279B	C4-310	C4277B
Mg Number	60	54	61	57	62	68	55	40	25	42
SiO2	51.50	48.30	46.80	49.30	48.00	48.00	46.70	52.90	51.20	47.70
TiO2	1.24	1.52	1.47	1.35	1.58	1.69	1.29	2.06	1.83	3.73
Al2O3	16.50	15.60	16.20	15.50	16.30	15.00	16.30	13.90	13.70	13.10
Fe2O3	1.27	1.49	1.53	1.37	1.43	1.37	1.53	1.67	2.15	2.22
FeO	6.47	7.59	7.80	7.00	7.27	6.97	7.82	8.51	10.94	11.34
MnO	0.19	0.14	0.17	0.17	0.13	0.17	0.13	0.14	0.12	0.26
HgO	6.42	5.91	8.03	6.09	7.93	9.59	6.25	3.76	2.36	5.34
CaO	6.26	10.48	8.10	9.80	6.32	5.70	9.54	5.14	5.56	9.08
Na2O	3.59	2.80	3.21	2.71	3.63	3.22	2.48	5.18	3.19	2.51
K2O	0.92	0.61	0.38	0.38	0.36	0.28	0.08	0.29	1.78	0.35
P2O5	0.17	0.26	0.24	0.23	0.42	0.45	0.15	0.25	0.24	1.02
LOI	3.35	3.60	3.48	3.43	4.28	5.31	5.90	4.32	5.78	2.14
Cr	200	242	0	105	319	265	159	41	35	49
Ni	1	121	0	44	176	150	100	0	0	19
Sc	0	0	0	0	0	0	0	31	0	53
V	250	227	0	199	201	213	200	348	348	358
Cu	9	61	0	25	47	0	37	16	0	0
Pb	0	2	0	9	0	13	0	6	7	5
Zn	75	69	0	63	69	75	66	81	101	86
Bi	0	0	0	0	0	0	0	0	0	0
Hf	0	0	0	0	0	0	0	25	0	7
Mb	0	0	0	0	0	0	0	1	0	2
K	0	0	0	0	0	0	0	2407	0	2905
Rb	19	9	0	9	7	6	0	7	45	5
Cs	0	0	0	0	0	0	0	1	0	0
Ba	692	229	0	256	409	360	78	146	430	370
Sr	575	464	0	467	817	764	313	536	184	393
Tl	0	0	0	0	0	0	0	0	0	0
Ga	17	16	0	20	20	17	32	25	22	18
Li	0	0	0	0	0	0	0	21	0	33
Ta	0	0	0	0	0	0	0	1	0	1
Nb	7	11	0	12	18	15	6	31	10	16
Hf	0	0	0	0	0	0	0	5	0	7
Zr	114	137	0	128	209	219	115	195	185	315
Ti	1	1	0	1	2	2	1	12349	2	22361
Y	37	40	0	31	46	47	32	39	41	64
Th	0	6	0	12	3	28	0	3	1	2
U	3	13	0	18	8	6	2	1	0	1
La	24.00	33.00	0.00	27.00	36.00	39.00	0.00	17.05	0.00	23.64
Ce	54.00	42.00	0.00	44.00	36.00	12.00	6.00	41.05	44.00	57.38
Pr	0.00	0.00	0.00	0.00	0.00	0.00	0.00	5.49	0.00	8.26
Nd	0.00	0.00	0.00	0.00	0.00	0.00	0.00	23.88	0.00	37.31
Sm	0.00	0.00	0.00	0.00	0.00	0.00	0.00	5.97	0.00	9.53
Eu	0.00	0.00	0.00	0.00	0.00	0.00	0.00	1.91	0.00	3.58
Gd	0.00	0.00	0.00	0.00	0.00	0.00	0.00	5.88	0.00	10.13
Tb	0.00	0.00	0.00	0.00	0.00	0.00	0.00	1.07	0.00	1.66
Dy	0.00	0.00	0.00	0.00	0.00	0.00	0.00	6.82	0.00	9.78
Ho	0.00	0.00	0.00	0.00	0.00	0.00	0.00	1.38	0.00	1.95
Er	0.00	0.00	0.00	0.00	0.00	0.00	0.00	3.96	0.00	5.53
Tm	0.00	0.00	0.00	0.00	0.00	0.00	0.00	0.57	0.00	0.75
Yb	0.00	0.00	0.00	0.00	0.00	0.00	0.00	3.60	0.00	4.59
Lu	0.00	0.00	0.00	0.00	0.00	0.00	0.00	0.53	0.00	0.70
Be	0.00	0.00	0.00	0.00	0.00	0.00	0.00	1.40	0.00	1.58

[illegible]

Sample Name	C41071	EL314	3-6350	3-6-38	3-6-60	3-6-5A	3-6-7	3-6-11	3-6-26	3-630A
Mg Number	58	48	76	61	58	56	67	59	50	47
SiO2	50.80	50.70	44.60	52.90	47.20	53.20	51.90	49.30	50.80	45.30
TiO2	1.32	1.48	1.08	1.12	1.72	1.20	1.00	1.04	2.00	1.52
Al2O3	16.10	15.50	12.20	17.00	15.50	15.20	15.70	15.20	14.20	15.40
Fe2O3	1.42	1.79	1.61	1.22	1.76	1.36	1.10	1.13	1.72	1.55
FeO	7.23	9.15	8.21	6.23	8.97	6.95	5.63	5.78	8.79	7.92
MnO	0.12	0.16	0.17	0.14	0.19	0.13	0.14	0.14	0.19	0.22
MgO	6.67	5.58	17.00	6.47	8.32	5.78	7.46	5.52	5.83	4.68
CaO	6.76	8.80	8.18	9.26	12.08	7.06	6.70	10.40	6.62	11.16
Na2O	5.04	3.13	1.10	2.98	2.37	3.79	3.01	2.16	3.88	3.80
K2O	0.32	0.69	0.26	0.41	0.10	1.13	0.74	0.19	1.11	1.35
P2O5	0.25	0.23	0.19	0.19	0.18	0.17	0.15	0.28	0.48	0.34
LOI	3.33	2.42	5.31	0.91	0.65	1.38	4.44	8.05	2.61	5.27
Cr	140	231	676	83	210	68	120	160	83	238
Ni	90	72	462	13	51	21	125	102	22	98
Sc	0	0	0	16	35	23	0	0	29	0
V	222	214	179	184	267	201	171	173	249	221
Cu	34	24	30	6	75	5	4	45	21	27
Pb	0	2	0	5	2	6	0	3	5	0
Zn	71	69	59	62	70	65	67	57	90	100
Bi	0	0	0	0	0	0	0	0	0	0
W	0	0	0	109	131	90	0	0	109	0
Mo	0	0	0	1	1	1	0	0	1	0
K	0	0	0	3403	830	9380	0	0	9214	0
Rb	8	14	9	11	1	33	17	3	24	43
Cs	0	0	0	1	0	2	0	0	3	0
Ba	146	230	114	136	29	388	510	203	516	452
Sr	511	324	145	350	229	304	408	404	361	489
Tl	0	0	0	0	0	0	0	0	0	0
Ga	14	15	7	16	12	15	14	15	16	12
Li	0	0	0	5	3	26	0	0	12	0
Ta	0	0	0	1	1	1	0	0	1	0
Nb	8	12	8	6	4	5	8	11	17	11
Hf	0	0	0	3	2	4	0	0	7	0
Zr	141	133	86	100	50	102	140	232	260	155
Ti	1	1	1	6714	10311	7194	1	1	11990	1
Y	31	42	25	17	26	26	29	29	37	33
Th	0	0	0	2	0	3	2	0	3	0
U	0	2	0	1	0	1	0	0	1	0
La	13.00	36.00	0.00	11.95	5.89	12.69	0.00	10.00	25.29	1.00
Ce	20.00	0.00	47.00	26.32	16.78	29.41	67.00	12.00	58.42	46.00
Pr	0.00	0.00	0.00	3.40	2.57	3.85	0.00	0.00	7.84	0.00
Nd	0.00	0.00	0.00	13.94	12.97	16.73	0.00	0.00	33.99	0.00
Sm	0.00	0.00	0.00	3.25	3.93	4.26	0.00	0.00	7.72	0.00
Eu	0.00	0.00	0.00	1.05	1.40	1.12	0.00	0.00	2.14	0.00
Gd	0.00	0.00	0.00	3.15	4.45	4.57	0.00	0.00	7.57	0.00
Tb	0.00	0.00	0.00	0.54	0.85	0.79	0.00	0.00	1.30	0.00
Dy	0.00	0.00	0.00	3.36	5.29	4.92	0.00	0.00	7.90	0.00
Ho	0.00	0.00	0.00	0.69	1.08	1.01	0.00	0.00	1.57	0.00
Er	0.00	0.00	0.00	1.98	3.03	3.12	0.00	0.00	4.48	0.00
Tm	0.00	0.00	0.00	0.28	0.42	0.45	0.00	0.00	0.62	0.00
Yb	0.00	0.00	0.00	1.89	2.65	3.02	0.00	0.00	4.01	0.00
Lu	0.00	0.00	0.00	0.27	0.37	0.44	0.00	0.00	0.61	0.00
Be	0.00	0.00	0.00	0.02	0.84	1.30	0.00	0.00	0.31	0.00

Sample Name	3-635B	3-635C	C4-100	C4-102	C4-166	C4-167A	C4-176B	C4-194	C4-208	C4-217
Mg Number	49	56	36	33	42	42	33	43	45	52
SiO2	53.60	48.00	61.80	66.40	60.40	57.10	66.80	58.70	62.00	59.70
TiO2	1.76	1.84	0.80	0.54	1.06	1.40	0.26	1.43	0.82	0.84
Al2O3	15.90	15.80	17.10	15.50	16.50	14.30	14.00	14.70	15.00	15.40
Fe2O3	1.53	1.62	0.72	0.52	0.85	1.18	0.35	1.27	0.82	0.96
FeO	7.79	8.28	3.67	2.63	4.34	6.00	1.78	6.47	4.17	4.91
MnO	0.16	0.18	0.07	0.05	0.14	0.15	0.11	0.16	0.09	0.11
HgO	4.90	6.86	1.34	0.87	2.09	2.81	0.58	3.26	2.27	3.47
CaO	4.82	8.20	4.52	3.48	3.10	5.30	4.78	4.08	4.22	5.30
Na2O	4.75	3.76	6.15	5.33	4.61	3.95	1.84	4.62	4.74	4.32
K2O	0.16	0.55	1.60	2.21	2.35	1.63	1.98	1.86	2.01	1.67
P2O5	0.40	0.31	0.15	0.12	0.22	0.32	0.06	0.33	0.18	0.15
LOI	3.33	3.00	2.36	1.66	3.67	5.21	6.72	1.98	1.94	2.30
Cr	11	47	57	20	16	22	25	13	32	85
Ni	0	43	11	0	5	0	0	1	0	38
Sc	0	28	0	0	0	0	0	0	0	0
V	3	238	127	83	110	214	72	213	112	134
Cu	7	17	7	3	0	4	6	1	2	37
Pb	16	5	18	9	11	11	16	6	25	16
Zn	89	80	21	27	89	79	25	100	51	63
Bi	0	0	0	0	0	0	0	0	0	0
W	0	55	0	0	0	0	0	0	0	0
Mo	0	1	0	0	0	0	0	0	0	0
K	0	4565	0	0	0	0	0	0	0	0
Rb	4	18	47	34	71	40	34	38	50	37
Cs	0	1	0	0	0	0	0	0	0	0
Ba	88	177	306	977	472	392	326	475	410	737
Sr	303	452	621	453	278	119	79	478	426	403
Tl	0	0	0	0	0	0	0	0	0	0
Ga	18	12	14	15	20	12	14	14	15	14
Li	0	17	0	0	0	0	0	0	0	0
Ta	0	1	0	0	0	0	0	0	0	0
Nb	10	6	6	10	9	11	7	9	12	7
Hf	0	4	0	0	0	0	0	0	0	0
Zr	197	133	107	139	193	162	87	191	153	122
Ti	2	11030	1	1	1	1	0	2	1	1
Y	44	30	24	31	58	53	26	50	41	32
Th	0	1	12	14	17	14	16	12	19	25
U	0	0	15	3	2	0	10	2	5	16
La	5.00	12.79	4.11	11.00	34.00	36.00	26.00	22.00	14.00	10.00
Ce	70.00	30.78	8.00	58.00	89.00	38.00	34.00	39.00	35.00	40.00
Pr	0.00	4.24	0.00	0.00	0.00	0.00	0.00	0.00	0.00	0.00
Nd	0.00	18.66	0.00	0.00	0.00	0.00	0.00	0.00	0.00	0.00
Sm	0.00	4.87	0.00	0.00	0.00	0.00	0.00	0.00	0.00	0.00
Eu	0.00	1.72	0.00	0.00	0.00	0.00	0.00	0.00	0.00	0.00
Gd	0.00	4.94	0.00	0.00	0.00	0.00	0.00	0.00	0.00	0.00
Tb	0.00	0.87	0.00	0.00	0.00	0.00	0.00	0.00	0.00	0.00
Dy	0.00	5.18	0.00	0.00	0.00	0.00	0.00	0.00	0.00	0.00
Ho	0.00	1.08	0.00	0.00	0.00	0.00	0.00	0.00	0.00	0.00
Er	0.00	3.03	0.00	0.00	0.00	0.00	0.00	0.00	0.00	0.00
Tm	0.00	0.44	0.00	0.00	0.00	0.00	0.00	0.00	0.00	0.00
Yb	0.00	2.73	0.00	0.00	0.00	0.00	0.00	0.00	0.00	0.00
Lu	0.00	0.40	0.00	0.00	0.00	0.00	0.00	0.00	0.00	0.00
Se	0.00	1.23	0.00	0.00	0.00	0.00	0.00	0.00	0.00	0.00

Sample Name	C4-66	C4-68	C4-76	C4-81B	C4-88C	C4-98	C4-99	C4-101	C4-167C	C4-233A
Mg Number	47	42	54	57	32	55	61	59	41	49
SiO2	63.50	66.60	63.40	61.00	66.80	56.40	65.60	61.60	60.10	60.90
TiO2	0.74	0.50	0.59	0.84	0.44	0.86	0.64	0.52	1.58	0.30
Al2O3	15.80	14.50	14.80	15.80	14.80	16.80	13.50	15.70	15.50	14.70
Fe2O3	0.73	0.58	0.68	0.86	0.62	0.97	0.67	0.76	1.12	0.54
FeO	3.72	2.95	3.46	4.37	3.14	4.96	3.40	3.89	5.69	2.74
MnO	0.06	0.06	0.08	0.14	0.09	0.10	0.09	0.08	0.12	0.15
HgO	2.17	1.39	2.67	3.76	0.97	4.03	3.50	3.63	2.60	1.76
CaO	1.22	4.40	3.36	4.64	1.54	3.26	3.96	2.00	3.40	3.90
Na2O	5.48	4.22	3.74	3.85	5.30	6.92	3.13	5.70	5.56	6.42
K2O	3.33	1.34	2.87	1.31	1.40	0.78	0.95	1.18	1.60	0.91
P2O5	0.25	0.14	0.17	0.22	0.20	0.19	0.14	0.15	0.34	0.11
LOI	2.13	2.13	2.23	2.83	2.59	2.71	3.29	3.16	1.79	5.99
Cr	24	47	80	44	9	40	44	102	0	7
Ni	9	20	23	25	0	36	24	18	0	3
Sc	0	0	0	0	0	0	0	0	0	0
V	113	79	84	147	37	151	124	121	0	18
Cu	12	21	28	18	9	26	19	17	0	4
Pb	12	2	12	8	13	0	0	0	0	9
Zn	68	32	53	56	81	74	44	66	0	106
Bi	0	0	0	0	0	0	0	0	0	0
W	0	0	0	0	0	0	0	0	0	0
Mo	0	0	0	0	0	0	0	0	0	0
K	0	0	0	0	0	0	0	0	0	0
Rb	64	25	63	12	31	8	16	11	0	8
Cs	0	0	0	0	0	0	0	0	0	0
Ba	1023	434	817	642	204	174	221	328	0	47
Sr	519	562	672	572	349	676	489	528	0	179
Tl	0	0	0	0	0	0	0	0	0	0
Ga	16	16	19	19	19	16	15	14	0	15
Li	0	0	0	0	0	0	0	0	0	0
Ta	0	0	0	0	0	0	0	0	0	0
Nb	13	5	11	10	8	7	5	9	0	9
Hf	0	0	0	0	0	0	0	0	0	0
Zr	199	104	180	155	156	114	95	157	0	295
Ti	1	0	1	1	1	1	1	1	0	1
Y	34	23	28	33	47	29	31	34	0	61
Th	16	6	10	7	22	0	7	6	0	8
U	7	3	4	1	40	0	8	4	0	2
La	44.00	33.00	41.00	41.00	35.00	33.00	29.00	41.00	0.00	27.00
Ce	94.00	56.00	77.00	73.00	39.00	50.00	37.00	64.00	0.00	48.00
Pr	0.00	0.00	0.00	0.00	0.00	0.00	0.00	0.00	0.00	0.00
Nd	0.00	0.00	0.00	0.00	0.00	0.00	0.00	0.00	0.00	0.00
Sm	0.00	0.00	0.00	0.00	0.00	0.00	0.00	0.00	0.00	0.00
Eu	0.00	0.00	0.00	0.00	0.00	0.00	0.00	0.00	0.00	0.00
Gd	0.00	0.00	0.00	0.00	0.00	0.00	0.00	0.00	0.00	0.00
Tb	0.00	0.00	0.00	0.00	0.00	0.00	0.00	0.00	0.00	0.00
Dy	0.00	0.00	0.00	0.00	0.00	0.00	0.00	0.00	0.00	0.00
Ho	0.00	0.00	0.00	0.00	0.00	0.00	0.00	0.00	0.00	0.00
Er	0.00	0.00	0.00	0.00	0.00	0.00	0.00	0.00	0.00	0.00
Tm	0.00	0.00	0.00	0.00	0.00	0.00	0.00	0.00	0.00	0.00
Yb	0.00	0.00	0.00	0.00	0.00	0.00	0.00	0.00	0.00	0.00
Lu	0.00	0.00	0.00	0.00	0.00	0.00	0.00	0.00	0.00	0.00
Be	0.00	0.00	0.00	0.00	0.00	0.00	0.00	0.00	0.00	0.00

Sample Name	C4-233D	C4-19	C4-70A	C4-263	C4-275	C4-275XA	C4-275XB	DS-84-88	C4-313A
Mg Number	55	46	35	33	21	20	20	60	48
SiO2	62.80	61.90	64.90	64.70	64.00	64.20	63.50	62.60	65.00
TiO2	0.46	0.94	0.72	0.78	0.58	0.53	0.53	0.98	0.45
Al2O3	15.50	15.10	14.70	13.40	14.60	14.80	14.80	15.30	14.70
Fe2O3	0.36	0.82	0.68	0.91	0.64	0.67	0.65	0.75	0.70
FeO	1.81	4.19	3.44	4.62	3.26	3.42	3.33	3.80	3.56
MnO	0.14	0.09	0.05	0.09	0.13	0.07	0.06	0.09	0.08
MgO	1.45	2.39	1.20	1.51	0.58	0.56	0.54	3.75	2.14
CaO	3.04	5.00	3.44	2.14	3.54	3.18	3.64	1.92	3.52
Na2O	7.48	4.02	4.08	4.78	2.28	4.93	4.89	5.33	4.15
K2O	1.08	1.75	3.08	0.63	2.54	1.91	1.90	0.69	1.89
P2O5	0.12	0.18	0.31	0.25	0.19	0.20	0.22	0.28	0.08
LOI	4.62	2.23	1.63	3.68	5.59	4.06	4.39	2.68	2.72
Cr	6	33	36	8	11	8	8	90	109
Ni	0	2	3	0	0	0	0	39	5
Sc	0	14	0	0	11	0	0	0	0
V	14	117	104	44	53	41	43	130	105
Cu	5	1	8	0	0	0	0	28	7
Pb	14	11	15	16	11	4	0	7	20
Zn	71	44	32	77	78	48	44	51	53
Bi	0	0	0	0	0	0	0	0	0
W	0	79	0	0	107	0	0	0	0
Mo	0	1	0	0	1	0	0	0	0
K	0	14526	0	0	21084	0	0	0	0
Rb	14	46835	60	8	72	32	34	8	30
Cs	0	1	0	0	3	0	0	0	0
Ba	187	398	1603	150	614	330	347	267	542
Sr	279	373	747	254	193	126	136	492	274
Tl	0	0	0	0	0	0	0	0	0
Ga	12	15	13	18	15	14	14	18	0
Li	0	17	0	0	44	0	0	0	0
Ta	0	1	0	0	1	0	0	0	0
Nb	11	6	13	10	26	10	10	14	7
Hf	0	4	0	0	5	0	0	0	0
Zr	308	145	196	227	162	150	147	182	149
Ti	1	5635	1	1	3477	1	1	1	1
Y	69	26	26	76	31	57	54	27	33
Th	20	6	9	17	6	19	9	19	5
U	5	2	0	0	2	2	0	2	5
La	34.00	19.95	52.00	47.00	17.86	47.00	48.00	41.00	3.00
Ce	50.00	42.51	88.00	63.00	40.13	21.00	42.00	61.00	46.00
Pr	0.00	5.07	0.00	0.00	5.20	0.00	0.00	0.00	0.00
Nd	0.00	19.56	0.00	0.00	21.39	0.00	0.00	0.00	0.00
Sm	0.00	4.52	0.00	0.00	5.17	0.00	0.00	0.00	0.00
Eu	0.00	1.14	0.00	0.00	1.28	0.00	0.00	0.00	0.00
Gd	0.00	4.59	0.00	0.00	5.06	0.00	0.00	0.00	0.00
Tb	0.00	0.77	0.00	0.00	0.91	0.00	0.00	0.00	0.00
Dy	0.00	4.76	0.00	0.00	5.68	0.00	0.00	0.00	0.00
Ho	0.00	1.01	0.00	0.00	1.19	0.00	0.00	0.00	0.00
Er	0.00	2.98	0.00	0.00	3.58	0.00	0.00	0.00	0.00
Tm	0.00	0.43	0.00	0.00	0.52	0.00	0.00	0.00	0.00
Yb	0.00	2.91	0.00	0.00	3.38	0.00	0.00	0.00	0.00
Lu	0.00	0.46	0.00	0.00	0.51	0.00	0.00	0.00	0.00
Be	0.00	0.97	0.00	0.00	1.44	0.00	0.00	0.00	0.00

[illegible]

Sample Name	C4011	C4012	C4052	C4095	C4222A	C4323	C4332A	C4332C	C4333A
Hg Number	68	53	33	44	56	38	21	24	30
SiO2	62.70	58.70	62.90	58.70	60.10	59.30	57.20	59.90	60.70
TiO2	0.55	0.53	0.65	1.31	0.78	1.97	0.27	1.29	1.32
Al2O3	14.10	14.90	12.30	14.50	14.80	14.40	14.20	16.50	14.40
Fe2O3	0.59	0.62	0.88	1.19	0.84	1.50	0.53	0.95	1.38
FeO	3.03	3.17	4.49	6.05	4.28	7.64	2.72	4.83	7.04
MnO	0.07	0.08	0.20	0.13	0.12	0.16	0.06	0.18	0.21
MgO	4.18	2.36	1.46	3.11	3.63	3.07	0.49	0.98	2.02
CaO	3.24	5.38	2.90	2.52	3.68	4.58	1.32	3.96	2.82
Na2O	3.76	4.98	5.10	6.16	3.40	4.03	3.79	5.97	4.84
K2O	0.72	0.65	2.84	0.33	2.12	1.74	3.00	2.06	1.60
P2O5	0.18	0.23	0.40	0.31	0.14	0.45	0.08	0.48	0.53
LOI	6.47	7.57	4.09	3.89	4.46	1.98	2.99	1.91	1.58
Cr	70	28	127	50	121	62	70	81	90
Ni	22	0	0	0	33	25	0	8	7
Sc	0	0	0	0	0	0	0	0	0
V	87	13	59	272	147	258	37	18	0
Cu	13	5	4	10	21	21	11	0	0
Pb	20	26	13	17	14	0	17	15	1
Zn	60	61	102	91	60	98	45	111	142
Bi	0	0	0	0	0	0	0	0	0
W	0	0	0	0	0	0	0	0	0
Mo	0	0	0	0	0	0	0	0	0
K	0	0	0	0	0	0	0	0	0
Rb	14	51	70	2	58	41	87	61	96
Cs	0	0	0	0	0	0	0	0	0
Ba	83	231	505	85	512	566	438	704	450
Sr	233	233	112	159	330	447	95	276	354
Tl	0	0	0	0	0	0	0	0	0
Ga	16	20	24	12	16	21	19	19	19
Li	0	0	0	0	0	0	0	0	0
Ta	0	0	0	0	0	0	0	0	0
Nb	8	13	21	9	7	15	7	23	16
Hf	0	0	0	0	0	0	0	0	0
Zr	117	380	465	186	122	279	235	723	349
Ti	1	1	1	2	1	2	1	1	1
Y	22	47	80	46	31	67	45	110	104
Th	10	8	11	0	9	0	6	1	0
U	3	0	0	0	0	10	0	20	9
La	15.00	45.00	63.00	18.00	15.00	43.00	29.00	73.00	62.00
Ce	41.00	11.00	54.00	59.00	0.00	47.00	0.00	0.00	19.00
Pr	0.00	0.00	0.00	0.00	0.00	0.00	0.00	0.00	0.00
Nd	0.00	0.00	0.00	0.00	0.00	0.00	0.00	0.00	0.00
Sm	0.00	0.00	0.00	0.00	0.00	0.00	0.00	0.00	0.00
Eu	0.00	0.00	0.00	0.00	0.00	0.00	0.00	0.00	0.00
Gd	0.00	0.00	0.00	0.00	0.00	0.00	0.00	0.00	0.00
Tb	0.00	0.00	0.00	0.00	0.00	0.00	0.00	0.00	0.00
Dy	0.00	0.00	0.00	0.00	0.00	0.00	0.00	0.00	0.00
Ho	0.00	0.00	0.00	0.00	0.00	0.00	0.00	0.00	0.00
Er	0.00	0.00	0.00	0.00	0.00	0.00	0.00	0.00	0.00
Tm	0.00	0.00	0.00	0.00	0.00	0.00	0.00	0.00	0.00
Yb	0.00	0.00	0.00	0.00	0.00	0.00	0.00	0.00	0.00
Lu	0.00	0.00	0.00	0.00	0.00	0.00	0.00	0.00	0.00
Be	0.00	0.00	0.00	0.00	0.00	0.00	0.00	0.00	0.00

Sample Name	C41051	C4086	C4-105	3-637C	3-6-44	3-6-65	DS-10A	DS-10C	3-6-98
Mg Number	52	53	52	54	45	32	35	15	38
SiO2	62.20	58.30	62.20	65.20	56.00	58.10	65.70	60.70	61.00
TiO2	0.48	0.86	0.48	0.64	1.64	1.92	1.16	0.88	1.00
Al2O3	14.80	16.60	14.80	14.10	15.10	13.30	12.80	13.70	15.30
Fe2O3	0.73	1.02	0.73	0.66	1.44	1.68	0.92	1.46	1.12
FeO	3.70	5.20	3.70	3.39	7.34	8.58	4.69	7.44	5.73
MnO	0.10	0.11	0.10	0.09	0.15	0.22	0.20	0.28	0.08
MgO	2.61	3.94	2.61	2.64	3.93	2.66	1.69	0.85	2.30
CaO	4.58	3.98	4.58	3.68	6.84	5.26	3.26	3.38	5.96
Na2O	3.01	3.88	3.01	4.34	3.86	4.24	3.88	5.98	4.19
K2O	3.31	1.31	3.31	1.25	1.71	2.26	1.34	1.20	0.44
P2O5	0.15	0.27	0.15	0.13	0.40	1.11	0.51	0.31	0.28
LOI	3.03	3.38	3.03	2.56	1.10	0.08	2.12	2.30	2.35
Cr	33	114	33	7	0	0	0	0	36
III	6	27	6	3	4	0	0	0	81
Sc	0	0	0	0	24	26	16	33	0
V	135	141	135	92	220	106	24	0	149
Cu	18	15	18	4	20	7	1	0	2
Pb	11	4	11	6	8	10	12	8	57
Zn	33	91	33	52	63	97	114	131	80
Bi	0	0	0	0	0	0	0	0	0
W	0	0	0	0	111	291	96	89	0
Mo	0	0	0	0	2	3	1	2	0
K	0	0	0	0	14194	18760	11123	9961	0
Rb	122	25	122	29	39	56	60	38	12
Cs	0	0	0	0	0	1	1	1	0
Ba	1263	301	1263	487	478	685	903	673	175
Sr	231	592	231	250	414	289	287	310	600
Tl	0	0	0	0	0	0	0	0	0
Ga	11	23	11	15	18	21	16	14	18
Li	0	0	0	0	12	5	30	13	0
Ta	0	0	0	0	1	2	1	1	0
Nb	8	10	8	10	13	19	16	19	10
Hf	0	0	0	0	6	53891	7	14	0
Zr	73	148	73	171	236	205	257	691	297
Ti	1	1	1	1	9831	11510	6954	5275	1
Y	21	28	21	35	34	64	42	68	31
Th	28	4	28	0	5	7	4	6	0
U	18	1	18	0	1	2	2	2	0
La	35.00	13.00	35.00	12.00	26.98	39.56	40.90	39.67	0.00
Ce	64.00	82.00	64.00	28.00	58.90	91.50	85.42	91.10	81.00
Pr	0.00	0.00	0.00	0.00	7.35	12.07	11.45	11.64	0.00
Nd	0.00	0.00	0.00	0.00	29.55	53.47	47.11	48.65	0.00
Sm	0.00	0.00	0.00	0.00	6.54	12.65	10.43	11.47	0.00
Eu	0.00	0.00	0.00	0.00	1.75	4.05	2.90	3.65	0.00
Gd	0.00	0.00	0.00	0.00	6.04	12.80	9.19	10.34	0.00
Tb	0.00	0.00	0.00	0.00	1.02	2.11	1.51	1.85	0.00
Dy	0.00	0.00	0.00	0.00	5.89	12.79	8.68	11.62	0.00
Ho	0.00	0.00	0.00	0.00	1.22	2.53	1.63	2.40	0.00
Er	0.00	0.00	0.00	0.00	3.54	7.20	4.41	7.05	0.00
Tm	0.00	0.00	0.00	0.00	0.50	1.00	0.58	1.05	0.00
Yb	0.00	0.00	0.00	0.00	3.21	6.41	3.60	6.93	0.00
Lu	0.00	0.00	0.00	0.00	0.50	0.97	0.49	1.10	0.00
Be	0.00	0.00	0.00	0.60	2.12	2.35	2.34	3.08	0.00

[illegible]

Sample Name	C4-169A	C4-169C	C4-253B	C4-211	HS-116	C4-288	C4-219	C4-255B	C4285
Hg Number	28	38	17	24	47	48	37	33	44
SiO2	71.80	71.50	68.40	70.10	68.70	72.00	71.60	70.40	71.10
TiO2	0.25	0.20	0.44	0.22	0.53	0.28	0.24	0.36	0.28
Al2O3	12.40	12.10	14.30	13.30	14.50	13.40	12.50	14.10	13.60
Fe2O3	0.38	0.29	0.61	0.50	0.43	0.32	0.28	0.71	0.37
FeO	1.95	1.50	3.10	2.52	2.20	1.64	1.45	3.62	1.87
MnO	0.12	0.09	0.04	0.08	0.02	0.08	0.09	0.07	0.06
HgO	0.49	0.60	0.43	0.53	1.28	0.98	0.56	1.19	0.97
CaO	2.06	3.16	2.36	1.06	0.22	0.84	2.32	0.22	1.84
Na2O	2.75	2.31	3.78	4.71	4.06	2.88	3.90	4.10	3.26
K2O	2.51	2.74	2.35	1.95	3.68	3.50	2.33	1.51	2.13
P2O5	0.05	0.05	0.13	0.05	0.05	0.04	0.00	0.07	0.02
LOI	3.82	4.47	3.33	2.26	2.68	2.52	3.39	2.82	4.01
Cr	5	5	6	3	15	64	75	37	71
Ni	1	1	0	0	1	0	0	0	1
Sc	9	0	0	11	0	0	0	0	0
V	6	18	15	0	71	25	15	95	57
Cu	7	9	5	4	0	6	6	6	18
Pb	8	10	10	14	28	20	8	16	27
Zn	58	32	45	64	48	42	38	55	37
Bi	0	0	0	0	0	0	0	0	0
W	94	0	0	166	0	0	0	0	0
Mo	1	0	0	2	0	0	0	0	0
K	20835	0	0	16186	0	0	0	0	0
Rb	70	76	48	55	125	96	49	34	49
Cs	2	0	0	3	0	0	0	0	0
Ba	571	289	425	480	583	765	631	109	602
Sr	87	71	211	294	157	287	135	110	309
Tl	0	0	0	0	0	0	0	0	0
Ge	14	16	16	14	18	18	4	23	193
Li	13	0	0	10	0	0	0	0	0
Ta	1	0	0	2	0	0	0	0	0
Nb	10	14	9	6	11	11	10	7	9
Hf	7	0	0	5	0	0	0	0	0
Zr	269	286	161	185	228	141	247	160	115
Ti	1498	0	1	1318	1	0	0	1	0
Y	34	66	49	30	30	32	43	27	23
Th	9	21	13	7	28	10	8	7	12
U	3	12	7	2	15	2	0	3	0
La	34.81	48.00	42.00	17.77	52.00	89.00	54.00	0.00	0.00
Ce	74.55	74.00	51.00	40.62	44.00	53.00	23.00	0.00	61.00
Pr	8.86	0.00	0.00	4.99	0.00	0.00	0.00	0.00	0.00
Nd	33.51	0.00	0.00	20.23	0.00	0.00	0.00	0.00	0.00
Sm	6.87	0.00	0.00	4.94	0.00	0.00	0.00	0.00	0.00
Eu	1.19	0.00	0.00	1.14	0.00	0.00	0.00	0.00	0.00
Gd	5.85	0.00	0.00	4.56	0.00	0.00	0.00	0.00	0.00
Tb	1.01	0.00	0.00	0.83	0.00	0.00	0.00	0.00	0.00
Dy	6.23	0.00	0.00	5.20	0.00	0.00	0.00	0.00	0.00
Ho	1.33	0.00	0.00	1.10	0.00	0.00	0.00	0.00	0.00
Er	4.08	0.00	0.00	3.45	0.00	0.00	0.00	0.00	0.00
Tm	0.62	0.00	0.00	0.53	0.00	0.00	0.00	0.00	0.00
Yb	4.15	0.00	0.00	3.59	0.00	0.00	0.00	0.00	0.00
Lu	0.65	0.00	0.00	0.56	0.00	0.00	0.00	0.00	0.00
Be	1.25	0.00	0.00	1.63	0.00	0.00	0.00	0.00	0.00

Sample Name	C4222C	DM571	DM621	EL325B	HS84	HS968	HS119	HS121	HS123
Hg Number	28	35	36	13	19	39	29	19	20
SiO2	70.70	72.20	72.20	72.80	73.30	68.10	71.80	69.50	68.60
TiO2	0.44	0.16	0.16	0.14	0.22	0.28	0.54	0.42	0.48
Al2O3	13.80	13.60	13.70	12.70	12.80	14.00	11.70	15.40	15.30
Fe2O3	0.44	0.29	0.26	0.36	0.34	0.47	0.57	0.60	0.65
FeO	2.25	1.47	1.31	1.82	1.71	2.42	2.91	3.04	3.30
MnO	0.05	0.04	0.06	0.25	0.05	0.04	0.06	0.05	0.08
MgO	0.57	0.52	0.49	0.18	0.27	1.02	0.77	0.47	0.53
CaO	2.00	1.16	1.52	1.32	1.04	2.78	2.22	0.66	1.32
Na2O	1.85	3.78	3.62	7.36	4.90	3.99	2.34	4.93	5.48
K2O	2.69	4.28	4.60	0.18	2.35	2.57	1.47	2.17	2.45
P2O5	0.06	0.06	0.06	0.03	0.03	0.11	0.13	0.10	0.12
LOI	5.01	0.88	0.61	1.67	1.80	3.76	5.31	2.42	1.77
Cr	58	74	86	104	84	0	77	28	48
Ni	10	0	0	0	0	0	0	0	0
Sc	9	0	0	0	0	0	0	0	0
V	90	25	25	5	29	48	49	13	10
Cu	7	6	6	8	5	3	17	5	5
Pb	15	23	17	39	11	16	16	26	19
Zn	61	14	10	57	40	12	39	61	61
Bi	0	0	0	0	0	0	0	0	0
W	7	0	0	0	0	0	0	0	0
Mo	1	0	0	0	0	0	0	0	0
K	22329	0	0	0	0	0	0	0	0
Rb	64	182	216	0	48	81	28	51	54
Cs	6	0	0	0	0	0	0	0	0
Ba	299	750	861	173	554	464	144	231	837
Sr	322	127	155	189	79	139	100	233	265
Tl	0	0	0	0	0	0	0	0	0
Ga	14	13	12	17	15	16	14	20	19
Li	14	0	0	0	0	0	0	0	0
Ta	1	0	0	0	0	0	0	0	0
Nb	10	9	8	26	11	8	9	13	13
Hf	7	0	0	0	0	0	0	0	0
Zr	232	102	146	533	268	196	192	380	387
Ti	2637	0	0	0	0	1	1	1	0
Y	33	17	17	99	58	37	38	47	59
Th	8	21	18	16	4	10	4	8	5
U	2	0	0	0	0	0	0	0	1
La	28.91	32.00	56.00	104.00	75.00	28.00	23.00	45.00	34.00
Ce	63.16	56.00	51.00	103.00	34.00	27.00	25.00	11.00	14.00
Pr	7.38	0.00	0.00	0.00	0.00	0.00	0.00	0.00	0.00
Nd	27.79	0.00	0.00	0.00	0.00	0.00	0.00	0.00	0.00
Sm	5.91	0.00	0.00	0.00	0.00	0.00	0.00	0.00	0.00
Eu	1.25	0.00	0.00	0.00	0.00	0.00	0.00	0.00	0.00
Gd	5.68	0.00	0.00	0.00	0.00	0.00	0.00	0.00	0.00
Tb	1.01	0.00	0.00	0.00	0.00	0.00	0.00	0.00	0.00
Dy	6.34	0.00	0.00	0.00	0.00	0.00	0.00	0.00	0.00
Ho	1.31	0.00	0.00	0.00	0.00	0.00	0.00	0.00	0.00
Er	3.91	0.00	0.00	0.00	0.00	0.00	0.00	0.00	0.00
Tm	0.58	0.00	0.00	0.00	0.00	0.00	0.00	0.00	0.00
Yb	3.96	0.00	0.00	0.00	0.00	0.00	0.00	0.00	0.00
Lu	0.58	0.00	0.00	0.00	0.00	0.00	0.00	0.00	0.00
Be	1.77	0.00	0.00	0.00	0.00	0.00	0.00	0.00	0.00

Sample Name	C4018	C4097	C4186	C4204	C4207	HS41	3-6-61	3-6-6	3-6-12
Mg Number	32	28	26	17	21	33	4	45	34
SiO2	72.10	71.90	70.20	69.80	69.10	68.70	73.30	68.50	67.20
TiO2	0.28	0.33	0.52	0.49	0.20	0.54	0.40	0.28	0.48
Al2O3	14.10	13.60	13.20	15.00	14.00	14.60	12.30	14.20	13.90
Fe2O3	0.31	0.47	0.43	0.53	0.44	0.61	0.56	0.45	0.61
FeO	1.58	2.41	2.20	2.72	2.22	3.11	2.85	2.31	3.09
MnO	0.05	0.05	0.07	0.05	0.04	0.10	0.09	0.04	0.08
MgO	0.49	0.61	0.52	0.38	0.39	0.99	0.08	1.27	1.04
CaO	1.40	0.88	2.22	1.16	1.64	1.60	0.54	2.30	2.30
Na2O	4.16	5.28	3.50	5.05	5.35	5.43	4.68	4.10	4.79
K2O	2.50	2.51	2.14	2.02	2.24	2.24	4.66	2.97	2.22
P2O5	0.09	0.06	0.08	0.10	0.03	0.10	0.03	0.09	0.13
LOI	1.64	1.55	3.94	2.48	2.59	1.38	0.34	2.95	2.48
Cr	95	160	44	77	69	136	0	0	4
Ni	0	0	0	0	0	2	0	0	0
Sc	0	8	0	0	0	0	0	0	12
V	26	23	17	31	18	12	3	39	24
Cu	8	7	8	7	3	0	1	2	0
Pb	26	13	12	11	29	11	2	11	14
Zn	41	58	63	40	39	52	65	14	84
Bi	0	0	0	0	0	0	0	0	0
W	0	8	0	0	0	0	0	0	135
Mo	0	2	0	0	0	0	0	0	1
K	0	20835	0	0	0	0	0	0	18428
Rb	54	57	45	59	51	50	68	83	53
Cs	0	1	0	0	0	0	0	0	1
Ba	649	570	179	124	393	452	178	510	461
Sr	377	142	98	113	77	224	21	147	186
Tl	0	0	0	0	0	0	0	0	0
Ga	18	18	24	17	15	17	25	17	17
Li	0	7	0	0	0	0	0	0	16
Ta	0	1	0	0	0	0	0	0	1
Nb	10	10	12	13	13	12	24	9	13
Hf	0	7	0	0	0	0	0	0	6
Zr	138	239	359	297	290	300	384	196	185
Ti	0	1978	1	1	0	1	0	1	2877
Y	30	35	58	49	59	72	50	41	38
Th	14	9	1	9	18	0	0	1	7
U	0	3	0	0	2	14	1	8	2
La	58.00	27.27	71.00	47.00	18.00	44.00	72.00	15.00	26.28
Ce	56.00	59.28	54.00	74.00	70.00	24.00	102.00	102.00	58.24
Pr	0.00	7.22	0.00	0.00	0.00	0.00	0.00	0.00	7.40
Nd	0.00	28.10	0.00	0.00	0.00	0.00	0.00	0.00	29.66
Sm	0.00	5.97	0.00	0.00	0.00	0.00	0.00	0.00	6.93
Eu	0.00	1.15	0.00	0.00	0.00	0.00	0.00	0.00	1.62
Gd	0.00	5.59	0.00	3.00	0.00	0.00	0.00	0.00	6.56
Tb	0.00	1.04	0.00	0.00	0.00	0.00	0.00	0.00	1.19
Dy	0.00	6.43	0.00	0.00	0.00	0.00	0.00	0.00	7.82
Ho	0.00	1.37	0.00	0.00	0.00	0.00	0.00	0.00	1.62
Er	0.00	4.25	0.00	0.00	0.00	0.00	0.00	0.00	4.78
Tm	0.00	0.61	0.00	0.00	0.00	0.00	0.00	0.00	0.69
Yb	0.00	3.97	0.00	0.00	0.00	0.00	0.00	0.00	4.75
Lu	0.00	0.62	0.00	0.00	0.00	0.00	0.00	0.00	0.74
Be	0.00	1.56	0.00	0.00	0.00	0.00	0.00	0.00	1.76

Sample Name	3-6-31	C4-281	C4-50	C4-181	HS-67A	DS-84-41	C4-239	C4-246A	C4-296
Hg Number	31	18	10	28	0	56	34	14	3
SiO2	67.00	77.90	76.60	76.50	75.50	79.20	76.60	76.50	76.20
TiO2	0.76	0.20	0.13	0.15	0.00	0.38	0.07	0.13	0.28
Al2O3	14.70	9.74	11.50	11.60	11.00	7.35	11.70	11.50	11.20
Fe2O3	0.61	0.34	0.34	0.29	0.00	0.58	0.19	0.33	0.55
FeO	3.10	1.72	1.72	1.48	0.00	2.94	0.99	1.70	2.79
MnO	0.06	0.05	0.02	0.02	0.03	0.05	0.02	0.04	0.04
MgO	0.90	0.25	0.12	0.38	0.08	2.48	0.34	0.19	0.06
CaO	2.42	0.44	0.04	0.24	0.24	1.10	0.22	0.02	0.08
Na2O	5.33	3.50	3.81	2.63	3.32	0.56	3.12	3.28	3.87
K2O	1.96	2.66	3.40	4.57	5.28	1.32	4.80	4.98	3.83
P2O5	0.17	0.00	0.00	0.02	0.02	0.12	0.00	0.00	0.00
LOI	1.60	1.08	0.93	1.39	0.47	3.11	1.10	0.68	0.52
Cr	0	2	1	0	1	64	136	97	189
Ni	0	7	5	3	9	37	13	3	0
Sc	0	1	0	0	0	0	0	0	0
V	38	0	0	9	0	78	4	2	11
Cu	1	0	4	0	7	10	8	6	7
Pb	4	11	9	18	27	12	39	34	25
Zn	20	72	89	71	104	30	55	87	57
Bi	0	0	0	0	0	0	0	0	0
W	0	229	0	0	0	0	0	0	0
Mo	0	1	0	0	0	0	0	0	0
K	0	22080	0	0	0	0	0	0	0
Rb	65	70	65	108	142	52	203	128	81
Cs	0	1	0	0	0	0	0	0	0
Ba	517	460	503	848	707	380	15	694	725
Sr	248	50	9	119	30	88	24	23	35
Tl	0	0	0	0	0	0	0	0	0
Ga	13	19	20	20	19	11	25	26	22
Li	0	10	0	0	0	0	0	0	0
Ta	0	3	0	0	0	0	0	0	0
Nb	9	21	28	25	31	11	29	26	25
Hf	0	13	0	0	0	0	0	0	0
Zr	219	451	606	386	618	95	103	519	531
Ti	1	1199	0	0	0	0	0	0	0
Y	46	82	134	80	142	19	79	94	80
Th	3	14	27	24	23	27	22	18	18
U	0	4	14	8	29	12	8	5	8
La	9.00	47.11	47.00	95.00	103.00	36.00	16.00	24.00	67.00
Ce	71.00	121.58	92.00	153.00	134.00	5.00	89.00	116.00	78.00
Pr	0.00	20.74	0.00	0.00	0.00	0.00	0.00	0.00	0.00
Nd	0.00	89.85	0.00	0.00	0.00	0.00	0.00	0.00	0.00
Sm	0.00	18.57	0.00	0.00	0.00	0.00	0.00	0.00	0.00
Eu	0.00	2.67	0.00	0.00	0.00	0.00	0.00	0.00	0.00
Gd	0.00	15.65	0.00	0.00	0.00	0.00	0.00	0.00	0.00
Tb	0.00	2.46	0.00	0.00	0.00	0.00	0.00	0.00	0.00
Dy	0.00	14.96	0.00	0.00	0.00	0.00	0.00	0.00	0.00
Ho	0.00	2.98	0.00	0.00	0.00	0.00	0.00	0.00	0.00
Er	0.00	9.02	0.00	0.00	0.00	0.00	0.00	0.00	0.00
Tm	0.00	1.30	0.00	0.00	0.00	0.00	0.00	0.00	0.00
Yb	0.00	8.51	0.00	0.00	0.00	0.00	0.00	0.00	0.00
Lu	0.00	1.34	0.00	0.00	0.00	0.00	0.00	0.00	0.00
Be	0.00	3.09	0.00	0.00	0.00	0.00	0.00	0.00	0.00

Sample Name	C4236A	C4241	C4297	C4301	C4305C	DM54	DM79	EL324	EL325A
Mg Number	7	32	3	2	31	23	10	1	22
SiO2	74.40	75.30	77.70	75.30	74.30	76.70	81.70	77.20	78.00
TiO2	0.36	0.07	0.20	0.26	0.10	0.14	0.18	0.20	0.20
Al2O3	12.70	11.80	11.60	11.20	11.50	12.10	9.02	11.60	11.20
Fe2O3	0.50	0.20	0.36	0.57	0.14	0.29	0.21	0.37	0.35
FeO	2.55	1.02	1.86	2.91	0.71	1.49	1.07	1.88	1.79
MnO	0.04	0.02	0.04	0.08	0.03	0.03	0.04	0.03	0.07
MgO	0.12	0.32	0.04	0.04	0.21	0.30	0.08	0.01	0.34
CaO	0.34	0.24	0.00	0.38	3.50	0.24	0.06	0.08	0.34
Na2O	5.73	3.08	4.06	4.76	3.53	3.46	1.11	5.54	2.59
K2O	1.47	5.29	4.31	3.00	1.89	4.91	5.88	2.44	2.38
P2O5	0.06	0.00	0.02	0.08	0.00	0.02	0.01	0.01	0.00
LOI	0.48	0.69	0.29	0.41	3.83	0.72	0.48	0.10	1.86
Cr	135	183	148	238	95	98	78	191	122
Ni	0	17	0	0	0	0	0	3	2
Sc	0	0	0	5	0	1	0	0	0
V	7	4	2	8	7	30	0	6	5
Cu	0	2	9	7	13	6	5	4	3
Pb	0	19	22	16	17	15	24	30	29
Zn	26	31	41	22	1	68	25	30	112
Bi	0	0	0	0	0	0	0	0	0
W	0	0	0	16	0	9	0	0	0
Mo	0	0	0	2	0	2	0	0	0
K	0	0	0	24903	0	40757	0	0	0
Rb	18	200	96	64	39	161	155	48	67
Ca	0	0	0	0	0	1	0	0	0
Ba	169	0	744	498	157	301	775	389	369
Sr	101	33	30	26	264	32	12	28	56
Tl	0	0	0	0	0	0	0	0	0
Ga	17	19	24	15	19	21	13	22	22
Li	0	0	0	1	0	2	0	0	0
Ta	0	0	0	9	0	2	0	0	0
Nb	10	28	26	15	7	23	21	26	28
Hf	0	0	0	11	0	11	0	0	0
Zr	264	112	606	401	104	290	501	590	608
Ti	1	0	0	1558	0	839	0	0	0
Y	62	83	106	49	30	58	68	100	108
Th	0	1	10	14	6	20	16	15	25
U	6	9	1	4	1	4	2	0	11
La	57.00	33.00	64.00	45.82	25.00	16.54	77.00	100.00	138.00
Ce	0.00	59.00	52.00	107.09	0.00	99.70	0.00	98.00	52.00
Pr	0.00	0.00	0.00	12.70	0.00	4.78	0.00	0.00	0.00
Nd	0.00	0.00	0.00	49.59	0.00	20.17	0.00	0.00	0.00
Sm	0.00	0.00	0.00	11.11	0.00	6.76	0.00	0.00	0.00
Eu	0.00	0.00	0.00	1.96	0.00	0.52	0.00	0.00	0.00
Gd	0.00	0.00	0.00	9.69	0.00	8.20	0.00	0.00	0.00
Tb	0.00	0.00	0.00	1.64	0.00	1.66	0.00	0.00	0.00
Dy	0.00	0.00	0.00	9.94	0.00	10.96	0.00	0.00	0.00
Ho	0.00	0.00	0.00	2.11	0.00	2.34	0.00	0.00	0.00
Er	0.00	0.00	0.00	6.30	0.00	7.21	0.00	0.00	0.00
Tm	0.00	0.00	0.00	0.96	0.00	1.10	0.00	0.00	0.00
Yb	0.00	0.00	0.00	6.33	0.00	7.18	0.00	0.00	0.00
Lu	0.00	0.00	0.00	0.94	0.00	1.12	0.00	0.00	0.00
Be	0.00	0.00	0.00	0.86	0.00	2.38	0.00	0.00	0.00

Sample Name	DS8401	3-637A	3-637B	3-6-63	3-6-58	3-6-8	3-6-33
Hg Number	40	30	38	2	13	18	32
SiO2	75.60	75.70	75.70	75.20	76.80	77.00	75.80
TiO2	0.40	0.28	0.24	0.32	0.00	0.08	0.28
Al2O3	12.20	12.20	12.20	11.20	12.90	13.30	12.60
Fe2O3	0.14	0.24	0.11	0.46	0.17	0.20	0.20
FeO	0.72	1.21	0.54	2.36	0.89	1.04	1.02
MnO	0.02	0.02	0.01	0.07	0.05	0.02	0.03
MgO	0.31	0.34	0.22	0.04	0.09	0.15	0.32
CaO	1.04	0.40	0.30	0.32	0.52	0.12	0.52
Na2O	5.78	3.65	3.52	4.34	4.91	2.22	4.00
K2O	0.51	4.16	3.92	4.94	2.96	2.50	3.82
P2O5	0.11	0.03	0.06	0.01	0.00	0.00	0.00
LOI	1.44	0.73	1.22	0.30	0.45	2.15	0.77
Cr	9	0	0	0	0	0	0
Ni	0	0	0	0	0	0	0
Sc	0	0	0	1	0	0	0
V	3	8	4	0	0	0	9
Cu	0	5	2	0	1	3	2
Pb	16	15	14	16	16	9	11
Zn	8	6	1	73	25	16	4
Bi	0	0	0	0	0	0	0
W	0	0	0	333	0	0	0
Mo	0	0	0	2	0	0	0
K	0	0	0	41006	0	0	0
Rb	0	118	118	86	85	74	108
Cs	0	0	0	1	0	0	0
Ba	64	739	798	104	713	671	754
Sr	140	71	85	7	53	51	92
Tl	0	0	0	0	0	0	0
Ge	12	11	14	27	17	18	14
Li	0	0	0	21	0	0	0
Ta	0	0	0	4	0	0	0
Nb	9	13	14	30	12	12	12
Hf	0	0	0	9	0	0	0
Zr	177	245	254	249	84	133	262
Ti	0	0	0	1918	0	0	0
Y	68	39	37	37	50	52	42
Th	21	11	13	15	6	7	14
U	5	1	0	4	0	0	7
La	44.00	44.00	24.00	23.51	9.00	28.00	37.00
Ce	42.00	95.00	74.00	53.81	124.00	108.00	157.00
Pr	0.00	0.00	0.00	6.63	0.00	0.00	0.00
Nd	0.00	0.00	0.00	24.78	0.00	0.00	0.00
Sm	0.00	0.00	0.00	5.18	0.00	0.00	0.00
Eu	0.00	0.00	0.00	0.76	0.00	0.00	0.00
Gd	0.00	0.00	0.00	4.61	0.00	0.00	0.00
Tb	0.00	0.00	0.00	0.94	0.00	0.00	0.00
Dy	0.00	0.00	0.00	6.61	0.00	0.00	0.00
Ho	0.00	0.00	0.00	1.51	0.00	0.00	0.00
Er	0.00	0.00	0.00	5.03	0.00	0.00	0.00
Tm	0.00	0.00	0.00	0.85	0.00	0.00	0.00
Yb	0.00	0.00	0.00	6.22	0.00	0.00	0.00
Lu	0.00	0.00	0.00	0.97	0.00	0.00	0.00
Be	0.00	0.00	0.00	3.86	0.00	0.00	0.00

APPENDIX E

LABORATORY PROCEDURES

FOR URANIUM/LEAD

ZIRCON DATING

APPENDIX E

Laboratory Procedures for Uranium/Lead (Zircon) Dating

The details of the methods used at the Jack Satterly Geochronology Laboratory of the Royal Ontario Museum for the selection and analysis of zircons for uranium/lead dating have been presented by Krogh (1982). This Appendix reviews the basic procedures and techniques for each of the five major steps: 1) sample selection and rock crushing; 2) mineral separation; 3) zircon picking and abrasion; 4) chemistry; 5) mass spectrometry.

E.1. Sample Selection and Rock Crushing

A representative suite of rock samples was collected specifically for the purpose of zircon age dating. Each sample weighed between 30 and 50 kilograms in an attempt to guarantee an abundant supply of zircons for analysis. Each sample was taken through a series of crushing procedures and reduced to a fine powder. The equipment and crushing room are completely cleaned with water and alcohol between every sample. A large filter vacuum is kept running in the room and individual vacuums are strategically placed around each piece of equipment during each phase of crushing.

The sequence of procedures is as follows:

- (1) Smash the sample with a sledge hammer on a metal plate until the entire sample consists of pieces a few centimetres across.
- (2) Pass the pieces produced individually through a jaw-crusher which produces "coarse sandy-gravel", this step is often repeated due to variation in the hardness of the rocks.
- (3) The sample is then passed through a disc mill which reduces it to a very fine powder, this step may also be repeated due to variation of hardness and how "wet" (i.e. hydrated or altered) the rock might be.

The final step in the crushing room is actually the first phase of mineral separation wherein the sample is passed across a Wilfley Table. This table can be inclined to differing degrees while water is passed across the entire surface. The sample is mounted near the "top corner" of the table and gently vibrated through a funnel and "fed-out" across the table. The table rocks back and forth thus producing two streaks of heavy minerals by gravity separation and settling, whereas the very light and fine minerals wash off the table with the sheeting water. This process produces a heavy mineral concentrate from the whole rock.

E.2. Mineral Separation Techniques

Two different types of mineral separation are necessary, magnetic separations and heavy liquid separations. The laboratory space is cleaned with alcohol and large sheets of clean paper are spread out on all counters and equipment. Sanitized containers are assembled and labeled for each sample. As in the cleaning procedure for the crushing room, the mineral separation laboratory and its equipment are disassembled and thoroughly cleaned between each sample. For each sample a primary sieving procedure produces two size fractions of +70 mesh and -70 mesh by passing the sample through a 70 mesh screen. The fine fraction (-70) is then used in the following separation steps, and a small glass vial of the +70 fraction is retained for reference or processing.

Magnetic Separation

The first step in the magnetic separation is to use the Frantz Isodynamic Separator rotated to a vertical position. The sample is mounted and allowed to free-fall at 0.5, 1.0, and 1.8 amps, thus eliminating the majority of hematite, magnetite and any silicate minerals with magnetic inclusions or coatings. At this stage it may be appropriate to run some samples through a Waller Solution which removes oxidation products in heavily oxidized rocks. The Waller Solution can be made up easily by combining 71 grams of sodium citrate with 8.5 grams of bicarbonate in 1 litre of

water as a stock solution. Add 1/2 teaspoon of the stock solution to 1 gram of sodium dithionate in 50 mls of water, and put sample in a beaker with the solutions; ultrasound then decant; ultrasound the sample in water twice (decant each time), then ultrasound the sample in alcohol; this should remove all oxidation products. At this stage the sample is put through a heavy liquid separation, described in the following section.

Upon completion of the first heavy liquid separation, the sample goes through a series of magnetic separations on the Frantz. The machine is balanced in a horizontal position then rotated back 10 degrees for the "initial Frantz". Successive runs are continued while increasing the amps from .25 A to full field by passing the non-magnetic split each time. Various magnetic minerals are removed at each stage of this separation and it is useful to keep the magnetic fractions from each run if other mineral separation might be considered. The "initial Frantzing" produces a "non-magnetic" heavy mineral separate. A second stage of heavy liquid separation takes place here.

The non-magnetic mineral separate is then passed through the Frantz which is rotated toward horizontal at settings of 5, 3, 2, 1 and 0 degrees all at full-field. At each stage a smaller fraction of "non-magnetic" minerals is produced until finally an almost pure population of zircons

results. It should be pointed out that not every sample will continue to split all the way down to 0 degrees, either because of a small population size or inclusions in and coatings on the zircons.

Heavy Liquid Separation

The first heavy liquid separation takes place after the freefall in most cases. Bromoform is used, with a density of 2.85. Clean air hoods are set up in the mineral separation laboratory, each chamber holding three heavy liquid stations. Each area is carefully cleaned and fresh paper covers the entire work space. From the top of each separatory apparatus the unit is as follows; funnel with filter to load bromoform into a separatory flask with a stopcock apparatus at its base; below this is another funnel through which the separated sample is released and washed down with alcohol into a beaker at the base. At this stage it may be necessary to use K-amylxanthate on the heavy separate to float pyrite out of the sample if it was present in the rock.

The second stage of heavy liquid mineral separation takes place after the initial Frantz. This procedure uses methylene-iodide (CH_2I_2) and the same apparatus as the first, although acetone is used for rinsing the sample through the funnels, not alcohol. At this stage a roughly 50/50 split of heavy and light minerals results. The heavy separate is then passed through the final Frantz stages

described above. The specific order of these steps can be altered depending on the rock sample and it's mineralogy.

E.3. Final Zircon Sample Selection

Upon completion of the steps outlined above a final selection of sub-milligram fractions are hand-picked in ethyl alcohol under a binocular microscope using care to select grains devoid of inclusions, foreign minerals and imperfections. The zircon fractions are polished in an air abrader (Krogh 1982) and cleaned in distilled water, hot 6N nitric acid and distilled acetone prior to dissolution (Krogh 1973).

E.4. Small Column Chemistry

The following steps are taken for zircon chemistry:

1. Wash resin in miniturized columns ie. four times with 3 X H₂O, three times in X1 6.2N HCl.
2. Condition the columns; 3.1N HCl, 0.15 ml., i.e. 16 drops
3. Convert sample with 3.1N HCl overnight, dry sample down on hot-plate to one tiny drop, not completely, add 10 drops of 3.1N HCl just before loading.
4. Load sample; 3.1N HCl, 0.10 ml ie. 10 or 16 drops (dep. on standards) Zr-Wash, 3.1N (2 or 3 drops) three times, then (10 or 16 drops) once for a total of 0.15ml.

5. Take the Pb off in 6.2N HCl 0.20 ml i.e. 15 or 21 drops (dependant on standard).
6. Take the U off in X 3 H²O 0.20 ml i.e. 16 or 19 drops (dependant on standard).

E.5. Mass Spectrometry

The zircon fractions are spiked using a mixture of ²⁰⁵Pb-²³⁵U isotopic tracer solution (Krogh and Davis 1975) and loaded into 0.5 ml, Krogh-type Teflon bombs. Extraction of U and Pb was explained by Krogh (1973), although mineraturized exchange columns are now employed which are scaled-down to one-tenth the originally published resin and reagent volumes. Average dissolution blanks for Pb and U measured in this study were 10 and 3 pg, respectively.

The lead and uranium were loaded onto outgassed, single Re filaments using silica gel and phosphoric acid (Cameron et al. 1969), and isotopic ratios were measured on a VG354 mass spectrometer. Lead and uranium isotopes were measured in single-collector mode and all ratios except ²⁰⁵Pb/²⁰⁴Pb, were measured on the axial Faraday collector. All Pb and U isotopic data were corrected for mass fractionation by a factor of +0.1%/AMU (+/-0.05%) determined from replicate analyses of NBS-SRM 981 common Pb and NBS-SRM U 500 standards. For ²⁰⁵Pb/²⁰⁴Pb ratios measured with a Daly photomultiplier detector, a

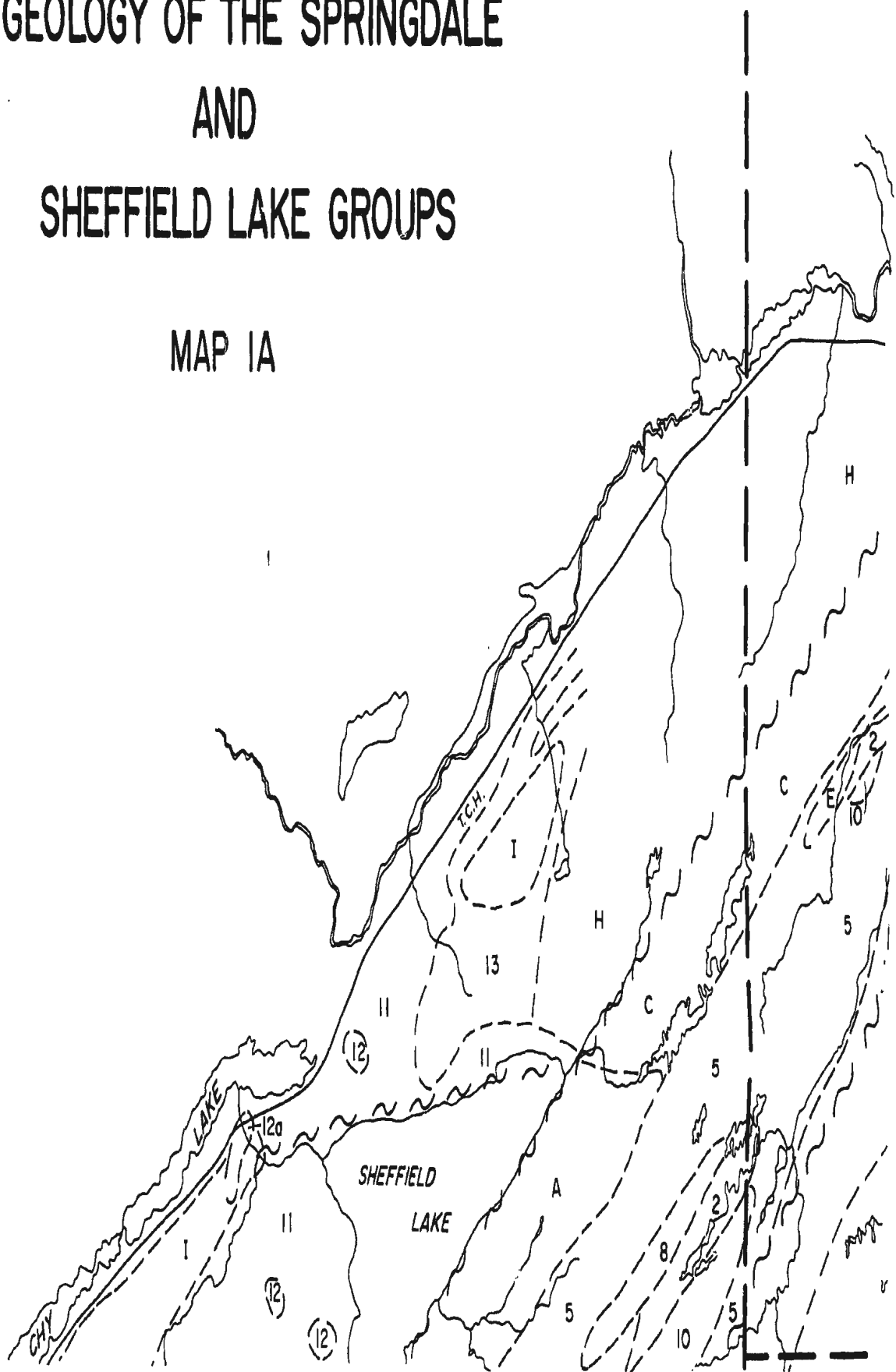
Daly-Faraday empirical correction factor of +0.35%/AMU was applied.

Analytical results are presented in Table 5.1 and Figures 5.1 to 5.5. Uncertainties in the Pb/U and $^{207}\text{Pb}/^{206}\text{Pb}$ ratios were calculated using a modified version of the error propagation program of Ludwig (1980); these errors are shown graphically in Figures 5.1-5.5. Common lead corrections were made by first correcting the measured ratios for instrumental fractionation and introduced spike, then subtracting lead equal in amount and composition to the dissolution blank; any remaining ^{204}Pb was assumed to represent ca.430 Ma model Pb with a composition given by Stacey and Kramers (1975). In all cases, the uncertainty in the amount and composition of common lead calculated in this manner represents an insignificant contribution to the error in the age calculation. Linear regression was carried out as outlined by Davis (1982) and errors on the calculated ages are quoted at the 95% confidence level for errors of 2-sigma. The decay constants and isotopic abundance ratios in all age calculations are those recommended by IUGS Subcommittee on Geochronology (Steiger and Jager 1977).

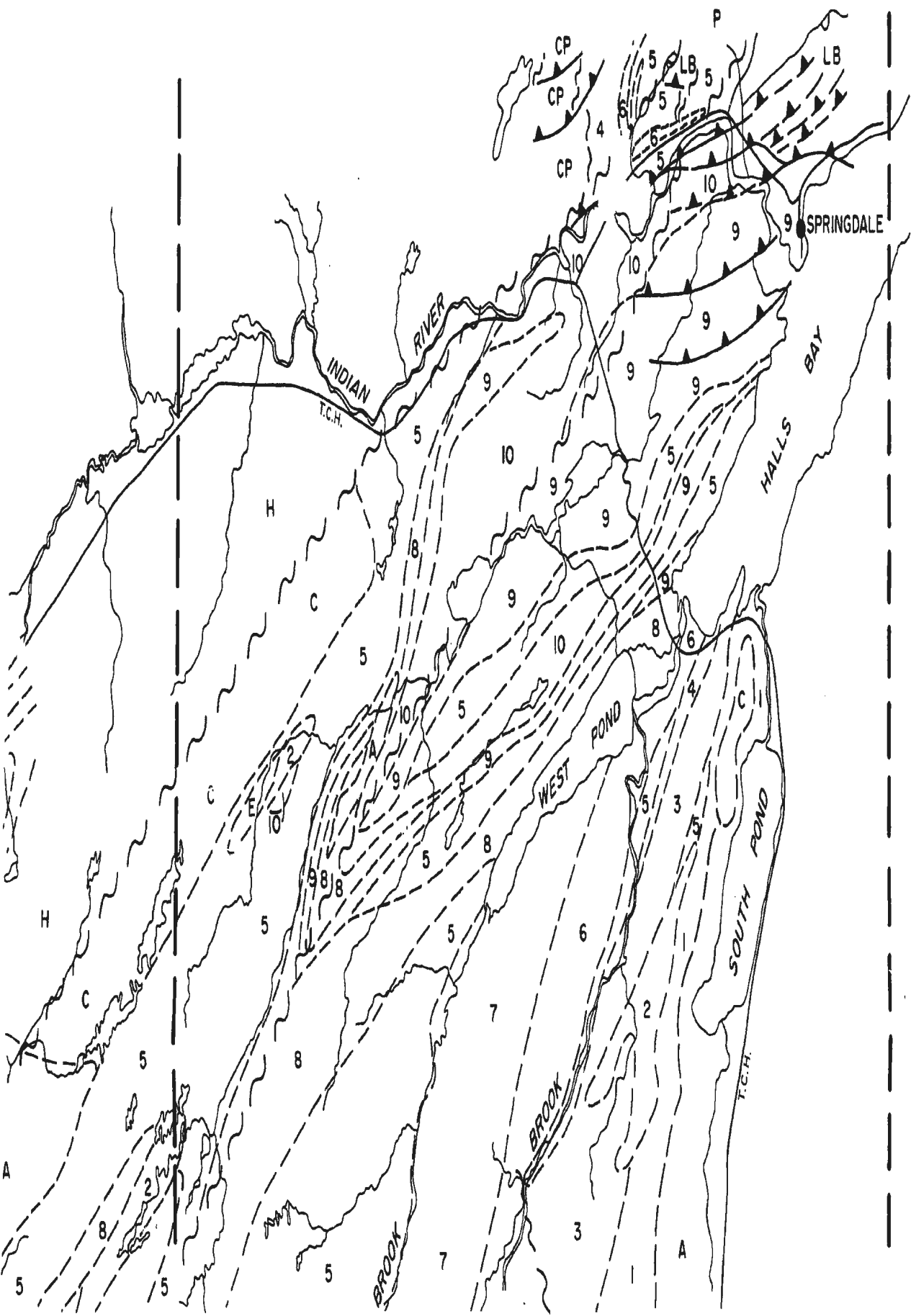
56°56'15"
49°32'

GEOLOGY OF THE SPRINGDALE AND SHEFFIELD LAKE GROUPS

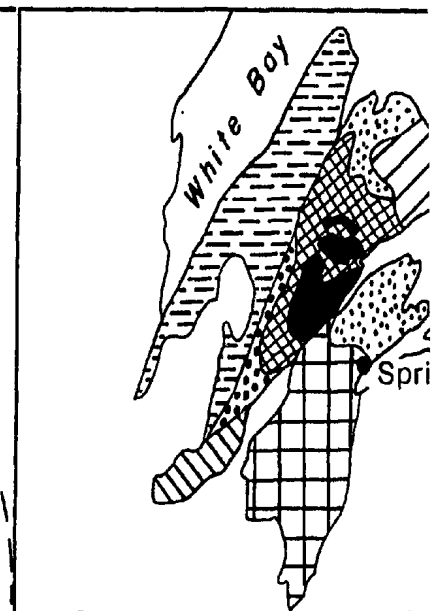
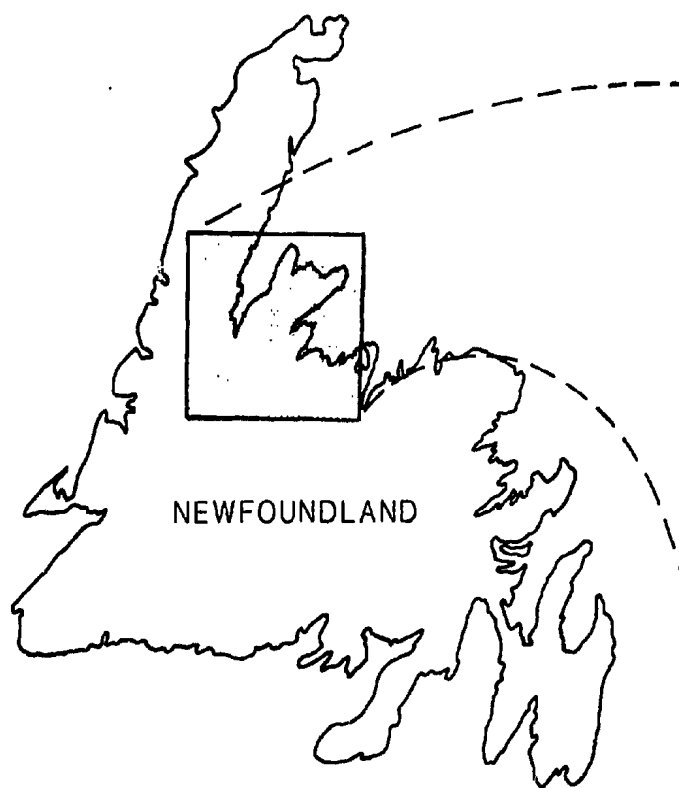
MAP 1A









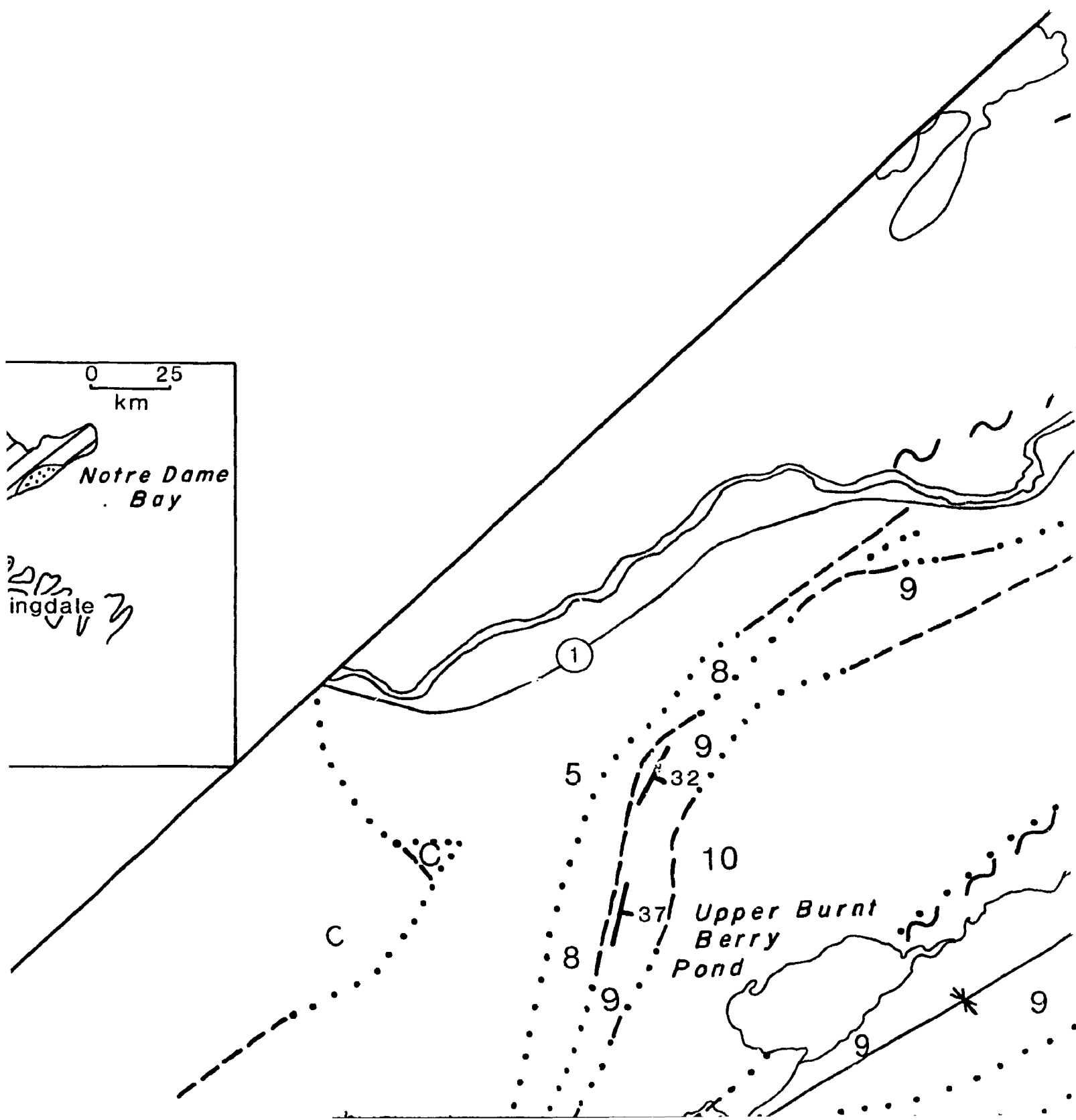
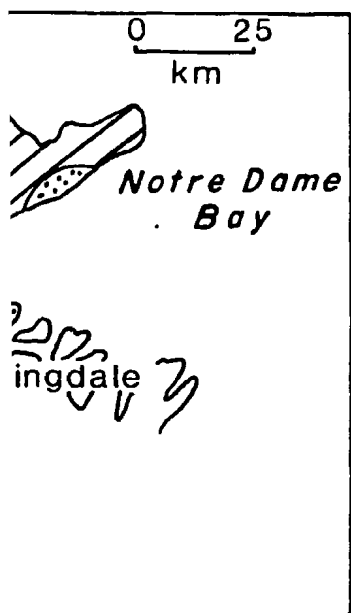
56°00'W
49°32'



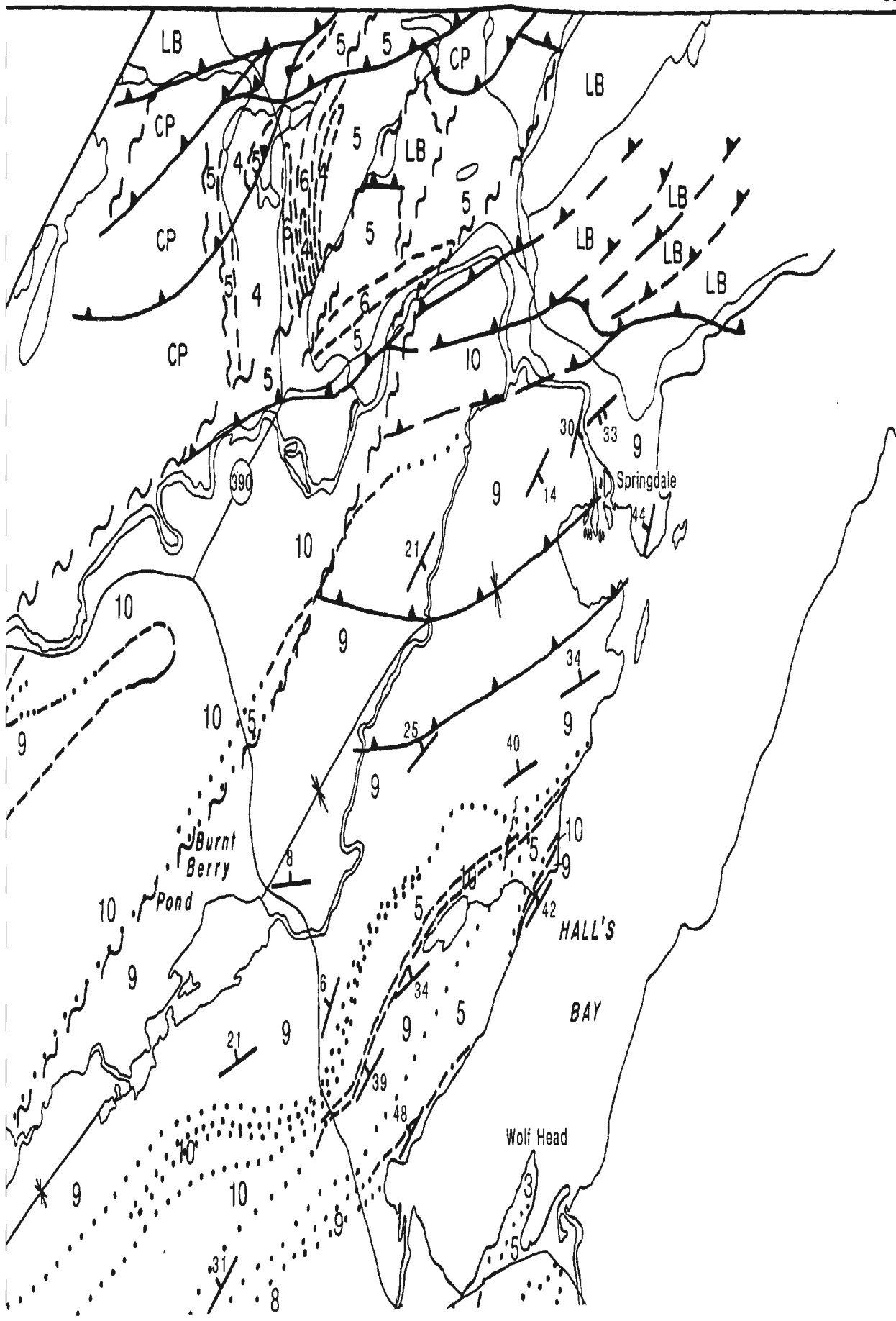
56° 30'
49° 32'

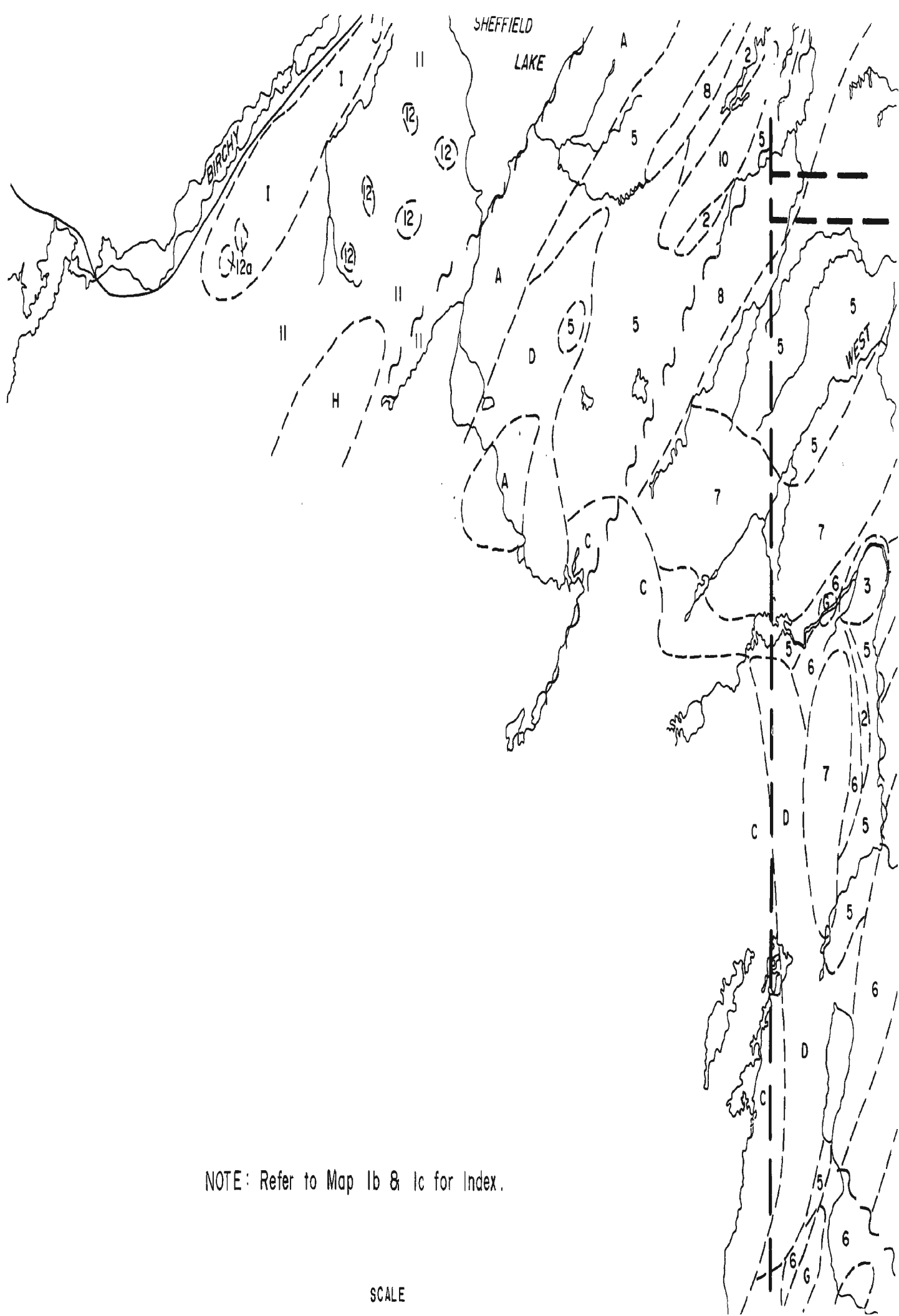


-  KING'S POINT COMPLEX
-  SHEFFIELD LAKE GROUP
-  MICMAC LAKE GROUP
-  HALL'S BAY GROUP
-  CAPE ST. JOHN GROUP
- 

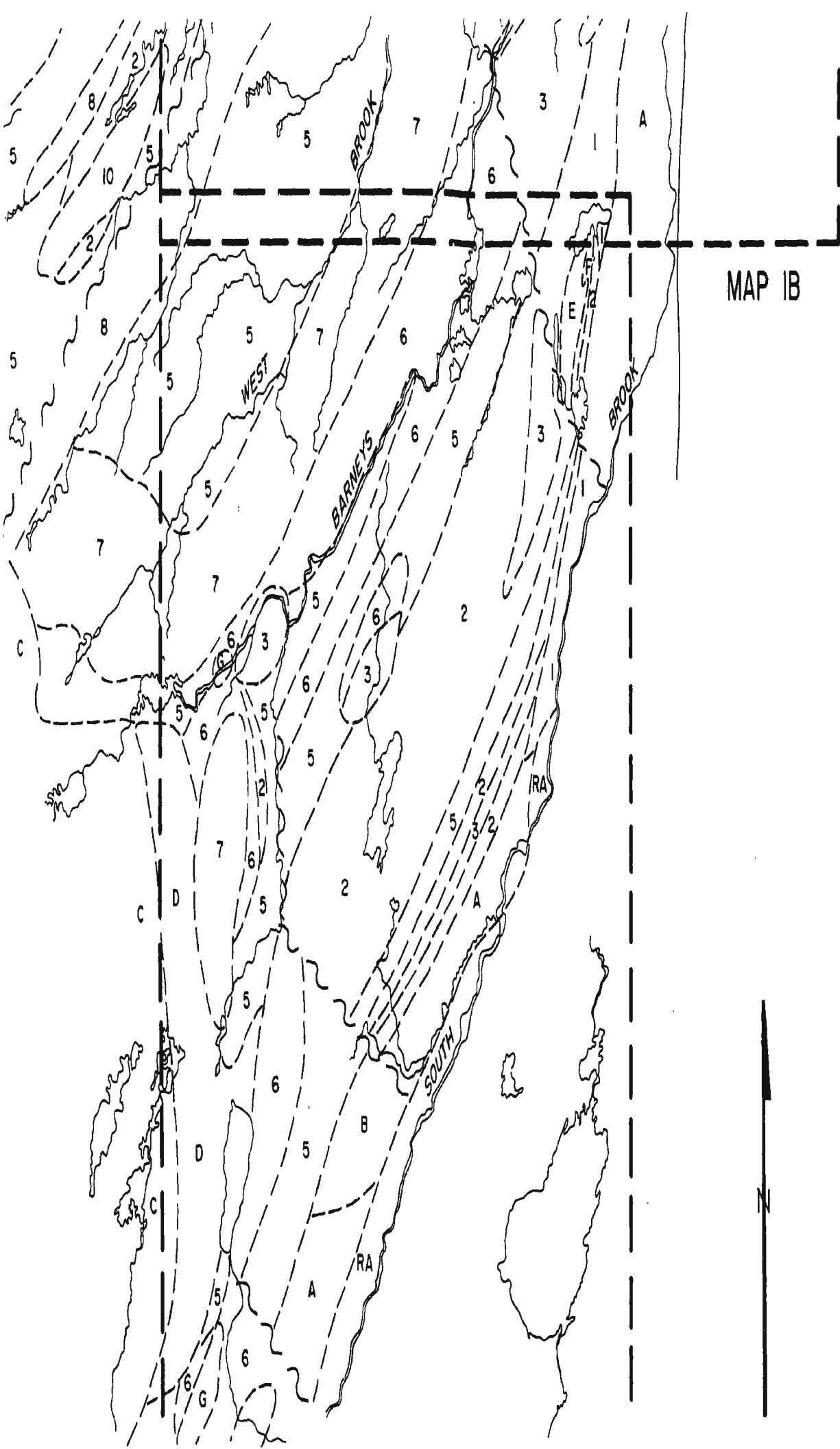


56°00'W
49°32'N







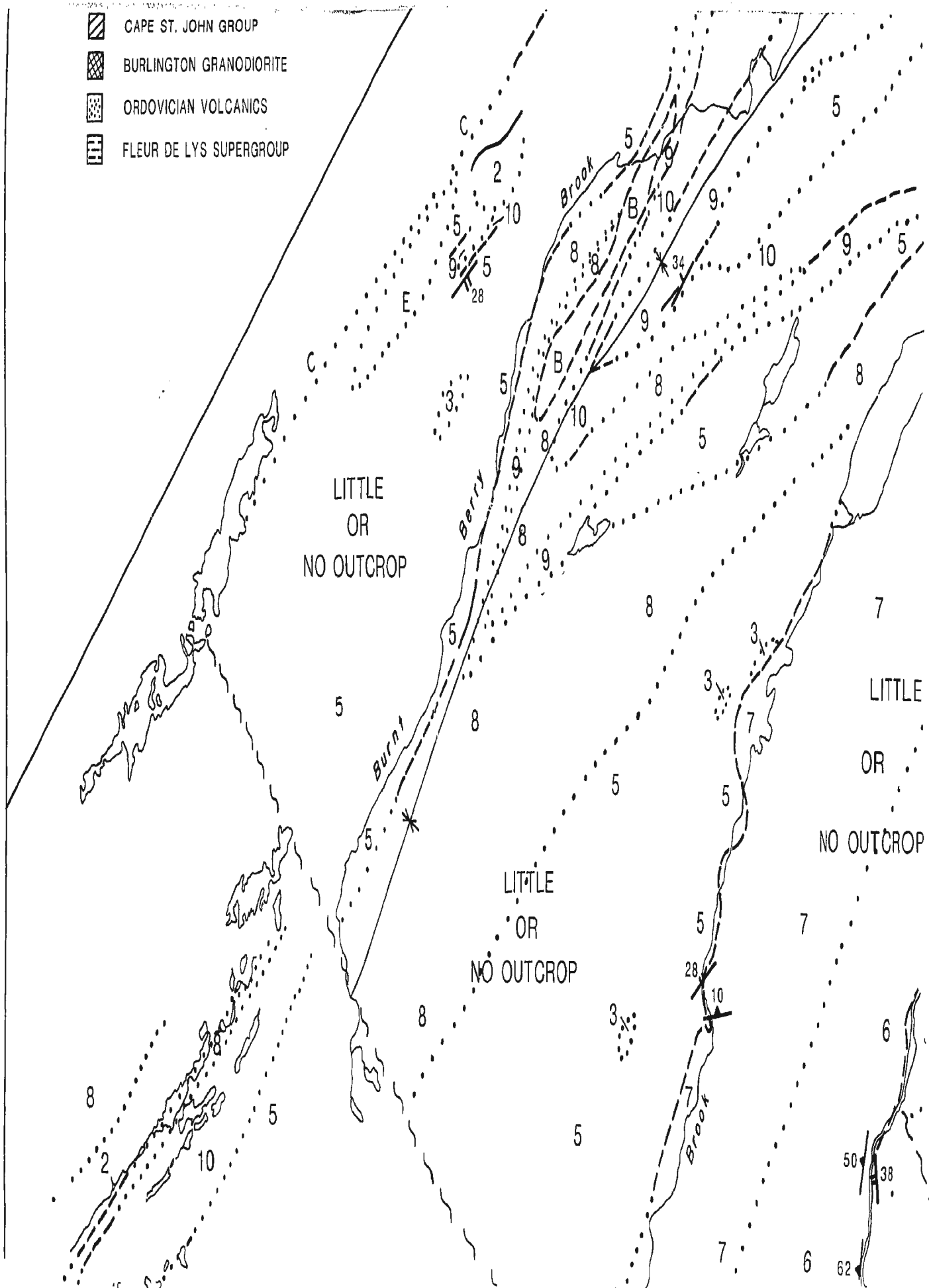


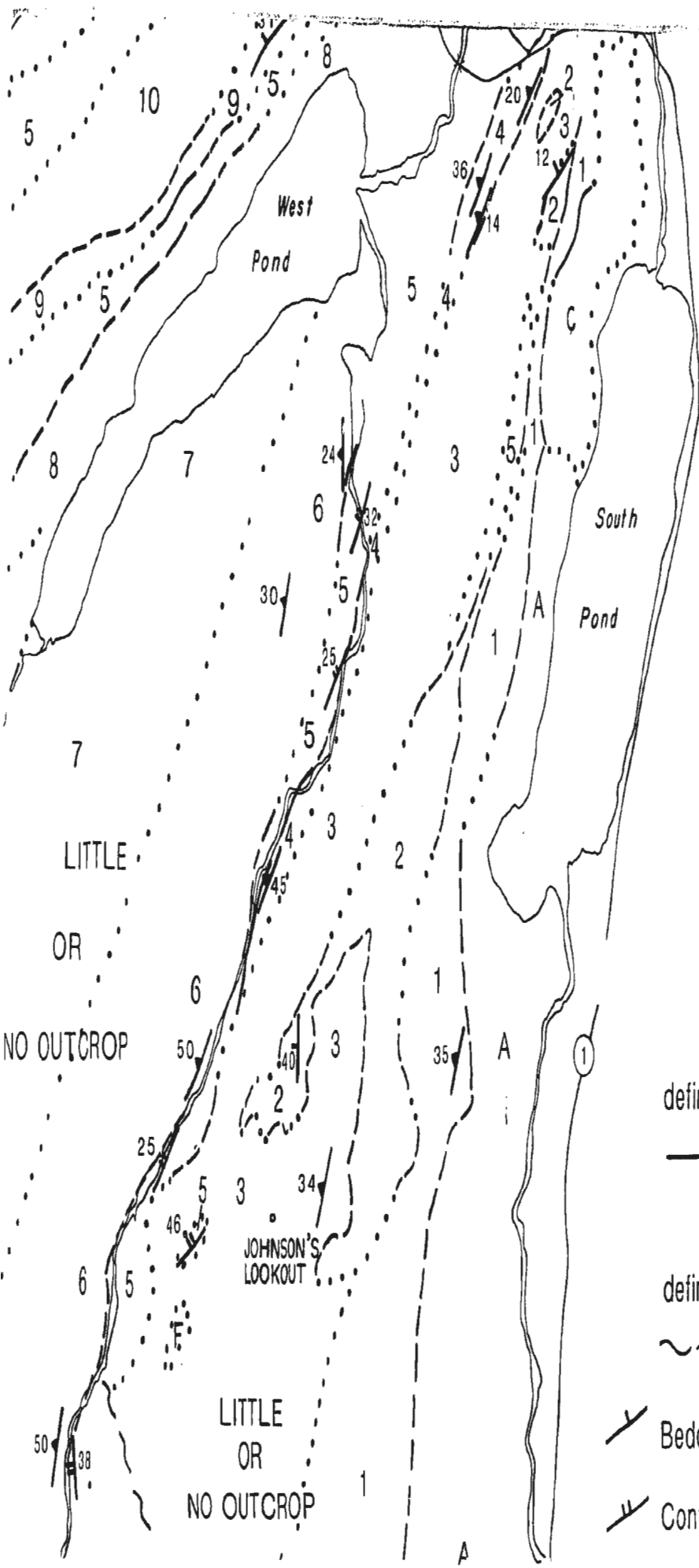
NOTE: Refer to Map 1b & 1c for Index.



MAP IB

-  CAPE ST. JOHN GROUP
-  BURLINGTON GRANODIORITE
-  ORDOVICIAN VOLCANICS
-  FLEUR DE LYS SUPERGROUP





MAP 1B
GEOLOGY OF THE
SPRINGDALE CALDERA
(Northern Margin)

SCALE

0 2000 4000 Metres

LEGEND

Geological contact
 defined, approximate, assumed

— — — — —

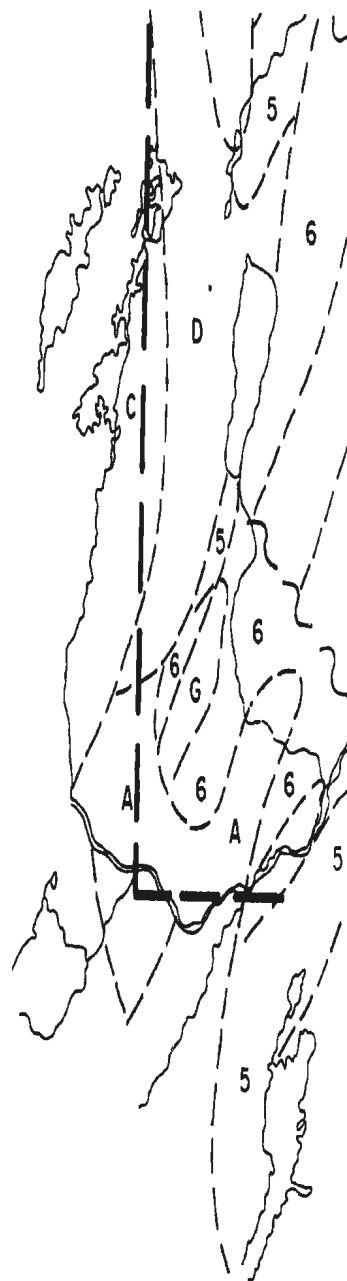
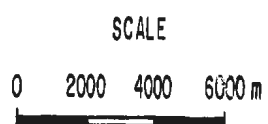
Fault
 defined, approximate, assumed

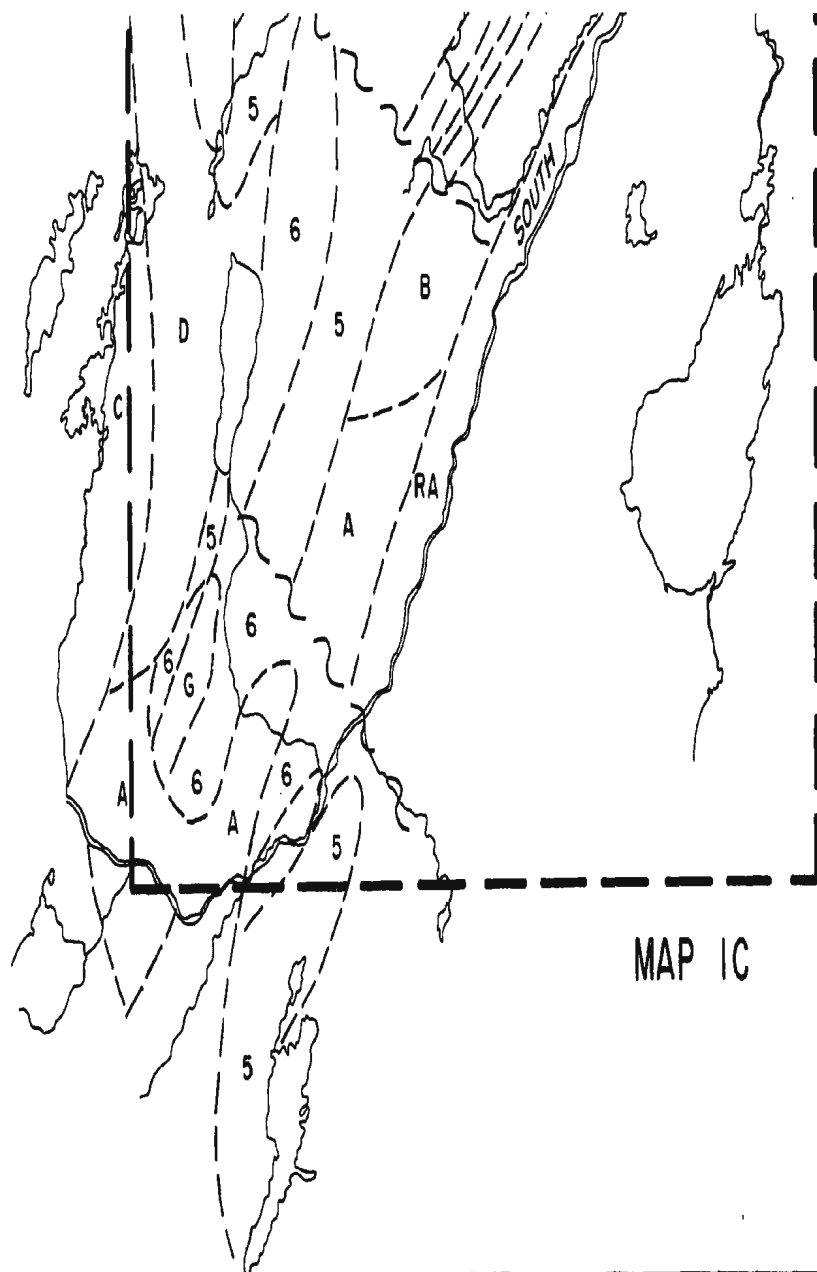
~~~~~

Bedding in sedimentary rocks

Contact or flow-structure in Basalt

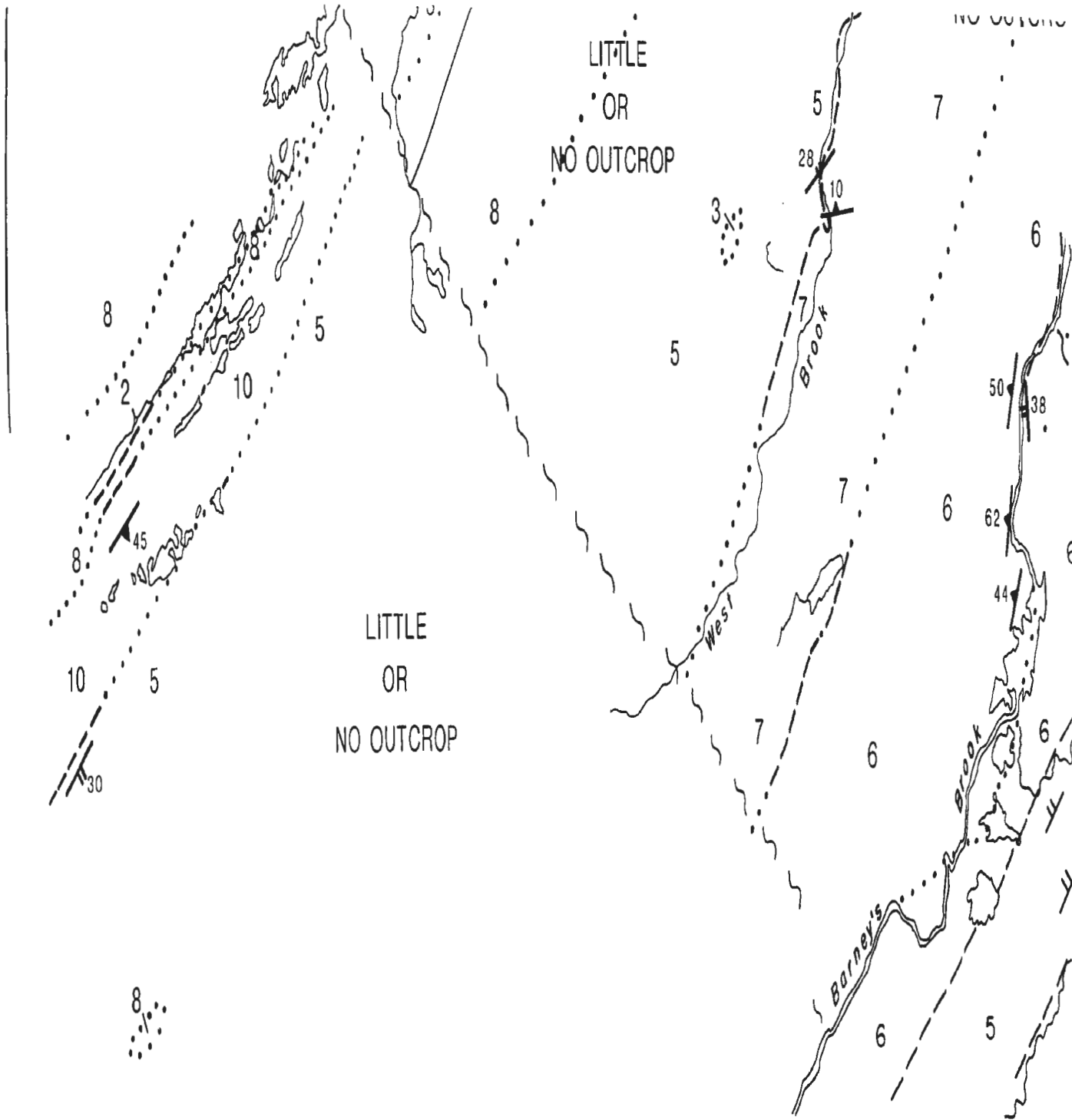
NOTE: Refer to Map 1b & 1c for Index.



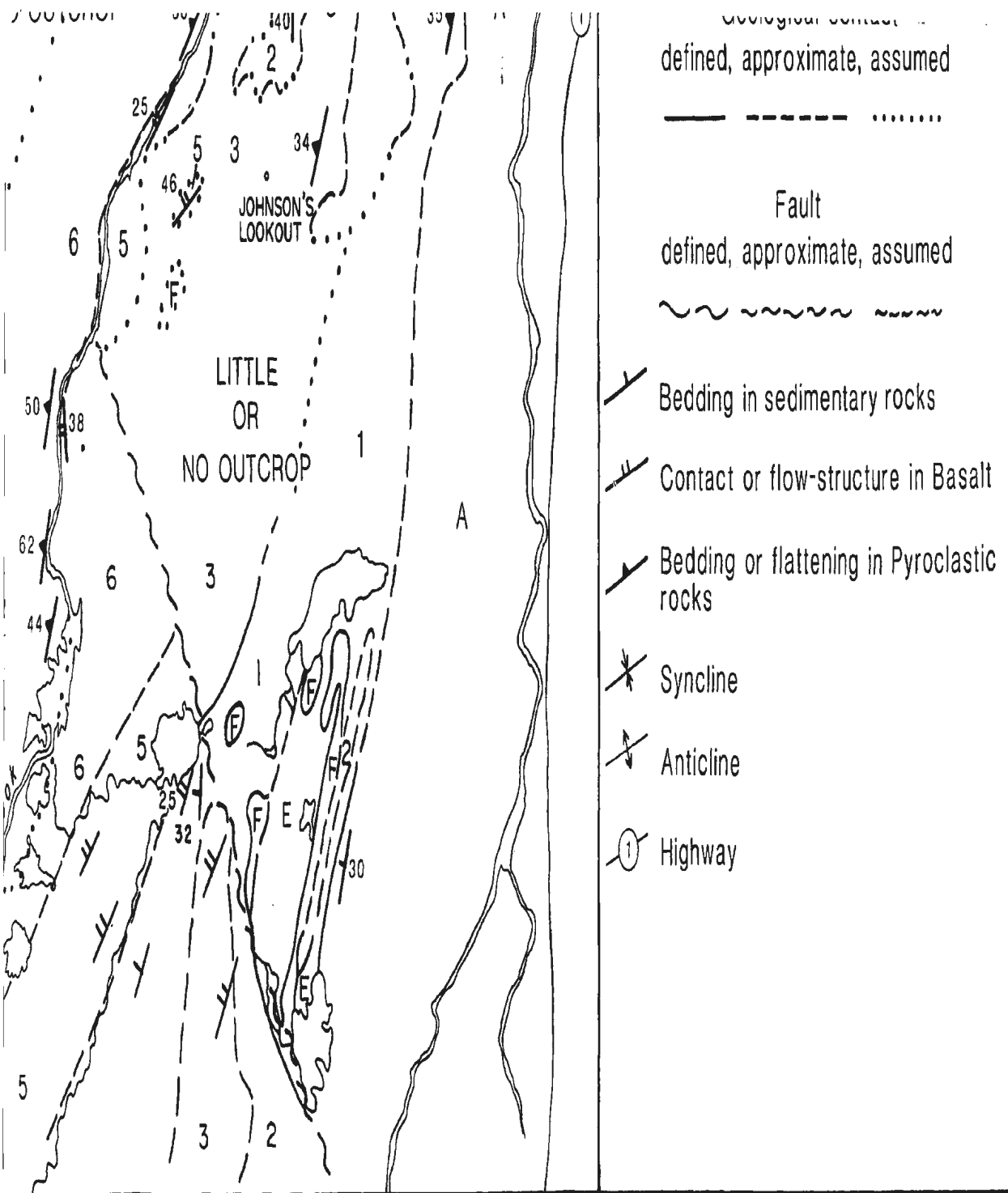


MAP IC

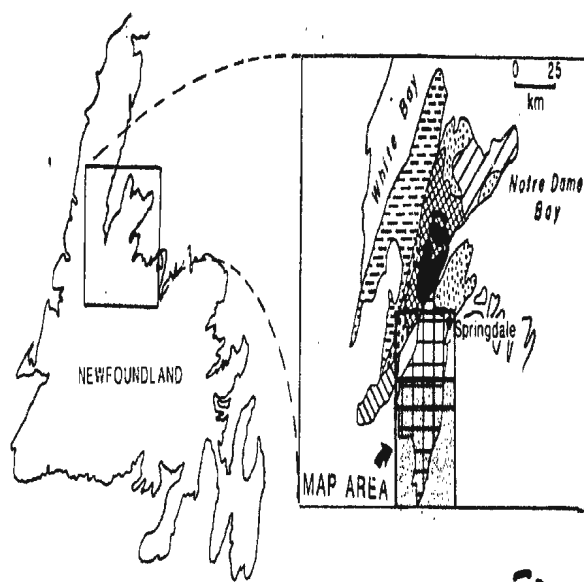
48°58'  
56°00'



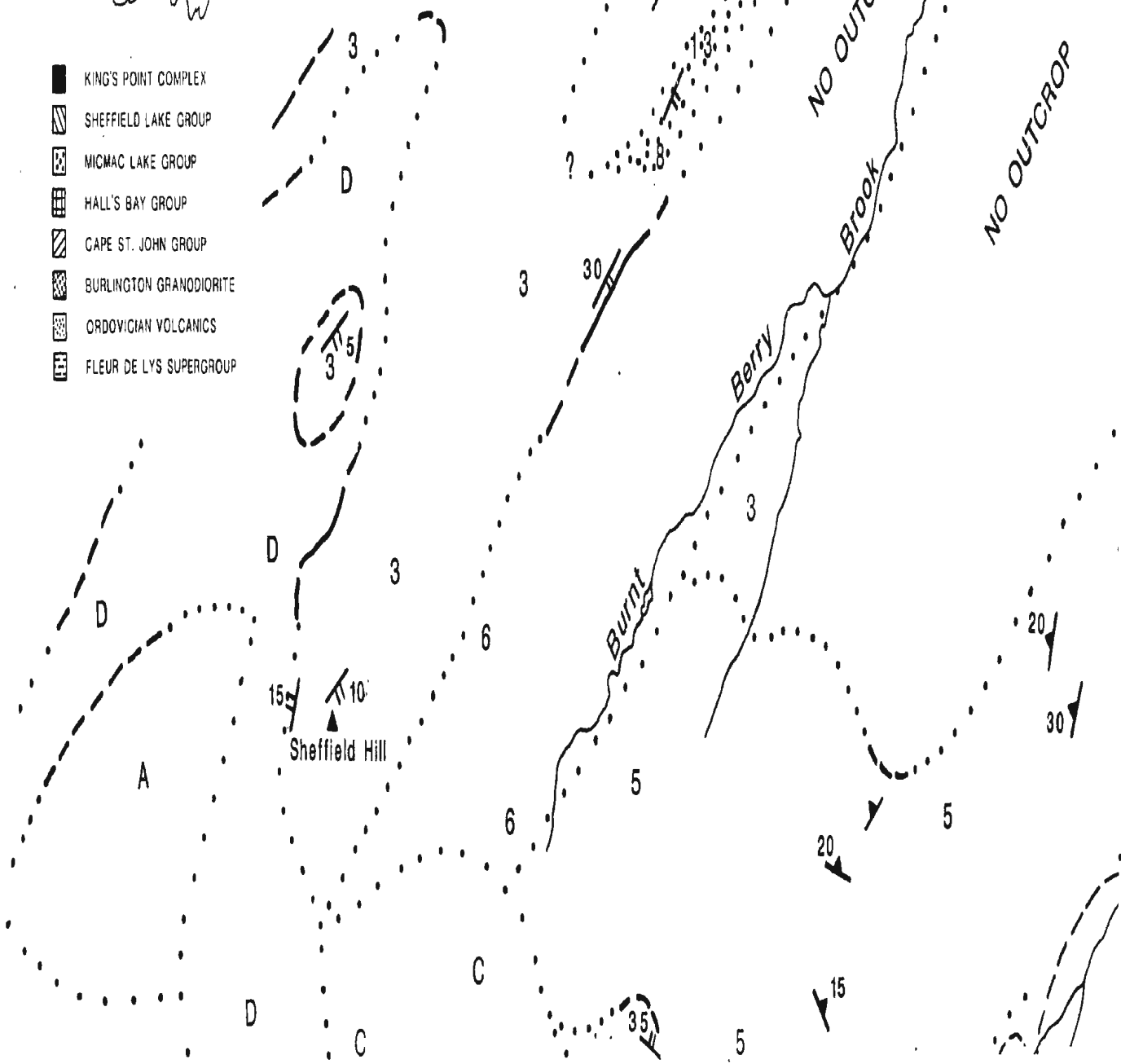


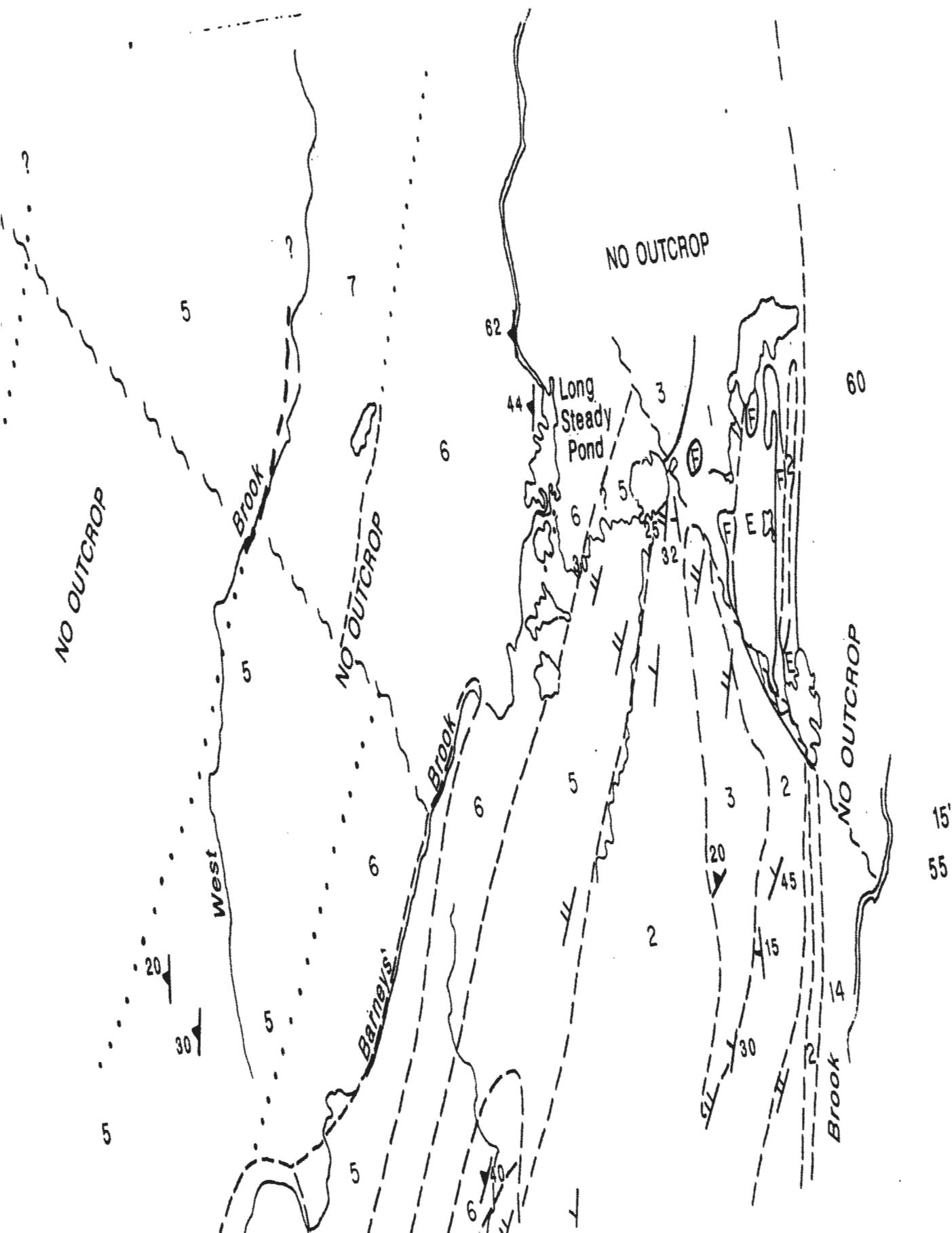


49°15'N  
 56°00'W



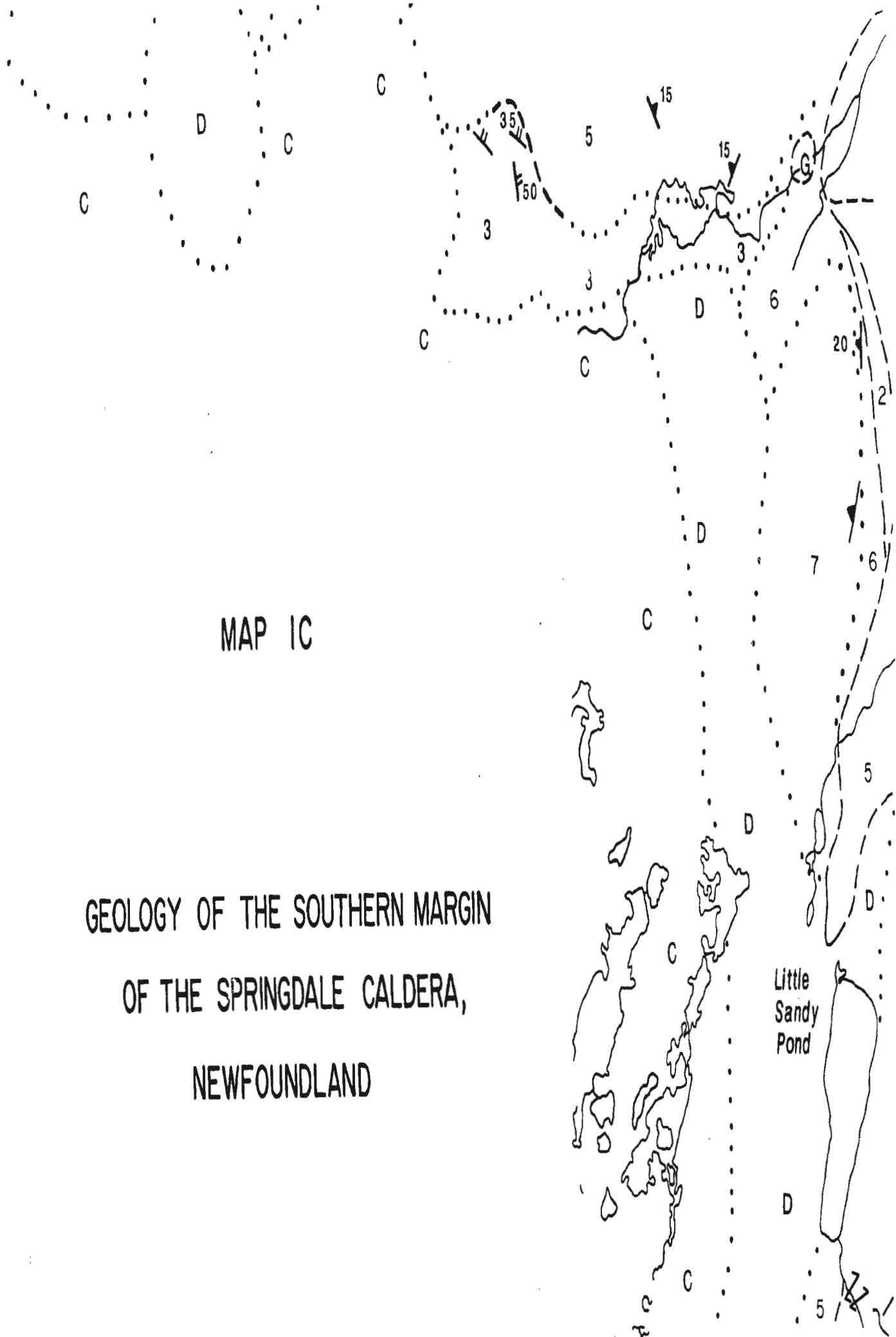
- KING'S POINT COMPLEX
- SHEFFIELD LAKE GROUP
- MICMAC LAKE GROUP
- HALL'S BAY GROUP
- CAPE ST. JOHN GROUP
- BURLINGTON GRANODIORITE
- ORDOVICIAN VOLCANICS
- FLEUR DE LYS SUPERGROUP

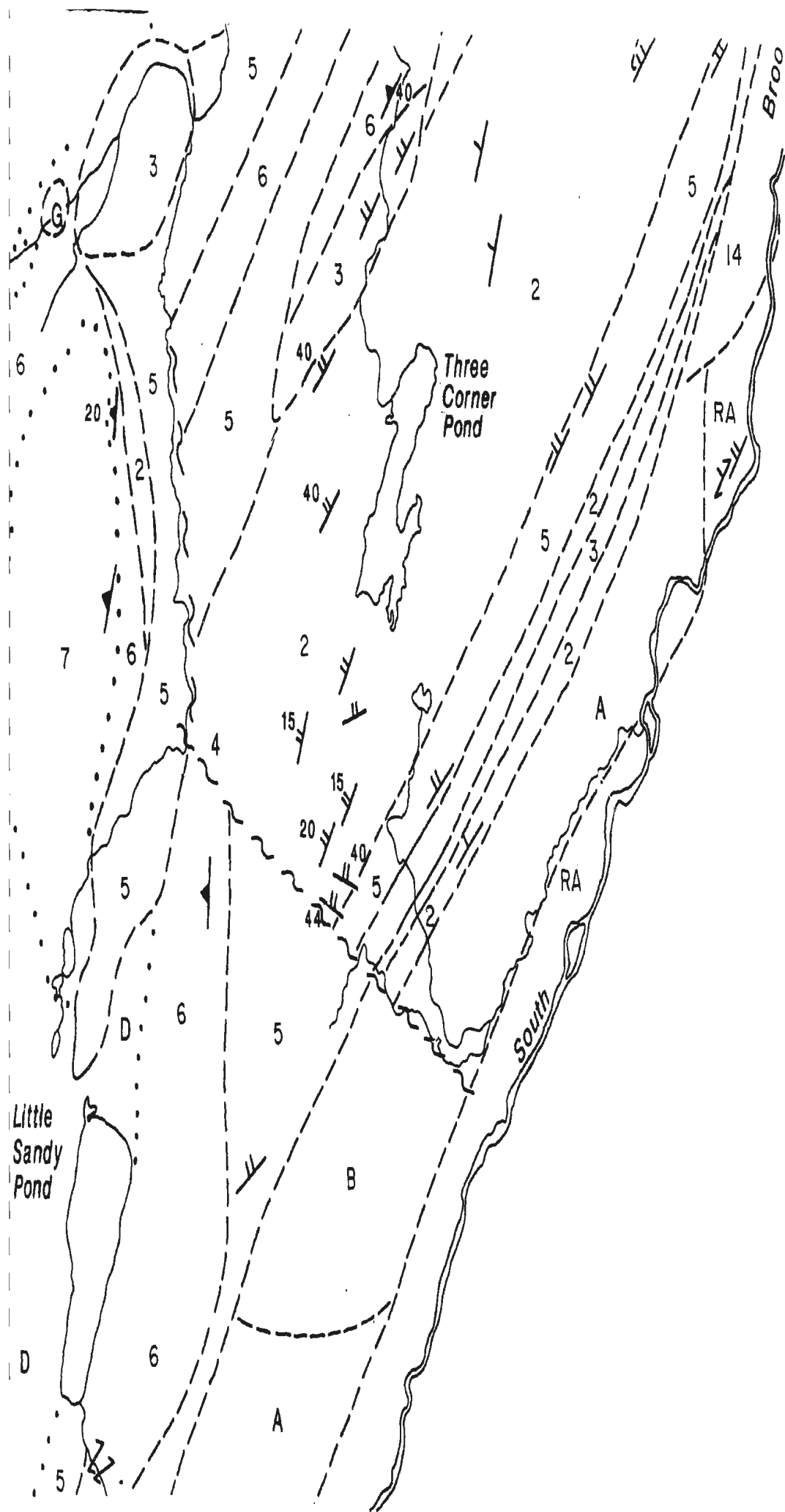




MAP IC

GEOLOGY OF THE SOUTHERN MARGIN  
OF THE SPRINGDALE CALDERA,  
NEWFOUNDLAND





# NEWFOUNDLAND

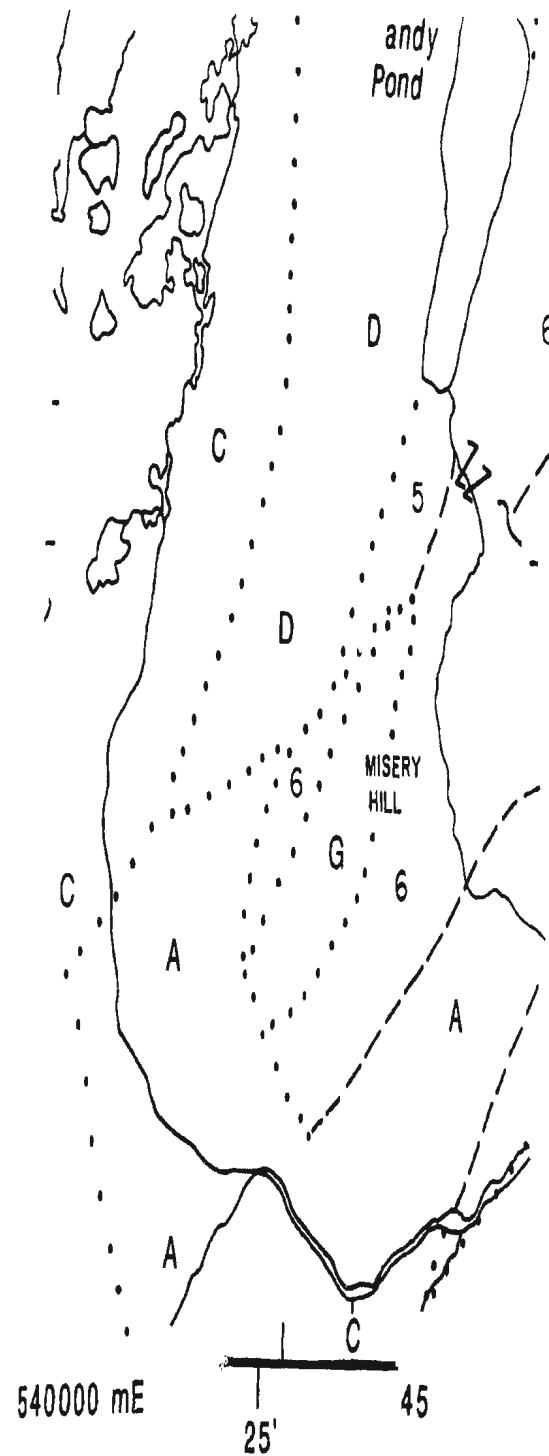
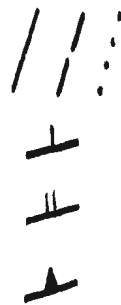
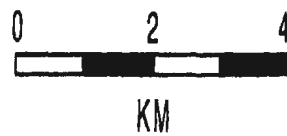
## SYMBOLS

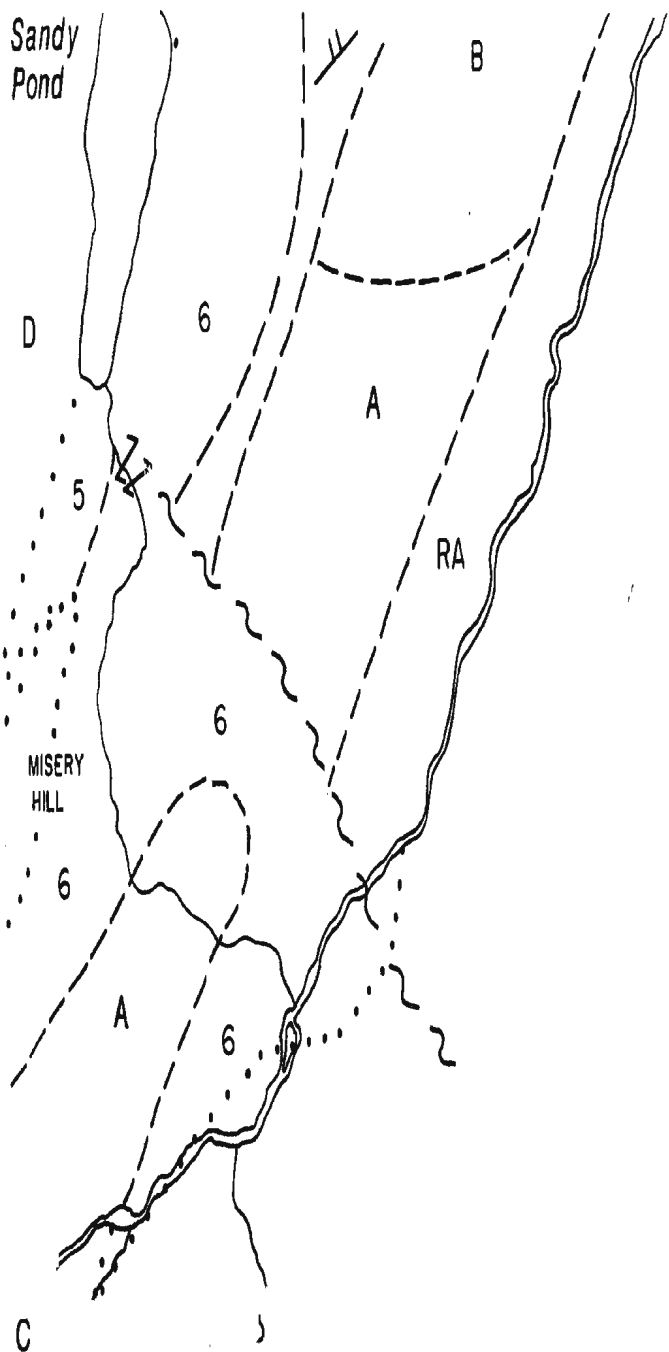
Geological contact: defined, approximate, assumed

Bedding in sedimentary rocks

Contact or flow-structure in Basalt

Bedding or flattening in Pyroclastic rocks





40

49°05'N

5435000 N



45

20'

50

55  
15'

56°10'W



**M. COYLE, PH.D. THESIS, 1990**

**GEOLOGY, GEOCHEMISTRY AND GEOCHRONOLOGY  
OF THE SPRINGDALE CALDERA**

**LEGEND FOR MAPS 1, 1A, 1B, 2, 3, 4**

**CARBONIFEROUS**

14. Red to grey mudstones to pebble conglomerates with local carbonate cement.

**SILURIAN-(DEVONIAN?)**

**SHEFFIELD LAKE GROUP**

13. Andesite. Aphyric to plagioclase-microphyric.
- 12a. Vitric tuff. Orange to red, welded. Characterized by large sodic amphibole oikocrysts with rare resorbed K-feldspar phenocrysts.

## **LEGEND (continued)**

12. **Ash-flow tuff.** Massive, maroon, aphanitic to flow-banded quartz- and feldspar-phyric.
11. Red and brown crystal, vitric and lithic-rich **ash-flow sheets.** **Laharic,** **fault and gas-breccias.** **Rhyolite domes** **and dykes.** **Minor basalt.**

## **SPRINGDALE GROUP**

10. **Crystal-lithic tuff.** Densely welded and massive large phenocrysts of quartz and feldspar, clasts of mafic and rare ultramafic lithologies.
9. **Clastic sedimentary rocks.** Red conglomerate, sandstone, and sandy siltstone, local caliche horizons; cross-bedding, ripples, laminations, rip-up horizons, scour channels, etc. indicate stream-flood and proximal and distal fluvial origin; clasts essentially volcanic or plutonic provenance.

## **LEGEND (continued)**

8. **Rhyolitic vitric ash-flow tuffs and breccias.** Welded, devitrified, locally massive; areas of unwelded vitroclastic tuffs with large individually devitrified shards with axiolitic texture; locally passes into sandstones; alternating thin basaltic and silicic bands in some horizons.
7. **Dacitic to rhyolitic ash-flow tuffs, vitroclastic breccia and domes.** Massive, vitric, strongly welded; curvilinear joint surfaces in the domes, with internal plastic shear zones, local brecciation, and flow folds; tuffs locally porphyritic, with small euhedral plagioclase and rare quartz phenocrysts in glassy matrix.

## **LEGEND (continued)**

6. **Silicic ash-flow tuffs.** Crystals, lithic fragments, and vitroclasts; basal lithophysae-rich horizons, grading up into a partially welded crystal-lithic lapilli tuff; broken phenocrysts of plagioclase, K-feldspar and quartz; flattened pumice bombs up to a metre long; clasts of silicic volcanics, andesite and rarely basalt.
5. **Mainly basaltic flows,** some of intermediate composition. Locally plagiophyric; with amygdales of quartz, calcite and chlorite; variably altered. Note that map units include large areas of no outcrop.
4. **Felsic to intermediate, dominantly dacitic, ash flow tuff.** Crystal-lithic and lapilli ash-flow tuffs; clasts of andesite, rhyolite, angular and flattened pumice; variably welded.
3. **Andesitic to dacitic flows.** Locally plagiophyric, massive to flow-foliated to brecciated; local intrusions of massive andesite.

## **LEGEND (continued)**

2. **Mesobreccia.** Laharic flows, tuffites and pepperites, volcanic conglomerates and breccias, red sandstones.
1. **Welded, lithic-crystal tuff.**  
Plagioclase and K-feldspar, accessory biotite, quartz, and rare opaques, clasts of granophyre, plagiophyric basalt, andesite, ultramafics, and jasper.

## **INTRUSIVE and BASEMENT ROCKS**

- I. **Quartz-K-feldspar porphyry.** Orange to green, with sodic amphibole oikocrysts and minor aegrine and altered fayalite.
- H. **Granite to quartz syenite.** Red medium-grained plagioclase, K-feldspar and amphibole porphyritic. Granophyric textured; heavily altered.

## **LEGEND (continued)**

- G. Rhyolite domes, dykes and sills.**  
High-silica. Microphenocrysts of quartz and feldspar, with finely disseminated riebeckite in groundmass; flow-foliated, auto-brecciated, zones of intense development of spherules and other indications of gas-streaming.
- F. Felsic microporphyry sills and dykes.**
- E. Microdiorite.** Black, fine-grained, massive.
- D. Granite.** Medium to coarse grained; characterized by quartz and pink feldspar with finer grained crystals of black amphibole, intruded by finer grained whitish grey granite, with locally riebeckite pegmatite and abundant amphibole-lined miarolitic cavities and fractures; offshoots of the Topsails Complex.
- C. One-feldspar granite.** White to red, medium to coarse grained, equigranular with amphibole  $\pm$  sodic pyroxene; in large part peralkaline.

## **LEGEND (continued)**

**B. Granite, granodiorite, minor diorite.**

**May in part be correlative with the Twin Lakes Complex.**

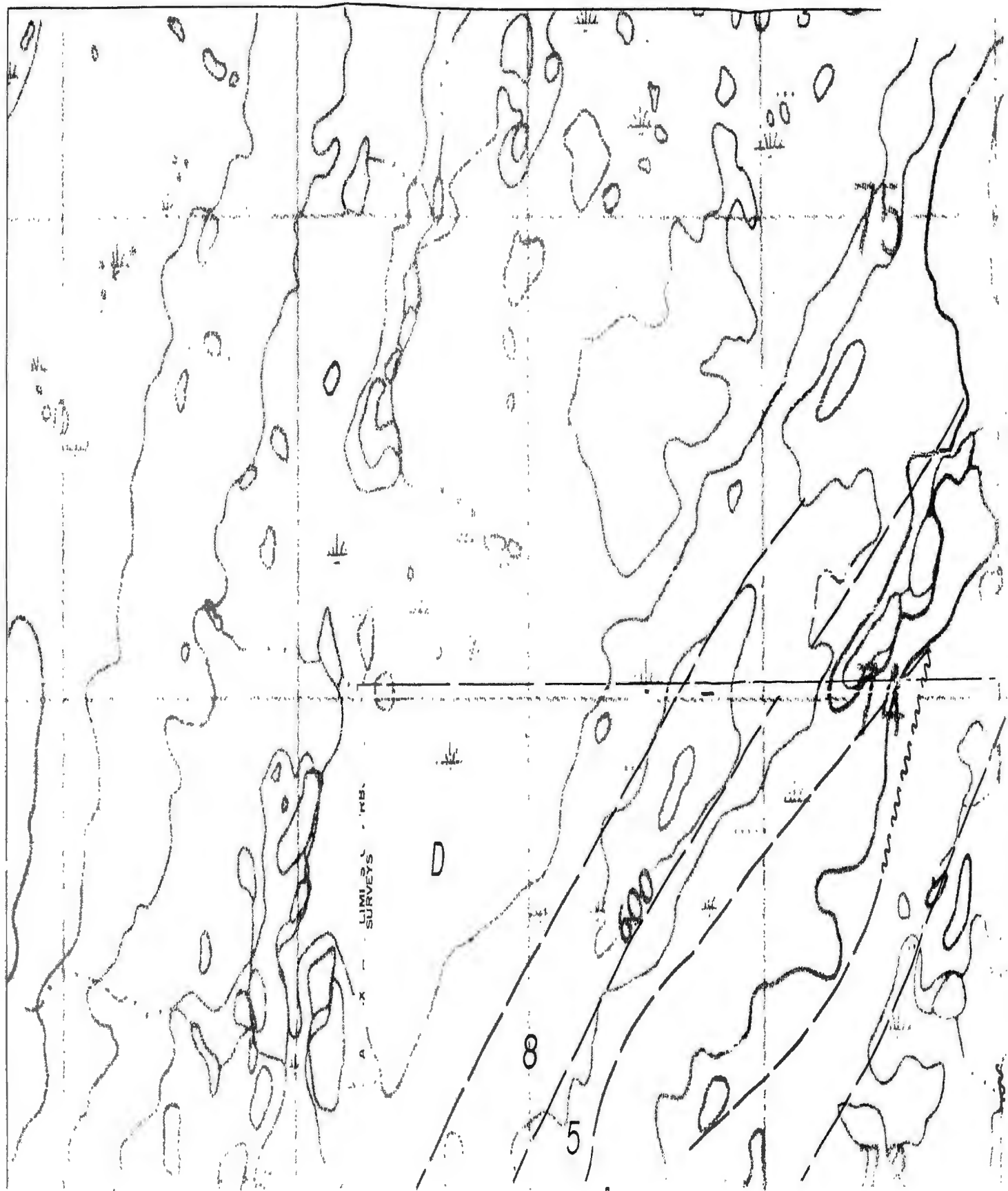
**A. Amphibolite, diorite, granodiorite, granite. Foliated amphibolite and gabbro occurring as large screens and xenoliths in foliated diorite and granodiorite; intruded by variably deformed tonalite and amphibolite-biotite granite; intruded or not veined by a pale fine-grained granite.**

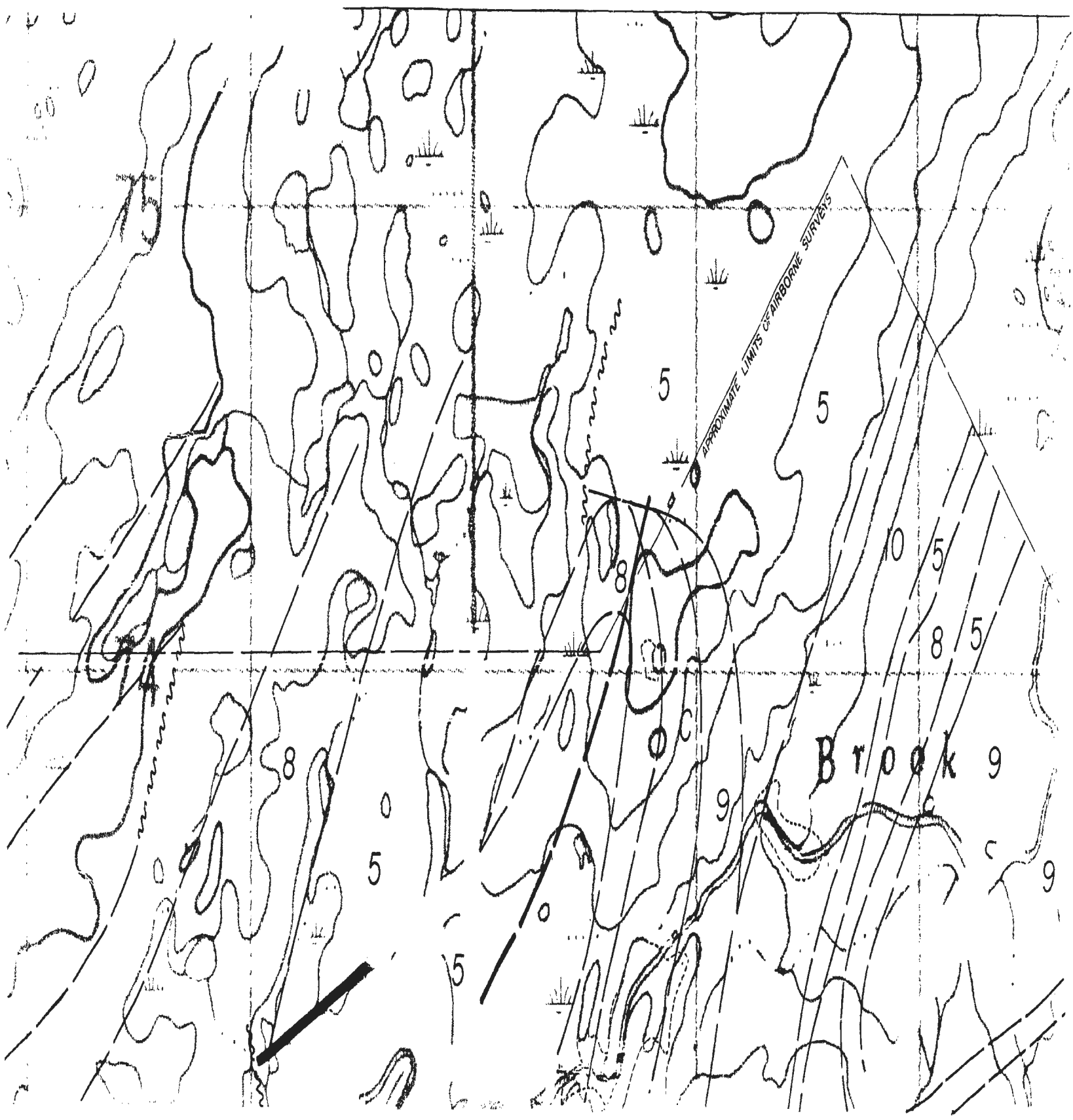
**RA. Roberts Arm Group. Mafic to felsic submarine volcanic rocks.**

**CP. Catchers Pond Group. Mafic to felsic submarine volcanic rocks.**

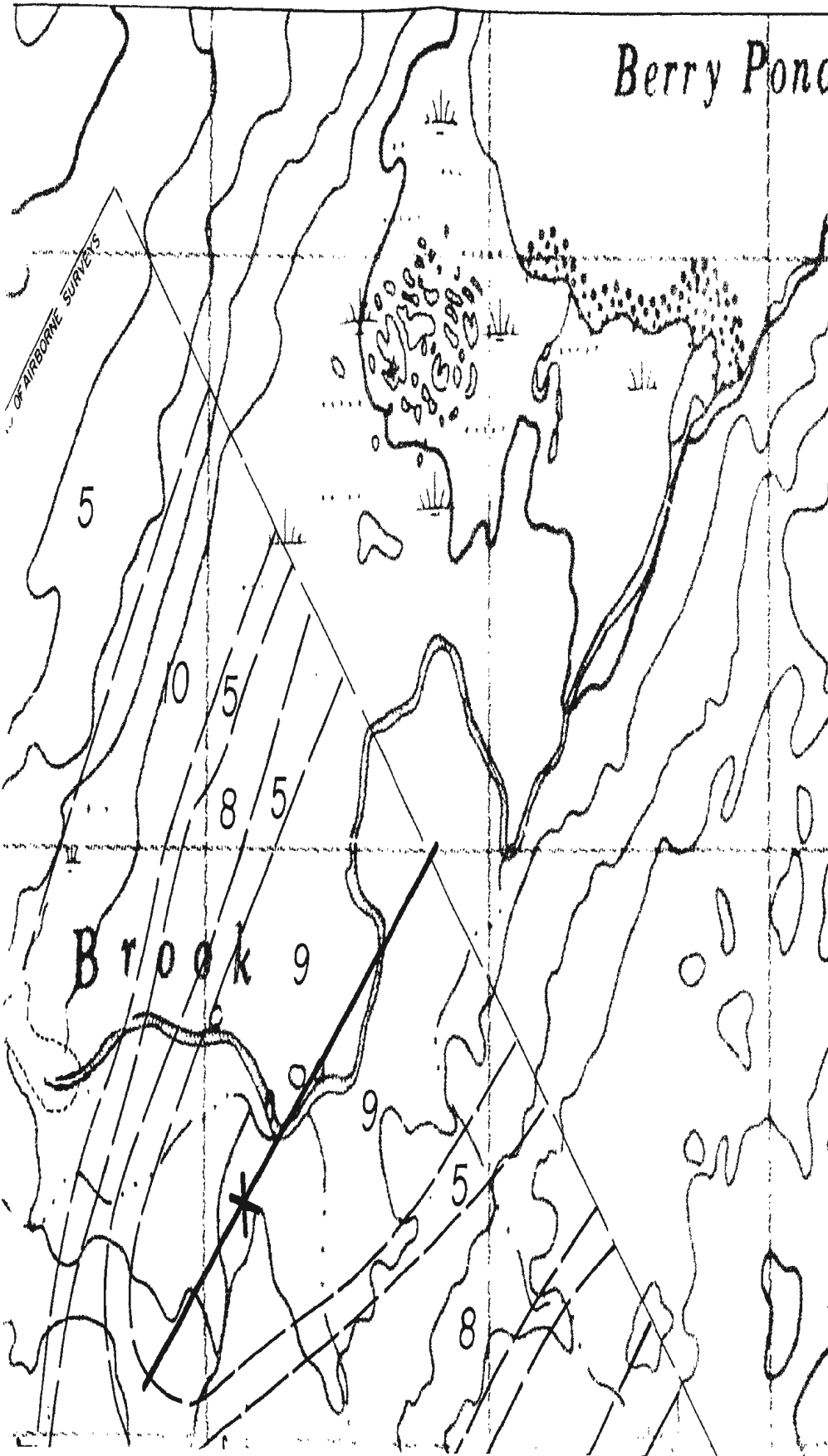
**LB. Lushs Bight Group. Mafic, ophiolite-related submarine volcanic rocks.**

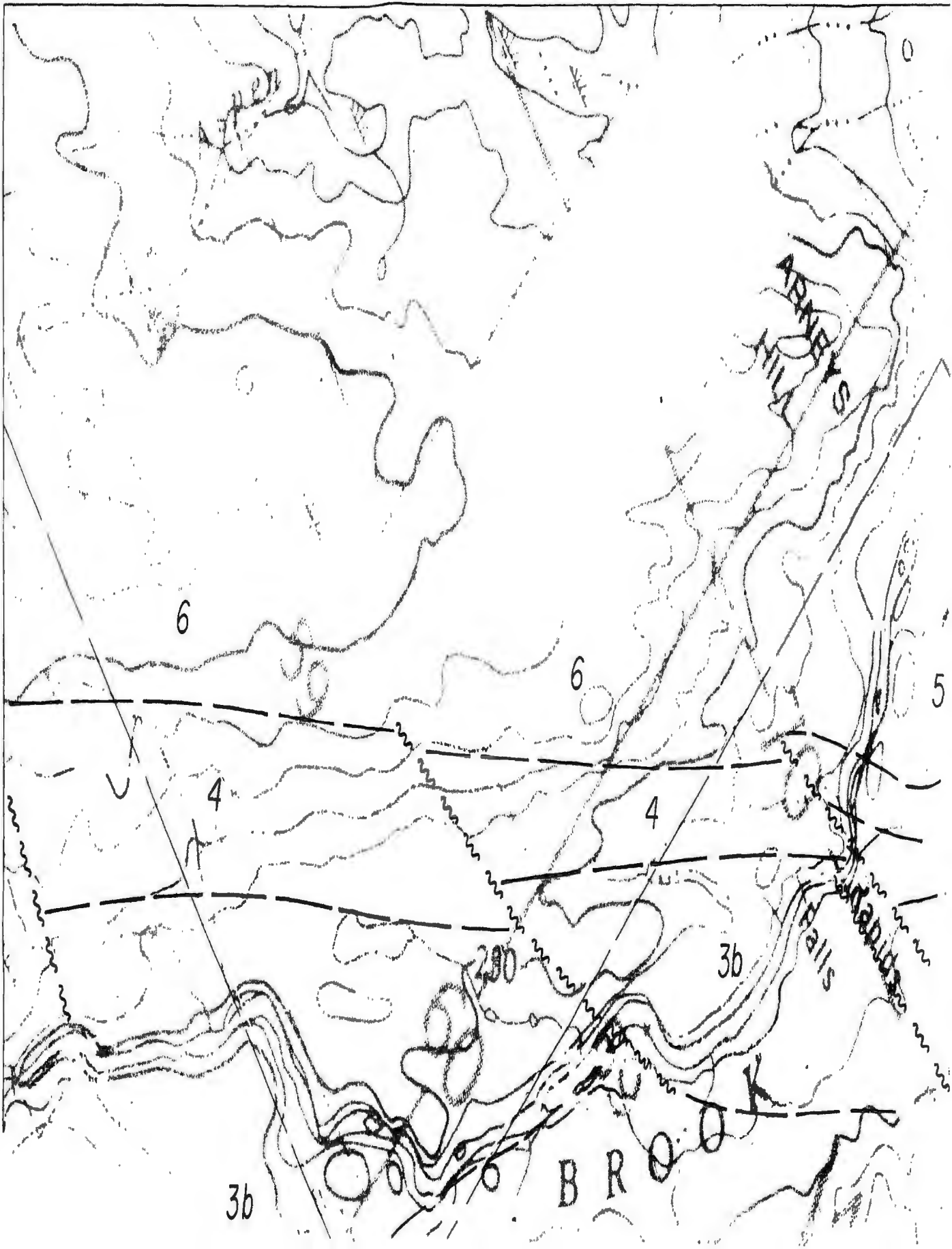


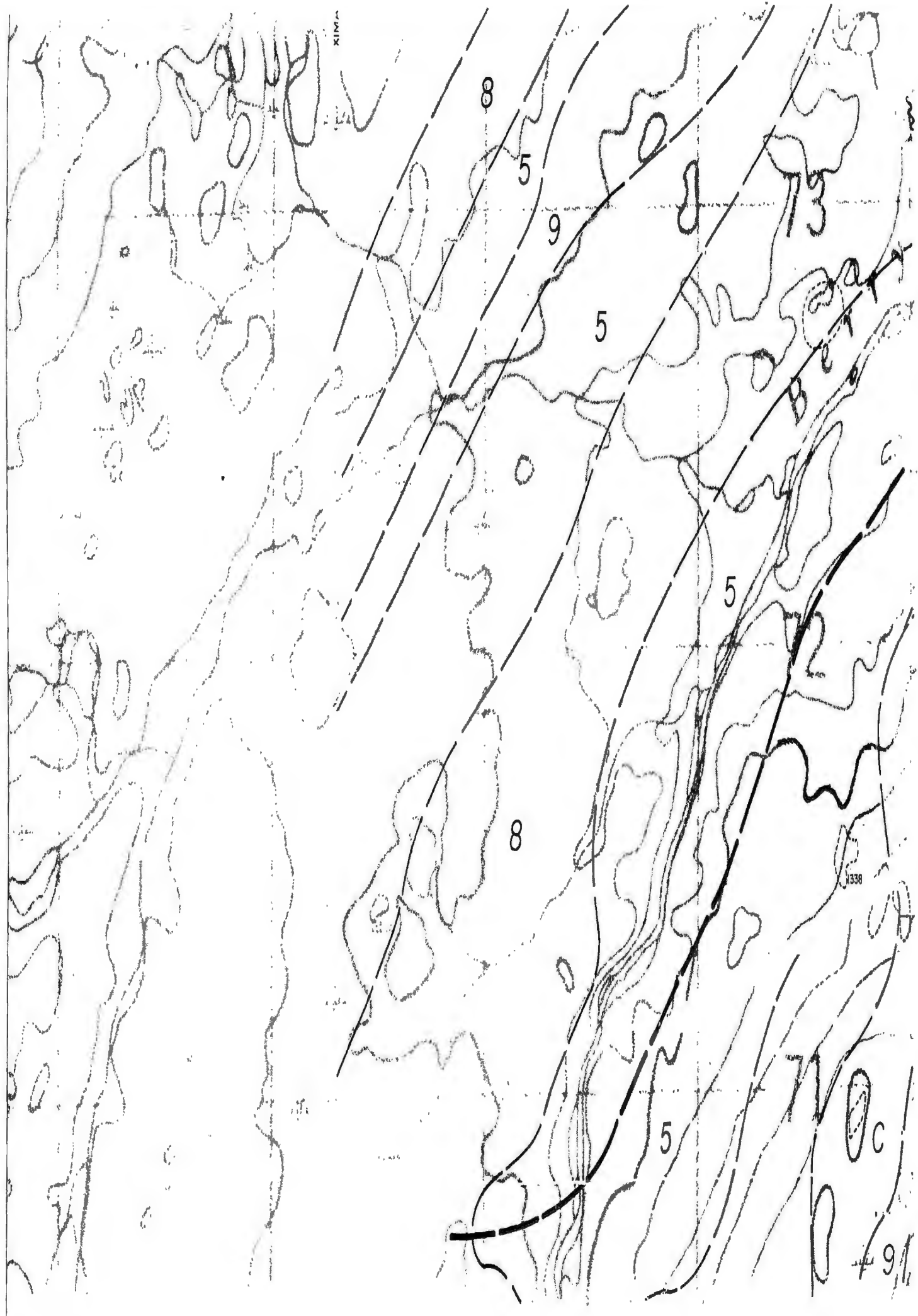


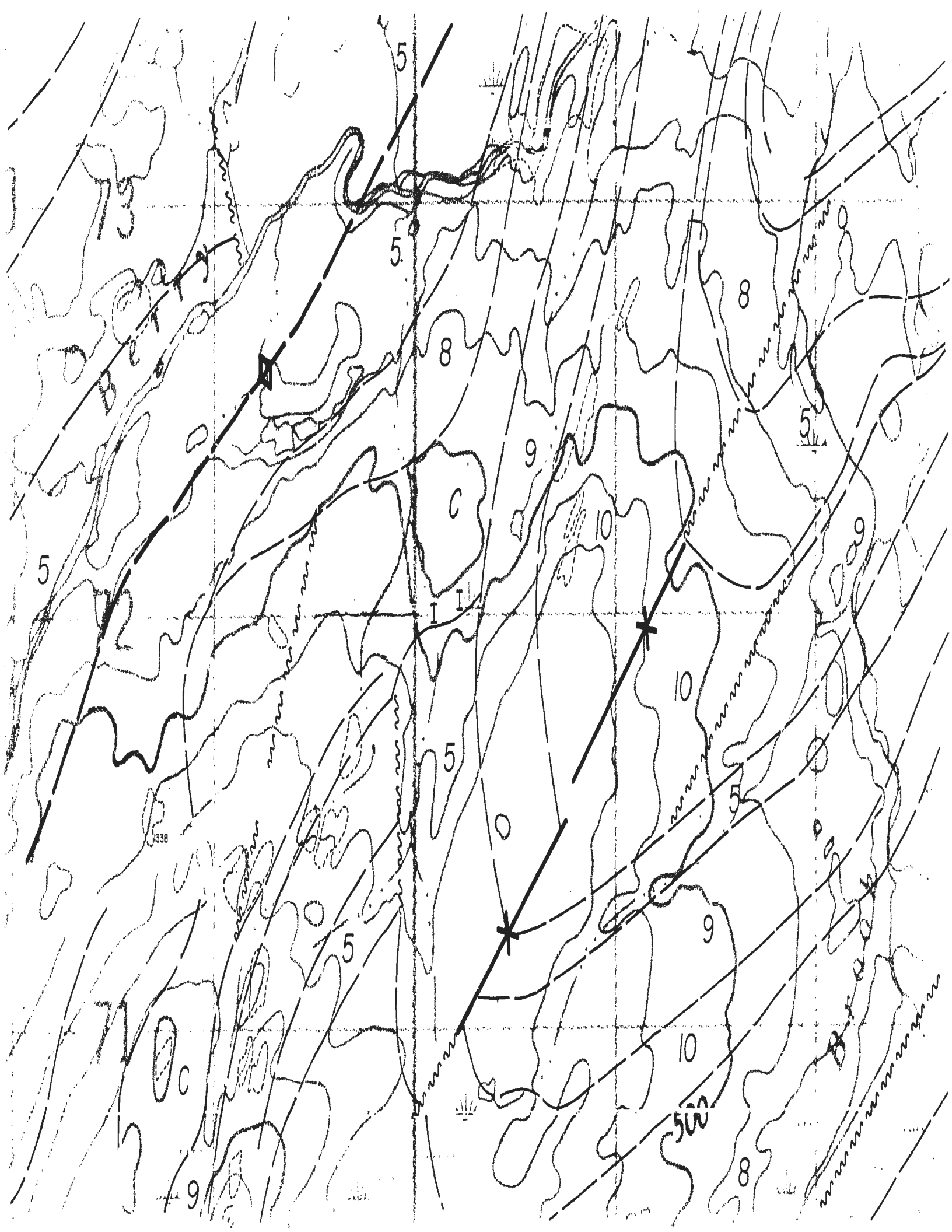


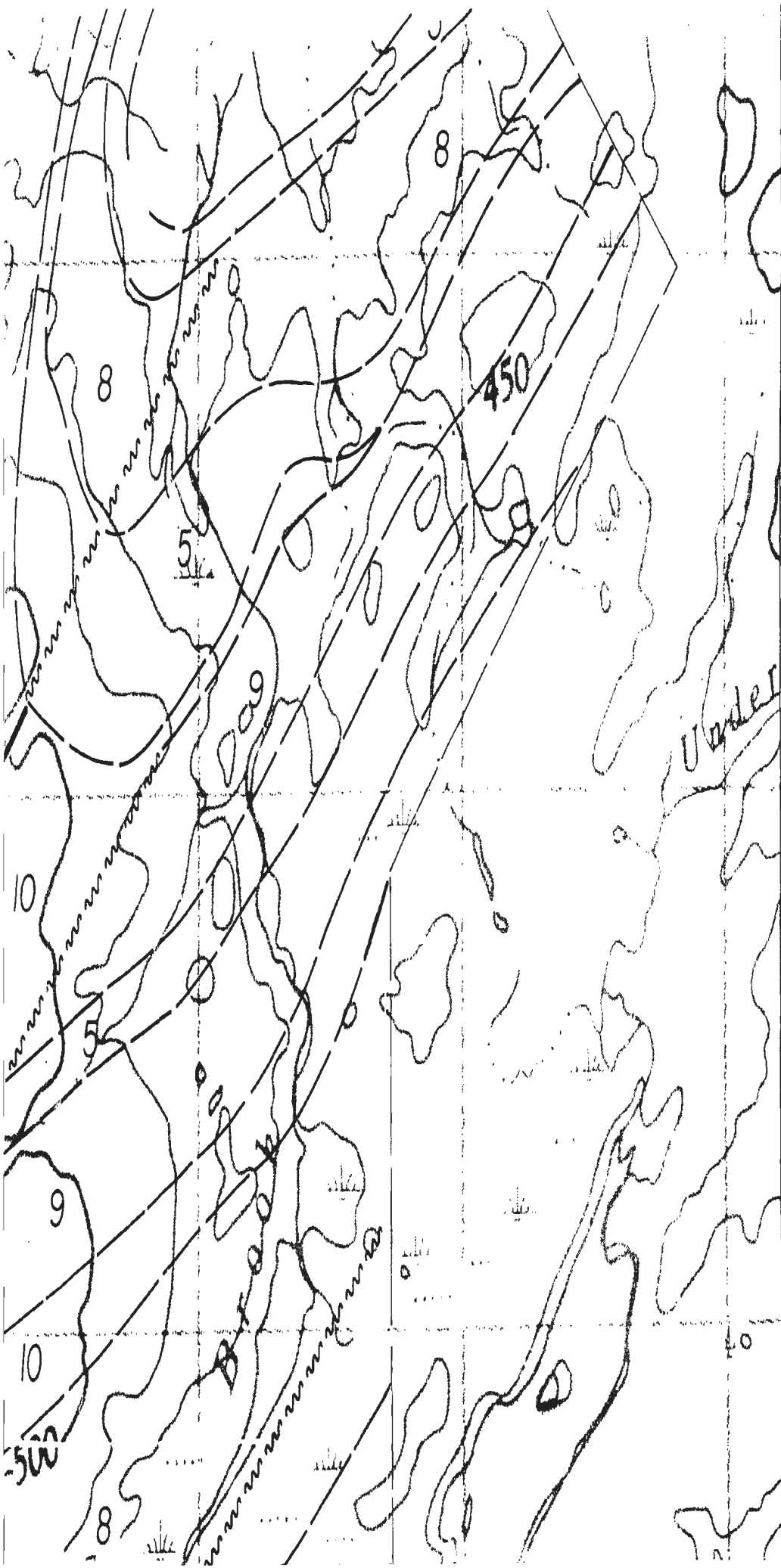
Berry Pond



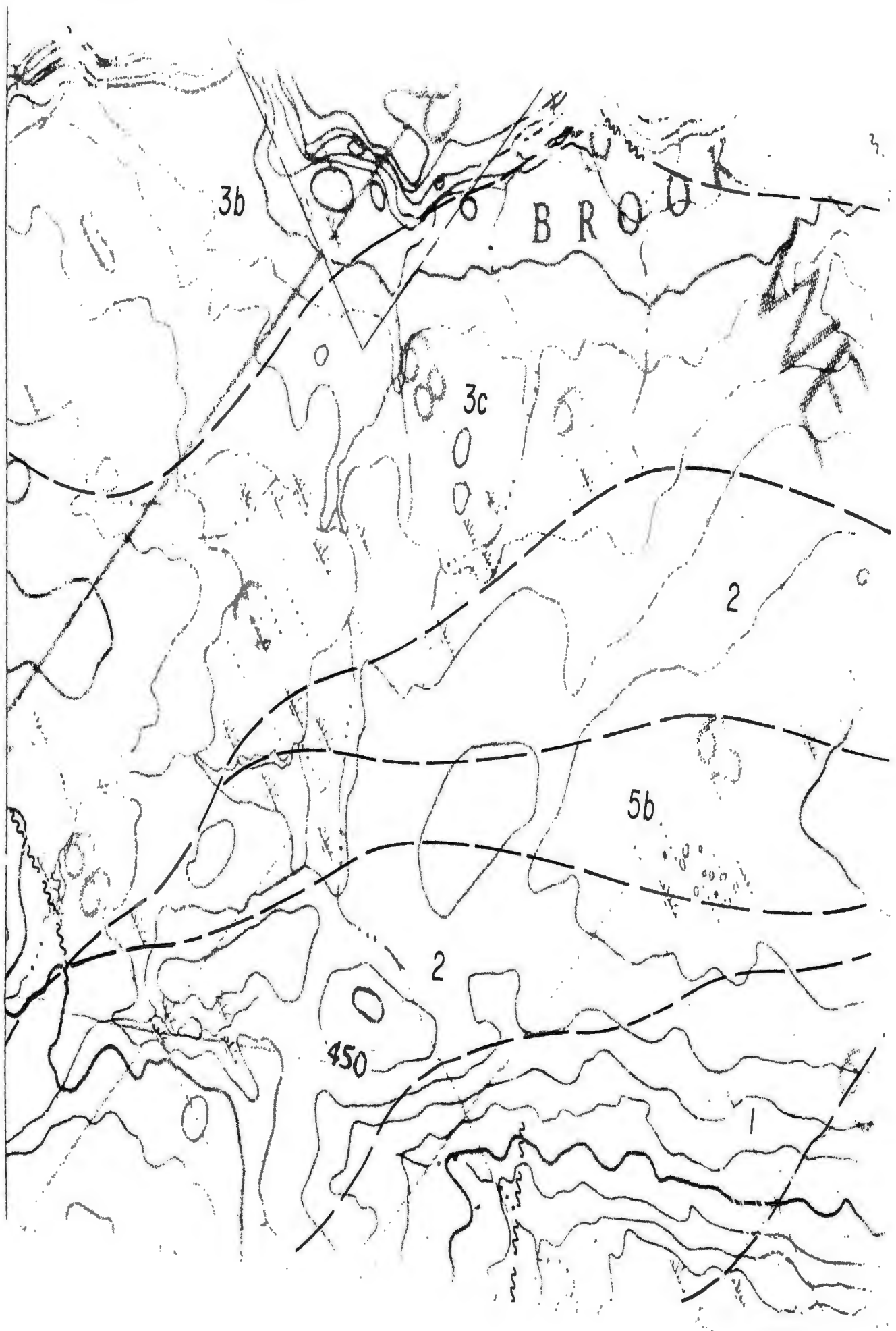


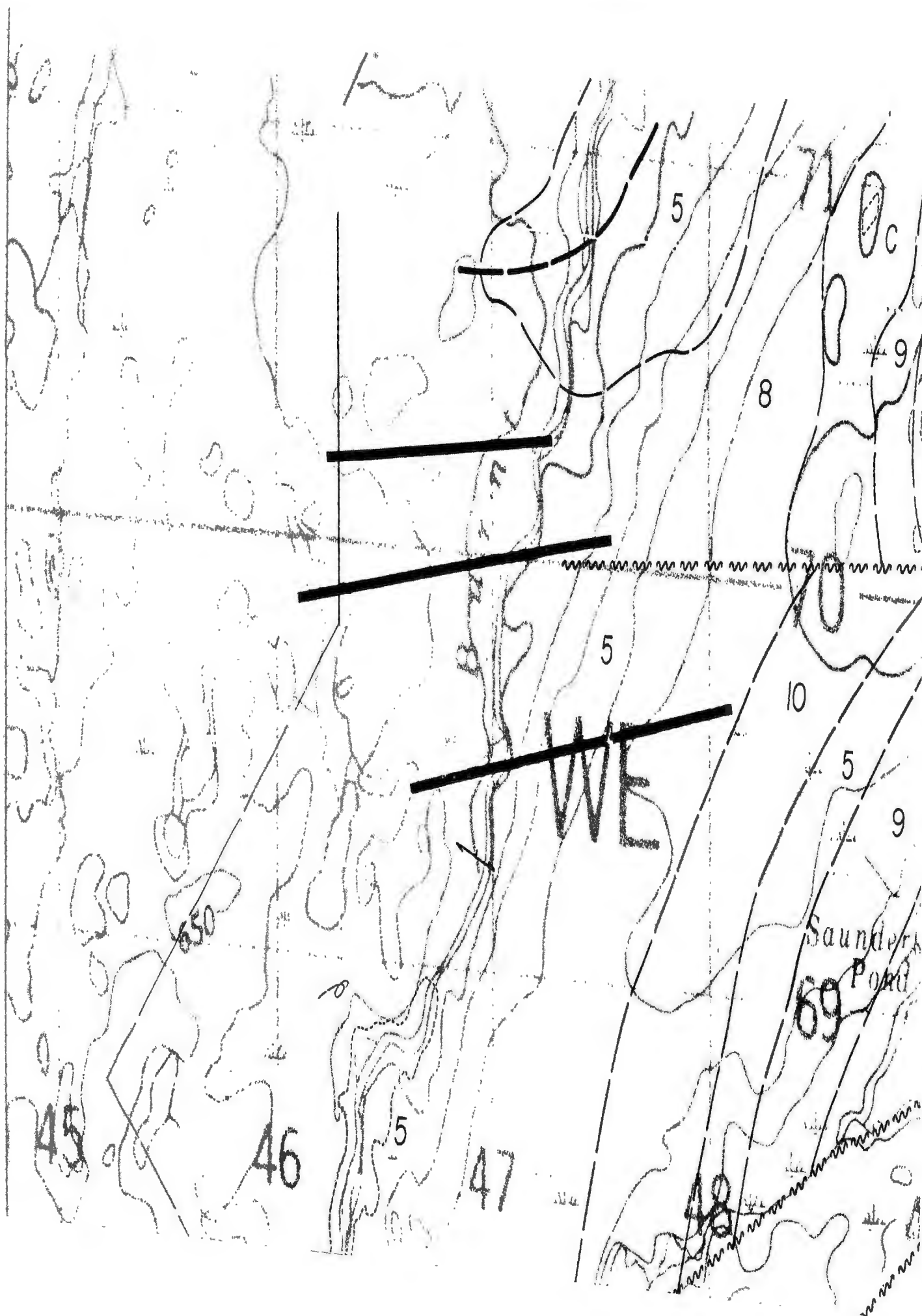


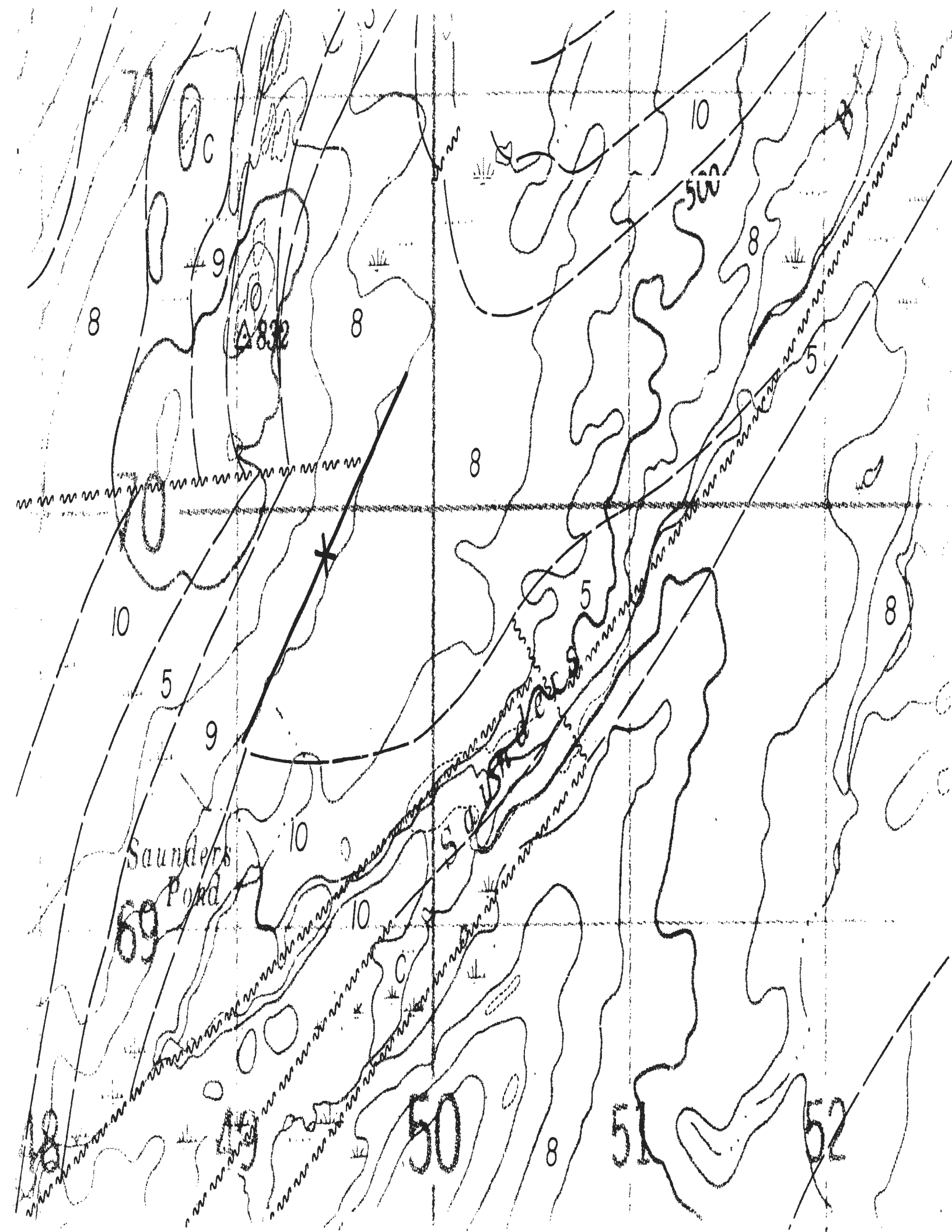


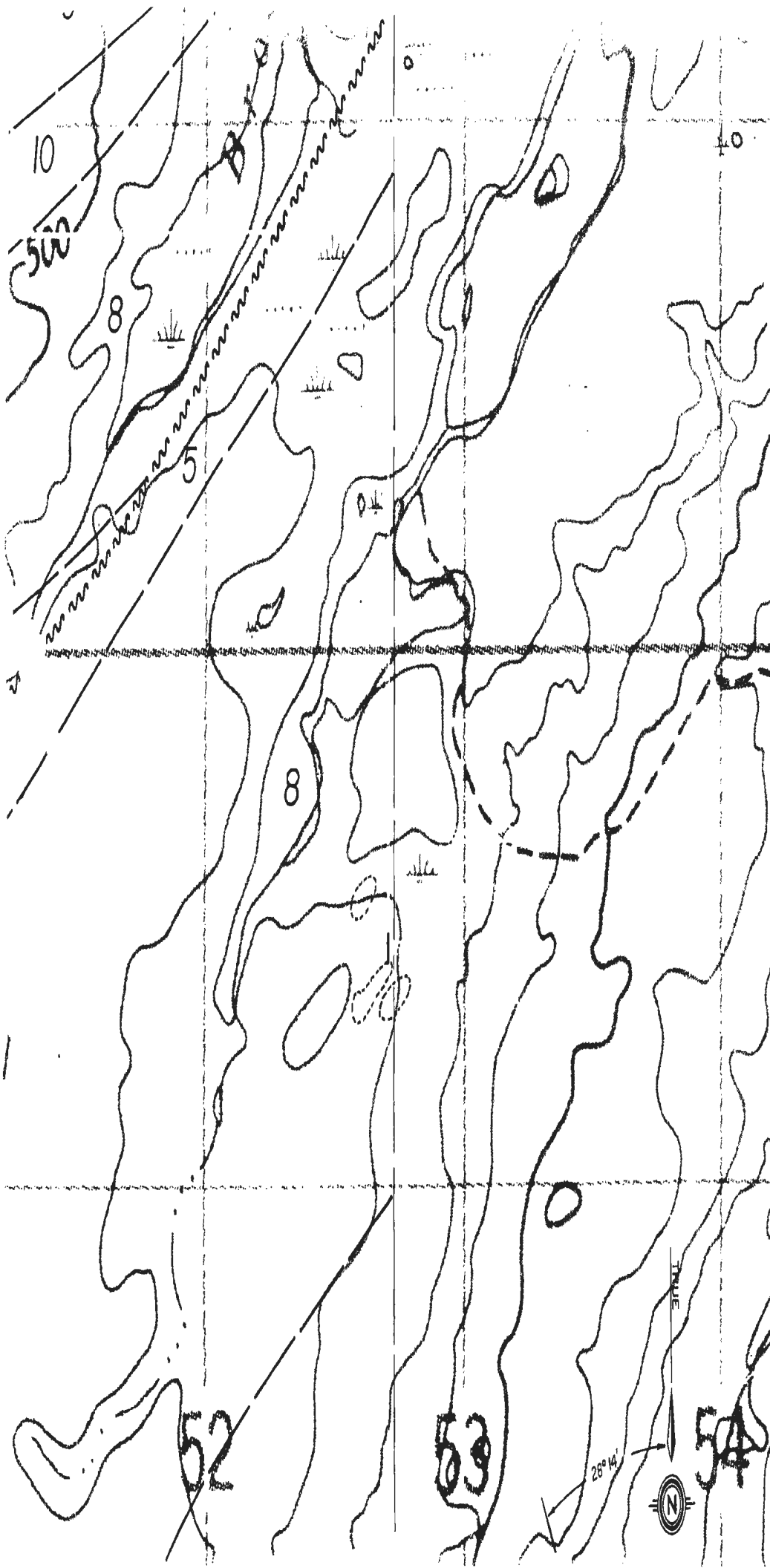


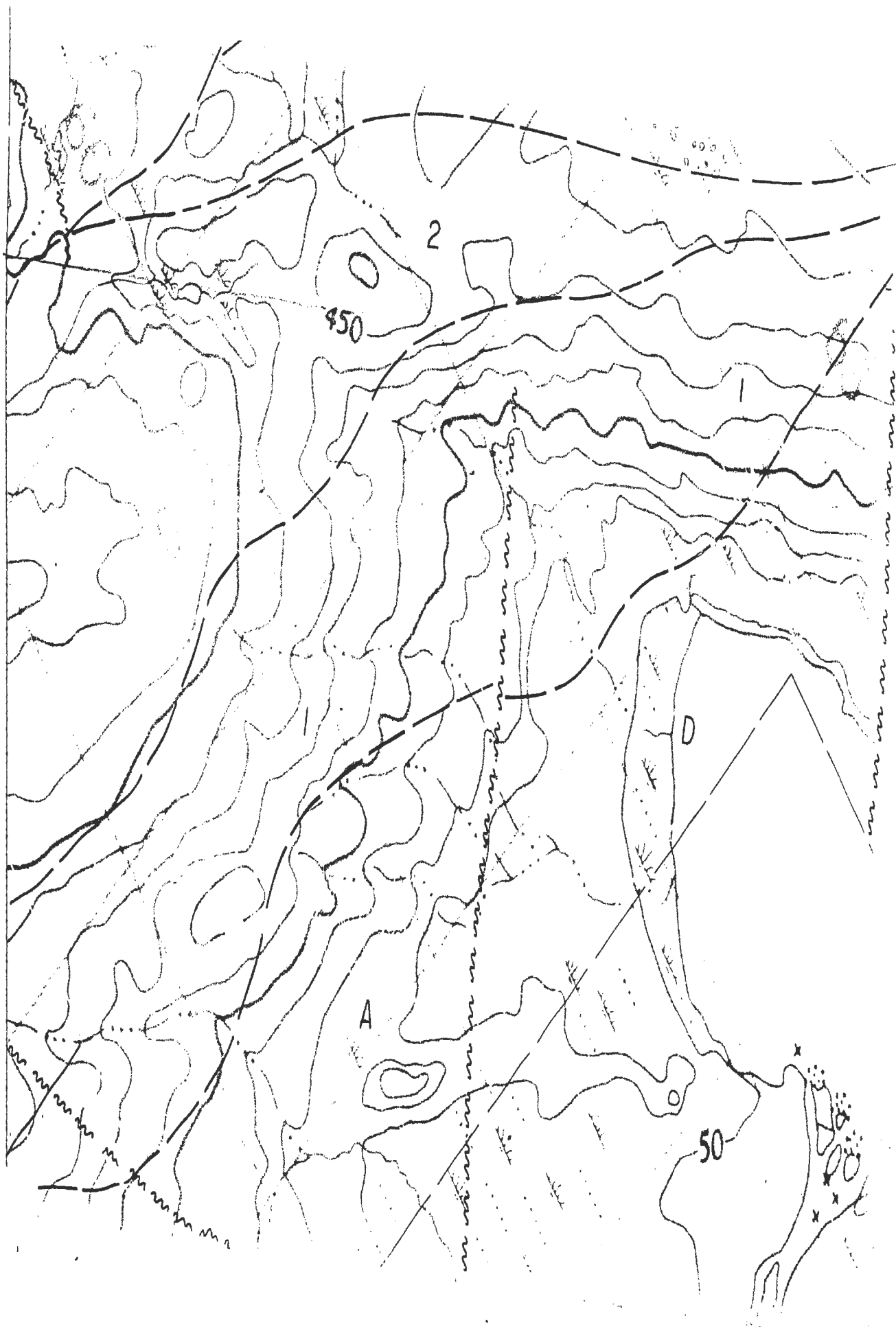


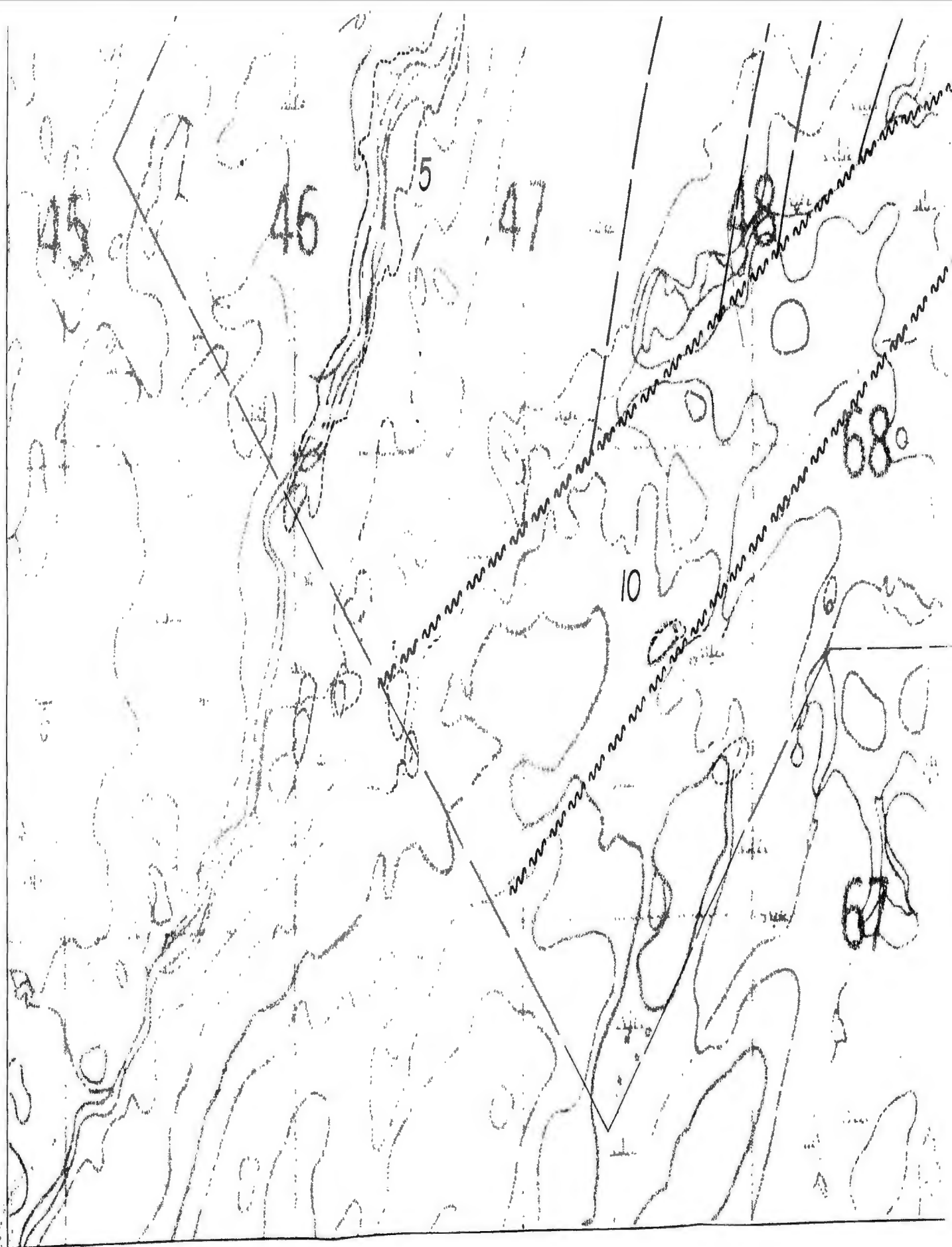












# LEGEND

## SHEPHERD LAKE GROUP

12: Orange to red welded vitric tuff characterized by large sodic amphibole oligoclase with rare resorbed K-feldspar phenocrysts.

11: Red and brown crystal, vitric and lithic ash-flow tuff - breccia. This unit is the most extensive and is the most recent.

6:

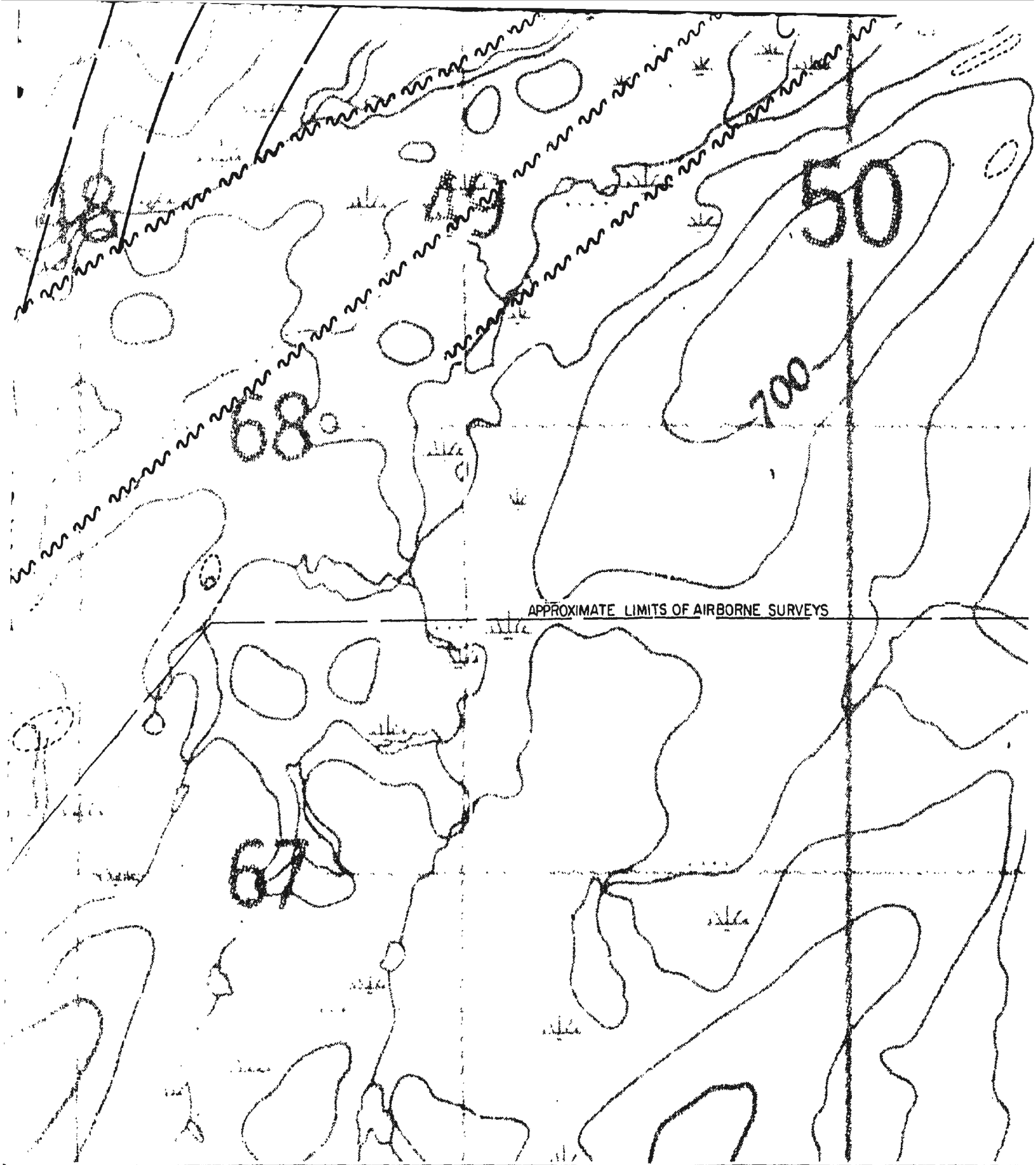
Silicic ash-flow tuffs. Crystals, lithic fragments, and vitroclasts; basal lithophase-rich horizons, grading up into a partially welded crystal-lithic lapilli tuff; broken phenocrysts of plagioclase, K-feldspar and quartz. Flattened pumice breccia up to a metre long; clasts of alkali feldspar, quartz and rarely basalt.

1:

Welded, basaltic andesite and basalt.

2:

Orange to red welded vitric tuff.

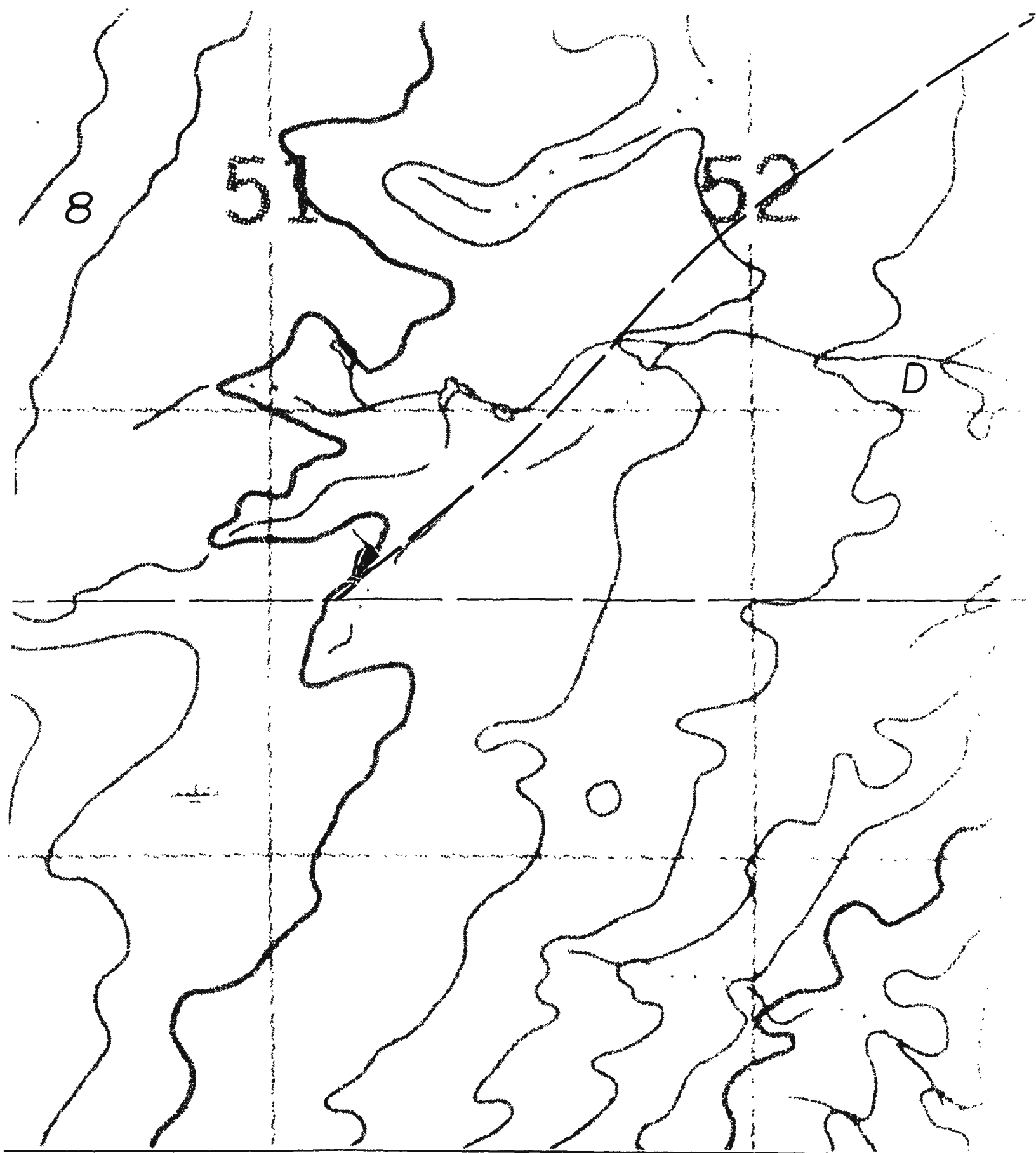


als, lithic fragments, and  
rich horizons, grading up  
stal-lithic lapilli tuff;  
se, K-feldspar and quartz;  
a metre long; clasts of  
rarely basalt.




1: Welded, lithic-crystal tuff. Plagioclase and K-feldspar,  
accessory biotite, quartz, and rare opaques, clasts of  
granophyre, plagiophyre basalt, andesite, ultramafics,  
and jasper.

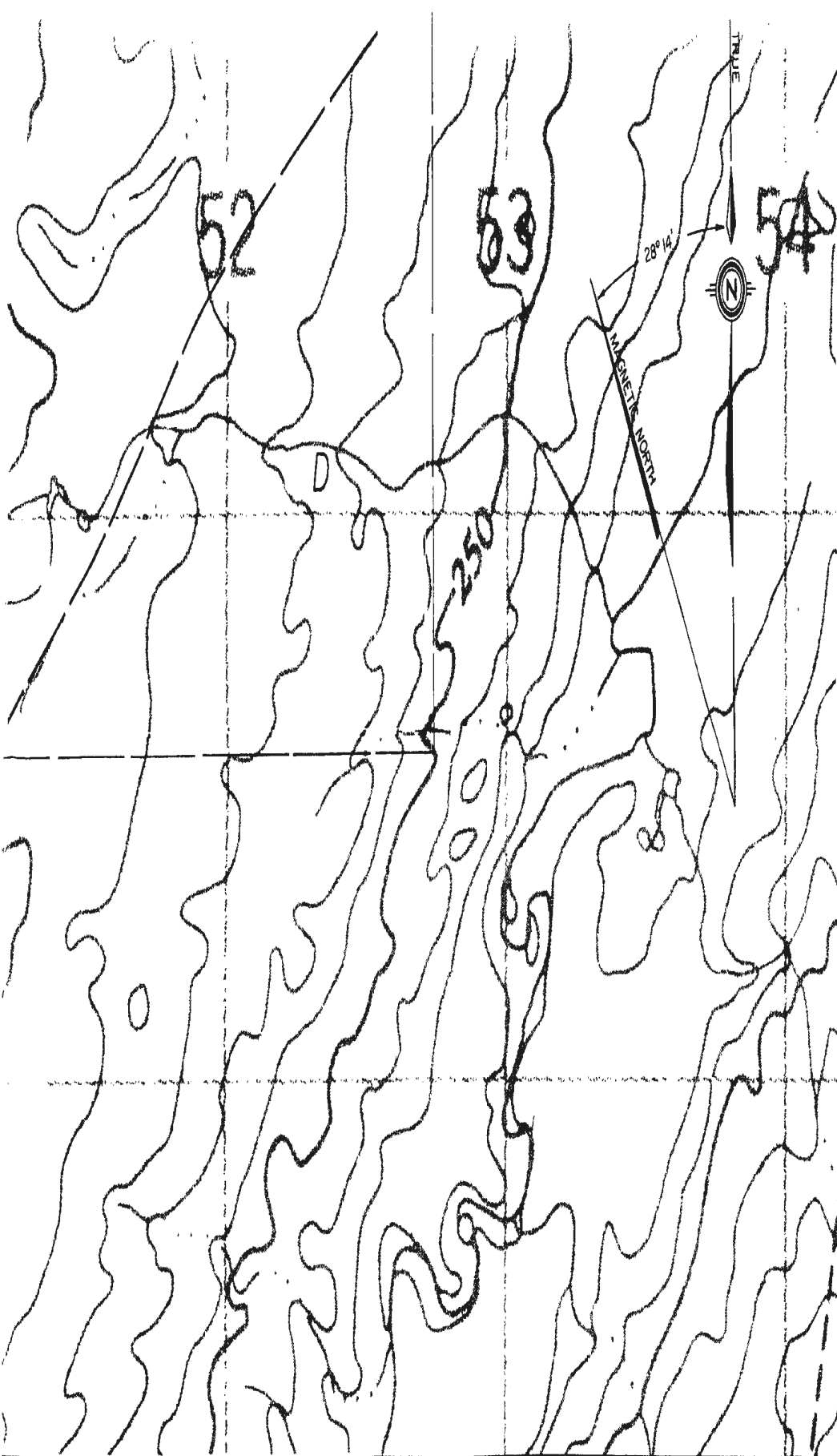
F: Orange to green quartz-K-feldspar porphyry with  
andesite, biotite and other acidine and related





SYMBOLS

- |                                                                                     |                                                      |
|-------------------------------------------------------------------------------------|------------------------------------------------------|
|  | MAJOR REGIONAL FAULT<br>(interpreted from magnetics) |
|  | FAULT                                                |
|  | BOUNDARY LINE                                        |



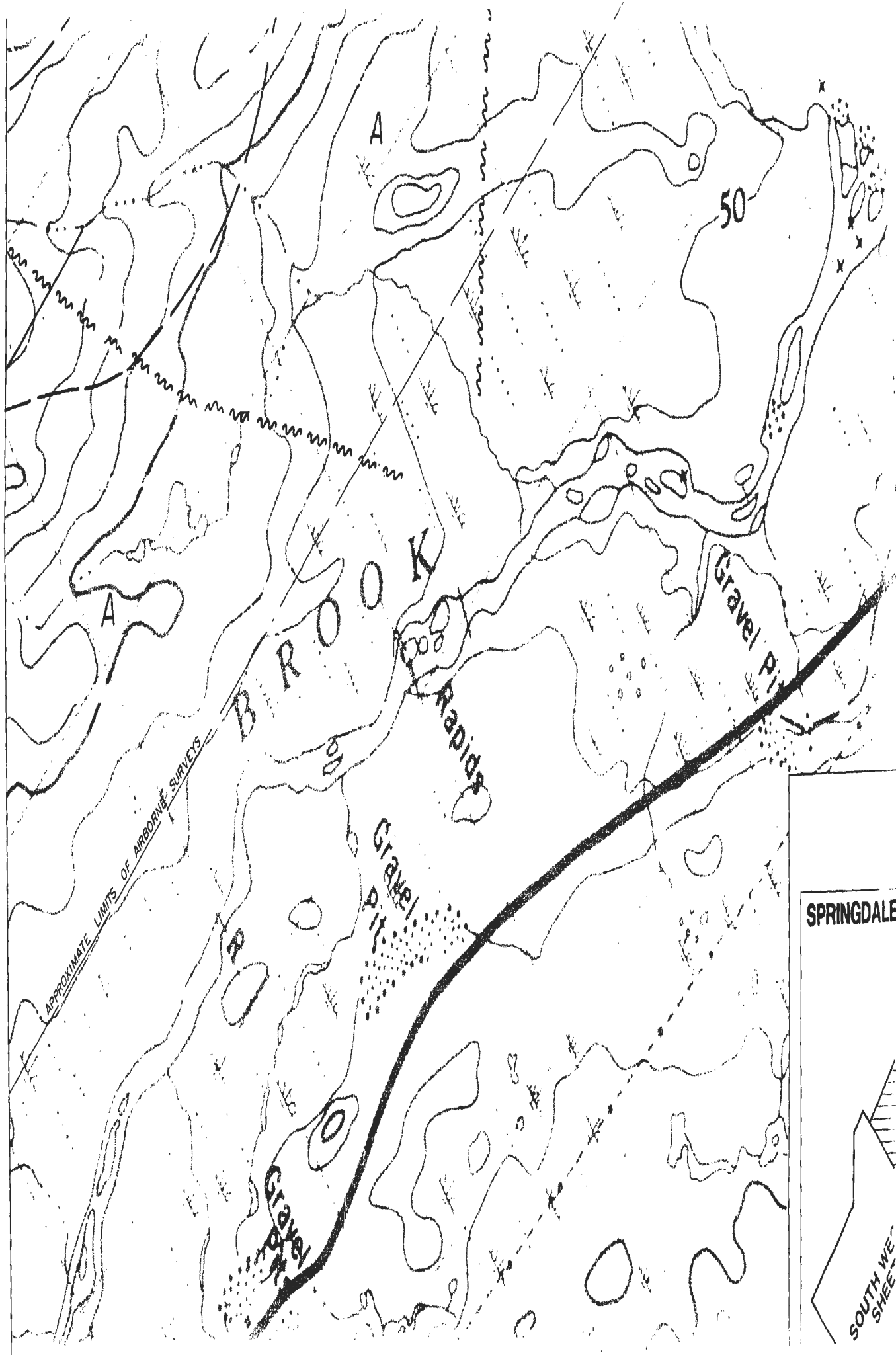
# **SYMBOLS**

MAJOR REGIONAL FAULT  
(interpreted from magnetics)

FAULT

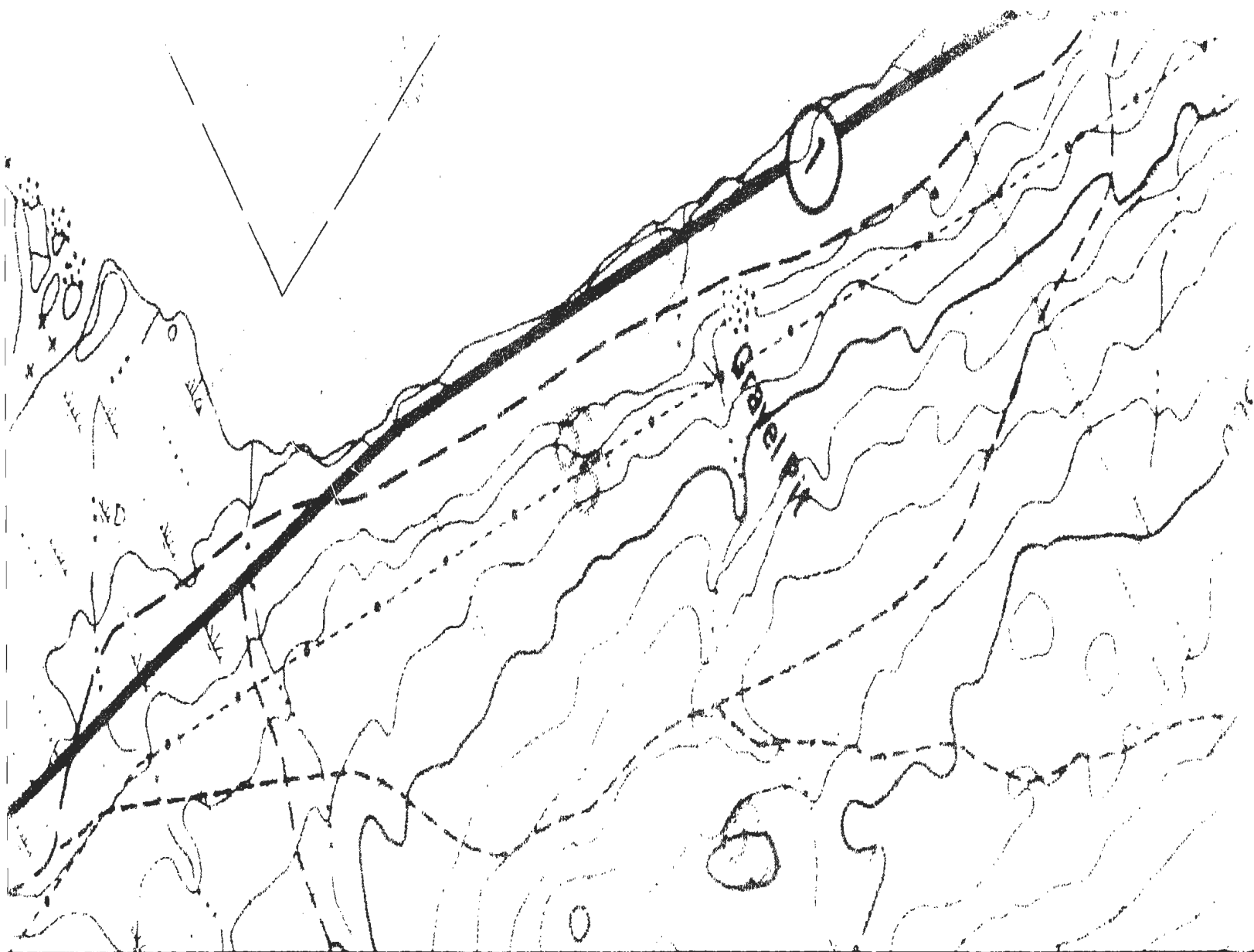
INDICATED CONTOUR

**MAP 2**



SPRINGDALE





# LEGEND

## SHEPHERD LAKE GROUP

- 12: Orange to red welded vitric tuff characterized by large sodic amphibole oikocrysts with rare resorbed K-feldspar phenocrysts.
- 11: Red and brown crystal, vitric and lithic ash-flow tuff sheets. Laharic, fault and gas breccias. Rhyolite domes and dykes and minor basalt occurrences.

## SPRINGDALE GROUP

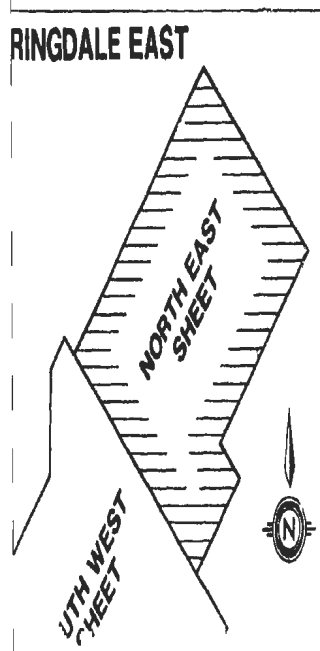
- 10: Crystal-lithic tuff. Densely welded and massive; large phenocrysts of quartz and feldspar, clasts of mafic and rare ultramafic lithologies.
- 9: Red clastic sedimentary rocks. Conglomerate, sandstone, and sandy siltstones, local caliche horizons; cross-bedding, ripples, laminations, rip-up horizons, scour channels, etc. indicate stream-flood, proximal and distal fluvial origin; clasts essentially volcanic or plutonic provenance.
- 8: Rhyolitic ash-flow vitric tuffs & breccias. Welded, devitrified, locally massive; areas of unwelded vitroclastic tuffs with large individually devitrified shards; locally passes into sandstone; alternating thin basaltic and siliceous bands indicate magma-mixing.
- 7: Dacitic to rhyolitic ash-flow tuffs, vitroclastic breccias and domes. Massive, vitric, strongly welded; curvilinear joint surfaces in the domes, with internal plastic shear zones, local brecciation, and flow folds; tuffs locally porphyritic, with small euhedral plagioclase and rare quartz phenocrysts in glassy matrix.
- 6: Siliceous ash-flow tuffs. Crystals, lithic fragments, and vitroclasts; basal lithology and textures, grading up into a partially welded vitroclastic breccia; the broken phenocrysts of quartz and feldspar and quartz

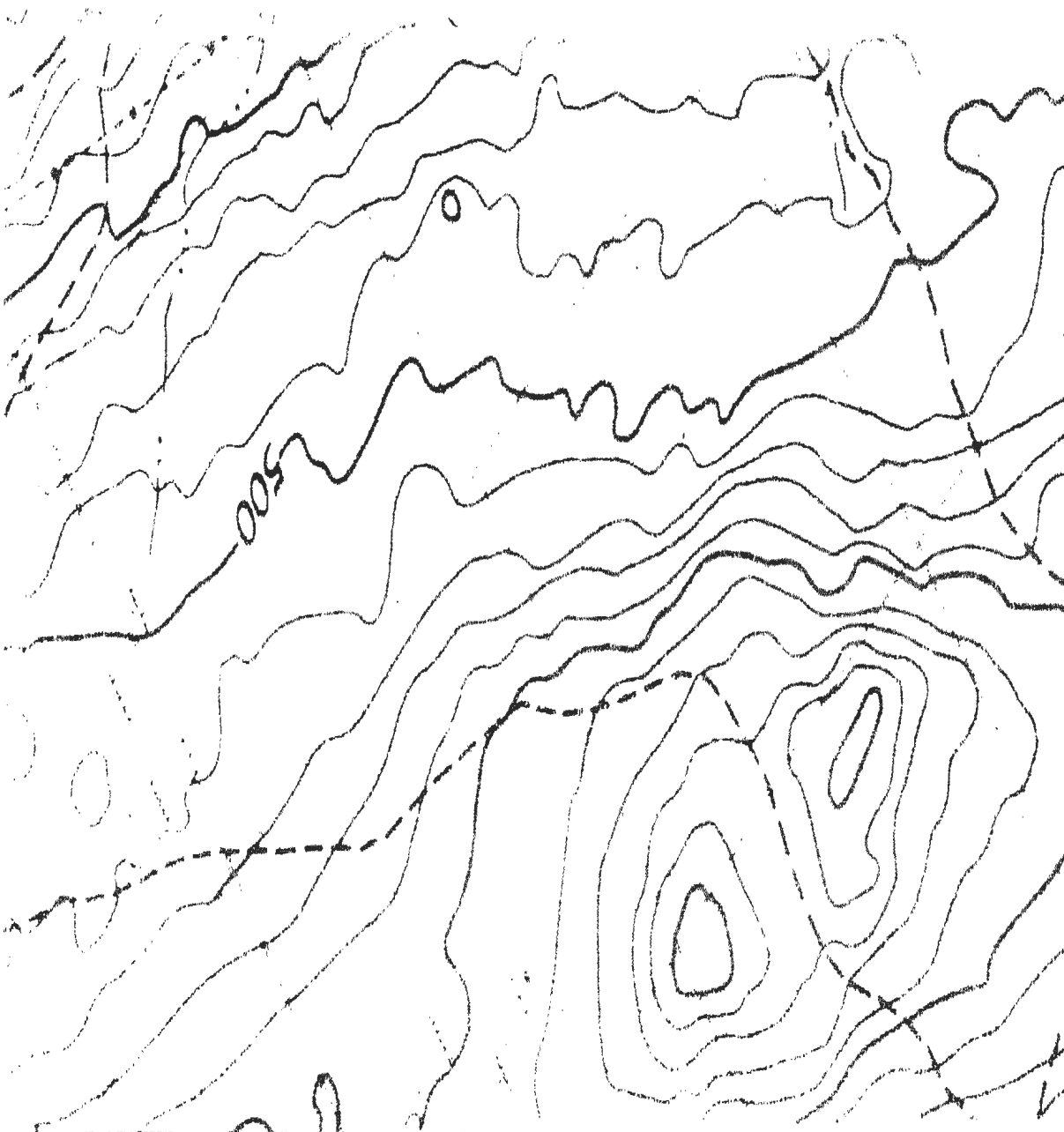
- 4: Felsic to intermediate, dominantly dacitic, tuff. Crystal-lithic and lapilli ash-flow tuffs; clasts of andesite, rhyolite, angular and flattened pumice; variably welded.
- 3: Andesitic to dacitic flows.
- 3a: Massive porphyritic andesite-dacite intrusive domes and flows.
- 3b: Lithic/lapilli andesitic-dacite ash-flow tuff with variable welding and weak argillite and carbonate-chlorite alteration.
- 3c: Dacitic-andesitic autoclastic apron of reworked volcanic debris around the domes of unit 3a.
- 2: Megabreccia. Laharic flows, tuffites and peperites, volcanic conglomerates and breccias, red sandstones.
- 1: Welded, lithic-crystal tuff. Plagioclase and K-feldspar, accessory biotite, quartz, and rare opaque, clasts of granophyre, plagiophyre basalt, andesite, ultramafics, and jasper.
- F: Orange to green quartz-K-feldspar porphyry with sodic amphibole oikocrysts and minor actinolite and altered fayalite.
- G: Medium to coarse grained granite, characterized by quartz and pink feldspar with finer grained crystals of black amphibole, intruded by finer grained whitish grey granite, with locally riebeckite pegmatite and abundant amphibole-lined staurolitic cavities and fractures; offshoots of the Topopahs Complex.
- D: Red medium grained granite to quartz syenite. Phenocrysts of K-feldspar, amphibole and biotite.
- C: High-silica domes, dykes and sills. Microphenocrysts of quartz and feldspar, with finely disseminated black-green amphibole (ferrohornblende) in matrix. Black feldspar and biotite, some of which may be part of the same phenocryst.

## SYMBOLS







- MAJOR FAULT
- FAULT
- TRAIL
- CONTOUR
- WATER
- ROAD

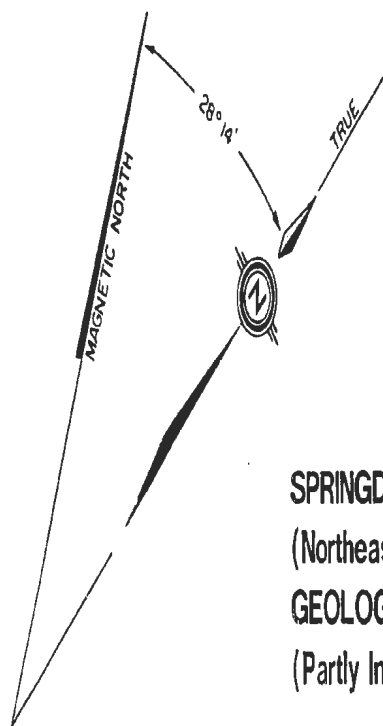
## RINGDALE EAST





#### SYMBOLS

-  MAJOR REGIONAL FAULT  
(Interpreted from magnetics)
-  FAULT
-  GEOLOGICAL CONTACT
-  SYNCLINE
-  ANTICLINE
-  FOLIATION (including, vertical)

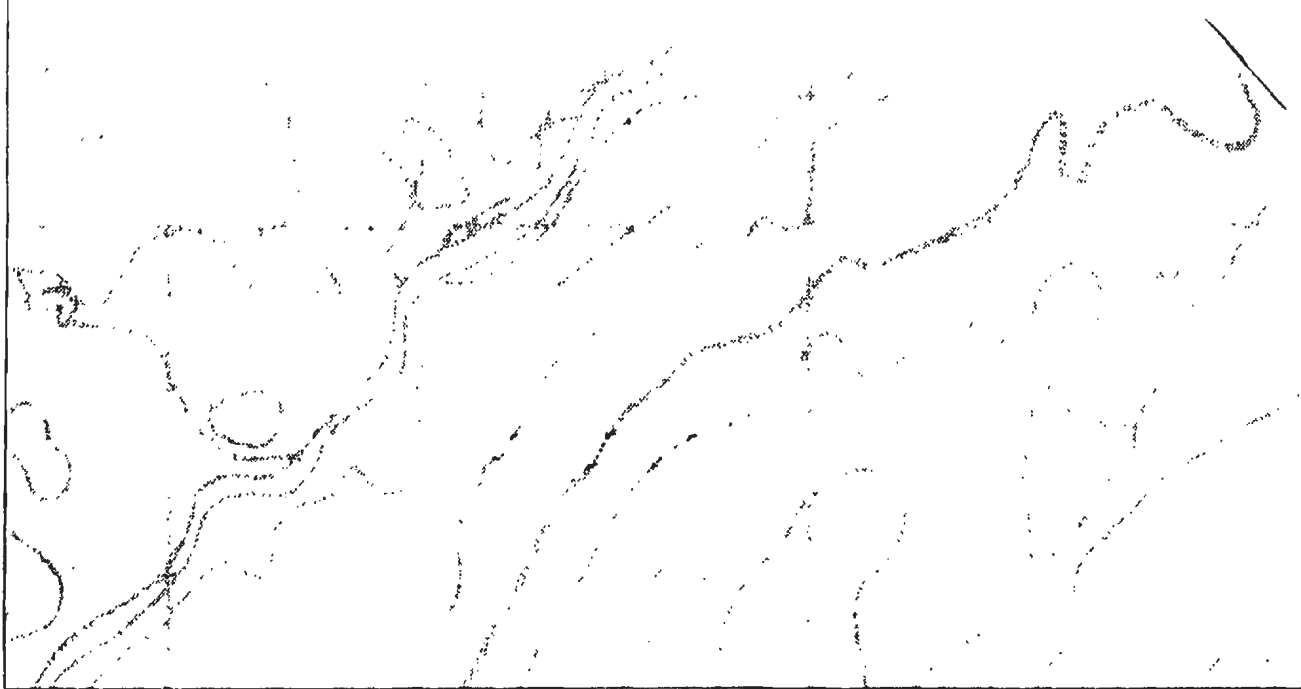


### MAP 3

SPRINGDALE EAST  
(Northeast Sheet)

GEOLOGY

(Partly Inferred from Aeromagnetics)



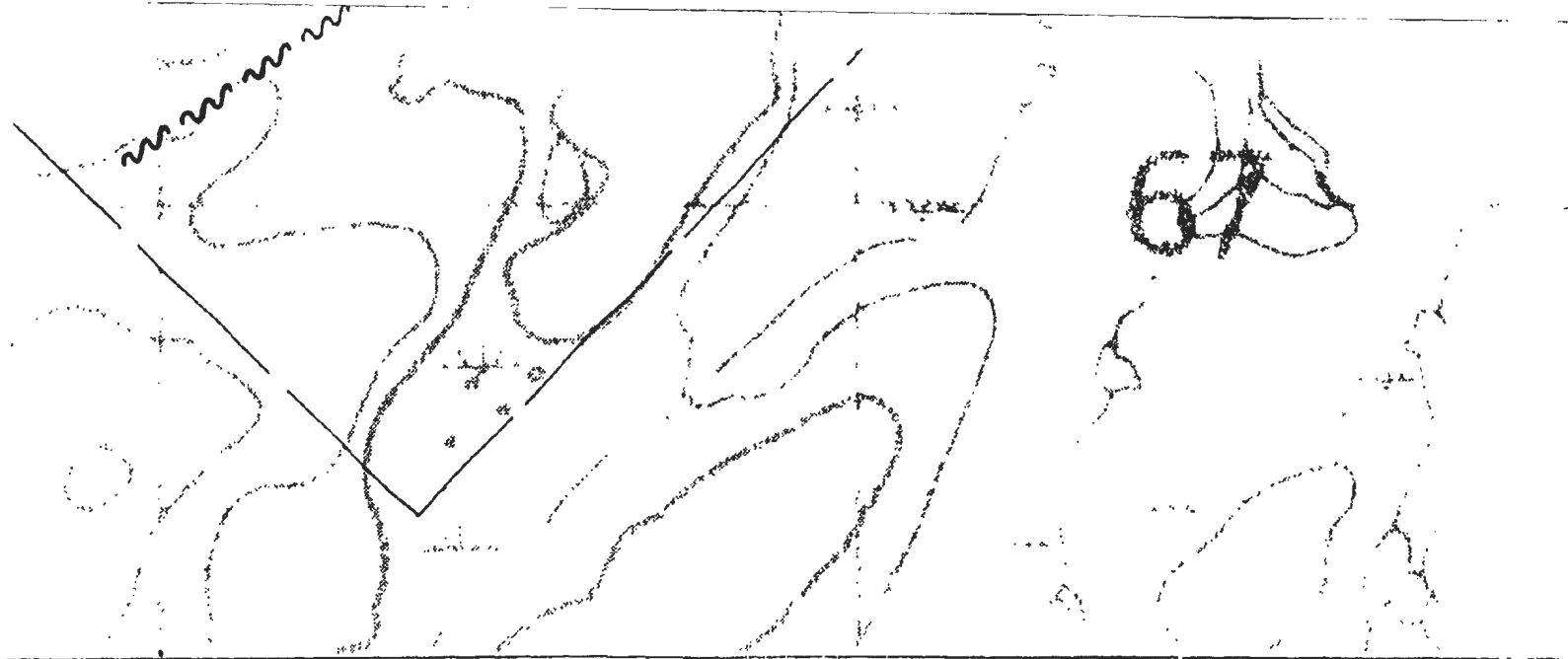
# **LEGEND**

## **SHEFFIELD LAKE GROUP**

- 12: Orange to red welded vitric tuff characterized by large sodic amphibole oligocrysts with rare resorbed K-feldspar phenocrysts.
- 11: Red and brown crystal, vitric and lithic ash-flow tuffs, Lahatic, fault and gas breccias. Rhyolite dikes and dykes and minor basalt occurrences.

## **SPRINGDALE GROUP**

- 10: Crystal-lithic tuff. Densely welded and massive; large phenocrysts of quartz and feldspar, clasts of mafic and rare ultramafic lithologies.
- 9: Red clastic sedimentary rocks. Conglomerate, sandstone and sandy siltstones, local caliche horizons; cross-bedding, ripples, laminations, slip-up horizons, sc channels, etc. indicate stream-flood, proximal and distal fluvial origin; clasts essentially volcanic and plutonic provenance.
- 8: Rhyolitic ash-flow vitric tuffs and breccias. Well devitrified, locally massive; areas of unwelded vitroclastic tuffs with large individually devitrified shards; locally passes into sandstone; alternating basaltic and silicic bands indicate magma-mixing.
- 7: Dacitic to rhyolitic ash-flow tuffs, vitroclastic breccias and domes. Massive, vitric, strongly welded; curvilinear joint surfaces in the domes, with internal plastic slip zones, local brecciation, and flow folds; tuffs locally porphyritic, with small euhedral plagioclase and quartz phenocrysts in glassy matrix.



large  
spat  
  
uff  
mes

large  
and

one,  
ss-  
our  
stal  
or

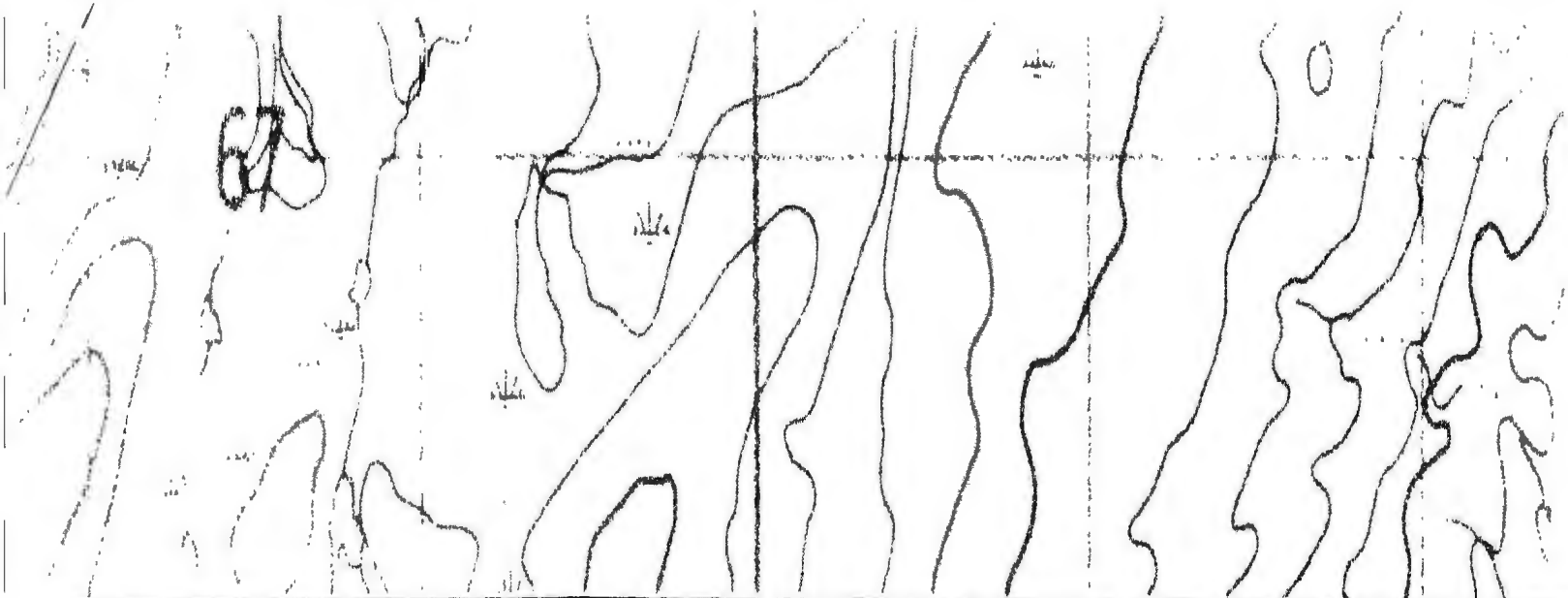
bed,  
lded  
ied  
thin

cia  
nar  
reat  
ally  
late

- 6: Silicic ash-flow tuffs. Crystals, lithic fragments, and vitroclasts; basal lithophysac-rich horizons, grading up into a partially welded crystal-lithic lapilli tuff; broken phenocrysts of plagioclase, K-feldspar and quartz; flattened pumice bombs up to a metre long; clasts of silicic volcanics, andesite and rarely basalt.
- 5: Mainly basaltic flows, some of intermediate composition.
  - 5a: Thin flows of basaltic andesite with plagioclase and minor amphibole phenocrysts, non-vesicular and massive to trachytic-textured.
  - 5b: Thick basaltic flows with plagioclase phenocrysts, and abundant quartz, chlorite, epidote and calcite in vesicles and fault zones.
- 4: Felsic to intermediate, dominantly dacite, tuff. Crystal-lithic and lapilli ash-flow tuffs; clasts of andesite, rhyolite, angular and flattened pumice; variably welded.
- 3: Andesitic to dacitic flows.
  - 3a: Massive porphyritic andesite-dacite intrusive domes and flows.
  - 3b: Lithic/lapilli andesitic-dacitic ash-flow tuff with variable welding and weak argillic and carbonate-chlorite alteration.
  - 3c: Dacitic-andesitic autoclastic apron of reworked volcanic debris around the domes of unit 3a.
- 2: Megabreccia. Laharic flows, tuffites and peperites, volcanic conglomerates and breccias, red sandstones.

- I: Welded, lithic crystal-lithic tuff. Accessory to 6A, granophyre, rhyolite and Jasper.
- F: Orange to green green amphibole andesite fayalite.
- B: Medium to coarse grained pink feldspar amphibole, quartz granite, with small amphibole-lithic offshoots.
- D: Red medium grained of F-feldspar, amphibole.
- C: High-silica domes, quartz and feldspar bluish-green, often foliated, and thin of spherulitic texture.
- B: Black fine-grained
- A: Amphibolite, horn amphibolite, and xenoliths in granite, locally granite.





thin, lithic fragments, and  
 7-10 inch boulders, grading up  
 to 1-2 foot lapilli tuff;  
 coarse, K-feldspar and quartz;  
 1-2 meter long; clasts of  
 and rarely basalt.

of intermediate composition.  
 andesite with plagioclase and  
 microcrystalline and massive to  
 plagioclase phenocrysts, and  
 epidote and calcite in

dominantly dacite, tuff.  
 ash-flow tuffs; clasts of  
 in and flattened pumice;

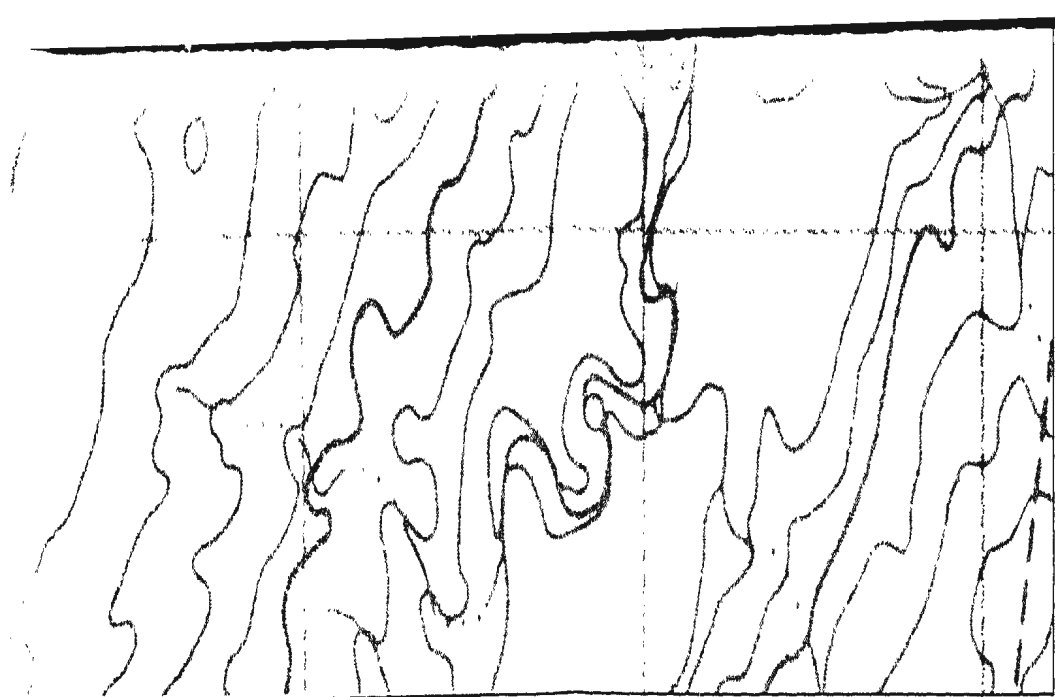
te-dacite intrusive domes and  
 typical ash-flow tuff with  
 plagioclase and calcite-chlorite  
 to apron of reworked volcanic  
 unit 1a.

pyroxenes and pyropeites,  
 nepheline, and sanidine.


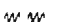






- 1: Welded, lithic-crystal tuff. Plagioclase and K-feldspar, accessory biotite, quartz, and rare opaques, clasts of granophyre, plagiophytic basalt, andesite, ultramafics, and jasper.
- F: Orange to green quartz-K-feldspar porphyry with sodic amphibole oikocrysts and minor aegirine and altered fayalite.
- E: Medium to coarse grained granite, characterized by quartz and pink feldspar with finer grained crystals of black amphibole, intruded by finer grained whitish gray granite, with locally riebeckite pegmatite and abundant amphibole-lined microlitic cavities and fractures; offshoots of the Topsails Complex.
- D: Red medium grained granite to quartz syenite. Phenocrysts of K-feldspar, amphibole and biotite.
- C: High-silica domes, dykes and sills. Microphenocrysts of quartz and feldspar, with finely disseminated bluish-green amphibole (riebeckite) in groundmass; flow-foliated, auto-brecciated, zones of intense development of spherules and other indications of gas-streaming.
- B: Black fine-grained massive microdiorite.
- A: Amphibolite, diorite, granodiorite, granite. Foliated amphibolite and gabbro occurring as large screens and xenoliths in foliated diorite and granodiorite; intruded by variably deformed tonalite and amphibole-biotite granite; intruded or net veined by a pale fine-grained granite.

# SYMBOLS

- MAJOR REGIONAL FAULT  
 (Interpreted from magnetics)
- FAULT
- GEOLOGICAL CONTACT
- SYNCLINE
- ANTICLINE
- FOLIATION (including, vertical)
- LIMIT OF OUTCROP
- TREND OF MAGNETIC HIGH



#### SYMBOLS

-  MAJOR REGIONAL FAULT  
(Interpreted from magnetics)
-  FAULT
-  GEOLOGICAL CONTACT
-  SYNCLINE
-  ANTICLINE
-  FOLIATION (including, vertical)
-  LIMIT OF OUTCROP
-  TREND OF MAGNETIC HIGH

## MAP 2

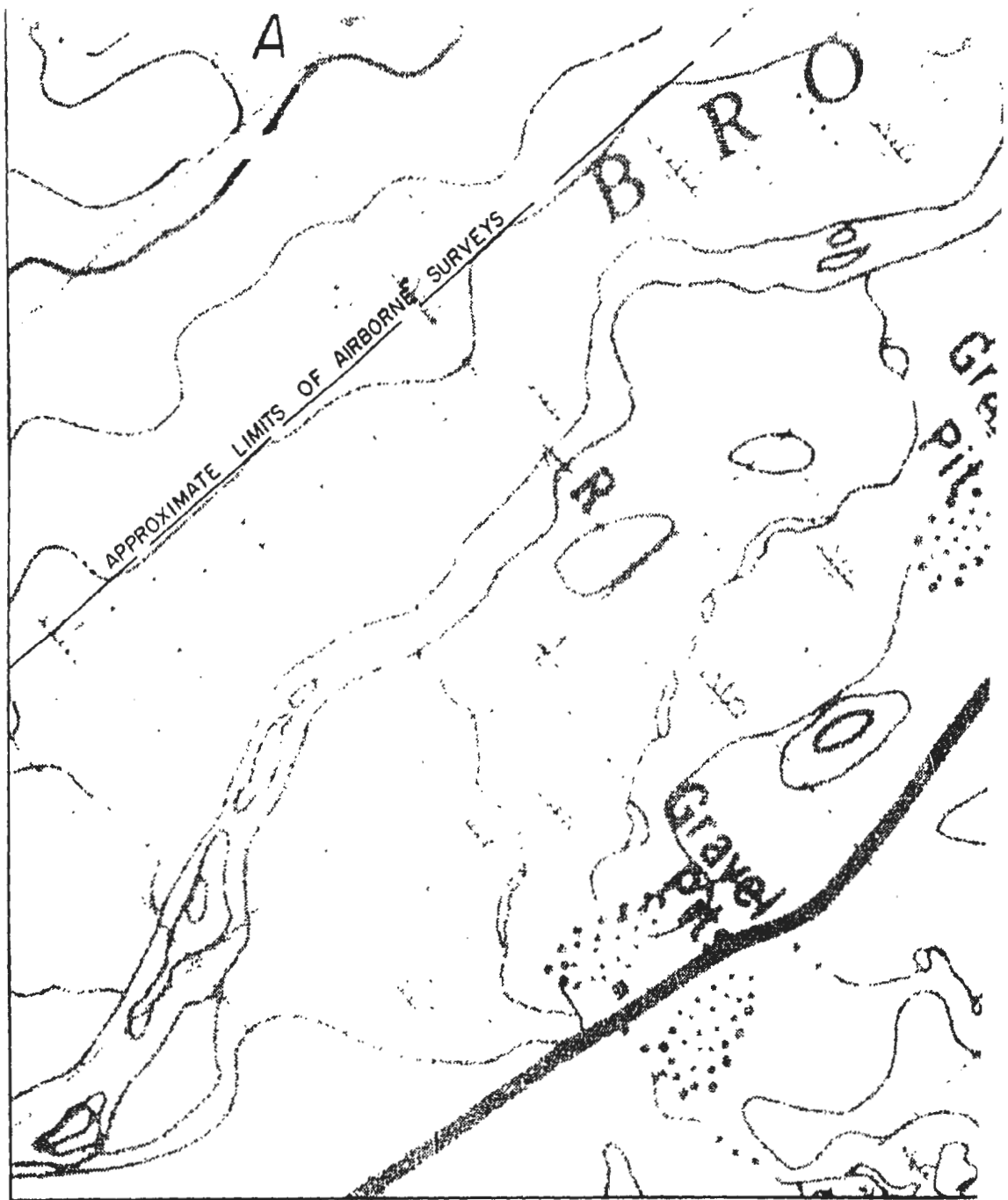
### SPRINGDALE CENTRE

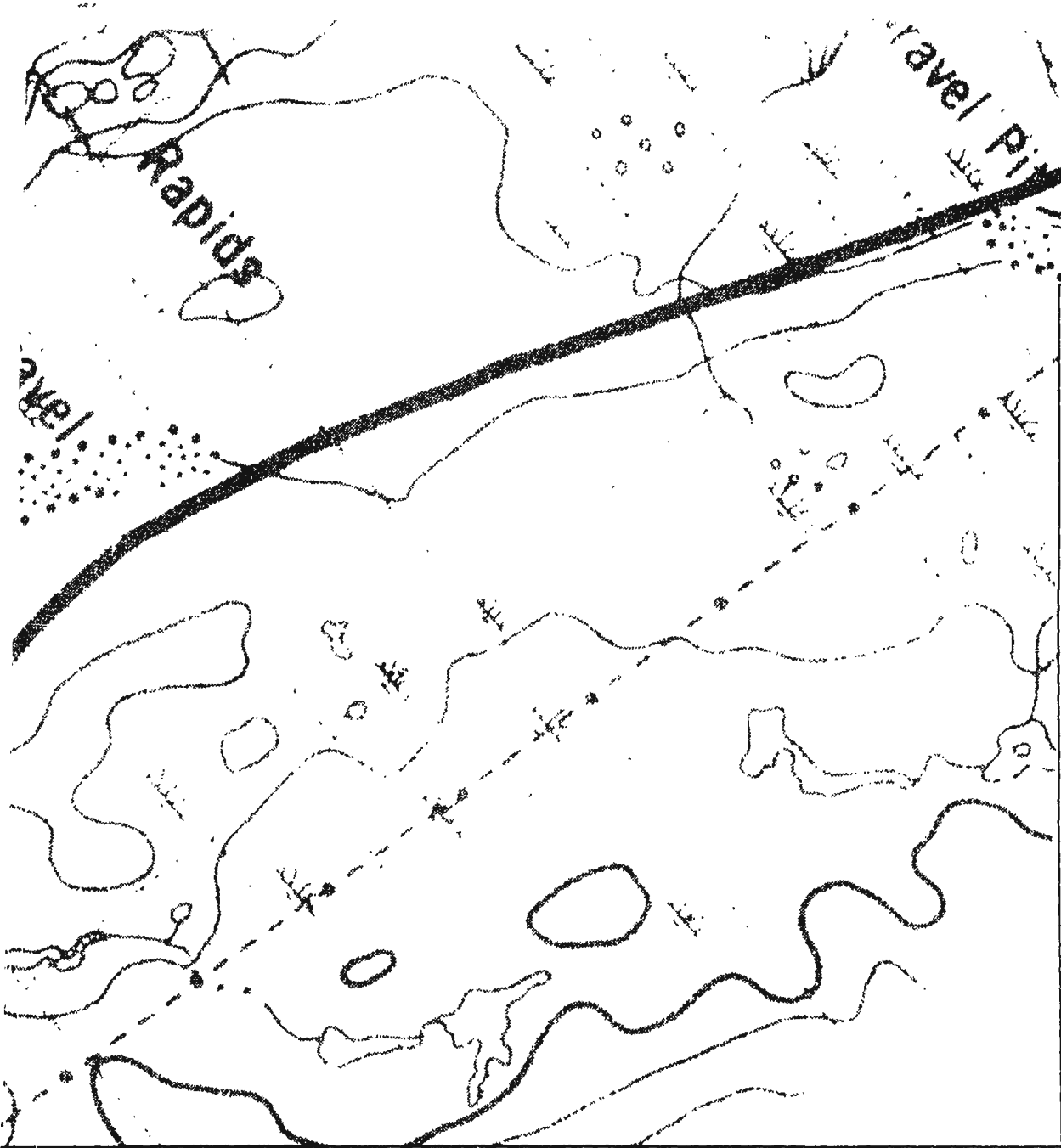
### GEOLOGY

(Partly Inferred from Aeromagnetics)

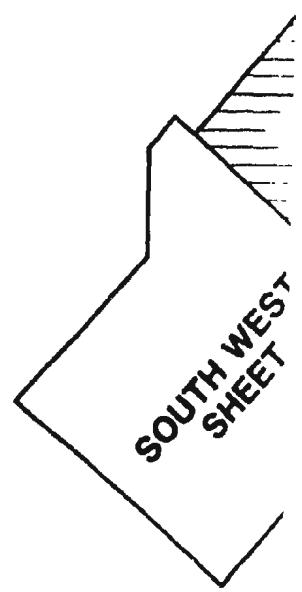
M. Coyle, Ph. D. Thesis, 1990.

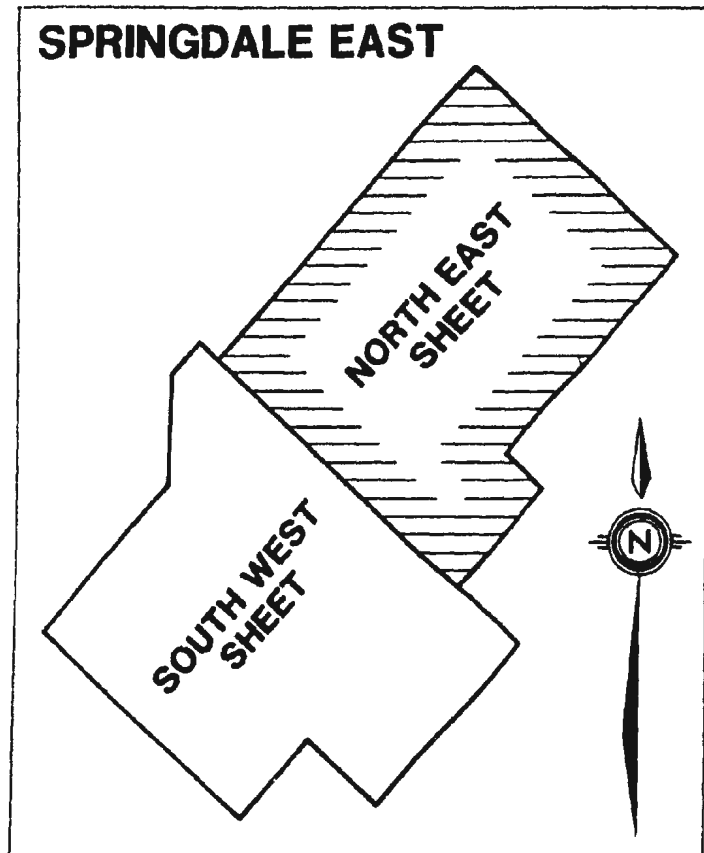






**SPRINGDALE**





## LEGEND

### SHEPPFIELD LAKE GROUP

- 12:** Orange to red welded vitric tuff characterized by sodic amphibole oikocrysts with rare resorbed K-feldspar phenocrysts.
- 11:** Red and brown crystal, vitric and lithic ash-flow sheets. Lahatic, fault and gas breccias. Rhyolite and dykes and minor basalt occurrences.

### SPRINGDALE GROUP

- 10:** Crystal-lithic tuff. Densely welded and massive; phenocrysts of quartz and feldspar, clasts of mafic rare ultramafic lithologies.
- 9:** Red clastic sedimentary rocks. Conglomerate, sand and sandy siltstones, local caliche horizons; bedding, ripples, laminations, rip-up horizons, channels, etc. indicate stream-flood, proximal and fluvial origin; clasts essentially volcanic plutonic provenance.
- 8:** Rhyolitic ash-flow vitric tuffs and breccias. Devitrified, locally massive; areas of vitroclastic tuffs with large individually devitrified shards; locally passes into sandstone; alternating basaltic and silicic bands indicate magma-mixing.
- 7:** Dacitic to rhyolitic ash-flow tuffs, vitroclastic and domes. Massive, vitric, strongly welded; curved joint surfaces in the domes, with internal plastic zones, local brecciation, and flow folds; tuffs porphyritic, with small euhedral plagioclase and quartz phenocrysts in glassy matrix.
- 6:** Silicic ash-flow tuffs. Crystals, lithic fragments, vitroclasts; basal lithophysae-rich horizons, gray into a partially welded crystal-lithic lapilli broken phenocrysts of plagioclase, K-feldspar and flattened pumice bombs up to a metre long; clastic silicic volcanics, andesite and rarely basalt.
- 5:** Mainly basaltic flows, some of intermediate composition.
- 5a:** Thin flows of basaltic andesite with plagioclase and minor amphibole phenocrysts, non-vesicular and massive trachytic-textured.
- 5b:** Thick basaltic flows with plagioclase phenocrysts, abundant quartz, chlorite, epidote and calcic vesicles and fault zones.

large  
feldspar

tuff  
domes

large  
lc and

stone,  
cross-  
scour  
distal  
lc or

welded,  
welded  
ified  
g thin









breccia  
planar  
shear  
locally  
d rate

ts, and  
ding up  
tuff;  
quartz;  
sts of








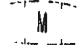
ition,  
se and  
sive to  
ts, and  
ite in

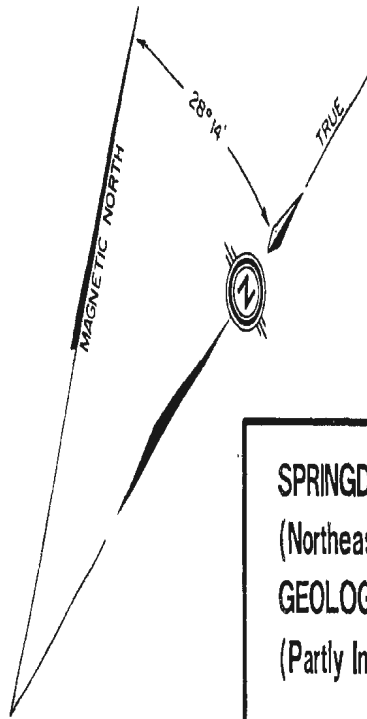
- 4: Felsic to intermediate, dominantly dacite, tuff. Crystal-lithic and lapilli ash-flow tuffs; clasts of andesite, rhyolite, angular and flattened pumice; variably welded.
- 3: Andesitic to dacitic flows.  
3a: Massive porphyritic andesite-dacite intrusive domes and flows.  
3b: Lithic/lapilli andesitic-dacitic ash-flow tuff with variable welding and weak argillic and carbonate-chlorite alteration.  
3c: Dacitic-andesitic autoclastic apron of reworked volcanic debris around the domes of unit 3a.
- 2: Megabreccia. Laharic flows, tuffites and pepperites, volcanic conglomerates and breccias, red sandstones.
- 1: Welded, lithic-crystal tuff. Plagioclase and K-feldspar, accessory biotite, quartz, and rare opaques, clasts of granophyre, plagiophytic basalt, andesite, ultramafics, and jasper.
- F: Orange to green quartz-K-feldspar porphyry with sodic amphibole oikocrysts and minor aegirine and altered fayalite.
- E: Medium to coarse grained granite, characterized by quartz and pink feldspar with finer grained crystals of black amphibole, intruded by fine grained whitish grey granite, with locally riebeckite pegmatite and abundant amphibole-lined miatolitic cavities and fractures; offshoots of the Topsails Complex.
- D: Red medium grained granite to quartz syenite. Phenocrysts of K-feldspar, amphibole and biotite.
- C: High-silica domes, dykes and sills. Microphenocrysts of quartz and feldspar, with finely disseminated bluish-green amphibole (riebeckite) in groundmass; flow-foliated, auto-brecciated, zones of intense development of spherules and other indications of gas-streaming.
- B: Black fine-grained massive microdiorite.
- A: Amphibolite, diorite, granodiorite, granite. Foliated amphibolite and gabbro occurring as large screens and xenoliths in foliated diorite and granodiorite; intruded by variably deformed tonalite and amphibole-biotite granite; intruded or net veined by a pale fine-grained granite.

SYMBOLS

-  MAGMA  
FLOW
-  FAULT
-  GULL
-  TONALITE
-  ANDERITE
-  DIORITE
-  LIMB
-  TONALITE

# **SYMBOLS**

-  MAJOR REGIONAL FAULT  
(interpreted from magnetics)
-  FAULT
-  GEOLOGICAL CONTACT
-  SYNCLINE
-  ANTICLINE
-  FOLIATION (including, vertical)
-  LIMIT OF OUTCROP
-  TREND OF MAGNETIC HIGH



## **MAP 3**

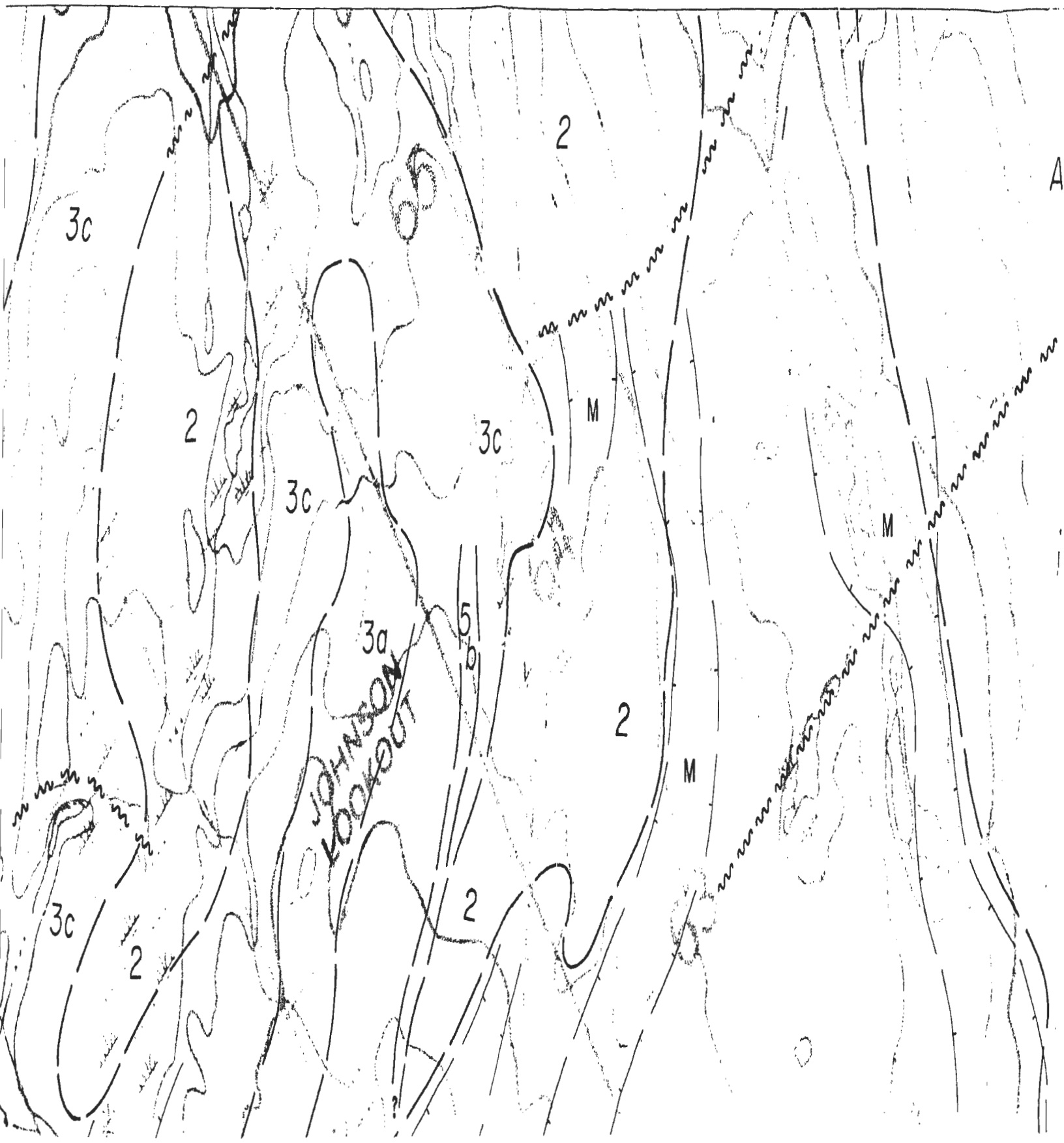
**SPRINGDALE EAST**  
 (Northeast Sheet)  
**GEOLOGY**  
 (Partly Inferred from Aeromagnetics)

**M. Coyle, Ph. D. Thesis, 1990.**









2013



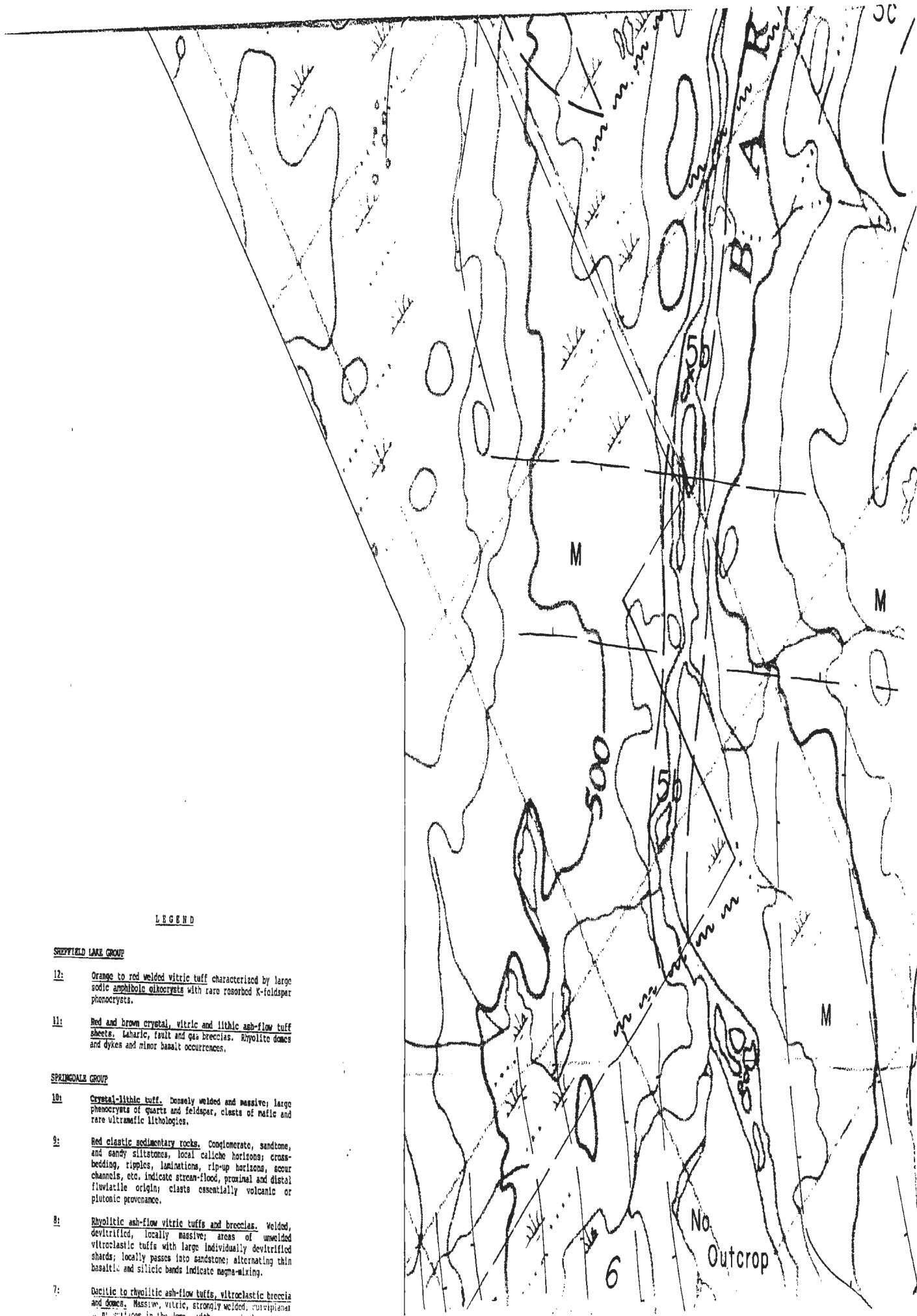
# LEGEND

## SHEPHERD LAKE GROUP

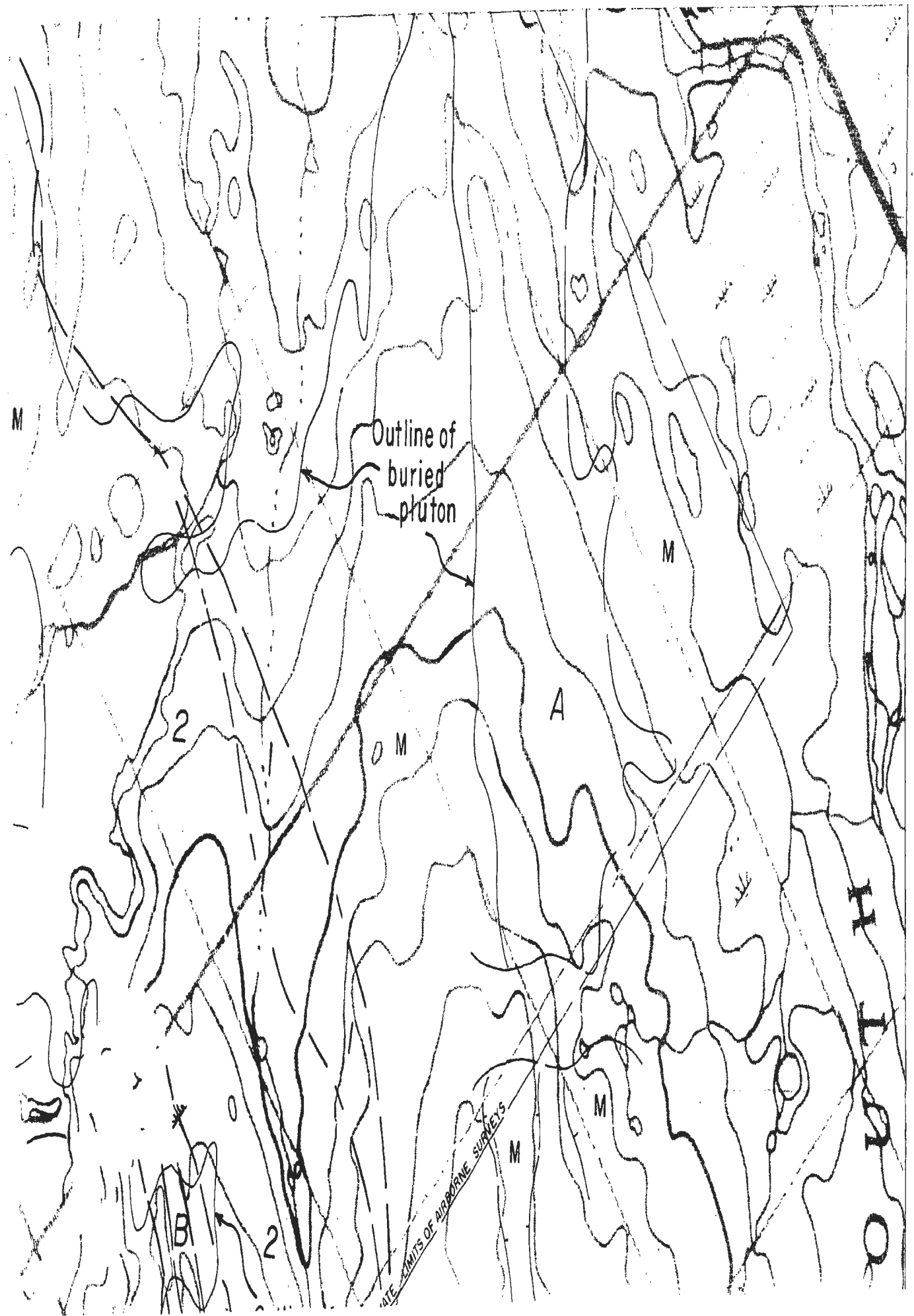
- 12: Orange to red welded vitric tuff characterized by large sodic amphibole oligoclase with rare resorbed K-feldspar phenocrysts.
- 11: Red and brown crystal, vitric and lithic ash-flow tuff sheets. Laharic, fault and gas breccias. Rhyolite domes and dykes and minor basalt occurrences.

## SPRINGMOUNT GROUP

- 10: Crystal-lithic tuff. Densely welded and massive; large phenocrysts of quartz and feldspar, clasts of mafic and rare ultramafic lithologies.
- 9: Red clastic sedimentary rocks. Conglomerate, sandstone, and sandy siltstones, local caliche horizons; cross-bedding, ripples, laminations, rip-up horizons, scour channels, etc. indicate stream-flood, proximal and distal fluvial origin; clasts essentially volcanic or plutonic provenance.
- 8: Rhyolitic ash-flow vitric tuffs and breccias. Welded, devitrified, locally massive; areas of unwelded vitroclastic tuffs with large individually devitrified shards; locally passes into sandstone; alternating thin basaltic and silicic bands indicate magma-mixing.
- 7: Dacitic to rhyolitic ash-flow tuffs, vitroclastic breccia and domes. Massive, vitric, strongly welded, outcrops as a surface in the dome, with



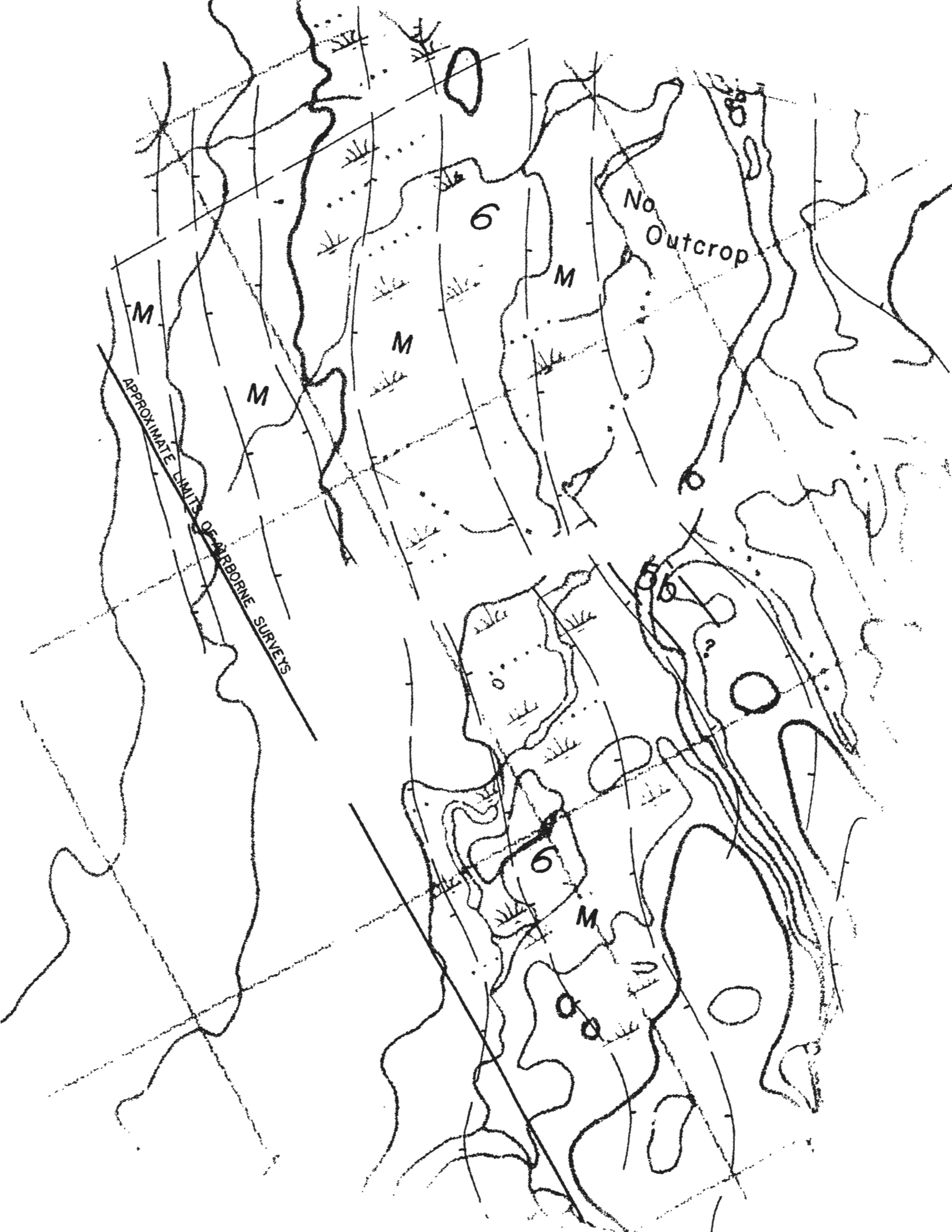




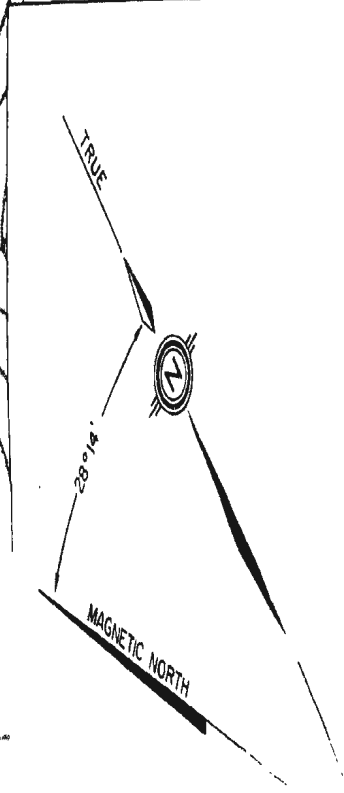
SPRINGDALE GROUP

- 10:** Crystal-lithic tuff. Densely welded and massive; large phenocrysts of quartz and feldspar, clasts of mafic and rare ultramafic lithologies.
- 9:** Red clastic sedimentary rocks. Conglomerate, sandstone, and sandy siltstones, local caliche horizons; cross-bedding, ripples, laminations, rip-up horizons, scour channels, etc. indicate stream-flood, proximal and distal fluvial origin; clasts essentially volcanic or plutonic provenance.
- 8:** Rhyolitic ash-flow vitric tuffs and breccias. Welded, devitrified, locally massive; areas of unwelded vitroclastic tuffs with large individually devitrified shards; locally passes into sandstone; alternating thin basaltic and silicic bands indicate magma-mixing.
- 7:** Dacitic to rhyolitic ash-flow tuffs, vitroclastic breccia and domes. Massive, vitric, strongly welded; curvilinear joint surfaces in the domes, with internal plastic shear zones, local brecciation, and flow folds; tuffs locally porphyritic, with small euhedral plagioclase and rare quartz phenocrysts in glassy matrix.
- 6:** Silicic ash-flow tuffs. Crystals, lithic fragments, and vitroclasts; basal lithophysae-rich horizons, grading up into a partially welded crystal-lithic lapilli tuff; broken phenocrysts of plagioclase, K-feldspar and quartz; flattened pumice bombs up to a metre long; clasts of silicic volcanics, andesite and rarely basalt.
- 5:** Mainly basaltic flows, some of intermediate composition.  
**5a:** Thin flows of basaltic andesite with plagioclase and minor amphibole phenocrysts, non-vesicular and massive to trachytic-textured.  
**5b:** Thick basaltic flows with plagioclase phenocrysts, and abundant quartz, chlorite, epidote and calcite in vesicles and fault zones.
- 4:** Felsic to intermediate, dominantly dacite, tuff. Crystal-lithic and lapilli ash-flow tuffs; clasts of andesite, rhyolite, angular and flattened pumice; variably welded.
- 3:** Andesitic to dacitic flows.  
**3a:** Massive porphyritic andesite-dacite intrusive domes and flows.  
**3b:** Lithic/lapilli andesitic-dacitic ash-flow tuff with variable welding and weak argillic and carbonate-chlorite alteration.  
**3c:** Dacitic-andesitic autoclastic apron of reworked volcanic debris around the domes of unit 3a.
- 2:** Megabreccia. Laharic flows, tuffites and pepperites, volcanic conglomerates and breccias, red sandstones.
- 1:** Welded, lithic-crystal tuff. Plagioclase and K-feldspar, al. m. biotite, quartz, and rare opaques, clasts of granophyre, plagiophytic basalt, andesite, ultramafics, and jasper.
- F:** Orange to green quartz-K-feldspar porphyry with sodic amphibole oikocrysts and minor aegirine and altered fayalite.
- E:** Medium to coarse grained granite, characterized by quartz and pink feldspar with finer grained crystals of black amphibole, intruded by finer grained whitish grey granite, with locally riebeckite pegmatite and abundant amphibole-linedmiarolitic cavities and fractures; offshoots of the Topsails Complex.
- D:** Red medium grained granite to quartz syenite. Phenocrysts of K-feldspar, amphibole and biotite.
- C:** High-silica domes, dykes and sills. Microphenocrysts of quartz and feldspar, with finely disseminated bluish-green amphibole (riebeckite) in groundmass; flow-foliated, auto-brecciated, zones of intense development of spherules and other indications of gas-streaming.
- B:** Black fine-grained massive microdiorite.
- A:** Amphibolite, diorite, granodiorite, granite. Foliated amphibolite and gabbro occurring as large screens and xenoliths in foliated diorite and granodiorite; intruded by variably deformed tonalite and amphibole-biotite granite; intruded or net veined by a pale fine-grained granite.







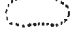



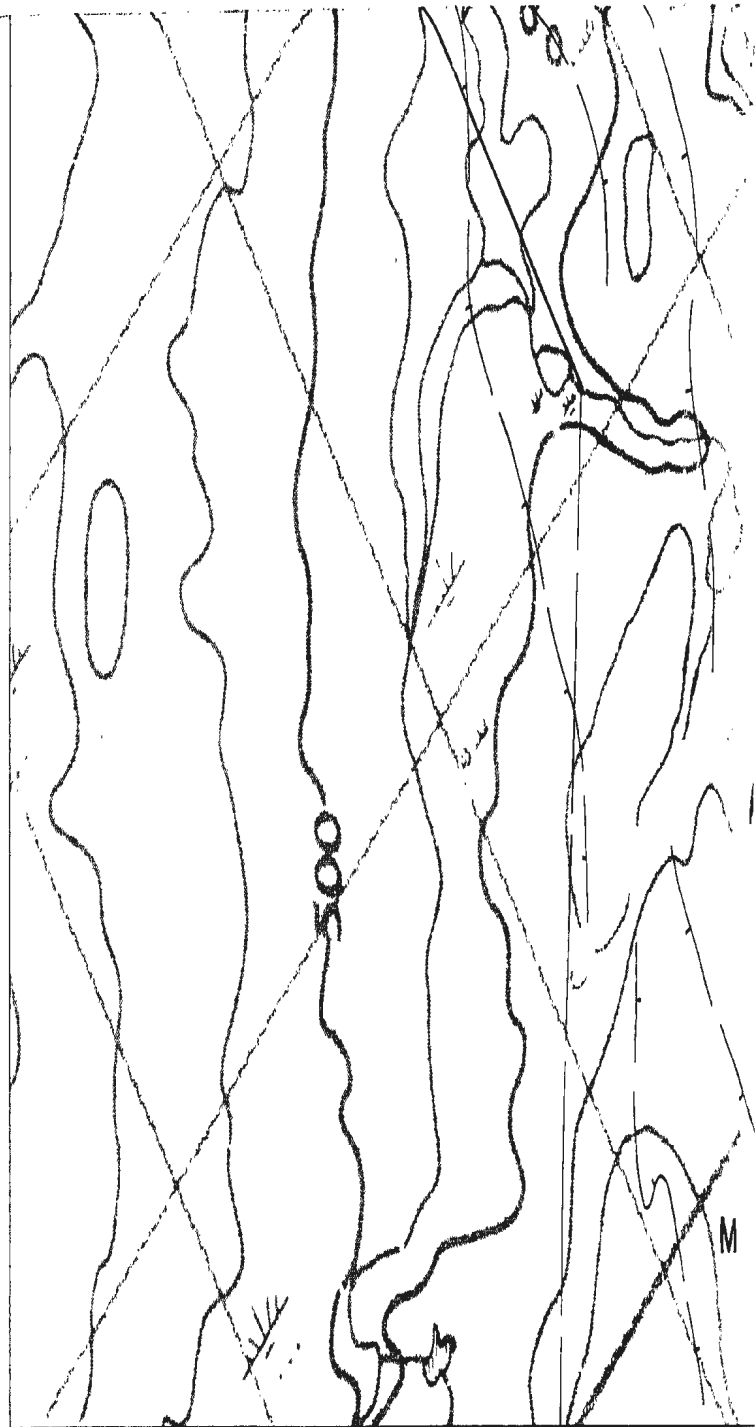


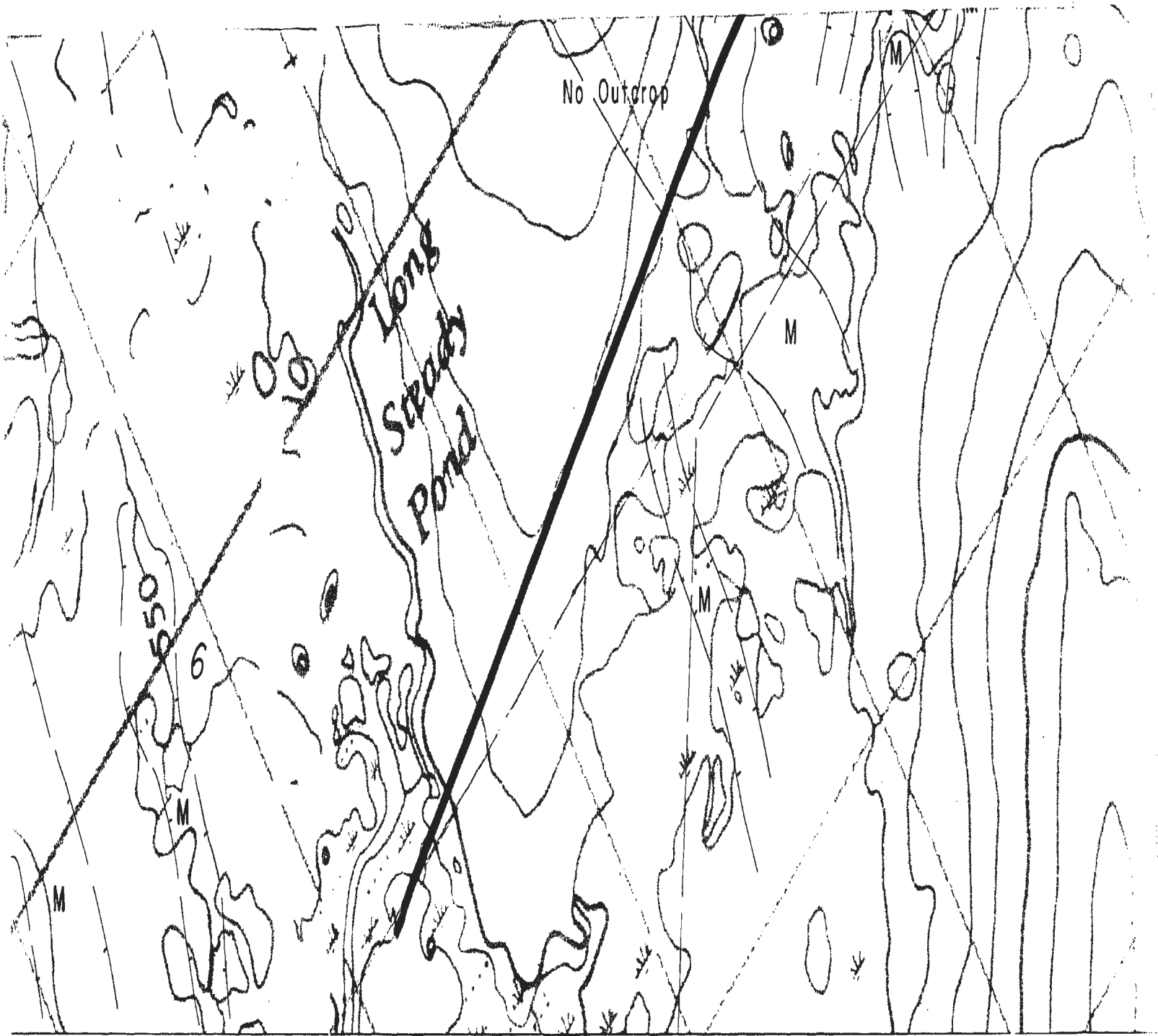


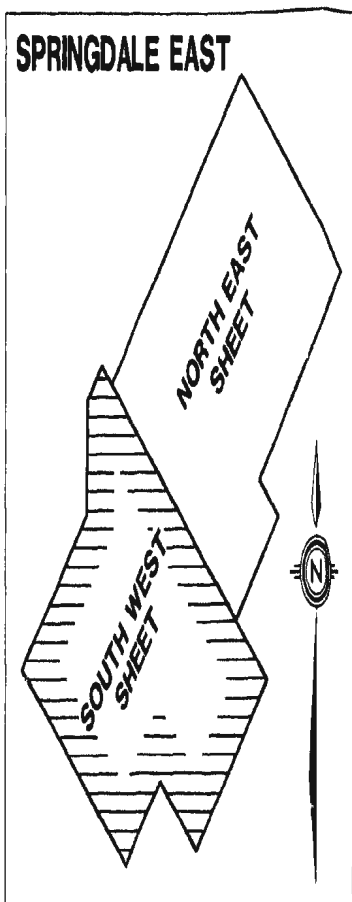
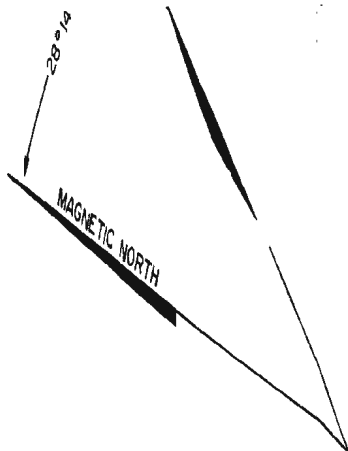


# **SYMBOLS**

|                                                                                     |                                                      |
|-------------------------------------------------------------------------------------|------------------------------------------------------|
|    | MAJOR REGIONAL FAULT<br>(Interpreted from magnetics) |
|    | FAULT                                                |
|    | GEOLOGICAL CONTACT                                   |
|    | SYNCLINE                                             |
|    | ANTICLINE                                            |
|   | FOLIATION (including, vertical)                      |
|  | LIMIT OF OUTCROP                                     |
|  | TREND OF MAGNETIC HIGH                               |







## MAP 4

SPRINGDALE EAST

(Southwest Sheet)

GEOLOGY

(Partly Inferred from Aeromagnetics)

M. Coyle, Ph. D. Thesis, 1990.



**M. COYLE, PH.D. THESIS, 1990**

**GEOLOGY, GEOCHEMISTRY AND GEOCHRONOLOGY  
OF THE SPRINGDALE CALDERA**

**LEGEND FOR MAPS 1, 1A, 1B, 2, 3, 4**

**CARBONIFEROUS**

- 14. Red to grey mudstones to pebble  
conglomerates with local carbonate  
cement.**

**SILURIAN-(DEVONIAN?)**

**SHEFFIELD LAKE GROUP**

- 13. Andesite. Aphyric to  
plagioclase-microphyric.**
- 12a. Vitric tuff. Orange to red, welded.  
Characterized by large sodic amphibole  
oikocrysts with rare resorbed  
K-feldspar phenocrysts.**



## **LEGEND (continued)**

12. Ash-flow tuff. Massive, maroon, aphanitic to flow-banded quartz- and feldspar-phyric.
11. Red and brown crystal, vitric and lithic-rich ash-flow sheets. Laharic, fault and gas-breccias. Rhyolite domes and dykes. Minor basalt.

## **SPRINGDALE GROUP**

10. Crystal-lithic tuff. Densely welded and massive large phenocrysts of quartz and feldspar, clasts of mafic and rare ultramafic lithologies.
9. Clastic sedimentary rocks. Red conglomerate, sandstone, and sandy siltstone, local caliche horizons; cross-bedding, ripples, laminations, rip-up horizons, scour channels, etc. indicate stream-flood and proximal and distal fluvial origin; clasts essentially volcanic or plutonic provenance.

## **LEGEND (continued)**

8. **Rhyolitic vitric ash-flow tuffs and breccias.** Welded, devitrified, locally massive; areas of unwelded vitroclastic tuffs with large individually devitrified shards with axiolitic texture; locally passes into sandstones; alternating thin basaltic and silicic bands in some horizons.
7. **Dacitic to rhyolitic ash-flow tuffs, vitroclastic breccia and domes.** Massive, vitric, strongly welded; curvilinear joint surfaces in the domes, with internal plastic shear zones, local brecciation, and flow folds; tuffs locally porphyritic, with small euhedral plagioclase and rare quartz phenocrysts in glassy matrix.

## **LEGEND (continued)**

6. **Silicic ash-flow tuffs.** Crystals, lithic fragments, and vitroclasts; basal lithophysae-rich horizons, grading up into a partially welded crystal-lithic lapilli tuff; broken phenocrysts of plagioclase, K-feldspar and quartz; flattened pumice bombs up to a metre long; clasts of silicic volcanics, andesite and rarely basalt.
5. **Mainly basaltic flows,** some of intermediate composition. Locally plagiophyric; with amygdales of quartz, calcite and chlorite; variably altered. Note that map units include large areas of no outcrop.
4. **Felsic to intermediate, dominantly dacitic, ash flow tuff.** Crystal-lithic and lapilli ash-flow tuffs; clasts of andesite, rhyolite, angular and flattened pumice; variably welded.
3. **Andesitic to dacitic flows.** Locally plagiophyric, massive to flow-foliated to brecciated; local intrusions of massive andesite.

## **LEGEND (continued)**

2. **Mesobreccia.** Laharic flows, tuffites and pepperites, volcanic conglomerates and breccias, red sandstones.
1. **Welded, lithic-crystal tuff.**  
Plagioclase and K-feldspar, accessory biotite, quartz, and rare opaques, clasts of granophyre, plagiophyric basalt, andesite, ultramafics, and jasper.

## **INTRUSIVE and BASEMENT ROCKS**

- I. **Quartz-K-feldspar porphyry.** Orange to green, with sodic amphibole oikocrysts and minor aegrine and altered fayalite.
- H. **Granite to quartz syenite.** Red medium-grained plagioclase, K-feldspar and amphibole porphyritic. Granophyric textured; heavily altered.

## **LEGEND (continued)**

- G. Rhyolite domes, dykes and sills.**  
High-silica. Microphenocrysts of quartz and feldspar, with finely disseminated riebeckite in groundmass; flow-foliated, auto-brecciated, zones of intense development of spherules and other indications of gas-streaming.
- F. Felsic microporphyry sills and dykes.**
- E. Microdiorite.** Black, fine-grained, massive.
- D. Granite.** Medium to coarse grained; characterized by quartz and pink feldspar with finer grained crystals of black amphibole, intruded by finer grained whitish grey granite, with locally riebeckite pegmatite and abundant amphibole-lined miarolitic cavities and fractures; offshoots of the Topsails Complex.
- C. One-feldspar granite.** White to red, medium to coarse grained, equigranular with amphibole  $\pm$  sodic pyroxene; in large part peralkaline.

## **LEGEND (continued)**

**B. Granite, granodiorite, minor diorite.**

**May in part be correlative with the Twin Lakes Complex.**

**A. Amphibolite, diorite, granodiorite, granite.** Foliated amphibolite and gabbro occurring as large screens and xenoliths in foliated diorite and granodiorite; intruded by variably deformed tonalite and amphibolite-biotite granite; intruded or net veined by a pale fine-grained granite.

**RA. Roberts Arm Group.** Mafic to felsic submarine volcanic rocks.

**CP. Catchers Pond Group.** Mafic to felsic submarine volcanic rocks.

**LB. Lushs Bight Group.** Mafic, ophiolite-related submarine volcanic rocks.





